ISSN (Print) : 2229-3574
ISSN (Online) : 2582-3485

Indian Journal of GEOSCIENCES

इण्डियन जरनल ऑफ जीओसाइन्सेस

Volume 74, No. 3, July - September 2020

K. Krishnanunni
(1941-2020)

A JOURNAL OF
EARTH SCIENCES FROM
GEOLOGICAL SURVEY OF INDIA

Indian Journal of Geosciences

A JOURNAL OF EARTH SCIENCE FROM GEOLOGICAL SURVEY OF INDIA

https://www.gsi.gov.in/IJG

SCOPE OF THE JOURNAL

INDIAN JOURNAL OF GEOSCIENCES invites original scientific contributions on any discipline of Earth sciences. The Journal also publishes review articles, short scientific communications, book reviews, announcements and letters to the editor. The official language of the Journal is English; however, original contributions in Hindi are also published.

PUBLICATION SCHEDULE

INDIAN JOURNAL OF GEOSCIENCES is a quarterly journal published in March, June, September and December. The management of the journal, however, reserves the right to release combined issue with or without prior announcement.

ADDRESS FOR CORRESPONDENCE

All correspondences (submission of manuscript, subscription, change of address, availability of back issues, advertisement, book review and other miscellaneous enquires) should be mailed to:

Director / Executive Editor, INDIAN JOURNAL OF GEOSCIENCES,
Publication Division,
Geological Survey of India,
29, Jawaharlal Nehru Road,
Kolkata 700 016, India.
E-mail: ijg@gsi.gov.in
directorpid@yahoo.co.in

Foreword

Sri K. Krishnanunni, former Director General (DG) of Geological Survey of India (GSI) fondly called Unni is known for his services to the domain of geoscience studies; the organisation and GSI to the nation. During his pioneering tenure as DG he undertook significant steps to enhance the activities of GSI and developed the field season programs as per the requirement of science as well as society.

DOVEMAP (Development of Village economy through Mineral Appraisal Programme); Project Vasundhara, a collaborative project between Geological Survey of India and ISRO aiming mineral targets; establishment of Regional Remote Sensing Service Centres (RRSSC) in GSI; National projects like preparation of lineament map and geomorphological map using Landsat imagery were the flagship initiated by Late Krishnanunni.

For his distinguished service in the field of remote sensing the Indian Society of Remote Sensing has conferred its highest award BHASKARA on Sri Krishnanunni in 2004.

It gives me pleasure to publish and dedicate this publication to the memory of Sri Krishnanunni as special volume of Indian Journal of Geosciences- inhouse journal of GSI. I convey, my heartfelt thanks to the Krishnanunni Memorial Charitable Trust for this beautiful initiative and idea of paying homage by publishing a dedicated volume housing technical papers from eminent scientists across the world.

My special thanks go to Padmashree C.P. Vohra, Dr. S.K. Acharya, Dr. Shailesh Nayak and Dr. Harsh Gupta who have contributed through messages, and all the authors for their contribution as technical papers.

I thank, Sri Anupendu Gupta, Editor-In-Chief, Indian Journal of Geosciences for his contribution as the technical reviewer for this special publication.

Last but not the least, I thank, the Mission-III team of GSI for making this volume a success.

(Dr. Ranjit Rath)
Director General

Preface

All volumes of GSI's internal journal 'Indian Journal of Geosciences' are special but the current volume dedicated to the memory of late K. Krishnanunni, former Director General, GSI is unique because of its nature, content and the overwhelming response received.

Late K. Krishnanunni was a person of rare qualities who inspired many geoscientists of the country to dedicate themselves for the service of the Nation. He has been a role model for many of us and he was like my elder brother since I first met him at Shillong in a wintery October morning of 1996.

At the outset, I thank Dr. Ranjit Rath, Director General, GSI for extending all the support in bringing out this special volume. I thank Dr. S. Raju, Additional Director General & National Mission Head-III for providing required logistics for publishing the volume. I thank Padmashree C.P. Vohra, former DG, GSI, Dr. S.K. Acharya, former DG, GSI, Dr. Shailesh Nayak, President, Krishnanunni Memorial Charitable Trust (KMCT), former Director, NIAS and former Secretary, Ministry of Earth Sciences and Dr. Harsh Gupta, former Secretary, DoD, former Director, NGRI and President, Geological Society of India for their kind messages sent in memory of Late K. Krishnanunni.

I am thankful, on behalf of GSI and on my own behalf, to the authors who are in top echelons in their respective fields. They include former DG's of GSI, eminent scientists and professors from across the country. Their valuable contributions, assimilated from various experiences in varied fields of geosciences have fortified this unique volume of Indian Journal of Geosciences.

I thank Sri E.V.R. Parthasaradhi, former DDG, GSI and Secretary, KMCT for his regular interactions and efforts to obtain papers from eminent geoscientists from India and abroad.

My special thanks go to Dr. Anupendu Gupta, former Dy. D.G., GSI, Editor in-Chief, IJG and Vice President of KMCT for his guidance, relentless work in editing the papers of highest standards for this volume.

Bringing out this special volume in record time would have been impossible but for the tireless efforts, for last two months, by my team mates, Smt. Pushp Lata, Director, Shri James Pebam and Shri M. Karthikeyan, Senior Geologists. I thank them from the bottom of my heart.

I am sure, this special volume will be a unique one and will be a guiding factor to its readers in scientific endeavour, policy making and planning for development of the Nation with appropriate usage of Geosciences.

(P.C. Patra)
DDG, Mission-III B

Message

I remember Sri Krishnanunni as a highly intelligent no-nonsense person with amiable behavior, having a vision for the introduction of the latest techniques in geological studies and their applications in applied fields. After having brilliant records in his studies he secured top position in the first UPSC examination held in 1964 for entering GSI.

Sri Krishnanunni soon developed an expertise in geological interpretation of air-photos and satellite imagery through his training and higher studies in India and abroad. His stints in ISRO and NRSA, on deputation, helped to build up a pioneering expert group who manned several centers (RRSSC) across the country for coordination with various Central and State agencies for the application of satellite data in their fields of study. In GSI, Sri Krishnanunni systematized computer applications in technical and management information systems. The project Vasundhara, initiated and steered by him led to the synthesis and interpretation of vast multi-disciplinary geoscientific data-sets collected over several decades in peninsular India. This was followed by programs of Informatics for a similar exercise in other selected parts of the country.

While in the Northeastern Region of GSI, Sri Krishnanunni initiated an innovative project on the development of the village economy through low-cost mineral appraisal (DOVEMAP) in the rural areas of the Northeastern States, which was soon adopted by other Regional offices of GSI.

The human approach of Sri Krishnanunni was unique. He was friendly and helpful to all his colleagues and friends. This is nice to see GSI's gesture to publish a special volume of IJG in his memory.

Lander P. Vohra

C. P. Vohra, *Padmashree*
Former Director General, GSI,
San Fransisco

Message

Sri Kalathinkal Krishnanunni, popularly known as Krishnanunni was one of my closest colleague in GSI. His all round brilliance and vision for modern geoscientific innovations and applications were well appreciated. His training in photogeology and remote sensing in IPI, Dehradun and DELFT, The Netherlands, early in his career, instilled a lifelong passion, love and authority on these fields of study and their utilization in diverse developmental arena.

Starting from Gujarat Circle in initial days, Sri Krishnanunni left distinctive mark wherever he was placed. In CHQ Kolkata as Director of PGRS Division and Geodata Division he infused new initiatives in launching Project Vasundhara for integrating all the data sets collected since several decades in Peninsular India. As DDG in North-Eastern Region he started DOVEMAP for rural development and employment generation.

On deputation to NRSA (1976-79), Sri Krishnanunni worked as Technical Staff Officer to the Director NRSA, assisting him in all technical matters of planning and implementation, which included facilities for remote sensing data procurement, processing and utilization and recruitment of suitable technical personnel. He was also actively involved in the discussions for procurement of airborne Modular Multispectral Scanner (M^2S) and Multispectral Data Analysis System by NRSA His expertise in the field drew him again to ISRO on deputation (1986-89) for establishing Regional Remote Sensing Service Centres (RRSSC) across the country. Sri Krishnanunni was highly appreciated by the then Chairman, ISRO Prof. U R Rao and Secretary, Ministry of Mines, Government of India Sri B K Rao.

When posted at CHQ, Kolkata as Sr. DDG, he was a great support to me in both technical and administrative matters. He prepared a document on project INDIGEO, a collaboration project with the I.T.C. The Netherlands aimed at capacity building of trained manpower in GIS, digital image processing and development of management skills in GSI and other Institutions. He was interacting with the Secretary, Additional Secretary and other officials of the Ministry of Mines and prepared a document on the role of the Ministry in the functioning of GSI.

I feel fortunate to have worked in close association with Sri Krishnanunni, who besides being a highly proficient geologist had great human qualities. His compassion and humane touch in dealing with people has left behind very large number of admirers, who have instituted a Trust in his memory. It is unfortunate that he had very short stint as DG, GSI and further suffered from major illness after superannuation. I appreciate DG, GSI for this Special volume of Indian Journal of Geosciences in remembrance of Sri Krishnanunni.

Dr. S.K. Acharyya
Former Director General, GSI
Emeritus Scientist
Department of Geological Sciences, Jadavpur University, Kolkata

Message

I am very pleased to learn that Geological Survey of India (GSI) is bringing out a special publication in memory of Shri. K. Krishnanunni, former Director General of GSI. Thanks to Shri Parthasaradhi to ask me to write a few words for my good friend Krishnanunni.

We both entered Indian School of Mines, Dhanbad in 1959. Krishnanunni was admitted for Mining. In those days, Mining was the most sought-after course of studies at ISM. Several students, who did not get Mining, would do a double diploma in Mining after doing masters in Geology, by studying for an additional year. However, Krishnanunni, after joining ISM, discovered that as he had done B.Sc. with Geology, he could get admission in the 2nd year of the 4- year M.Sc. course in Geology and opted for it. His has been the first and only case of a student switching from Mining to Geology at ISM. This simply describes his love for Geology. Another worth remembering happening at ISM is Krishnanunni's bringing out a special publication dedicated to Dr. S.K. Roy, the first head of the Department of Applied Geology at ISM, almost single handed where among others, Dr. B.C. Roy, Director General of the GSI, also contributed.

We kept in contact of one-another. During, 1976-1977, when he was deputed to NRSA, I was at Hyderabad with the National Geophysical Research Institute, and that provided us ample opportunities to interact. During 1982 to 1990, I was at Trivandrum and Cochin. Krishnanunni made a point to look me up on his visits to Kerala. I was always impressed with his vision, hunger and commitment to do new things which are amply reflected in his illustrious career.

His dedicated work for GSI, NRSA and AMD lead to many new initiatives for which he would always be remembered.

Officers of GSI deserve appreciation in bringing out this volume. I wish well to the family members of Shri K. Krishnanunni.

(HARSH K GUPTA)
President
Geological Society of India, Banglore

Message

Shri K Krishnanunni, former Director General of the Geological Survey of India (GSI) has pioneered the remote sensing applications, especially related to geosciences in the country. He made significant contributions during early phases of the then National Remote Sensing agency (NRSA) and built very strong team of advancing geoscience applications of satellite data. Later, he conceptualised and set up Regional Remote Sensing Service Centres, in close association with major user institutions, Geological Survey of India, National Bureau of Soil Science and Land Use Survey, Central Arid Zone Research Institute and Indian Institute of Technology, Kharagpur. He was instrumental in introducing remote sensing, especially satellite remote sensing in GSI. One of the greatest contributions to the field of remote sensing was launching the project 'Vasundhara'in eighties for demonstrating use of remote sensing in mineral exploration. For the first time, an integrated survey using satellite remote sensing, air-borne geophysical survey, field-based geological and geophysical survey and lab-based geochemical analysis was undertaken. All these scientific data was organised in indigenously developed INGIS and aided in mineral search and prognostication. This project had laid foundations for many national projects in different fields as part of Remote Sensing Application Mission. For his distinguised services to the field of remote sensing, the Indian Society of Remote sensing has conferred its highest award 'Bhaskara' in 2004. Dr. Krishnanunni has left us but his legacy will continue forever.

(Shailesh Nayak)
Chair,
Krishnanunni Memorial Charitable Trust,
Hyderabad

From Editor's Desk

I am thankful to GSI for bestowing on me the responsibility of editing this Special Volume of Indian Journal of Geoscience to be published in the memory of Sri K. Krishnanunni, Former DG, GSI, who departed recently. It is certainly a priviledge to get associated with this act of paying tribute to the esteemed personality, who was my close friend and senior colleague in GSI for many years.

In course of editing, I was fortunate to have glimpses of so many valuable contributions made by eminent scientist from different Institutions of India and abroad on variety of sub-disciplines of geosciences and beyond. Some of the contributors were course mates of Sri. Krishnanunni in ISM, Dhanbad and some were his associates in many departments, other than GSI. In total 21 papers are accommodated in this volume, in addition to a brief life sketch of Sri Krishnanunni and a few messages commending the befitting efforts of GSI in remembrance of this widely admired man.

I am grateful to Sri P.C.Patra, DDG, M III-B and to the editorial group of Publication Division, GSI, headed by Smt. Pushp Lata, Director for help and coordination. The constant support and guidance received from Sri. E. V. R. Parthasaradhi, former DDG, GSI and Secretary of Krishnanunni Memorial Chartable Trust, Hyderabad, is gratefully acknowledged.

Dr. Anupendu Gupta,
Ex-DDG, GSI,
Editor-in Chief,
Indian Journal of Geosciences

Krishnanunni - A life sketch

Kalathinkal Krishnanunni, popularly known as Krishnanunni was born on 23rd March 1941 at Paravur, near Ernakulam, in Kerala. His father Prof. P. Kochunni Panicker was a history Professor and Principal of Victoria College, Palakkad and his mother Smt.Sarojini Amma was a housewife. His school education was from his native place Paravur and graduation from University College, Trivendrum. He obtained his M.Sc (Applied geology) degree in 1962 from the Indian School of Mines (ISM), Dhanbad. All through his career he had a brilliant academic record.

After a short stint as demonstrator in ISM, Sri Krishnanunni worked as a Scientist in Atomic Minerals Directorate (AMD) during 1963-65. While working in AMD, he appeared for the first UPSC examination for recruitment as Geologist in the Geological Survey of India (GSI) in 1964 and topped the list of 110 successful candidates.

He started his career in the GSI at Gujarat Circle, Ahmedabad in 1965. In 1968-69 he was deputed to the then Indian Photo-interpretation Institute (IPI), Dehradun presently known as IIRS, for training in air photo interpretation for geology. He stood first in the batch in the qualifying examination, by virtue of which, he was awarded a fellowship at the International Institute for Aerial Surveys, popularly known as ITC at Delft, the Netherlands during 1969-71 for pursuing Master's course which he accomplished with distinction. In early 1973 he was transferred to Map Division, Central Headquarters, Kolkata, which also included Photo geology Division and continued there till 1984 but for break of two years 1976-77, when he was deputed to the newly formed National Remote Sensing Agency (NRSA). During his long stay in Kolkata he was responsible for popularising the use of photo geology and remote sensing in GSI. After this initiative each of the Regions had started P G R S Divisions and included several investigations in their annual field programme involving the use of photo geology and remote sensing. From CHQ Sri Krishnanunni has initiated National projects like preparation of lineament map and geomorphological map using Landsat imagery. Prof. Satish Dhavan, Chairman ISRO and Prof. Pisharoty, father of remote sensing in India were highly appreciative of GSI and its scientists for their early initiative and commitment to the use of remote sensing techniques. Much of the credit for this goes to Sri Krishnanunni.

Apart from his technical achievements, Sri Krishnanunni was equally involved in the welfare measures for fellow earth scientists. He was actively associated with GSI Scientific Officers Association (GSISOA). He along with a few colleagues created GSISOA Welfare Fund aimed at rehabilitation of families of officers who lost lives while in service. The fund was financed by annual subscription from members of SOA, with the bulk of collections going towards payment of premium of LIC Group Insurance scheme, and the balance forming a corpus to meet operational expenses.

Though the institution of Central Government Employees Group Insurance Scheme (CGEGIS) by the GOI in 1980-81 (which was almost a replica of GSISOA WF, but with financial benefits several times higher) has reduced the attraction of GSISOA Welfare Fund, Sri Krishnanunni made it possible to make some constitutional changes and by delinking LIC ensured that all the additional benefits were passed on to only the families of deceased members.

Sri Krishnanunni was deputed as staff officer to the Director of National Remote Sensing Agency (NRSA) in 1976. It was a new organization formed by the Government of India, for collection, processing, utilisation and dissemination of remotely sensed data in the country. Sri Krishnanunni assisted the Director NRSA on all technical matters, their planning and realisation, which included facilities for remote sensing data procurement, processing and utilization and recruitment of suitable technical personnel. He was also associated with planning of indigenous facilities for collection of aero magnetic data and also in the procurement of airborne Modular Multispectral Scanner (M^2S) and Multispectral Data Analysis System by NRSA.

Sri Krishnanunni was deputed to ISRO during 1986-89 mainly with the task of establishing Regional Remote Sensing Service Centres (RRSSC) with the main objectives of providing support of digital infrastructure in processing Remote Sensing data, taking up of collaborative projects, training and capacity building exercises in their respective regions. He was successful in establishing RRSSC's at Bengaluru, Nagpur, Jodhpur, Kharagpur and Dehradun with the State of the art hardware and software facilities and competent technical manpower with the support and co-operation from the stake holding Ministries and Departments of Government of India. One of the prestigious projects taken up at that time was Project Vasundhara, a collaborative project between Geological Survey of India and ISRO aimed at prognosticating mineral targets by multi-theme data integration including digital image processing. That the RRSSCs conceived and commissioned by Sri Krishnanunni, have now become Centres of Excellence for the application of geospatial technologies in the country is a fitting tribute to Krishnanunni.

On repatriation to GSI in 1989, he was posted first in Geodata Division and then in the International Wing at Kolkata. On promotion as Deputy Director General in 1992, he was posted in the Northern Region, Lucknow. In 1994 he was transferred to North-Eastern Region, Shillong where he continued upto 1998. He conceived a project called DOVEMAP (Development of Village Economy through Mineral Appraisal Programme) aimed at improving village economy and increasing rural employment. The project was successfully implemented in 400 villages of different states of the North-east and the results shared with concerned local officials. He was promoted as Sr. DDG. in 1997 and continued in Shillong. In March 1998, he was transferred to the Central Headquarters, Kolkata where he assisted the then Director General Dr. S.K. Acharyya in both technical and administrative matters relating to the Department. He was also interacting with the Secretary and other officials of Ministry of Mines, Government of India. He was Chairman of the experts panel constituted by the Ministry of Mines for modernization of GSI in March 2000. Experts from GSI and other scientific and user organizations were the other members of the panel. The panel gave its report in three months time and suggested several far reaching recommendations on the type of facilities to be created and managed for modernization of the Department.

Sri Krishnanunni was promoted as Director General on 1-12-2000 and his first job was to plan celebrations on 150 years completion of the Geological Survey of India which he successfully organized in Central Headquarters, Regions and States. He authored a number of technical papers which were published in national and international journals of repute.

After 36 years of yeoman service in the Department, Sri Krishnanunni superannuated on 31-3-2001 and settled in Palakkad in Kerala.

For his distinguished service in the field of remote sensing the Indian Society of Remote Sensing has conferred its highest award BHASKARA on Sri Krishnanunni in 2004.

He expired on 4-6-2020 after a brief illness, leaving behind his wife Ms. Latha, two sons and their families and a host of his admirers in sorrow.

Sri Krishnanunni was a great intellectual and visionary besides being a good human being. Through his informal attitude and generous nature he attracted many admirers from all walks of life. To perpetuate his vision and propagate his ideals his admirers formed Krishnanunni Memorial Charitable Trust. The main activities proposed by the Trust include organising memorial lectures, awarding financial grant to needy students and through publications. This special publication by GSI is a humble effort by the trust, vigorously followed by Sri P.C.Patra, DDG, GSI and himself a great admirer of Sri Krishnanunni.

E.V.R. Parthasaradhi
Former DDG, Geological Survey of India

Contents

Invited Papers

Indian Journal of Geosciences, Volume 74, No. 3
July - September, 2020; pp. 191-196

Invited Paper

Towards Blue Economy: A Perspective

Shailesh Nayak

National Institute of Advanced Studies (NIAS), Bengaluru - 560094
Former Secretary, Ministry of Earth Sciences
Email: shailesh@nias.res.in

Abstract: The term 'Blue Economy' emphasizes essentially an ocean-dependent economic development to improve quality of life of people. India committed to advance the "Blue Economy" and several programs have been initiated to promote blue economy in the country. One of the important components of promoting blue economy is to have adequate information about sea bed and mineral resources, in the Exclusive Economic Zone (EEZ), Legal Continental Shelf as well as High Seas. Apart from placer minerals on the coast, we need to explore for minerals, such as manganese nodules, polymetallic sulphides and cobalt crusts in High Seas. The availability of gas hydrates on our continental shelf has huge potential to satisfy our ever-increasing energy requirements. We need to invest in developing technology and human resources to utilize these resources. At the same time, the development of offshore mineral and energy resources will need setting up of infrastructure facilities on the coast. As coastal zone is vulnerable to many hazards such as cyclones, storm surges, tsunamis, coastal erosion, sea level rise, etc., an assessment of coastal vulnerability to understand risks involved, has to be undertaken. Various environmental data will be required to utilize ocean resources. An institutional framework for implementing activities related to blue economy to be set up so that investments in building infrastructure, developing human resources, and setting up governance system shall pay rich dividends for future generations and ensure sustainability.

Keywords: Blue economy, polymetallic nodules and sulphides, gas hydrate, coastal zone management.

Introduction

Oceans provide energy, food and mineral resources, facilitate trade and commerce, control weather, climate and hazards as well as present an ecosystem to survive. Our economic dependence on ocean has been increasing and will continue to increase in future. Prof. Guntar Pauli was first to introduce the term 'Blue Economy' to reflect the needs of people for growth and prosperity in view of impacts of climate change (Pauli, 2010). The term 'Blue Economy' has been defined as an ocean-dependent economic development for improving quality of life of people while ensuring inclusive social development as well as environmental and ecological security. It means that there should be certain limitations on the technology-based economic development and emphasis should be on social obligations to protect and conserve coastal and marine ecosystems. The Third World Summit Conference UN+20 in 2012 had also focused on expanding the "Green Economy" to "Blue Economy" and subsequently UN advocated conservation and sustainable use of ocean resources as one of goals under Sustainable Development Goals (SDGs). UN has also declared 2021-2030 as the "Decade of Ocean Science for Sustainable Development." Hence, it is very apt to discuss about the role of geoscience in development of blue economy.

The major components of the Blue economy are 1. Sustainable use of living resources, 2. Exploration and utilization of minerals, hydrocarbons and develop renewable energy resources, 3. Development of deep ocean technologies for harnessing resources, 4. Development of shipping and ports to facilitate trade, 5. To encourage eco-friendly tourism along the coast and 6. Assessment of hazards and response mechanism (cyclone, tsunami, sea level rise, coastal erosion, etc.).

The issues related to geoscience such as surveying of sea bed, exploration of mineral and energy resources, and coastal zone management are briefly discussed in this article.

Survey of the Exclusive Economic Zone and Legal Continental Shelf

The marine geophysical survey of a sea bed is one of the prime requirements for assessing potential for mineral and energy resources. The United Nations Convention on the Law of the Sea (UNCLOS) established different maritime zones for coastal states with corresponding duties and obligations, viz. Exclusive Economic Zone (EEZ), Continental Shelf and High Seas (International Seabed area). The EEZ extends up to 200 nautical miles from baseline and Indian EEZ covers 2.02 million sq km. India has sovereign rights over the waters, sea bed and sub-soil for the purpose of exploring and exploiting, conserving and managing living and non-living resources and other economic activities. Multibeam bathymetry and geophysical surveys have been undertaken by the Earth System Science Organization (ESSO) – National Centre for Polar and Ocean Research (NCPOR), ESSO-National Institute of Ocean Technology (NIOT) as well as Geological Survey of India (GSI). These surveys mapped topographical and geomorphological features such as sea mounts, channel levees, abyssal plains, slumps, etc. Systematic samples were drawn and analyzed to understand resource potential. About 80 per cent of survey of EEZ has been completed and maps of 2° x 2° are under preparation (M. Ravichandran, Personal Communication).

The continental shelf comprises the seabed and subsoil of the submarine areas that extend beyond the territorial sea and as natural prolongation of land territory to the outer margin of the continental margin. India can assert their sovereign rights over resources of the legal continental shelf, up to an outer limit of 350 nautical miles from the baseline upon fulfilling certain conditions and based on the recommendations of the Commission on the Limits of the Continental Shelf (CLCS). A reconnaissance marine geophysical survey, viz. multi-beam bathymetry, gravity and magnetic profiling, and multi-channel seismic reflection and refraction, measuring 31,000 line km, along with 90 ocean bottom seismometer, on the continental shelf of India was carried out (Nayak, 2014). These surveys were conducted by ESSO-NCPOR, Council of Scientific and Industrial Research (CSIR) – National Geophysical Research Institute (NGRI) and CSIR-National Institute of Oceanography (NIO). These data were used to prepare a claim of about 0.6 million sq. km in the Arabian Sea and submitted the CLCS in 2010. The second submission to CLCS in the Bay of Bengal is yet to be done. All these data related to EEZ and CLCS have been organized as Marine Geo-scientific Database at ESSO-NCPOR.

The High Seas are areas beyond EEZ and beyond the limits of national jurisdictions. The exploration and exploitation of mineral resources of sea bed and ocean floor in the High Seas are to be undertaken after concurrence of the International Seabed Authority (ISBA) established under UNCLOS. Three categories of the deposits have been identified, polymetallic manganese oxide nodules (PMN), polymetallic sulphides (PMS) and cobalt-rich ferromanganese crusts (Co-Fe-Mn) by ISBA to undertake exploration surveys by nations. The details about the surveys undertaken by India are discussed in the next section.

Mineral and Energy Resources

The development of offshore mineral and energy resources is complimentary to replenish the country's requirements for its industrial and economic growth. The assessment of mineral and energy resources has been undergoing since last couple of decades, however, the exploration and assessment of these resources and development of suitable technologies need to be stepped up. Considerable investments in terms of human and financial resources are required to meet these challenges. Such investments will be beneficial to the country in the long run for sustained economic growth.

Mineral Resources: Coastal and offshore minerals offer many strategic metals, such as nickel, cobalt, copper, uranium, thorium, titanium, etc. India does not have resources for key metals such as nickel and cobalt and copper resources are dwindling. The reserves of these metals on land may not last more than few decades and we will have to depend on supplementary offshore resources. These minerals are distributed right from coast to deep sea, to the depth of 6000 m.

Coastal placer minerals, such as ilmenite, rutile, magnetite, garnet, zircon are extensively available on the Kerala, Tamil Nadu, Andhra Pradesh, Orissa and Maharashtra coasts and nearshore waters (Loveson and Misra 2004; Loveson et.al. 2005; Loveson et.al. 2007). The Geological Survey of India (GSI), Atomic Mineral Division (AMD) of the Atomic Energy Department (AEC) and CSIR-NIO have been involved in exploration and survey of these minerals. The reserves of ilmenite, rutile, garnet, zircon, kainite and sillimanite are estimated to be about 600, 30, 60, 35, 2 and 4 million tons, respectively, which is worth of approximately US $ 120 billion (Indian Mineral Yearbook, 2017). The enormous presence of offshore ilmenite and other placers deposits has led the Govt. of India to encourage offshore mining through "Offshore Area Minerals (Development and Regulation) Act 2002" and "Offshore Mineral Concession Rules 2016". The Ministry of Mines in 2010 have notified specified offshore blocks of 5' x 5' size, 26 in the Bay of Bengal and 37 in the Arabian Sea for exploration (The Gazette of India No. 1126 dated June 9, 2010). Many private companies have shown interest and have signed MoU with the concerned state governments such as Tamil Nadu and Orissa to utilise these resources. Various indigenous technologies for mining and beneficiation of these minerals have been developed.

Poly-metallic nodules are scattered on sea floor in the Central Indian Ocean (CIO) beyond the depth of 4000 m. India has exploration rights, as granted by the International Sea Bed Authority (ISBA) over 75,000 sq. km in the CIO. India has been recognized as the 'Pioneer Investor.' It has entered into a contract with ISBA for exploration of polymetallic nodules (PMN) and is valid up to 2022. Detailed exploration geophysical and geological surveys have been carried out by CSIR-NIO since 2002. The first mining site of about 12.5 x 12.5 km has been identified. The environmental data for baseline conditions have been collected. The environmental impact assessment (EIA) has been carried by simulating mining and predicting its impacts as well as suggesting mitigation measures (Sharma, 2011). The total reserves are 380 million tons, comprising Mn, Ni, Cu, Co, etc. (Jauhari and Pattan, 2000). The total worth of these reserves initially estimated to be about US $ 45 billion (based on average metal process in June 2018). However, recent estimates by ISBA puts their worth to be around US $ 187 billion.

Metallurgical processes for extraction of metals, Mn, Cu, Ni, Co, have been developed using different approaches by CSIR-Institute of Mineral and Metals Technology (IMMT) and CSIR- National

Mineral Laboratory (NML). A pilot plant of 500 kg capacity was set-up at the Hindustan Zinc Ltd, Udaipur to demonstrate the hydro-metallurgical process for extraction of copper, nickel and cobalt. Efforts are to be initiated to extract other metals also.

The poly-metallic sulphides, associated with mid-oceanic ridges, have kindled lot of interest due to high concentrations of the base metals (Cu, Pb, Zn) and noble metals (Au, Ag. Pd, Pt). India has entered into an exploration contract in 2016 with the ISBA covering an area of 10,000 sq. km for 15 years in the SW Indian Ocean. ESSO-NCPOR has been leading these efforts. Preliminary surveys have been undertaken to study various oceanographic, chemical, geological and biological studies to identify potential sites. The exploration work is under progress and analysis and interpretation of data/samples are underway.

The rare metals (metals having concentration of few milligrams per ton in the Earth's crust), such as cobalt (Co) which have applications in high-tech industries, are found in abundance on the seamount ferromanganese crusts. Cobalt is mostly associated with copper, nickel and arsenic. The first Co-enriched ferromanganese encrustations (SFMC) was reported in the equatorial Indian Ocean Seamount, called Afanasiy Nikitin sea mount (Banakar, *et al.* 1997; Parthiban and Banakar, 1999). The most dominant metals in SFMC are Mn, Fe, Co, Ni, Cu, V, Pb, Zn, followed by Rare Earth Elements (REE) and followed by Platinum Group Elements (PGE). These expeditions have revealed that Co content varies from 0.3 to 0.9 % while Pt ranged from 200-900 ppb (Banakar *et al.* 2007; Rajani *et al.* 2005). Cobalt being strategic importance, it is crucial for India to seek exploration rights in this region to understand their mode of occurrence, estimate their resources, assess economic potential and develop technology to harness them.

Energy Resources: The Ocean has been providing most of energy requirements of mankind. India, is one of the largest consumers of fossil fuel, however, indigenous production is only 30 per cent of requirement. Gas hydrates, ice-like crystalline form of methane (99.9%) and water, are considered as a major future hydrocarbon energy resource and occurs in shallow sediments along continental margins of India where water depth is more than 500 m. The volume of methane gas in the deep ocean located gas hydrates reservoirs of India is prognosticated to be 1900 TCM. It is presumed that only 10% recovery can meet India's energy requirement for 100 years (Sain and Gupta, 2008; Sain and Gupta, 2012). A detailed program for understanding formation of gas hydrate as well as development of technology to harness same has been launched.

Under the aegis of the Ministry of Earth Sciences, ESSO-National Institute of Ocean Technology (NIOT), CSIR-NGRI and CSIR-NIO are pursuing activities towards delineation and resource estimation at prospective targets. CSIR-NIO has commenced many cruises in Krishna, Godavari and Mahanadi basins and other places and subsequently generated a huge database on geological and geophysical information for gas hydrates exploration studies (Dewangan *et al.* 2010; Mazumdar *et al.* 2009; Muralidhar *et al.* 2006). CSIR-NGRI has set up a state-of-art Gas Hydrate Research Centre comprising inversion, processing, modelling & interpretation of seismic data for detection and assessment of gas hydrates along with laboratory studies to understand formation and dissociation kinetics to provide inputs for developing suitable production technology. The decade long research has led to characterize gas hydrate reservoirs, development of methods for quantification and assessment of gas hydrates, identification of prospective zones in the Krishna-Godavari, Mahanadi and Andaman offshore basins (Sain, 2017). The development of full waveform tomography (FWT) has facilitated estimation of critical parameters such as porosity, permeability, pore pressure and geo-technical properties that are required for the development of viable production technology. ESSO-NIOT has been engaged in developing numerical models towards extraction of methane gas from gas hydrate reservoirs. Various models for thermal simulation, gas hydrate reservoir modelling, methane gas bubble dissolution model, etc. have been developed and a patent has been obtained (Vedachalam *et al.,* 2016).

The National Gas Hydrate Program (NGHP), spearheaded by the Directorate of Hydrocarbons (DGH) and Oil and Natural Gas Commission (ONGC) have completed two drilling expeditions NGHP-01 and 02 in Mahanadi basin and near Andaman Islands, utilising Joides Resolution of USA and Chikyu of Japan, respectively, in KG basin. The expeditions have identified two distinct gas hydrate accumulations in the KG basin with layer type and fracture type settings with thickness ranging from 20-100 m, within 200 m below sea floor at 2200 m depth. ONGC has set up a Gas Hydrate Research & Technology Centre (GHRTC) at Panvel, Maharashtra for R&D works relating to exploration and exploitation of gas hydrate resources. The proposed NGHP-03 aims at pilot production testing for understanding of the environmental impacts.

Ocean Technology: India has been planning to harness ocean mineral and energy resources. This requires development of a set of equipments, viz., in-situ soil tester, remote operable vehicle, autonomous coring machine, autonomous vehicles, manned submersible and mining equipment. ESSO-NIOT is actively engaged in developing suitable technologies. The visual observation of sea floor, measurement of characteristics of sea bed and environs is one of the important requirement of exploration for minerals.

Remotely operated vehicle (ROSUB 6000) has multifunctional sampling tools operated with robotic arm, high-resolution video imaging systems, scientific payloads and multi-beam sonar and can operate up to 6000 m depth (Ramadass *et al.* 2020). ROV is proved to be very useful for collecting scientific data and seabed samples towards mineral exploration, seabed imaging, gas hydrate exploration, pipeline routing, submarine cabling, etc. A remotely operable soil tester (ROSIS) have been developed for obtaining soil properties and tested at 5500 m depth (Muthukrishna *et al* 2014). The strength of soft sea-bed, especially the bearing strength and shear strength parameters for designing mining equipment. An acoustic positioning system which facilitates deep sea positioning and track keeping has been developed.

Deep water Wire-line Autonomous Coring Machine (WACS) has been developed for obtaining core up to 100 m at the depth of 3000 m water depth for geotechnical investigations and assessment of ocean resources (Ramesh *et al.* 2020). The coring system has unique capability to collect gas hydrates with custom-built in situ pressure core sampler.

Polymetallic nodules are available in deep sea having pressure of 550 bar and very soft soils 2.5 kPa (similar to heavy grease). The development technology for mining these nodules is a major challenge and has been underway at the ESSO-NIOT. The system comprises seabed-based crawler, vertical riser and surface facility for collecting produced minerals. A mining machine, a tracked vehicle, developed and demonstrated at water depth of about 500 m, where nodules were collected, pushed and pumped to the mother vessel (Varshney *et al.* 2015). These results are being used to develop a mining machine system for 6000 m is being developed.

Freshwater from Sea: All developmental activities along the coast and in high seas, will require freshwater, which is scarce. Freshwater from sea is a very attractive solution; however, plants based on reverse osmosis technology are ecologically unfriendly. A Low Temperature Thermal Desalination, an environment-friendly technology that utilizes natural ocean thermal gradient, is found to be suitable for this purpose. Three plants, in Kavaratti, Agatti and Minicoy, each generating 100,000 l/day, based on this technology has been under operation on the Lakshadweep Islands (Nayak, 2010) during last 15 years. Water-borne diseases have reduced considerably on the Islands. Similar plants are being set up in remaining islands. Power plants also generate hot waste water and can be used to generate drinking water or boiler quality water. The technology was successfully demonstrated at the North Chennai Thermal Power Station (Jahihal and Prabhakaran, 2019). The technology is now being scaled up and a plant for 1.5 million l/day is being set up at the Tuticorin Power Plant. An offshore plant for generating 10 million l/day freshwater is being planned. The challenge is to design suitable seawater intake and appropriate ocean platform and experiments are underway. The successful implementation of this technology will ensure freshwater availability for developmental activities.

Coastal Zone Management

All above mentioned developmental activities will increase pressure on the coastal zone. Hence, an effective coastal zone management plan, comprising a regulatory mechanism for conserving coastal and marine ecosystem, ocean state advisory for safe shipping and navigation system, vulnerability assessment of coastal hazards and warning systems for these hazards, has been developed. In India the areas between high and low tides and 500 m from high tideline are declared as 'Coastal Regulation Zone (CRZ)' and in this zone, certain activities are restricted or prohibited in order to preserve and conserve coastal ecosystems. This regulation has helped to conserve vital and critical ecosystems, provide livelihood security to coastal communities and promote socio-economic development (Nayak, 2017). The management plans for the entire Indian Coast have been prepared which will help to build necessary infrastructure for 'Blue Economy'.

The information on sea state (sea surface temperature, currents, mixed layer depth, waves, tides, etc.) is required for economic activities such as shipping, fishing, oil and gas production. Numerical models have been customized to forecast waves, ocean currents, sea surface temperature, etc. on a daily basis. A three to six-hourly forecast for waves (height and direction), sea surface temperature, mixed layered depth, depth of thermocline, surface currents are provided 5 days in advance for the entire Indian coast and Indian Ocean at various spatial scales (Balakrishnan Nair *et al.* 2013) and can be accessed on www.incois.gov.in.

The coast is also vulnerable to many hazards such as cyclones, storm surges, tsunamis, coastal erosion, sea level rise, etc. The prediction of landfall point has been is about 40 km and intensity is accurate in 85% cases (Goyal, *et al*, 2013) and forecast are provided at least 5 days in advance to all stakeholders. The prediction of associated storm surge to assess likely areas of inundation is very accurate. A state-of-the-art tsunami warning system, capable of receiving and analyzing seismic and sea level, in real time and provides advisories about travel time, and run up height at 1800 coastal forecast points within 10 minutes to all concerned within India and the Indian Ocean Rim countries (Nayak and Srinivasa Kumar, 2011; Nayak *et al*., 2020).

Coastal vulnerability maps (cyclone, tsunami, and sea level rise) for the entire Indian coast have been produced on 1:100,000 scale (www.incois.gov.in). The methodology is based on projected long-term rise in sea level, climatological data on tidal range and wave height, coastal elevation and slope, long-term shoreline changes (rate of erosion and accretion) along with geomorphological setting has been developed (Srinivasa Kumar *et al.* 2010). The vulnerability has been defined in terms of an index indicating likelihood of physical changes that may occur and the natural ability of coastal system to change environmental conditions. Such maps can provide base level information for coastal management.

Tourism is one of important economic activity on the coast. In order to promote a safe and environment-friendly tourism, the process of obtaining 'Blue Flag' certification from the Foundation for Environment Education (FEE), not-for-profit non-governmental organization, based in Denmark has been initiated. The Blue Flag criteria includes specific standards for the water quality, safety, environment management and education. India has submitted applications for eight beaches, viz. Shivrajpur (Gujarat), Ghoghla (Diu), Kasargod and Padubidri, (Karnataka), Kappad (Kerala), Rushikonda (Andhra Pradesh), Golden beach (Orissa and Radhanagar (Andaman and Nicobar Islands) for blue flag certification to FEE. It is expected that these beaches will promote high-value tourism in the country.

The Way Ahead

It is likely that the economic growth prospects in India beyond 2030 will be limited without large investments in coastal and ocean environments. Realizing the importance of the ocean resources, the Govt. of India has announced a 'Deep Sea Mission' in order to gain knowledge about resources in the Indian Ocean and development of technologies to harness them (MoES, 2018). Ocean environmental data will be crucial to make macro-economic decisions about the blue economy. Oceans will have to be managed and accounted for in the same way as other valuable assets on land for sustainable growth.

Large volume of scientific data of the Indian Ocean collected during last fifty years or so, has been organized around GIS as the Ocean Data and Information System (ODIS) (Rama Rao *et al.* 2018). However, these outputs are not stored / represented in formats, systems and structures that finance, economy or other decision-makers understand or can use. We need to develop a framework to bring together these disparate data sources by developing an accounting system for oceans resources and environment. These ocean data sets are to be integrated with environmental, social and economic data to develop an accounting framework as a part of strategy for ushering blue economy. Such exercise will help to strengthen "societal relevance" of ocean.

An institutional framework for implementing activities related to blue economy has to be planned and set up. Under this framework, the decisions about investments in building infrastructure, human resources, finances and governance system for ocean environment have to be made.

An effective communication with various stakeholders including policy makers about the scope and objectives of such development, which are relevant to society, should be established. The primary focus of ocean governance should be sustainable development through the utilization of ocean resources taking into account conservation needs and protection and preservation of the marine environment. Such a responsible stewardship of oceans will pay dividends for generations to come and renew our commitments to ensure sustainability of oceans and thus of the planet Earth, for the benefit of mankind.

Acknowledgements

The author is extremely grateful to his colleagues, Dr. M. Atmanand, Purnima Jalihal and Dr. G.A. Ramadass of ESSO-NIOT, Dr. M. Ravichandran of ESSO-NCPOR and Dr. Milind Wakdikar, MoES for useful discussions. Thanks are due to Ms V. B. Mariyammal, NIAS for helping in preparing the manuscript.

References

Balakrishnan Nair, T. N., Sirisha, P., Sandhya, K. G., Srinivas, K., Sanil Kumar, V., Sabique, L., Arun Nherakkol, Krishna Prasad, B., Rakhi Kumari, Jeyakumar, C., Kaviyazhahu, K., Ramesh Kumar, M., Harikumar, R., Shenoi, S. S. C. and Shailesh Nayak, 2013: Performance of the ocean state forecast system at Indian National Centre for Ocean Information Services. *Current Science*, **105(2):** 175-181.

Banakar, V. K., Pattan, J. N., Mudholkar, A. V., 1997: Palaeoceanographic conditions during the formation of a ferromanganese crust from the Afanasiy-Nikitin Seamount, North Central Indian Ocean: Geochemical evidence. *Marine Geology*, **136(3-4):** 299–315.

Banakar, V.K., Hein, J. R., Rajani, R.P., and Chodankar, A. R., 2007: Platinum group elements and gold in ferromanganese crusts from Afanasiy-Nikitin seamount, equatorial Indian Ocean: Sources and fractionation. *Journal of Earth System Science*, **116(1):** 3-13.

Dewangan, P., Ramprasad, T., Ramana, M. V., Mazumdar, A., Desa, M., Badesab, F.K., 2010: Seabed morphology and gas venting features in the continental slope region of Krishna-Godavari basin, Bay of Bengal: implications in gas-hydrate exploration. *Marine and Petroleum Geology*, **27(7):** 1628-1641.

Goyal, S., Mohapatra, M., and Sharma, A. K., 2013: Comparison of best track parameters of RSMC, New Delhi with satellite estimates over North Indian Ocean. *Mausam*, **64(1):** 25-34.

Indian Mineral Year Book, 2017: Reviews on Minerals. Indian Bureau of Mines, Nagpur.

Jalihal, P. and Prabhakar, S. 2019: Desalination technologies. *In:* Mujumdar, P.P., and Tiwari, V.M., (Eds.), *Water Futures of India: Status of Science and Technology, Indian National Science Academy and IISc Press*, 361-400.

Jauhari, P.J., and Pattan, J. N., 2000: Ferromanganese Nodules from the Central Indian Ocean Basin. *In:* Cronan, D.S., (Ed.), *Handbook of Marine Mineral Deposits*, *CRC Press, Boca Raton, Florida.* 171–195.

Kocherla, M., Mazumdar, A., Karisiddaiah, S. M., Borole, D.V., Rao, B. R., 2006: Evidences of methane-derived authigenic carbonates from the sediments of the Krishna-Godavari basin, eastern continental margin of India. *Current Science*, **91(3):** 318-323.

Loveson, V. J., and Misra, D.D., 2004: Sustainable Development of Coastal Placer Minerals. *Allied Publishers Pvt. Ltd.*, New Delhi, 308p.

Loveson, V. J., Sen, P. K., and Sinha, A., 2007: Exploration, Exploitation, Enrichment and Environment of Coastal Placer Minerals. *MacMillan (India) Ltd.*, New Delhi, 297p.

Loveson, V.J., Chandrasekar, N. and Sinha, A., 2005: Development Planning of Coastal Placer Minerals. *Allied Publishers Pvt. Ltd.*, New Delhi, 272p.

Mazumdar, A., Dewangan, P., Joao, H. M., Peketi, A., Khosla, V. R., Kocherla, M., Badesab, F.K., Joshi, R. K., Roxanne, P., Ramamurty, P. B., Karisiddaiah, S. M., Patil, D. J., Dayal, A. M., Ramprasad, T., Hawkesworth, C. J., Avanzinelli, R., 2009: Evidence of paleo-cold seep activity from the Bay of Bengal, offshore India. *Geochemistry, Geophysics, Geosystems*, **10(6):** 1-15.

MoES, 2018: Deep Ocean Mission. *Ministry of Earth Sciences, Govt. of India*, New Delhi, 165p.

Muthukrishna Babu, S., Ramesh, N. R., Muthural, P., Ramesh, R., Deepak, C. R., and Atmanand, M. A., 2013: In-situ soil testing in the Central Indian Ocean Basin at 5462 m water depth. *International Society of Offshore and Polar Engineers*, **24(3):** 213-217.

National Institute of Ocean Technology (NIOT), 2012: A process and a system for controlled production and collection of methane gas from an unconsolidated marine system, Patent Number: 4234/CHE 2012. *The Patent office Journal,* 30/11/2012

Nayak, S., 2010: Societal benefits of Earth System Science. *Journal of the Indian Institute of Science*, **90(4):** 503-513

Nayak, S., 2014: Towards stewardship of oceans. *In:* India Culture of Science: Glorious Past and Bright Future, R. C., Sobti and G. S., Rautela (Eds.), *Narendra Publishing House*, Delhi, 735-756.

Nayak, S., 2017: Coastal zone management in India – present status and future needs. *Geo-spatial Information Science*, **20(2):** 174-183.

Nayak, S., and Srinivasa Kumar, T., 2011: Tsunami Watch and Warning Centres. *In:* Harsh K. Gupta (Ed.), *Encyclopedia of Solid Earth Geophysics, Springer*, Dordrecht, **2:** 1498-1505.

Nayak, S., Srinivasa Kumar, T., and Rama Rao, E. P. 2020: Tsunami Watch and Warning Centres. In Encyclopedia of Solid Earth Geophysics (Harsh K. Gupta. Ed.). *Encyclopedia of Earth Science Series*.

Parthiban, G., and Banakar, V.K., 1999: Chemistry and possible resource potential of cobalt rich ferromanganese crust from Afanasiy-Nikitin seamount in the Indian Ocean. *The Indian Mineralogist*, **33(1):** 125-132.

Pauli, G., 2010: The Blue Economy: 10 Years, 100 Innovations, 100 Million Jobs. *Paradigm Publications*, Taos, New Mexico, 107p.

Rajani, R. P., Banakar, V. K., Parthiban, G., Mudholkar, A. V., and Chodankar, A. R., 2005: Compositional variation and genesis of ferromanganese crusts of the Afanasiy–Nikitin Seamount, Equatorial Indian Ocean. *Journal of Earth System Science*, **114:** 51-61.

Rama Rao, E. P., Uday Bhaskar, T. V. S., Venkat Seshu, R., Srinivasa Rao, N., Suprit, K., and Geetha, G., 2018: Marine data services at National Oceanographic Data Centre-India. *Data Science Journal*, **17(2):** 1-7.

Ramadass, G. A., Ramesh, S., Vedachalam, N., Subramanian, A. N., and Sathianarayanan, D., Ramesh, R., Harikrishnan, G., Chowdhury, T., Jyothi, V. B. N., Pranesh, S. B., Doss Prakash, V., and Atmanand, M. A., 2020: Unmanned underwater vehicles: Design considerations and outcome of scientific expeditions. *Current Science*, **118(11):** 1681-1686.

Ramesh, S., Murthy, K. N. V. V., Hussain, S. M., Ramasamy, S., and Ramadass, G. A., 2020: Occurrence of Nummulitic coralline limestone from offshore Palar Basin, Bay of Bengal, India. *Marine Georesources and Geotechnology*, **38(1):** 57-63.

Sain, K., 2017: Gas hydrates: a possible future energy resource. *Journal of the Geological Society of India*, **89:** 359-362.

Sain, K., and Gupta, H. K., 2008: Gas hydrates: Indian scenario. *Journal of the Geological Society of India*, **72(3):** 299-311.

Sain, K., and Gupta, H. K., 2012: Gas hydrates in India: Potential and development. *Gondwana Research*, **22(2):** 645-657.

Sharma, R., 2011: Deep Sea Mining: Economic, technical, technological and environmental considerations for sustainable development. *Marine Technology Society Journal*, **45(5):** 28-41.

Srinivasa Kumar, T., Mahendra, R. S., Nayak, S., Radhakrishnan, K., and Sahu, K. C., 2011: Coastal vulnerability assessment for Orissa state, East coast of India. *Journal of Coastal Research*, **26(3):** 523-534.

Varshney, N., Rajesh, S., Aarthi, A. P., Ramesh, N. R., Vedachalam, N., Ramadass, G. A., and Atmanand, M. A., 2015: Estimation of reliability of underwater polymetallic nodule mining machine. *Marine Technology Society Journal*, **49(1):** 131-147.

Vedachalam, N., Ramesh, S., Srinivasalu, S., Rajendran, G., Ramadass, G. A., and Atmanand, M. A., 2016: Assessment of methane gas production from Indian gas hydrate petroleum systems. *Applied Energy*, **168:** 649-660.

Indian Journal of Geosciences, Volume 74, No. 3
July - September, 2020; pp. 197-204

Invited Paper

Grey areas in the Palaeogene of the Lesser Himalaya: a review of various controversies

O. N. Bhargava

Department of Geology (CAS), Panjab University, Chandigarh - 160014
Former Director, Geological Survey of India
Email: onbhargava@gmail.com

Abstract: The Palaeogene in the Lesser Himalaya of the western sector is represented by the Subathu and Dagshai formations - two subdivisions of the Sirmur Group. Several aspects of these two formations are enmeshed in numerous controversies. The controversies are: (i) Was the basin continuous from east to west or fragmented? (ii) Was it continuous from the Indus Suture zone to the Sub-Himalaya and even extending to Jaisalmer or two separate basins? (iii) Problem of multiple nomenclature. (iv) Was the sedimentation from the Subathu Formation to the Dagshai Formation uninterrupted or a hiatus exists between the Subathu and the Dagshai formations? (v) Is the Chert breccia in Jangal Gali (Jammu) – a paleosol or rhyolite? (vi) Is Subathu Formation a shallow marine sequence or a flysch? (vii) Is the spatial repetition of the Subathu and Dagshai formations due to folding and thrusting or owing to facies variation? Decoding the script of the Palaeogene sediments shall reveal the history of collision of the Indian Plate and enable assessment of oil and gas potential.

Key words: Foreland basin, Subathu, Dagshai, Palaeogene

Introduction

The Palaeogene period (~65.5 - 23 Ma) commenced at the end of the Cretaceous, which is known for mass extinction of life, most conspicuously the dinosaurs. It was the most exciting period in the Earth's history. The Indian Plate, like a Noah's Ark, embarked on its spectacular journey carrying flora and fauna of southern latitudes to the northern latitudes. It was during this period that the Indian Plate docked and collided with the Asian Plate to form the Himalaya. The collision led to creation of the Himalaya Foreland Basin (HFB), which was inundated by the sea. The Palaeogene-Neogene sediments of the HFB in the Western Himalaya are classified under the Sirmur Group and the Neogene-Quaternary succession throughout the Himalaya is designated as the Siwalik Supergroup (Medlicott, 1864); the rocks of Sirmur Group and the Siwalik Supergroup together constitute the Sub-Himalayan Range.

Simultaneously, the marine transgression was registered in several parts of the Indian Subcontinent (Krishnan, 1982). Globally, it was a period of warm climate, with several transient hyperthermal events of extreme warmth. During the late Palaeogene and the Miocene the monsoon became active together with development of grasslands. Palaeocene-Eocene boundary witnessed advent of many mammals, particularly the Artiodactyls, Perissodactyls and Primates. Carbonaceous shale, coal and lignite deposits flourished around ~55.5-5 Ma in the western and north-eastern margins of the Indian subcontinent. The Palaeocene-Eocene sediments in the Indian Plate constitute source rock for the hydrocarbons.

The Sirmur Group in ascending order is divisible in the Subathu, Dagshai and Kasauli formations (Medlicott, 1864), of these the first two represent the Palaeogene sequence. The study of the Palaeogene sediments is of great importance; it shall reveal the history of collision of the Indian Plate and permit assessment of oil and gas potential in HFB. Despite applied and academic aspects, there are several lacunae and controversies surrounding the Palaeogene successions of the Himalaya. In the present paper the controversial issues are highlighted so that future studies are focussed to resolve these problems.

Controversies

Various controversies that need resolution are enumerated below:

1. Extent of the Basin, 2. Nomenclature, 3. Nature of contact between the Subathu and Dagshai formations, 4. Stratigraphic range of the Dagshai Formation, 5. Environment of deposition, 6. Structural disposition and 7. Paleogeographic reconstruction of the Palaeogene basin.

Extent of the Palaeogene Basin

Lateral Extent

The Palaeogene successions are exposed in the Sub-Himalaya between Jammu and Himachal Pradesh (Bhatia and Bhargava, 2006). Further east, the Palaeogene sequences, particularly the Subathu Formation, are exposed in the Lesser Himalaya, as windows or outliers in Uttarakhand, Nepal and Assam. So far there has been no report of any Palaeogene in Darjeeling and Bhutan sectors, though Nummulitic rock as a float has been recorded in Bhutan (Acharyya, 1994). The absence of the Palaeogene east of Himachal Pradesh has been interpreted as termination of the basin, delimited by Delhi-Haridwar-Harsil Ridge (Pal *et al*., 2000).

The fact that the Subathu Formation is found in the Bidhalana and Pharat windows (Fig. 1) and as outliers in the Mussoorie and Lansdowne synclines (Uttarakhand) and in the Tansen area (Nepal) demonstrates that the Palaeogene basin did extend in the Lesser Himalaya. A foreland basin created due to the collision of the plates has to be a regional feature and is expected to have developed over the entire length of the Himalaya. Identical lithology and faunal contents of the Subathu and its equivalents up to Assam are suggestive of one continuous basin throughout the Himalaya. Irregular development of the Palaeogene in the Sub-Himalaya, east of Himachal, thus could be due to concealment under the thrust sheets, as is evident by the presence of the Subathu Formation in the windows at Solan, Bidhalana and Pharat in the Krol Belt and in the Deoban area.

Connection between the Indus Valley and Sub-Himalayan basin and its southward extension

Also disputable is the relationship between the Paleogenae Sea in the Indus Valley and in the Sub-Himalaya. According to Najman *et al*. (1994) and Virdi (1994) there was one continuous basin that extended from the Indus Valley to the Sub-Himalaya (Fig. 2). Virdi (1994) even extends this basin further south up to the Jaisalmer area in the peninsular part. Had the basin been continuous from the Indus Valley to the

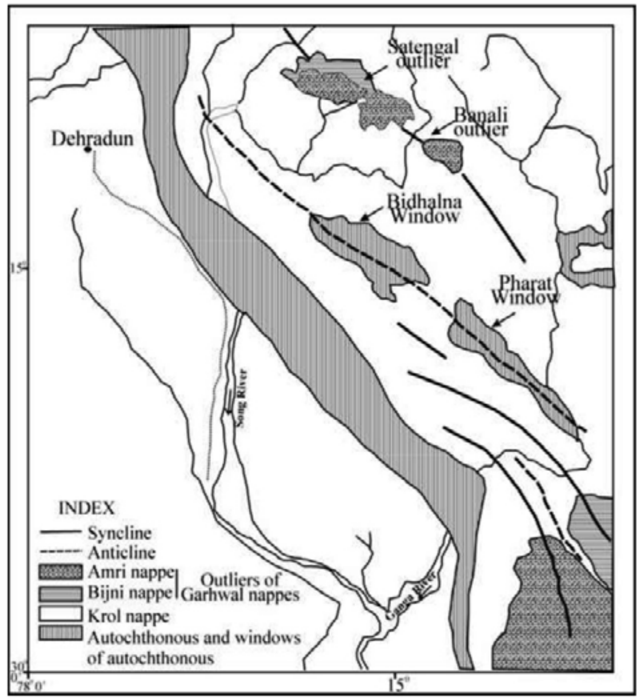

Fig. 1: Generalised map showing Bidhalana and Pharat windows (Redrawn after Auden, 1937).

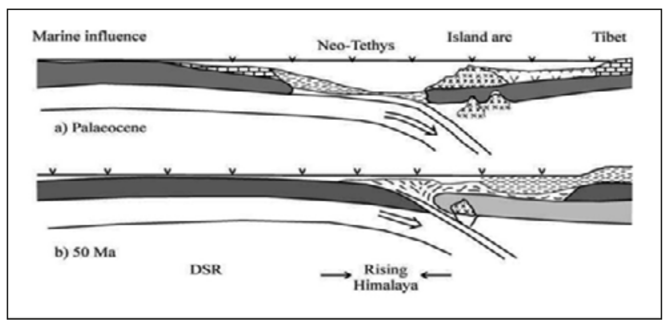

Fig. 2: Basin of the Subathu period as proposed by Najman *et al*. (1994).

Sub-Himalaya, one would expect the Subathu outliers all along this stretch, particularly in windows like Rampur, Larji, Pithoragarh etc., exposed towards the Higher Himalaya. Likewise, had the same basin extended up to Jaisalmer in the peninsular part, the Subathu Formation would have been encountered below the Siwalik sediments in the foot-hill region in various bore holes drilled by the ONGC.

The Foreland Basin was created as a result of collision of the Indian Plate and consequent rise of thrust sheets, thus, the Sub-Himalaya basin is likely to have been delimited by the rising thrust sheets, which would have acted as barrier (ridge) between the Indus and Sub-Himalaya basins as envisaged by Singh, *et al*. (2016) who consider Indus and Sub-Himalayan as two separate basins (Fig. 3).

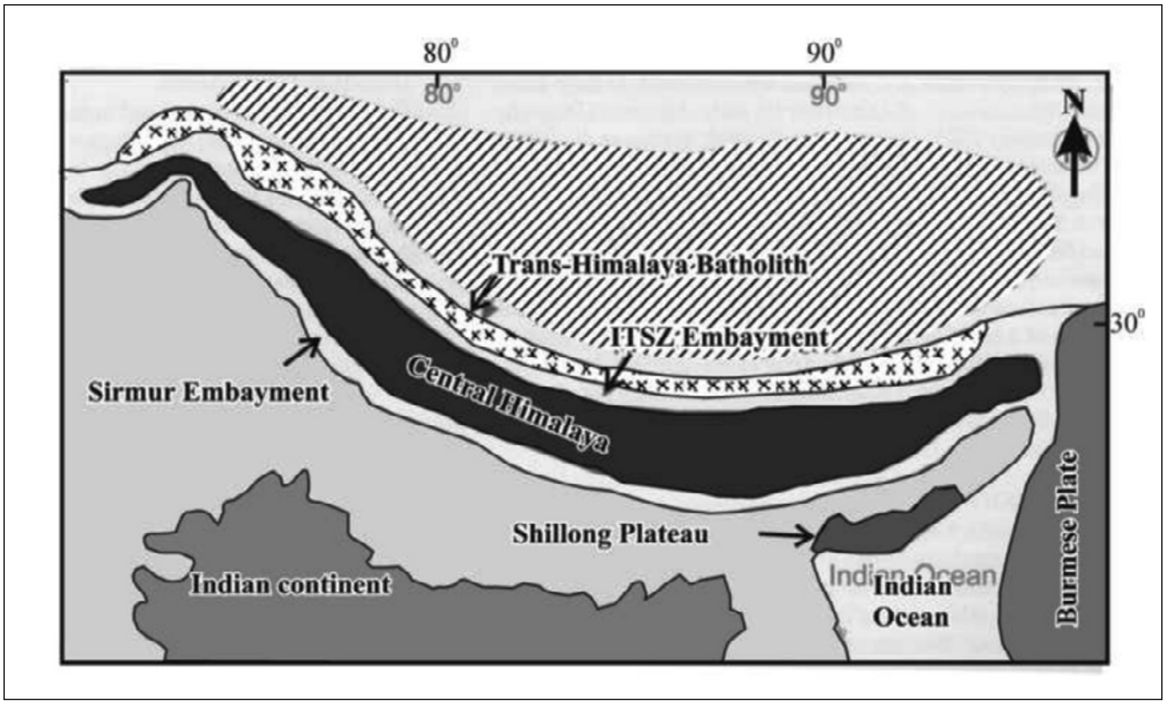

Fig. 3: Palaeogene basins as proposed by Singh, I.B. *et al*. (2016).

Direction of transgression

According to Najman *et al*. (1994) and Virdi (1994) the sea invaded from the North and extended to the south. Singh *et al*. (2016) showed a continuous basin connected to open sea on west and also in the east for the southern basin and the Indus basin connected to northern sea. No serious work on this aspect has been undertaken so far.

Nomenclature

In the Shimla Hills, Medlicott (1864) proposed Sirmur Series to include the Subathu, Dagshai and Kasauli stages, which as per stratigraphic code now designated as the Sirmur Group divisible in the Subathu, Dagshai and Kasauli formations. In the Murree section, the Palaeogene sequence was designated as the Nummulitic Limestone, the Lower Murree and Upper Murree (Wynne, 1874), their type sections are located in Pakistan. These terms were extended to Kashmir and Dharamsala (NW Himachal Pradesh) sectors also. Much later, Lahiri (1939) introduced Nummulitic and Dharamsala Beds, the latter divisible in the Upper Dharamsala and Lower Dharamsala.

Completion of the mapping from Sirmur to Jammu establishes that the Nummulitics and Murree/Dharamsala are strike extension of the Sirmur Group. As per the Code of Stratigraphic Nomenclature of India, the Sirmur Group and its subdivisions should have priority and terms, Nummulitics and Lower and Upper Murree/Dharamsala should be dropped, though some workers still use these terms (Singh, *et al*. 2013). Moreover, use of same name for two units, viz., Lower Murree/Lower Dharamsala and Upper Murree/Upper Dharamsala violates the stratigraphic code. It is time that the nomenclature of the Palaeogene sequences is standardised.

Nature of contact between the Subathu and Dagshai formations

Conformable or unconformable?

In Himachal Pradesh, Medlicott (1864) considered a normal and conformable stratigraphic contact between the Subathu and the Dagshai formations. Subsequently, Pilgrim (1910, 1912) discovered vertebrate fossils in the Bugti Beds, designated as the Fatehjung Fauna, in the Suleiman Range and assigned a Lower Miocene age. The Bugti Beds were correlated with the Dagshai Formation. Since the youngest fossils in the Subathu are of Middle Lutetian age, a major break involving the absence of entire Oligocene was envisaged. In the Salt Range and Kohat section, reworked Eocene fossils are recorded in the Upper Murree (Burdigalian) sequence, in the Potwar area, a sequence equivalent to the upper part of the Dagshai Formation rests over the Chorgali Formation (= part of the Subathu). In Nepal, a ferricrete horizon intervenes between the Bhainskati (=Subathu) and the Dumri (=Dagshai) formations, signifying a sedimentological break, whereas in the Suleiman Range a continuous Palaeogene sequence is observed

In undisturbed sections observed at Subathu, Garkhal and Dharampur, the green shale in upper part of the Subathu Formation alternates with red shale which finally passes into the predominantly red Dagshai sequence (Fig. 4a, b). Raiverman (1979) observed a conformable contact between the Subathu and the Dagshai formations. Later, Raiverman (2002) revised his earlier opinion and marked an unconformity between the two formations. In a written communication he mentioned, "the hiatuses do not apply all over the basin in variable structural settings". The paleontological investigations by Prof. S. B. Bhatia and his students negated such a break, they delineated a sequence designated as the Passage Beds to mark continuous succession between the Subathu and the Dagshai formations, which show biochronological continuity (Table 1) (for details see Bhatia and Bhargava, 2006). Marivaux *et al*. (1999) recorded Oligocene Cricetidae (Rodentia, Mammalia) and re-evaluated the Bugti Bone Bed fauna (=Fatehjung Fauna; Bugti Member, Chitrawata Formation) and assigned an Oligocene age to it. Welcomme *et al*. (2001) recorded species of *Pseudocricetodon,* which is known only from the Early Oligocene. They also recorded typical Oligocene neritic foraminifer *Nummulites bouillei, Nummulites clypeus* (= *N. intermedius-fichteli*), associated with molluscs (*Pecten substriatus*, oysters), selachians, sirenians and remains of rhinocerotoids (*Cadurcotherium indicum* and large-sized *Paraceratherium bugtiense*). Welcomme *et al*. (2001, p. 403) concluded "....that the continental Oligocene hiatus does not occur in the Suleiman geological province as traditionally accepted...". On contrary they suggested an intra-Oligocene break. Antoine *et al.* (2003) while reporting Elephantoidea from the Bugti Hill recorded five successive ''bone beds'' that bridged the supposed Oligocene sedimentary hiatus. Thus, the fossil contents and contact relationship observed in the field suggest a continuous succession from the Subathu Formation to the Dagshai Formation. The conformable relationship was substantiated by paleomagnetic data (Najman *et al*., 1994). Najman *et al.* (1997), based on $^{40}Ar/^{39}Ar$ dates of single detrital muscovite from the Jamuna Valley and Morni areas (Fig. 5), advocated a 10 Ma break between the Subathu and the Dagshai. At both these localities (Figs. 6, 7) the outcrops are of the Nahan Formation (Siwalik Group) (Auden, 1934). The $^{40}Ar/^{39}Ar$ dates of Najman *et al*. (1997), therefore, pertain to the muscovite of the Nahan Formation and are not relevant to the Dagshai Formation. Later, Jain *et al*. (2009) based on fission track date of detrital zircons also suggested a >10 Ma gap between these two formations on the premise that the Dagshai sediments never reached the annealing temperature of zircons in the range of 175-250^{o} C. The exact stratigraphic position of the samples collected by Jain *et al.* (2009) is not known.

Studies by Raiverman *et al*. (1979; 2002) of the Dagshai sandstone (he calls them quartzite) reveal: reduced porosity, increased density with sutured to concavo-convex grain fabric, silica cement and silica veins-some veins cut across quartz grains—possible only if individual grains lost their discrete status and got fused. In more argillaceous varieties,

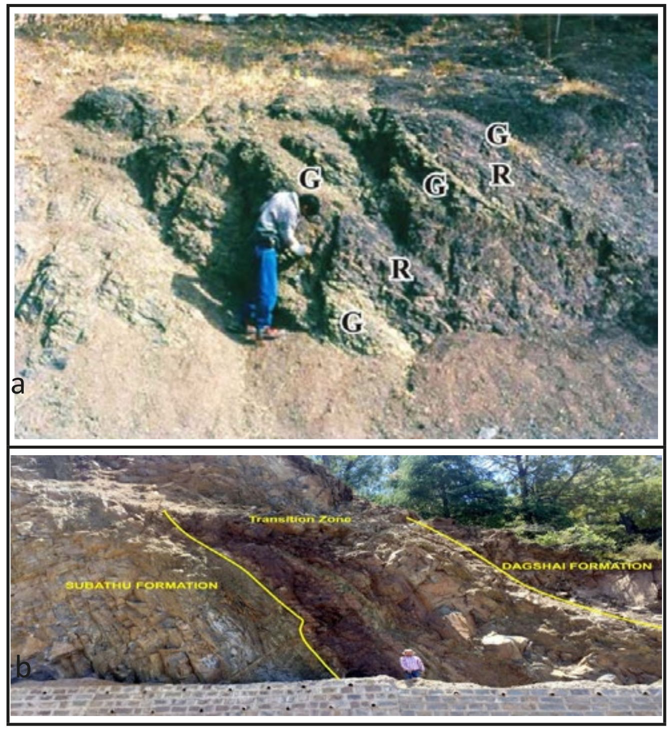

Fig. 4: (a) Field photograph about 500 m from Dharampur town towards Shimla along the NH 22. (R-red beds; G-green beds) and (b) Field photograph near Shiv temple beyond Dharampur.

Table 1. Fossil contents of the Subathu and Dagshai formations showing a biochronological continuity.

Dagshai Fm.	*Leptomeryx* sp., *Pseudocricetodon*	Priabonian-Rupelian
Passage Beds	*Harrischara* cf. *vasiformis*	M. Bartonian-M.Priabonian
	Linderina sp.	M. Bartonian-M.Priabonian
	Chlamyspa kistanika	Priabonian
	Alcopocythere tracscendens	Bartonian
	Alcopocythere abstracta	Bartonian
	Raskyellapeckii	Lutetian-?Bartonian
Subathu Fm.	*Assilina exponens*	M Lutetian-?Bartonian
	Nummulites discorbinus	E-M Lutetian
	Nummulites obesus	E-M Lutetian
	Nummulites lehneri	E-M Lutetian
	Assilina spiraabradi	E-M Lutetian

clay and more labile constituents have crystallised and formed muscovite-biotite lamellae with development of schistocity-representing phyllomorphic stage of diagenesis or anchimetamorphism, where a temperature range of 200^{o}-300^{o} C is expected (cf. Dapples, 1967). The study thus questioned the >10 Ma hiatus suggested by Jain *et al*. (2009) on the basis of fission track date. Bera *et al*. (2008), without any isotope data conjectured a 3 Ma break between the Subathu and Dagshai formations. Retallack *et al*. (2018) based on a paleosol horizon observed by them above the Subathu Formation near the Chakki-ka-Mor favoured a break at Subathu-Dagshai level, though have not specified the duration of the break. The identification of the paleosol at Chakki-ka-Mor is far from convincing.

Viewed regionally, the Subathu-Dagshai sequences south of the Surajpur Thrust, being nearer to the coast, selectively do

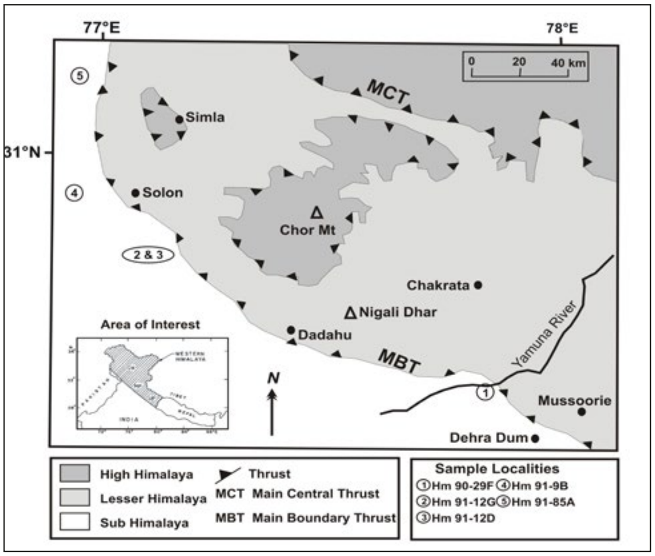

Fig. 5: Map showing the location of samples collected by Najman *et al*. (Redrawn after Najman *et al*., 1994).

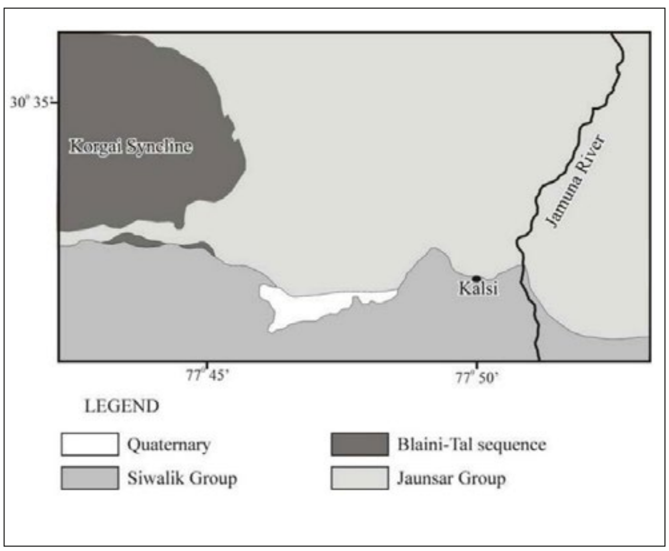

Fig. 6: Map around Jamuna Valley (Simplified after Auden, 1934).

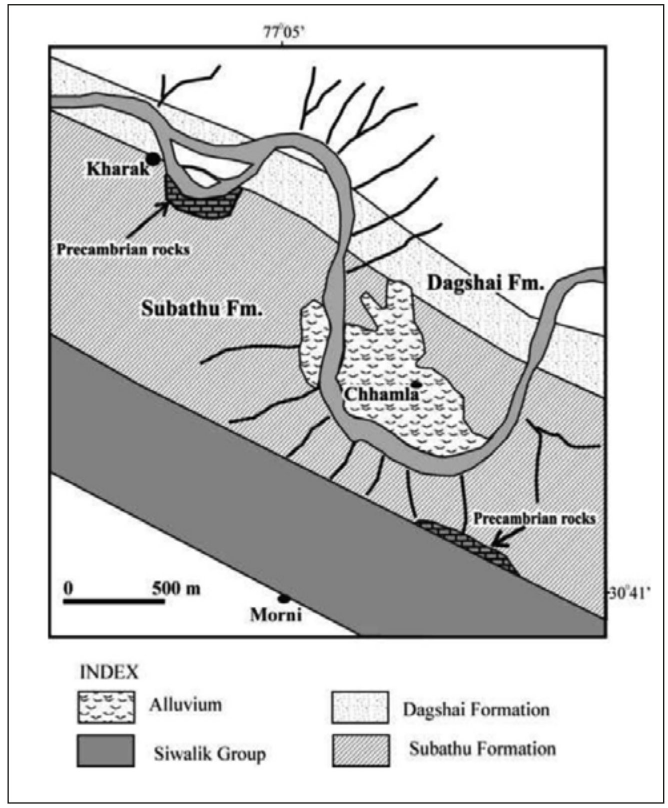

Fig. 7: Geological map of Morni area (after Narain, 1967).

show an unconformable relationship, to the extent reworked Nummulites are found in the Dagshai Formation. In the areas north of the Surajpur Thrust, the sequence seems to be continuous. Fresh samples for dating should be collected from different localities with unambiguous geological sections. The samples thus collected should be precisely located on detailed lithocolumn

Stratigraphic position of the white sandstone

A white sandstone was identified as a marker between the Subathu and the Dagshai formations (Auden, 1934). Most of the workers (see Bhatia *et al*., 2013 for detailed references) considered it a part of the Dagshai Formation. Bera *et al.* (2008) classified it with the Subathu Formation and considered it to represent forced regression. This well sorted sandstone is of marine origin and was classified with the Subathu Formation by (Bhatia *et al*., 2013), representing the culmination of Subathu cycle (Bhatia *et al*., 2013). The sandstone is not present in all the sections. Does it form part of the Subathu Formation or of the Dagshai Formation and is it a marker in real sense? And if a break exists between the Subathu and Dagshai formations, is it below or above this sandstone? Detrital zircons from the sandstone should be dated for a definite answer.

Is the Dagshai Formation younger to the Subathu Formation or its age equivalent?

Medlicott (1864) and most of the subsequent workers regarded the Dagshai Formation to stratigraphically succeed the Subathu Formation. However, Raiverman and Raman (1971) suggested that the Dagshai Formation is a facies variant of the Subathu Formation. The Charring Crossing in Dagshai town was cited by these authors as a locality where the Subathu Formation can be seen to pass laterally into the Dagshai Formation. This locality was examined by Bhatia *et al*. (2013) and found that the outcrops at this locality are poor and full of slickensides. The contact was interpreted as tectonic (Bhatia *et al*., 2013) (Fig. 8). The fossils indicate younging from the Subathu Formation to the Dagshai Formation, thus refuting the concept of facies variation between the two.

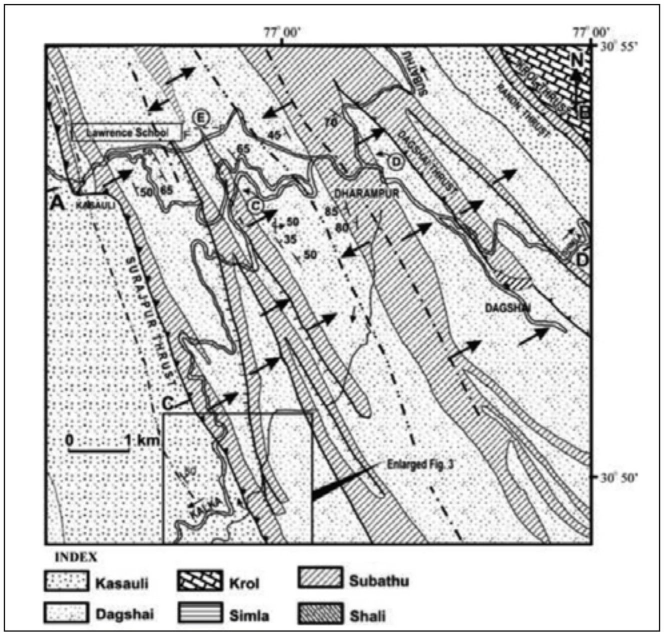

Fig. 8: Geological map around Charring Crossing (Modified after Bhatia *et al*., 2013).

Chert breccia vs. rhyolite

In the Jammu area, a chert breccia described from the Subathu Formation (Singh, 2003) was reinterpreted as rhyolite (Shukla and Siddaiah, 2011). The work carried out by the Geological Survey of India, supervised by S. K. Tangri (personal communication to ONB) found stratigraphic position of the breccia below the pre-Subathu bauxite, hence was not regarded as a part of the Subathu Formation. The GSI regarded chert breccia as a paleosol developed over the Riyasi Limestone. The breccia types identified in and around the Sirban Limestone Formation include: i) Dolomite-Quartzarenite-Chert Breccia (tectono-sedimentary origin), ii) Slump Breccia (part of olistostrome), iii) Tectonic (fault) Breccia, iv) Collapse Breccia-Authigenic (with dolostone clasts), v) Collapse Breccia-Transported (with dolostone and quartzarenite clasts).

The so called 'Rhyolitic Breccia' is sporadic and limited to a few outcrops, and also has laminated dolostone clasts. The breccia has been subjected to large scale silicification during late stage diagenesis, and the tectonic activities have mobilized fluids of varying compositions thereby resetting the mineralogical compositions. The latest information is that both, the Chert Breccia as well as rhyolite occur, while the former has extensive development, the latter is confined to local sections and occurs above the breccia. If so, the 'rhyolite' is an equivalent to the Darla-Tattapani Volcanics, which occupies a position above the Shali Group (= Riyasi Limestone). A more detailed mapping with isotopic dating of the "rhyolite" should be carried out to solve this problem. The genesis and stratigraphic position of the Chert Breccia and rhyolite respectively remains to be resolved satisfactorily.

Depositional history

Most workers interpreted the Subathu Formation as a shallow marine sequence and the Dagshai—a deltaic-estuarine deposit (for detailed references see Bhatia *et al*., 2013). However, Bera *et al*. (2008) considered the Subathu a flysch deposit, in which shallow marine fossils were thought to have been derived from the shallower parts located towards the craton. These observations were made mainly at the Tal locality (Arki area), which is a highly tectonised belt involving the Kakara, Simla and Shali sediments (Fig. 9) (Srikantia and Sharma, 1970). It is quite likely that the Simla sediments, which superficially simulate flysch and closely resemble the Subathu rocks were mistaken for the Subathu Formation by Bera *et al.* (2008). The fossils in the Subathu occur in the same and standard stratigraphic order in all the sections, which is rather an unusual situation, had the fossils been reworked.

Balanced sections

Three balanced cross-sections are presently available:

(i) Dubey *et al*. (2001) suggested that in the tensional phase, during the first stage basement faults were formed. Increased tectonic displacement led to subsidence of the basin.

(ii) Mukhopadhay and Misra (2005) proposed that the spatial repetition of the Subathu and the Dagshai formations is due to thrusting. Increased compression led to thrust propagation and formation of thrust propagated folds.

(iii) Baruah and Joshi (2011) advocated a two-tier decollement system.

A final picture and updated structural interpretation in light of latest drilling by the ONGC is still awaited.

Recommendation

1. An integrated litho- and biostratigraphic studies involving various elements in the Lesser Himalaya of Jammu, Bilaspur, Kalka-Shimla, Nepal and Arunachal and their comparison with the Salt Range, the Suleiman Range, Jaisalmer and Kutch are necessary. Similar studies of the Subathu Formation exposed at various tectonic levels i.e., over (i) the Shali and Deoban groups, (ii) the Simla Group, (iii) the Krol and Tal groups and (iv) in the windows of Solan, Bidhalana, Pharat are required. The result of these studies when plotted after correcting the crustal shortening will reveal information that will be useful in basin reconstruction.

2. Sedimentological studies in palaeontologically controlled sections, to include isopach maps and study of heavy mineral and dating of detrital zircons at different levels to reconstruct the Palaeogene basin in the Indian Plate shall be useful for oil prospecting.

3. Structural analysis in the light of drilling and geophysical data.

Acknowledgement

I am thankful to Shri E.V. R. Parthasaradhi, to have invited me write this article to a volume of Indian Journal of Geosciences dedicated to Late K. Krishnanunni, a former Director General, Geological Survey of India.

References

Acharyya, S.K., 1994: The Cenozoic foreland basin and tectonics of the Eastern Sub-Himalaya: problems and prospects. *In: Kumar, S., Ghosh, S.K., Phadtre, N.R., Siwalik Foreland Basin of Himalaya. Himalayan Geology,* **15:** 3-21.

Antoine, P-O., Welcomme, J-L., Marivaux, L., Baloch, I., Benammi, M. and Tassy, P., 2003: First record of Paleogene Elephantoidea (Mammalia, proboscidea) from the Bugti Hills of Pakistan. *Journal of Vertebrate Paleontology*, **23(4)**:977–980

Auden, J.B., 1934. The geology of the Krol Belt and associated formations. *Records of the Geological Survey of India*, **67(4)**:357–454.

Auden, J.B. 1937. The Structure of the Himalaya in Garhwal. *Records of the Geological Survey of India*, **71(4)**: 407-433.

Baruah, M. and Joshi, G., 2011: Section balancing in the area south of Solan, H.P., India for reinforcing subsurfacing model related to ongoing Hydrocarbon Exploration in the area. *Journal of Indian Association of Sedimentologists*, **30(1):** 1-10.

Bera, M.K., Sarkar, A., Chakraborty, P.P., Loyal, R.S. and Sanyal, P., 2008: Marine to continental transition in Himalayan foreland. *Geological Society of America Bulletin,* **120 (9/10)**: 1214–1232.

Bhatia, S.B. and Bhargava, O.N., 2006: Biochronological continuity of the Palaeogene sediments of the Himalayan foreland basin: Paleontological and other evidences. *Journal of Asian Earth Sciences,* **26(5)**: 477–487.

Bhatia, S.B., Bhargava, O.N., Singh B.P. and Bagi, H., 2013: Sequence stratigraphic framework of the Palaeogene succession of the Himalayan Foreland Basin: a case study from the Shimla Hills. *Journal of the Palaeontological Society of India*, **58(1)**: 21-38.

Dapples, E.C., 1967: Diagenesis of sandstones. *In:* Diagenesis in Sediments. (Eds.) G. Larsen, G.V. Chilingar*, Development in Sedimentology,* **8**: 91-125.

Dubey, A.K., Misra, R. and Bhakuni, S.S., 2001. Erratic shortening from balanced cross-sections of the western Himalayan Foreland basins: causes and implications for basin evolution. *Journal of Asian Earth Sciences*, **19(6)**, 765-775.

Jain, A.K., Lal, N., Sulemani, B., Awasthi, A.K., Singh, S., Kumar, R. and Kumar, D., 2009: Detrital-zircon fission-track ages from the Lower Cenozoic sediments, NW Himalayan foreland basin: Clues for exhumation and denudation of the Himalaya during the India–Asia collision. *Geological Society of America Bulletin*, **121(3-4)**: 519–535.

Krishnan, M.S., 1982: Geology of India and Burma. 4th Edition Higginbothams (Private) Ltd Madras*,* 1-536.

Lahiri, H. M., 1939: Kangra district and Chamba State. *In*: General Report for the Year 1938, (Eds.) Heron, A.M. *Records of the Geological Survey of India,* **74(1)**: 70-72.

Marivaux, L., Vianey-Li and Welcomme, J-L., 1999: First discovery of Oligocene Cricetidae (Rodentia, Mammalia) in South Gandoin Syncline, Bugti Hill, Balochistan, Pakistan. *Compte Rendu Academy Science, Paris, Earth and Planetary Science,* **329**: 839-844.

Medlicott, H.B., 1864: On the geological structure and relation of thesouthern portion of the Himalayan Range between the rivers Ganges and Ravee. *Memoirs of the Geological Survey of India*, **3(2)**: 1-212.

Mukhopadhyay, D.K. and Mishra, P., 2005: A balanced cross section across the Himalayan frontal foreland belt, Subathu area, Himachal Pradesh, India: thrust sequence, structural evolution and shortening. *Journal of Asian Earth Sciences*, **25(5)**: 735-746.

Najman, Y., Clift, P., Johnson, M.R.W., and Robertson, A.H.F., 1994: Early stages of foreland basin evolution in the Lesser Himalayas, North India, *In:* Himalayan Tectonics, (Eds.) Treloar, P.J., and Searle, M.P. *Geological Society London Special Publication,* **74**: 541-558.

Najman, Y.M.R., Pringle, M.S., Johnson, M.R.W., Robertson, A.H.F. and Wijbrans, J.R., 1997. Laser 40Ar/39Ar dating of single detrital muscovite grains from early foreland-basin sedimentary deposits in India: implications for early Himalayan evolution. *Geology*, **25 (6)**: 535–538.

Narain, K., 1967: Tectonic position of certain limestone bands between Dabsu and Tundapathar. *Publication Centre of Advanced Study in Geology. Panjab University, Chandigarh*, **3**: 131-139

Pal, D., Srivastava, R.A.K. and Mathur, N.S., 2000: Influence of Delhi-Hardwar-Harsil Ridge (DHHR) on Basin Configuration in Himalayan Foothills Belt during Tertiary. *Himalayan Geology,* **21(1-2)**: 133-144.

Pilgrim, G.E., 1910: Notices of new mammalian genera and species from the Tertiaries of India. *Records of the Geological Survey of India,* **40 (1):** 63–71.

Pilgrim, G.E., 1912: The vertebrate fauna of the Gaj Series in the Bugti Hills and Punjab. *Palaeontologica Indica*, **4 (2):** 1-83.

Raiverman, V., 1979: Stratigraphy and facies distribution, Subathu sediment, Simla Hills, Northern Himalaya. *Miscellaneous Publications, Geological Survey of India*, **41(5)**: 111-125.

Raiverman, V., 2002: Foreland sedimentation in Himalayan tectonic regime: a re-look at the orogenic process. Bishen Singh Mahendra Pal Singh Publisher, Dehradun, 378p.

Raiverman, V., and Raman, K.S., 1971, Facies relations in the Subathu sediments, Simla Hills, northwestern Himalaya, India: *Geological Magazine,* **108(4)**: 329–341.

Retallack, G. J., Bajpai, S., Liu, X., Kapur, V.V. and Pandey, S. K. 2018: Advent of Strong South Asian Monsoon by 20 Million Years Ago. *Journal of Geology*, **126(1)**: 1–24.

Shukla, M.K. and Siddaiah, S., 2011: Is Chert Breccia at Kalakot, J & K sedimentary in origin? *Himalayan Geology*, **32 (2)**: 169-171.

Singh, B.P., 2003: Evidence of growth fault and forebulge in the Late Palaeocene (~57.9-54.7 Ma), western Himalayan foreland basin, India. *Earth and Planetary Science Letters*, **216(4)**: 717–724.

Singh, B.P. 2013: Evolution of the Palaeogene succession of the western Himalayan foreland basin. *Geoscience Frontiers,* **4**: 199-212.

Singh, I.B., *et al.*, 2016. Post-collision sedimentation in the Indus Basin (Ladakh, India): implication for the evolution of the Northern margin of the Indian Plate. *Journal of the Palaeontological Society of India*, **60(2)**: 97-146.

Srikantia, S.V. and Sharma, R.P., 1970. The occurrence of Kakara (Palaeocene) affinity in the Bakhalag Bugher belt, Himachal Pradesh. *Journal of Geological Society of India*, **11(2)**: 185-188.

Virdi, N. S., 1994. The floor of the Tertiary Basin of northwest India—control of basement highs and paleotopography on the basin evolution. *Himalayan Geology,* **15**: 231-244.

Welcomme, J.-L., Benammi, M., Crochet, J.-Y., Marivaux, L., Metais, G., Antoine, P.-O., and Baloch, I., 2001. Himalayan Forelands: paleontological evidence for Oligocene detrital deposits in the Bugti Hills (Balochistan) Pakistan). *Geological Magazine,* **138 (4)**: 397–405.

Wynne, A. B., 1874. Notes on the geology of the neighbourhood of Mari Hill section in the Punjab. *Records of the Geological Survey of India,* **7**: 64-74.

Indian Journal of Geosciences, Volume 74, No. 3
July - September, 2020; pp. 205-215

Invited Paper

A review of tectonometamorphic evolution of Himalayas

Naresh Chandra Pant* and Preeti Singh

Department of Geology, University of Delhi, New Delhi
**Corresponding author's email: pantnc@gmail.com*

Abstract: Himalayas represent the highest and the youngest, "still active" orogenic continental mountain belt on the planet earth. The ~2500 long and a few hundred-kilometer-wide belt is linked with a mountain system involving several other associated ranges. The northern limit, marked by sporadically exposed high-pressure rocks (e.g. Indus Tsangpo Suture Zone) is followed south ward by the Tethyan Himalayan Sequence (THS), Greater Himalayan Sequence (GHS), Lesser Himalayan Sequence (LHS) and Sub-Himalayan Sequence. There is remarkable lateral continuity in many of these divisions and structures marking these sequences. The process of crustal shortening and rise of the Himalayas involved leading elements of the Indian continental crust as well as the sediments of the Tethyan basin and the continental deposits subsequent to the marine to continent transition. Metamorphism and associated Tertiary magmatism allows lateral correlation of the orogenic process.

Keywords*:* Himalayas, metamorphism, crustal shortening, Tethyan basin, Magmatism

Introduction

The Himalaya represents the youngest and the most spectacular example of all the continent-continent collisional zones on the Earth. Formation and rise of Himalaya has been of interest to geologists for a very long time but it has assumed even more significance in the last few decades as its critical role is increasingly recognized in influencing the global climate (as well as regional climate too) especially in the context of global warming (e.g. Richter *et al*., 1992). It is well understood that the evolution of the Himalayan orogen followed subduction of NeoTethys after the closure of SSZ towards north and Indus Tsangpo Suture Zone (ITSZ) towards south and was caused by the subduction of continental Indian plate (Dewey and Burke, 1973; Le Fort, 1975; Searle *et al*., 1988). The process involved the Paleo-Mesozoic sedimentary cover of Tethys as well as older leading segment of the Indian plate. This event led to the formation of distinct lithotectonic elements including Tethyan Himalayan Sequence (THS), Himalayan Metamorphic Belt (HMB) (within which three crystalline sequences of Tso Morari (TMC), Higher Himalayas (HHC) and Lesser Himalayas (LHC) are distinguishable), Lesser Himalaya Sedimentary Belt (LS) besides Sub-Himalayan Cenozoic belt (SH) (Jain *et al*., 2016).

Many geologist and geophysicist have investigated and produced numerous work on the tectonics and evolution of this great orogenic system for the last four decades (Gansser, 1964; Dewey and Bird, 1970; Srikantia and Bhargava, 1983; Valdiya, 1995; Le Fort, 1996; Searle *et al*., 1988; Searle and Tirrul, 1991; Thakur, 1993; Searle *et al*., 1988 Le Fort, 1996; Voo *et al*., 1999; Hodges, 2000; Chemenda *et al.,*2000; Rolland *et al*., 2000; Yin and Harrison, 2000; Jain and Singh, 2009; Jain *et al*., 2016; Searle and Treolar, 2019; Pant *et al*., 2020. Present article is an attempt to lay out a summarized review in a coherent manner on the Himalayan evolution journey.

Regional Setting of the Himalayas

World's largest concentration of mountain ranges is found in the central parts of the Eurasia and comes under the Alpine Himalayan orogenic process. The Himalayas, Karakoram, Hindu Kush and Pamirs together with the high plateau of Tibet represents the most actively deforming parts of the continental crust. From the Pamir's some of the world's largest mountain ranges branch off to the north, south, west and to the east (Searle, 1991; Le Fort, 1996; Hodges, 2000). The Himalayas follow the south of the Pamir mass, and, bordering the Tibetan high plateau to the south (Fig.1).

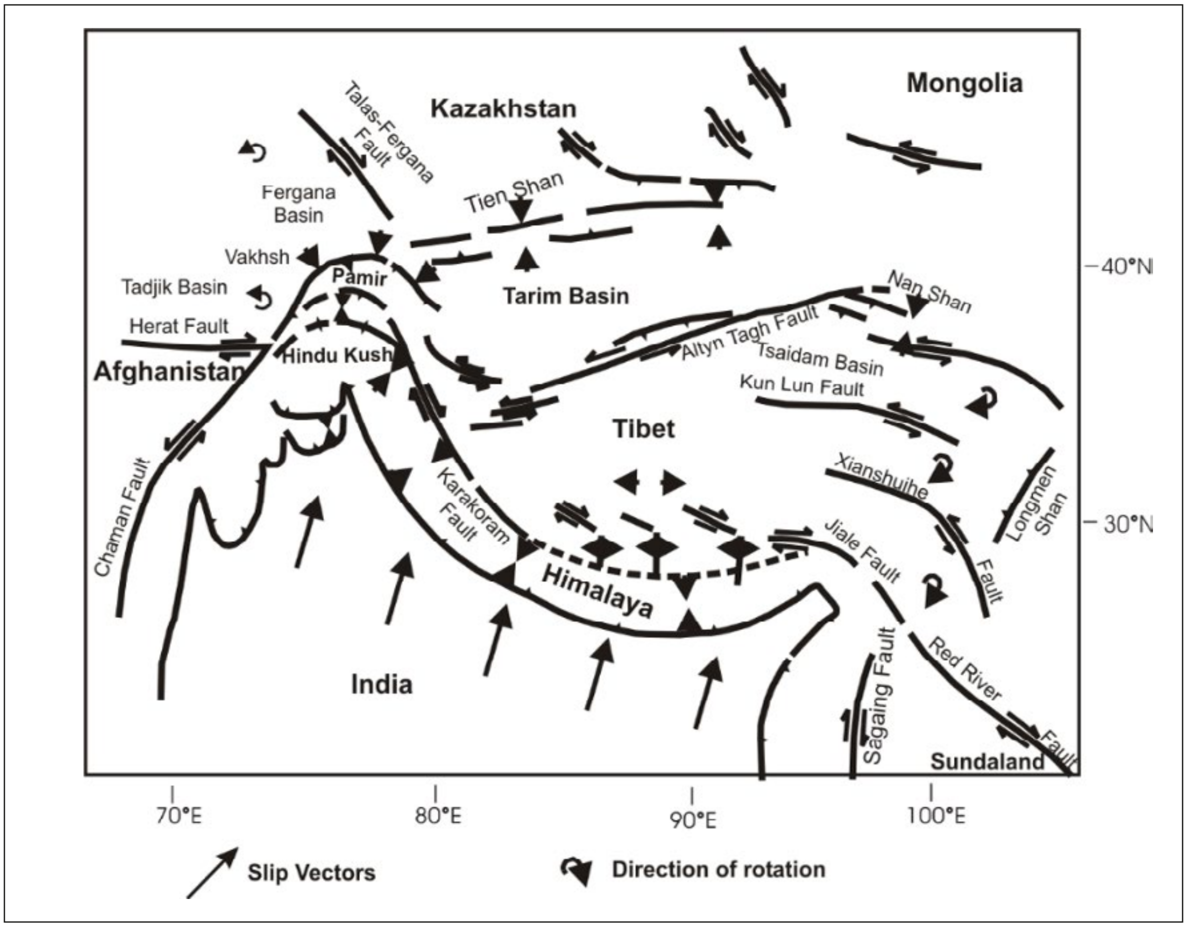

Fig. 1: A map of the Himalayas and the Central Asia, showing major structures and tectonic zones (modified after Searle, 1991)

The other mountain ranges, present along the Pamir mass whose position defines the regional geological setting of the Himalayas includes:

The Tien Shan mountain range is present in the north and east of the Pamirs. It meets with the Gobi Desert towards east of Mongolia and borders against the Tarim Basin in China. The Tarim Basin is followed by the Kunlun Mountains in the southern side and meets the Tibetan Plateau in the north. It merges into the Alai Tag mountain range in the north of the Pamirs. The Hindu-Kush mountain range occurs towards south west side of the Pamirs in the Afganistan. These mountains continue upto Kubul region and towards west gradually plunges into the Hemland river basin. The southern border of the Hindu-Kush is exposed as mélange in the east of the Kubul River, and has been considered to demarcate the tectonic contact between Himalayas and Karakoram by some workers (Searle and Tirrul, 1991; Avouac and Tapponnier, 1993*)*. The Karakoram mountain range also called Mustagh Karakoram extends in an ESE-WSW direction for over 350km from the confluence of the Siachin and Shyok near NW of Gilgit. The SE Karakoram can be traced into the Kailas Range, while the NW Karakoram follows the Himalayan syntaxis along south of the Pamirs and continues into the Hindu-Kush. In general, it is regarded as an important link between the Pamirs and the Alpine Himalayas; The Eastern and western continuation of the Himalayas is marked by the syntaxial bends. These syntaxial bends formed due to northward movement of the Indian Shield. In the eastern side of the Himalayas there are Tertiary and Cretaceous Burmese ranges (Arakan Yoma, Naga and Patkai-Chin hills) which are considered as related to the Himalayan orogeny by some workers (Valdiya, 1984*)*. This Indo-Burman orogenic belt forms a conspicuous boundary between India and Myanmar. It starts from the southern tip of the Mishimi massif and extends up to the Andaman and Nicobar of the Matawai Island, S-W Sumatra. The tectonic development of this orogen is linked with the eastern subduction of the Indian Plate beneath the Burmese plate which leads to the closure of late Jurassic-Tertiary ocean. The evidence for the existence of a suture zone along the Indian-Myanmar boundary is provided by the deposition of synorogenic flysch, ophiolitic rocks, trench mélange, radiolarite cherts, metamorphic rocks of blueschist facies and arc type igneous rocks. In the western continuation of the Himalayas, there lies a Salt Range to the west of the Indus and is offset by the Sulaiman range. The

Hazara range, which forms the western continuation of the main Himalaya, continues southwestwards but diminishes greatly in magnitude. The Sulaiman Range is not a direct continuation of the Lower Himalayas, but is a fold system of younger sediments that develops out of the Hazara ranges in the west. Westward the Sulaiman belt is sharply limited by an ophiolitic tectonic line. This suture line may be a continuation or a branch of the Indus Suture Zone. In the southern side, the Himalayan range is limited by the foreland called Indian shield or the Peninsular shield. A thrust called Himalayan frontal thrust (HFT) marks the boundary between the southernmost divisions of the Himalayas, i.e. Siwaliks from the Indo-Gangetic plain.

Geological subdivisions of the Himalayas

Geologically, the whole Himalayas can be subdivided into different parallel lithounits that extends from western to the eastern end of the Himalayan mountain range. The Nanga Parbat (33°15′ N: 74°36′ E and 8119 m) and the Namcha Barwa (29°37′ N: 95°15′ E and 7761 m) are the geographic western and eastern limits of the Himalayas respectively, spanning nearly 2500 km in length and about 320 km in width (Gansser, 1964; Verma, 1989; Jain *et al*., 2016, 2020; Searle *et al*., 2019).

The extensive linear belts comprise of southernmost Sub-Himalayan zone, followed by autochthonous-para-autochthonous units of Lesser Himalayan zone; the Central Crystalline zones and the Tethyan Himalayan zone as the northern most unit. Other than these linear belts there are ophiolites, high pressure to ultrahigh pressure metamorphic rocks (HP/UHPM) and granites that occur as isolated bodies throughout the Himalayas. Each of these zones from north to south are marked by tectonic contact which are fairly continuous throughout the Himalayas, viz., HFT, MBT, MCT and STD along with Indus Suture Zone (Fig.2).

The Sub-Himalaya: or the Siwalik Himalayas mainly consists of the several molasses deposited in the peripheral foreland basin in front of the mountain belt and distributed through the Himalayas. Their width ranges from 50 km in the western part of the Himalayas to a narrow strip in the eastern part. Lithologically, mainly comprises of sandstones, mudstones and carbonate rocks. The Siwalik sedimentation range in age ~Paleogene -Neogene. The Sub Himalayas are bounded in the south by the *Himalayan Frontal Thrust (HFT),* which separates it from the Indo Gangetic Plain. Some researchers believed that it is likely that the HFT led to the deformation in the Sub-Himalaya and has evolved during Pleistocene-Holocene. It has caused growth of longitudinal, front-parallel intermontane valleys (the Duns), and imbricated thrust system (Jain *et al*., 2020 and references therein).

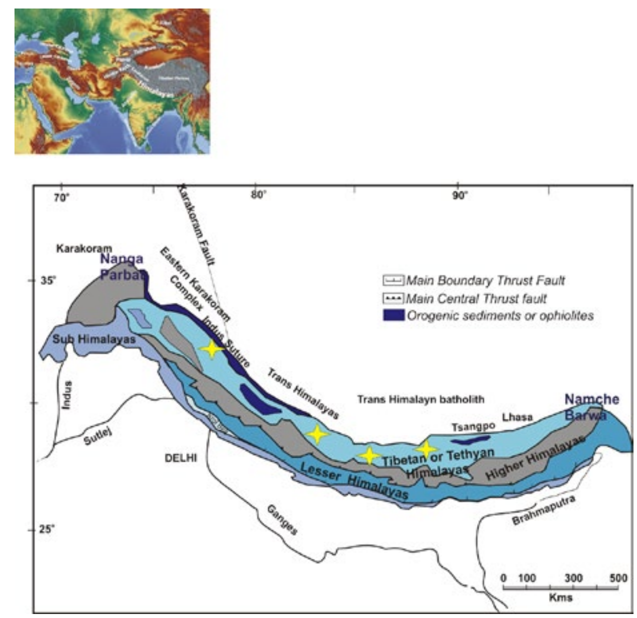

Fig 2: A geological map showing four major subdivisions of the Himalayas (modified after Gansser, 1964), some granite locations are marked as Gangotri ~22 Ma (Harrison *et al*., 1997); Manaslu `22-19 Ma (Harrison *et al*., 1999); Everest-Makalu ~23Ma(Schaerer, 198); Lhagoi Kangri ~15 Ma (Schaerer *et al*., 1986).

Main Boundary Thrust: or the MBT is a north-dipping thrust that demarcates the contact between the Lesser Himalayas and the Sub-Himalayas (Pilgrim and West, 1928; Valdiya, 1992). The Slip along MBT is ~ 10Ma old and considered to be active upto Pleistocene. After its formation ~11Ma, the MBT exhibits neotectonic activation in certain localized areas. Different names have been assigned in different geographical location for this vast extended thrust from western to the eastern end of the whole Himalayas, like Krol Thrust, Muree Thrust and Medlicott Wadia Thrust (Jain *et al.*, 2020).

The Lesser Himalayas: or the Lower Himalayas mainly consists of quartzite, dolomite and phyllite together with acid volcano-sedimentary rocks and basic lava flows in the para-autochthonous zone and unmetamorphosed authochthonous zone, that range in age from Precambrian to Eocene. Some tectonometamorphic zone belongs to this unit represent nappe zone that have underwent deformation and exhibits medium to high grade metamorphic rocks as in Kishtwar, Chor and Darjeeling.

Main Central Thrust: or MCT is defined as one of the most significant and largest tectonic discontinuities as a ductile shear zone in the Himalayas. It demarcates the tectonic boundary between Lesser Himalayas and Higher Himalayas accommodated with a displacement ranging from ~150 to 500 km. Geochronological record estimates an age of ~22 Ma for the initiation of anataxis and shearing deformation along

MCT. A NNE trending stretching lineation is characteristics of this zone and is parallel to Lesser Himalayas, Higher as well as Tethyan Himalayas. Folds are also parallel to this lineation and it is surmised that a strong compressional regime at continental crustal level operated in ductile to brittle environment to give rise to this large scale structure. The activity time span ranges from 23–20 to 15 Ma in different areas of the belt down to much younger ages in central Nepal (Mukhopadhyay *et al.*, 2017; Searle *et al*., 2008).

At some places in the Himalayas, MCT is divided into MCT I and MCT II, where, MCT I separates the rocks of the Lesser Himalayas from the Higher Himalayas and MCT Π or the Vaikrita thrust which is a duplex structure separates the rocks of higher metamorphic grade (lower to upper amphibolite) from the lower metamorphic grade (lower to upper green schist) of rocks (Thakur, 1993; Yin *et al*., 2006; Searle *et al*., 2008).

The Greater Himalayas *or Higher Himalayas or Central Crystalline zone:* comprises of metamorphic rocks of varied grade. This zone, believed to be a part of Indian Precambrian shield, has been metamorphosed as a result of the Himalayan oogenesis during Tertiary time. The Higher Himalayan zone has suffered the maximum crustal shortening and represents the region of the highest uplift in Himalayas and constitutes some of the highest peaks like the Mount Everest, Nanga Parbat, Kanchenjunga etc. This zone comprises rocks from Late Proterozoic–Cambrian ages. Granites of the Neogene age also intrude this unit. Thickening in the lower crust followed by India-Asia collision resulting in Barrovian metamorphism at deeper levels along the Greater Himalayas. The HHC made up of the most part of Himalayan Metamorphic Belt (HMB). Details on Himalayan metamorphism have been discussed by many geologist (Verma, 1989; Miller *et al.*, 2000; Pant *et al*., 2006; Searle *et al*., 2003; Kohn, 2014; Pant *et al*., 2020).

Kyanite- and sillimanite-grade metamorphic rocks are present along the entire 2500 km length of the Greater Himalaya except the two syntaxial regions in the far NW (Nanga Parbat syntaxis) and far NE (Namcha Barwa syntaxis). The Nanga Parbat–Haramosh massif occupies the core of the Nanga Parbat syntaxis comprises of relatively high-P rocks viz., granulites, Ky+ Kfs gneisses, and the Stak eclogite. High grade metamorphic rocks including granulites and Crd+ Spl–bearing assemblages have been reported from core of the Namche Barwa massif along with leucogranites (Pognante *et al*., 1993, Le Fort *et al*., 1996; Burg *et al*., 1996; Booth *et al*., 2009, Guilmette *et al*., 2011).

The South Tibetan Detachment Fault/System: *or STDF/ STDS, also known as Trans Himadri Thrust* is a low-angle normal fault that marks the contact between the Higher Himalayas and Tethyan Himalayas. Throughout the Himalaya, the STDS is now a well-established top-to-the-north-down structure, having ductile to brittle normal shear zones of variable thickness (Burg and Chen, 1984; Hodges *et al*., 1996; Carosi *et al*., 1998; Jain *et al*., 2005). One of the characteristics feature associated with this detachment fault is the occurrence of deformed leucogranites, along the footwall and hanging wall of the fault. Crystallization ages of these granites imply an age of ~12-20Ma for this fault system (Spencer *et al*., 2012; Jain *et al*., 2014; Sen *et al*., 2015; Montemagni *et al*., 2018).

The Tethyan Himalaya: The Tethyan zone is made up of a nearly complete stratigraphic section and range in age from late Precambrian to Cretaceous and Lower Eocene. The leucogranites of the Higher Himalayas are considered to be an origin of partial melting of the Indian continental crust. The THT is recognizable over a distance of 1600 km from west of the Zanskar through Lahaul, Spiti and Kumaon to northern Nepal. The Paleozoic-Mesozoic sequence of the Zanskar Supergroup is unmetamorphosed in the Zanskar range, but have been metamorphosed to Ultra High Pressure metamorphism in the Tso Morari Crystalline Complex (Gansser, 1964; Thakur, 1983; Laskowski *et al*., 2016)

Other important units in north of the Tethyan Himalayas: The Zildat Thrust separates the *Indus-Suture Zone (ISZ)* from the Tso Morari Complex in the north. This zone consists of components of Trans Himalayan zone, Neo-Tethyan ocean floor components and the Indian Plate components. The southernmost unit of the Indus Suture Zone consists of an ophiolitic mélange, referred to as the Zildat ophiolitic mélange. The Zildat ophiolitic mélange thrust over the Tso Morari Crystallines and in turn is overlain by the Nidar ophiolites, this ophiolitic belt consists of thrust slice of basic volcanic rocks, deformed garnet schist with lenses of serpentinite and limestone. The Indus Formation overlies the Nidar Ophiolite, which in turn is overlain by the molassic sediments of the Kargil Formation. These sediments are seen to overlie unconformably the granitoids of the Ladakh Plutonic Complex (LPC). The LPC is a composite batholith that consists of plutons of varying composition of two mica granite, pink porphyritic granite, and Ca-amphibole granite and is exposed immediately to the north of the ISZ. The Shyok Suture Zone (SSZ) rocks lies between the LPC and the Karakoram Zone. It extends in NW-SE direction. This unit can broadly be divided into the Shyok Group locally known as Luzarmu Formation, consisting of andesite and chert etc. Above the SSZ there lies a NW-SE trending zone called the Karakoram Zone. The two Zones are separated from each other by a thrust called Karakoram Thrust. This Zone is demarcated by the mylonitic gneissic bands with metamorphic rocks of greenschist-amphibolite grade and is also modified by later granitic activity of Karakoram Plutonic Complex (Fraser *et al*., 2001; Maheo *et al.*, 2002; Jain and Singh, 2008; Searle *et al*., 2015).

Evolution of the Himalayas

The whole evolutionary history of the Himalayan orogenesis can be divided into different chronical periods as evidenced by different workers on the basis of stratigraphic, paleomagnetism, tectonic, lithological and experimental proofs (Dewey and Burke, 1973; Le Fort, 1975; Searle, 1991, 1996, 2019; Jain *et al*., 2016, 2020):

(a) The breakup of the Gondwana land from the Laurasian can be considered as the beginning of the evolution of the Himalayan orogenetic history. The breakup of Gondwana (~140 Ma) is marked by multiple events of rifting (in the continental block) resulting in the separation of India and Tibetan block (or Lhasa) from the main Gondwana land. This separation was marked by Panjal Volcanism ~200-250 Ma; further the Lhasa block collided with Eurasia (marked by Banggong-Nujiang suture). This process was followed by the northward movement of the continental plate across the oceanic Tethyan plate. The northward movement of India for some 100 my progressively down the Tethyan Ocean. The closure of the ocean was accompanied by subduction of the ocean floor under the crust of Eurasia. The subduction produced a large amount of magmatic rocks and the magma formed the mountain range known as Trans-Himalayas on to the southern margin of the Eurasia and intra oceanic subduction within the Neo-Tethys. In the western side, intra-oceanic subduction there formed a paleo-arc, which is presently outcropping on the surface of the earth as the Ladakh-Kohistan arc.

(b) The closure of the Tethys started with suturing of Ladakh-Kohistan arc with southern Eurasia c.a. 70-80 Ma in the form of Shyok Suture Zone (SSZ), followed by collision of the Indian plate (Indian and Australian) with the accreted Eurasia, leading to the development of a suture zone at the fringes of the two plates, known as Indus Suture Zone. It is accompanied by a number of tectonic and metamorphic processes, including the obduction of the ophiolites along the Indian margin and the very high pressure rocks i.e., eclogites facies metamorphism of part of Indian continental edge. The present day ophiolitic remains are best exposed along three segments. viz., Spongtang in Ladakh, Koigar in Kumaon and Xigaze in SE Tibet. Eclogites have been reported from Kaghan valley in Pakistan (Pognante and Spencer, 1991), Tso Morari Complex (TMC) in SE Ladakh (Guillot *et al*., 1997; Sachan *et al*., 1999; Singh *et al*., 2013) and the Ama Drime, near Mt.Everest, Nepal (Lombardo *et al*., 2000; Groppo *et al*., 2007). The collision did not occur uniformly and appears to have moved progressively from W to E for a period of several million years, ending by ca 50 Ma, accompanied by a decrease of convergence rate. The presence of UHP rocks in the TMC symbolize with the marking of first step of the continental Indian Plate subduction down to depth of ~120 km. UHPM is followed by subsequent retrogression to HP and amphibolite facies between ~ 50 Ma to greenschist facies at ~30 Ma during exhumation of these rocks to the surface (Guillot *et al.*, 2008; Singh *et al*., 2013; O'Brien, 2018. This exhumation rate witnessed at the TMC is considered to be quite fast and can be marked as the rise of Himalayas.

(c) The Era post-dating the collision and suturing included two successive periods; first is characterized by the formation of south vergent nappes originating within the Suture Zone, and, second is characterized by crustal shearing and crustal doubling. The formation of south directed thrusting was responsible for the stacking of nappes on the Indian margin and which was also accompanied by the metamorphism of the underlying formation up to the kyanite-sillimanite grade. The major Himalayan orogenic event resulted in the doubly thickened continental crust. The large scale overthrusting of metamorphic and crystalline units of the Higher Himalayan Crystallines over less metamorphosed Lesser Himalayan sediments and volcanic formation has been termed as Main Central Thrust (MCT). Metamorphism and partial melting within the HHC belt (of ~25 Ma) led to the generation of leucogranites and leucosome melt. These melts appear to have evolved in a southward extruding Himalayan orogenic channel, bounded by the MCT and STDS. Subsequent Miocene–Pleistocene exhumation is wide spread in the HHC followed by its extensive erosion to produce detritus for the Cenozoic Himalayan foreland and Indo-Gangetic–Bengal basin (Jain *et al*., 2020 and references within).

(d) The ongoing convergence of the Indian and the Eurasian plate has been continually accompanied by rearrangements of continental masses along major thrusts and faults. After MCT, a thrust called Main Boundary Thrust (MBT) was formed in the Himalayas. This thrust separates the Lesser Himalayas from the Sub-Himalayas or the Siwaliks. Thrust activity has been discontinuous with pulses of rapid movement lasting less than 0.5 Ma. After the formation of MBT a thrust called Himalayan Frontal Thrust (HFT) formed. It separates the Sub Himalayan units from the Indo-Gangetic Planes.

(e) As convergence proceeds the mountain ranges rises, but in discontinuous way. Uplift is counteracted by erosion and the detritus produced by it is partially trapped in large intermontane basins (like Siwalik basin) and partly in the Indo-Gangetic plains and fans.

Himalayan Metamorphism

Though the Himalayan metamorphism is generally considered to be a Cenozoic event with the peak metamorphism attributed to have occurred ~22 Ma (Kohn, 2014; Verma, 1989), it has also been proposed that the Himalayan orogen had an early Paleozoic beginning with accompanying deformation, metamorphism and magmatism (Gehrels *et al*., 2003). Kohn (2014) considered Greater Himalayan Sequence (GHS) to be a "sandwich" between Tethyan Himalayan Sequence (THS) and LHS) with lateral continuity of the combined sequence of the order of ~2000 km. He also attributed telescoping of metamorphic grades by the South Tibet Detachment System (STDS). The northern limit of the Himalayan metamorphism is marked by the detached occurrences of high pressure assemblages of Indus Tsangpo Suture Zone (ITSZ) and equivalents.

Vadlamani and Pant (2020) summarized pre-Himalayan metamorphic imprints. There were also reports of much older pre- Himalayan metamorphism (e.g. Pant *et al*., 2006). In a recent review, Pant *et al*., (2020) identifying three elements of Transhimalaya, suture zone and Himalayas, considered Himalayan metamorphism to be affecting the Himalaya as well as Transhimalaya rocks. They distinguished three metamorphic domains with characteristic P-T-t paths from Transhimalaya in the north to the sporadic occurrence of suture zone (i.e. ITSZ) defining the limit of Indian continental component and Himalayan metamorphism. They considered the Himalayan metamorphism to represent the most prominent manifestation of this youngest orogeny with a clockwise P-T-t path typically representing continental curst thickening event (Fig.3)**.**

Nearly 100 years ago (pre-plate tectonic era) Argand (1924) proposed underthrusting of India beneath Asia leading to doubling of continental crust for rise of the Himalaya and concomitant ductile deformation of Indian continental crust. In one of the early application of the plate tectonic theory, collision type mountain belt was proposed for the Alpine-Himalayan belt (Dewey and Bird, 1970). Considering Transhimalayan lithotectonic package, Himalaya was considered to be produced by the underthrusting of Indian continent beneath Asia along Indus Tsangpo Suture Zone (ITSZ) but not directly by continent-continent collision by some workers (Powell and Conaghan, 1975). Others also proposed detachment of Indian continental crust during the subduction and followed by the buoyant rise of the detached segment (e.g. Chemenda *et al*., 2000). Some of the well discussed models of exhumation include wedge-extrusion model in which extrusion towards south through MCT and other north dipping low angle dislocations of tapered wedge/s of high grade metamorphic rocks was proposed (Burchfiel and Royden, 1985) and channel-flow model which envisaged extrusion of these rocks on account of mid-crustal channel of low-viscosity (fully or partially molten crust) between MCT and STDS (Beaumont *et al*., 2001; Godin *et al*., 2006). Another striking and related feature of the Himalayan belt is

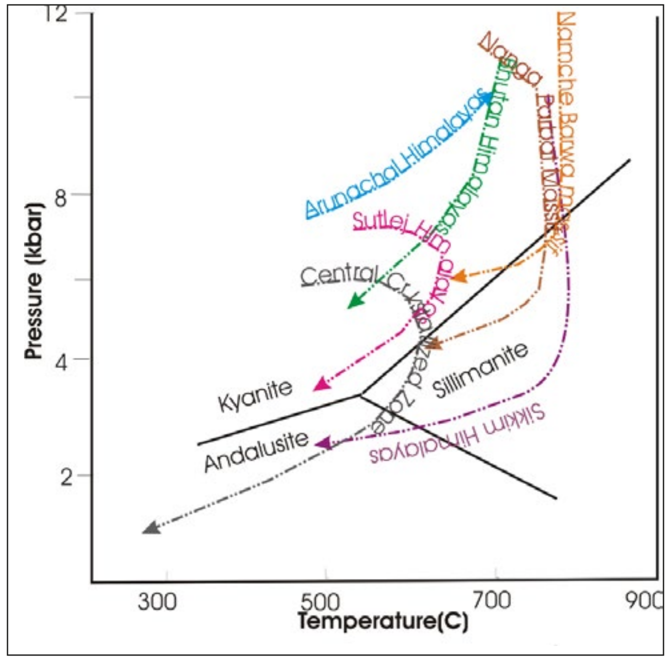

Fig. 3: The proposed P-T path for different metamorphic terrains from the Himalayas, Arunachal Himalayas (Wallis *et al*., 2014); Bhutan Himalayas (Daneil *et al*., 2003); Syntaxial zones (Zeitlier *et al*., 1993 and Booth *et al*., 2009); Sutluj section (Caddick *et a*l., 2007); Sikkim Himalayas (Ganguly *et al.*, 2000; Central Crystalline Zone (Verma, 1989); Univariant reactions marked are from Pattison(1992; Ky-Sill-And)*(adopted from Pant et al., 2020)*

the presence of inverted metamorphic sequence across several sections from west to east (Hubbard, 1996; Harrison *et al*., 1999; Stephenson *et al*., 2002; Dasgupta *et al*., 2004). Several of the exhumation models (e.g. channel-flow) attempted to incorporate explanation of this feature. Ductile shear model was invoked by Jain *et al., (*1993) and Jain *et al*. (2005) to invoke transposition of metamorphic isograds by simple or general shear through frictional heating along the MCT. The exhumation of GHS has been proposed by contemporaneous shearing along two major tectonic features i.e. MCT and STDS in ~40 Ma (major movement dated at ~25 and ~17 Ma) through tectonometamorphic shear zones (Carosi *et al*., 2018) by southward propagating "in-sequence" thrusting. A summary and schematic diagram illustrating these models has recently been described by Jain *et al*. (2020).

Himalayan leucogranites

Several granites broadly representing three age groups, namely, a Paleoproterozoic age, a late Proterozoic to early Paleozoic age and a Cenozoic age, are present in the Himalaya (Honegger *et al.*, 1982; Singh and Jain, 2003 and references therein; Singh, 2020; Weinberg, 2016). In the present context, only the youngest groups are relevant. These are leucogranites (often tourmaline bearing, two-feldspar two-mica type) and generally represent low crystallization temperatures (~700-750^{o}C; Montel, 1993). The emplacement ages for these vary between 24-17 Ma; Harrison *et al*., 1998 and 1999) and are nearly coincident with the peak metamorphic ages of the Himalayan metamorphism and represent partial melting product of the Himalayan orogeny (Fig.2).

Two subdivisions of the magmatic rocks were reported from the Himalayan ranges: viz., the High Himalayan leucogranites and the North Himalayan granite, suggested to have differences in terms of emplacement style, temperature and age data were proposed (Weinberg, 2016; Harrison *et al*., 1997). The High Himalayan leucogranites form a discontinuous chain of sills and dikes that are exposed adjacent to the South Tibetan detachment, which separates Indian gneisses of the Tibetan slab from lower-grade Tethyan shelf deposits in the hanging wall. These include the plutons of the Zanskar, Garhwal, Manaslu, and Everest-Makalu regions (age ~ 24-17 Ma). The North Himalayan granite belt runs parallel to, and ~100 km to the north of, the High Himalaya. They differ from the High Himalayan leucogranites in their emplacement style, younger ages (17–9Ma), and higher melting temperatures (>750 °C) suggested by noneutectic compositions and high light rare earth contents coupled with low monazite inheritance (Debon *et al*., 1986; Schärer *et al*., 1986; Montel, 1993). However, modelling results indicate that slip along a shallowly dipping fault within a metamorphically stratified crust can produce two horizontally separated granite belts through discontinuous partial melting reactions. Critically analyzing the age data of the granites, Harrison *et al*., (1997, 1999) considered the two belt of granites to have been produced by the northward propagating melting process occurring in segregated clusters on account of variable exposures. On the basis of a generalized clockwise P-T paths recorded along different Himalayan metamorphic sections (Fig.3) it can be suggested that Himalayan granites formed as a result of decompression melting (muscovite as well as biotite dehydration melting) at an average P-T ~ 4-9 kbar and 650-750° C.

Concluding remarks

The story of evolution of the youngest and evolving continental mountain chain on the planet is a result of a complex plate tectonic convergence involving two continental segments, an arc in-between and closure of the Tethys. Multiple geological processes including sedimentation (marine to continental and transition and attendant paleontological record), multiple magmatism, deformation and metamorphism preserve clues of this evolution. This paper addresses only a very limited of these aspects as would be the case with any such limited review. The authors acknowledge the immense other contributions not discussed and mentioned in the present review.

Acknowledgement

Shri E.V.R. Parthasaradhi is thanked for inviting the contribution for this commemorative volume. Support of the MoES funded project "Age Constraints on metamorphic evolution of the Trans-Himalayas': 'MoES/P.O. (Geol/101(b)/2017)" is thankfully acknowledged.

References

Argand, E., 1924: La Tectonique de L'Asie. *International Geological Congress* -1922**,** *Session -XIII*: 170–732.

Avouac, J.P. and Tapponier, P., 1993: Kinematic model of active deformation in central Asia. *Geophysical Research Letters*, **20(10)**: 895-898.

Beaumont, C., Jamieson, R. A., Nguyen, M.H. and Lee, B., 2001: Himalayan tectonics explained by extrusion of a low-viscosity channel coupled to focused surface denudation. *Nature*, **414**: 738 – 742.

Booth, A.L., Chamberlain, C.P., Kidd, W.S.F. and Zeitler, P.K., 2009: Constraints on the metamorphic evolution of the eastern Himalayan syntaxis from geochronologic and petrologic studies of Namche Barwa. *Geological Society of American Bulletin*, **121(3-4)**: 385–407.

Burchfiel, B. C. and Royden, L. H., 1985: North-south extension within the convergent Himalayan region. *Geology*, **13(10)**: 679-682.

Burg, J. P. and Chen, G. M., 1984: Tectonics and structural zonation of sourthern Tibet, China. *Nature,* **331**: 219-223.

Burg, J. P., Chaudhry, M.N., Ghazanfar, M., Anczkiewicz, R. and Spencer, D., 1996: Structural evidence for back sliding of the Kohistan arc in the collisional system of northwest Pakistan. *Geology*, **24(8)**: 739– 742.

Caddick, M.J., Bickle, M.J., Holland, T.J.B., Harris, N.B.W., Horstwood, M.S.A., Parrisch, R.R. and Ahmad, T., 2007: Burial and exhumation history of a Lesser Himalayan schist: Recording the formation of an inverted metamorphic sequence in NW India. *Earth and Planetary Science Letters*, **264(3-4)**: 375–390

Carosi, R., Lombardo, B., Molli, G., Musumeci, G. and Pertusati, P.C., 1998: The south Tibetan detachment system in the Rongbuk valley, Everest region. Deformation features and geological implications. *Journal of Asian Earth Sciences*, **16(2-3)**: 299–311.

Carosi R., Montomoli C., Iaccarino S. & Visonà D., 2018: Structural evolution, metamorphism and melting in the Greater Himalayan Sequence in central-western Nepal. In: Treloar P.J. & Searle M.P. (Eds.) Himalayan Tectonics: A Modern Synthesis. *Geological Society, London, Special Publications,* 483.

Chemenda, A.I., Burg, J. and Mattauer, M., 2000: Evolutionary model of the Himalaya-Tibet system: geopoem based on new modelling, geological and geophysical data. *Earth and Planetary Science Letters,* **174**(3-4): 397-409.

Debon, F., Le Fort, P., Sheppard, S.M.F. and Sonet, J., 1986: The four plutonic belts of the Transhimalaya - Himalaya: A chemical, mineralogical, isotopic, and chronological synthesis along a Tibet-Nepal granite section. *Journal of Petrology,* **21(1)**: 219–250.

Daniel, C.G., Hollister, L.S., Parrish, R.R., Grujic, D., 2003: Exhumation of the Main Central Thrust from lower crustal depths, eastern Bhutan Himalaya. *Journal of Metamorphic Geology,* **21(4)**: 317–334

Dasgupta, S., Ganguly, J. and Neogi, S., 2004: Inverted metamorphicsequence in the Sikkim Himalaya: crystallization history, P–T gradient and implications. *Journal of Metamorphic Geology,* **22(5)**: 395–412.

Dewey, L.F. and Bird, J.M., 1970: Mountains belts and the new global tectonics. *Journal of Geophysical Research,* **75(14)**: 2625-2647.

Dewey, J. F. and Burke, K. C. A., 1973: Tibetan, Variscan and Precambrian basement reactivation: products of a continental collision. *Journal of Geology*, **81(6)**: 683-692.

Fraser, J.E., Searle, M.P., Parrish, R.R. and Noble, S.R., 2001: Chronology of deformation, metamorphism, and magmatism in the southern Karakoram Mountains. *Geological Society of America Bulletin*, **113(11)**: 1443–1455.

Ganguly, J., Dasgupta, S., Cheng, W. and Neogi, S. (2000) Exhumation history of a section of the Sikkim Himalayas, India: records in the metamorphic mineral equilibria and compositional zoning of garnet. Earth and Planetary Science Letters 183,471–486

Gansser, A., 1964: Geology of the Himalayas. Interscience Publication, John Wiley and Sons Ltd, London, 289p.

Gehrels, G.E., DeCelles, P.G., Martin, A., Ojha, T.P., Pinhassi, G. and Upreti, B.N., 2003: Initiation of the Himalayan Orogen as an Early Paleozoic Thin-skinned Thrust Belt. *GSA Today*, 1-9.

Godin, L., Grujic, D., Law, R.D. and Searle, M.P., 2006: Channel flow, extrusion, and exhumation in continental collision zones: an introduction. *In*: Channel Flow, Extrusion, and Exhumation in Continental Collision Zones, (Eds.) Law, R.D., Searle, M.P. & Godin, L. *Geological Society, London, Special Publication*, **268**: 1–23.

Groppo, C., Lombardo, B., Rolfo, F. and Pertusati, P., 2007: Clockwise exhumation path of granulitized eclogites from the Ama Drime range (Eastern Himalaya). *Journal of Metamorphic Geology*, **25(1)**: 51-75.

Guilmette, C., Indares, A., H´ebert, R., 2011: High-pressure anatectic paragneisses from the Namche Barwa, Eastern Himalayan Syntaxis: textural evidence for partial melting, phase equilibria modeling and tectonic implications. *Lithos,* **124(1-2)**: 66–81

Guillot, S., de Sigoyer, J., Lardeux, J. M, and Mascle, G., 1997: Eclogitic metasediments from the Tso Morari area (Ladakh, Himalaya): evidence for continental subduction during India-Asia convergence. *Contributions to Mineralogy Petrology*, **128**: 197-212.

Guillot, S., Maheo, G., de Sigoyer, J., Hattori, K.H. and Pecher, A., 2008: Tethyan and Indian subduction viewed from the Himalayan high to ultra-high pressure metamorphism. *Tectonophysics*, **451(1-4)**: 225-241.

Hodges, K.V., Parrish, R.R. and Searle, M.P., 1996: Tectonic evolution of the central Annapurna Range, Nepalese Himalayas*. Tectonics*, **15(6)**: 1264– 1291.

Hodges, K.V., 2000: Tectonics of the Himalayas and southern Tibet from two perspectives. *Geological Society of American Bulletin*, **112(3)**: 324-350.

Honegger, K., Dietrich, V., Frank, W., Gansser, A., Thöni, M., and Trommsdorff, V., 1982: Magmatism and metamorphism in the Ladakh Himalayas (the Indus-Tsangpo suture zone). *Earth and Planetary Science Letter*s, **60(2)**: 253-292.

Harrison, T.M., Grove, M., Lovera, O.M., Catlos, E.J., 1998: A model for the origin of Himalayan anatexis and inverted meta- morphism. *Journal of Geophysical Research*, **103(B11)**: 27,017-27,032.

Harrison T.M., Lovera, O.M., Grove, M., 1997**:** New insights into the origin of two contrasting Himalayan granite belts. *Geology,* **25(10)**: 899–902

Harrison T.M., Grove M., Lovera O.M., Catlos, E.J. and D'andrea J., 1999: The origin of Himalayan anatexis and inverted metamorphism: Models and constraints. *Journal of Asian Earth Sciences*, **17(5-6)**: 755–772.

Hubbard, M.S., 1996: Ductile shear as a cause of inverted metamorphism: example from the Nepal Himalaya. *Journal of Geology*, **104(4)**: 493-499.

Jain, A. K., Singh, S. Manickavasagam, R. M., Joshi, M. and Verma, P. K., 2003: HIMPROBE Programme: Integrated studies on geology, petrology, geochronology, and geophysics of the Trans Himalaya and Karakoram. *Memoir of Geological Society of India,* **53**: 1-56.

Jain, A.K., Manickavasagam, R.M., Singh, S. and Mukherjee, S., 2005: Himalayan collision zone: new perspectives-its tectonic evolution in a combined ductile shear zone and channel flow model. *Himalayan Geology*, **26(1)**: 1-18.

Jain, A.K. and Singh, S., 2008: Tectonics of the southern Asian plate margin along the Karakoram Shear Zone. Constraints from field observations and U-Pb Shrimp ages: *Tectonophysics,* **451**:186-205.

Jain, A.K. and Singh S., 2009: Geology and Tectonics of the Southeastern Ladakh and Karakoram. Geological Society of India, Bangalore, India, 179p.

Jain, A.K., Shrestha, M., Seth, P., Kanyal, L., Carosi, R., Montomoli, C., Iaccarino, S., Mukherjee, P.K., 2014: The Higher Himalayan Crystallines, Alaknanda–Dhauli Ganga Valleys, Garhwal Himalaya, India*. In*: Geological field trips in the Himalaya, Karakoram and Tibet, (eds) Montomoli C, Carosi R, Law RD, Singh S, Rai SM. *Journal of Virtual Explore*, **47(8)**.

Jain, A.K., Dasgupta, S., Bhargwa, O.N., Patel, R. and Mukul, M., Md. Israil, Perumal, J.R., Patel, R.C., Mukul, M., Parcha, S.K., Adlakha, V., Agarwal, K.K., Singh, P., Bhattacharya, K., Pant N.C. and Banerjee, D.M., 2016: Tectonics and Evolution Of the Himalaya. *Proceedings of Indian National Science Academy*, *Special Issue*, **82(3**): 581-604.

Jain, A.K., Banerjee, D.M. and Kale, S.V., 2020: Tectonics of Indian subcontinent. Springer Publication, 295-448.

Kohn, M.J., 2014: Himalayan Metamorphism and Its Tectonic Implications. *Annual Review of Earth and Planetary Sciences*, **42:** 381-419.

Laskowski, A. K., Kapp, P., Vervoort Jeff, D. and Ding L., 2016: High-pressure Tethyan Himalaya rocks along the India-Asia suture zone in southern Tibet. *Lithosphere,* **8(5):** 574-582.

Le Fort, P., 1975: Himalayas: the collided ranges. Present knowledge of the continental arc. *American Journal of Science*, **275A**: 1-44.

Le Fort, P., 1996: Evolution of the Himalayas. *In*: The Tectonics of Asia, (Eds.) Yin, A., Harrison, T.M. Cambridge University Press, New York, 95-106.

Lombardo, B., Rolfo, F. and Compagnoni, R., 2000: Glaucophane and barroisite eclogites from the upper Kaghan nappe: implication for the metamorphic history of the NW Himalaya. *In*: Tectonics of the Nanga Parbat syntaxis and the W Himalayas (Eds.) M.A. Khan, P.J. Treloar, Searle, M.P. and Jain, M.Q. *Geological Society, London, Special Publication***, 170**: 411-430.

Mahe´o, G., Guillot, S., Blichert-Toft, J., Rolland, Y. and Pecher, A., 2002: A slab breakoff model for the Neogene thermal evolutionof South Karakoram and South Tibet. *Earth and Planetary Science Letters,* **195(1-2)**: 45–58.

Montemagni, C., Montomoli, C., Iaccarino, S., Carosi, R., Jain, A.K., Massonne, H.-J., Villa, I.M., 2018: Dating protracted fault activities: microstructures, microchemistry and geochronology of the Vaikrita Thrust, Main Central Thrust zone, Garhwal Himalaya, NW India. *Geological Society of London, Special Publication,* **481**: 127-146.

Montel, J.-M., 1993: A model for monazite/melt equilibrium and application to the generation of granitic magmas. *Chemical Geology*, **110(1-3):** 127–146

Miller, C., Klotzli, U., Frank, W., Thoni, M., Grasemann, B., 2000**:** Proterozoic crustal evolution in the NW Himalaya (India) as recorded by circa 1.80 Ga mafic and 1.84 Ga granitic magmatism. *Precambrian Research*, **103(3-4):**191–206

Mukhopadhyay, D., Chakraborty, S., Trepmann, C., Rubatto, D., Anczkiewicz, R., Gaidies, F., Dasgupta, S., Chowdhury, P., 2017: The nature and evolution of the Main Central Thrust: Structural and geochronological constraints from the Sikkim Himalaya, NE India. *Lithos*, **282-283**: 447-463.

O'Brien, P.J., 2018: Eclogites and other high-pressure rocks in the Himalaya: a review. *In*: Himalayan Tectonics: A Modern Synthesis, (Eds.) Treloar, P.J. and Searle, M.P., *Geological Society, London, Special Publications*, **483(5)**: SP483.13.

Pant, N.C., Kundu, A., Kumar, R., Dorka, B.S., Prasher, S., 2006: Paleoproterozoic metamorphism in the Jeori-Wangtu Gneissic Crystallines (JWGC), Western Himalaya. *Journal of Asian Earth Science*, **26(6)**: 585–604.

Pant, N.C., Singh, P., Jain, A.K., 2020: A Re-look at the Himalayan metamorphism. *Episodes,* **43(1)**: 369–380.

Pattison, D.R.M., 1992: Stability of andalusite and sillimanite and the Al_2SiO_5 triple point; constraints from the Ballachulish aureole, Scotland. *Journal of Geology,* **100(4)**: 423–46.

Pilgrim, G.E. and West, W.D., 1928: The structure and correlation of the Simla rocks. *Memoir of Geological Survey of Indi*a**, 53**:1–150.

Pognante, U. and Spencer, D.A., 1991: First report of eclogites from the Himalayan belt, Kaghan valley (Pakistan). *European Journal of Mineralogy*, **3(3):** 613-618.

Pognante, U. & Benna, P., 1993: Metamorphic zonation, migmatization and leucogranites along the Everest transect of Eastern Nepal and Tibet: record of an exhumation history. *Geological Society London, Special Publication,* **V (74)**, 323–340.

Powell, C.Mc.A. and Conaghan, P. J., 1975: Polyphase Deformation in Phanerozoic Rocks of the Central Himalayan Gneiss, Northwest India**.** *The Journal of Geology***, 83(3)**: 403-406.

Richter, F. M., Rowley, D. B. and DePaolo, D. J., 1992: Sr isotope evolution of seawater: The role of tectonics. *Earth and Planetary Science Letters*, **109(1-2)**: 11-23.

Rolland, Y., Pêcher, A., Picard, C., 2000: Middle Cretaceous back-arc formation and arc evolution along the Asian margin: the Shyok Suture Zone in northern Ladakh NW Himalaya. *Tectonophysics*, **325(1-2)**:145–173.

Sachan, H. K., Bodnar, R. J., Islam, R., Szabo, C. and Law, R.D., 1999: Exhumation history of eclogites from the Tso Morari Crystalline complex in Eastern Ladakh: Mineralogical and Fluid inclusion constraints. *Journal of Geological Society of India*, **30(2)**:181-190.

Schärer, U., 1984: The effect of initial ^{230}Th disequilibrium on young U-Pb ages: The Makalu case, Himalaya. *Earth and Planetary Science Letters*, **67(2)**: 191–204.

Schärer, U., Xu, R. H., and Allègre, C. J., 1986: U-(Th)-Pb systematics and ages of Himalayan leucogranites, south Tibet. *Earth and Planetary Science Letters*, **77(1)**: 35–48.

Searle, M.P. and Tirrul, R., 1991: Structural and thermal evolution of the Karakoram crust. *Journal of the Geological Society, London*, **148**: 65–82.

Searle, M. P., Windley, B. F. Coward, M. P. Cooper, D. J. Rex, A. J., *et al.*1988: The closing of Tethys and the tectonics of the Himalaya. *Geological Society of America Bulletin*, **98(6)**: 678-701.

Searle, M.P., 1996: Cooling history, erosion, exhumation, and kinematics of the Himalaya-Karakoram-Tibet orogenic belt. *In*: The Tectonic evolution of Asia, (Eds.) A. Yin and T. M. Harrison, 110–137. New York: Cambridge University Press.

Searle, M.P., Simpson, R.L., Law, R.D., Parrish, R.R. and Waters, D.J., 2003: The structural geometry, metamorphic and magmatic evolution of the Everest massif, High Himalaya of Nepal – South Tibet. *Journal of the Geological Society, London*, **160:** 345–366.

Searle, M.P., Law, R.D., Godin, L., Larson, K.P., Streule, M.J., Cottle, J.M. and Jessup, M.J., 2008: Defining the Himalayan Main Central Thrust in Nepal. *Journal of the Geological Society,* **165:** 523–534.

Searle, M. P., 2015: Mountain Building, Tectonic Evolution, Rheology, and Crustal Flow in the Himalaya, Karakoram, and Tibet. *In*: Treatise on Geophysics, (Editor-in-chief): Gerald Schubert), 6, Oxford, Elsevier, 469-511.

Searle, M. P. and Treloar, J. P., 2019: Introduction to Himalayan tectonics: a modern synthesis. *Geological Society, London, Special Publications*, **483**:1-17.

Sen, K., Chaudhury, R. and Pfänder, J., 2015: ^{40}Ar–^{39}Ar age constraint on deformation and brittle–ductile transition of the Main Central Thrust and the South Tibetan Detachment zone from Dhauliganga valley, Garhwal Himalaya, India. *Journal of Geodynamics*, **88**:1–13.

Singh, P., Saikia, A., Pant, N.C. and and Verma, P.K., 2013: Insights into the P–T evolution path of Tso Morari eclogites of the northwestern Himalaya: Constraints on the geodynamic evolution of the region. *Journal of Earth System Science*, **122(3)**: 677–698.

Singh, S., and Jain, A. K., 2003: Himalayan granitoids. *Journal of the Virtual Explorer*, **11**: 1-20

Singh, S., 2020: Himalayan magmatism through space and time. *Episodes,* **43(1)**: 358-368

Spencer, C.J., Harris, R.A., Dorais, M.J., 2012: The metamorphism and exhumation of the Himalayan metamorphic core, eastern Garhwal region, India. *Tectonics*, **31:** TC1007.

Srikantia, S.V. and Bhargava, O.N., 1983: Geology of the Paleozoic sequence of Kashmir Tethys Himalayas in the Lidar valley. *Journal of Geological Society of India,* **24(7)**:363-377.

Stephenson, B.J., Waters, D.J. and Searle, M.P., 2002: Inverted metamorphism and the Mail Central Thrust: field relations and thermobarometric constraints from the Kishtwar Window, NW Indian Himalaya. *Journal of Metamorphic Geology*, **18(5)**: 571–590

Thakur, V. C., 1983: Deformation and Metamorphism of the Tso Morari crystalline complex. *In*: Geology of the Indus Suture Zone of Ladakh, (Eds.) V. C. Thakur and K. K. Sharma. Wadia Institute of Himalayan Geology, Dehradun, India, 1-8.

Thakur, V.C., 1993: Geology of the Western Himalaya. Pergmon Press, Oxford, 1–355

Vadlamani, R. and Pant, N.C., 2020: Precambrian/Early Paleozoic orogenic rocks in the Himalaya - Remnants of the leading edge of the Indian plate. *Proceedings of the Indian National Science Academy*, 86: 167-173.

Valdiya, K.S.,1984**:** Evolution of the Himalayas. *Tectonophysics,* **105(1-4)**: 229-248.

Valdiya, K.S., 1992: The Main Boundary thrust zone of the Himalaya, India. In: Bucknam RC, Hancock PL (eds) Major active faults of the world: results of IGCP Project 206. *Annales Tectonicae*, **6**:54–84.

Valdiya, K.S., 1995: Proterozoic sedimentation and Pan-African geodynamic development of the Himalaya. *Precambrian Research*, **74(1-2)**: 35–55.

Voo, D.D.R., Spakman, W. and Bijwaard, H., 1999: Tethyan subducted slab under India. *Earth and Planetary Science Letters*, **171(1)**: 7-20.

Verma, P.K., 1989: The Himalayan Metamorphism. *Geological Society Special Publication*, **43**: 377-383.

Wallis, D., Phillips, R.J. and Lloyd, G.E., 2014: Evolution of the Eastern Karakoram Metamorphic Complex, Ladakh, NW India, and its relationship to magmatism and regional tectonics. *Tectonophysics*, **626**: 41-52.

Weinberg, R.F., 2016: Himalayan leucogranites and migmatites: nature, timing and duration of anataxis. *Journal of Metamorphic Geology*, **34(8)**: 821-843.

Yin, A. and Harrison, T.M., 2000: Geological evolution of the Himalayan–Tibetan orogen. *Annual Reviews of Earth Planetary Sciences*, **28:** 211–280.

Yin, A., Dubey, C.S., Kelty, T.K., Gehrels, G.E., Chou, C.Y., Grove, M. and Lovera, O., 2006: Structural evolution of the Arunachal Himalaya and implications for asymmetric development of the Himalayan orogen. *Current Science,* **90(25)**: 195–206.

Zeitler, P.K., Chamberlain, C.P. and Smith, H.A., 1993: Synchronous anatexis, metamorphism, and rapid denudation at Nanga Parbat (Pakistan Himalaya). *Geology,* **21(4)**:347–50.

Indian Journal of Geosciences, Volume 74, No. 3
July - September, 2020; pp. 216-222

Invited Paper

Some Undiscovered Greenfield Mineral Potential in India: Need for Concerted Exploration Efforts with a Mission Mode

Anupendu Gupta

Former Deputy Director General, Geological Survey of India, Kolkata
Email: anupendu@yahoo.com

Abstract: Undiscovered mineral potential visualized through geological concepts exists in many countries, as also in India. Concept based search in many domains has lead to significant discoveries, some of which unraveled new metallogenic realms unknown theretofore. In Indian perspective, three conceptual metallogenic milieus are highlighted in this paper to attract the attention of the exploration agencies and concerned governments. These are Trans-Himalayan region, the vast Deccan Trap covered area and the Bundelkhand Granite-Gneiss massif in the peninsular India.

Ophiolite related metallization along Indus-Tsangpo suture within Indian territory in north Ladakh is a distinct possibility, though the overriding hinterland plate offers much greater metallogenic potential as discovered in Tibet. Underplating of foreland plate along the collision zone may comprise several smaller thrust zones, having multiple loci of metallization. This zone needs serious exploration efforts.

About half a million sq. km of the peninsular India is covered by Mesozoic continental flood basalt, called Deccan Trap. The terrain remains totally unexplored in respect of the possible sub-trap volcanogenic or hydrothermal metallization similar to Ni-Cu-PGE deposits of Noril'sk and Talnakh located below Siberian flood basalt in Russia.

The Bundelkhand Granite-Gneiss massif presents a highly favourable domain for Precambrian Porphyry type mineralization. The only known Precambrian (~2500 Ma) Porphyry copper-molybdenum deposit in India is at Malanjkhand. A serious effort is needed to find out more Precambrian Porphyry deposits like Malanjkhand in Bundelkhand province.

Key words: Trans-Himalaya, Indus-Tsangpo suture, Deccan Trap, Sub-trap metallization, Bundelkhand granite-gneiss massif, Porphyry deposit.

Introduction

Greenfield mineral potential visualized through geological concepts but yet to be discovered exists in many countries, as also in India. Concept based investigations in many of such domains have led to significant discoveries, some of which unraveled new metallogenic realms unknown theretofore, like IOGC type deposits (Gupta, 2011).

In Indian perspective, three conceptual metallogenic milieus are highlighted here to attract the attention of the exploration agencies and concerned governments. These are Trans-Himalayan region in northern Ladakh, the vast Deccan Trap covered area in west-central peninsula and the Bundelkhand Granite-Gneiss massif located in the north-central edge of the peninsular India (Gupta, 2018).

Trans-Himalayan region in north Ladakh

It is rather intriguing that the most impressive mountain range on the face of the earth has a dismal record of metallogeny and should consequently stand written-off as a non-potential crustal segment. Both from the view point of plate tectonic status of this continent-continent collision zone and its comparison with Alpine belt, it is difficult to believe that all the possible negative factors could conjure in a unique manner to make the Himalaya barren of any significant metal accumulation. It will be regarded as a freak of nature even if theoretical explanations are presented to justify insignificant metallization in all segments of Himalaya ranging in age from Proterozoic to Tertiary. Therefore, with an optimistic outlook, the Himalaya deserves a thorough scanning for possible but varied metallogeny ranging from sedimentary-diagenetic types in the Frontal belt, SEDEX type and hydrothermal deposits in Lesser Himalaya, Tertiary granitic pluton related metallization in Central crystalline, bedded deposits in Tethyan sediments, ophiolite related metallization along Indus-Tsangpo suture zone and Shyok-Nubra tectonic belt and also the Porphyry type deposits in Trans-Himalayan region. The hot spring system of Puga valley, Ladakh, perhaps presents evidence of a live epithermal process at depth. There are many prominent hydrothermal alteration zones with or without mineral shows which may also lead to metal concentration in deeper levels (Sarkar and Gupta, 2012).

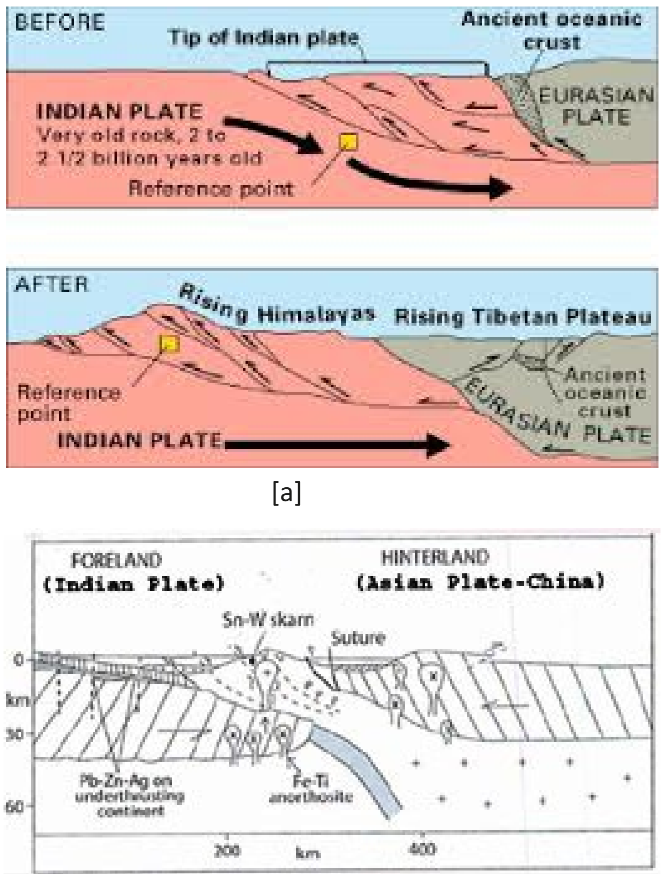

[a]

[b]

Fig. 1: (a) Northern tip of Indian plate before and after the collision in Trans-Himalayan Indus-Tsangpo suture zone, (b) Cartoon of foreland-hinterland in collisional setting with locations of some deposit types (Mitchell and Garson, 1981; Deb and Sarkar, 2017).

Mitchel and Garson (1981) assigned several tectonic elements in a collision zone as depicted in the cartoon (Fig. 1 b). The zone of our interest in this cartoon is the Foreland (underthrusting Indian Plate), which shows the inherited Precambrian Pb-Zn-Ag deposits, syn-collisional Tertiary Fe-Ti anorthosite and Sn-W skarns in granite plutons.

The prospect for ophiolite related metallization along Indus-Tsangpo suture zone and Nubra-Shyok tectonic belt in the Trans-Himalayan region of northern Ladakh arises from the distinct possibility of multiple shear zones in the foreland wedge of Indian plate within geographical territory of the country. It is well understood now that the highly tectonised collision zone, having possibility of metallogenic conduits, affect significant width of underthrusted Foreland, besides the obvious potential of the overriding Hinterland.

The Indus-Tsangpo suture zone, passing through the south of Ladakh range (granitic batholith), comprises flyshoidal (Cretaceous-Eocene) and molasses sediments (Mio-Pliocene), with thrust contact in between. The Shyok - Nubra tectonic belt, lying to the north of Ladakh range and south of Karakoram Range, comprises acid to intermediate volcanics with interbedded sediments of Lower Cretaceous age and ophiolite mélange (Khardung volcanics) consisting of mafic lava flows and ultramafic intrusives alternating with metasediments (Shyok Formation). The tectono-stratigraphy of the Shyok area suggests that they probably represent the components of a marginal basin in an island-arc system (Thakur *et al*., 1981; Thakur, 1990; Srimal, 1990). Indus and Shyok tectonic belts had the same Cretaceous–Oligocene history. However, the post-Oligocene volcanic eruptions noted at places in the Shyok valley is the youngest igneous activity in the whole of the Ladakh Himalaya (Hakim Rai, 1982). In spite of the continuing debate that Shyok –Nubra tectonic belt represented a Cretaceous palaeo-suture or was active during Tertiary (Borneman *et al*., 2015), the entire package of Late Cretaceous – Tertiary formations exposed in the Indus and Shyok valleys, on the south and north of Ladakh granitic batholith should be the target for concerted exploration efforts (Fig. 2 & 3).

More commonly an island arc forms on the overriding Hinterland (which is beyond Indian territory) with much greater metallogenic potential for Porphyry type deposits, as discovered in Tibet (China). The recent discoveries of Qulong/ Yulong and Jiama giant porphyry Cu-Mo (1430 Mt) and Cu-Mo-Ag (1054 Mt) deposits in Miocene Gangdese in Tibet have removed the earlier impression that the Himalayan belt was largely sterile (Sarkar and Gupta, 2012). It is opined that the aforesaid deposits are related to post-collisional magmatism. But unfortunately none of these discoveries are in the Indian segment of the Himalayan collision zone. However, syn- to post-collisional Tertiary granitic plutons are plenty in the Shyok –Nubra tectonic belt, besides young ophiolites (Srimal, 1982, 1990; Srimal *et al*., 1986, 1987; Upadhyay, R. 2009, Nathaniel L., 2015).

Although PGE and podiform chromite mineralization are reported from Indus-Tsangpo suture zone, the preliminary data are not very encouraging. Nevertheless, it is highly potential for ophiolitic Cyprus type Cu-deposit. The Trans-Himalayan tonalitic granitoids in the Ladakh belt are potential rocks for the discovery of Porphyry copper mineralization, but none has been discovered to date within Indian territory. It goes without

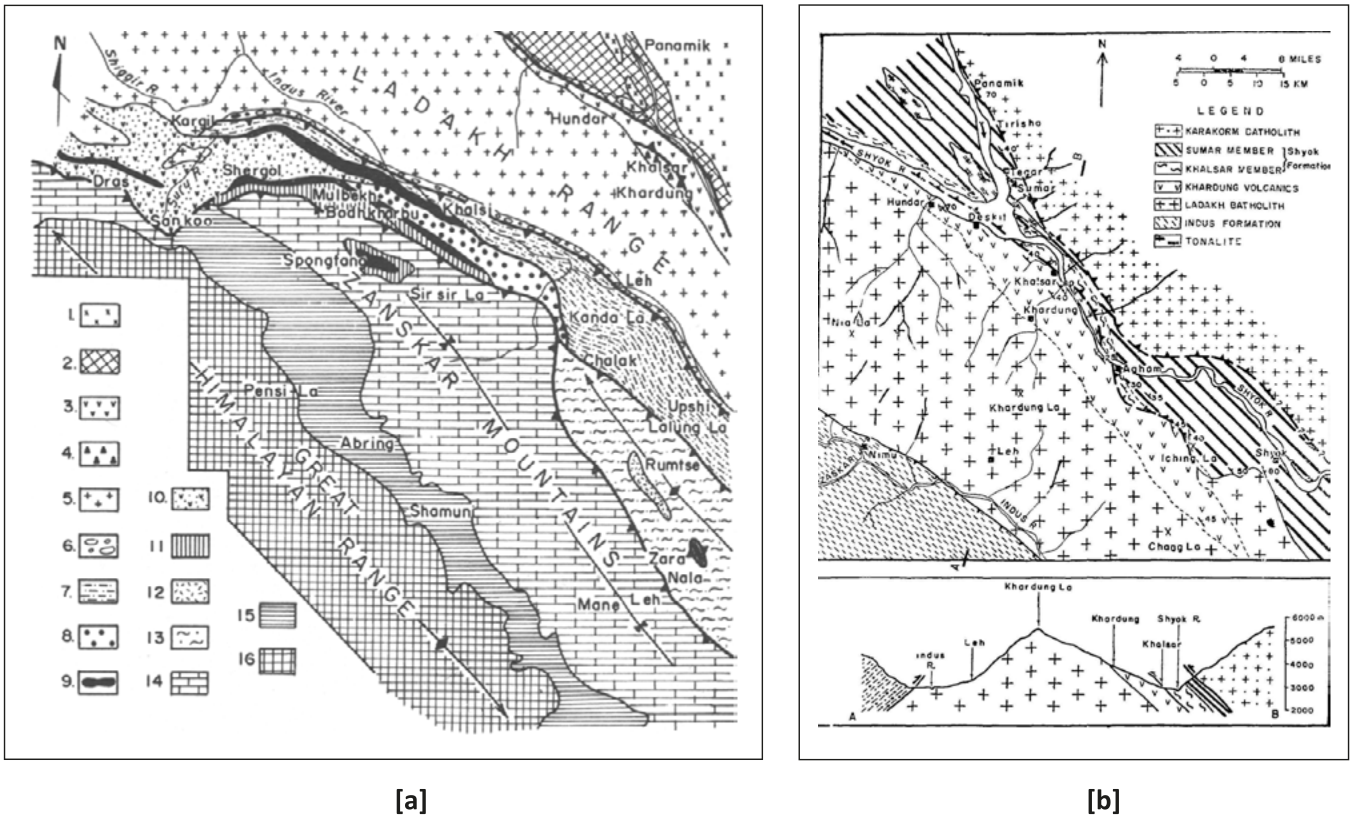

Fig. 2: (a) Geological map of Indus Suture Zone in Ladakh. Index. 1. Karakoram plutonic complex; 2. Shyok group. 3. Nubra group; 4. Khardung Formation; 5. Ladakh plutonic complex; 6. Kargil Formation; 7. Indus Formation; 8. Nindam Formation; 9. Shergol ophiolite mélange; 10. Dras Formation; 11. Lamayuru Formation; 12. Polokong granite; 13. Tso-Morari crystalline complex; 14. Mesozoics of Tethyan Himalaya; 15. Paleozoics of Tethyan Himalaya; 16. Zanskar crystallines of Higher Himalaya (after Thakur, 1990). **(b)** Geological map of southern (Indus suture zone) and northern flank (Shyok tectonite) of Ladakh Batholith and a cross section (Thakur *et al.*, 1981).

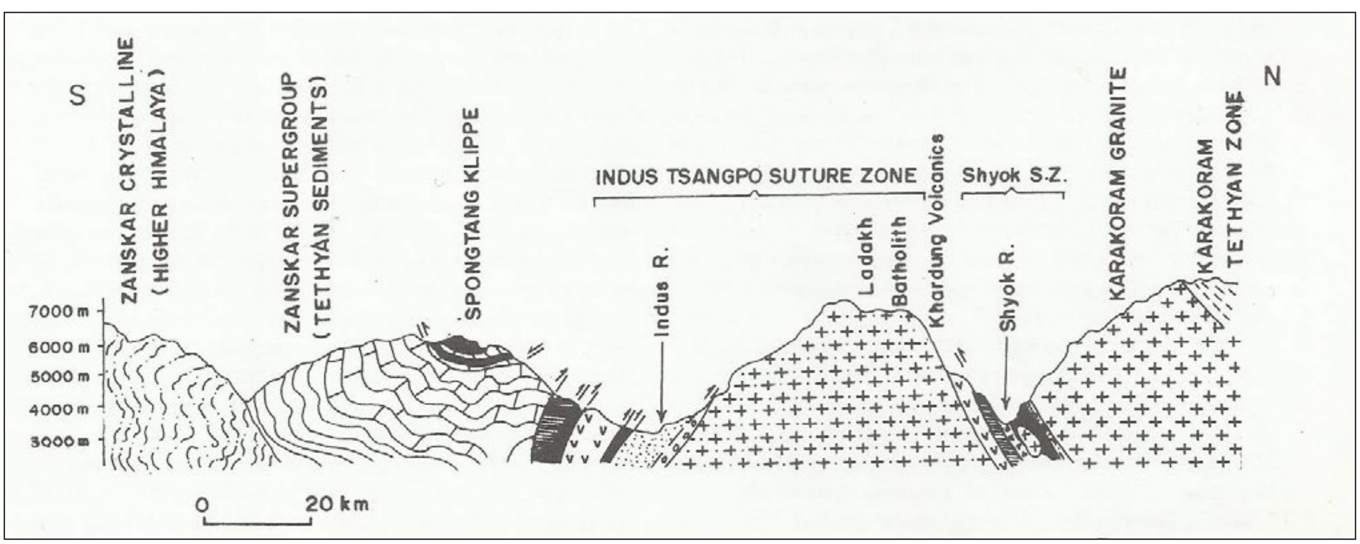

Fig. 3: Cross section across Zanskar crystallines & sediments – Indus-Tsangpo suture zone – Ladakh Granite – Shyok tectonic belt – Karakoram Granite (Sinha *et al*., 1999).

special mention that explorers will have a serious task ahead to attain a break through in this inaccessible high altitude terrain of Trans-Himalayan region in Ladakh.

Deccan Trap covered region

About 0.5 million square kilometres of west-central part of peninsular India is covered by the largely Mesozoic continental flood basalts known as Deccan Traps. The main spread of Deccan volcanics extends from the northern fringe of Karnataka, to large tracts of western and central Maharashtra, parts of Madhya Pradesh in north and Gujarat in the west. The maximum thickness of the flood basalt is about 3000 m in the Western Ghats of Maharashtra, petering down to a few hundred metres or even tens of meters in the fringe areas.

The original spread of this extensive Phanerozoic volcanic suite could be much larger than the present extent, as obvious from its scattered surface and sub-surface occurrences both on-land and in the off-shore regions around the peninsula. Coffin and Eldholm (1993) estimated the original spread of Deccan traps as 1.5 million sq km. It is quite apparent that the northern extension of Dharwar craton and the western continuity of Bastar craton, both being repository of many metalliferous deposits, are covered by the thick volcanic pile of Deccan Trap.

The continental flood basalt provinces like Deccan Trap are found across many continents which are formed by extremely large accumulation of extrusive volcanic rock formations, variously attributed to mantle plumes or/and plate tectonic processes. The formations just below the flood basalts have two major economic implications, viz. the trapped hydrocarbons and/or copper-nickel mineralisation in the sub-trap sedimentary formations.

Geophysical imaging of sub-basalt strata followed by drilling has resulted in discovery of immense hydrocarbon potential in many parts of the world. There are series of success stories of locating sizeable hydrocarbon resource below basal flows, such as North Atlantic volcanic province (NAVP) – 2003, Paleozoic off shore basin, Brazil viz. Amazon and Parana basins – 2000, Columbia River Basalt Group (CRB) in NW USA – 2007, and younger basins in south Atlantic. In India, the Directorate of Hydrocarbons (DGH), some oil companies and NGRI have conducted geophysical investigations (seismic tomography and other methods) aided by surface geochemical studies and limited drilling to locate favourable structures for oil & gas accumulation in the Mesozoic sediments underlying the Deccan Trap. Encouraging results were obtained in respect of favourable structures in sub-trap strata of Saurashtra and Kutch basins (2009-10).

A broad estimation of potential global reserve stands in the range of ~800 tcf gas and around ~ 30 billion barrels of oil below all the basalt covered basins of the world (Gupta, 2018).

Other than the mentioned efforts towards locating hydrocarbon traps below the Deccan Trap, this vast terrain remains almost entirely unexplored, so far as prognostication for metalliferous deposits is concerned. No effort was directed towards building up of database in regard to the possible existence of (i) mineral deposits in the basement, (ii) hydrothermal activities in the trap or (iii) in respect of probable sub-trap metallogeny related to the volcanism in this vast terrain. It does not need overemphasis to consider this region as an appropriate Greenfield for launching massive search for minerals.

There are three most crucial factors for the formation of large and super-large magmatic sulphide deposits in sub-trap formation, viz. i) large volume of mantle-derived mafic-ultramafic magmas, ii) fractional crystallization and crustal contamination, iii) Input of sulfur from crustal rocks, resulting in immiscibility between metal rich silicate magma and sulphur rich contaminated melt and segregation due to inefficient equilibration (Sarkar and Gupta, 2012). All magma plumbing systems are to be located near regional deep faults, through which the mantle-derived magma could move up. Besides the favourable location, the timing of magma separation and sulphide concentration is also important.

Other than the possibility of locating mineralized tracts in the Precambrian basement rocks, there are two broad possibilities of metallization within the Deccan volcanics, i.e. 1) magmatic sulphide and 2) hydrothermal mineralization. Situation similar to Noril'sk-Talnakh Ni-Cu sulphide deposits in Siberia, where ore accumulation has taken place at the interface of the continental basalt with the underlying Permo-Triassic sediments is a distinct possibility.

It is necessary for GSI to collaborate with DGH, NGRI and Oil Companies for identifying potential blocks for possible Ni-Cu sulphide concentration in lower Trap and sub-Trap strata and to launch dedicated exploration efforts by drawing state-of-the-art global expertise.

Bundelkhand granite-gneiss complex

It was observed that the Pearl Lake Porphyry, McIntyre Mine, Canada, "demonstrates not only porphyry copper deposits formed during early Precambrian time, but that the level of erosion has not been as great as to remove these deposits". This discovery opened up new avenues for the geologists to look for Porphyry-type deposits in the Precambrians, which till 1971 were considered almost by definition to be confined to Late Mesozoic-Tertiary rocks occurring in Island arc setting. Since then many more Precambrian Porphyry deposits from Australia, Finland, Canada, China, Sweden and many other countries have been added to the list. The Malanjkhand Cu-deposit in M.P., India was recognised as one of the largest of this type much later than its discovery (Sikka, 1989; Stein *et al*., 2004), though the uppermost stock-work zone seems absent according to the later researchers (Sarkar and Gupta, 2010).

Could the vast Bundelkhand granitoid complex host Porphyry sulphide or shear controlled hydrothermal mineralization remains a moot question of great relevance.

The general characteristics of the Precambrian Porphyry deposits are 1) association with calc alkaline/ alkaline magma in subduction zones, 2) typical presence of I-type syn-kinematic granitoids as host rocks, 3) association with high level porphyritic intrusives along faults and shears, 4) weak to strong hydrothermal alteration (kaolinite, sericite, propylitic, phyllic etc.), 5) development of enriched oxidation zones in some cases, and 6) mineralogical zoning of the ore body. At least three of the above criteria (1, 2 & 4) are satisfied by the Bundelkhand complex and age-wise also it matches with one of the global age clusters of Precambrian Porphyry deposits (2500-2800 Ma) including the Malanjkhand deposit (2500 Ma). Evidence of hydrothermal activity is spread over the entire terrain as prominent linear zones of clayey alteration comprising pyrophyllite, diaspore, sericite, chlorite and kaolin. There is also the evidence of oxidation in form of ferruginous zones within the granitoid complex. Occurrences of pyrite, chalcopyrite, galena and molybdenite are reported from a number of places, sometimes in close proximity of quartz reefs and zones with pyrophyllite-diaspore mineralization.

Three distinct granitoid suites in order of decreasing age have been identified within the Bundelkhand Granite-gneiss massif of Paleoproterozoic age – 1) Hornblende granitoids, 2) Biotite granitoids, 3) Leucogranitoids. These granitoids were emplaced in previously deformed basement consisting of gneisses, banded iron formations and other metasediments, mafic to felsic volcanics. These granites are of I-type with wide compositional range and indicate affinity with subduction related Island Arc type basaltic source. The southern part of the massif represents subduction related magmatism of an ocean similar to an Andean plate margin (Mondal and Zianuddin, 1996). Similar Subduction related tectono-magmatic evolution is also suggested for the Malanjkhand I-type granite, which hosts porphyry Cu-Mo deposit (Stein *et al*., 2004). As such, there is hardly any reason for ruling out the Bundelkhand granitoid complex as a prospective repository of porphyry-type sulphide mineralization.

So far, the mineral prospecting efforts in this region have been mainly directed towards assessing the mineralized

Noril'sk & Talnakh Group of deposits (Russia)

Examples include more than 20 intrusions occurring in three areas: Talnakh, Noril'sk and Imangda, along the Noril'sk-Kharaelakh fault, Siberian basalt region.

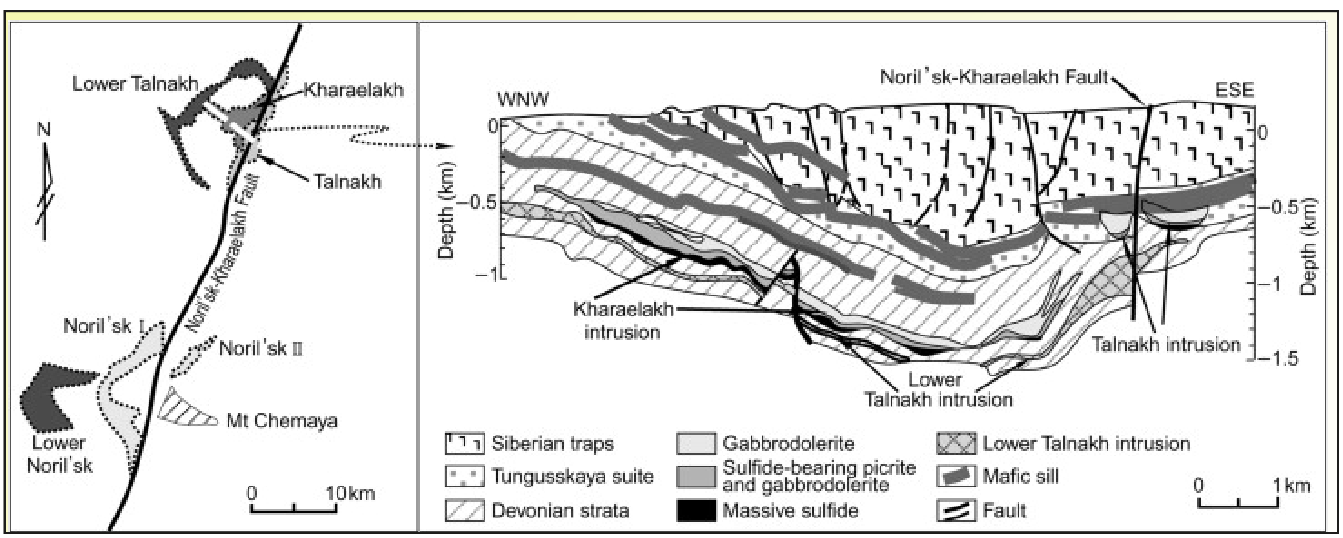

Combined Talnakh and Noril'sk ores reserves - 338.98 Mt @ 1.33% Ni, 2.26% Cu, 5.38 g/t Pd, 1.42 g/t Pt, 0.28 g/t Au, (data: dated 2000)

Fig. 4: Noril'sk-Talnakh giant Ni-Cu deposits, Russia. Latest reserve figures (2004) are 478.7 Mt ores, containing metal contents of 6.27 Mt of nickel, 9.37 Mt of copper, 62.2 Moz of palladium and 16 Moz of platinum.

Deeper search in Bundelkhand Granite-Gneiss massif

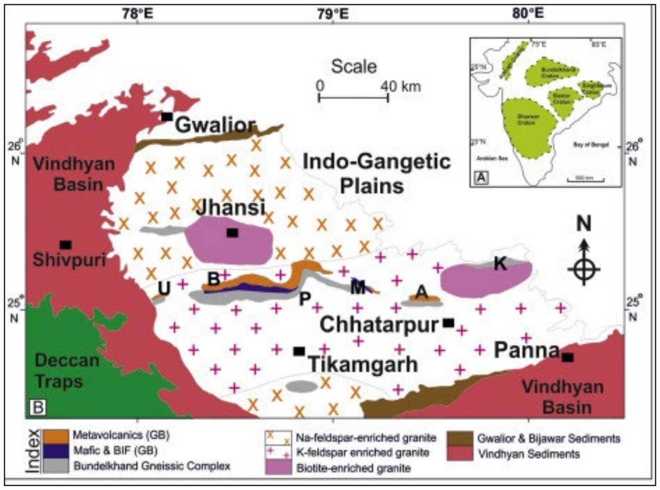

Bundelkhand Granite Complex (250 km x 200 km) shows many indicators for Precambrian Porphyry Cu-Mo deposit at depth.

Only known deposit of this type in India is at Malanjkand, MP .(221 Mt x 1,31 % Cu)

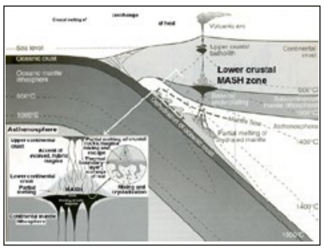

Porphyry Cu-deposit – genetic MASH diagram

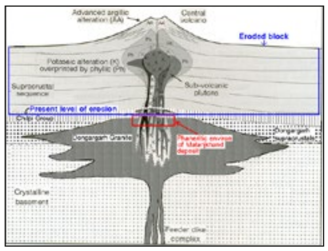

Malanjkhand model

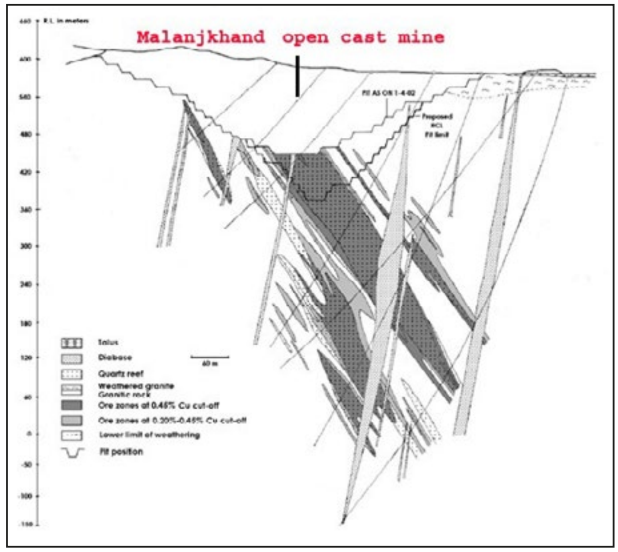

Cross section of Malanjkhand Cu-Mo deposit

Fig. 5: Regional map of Bundelkhand Granite-Gneiss massif, Genetic models of Porphyry deposits and cross section of Malanjkhand Cu-Mo deposit.

volcanisedimentary enclaves of older supracrustals and the sporadic vein quartz hosted mineralization within the granitoid complex by shallow probes. Concept oriented deeper probe should be a priority task in this region to locate concealed Porphyry type mineralization. GSI has recently contemplated launching of investigations for locating deep seated mineralization in Bundelkhand terrane (GSI, 2018). However, it would be necessary to pursue the objective with robust concept base and by applying globally available state-of-the-art multidisciplinary exploratory methods.

Acknowledgement

I am greatly thankful to Sri E.V.R. Parthasaradhi, Secretary, Krishnanunni Memorial Charitable Trust, for inviting me to contribute a paper in the proposed Special Volume of the Indian Journal of Geosciences, GSI, to be published in the memory of Late K. Krishnanunni, former Director General, GSI. I am also grateful to Sri P.C. Patra, DDG, Mission IIIB, GSI for accepting the paper for publication.

References

Borneman, N.L., Hodges, K.V., Van Soest, MUCH., Bohon, W. , Wartho, J.A., Cronk, S.S. and Ahmad, T., 2015: Age and structure of the Shyok suture in the Ladakh region of northwestern India: Implications for slip on the Karakoram fault system. *Tectonics,* **34 (10)**: *2011-2033.*

Coffin, M.F. and Eldholm, O., 1993: Scratching the surface: Estimating dimensions of large igneous provinces. *Geology*, **21(6)**: 515–518.

Deb M. and Sarkar S.C, 2017: Minerals and Allied Natural Resources and their Sustainable Development. Springer, 569 p.

Gupta, A., 2011: Contributed in Position Paper on Location and Development of Deep Seated Metalliferous Deposits in India. *Centre for Techno-Economic Mineral Policy Options* (*C-TEMPO), Ministry of Mines. 48 p.*

Gupta, A., 2018: Non-Renewable Solid Mineral Resources are heading for exhaustion within foreseeable future – a reality or myth: A critical appraisal of the present status and future perspective of the mineral resources in India. *Journal of Asiatic Society,* **LX(3)**: 39-66.

GSI, 2018: Programme for Enhancing Visibility, Activity and Quality (VAQ) of Geological Survey of India.

Hakim Rai, 1982: Geological evidence against the Shyok palaeo-suture, Ladakh Himalaya. *Nature*, **297**: *142–144.*

Hakim Rai, 1997: Geology of the Shyok Tectonic Zone in Eastern Ladakh, India. *Journal Geological Society of India***, 49**: *727-730.*

Mitchell, A.H.G and Garson M.S, 1981: Mineral deposits and global tectonics. Academic Press, London, 405 p.

Mondal, M.E.A. and Zainuddin S.M., 1996: Evolution of the Archean-Palaeoproterozoic Bundelkhand Massif, central India - evidence from granitoid geochemistry. *Terra Nova,* **8 (6)**: 532-539

Sarkar, S.C and Gupta A, 2012: Crustal Evolution and Metallogeny in India. Cambridge University Press, 850 p.

Sikka, D.B., 1989: Malanjkhand Proterozoic porphyry copper deposit, M.P., India. *Journal Geological Society of India*, **34(5)**: 487–504.

Sinha, A.K., Hakim Rai, Upadhyay, R., Chandra, R. 1999: Contribution to Geology of the eastern Karakoram. *In*: Himalaya and Tibet: Mountain Roots to Mountain Tops. Macfarlen A, Sorkhabi, R. B. and Quade, J. (eds). The *Geological Society of America, Special Paper,* **328**.

Srimal, N. 1986: India-Asia collision implications from the geology of the eastern Karakoram. *Geology,* **14(6)**: *523-27.*

Srimal, N., Bhandari, A.K. and Chakravarti, S.K. 1982: Island-arc volcanism in the Ladakh Himalaya. *Indian Journal of Earth Science,* **9(1)**: *44-58.*

Srimal. N., Basu, A.R. and Kyser, T.K. 1987: Tectonic inferences from oxygen isotopes in volcano-plutonic complexes of the India-Asia Collision zone, NW India. *Tectonics,* **6(3)**: *261-273.*

Srimal N. 1990: Evolution of Shyok Tectonic belt. *Extended Abstract, Group Discussions on Suture Zones – Yong and Old, Organised by WIHG and GSI, Dehradun.*

Stein, H.J., Hanna, J.L., Zimmerman, A., Markey, R.J., Sarkar, S.C. and Pal, A.B., 2004: A 2.5 Ga porphyry Cu–Mo–Au deposit at Malanjkhand, central India: implications for late Archean continental assembly. *Precambrian Research*, **134(3-4)**: 189–226.

Thakur, V.C, 1990: Indus-Tsangpo Suture Zone in Ladakh – Its Tectonostratigraphy and Tectonics *Proceedings of the Indian Academy of Sciences - Earth Planetary Sciences,* **99**: 169-185.

Thakur, V.C, Virdi, N. S, Hakim Rai, Gupta, K. R, 1981: A note on the geology of Nubra-Shyok area, Ladakh. *Journal Geological Society of India,* **22(1)**: 46-50.

Upadhyay, R., 2009: U–Pb zircon age for a granite intrusion within the Shyok suture zone, Saltoro Hills, northern Ladakh. *Current Science,* **97(8)**: 1234-1239.

Indian Journal of Geosciences, Volume 74, No. 3
July - September, 2020; pp. 223-239

Invited Paper

Seven Decades of Developments in Uranium Exploration Strategy and Emerging Concepts in Singhbhum Uranium Province, Jharkhand, India

D. K. Sinha

Atomic Minerals Directorate for Exploration and Research, Hyderabad-500 016
Email: director.amd@gov.in

Abstract: Sustained exploration by AMD over last seven decades has established five (05) generations of uranium metallogeny in India ranging from 2.8 Ga to recent and a total of forty-four (44) uranium deposits in different states of the country. The Singhbhum Shear Zone (SSZ) is the oldest known uranium province of the country and still is the largest production centre and a promising exploration domain.

Recent exploration efforts by AMD in SSZ are oriented to augment additional resources in the blocks adjacent to the established deposits and the existing mining centres in order to extend the lifespan of the mines. Reappraisal of the 35 km stretch between Jaduguda and Khejurdari in the South-Eastern part of SSZ, which hosts the major copper deposits with significant uranium mineralisation in some known sectors is being extensively worked by AMD. Conceptual model based exploration strategy has given encouraging results and has helped to identify new deposits.

The focused exploration efforts have resulted in significant enhancement of the uranium resources. The potentiality of the quartz pebble conglomerate (QPC) at the base of IOG and Dhanjori Group is being evaluated for U ± Au mineralisation in the western and central part of the shear zone. The recent path breaking discovery of a globally unique serpentinized peridotite hosted, polymetallic deposit (U–Cr–Ni–Mo–REE–Fe–Mg) in Kudada area, south of Turamdih mines has opened up huge avenues for the enhancement of strategic mineral resources and is helping to develop a new exploration model for uranium in the domain of SSZ. Integrated modelling of the geophysical, geological and subsurface exploration data has established the extent and trend of slip, lateral displacement and separation of blocks along the Tirukocha fault. The developed model has provided inputs for further planning of boreholes in Jaduguda Bhatin link area to augment additional unexplored resources. Subsurface exploration aided by geophysical data modelling has led to a new concept of Arkasani Granophyre related magmatic-hydrothermal uranium mineralization in the western part of SSZ.

With all these promising leads and proposed exploration inputs, SSZ continues to a potential domain for augmentation of uranium resources and centre for focused geological research by AMD.

Keywords: Singhbhum Shear Zone, Uranium, Exploration, Conceptual model, Polymetallic

Introduction

India is pursuing a comprehensive three-stage nuclear power programme to cater to the country's long term energy security, which demands an uninterrupted supply of atomic minerals. Following the vision and foresight of Dr. Homi J. Bhabha, Atomic Minerals Directorate for Exploration and Research (AMD), a constituent unit of Department of Atomic Energy (DAE) has reached great heights since its inception and has taken giant leaps to attain self-sufficiency in resources of atomic minerals for the nation's nuclear power programme.

Uranium exploration by AMD is primarily concerned with the knowledge of various processes of uranium mineralisation in a geological domain and with contemplating the possibilities of locating economically viable deposits in a particular domain. Exploration is primarily focused on delineation of the anomalies with regard to the geochemical and the geophysical properties as a result of mineralising processes. Sustained exploration by AMD over last seven decades (1949-2010) has established a total of 44 uranium deposits in different states of the country *(Sinha, 2020)*. Survey and exploration for Uranium in India was initiated in 1949 in the Singhbhum

Thrust belt (now referred to as Singhbhum Shear Zone-SSZ) of eastern India *(Vasudeva, 1965)*. Over the last seven decades, exploration efforts by the Directorate has established 17 uranium deposits spread over different sectors of this ~120 km linear belt of intense deep tectonism, which is also a renowned store house of other associated polymetallic mineral (Cu, U, Mo, Ni, Te etc.) resources *(Sarkar, 1982, 2000; Banerji, 1981; Rao and Rao, 1983a; Pal, et al., 2009, 2011)*. The Uranium Corporation of India Ltd. (UCIL) under the DAE carries out mining and milling of uranium from Jaduguda, Bhatin, Narwapahar, Turamdih, Bagjata, Mohuldih (all underground mines), and Banduhurang (opencast mine) uranium deposits in SSZ *(Gupta and Sarangi, 2011)*.

Recent exploration efforts by AMD have paved the way for identification of additional resources in SSZ in the blocks adjacent to the existing mining centres, thereby extending the lifespan of the mines. Conceptual modelling based exploration strategy has also given encouraging results and has helped to identify new potential zones. Some recent discoveries have helped to reorient the exploration programme to enhance the resource base of the SSZ significantly. The present paper describes some of these results and the plan for future exploration by the Directorate.

Historical Perspective

The first surveys for uranium were started in 1949 in Singhbhum region of eastern India by a joint team of geologists from the Atomic Energy Commission, Geological Survey of India and Damodar Valley Corporation under the leadership of Khedkar from GSI *(Rama Rao, 2013)*. The assignments included geological mapping and radiometric checking with Geiger Muller counters of the entire Singhbhum Thrust Belt over ~120 km with a width about 2 to 5 km. The Singhbhum region was the obvious first preference since torbernite and autunite were reported here in 1919 and documented in the records of the Asiatic Society of Bengal *(Fermor, 1919)*. Some 57 uranium anomalies were discovered by this team *(Khedkar, 1951; Krishnamurthy, 2006)*. The location of the uranium anomalies were subsequently followed up with exploratory drilling which commenced in December 1951 by contracting the services of M/s. Associated Drilling & Supply Company, London at Jaduguda and at Kanyaluka with four (04) Calyx drill boreholes. Subsequently, IBM joined the drilling programme in December 1953 at Jaduguda *(Vasudeva, 1965)*. Core drilling by Raw Material Division (RMD, now AMD) commenced in 1955 with L&T rigs that were procured through the Tatas. By 1963, ~70 km long stretch had been drilled in 33 different anomalous uranium-bearing localities. Major part of the drilling (~75%) was concentrated in four major prospects namely Jaduguda, Bhatin, Narwapahar and Keruadungri *(Bhola, 1965; Bhola, et al., 1966)*. RMD was later renamed as Atomic Minerals Division in 1958 and rechristened as Atomic Minerals Directorate for Exploration and Research (AMD) in 1998. Subsequent exploration efforts by AMD have brought out several uraniferous occurrences and a total of fourteen (14) low to medium grade mineable uranium deposits along the SSZ. The copper rich belt along Rakha – Surda - Mosabani – Badia tract in the eastern part of SSZ was also explored intensively and it was observed that, uranium and copper lodes coincide at Surda-Pathargarah while the other sectors of the copper belt are characterised by development of separate uranium and copper lodes *(Sharma, 1969)*. In Roam – Sideshwar area, indiscernible coexistence of uranium and copper lodes was reported by mapping of underground mine development *(Krishnanunni, 1964)*.

The uranium mining and production in India had an exciting beginning with the formation of Uranium Corporation of India Ltd. (UCIL) in 1967 under the DAE. The corporation launched its operation with the commissioning of an underground mine and an ore processing plant at Jaduguda in 1968. Subsequently, underground mining at Bhatin, Narwapahar, Bagjata, Turamdih (with a processing plant), Mohuldih and open cast mine at Bandhuhurang were commissioned between 1987 to 2012. Singhbhum went on to be the only uranium mining production centre till another underground mine and processing plant was commissioned in 2012 to mine the globally unique and country's largest stratabound dolostone hosted uranium mineralisation at Tummallapalle, Kadapa district Andhra Pradesh *(Gupta and Sarangi, 2011; Sinha and Verma, 2018)*.

Uranium exploration in India: present status

Sustained efforts by AMD over last seven (07) decades have established five (05) generations of uranium metallogeny in India, which are closely related to the crustal and atmospheric evolution. Between 2.8 – 2.2 Ga, paleoplacer type mineralisation involving mechanically concentrated uraninites, occurs in basal pyritiferous quartz pebble conglomerates of the greenstone belts in Dharwar, Singhbhum and Aravalli Cratons *(Mahadevan, 1988a; Pandit, 2002)*. Post 2.2 Ga, the Great Oxygenation Event led to the release of a copious amount of oxidised uranium into geochemical system. The period between 0.8-2.2 Ga, greatly favoured the source-mobilisation-precipitation trinity essential to form different types of uranium deposits. Syn-diagenetic uranium concentration is recorded in dolostone of Vempalle Formation in south western part of Cuddapah Basin *(Sinha and Babu, 1986; Sundaram, et al., 1989)*. AMD has already established a large tonnage stratabound carbonate hosted uranium deposit at Tummalapalle and in adjacent areas, Kadapa district. Further exploration by AMD and proposed exploitation through mine developments by Uranium Corporation of India Ltd. (UCIL) is in advanced stages. In northern part of the Cuddapah Basin, soluble uranium got concentrated along the unconformity between the basement granitoids and overlying Srisailam Formation and Kurnool Group to form fracture controlled, epigenetic unconformity type deposits *(Sinha et al., 1995; Jeyagopal, 1996)*. Exploration by AMD has established four (04) sizable unconformity-proximal, fracture controlled uranium deposits in north eastern part of the Cuddapah Basin at Lambapur, Peddagattu and Chitrial in Telangana and Koppunuru in Andhra Pradesh *(Sinha, 2020)*.

Polyphase re-mobilisation, metasomatism and magmatic/ metamorphic fluid activity has also led to the formation of several hydrothermal, vein-type, epigenetic deposits along favourable structural locales in the Singhbhum Shear Zone (SSZ), Kotri - Dongargarh Belt (KDB) in central India, albitite line of North Delhi Fold belt (NDFB) in Aravalli Craton *(Saraswat, 1988)* and Gogi-Kanchankayi in Bhima basin *(Pandit et al., 2002, Roy et al., 2016)*. In western India, two (02) low grade, medium tonnage deposits near Rohil and Jahaz, Rajasthan have been established in the NDFB of Aravalli craton *(Yadav, 2002)*. Several small and isolated hydrothermal, vein-type uranium deposits have been established in varied geological terrains of India viz., Bodal-Bhandaritola, Jajawal, Dumath- Dhabi in Kotri-Dongargarh Belt *(Sen, 1977; Saxena et al., 1998)*, Naktu in Chottanagpur Granite Gneiss Complex *(Bhattacharya, et al., 1992; Mahendra Kumar, et al., 1998)*, Umra in Aravalli Fold Belt *(Kaul, et al., 1991a)* and Kasha-Kaladi in higher Himalayan crystalline belt *(Kaul, et al., 1991b)*.

The Cretaceous period during 0.65 Ga witnessed the formation of tabular sandstone-type uranium deposits in the Mahadek Basin in the NE part of India, where the uranium released from fertile Neoproterozoic granites got concentrated as tabular lodes in carbonaceous matter impregnated sandstones *(Saraswat, et al., 1977, Sengupta, 1991)*. Exploration in parts of Meghalaya has established several low to medium tonnage Cretaceous sandstone-type uranium deposits *(Sen, et al., 2002)*.

During 0.011-0.6 Ga, appreciable uranium concentration was generated along the contact of Middle and Upper Siwalik Group *(Swarnakar, 2002)*. The last generation of uranium mobilisation process and concentration (post 0.011 Ga) is observed in the Quaternary calcrete / playa deposits of Western Rajasthan *(Misra, et al., 2011; Rao, et al., 2015)*. A total of 44 uranium deposits located in different parts of the country (Fig. 1) have been established till date by AMD *(Sinha, et al., 2020)*.

Developments in exploration strategy for Singhbhum Uranium Province

Geological Setting

The eastern Indian shield comprises of the Chhotanagpur Granite-Gneiss Complex (CGGC) in the north, the Singhbhum Archean Craton in the south and the E-W trending Proterozoic North Singhbhum Mobile Belt between the two. The Singhbhum Craton is roughly a triangular shaped region, bounded by the arcuate shaped Singhbhum Shear Zone (SSZ) on the north, the Sukinda Thrust on the south, and Tertiary sediments of the Bengal Basin to the east. The SSZ is a 200 km long arcuate belt of high strain characterized by multi-phase deformation, intense ductile shearing, multiple metasomatic features including imprints of sodic metasomatism and polymetallic mineralisation *(Dunn and Dey, 1942; Mahadevan, 2002)*. Existing geochronological and isotopic (whole rock and mineral) data generated for over three decades from different parts of the Singhbhum Craton (SC) suggests that the crustal growth of the craton extended over a protracted period of ~1.5 Ga from Hadean (>4 Ga) to the end of Neoarchean (2.5 Ga) *(Chaudhuri, 2020 and references therein)*.

The oldest rocks exposed in the craton include Older Metamorphic Group (OMG), Older Metamorphic and Tonalite Gneiss (OMTG), unclassified mafic-ultramafic rocks occurring as enclaves within Singhbhum Granitoids, Banded Iron Formation (BIF) of Badampahar – Gorumahisani Belt, acid volcanics and ultramafic dykes which have suffered the SSZ related deformation especially along the arcuate belt (Fig. 2). The Archean basements are overlain by Quartz-Pebble-Conglomerate (QPC), occurring at the base of Iron Ore Group (IOG) and also Dhanjori Group *(Mukhopadhyay, 2001)*. The IOG comprises of conglomerate, phyllites-shale-wacke, quartzite, Banded Magnetite Quartzite (BMQ), ultramafics, acid volcanics, tuffaceous units, grits, etc. The Dhanjori Group comprises of volcano-sedimentary sequence containing quartzite-conglomerate, mafic-ultramafic flows and intrusives with tholeiitic (pillowed) basalt interlayered with tuffs (2.1 Ga) overlying the IOG. The rocks of Dhanjori Group are overlain by Singhbhum Group which comprises quartzite-conglomerate (oligomictic and polymictic), feldspathic schist, granite mylonite, sericite-quartz-schist, chlorite-quartz-schist (and their mineralogical variants), metabasic sills, mica schists and quartzites. The lower part of the Singhbhum Group comprising the Chaibasa Formation represents a metasedimetary package in which non-diastrophic structures are preserved despite many deformational episodes. The upper part of the Singhbhum Group constitutes the Dhalbhum

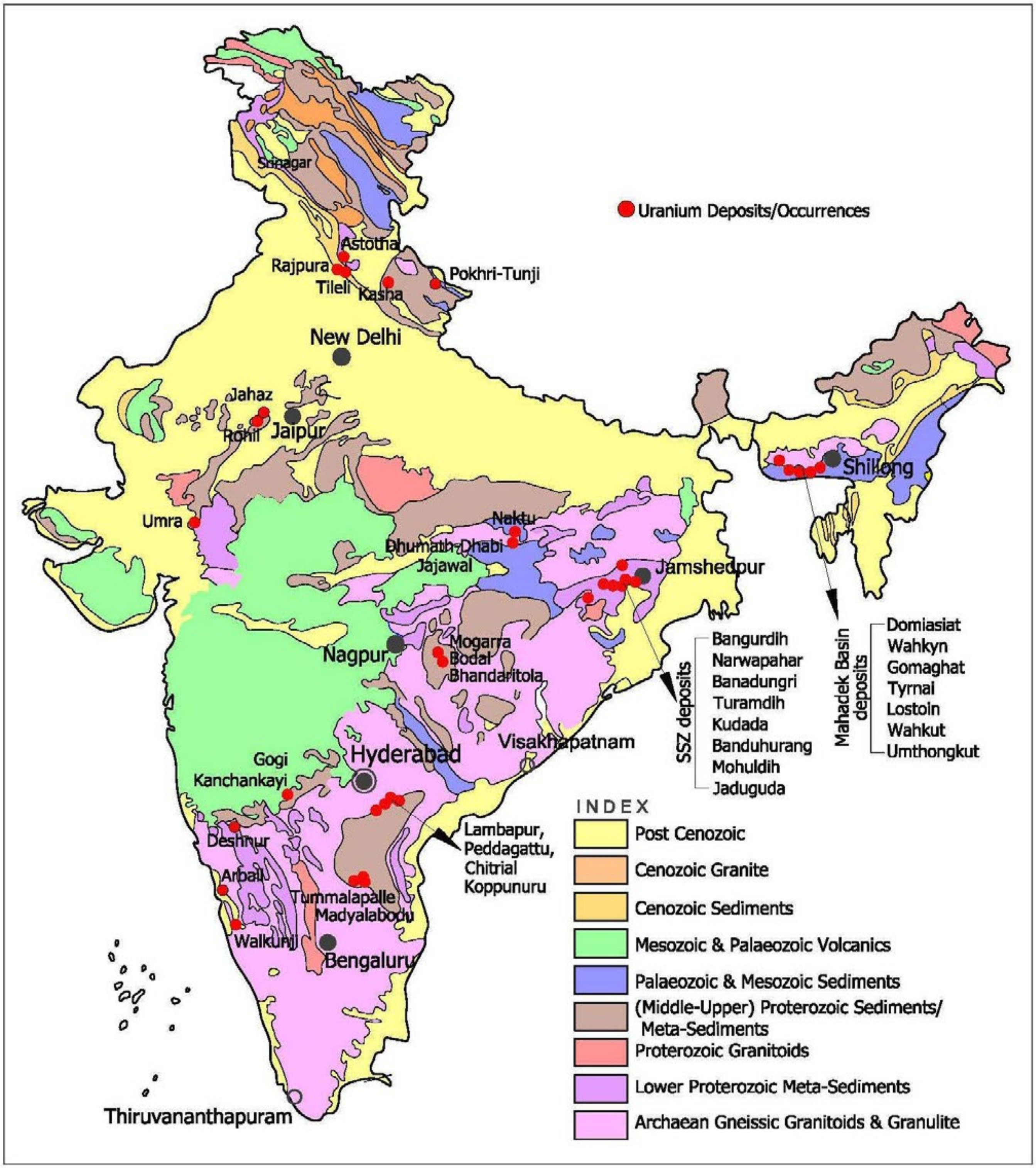

Fig. 1: Uranium deposits in India.

Formation comprising phyllites and ortho-quartzites which have been interpreted as a meandering channel system *(Mahadevan, 2002; Mazumdar, et al., 2012)*. Apart from the extensive Singhbhum Granite of three different phases, several younger isolated granitic bodies are also exposed along the SSZ, such as Chakradharpur Granite (CKPG), Arkasani Granophyre (AG) and Soda Granite (SG) (now seen as feldspathic schists). Several younger mafic and ultramafic bodies have been emplaced all along the shear zone. These bodies vary in age, and therefore, show repeated tapping of the mantle during the process of shearing or even in post-shearing period. The shear zone rocks have been affected by progressive as well as retrogressive metamorphism. The early prograde metamorphic (M1) event culminated at 480 ± 40°C, 6.4±0.4 kbar in epidote-amphibolite facies which led to the formation of garnet and chloritoid porphyroblasts in the pelitic schists. The second metamorphic event (M2) caused retrogression of the M1 assemblages by infiltration of boron– rich fluid from a deep–seated magma *(Sengupta, et al., 2005)*.

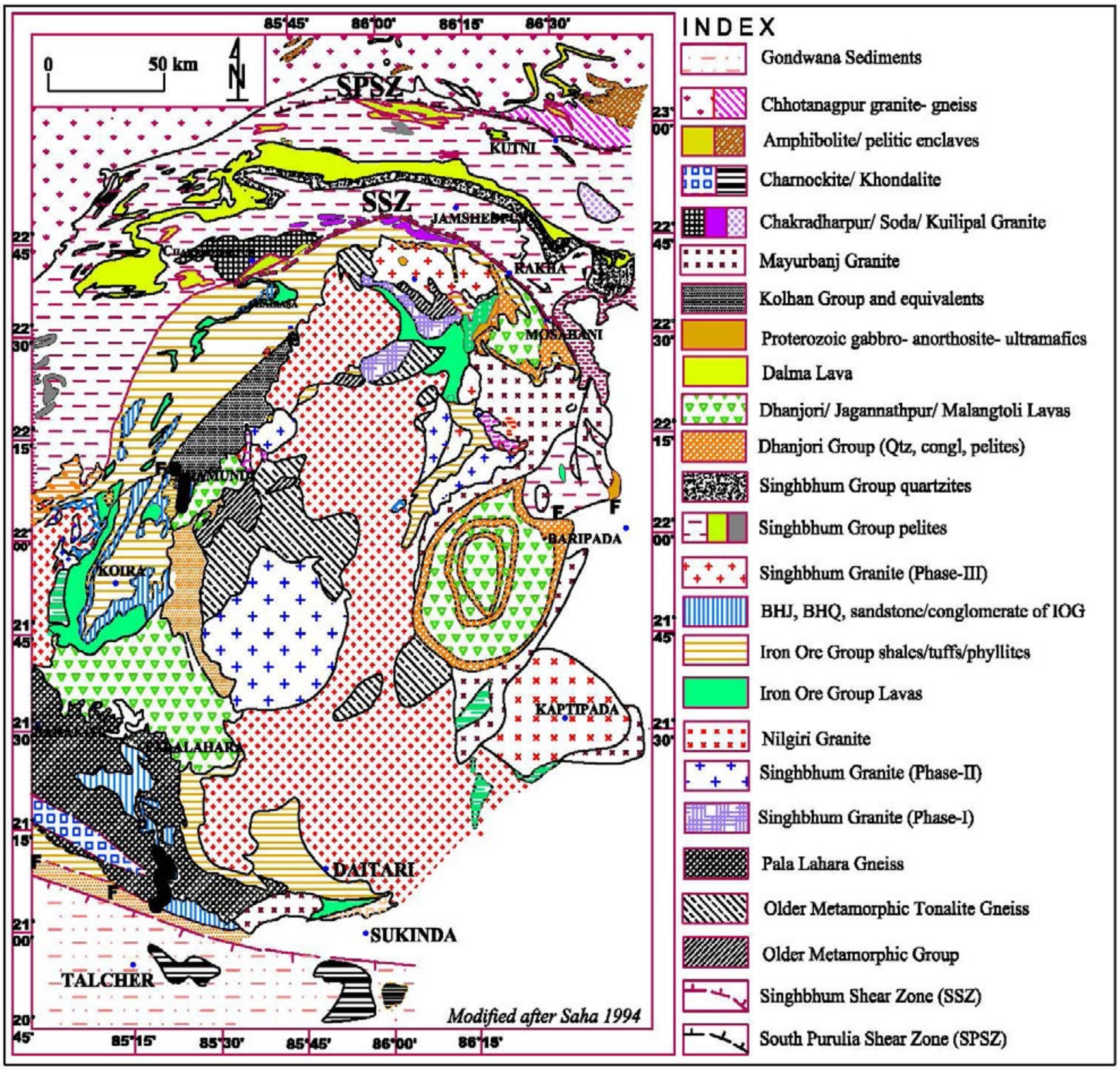

Fig. 2: Regional geologiocal map of Singhbhum-Odisha craton (modified after *Saha, 1994*)

Structural deformation in SSZ is in general, attributed to repeated folding, mylonitisation, and rotation of pre-existing structures along the NE to SW trending tectonic transport direction in an environment of prolonged progressive deformation *(Mukhopadhyay and Deb, 1995; Gupta and Basu, 2000; Matin, et al., 2012)*. Compression and progressive ductile shearing resulted in initial south-vergent isoclinal folds (F1) with NW–SE/E–W fold axes, development of pervasive mylonitic foliation that dips steeply to the NE/N, and formation of down-dip mineral lineation. Open, sub-horizontal asymmetric folds (F2), parallel to the SSZ, with shorter southern and longer northern limbs mark the waning stage of this southward crustal movement. A third generation of less intense, locally developed gentle upright folds (F3), transverse to the shear-zone trend, occur either as fine crenulations or locally mappable warps *(Ghosh and Sengupta, 1990)*. Mylonites are commonly present in almost all rock types that are involved in shearing. These can be classified as L-S type tectonites *(Sarkar, 1985)*. Following the ductile deformation, the rocks in the SSZ underwent brittle deformation, which is expressed as extensional brittle fractures parallel as well as normal to the shear zone, presumably at shallower crustal levels *(Srivastava and Pradhan, 1995)*.

Nature of mineralisation

The uranium mineralization is confined to the arcuate SSZ from Duarpuram in the west to Baharagora in the southeast (Fig. 3). Uranium proto-ore was probably supplied from the Archaean lithologies and got concentrated in the overlying QPC, occurring at the base of Iron Ore Group (IOG) and also in Dhanjori Group. The arcuate shape is possibly due to the fact that Singhbhum Craton acted as buttress against stresses from NNE direction. The resultant structure is an anticlinorium of isoclinally folded rocks dipping consistently north and marked by a prominent shear zone with crushed and mylonitised rocks *(Bhola, 1965)*. This has provided an ideal situation for mineralizing fluids to form shear controlled hydrothermally generated metamorphite type of deposits in addition to the proto-ore and QPC environment. The metamorphite deposits occur as disseminations, impregnations and veins along the shear planes within or affecting metamorphic rocks of various ages. The uranium and copper deposits in different sectors of SSZ are highly variable in size, resource and grade. The uranium mineralization, in particular are hosted by the chlorite-quartz schist, biotite-chlorite-quartz schist, feldspathic schist, quartzites and conglomerates of Singhbhum Group with minor amount of magnetite, apatite and tourmaline *(Rao and Rao, 1983a)*.

Based on the spatial relationship and association of uranium and copper mineralisation in SSZ, three (03) broad zones have been identified *(Sharma, 1969).* The Central zone comprising the Surda-Pathargarah area show sympathetic distribution of uranium and copper mineralisation where the U- Cu lodes coincide with each other. The intermediate zone extending to SE (Mosaboni - Badia area) and to the NW (Tamapahar, Rakha and Roam- Sidheswar) side of the central zone is characterised by the development of individual uranium lode, although the uranium and copper lodes coincide at places *(Krishnanunni, 1964).* The Outer zone flanks the intermediate zone along SSZ, extending from Jaduguda–Narwapahar-Keruadungri towards the NW and Kanyaluka-Bhalki towards SE. In the outer zone, copper lodes occur either to the hangwall or to the footwall side of uranium lode.

The uranium deposits of the Central Sector of SSZ (Nimdih, Rajdah, Narwapahar, Banadungri and Mohuldih) are peneconcordant, gradational strata bound and hosted in relatively lower metamorphic grade of rocks, except in Turamdih group of deposit where the superposition of the deformational events have accounted for repetition of mineralized lodes, apparent gaps in mineralization between blocks and has also contributed to bringing the lodes to shallower level in Turamdih south and Nandup block *(Mohanty and Verma, 1989; Pandey, et al., 1994).* The deposits of eastern sector (Jaduguda, Bhatin, Bagjata and Kanyaluka) are discordant and vein-like associated with host rocks of relatively higher grade of metamorphism. Uranium mineralization is confined to Chaibasa-Dhanjori interface depending upon the intensity of shear. In most of the cases mineralization is bottomed at the lowest unit of Chaibasa Group or the upper part of Dhanjori metasediments. Quartz-sericite to sericite-quartz schists have been considered as the marker for bottom of uranium mineralization *(Pandey, et al., 1994)*. The uranium mineralization in SSZ is present in sheared low grade metamorphic rocks, viz., quartz-chlorite schist or quartz-biotite schist. However, it is absent in hornblende – (or actinolite) schist. This feature indicates that favourable rocks for U-mineralization are of green schist facies rather than epidote-amphibolite facies or rocks of ultrabasic (actinolite schist) composition *(Dhanaraju, et al., 1988)*. Uranium mineralization is represented by uraninite, minor pitchblende, brannerite, U-Ti complex, refractory uranium bearing minerals (viz. allanite, sphene, davidite, xenotime and rare monazite) and uraniferous iron oxides which occur in many instances in association with sulphide mineralization of chalcopyrite, minor bornite, chalcocite, covellite and molybdenite and oxides like magnetite, ilmenite, titano-magnetite, etc. *(Rao and Rao, 1983a)*. The mineralogy is complex and the chemistry of the ores, particularly U and Cu, is greatly influenced by the host rock involved in shearing. Shear zone transgressing to Dhanjori Group (Jublatola) is rich in U, Cu, Ni, Mo [(±) Bi, Au, Ag, Te & Se], whereas in schists and quartzite of Chaibasa Formation it is poor in above metals.

Ore genesis

Unfolding the genetic aspects of polymetallic mineralisation in SSZ is ever challenging because of polyphase volcanism,

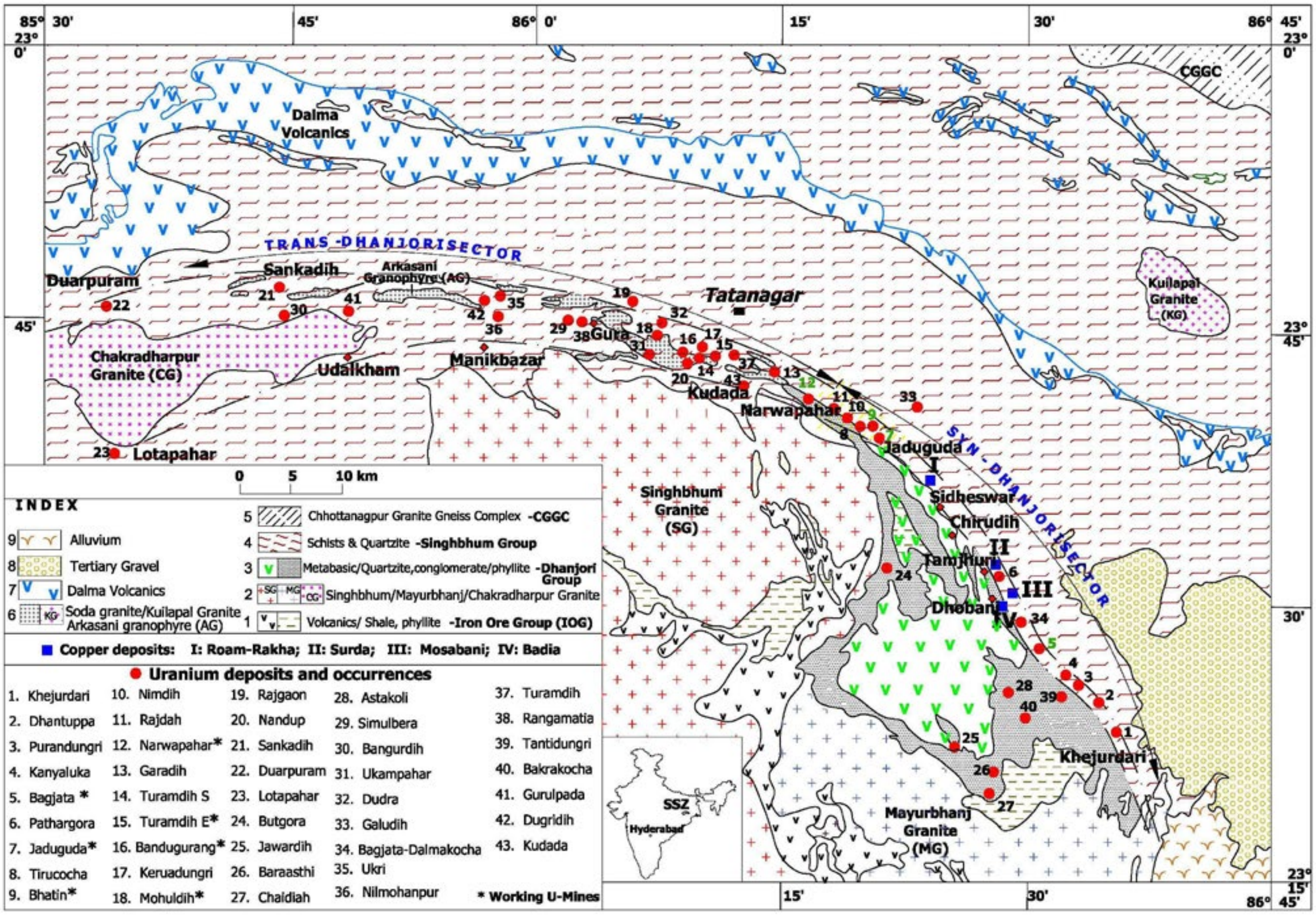

Fig. 3: Geological map of Singhbhum Shear Zone (SSZ) showing the uranium deposits/occurrences and copper mines.

metasomatism, overprinted structural deformations and intense shearing has been addressed by many authors *(Banerji, 1962, 1981; Sarkar, 1982; Sinha, et al. 1990)*. Various modes of occurrence for uranium mineralization have been reported from SSZ. Titanium oxide-uranium oxide grain aggregates found in Jaduguda-Bhatin deposits are related to QPC-type of environment where primary and secondary brannerite have also been reported *(Rao and Rao, 1983b)*. Three generations of uraninite have been seen in SSZ in which the last phase is post-sulphide mineralization. The refractory uranium bearing minerals (allanite, xenotime, monazite, sphene, etc) and uranium associated with apatite-magnetite veins are the product of pneumatolytic – hydrothermal metasomatism probably related to younger granitic phases referred earlier (AG and SG). The uraninite associated with feldspathic schist (~SG) in Narwapahar-Turamdih sector has been correlated with metasomatic feldspathization process and subsequent remobilization to form ore bodies. On the basis of various observations, it was proposed that geochemical source of U was Singhbhum Granitoid, whereas the basic rocks of Dhanjori Group provided Cu, Ni and Mo for the formation of U-Cu deposits of SSZ *(Rao and Rao, 1983c)*. Uranium was probably enriched in Singhbhum Granite by partial melting of the upper mantle/ lower crust around 2900-3000 Ma and continued till 1900Ma (Mayurbhanj and Nilgiri Granitoid) to 1420 Ma (SG) *(Mahadevan, 1988b)*. This is also corroborated by the fact that the age of initial uraninite mineralisation in the SSZ obtained from the concordia plot of the lead isotopic ratios of uraninites is 1600 Ma while the feldspathic schists of Narwapahar is 1580 Ma. Uraninite from Bhatin, Rakha and Surda gave Pb-Pb age of 1478 ±14 Ma *(Rao, et al., 1979).* Recently, AMD has dated uraninite from Kudada deposit (1798 ±14 Ma, Sm-Nd) and Banadungri deposit (1686 ±180 Ma, Sm-Nd; 1616±54 Ma, U-Pb), which are close to the above age brackets.

QPCs at the base of IOG and Dhanjori Group show evidence of detrital accumulation of uranium bearing minerals. These U-concentrations along with host rocks got folded into a major synclinal sequence prior to involvement in shearing episodes. Shearing episodes have further remobilized and reconstituted the uranium mineralization concomitant with the early folding events. The localization of U-Cu lodes with predominant platy minerals, particularly chlorite, is controlled by the deformation and metamorphism of Chaibasa and Dhanjori rocks simultaneously. The younger granites namely CKPG, AG and SG along with younger basic units, formed by the partial melting of lower crust – upper mantle interface generated geothermal gradient *(Mahadevan, 1988b)*. Mantle metasomatism or crustal contamination of upheaving melts cannot be ruled out in such cases, which could have generated diverse type of uranium mineralization hitherto not known. The chemical and structural characteristics of various uraninites differ from east to west and from north to south i.e. along and across the strike of the SSZ. The uraninite composition varies from $UO_{2.31}$ to $UO_{2.44}$ and cell dimension from 5.42 Å to 5.45 Å *(Rao and Rao, 1983a)*. Recent data generated by AMD show compositional values of $UO_{2.00}$ to $UO_{2.29}$ and cell dimension from 5.43 Å to 5.47 Å in accordance with previous observations. Larger cell dimension has been found in eastern and western part of the SSZ while it is comparatively smaller in Central Sector (Jaduguda).

Tracing the spatial disposition of the ubiquitous metapelites and metabasics emplaced within the sheared metasediments of SSZ through geological mapping, correlation in borehole sections and integrated petromineralogical-geochemical-mineral chemistry-thermobarometric studies have provided insight to understanding their emplacement history. These metabasics have been characterised as amphibolites (edenite and pargasite) metamorphosed from dolerite/gabbro suite with metamorphic temperature of ~650°C and pressure around 7kbar corresponding to a depth of 24-27 km. These rocks show syn-shearing characteristics and are pre-mineralisation indicating precursor to hydrothermal processes. The mode of occurrence of amphibolites with uranium lodes implies that while the original mafic rock was undergoing transformation to amphibolites, the overthrusting in SSZ was at its peak and probably the original mafic emplacement must be during the early onset of deformation/shearing. The high temperature conditions in this process definitely might have generated sufficient hydrotherms which could have played a role in remobilisation of uranium mineralisation.

Present focus and Emerging new concepts

Conceptual modelling based exploration, integrating available heliborne geophysical, geochemical and geological data generated over the period of seven decades is the present strategy which is the focus of all new concepts. Such strategy is targeted to identify new potential zones within the Singhbhum Uranium Province (SUP). Certain exploration domains in the SUP have led to major breakthrough.

QPC Related U-Mineralisation

QPCs at the base of the IOG and the Dhanjori Group show evidence of detrital accumulation of uranium bearing minerals as already stated. However, the potentiality of QPC as a paying horizon for U ± Au is yet to be established in Singhbhum Province. Recent attempt has provided insight to QPC-related horizons and their continuity in lenses in the western part of the SSZ in Gura area, Saraikela-Rajkharswan district. Reconnoitory drilling has resulted in the identification of subsurface conglomerate bands with U-Th mixed anomalies at a shallower level while uraniferous bands are found at deeper level (250-300m depth). Repeated nature of Th, U+Th and U-enriched bands at Gura and the occurrence of intermittent yet significant QPC horizon over a considerable stretch of 35 km along Udalkham-Manikbazar-Simulbera sector has strengthened the concept of exploration for QPC type of mineralization (Fig. 4). Magnetite is predominant in these conglomerates and hematite is absent. Similarly, deformed uraniferous conglomerate of Jaduguda occurring above the Dhanjori meta-basic/ basalt and its probable western continuity at Nimdih is also being probed. Moreover, consideration of its QPC nature is doubtful though looked up as a potential host rock.

Further west of Nimdih, to the SW of Narwapahar, a 2.8 km long potential uraniferous zone between Chirugora and Kudada village has been delineated based on the inputs from recent heliborne geophysical survey. The follow up ground surveys have delineated encouraging uraniferous anomaly in quartzite of Singhbhum Group at Chirugora close to the unconformity between the psammopelitic sediments of Singhbhum Group and the basement comprising Singhbhum Granite/diorite and ultramafic suites. The unconformity is marked by a NW–SE trending, intermittently exposed stretched pebble conglomerate (20- 35m) extending over 2 km in strike from Lailam to further eastward to Damudih area behind Narwapahar hill. Further eastern continuity of the conglomerate is not traceable beyond Narwapahar. The unconformity contact between the Singhbhum granitoids and the overlying Singhbhum Group of rocks to the south of Chirugora is a prime target for drilling as a potential uranium horizon. Subsurface exploration in this area is suspended due to logistics.

Serpentinised Peridotite hosted polymetallic mineralization

A path breaking discovery of a globally unique serpentinized peridotite host for uranium deposit with polymetallic affinity (U–Cr–Ni–Mo–REE–Fe–Mg) in Kudada area, south of Turamdih mines (Fig. 5) has opened up huge avenues for enhancement of indigenous strategic mineral resources of India *(Sinha and Verma, 2018; Sinha, et al., 2019)*. Globally, there is no known report of uranium deposit in such ultramafic host rock.

The discovery is accidental where the recent phase of exploration was initiated with the background to probe the base of the IOG through the Singhbhum Group, for

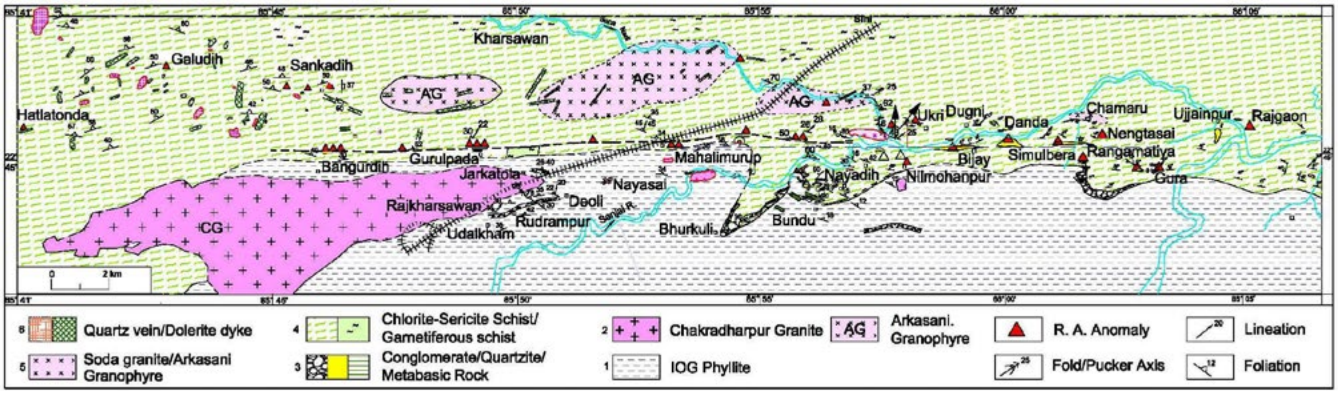

Fig. 4: Geological map of western part of SSZ showing uranium potential areas around Gura- Udalkham area, Saraikela-Rajkharswan district, Jharkhand.

QPC type of uranium mineralization at a depth of more than 500 m. The boreholes have intercepted serpentinized peridotite with polymetallic (U–Cr–Ni–Mo–REE–Fe–Mg) nature intruded into the phyllites of IOG. Exploratory drilling has so far established nearly 1 km dip continuity of 300m thick mineralised host rock with multiple uranium ore lodes at deeper levels (up to 650 m) compared to the depths of mineralized lodes (300–350 m) explored during earlier phases of exploration in the Singhbhum Group. Ore microscopy, XRD and SEM studies of borehole core has confirmed the presence of discrete Uraninite (600 - 2000 microns), magnetite, chrome-spinel, pyrite, chalcopyrite, galena, molybdenite, cobaltite, millerite, nickeline, vaesite, pentlandite and skutterudite and traces of gold, platinum and silver. Chemical analysis (n=175 from 12 boreholes) indicated significant concentration of U3O8 (0.010–4.20%) MgO (Av. 25%), Cr (Av.2300 ppm), Cu (Av.570 ppm), Ni (Av.500 ppm), Mo (Av.400 ppm) with traces of Au (upto 30 ppb) and PGE (upto 95 ppb). Uraniferous host also analysed high total REE (Av.1558 ppm; n=5). The polymetallic nature of this upcoming uranium deposit has added enormous value to the cumulative tenor and its economic potential. The dimension of the deposit and its locational proximity to the Turamdih Uranium mines is of utmost significance to the mining economics as this will facilitate UCIL to exploit this upcoming uranium deposit in the heart of Singhbhum province by using the existing mining infrastructure available nearby.

The discovery of the polymetallic (U-Cr-Ni-Mo-REE-Fe-Mg) mineralization sets up a new exploration model for uranium in the domain of SSZ and scope for further research. Syngenetic Cr-Ni-Mo-Fe-Mg concentration in ultramafic host is acceptable but uranium and REE concentration need to be accounted for by the epigenetic process, if in case, they are not syngenetic. Evidences favouring genetically related uraninite and chromite are observed and hence intensive studies are continued to solve the mystery. Unit cell dimension of uraninite (5.4498 to 5.4650Å) in serpentinized peridotite are comparable with the values reported from other uranium deposits of SSZ which is indicative of high temperature (~ 500°C) of crystallization of uraninite. In this background, epigenetic hydrothermal process of formation, akin to SSZ type of uranium mineralization is acceptable for the subsequent uraninite which is after the high temperature uraninite (with 5.10 – 9.45% ThO2) in serpentinized peridotite of Kudada area. The observations like large size of uraninite grains upto 2000 microns, occurrence of discrete uraninite in interstitial spaces of olivine pseudomorphs support the unique syngenetic uranium metallogeny prior to epigenetic U-Cu metallogeny. The understanding in this regard is not yet clear however, it has helped to explore ultramafic bodies of IOG in SSZ for multi-metal type of mineralisation.

Tirukocha Fault related Exploration

The eastern part of SSZ records a few prominent faults related to brittle deformation as a post-shearing phenomenon. The Tirukocha Fault between Bhatin and Jaduguda, and Gohala Fault between Bagjata and Kanyaluka have affected the uranium mineralization. Both the faults have been represented in Total Magnetic Intensity (TMI) Image for the central part of SSZ prepared recently by AMD (Fig. 6). The integrated studies carried out based on geological mapping and the collection of subsurface data from boreholes and underground Jaduguda mines, suggests its oblique slip nature. The surface manifestation of Tirukocha fault is identified by the clear displacement of the quartzite unit of Chaibasa Formation in Jaduguda by ~1 km dextrally on plan (Fig. 7). The level plan made on the marker quartzite depicts a lateral displacement of ~1 km with a vertical separation of 570 m. These measurements are significant to understand the exploration in Jaduguda-Tirukocha area where substantial tonnage is unexplored *(Sinha and Verma, 2018)*. The concept is tested and a few boreholes have picked up mineralization based on the above understanding. Exploration so far indicates that the richer grades are extending further east. This calls for meticulous planning in the east, where the ore body and the fault plane make an intersection line plunging steeply towards northeast direction. Calculation of the intersection of the two planes indicates that intercepts of better grade and

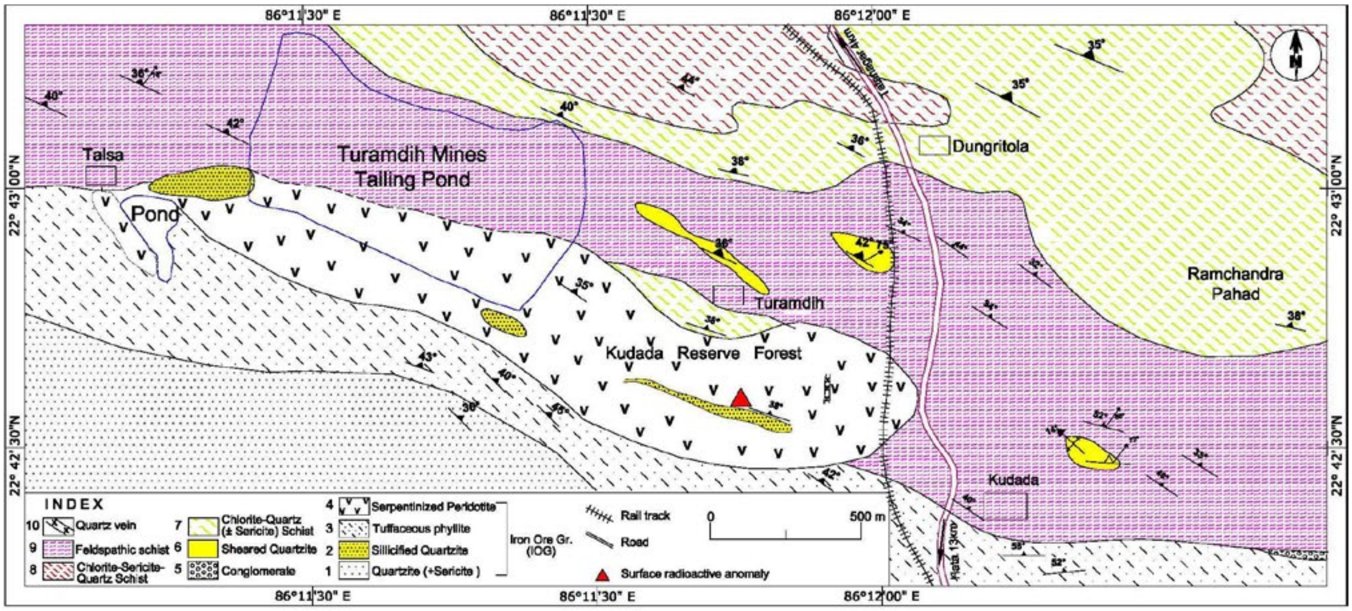

Fig. 5: Geological map of Kudada area, south of Turamdih mines, East Singhbhum district, Jharkhand.

thickness values can be expected further eastward with each deeper series. On similar analogy, Gohala fault has also been taken up for exploration (Fig. 8). The uranium mineralized lodes of Bagjata and Kanyaluka deposits are considered to be time separated bodies with a probable slip of 3 km. The understanding developed due to recent subsurface exploration has paved the way for establishment of many new deposits at depth in this sector.

Arkasani Granophyre Related U-Mineralisation

The SSZ bifurcates into two arms at Narwapahar and continues further westwards where the Bangurdih-Gurulpada sector forms the southern segment of the shear while the Sankadih-Galudih forms the northern shear plane of SSZ (Fig. 3 & 4). The surface uranium occurrences defining an E-W trend along Banaykela, Gurulpada, Mahalimurup, Dhadkidih, Dugridih, Nilmohanpur, Ukri and Bijay areas are confined to southern shear while Sankadih, Saharbera, Sarmali and Tirildih are situated along northern segment. The northern shear has association of Arkasani Granophyre (AG) and Soda Granite (SG) as evidenced on outcrop level. Pb-Pb age of 1721 Ma is considered to be the emplacement age of AG while Rb-Sr age of 1052 Ma is assigned as its recrystallization age. For SG, Pb-Pb age of 2230 Ma is considered to be the emplacement age while 1430 Ma is the metamorphic reset time of Rb-Sr clock. Recent efforts in exploring the soil covered area between Sankadih and Galudih by non-core drilling has established low to medium grade (0.021-0.043% U3O8) uranium mineralization over a strike length of 360m upto depth of 120m in two series. Heliborne and ground geophysics has helped in planning of boreholes and understanding of target depths. This has established 800m strike length located west of the main Sankadih block. The correlatable uraniferous mineralization is confined to Arkasani Granophyre/Feldspathic schist. The subsurface continuity in this unit has generated a new concept to explore the Arkasani Granophyre magmatic-hydrothermal related mineralization adjacent to SSZ *(Sinha and Verma, 2018)*. The shear-controlled chlorite-biotite-quartz schist hosted uranium mineralization at Sankadih occurs near the contact of AG. Even schistose rocks occurring within the AG show the presence of uranium. The emplacement of AG and SG is syn- to post-major shearing phenomenon. Cu content of Arkasani Granophyre ranges between 16 to 103 ppm (n=26). In boreholes drilled at Sankadih, Cu values upto 423 ppm were recorded in the uranium mineralised zone (n=23). The chalcopyrites developed in the schist show magmatic (+0.9 to + 1.4δ 34So/oo, n=2) and metamorphic (+2.6 to 3.4δ 34So/oo, n=3) parentage, indicating later remobilisation under metamorphic conditions *(Kumar, 2006)*. In other words, it is interpreted that AG has brought magmatic and metamorphic effects to the shear zone rocks and supported in recycling of U-Cu mineralisation in subsequent episodes. The concept so developed has been tested and investigations have resulted in encouraging values of AG related uranium mineralisation.

Reappraisal of exploration in the SE part of SSZ

The arcuate shaped SSZ takes a southwesterly bend near Kesarpur and continues upto Tilogoria-Dumurdiha in Odisha. Recent exploration inputs have initiated interest for further probing of the tract between Kanyaluka to Kuliana. The Kuliana area was explored during the early seventies when uranium was reported in boreholes drilled for copper. Copper deposits of 2.16 million tonne of ore with average grade of 1.54% Cu was established by GSI during 1971 to 1975 and

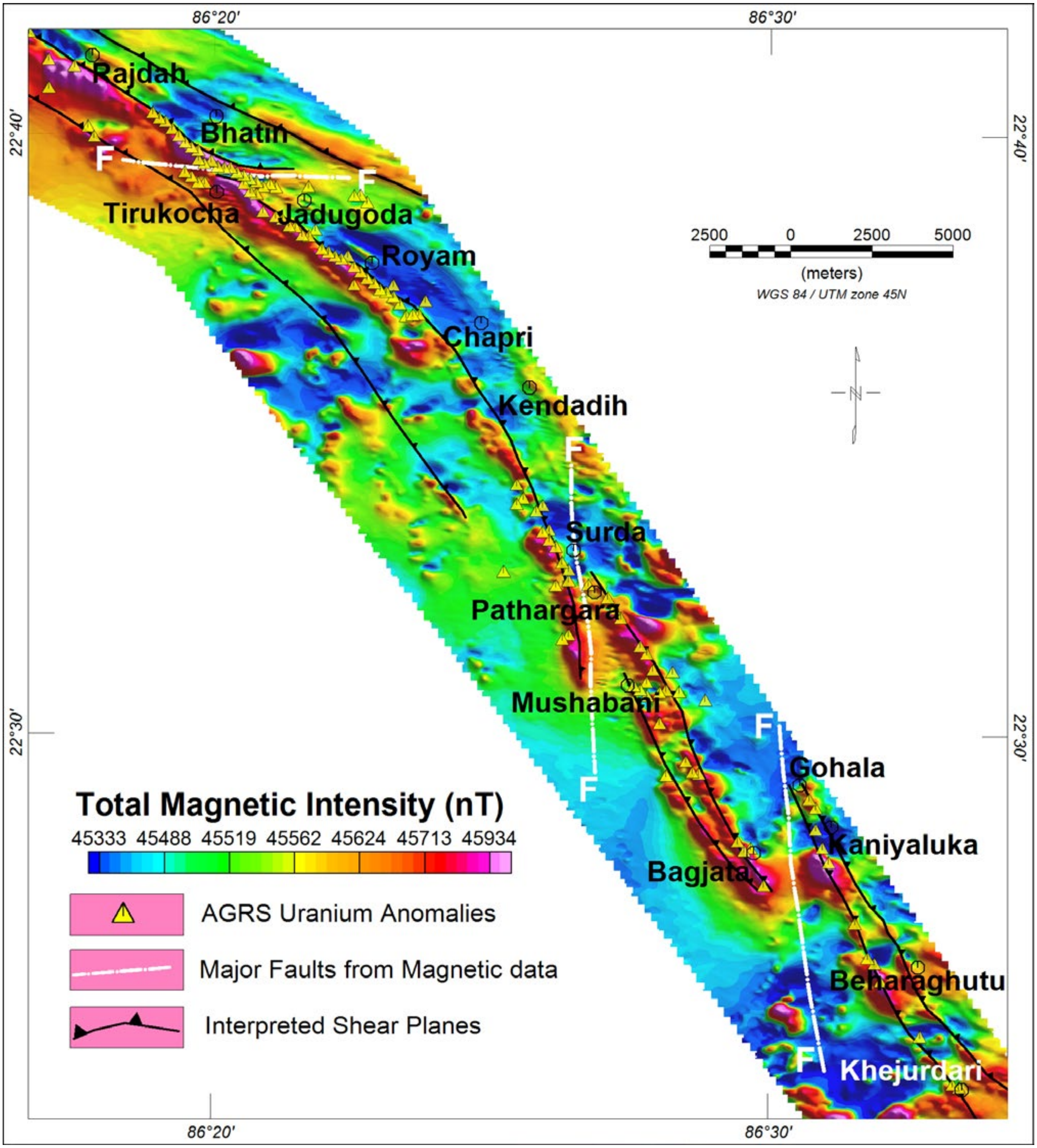

Fig. 6: Total Magnetic Intensity (TMI) image of central part of SSZ showing signatures of Tirukocha, Pathargora and Gohala faults.

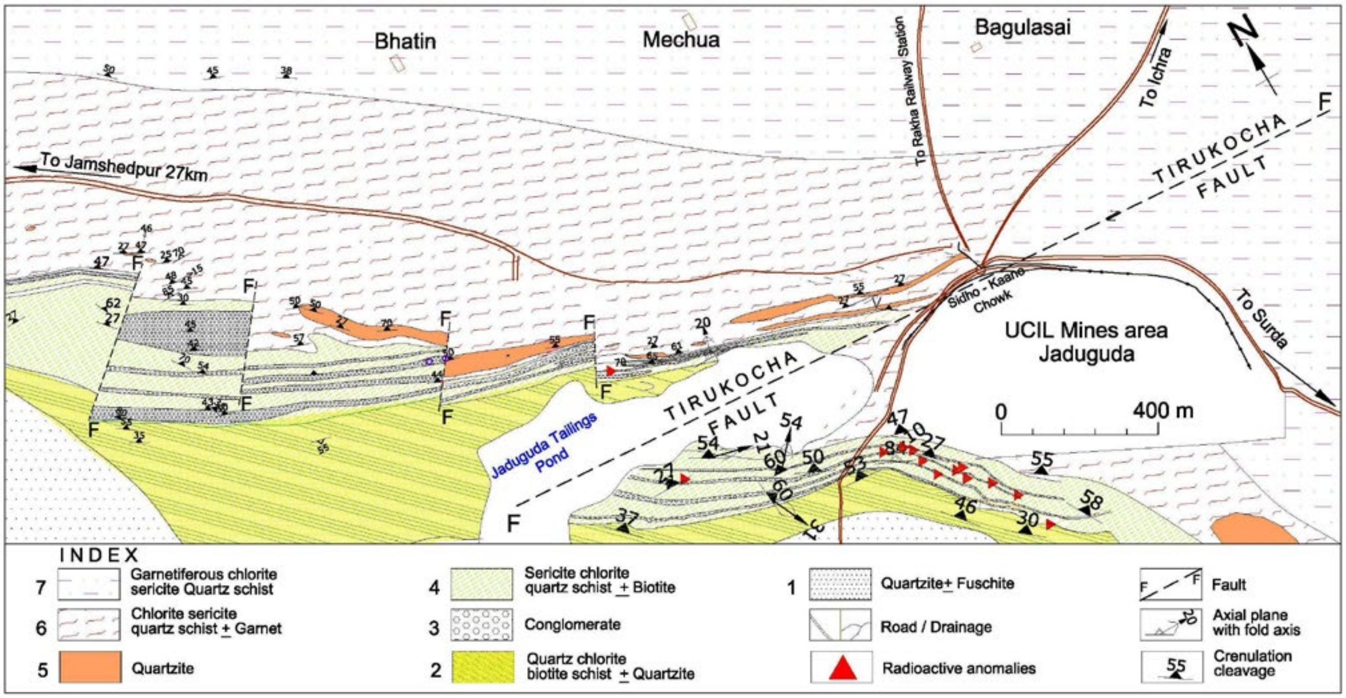

Fig. 7: Geological map of Jaduguda – Bhatin area in the central part of SSZ showing displacement of uranium mineralisation along Tirukocha fault.

taken up by MECL for the development of two stage mining during 1977 to 1981. The copper mining was suspended due to its inferior grade; however interest has been revived because of the policy decision on lowering of the cut-off grade for Cu. In the new economic perception, with lowered cut-off grade to 0.5% Cu, Central agencies are interested to take up the blocks. AMD has already initiated exploration programme and recorded persistence of uranium mineralisation in quartz-biotite-chlorite schists and feldspathic schist akin to the northern continuity of SSZ. A massive exploration has been taken up recently to bridge the gap between Kuliana and Kanyaluka due to favourable logistics. The stretch of 60 km shows presence of uraninite-magnetite association similar to the uraniferous belt in the central part of SSZ with a change in strike. Shearing of varying intensity is observed within the schistose and quartzite variants of Singhbhum Group. The focus is on the 35 km stretch between Jaduguda and Khejurdari which hosts the major copper deposits at Rakha, Sidheswar, Surda, Mosabani and Badia. Several known sectors of uranium mineralisation associated with copper are Sidheswar, Chirudih, Tamajhuri and Dhobani where uraniferous bands are recorded in departmental and GSI boreholes (Grades - 0.030% to 0.340% eU3O8; thickness 1.30 – 5.00m). The subsurface exploration in the light of the concepts described above (5.1 to 5.4) is continuing in the southern extension of SSZ and AMD is hopeful for addition of substantial tonnage even to the south of Bagjata – Kanyaluka where no uranium deposit have been established so far.

Conclusion

Even after seven decades of exploration, exploitation and research, the unfolding of the genetic aspects of polymetallic mineralisation in SSZ remains ever challenging because of polyphase volcanism, metasomatism and overprinted structural deformations. Multidisciplinary techniques adopted in AMD for survey and prospecting of uranium mineralisation in SSZ have paved the way for additional resources in SSZ, particularly in the blocks adjoining the existing mining centres, thereby extending the lifespan of the Narwapahar, Jaduguda and Bhatin uranium mines. AMD's recent focus on reappraisal of exploration along the belt of major copper deposits between Roam-Sidheswar to Dhantuppa-Khejurdari where U-Cu mineralisation was reported (*Krishnanunni, 1964*; Fig. 9) is expected to establish additional uranium resources. Conceptual modelling based exploration strategy has led to major breakthroughs in identifying new potential zones within as well as away from the known sectors of uranium mineralisation. The model to probe the base of the IOG through the Singhbhum Group has led to the discovery of a globally unique, serpentinized peridotite hosted polymetallic deposit (U–Cr–Ni–Mo–REE–Fe–Mg) in Kudada area, near Turamdih mines and thereby a new exploration model for uranium in SSZ is developed. Additional unexplored resources have been augmented in Jaduguda Bhatin link area by constraining the slip, lateral displacement and separation of blocks along the Tirukocha

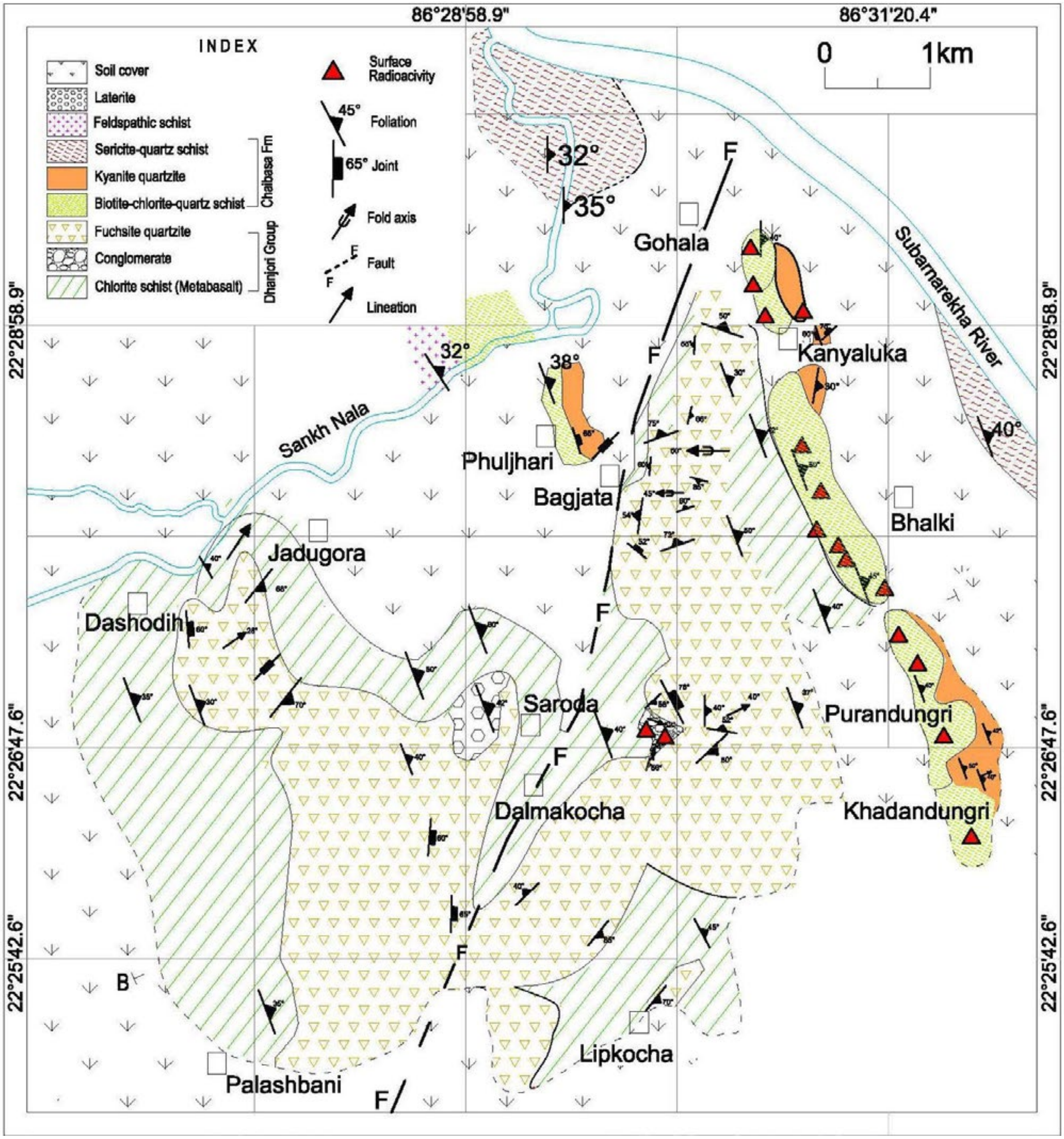

Fig. 8: Geological map of Bagjata – Kanyaluka area in the eastern part of SSZ showing signatures of Gohala Fault.

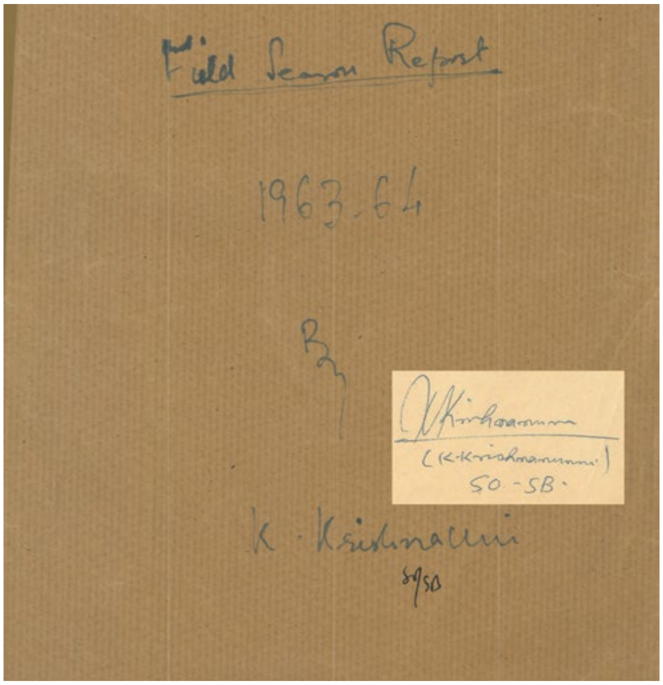

Fig. 9: From the AMD records: Report submitted by late Shri K. Krishnanunni, Field Season 1963-64.

fault through integrated modelling of geophysical, geological and subsurface exploration data. Further, the potentiality of QPC at the base of IOG and Dhanjori Group for U ± Au and the magmatic-hydrothermal related mineralization related to Arkasani Granophyre are being considered as challenges to exploration strategy and likely to provide surprises in the form of multi-metallic deposits. By virtue of the recent discoveries, promising leads and proposed huge exploration inputs, SSZ continues to be in the limelight for augmentation of additional uranium resources and focused geological research by AMD.

Dedication

This paper is dedicated to the fond memory of late Shri K. Krishnanunni, former AMD and GSI geoscientist. Shri Krishnanunni served AMD for a short span of two years (1963-64) and made significant contribution to uranium exploration in Roam – Sidheshwar sector of SSZ in Jharkhand. He had carried out geological mapping, triangulation survey, trenching, channel sampling, shielded probe logging and mapping of underground mine development by Indian Bureau of Mines (IBM) in this area. His work established that unlike other sectors of the SSZ, uranium and copper lodes co-exist in Roam – Sidheshwar sector. His work brought to light the continuity of three (03) uranium ore lodes in this sector. In his annual assignment report submitted to AMD, he indicated the possibility of further subsurface continuity and enrichment of these lodes. AMD is relooking into the possibility of exploration in the south-eastern part of SSZ and his recommendations will definitely serve as a guiding light for the exploration programme.

References

Banerji, A.K., 1962: Cross folding, migmatization and ore localization along part of the Singhbhum Shear Zone, south of Tatanagar, Bihar, India. *Economic Geology*, **57(1)**: 50–71.

Banerji, A.K., 1981: Ore genesis and its relationship to volcanism, tectonism, granitic activity, and metasomatism along the Singhbhum Shear Zone, Eastern India. *Economic Geology*, **76**: 905–912.

Bhattacharya, A.K., Gorikhan, R.A., Khazanchi, B.N., Fahmi, S., Singh, J., and Kaul, R., 1992: Uranium mineralisation hosted by migmatite-mobilizates and breccia zone in the northwestern part of Chhotanagpur Granite Gneiss complex, Rihand valley, Sonbhadra district, Uttar Pradesh. *Indian Journal of Geology*, **64(3)**: 259-275.

Bhola, K.L., 1965: Radioactive deposits in India. Symposium on Uranium Prospecting and Mining in India, *Jaduguda Mines Project*, 1-41.

Bhola, K.L., Rama Rao, Y.N., Sastry, C.S., and Mehta, N.R., 1966: Uranium mineralization in Singhbhum Thrust Belt, Bihar, India. *Economic Geology*, **61(1)**: 162-173.

Chaudhuri, T., 2020: A review of Hadean to Neoarchean crust generation in the Singhbhum Craton, India and possible connection with Pilbara Craton, Australia: The geochronological perspective. *Earth-Science Reviews*, 202: 1-25.

Dhana Raju, R., and Das, A.K., 1988: Petrography and uranium mineralisation of the Proterozoic schistose rocks from Jublatola, Singhbhum district, Bihar, Eastern India. *Exploration and Research for Atomic Minerals*, **1**: 41-56.

Dunn, J.A., and Dey, A.K., 1942: The Geology and petrology of Eastern Singhbhum and surrounding areas. *Memoirs of the Geological Survey of India*, **69(2)**: 281–456.

Fermor, L.L. 1919: Epigenetic ore deposits due to granitic intrusions: Singhbhum. Proceed. Asiatic Society Bengal, v. **15.**, p. clxxxviii.

Ghosh, S.K., and Sengupta, S., 1990: Singhbhum shear zone: structural transition and a kinematic model. Proceedings of the Indian Academy of Sciences - *Earth and Planetary Sciences*, **99**: 229–247.

Gupta, A., and Basu, A., 2000: North Singhbhum Proterozoic mobile belt Eastern India - a review. *Geological Survey of India Special Publication*, **55**: 195–226.

Gupta, R., and Sarangi, A.K., 2011: Overview of Indian Uranium Production Scenario in coming decades. *Energy Procedia*, **7**: 146-152.

Jeyagopal, A.V., Kumar, P., and Sinha, R.M., 1996: Uranium mineralization in the Palnad sub-basin, Cuddapah Basin, Andhra Pradesh, India. *Current Science*, **71(12)**: 957–959.

Kaul, R., Yadava, R.S., Gupta, K.R., Govind Singh, and Bahuguna, R., 1991a: Structure and uranium mineralization in the Proterozoic Aravalli Supergroup of Umra area, Udaipur district, Rajasthan, India. *Exploration and Research for Atomic Minerals*, **4**: 13-25.

Kaul, R., Singh, R., Sen, D.B., and Gupta, R.K., 1991b: Uranium exploration in the Proterozoic rocks of northwestern Himalaya, India. *Exploration and Research for Atomic Minerals*, **4**: 1-12.

Khedkar, V.R., 1951: Report on the iso-rad survey and prospecting for uranium in the belt of uraniferous rocks in Singhbhum district, Bihar. Field Season Report for 1950-51. *RMSU (AEC) Report* (Unpublished).

Krishnamurthy, P., 2006: The saga of Singhbhum uranium discoveries and exploration. Centenary Volume, *Transactions of the Mining, Geological and Metallurgical Institute of India*, **102-103(1&2)**: 151-169.

Krishnanunni, K., 1964. Report for Field Season 1963-64., AMD, (Unpublished), pp. 1-7.

Kumar, Shailendra, Chauhan, K.R., Gupta, K.R., and Bagchi, A.K., 2006: Sulphur isotopic study on chalcopyrite from Sankadih, western Singhbhum Shear Zone, Jharkhand, India. *Exploration and Research for Atomic Minerals*, **16**: 45-49.

Mahadevan, T.M. 1988a: Exploration for quartz-pebble type uranium deposits in India- Problems and prospects. *Geological Society of India, Memoirs,* **9**, P. 19-28.

Mahadevan, T.M., 1988b: Characterization and genesis of the Singhbhum uranium province, India. *International Atomic Energy Agency*, Vienna (Austria), Panel proceedings series, 337-368.

Mahadevan, T.M., 2002: Geology of Bihar and Jharkhand. *Geological Society of India*, Bangalore, 564p.

Mahendra Kumar, K., Gorikhan, R.A., Mathur, D.K., Sengupta, B., and Bhattacharya, A.K., 1998: Uranium mineralisation hosted by albite-rich leucosomes in the migmatised early Proterozoic metasedimentary rocks around Naktu, Son Valley, Sonbhadra district, Uttar Pradesh, India. *Exploration and Research for Atomic Minerals*, **11**: 55-60.

Matin, A, Banerjee, S., Dutta Gupta, C., and Banerjee, N., 2012: Progressive deformation across a ductile shear zone: an example from the Singhbhum Shear Zone, eastern India. *International Geology Review*, **54(3)**: 290–301.

Mazumder, R., Eriksson, P. G., De, S., Bumby, A. J., and Lenhardt, N., 2012: Palaeoproterozoic sedimentation on the Singhbhum Craton: global context and comparison with Kaapvaal. *Geological Society, London, Special Publications*, **365**: 51–76.

Misra, A., Pande, D., Ramesh Kumar, K., Nanda, L.K., Maithani, P.B., and Chaki, A., 2011: Calcrete-hosted surficial uranium occurrence in playa-lake environment at Lachhri, Nagaur District, Rajasthan, India. *Current Science*, **101(1)**: 84-88.

Mohanty, R., and Verma M.B., 1989: Structure as a guide for uranium exploration in the Turamdih–Mohuldih area, Singhbhum district, Bihar. Proceedings National Symposium on uranium technology. *Bhaba Atomic Research Center*, Bombay, 1–18.

Mukhopadhyay, D., 2001: The Archaean nucleus of Singhbhum: the present state of knowledge. *Gondwana Research*, **4(3)**: 307– 318.

Mukhopadhyay, D., and Deb, G.K., 1995: Structural and textural development in Singhbhum Shear Zone, eastern India. Proceedings of the Indian Academy of Sciences - *Earth and Planetary Sciences*, **104**: 385–405.

Pal, D.C., Barton, M.D., and Sarangi, A.K., 2009: Deciphering a multistage history affecting U-Cu (-Fe) mineralization in the Singhbhum Shear Zone, eastern India, using pyrite textures and compositions in the Turamdih U-Cu (-Fe) deposit. *Mineralium Deposita*, **44**: 61–80.

Pal, D.C., Sarkar, S., Mishra, B., and Sarangi, A.K., 2011: Chemical and sulphur isotope compositions of pyrite in the Jaduguda U (-Cu-Fe) deposit, Singhbhum shear zone, eastern India—implications for sulphide mineralization. *Journal of Earth System Science*, **120**: 475–488.

Pandey, P., Kumar, P., and Upadhyay L.D., 1994: Uranium deposits of Turamdih-Nandup area, Singhbhum district, Bihar and their spatial relationship.

Exploration and Research for Atomic Minerals, **7**: 1–13.

Pandit, S.A., 2002: Uranium occurrences in the quartz pebble conglomerate in Karnataka. *Exploration and Research for Atomic Minerals*, **14**: 131-146.

Pandit, S.A., Natarajan, V., and Dhanaraju, R., 2002: Exploration for Uranium in the Bhima Basin in parts of Karnataka, India. *Exploration and Research for Atomic Minerals*, **14**: 59-78.

Rama Rao, Y.N., 2013: Conceptual approaches and changing philosophies in uranium exploration through time in India. *Journal of the Geological Society of India*, **82**: 192-197.

Rao, A.Y., Vijay Raj, K., Yadav, O.P., Nanda, L.K., Rai, A.K., and Parihar, P.S., 2015: Uranium-bearing magnesian-calcrete in surficial environment from Khemasar, Churu district, Rajasthan, India. *Current Science*, **108(8)**: 1540-1544.

Rao, N.K., Rao, G.V.U., and Aggarwal, S.K., 1979: Lead isotopic ratios of uraninites and the age of uranium mineralization in Singhbhum Shear Zone, Bihar. *Journal Geological Society of India*, **20(3)**: 124–127.

Rao, N.K., and Rao, G.V.U., 1983a: Uranium mineralization in Singhbhum Shear Zone, Bihar: I. Ore Mineralogy and petrography. *Journal of the Geological Society of India*, **24(9)**: 437–453.

Rao, N. K., and Rao G.V.U., 1983b: Uranium mineralization in Singhbhum Shear Zone, Bihar: II. Occurrence of 'Brannerite'. *Journal of the Geological Society of India*, **24**: 489-501.

Rao, N. K., and Rao G.V.U., 1983c: Uranium mineralization in Singhbhum Shear Zone, Bihar: IV. Origin and geological time frame. *Journal of the Geological Society of India*, **24**: 615-627.

Roy, D., Bhattacharya, D., Mohanty, R., Patnaik, S., Pradhan, A.K., Chakrabarti, K. and Zakaullah, S., 2016: Study of Deformation pattern in Gogi–Kurlagere fault zone at Gogi–Kanchankayi sector of Proterozoic Bhima basin of northern Karnataka: its implication in control of uranium mineralisation. *Exploration and Research for Atomic Minerals*, **26**: 157-176.

Verma, S.C., Nagabhushana, J.C., Sinha, K.K., Viswanath, R.V., and Saraswat, A.C., 1991: Uranium exploration in India - Perspective and strategy. *International Atomic Energy Agency*, Vienna: 121-122.

Saha, A., 1994: Crustal evolution of Singhbhum-North Orissa, India. *Memoirs Geological Society of India*, **27**: 341p.

Saraswat, A.C., Rishi, M.K., Gupta, R.K., and Veerabhaskar, D., 1977: Recognition of favourable uraniferous areas in sediments of Meghalaya, India: A case study. *In:* Recognition and Evaluation of Uraniferous Areas. Proceedings of the Technical Committee Meeting, *International Atomic Energy Agency*, Vienna, 165-182.

Sarkar, S.C., 1982: Uranium (-nickel-cobalt-molybdenum) mineralization along the Singhbhum copper belt, India, and the problem of ore genesis. *Mineralium Deposita*, **17**: 257–278.

Sarkar, S.C., 1986: The problem of uranium mineralization in Precambrian metamorphic shear tectonites - with particular reference to the Singhbhum Copper-Uranium Belt, Eastern India". *International Atomic Energy Agency*, Vienna, 9–20.

Sarkar, S.C., 2000: Crustal evolution and metallogeny in the eastern Indian craton: *Geological Survey of India Special Publication*, **55**: 169–194.

Saxena, V.P., Bahukhandi, N.K., Reddy, S.V.S., Sabot, H.K., and Verma, S.C., 1998: Uranium mineralisation in Surguja Crystalline Complex, Madhya Pradesh, India - a review for evolving new exploration strategy. *Exploration and Research for Atomic Minerals*, **11**: 61-75.

Sen, D.B., 1977: A brief note on the geology and occurrence of uranium at Badal, Rajnandgaon district, Madhya Pradesh. *Current Science*, **46**: 605.

Sen, D.B., Sachan, A.S., Padhi, A.K., and Mathur, S.K., 2002: Uranium exploration in the Cretaceous Mahadek sediments of the Meghalaya Plateau. *Exploration and Research for Atomic Minerals*, **14**: 29-58.

Sengupta, B., Bahuguna, R., Sunil Kumar, Singh, R., and Kaul, R., 1991: Sandstone-type uranium deposit at Domiasat, West Khasi Hills District, Meghalaya, North-east India. *Current Science*, **61(1)**: 46-47.

Sengupta, N., Mukhopadhyay, D., Sengupta, P., and Hoffbauer, R., 2005: Tourmaline-bearing rocks in the Singhbhum shear zone, Eastern India: evidence of boron infiltration during regional metamorphism. *American Mineralogist*, **90(8-9)**: 1241–1255.

Sharma, K.K., 1969: Some observations on uranium-copper relationship in the Surda copper mines and their bearing on the zoning of mineralisation in the Singhbhum Thrust belt, Bihar. *Proceedings of the Indian National Science Academy,* **36A(5)**: 319-330.

Srivastava, D.C., and Pradhan, A., 1995: Late brittle tectonics in a Precambrian ductile belt: evidence from brittle structures in the Singhbhum Shear Zone, eastern India. *Journal of Structural Geology*, **17(3)**: 385–396.

Sinha, D.K., 2020: Atomic Minerals Directorate for Exploration and Research. Institutional Report. *Proceedings of the Indian National Science Academy,* **86(1)**: 755-758.

Sinha, D.K., and Verma, M.B., 2018: Uranium Potential of Singbhum Shear Zone, India: Future Prospects. International Symposium on Uranium Raw Material for the Nuclear Fuel Cycle: *Exploration, Mining, Production, Supply and Demand, Economics and Environmental Issues (URAM-2018)*, 393-398.

Sinha, D. K., Gupta, Shekhar, Nautiyal, K., Akhila, V. R., Shrivastava, V. K., Padhi, A. K. and Verma, M.B., 2019: Serpentinized peridotite-hosted uranium mineralization (U–Cr–Ni–Mo–REE–Fe–Mg) in Kudada–Turamdih area: A new environment of Metallogeny in Singhbum Shear Zone, India. *Current Science*, **117(5)**, 830 – 838.

Sinha, K, K., Das, A.K., Sinha, R.M., Upadhyay, L.D., Pandey, P., and Shah, V.L., 1990: Uranium and associated copper-nickel-molybdenum mineralization in the Singhbhum Shear Zone, Bihar, India: present status and exploration strategy. *EARFAM*, **3**: 27–43.

Sinha, R.M., Shrivastava, V.K., Sarma, G.Y.G., and Parthasarathy, T.N., 1995: Geological favourability for unconformity-related uranium deposits in northern parts of the Cuddapah basin: Evidences from Lambapur uranium occurrence, Andhra Pradesh, India. *Exploration and Research for Atomic Minerals*, **8**: 111-126.

Sinha, P.A. and Babu, R., 1986: New find of radioactive mineralisation in Cuddapah Basin. Geol. Surv. Ind. Southern Region News, v. **5(2)**, p. 17.

Sundaram, S.M., Sinha, P.A., Ravindrababu, B., and Muthu, V.T., 1989: Uranium mineralisation in Vempalle dolomite and Pulivendla conglomerate/quartzite of Cuddapah Basin, Andhra Pradesh. *Indian Minerals*, **43**: 98–103.

Swarnkar, B.M., Kothari, P.K., Umamaheswar, K., and Srinivasan S., 2002: Exploration for sandstone-type uranium mineralisation in the Siwaliks of northwestern Himalaya, India. *Exploration and Research for Atomic Minerals*, **14**: 1-27.

Vasudeva, S.G., 1965: Preliminary geological observations on the drill cores in Singhbhum thrust belt. *In:* Y.N.Rama Rao (Ed.), Proceedings Symposium on' uranium prospecting and mining in India -1964. *Jaduguda Mines Project*, 88-95.

Yadav, O.P., Hamilton, S., Vimal, R., Saxena, S.K., Pande, A.K., and Gupta, K.R., 2002: Metasomatite-Albitite hosted Uranium mineralisation in Rajasthan. *Exploration and Research for Atomic Minerals*, **14**: 109-130.

Indian Journal of Geosciences, Volume 74, No. 3
July - September, 2020; pp. 240-256

Invited Paper

Geophysical Tools for Oil and Gas Exploration of Geologic Structures

M. R. Thapar[1] and J. K. Thapar

International Geophysical Company, Tulsa, OK 74135, USA
Corresponding author's email: igctul@att.net

Abstract: Geologic structures have been the target for oil and gas exploration since the discovery of oil in the mid-1800s. Our goal is to present new geophysical tools which will help improve the exploration success, starting with seismic survey design, seismic data acquisition, seismic data processing, seismic data interpretation and mapping. The discussion of each tool highlights a key and specific area of oil and gas exploration.

Keywords: Structure, seismic, mapping, modeling, contour, magnetic, gravity, variation, surface, linear, exploration

Introduction

Geological Structure Contour Modeling©2 (GSCM): 3D rays are traced along Linear or curved paths from each structure contour. Curved ray paths are used when there is a velocity gradient in the subsurface. Linear ray paths when velocity gradients are small. The areal extent of the structure is derived from 3D ray tracing along with migrated and unmigrated structure maps for the structure. Correctly calculated areal extent of a structure is a must for successfully imaging, interpreting of the structure during seismic exploration. Migrated and unmigrated structure maps help in recognizing potential pitfalls in interpretation and in the estimation of resources. Structure depths for GSCM are obtained by parametrically modeling a structure or from wells and seismic interpretation. The results include areal extent of the structure, migrated and unmigrated maps, and quality control dip, strike, and curvature maps.

Acquisition Footprints Analysis Tool©3: Studies of amplitude variation with offset distance from the source are used by interpreters for direct detection of hydrocarbon saturation. The first step is to reformat the data from the field format to standard SEGY format. The second step is to remove the variations in source and receiver responses leaving the geological effects, i.e., AVO in the seismic data. This method calculates the seismic data acquisition footprints and applies the footprint correction and extracts the AVO response for the target horizon. The extracted AVO response is then compared with the AVO model response for hydrocarbon prediction. This method uses real seismic data for acquisition footprints analysis, or it can model seismic data acquisition and then conduct acquisition footprints analysis to extract AVO.

Structure Mapping Tool©4 (StrucMap): It includes modeling and mapping tools for fault polygon, Pinch-outs, and Unconformity. This paper includes a tool for testing and analyzing mapping methods and parameters. This tool is useful to efficiently determine the right variogram for Kriging method to generate a structure map. Restore-Tops is the well-known method of contouring faulted structures (Jones *et al*, 1986; Tearpock and Bischke, 1991, 2002.). A computerized and automated version of this method is used for contouring and mapping faulted structure and conducting volumetric calculations. In many parts of India and the world, seismic statics are a major obstacle in seismic data processing and in seismic interpretation. Seismic statics and mis-ties modeling and mapping tool is useful for understanding and detecting the pitfalls on seismic structure maps due to statics. This presentation also includes a structure contouring and volumetrics calculations.

Gravity Modeling and Mapping (GravMod)* ©5*: This is a tool for Modeling and Mapping gravity anomalies of geometric shapes. Modeled data are calculated in 3D to generate line profiles and gravity anomaly map for the selected shape. Gravity maps (2D and 3D) are generated and displayed for variations of selected model parameters and Profiles are displayed and stored as Excel Charts. Only maps are discussed in this presentation.

Magnetic Modeling and Mapping (MagMod)* ©6*: This is a tool for Modeling and Mapping magnetic anomaly of a geometric shape. Modeled data is calculated in 3D to generate 3-Component magnetic anomaly profiles and maps for the selected shape. Magnetic Maps are generated and displayed for variations of selected model parameters and Profiles are displayed as Excel Charts. Only maps are discussed in this presentation.

Geological Structure Contour Modeling (GSCM) ©7: Seismic energy generated at the source is propagated to the target horizon and back to the receivers at the surface. The transmission of seismic energy from point on the surface to a deeper horizon is along a linear path in constant velocity layers; this transmission takes place along a curved path in layers with increasing velocity with depth. This method carries out 3D ray tracing from each structure contour using linear or curved ray paths (Fig. 1 and Fig. 2). Curved ray paths are required in older geological strata because of higher velocity gradients in the subsurface.

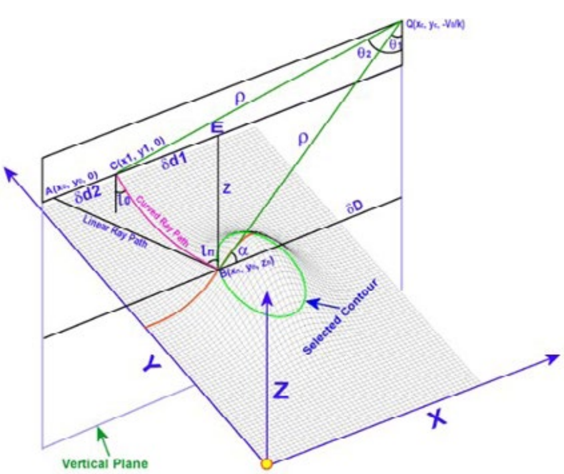

Fig. 1: Shows 3D ray tracing along linear and curved ray paths from a structure

The structure depth data are obtained from well information or parametrically modeled structure. The key steps in this method are as follows:

(1) First step is to specify the shallowest and deepest contours, and contour interval between successive contours for ray tracing.

(2) 3D ray trace from finely spaced points along each contour to the surface, e.g., ray trace from point B to location A or C for linear or curved raypath respectively (Fig. 2).

To determine the areal extent of the structure for 3D survey design, outline the extent of all 3D rays traced for the structure. Add the maximum offset distance to x and y dimenstions of areal extent for designing a 3D survey and imaging the structure, as in Fig. 3 for linear raypaths and Fig. 4 for curved raypaths. The x and y dimensions using **linear ray tracing** are given in Table I. The areal extent for the 3D survey is calculated by adding the maximum offset distance to the x and y dimensions of the inside rectangle in Fig. 3. This rectangle encloses all ray traces from the 3D structure.

Table I: Areal extent parameters with linear ray tracing.

XLen-in (km)	YLen-in (km)	Area-in (km)²	XLen-out (km)	YLen-out (km)	Area-out (km)²
14.27	13.94	199	18.27	17.94	327.86

The x and y dimensions using curved ray tracing are given in Table II:

Table II: Areal extent parameters with curved ray tracing.

XLen-in (km)	YLen-in (km)	Area-in (km)²	XLen-out (km)	YLen-out (km)	Area-out (km)²
10.67	12.38	132.08	14.67	16.38	240.28

The linear ray tracing in lower velocity younger rocks will produce a larger areal extent as compared to the curved ray tracing in higher velocity older rocks. Offshore rocks are younger, lower velocity, and negligible velocity gradient. The raypaths are linear in this case as compared to older geological strata with higer velocities.

(1) Generate unmigrated maps. All 3D ray trace points similar to A or C in Fig. 1 and Fig. 2 are used to map the unmigrated location of each contour.

(2) Generate the migrated maps using the depth data for the structure and compare it with unmigrated map.

(3) Generate quality control maps, e.g., dip, strike and curvature maps for the structure.

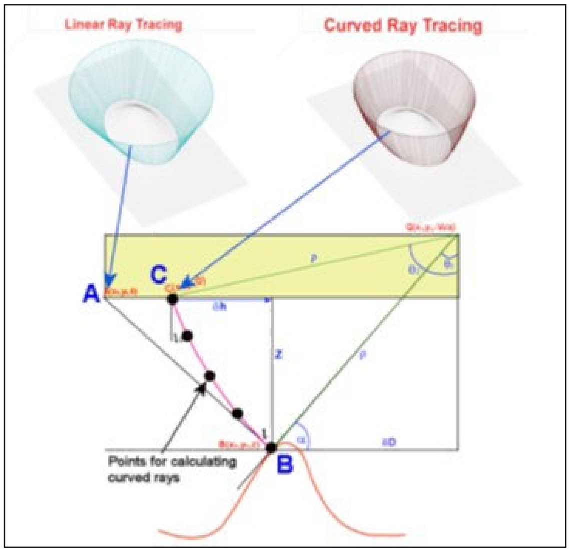

Fig. 2: Shows ray tracing along linear and curved ray paths from a structure in 2D

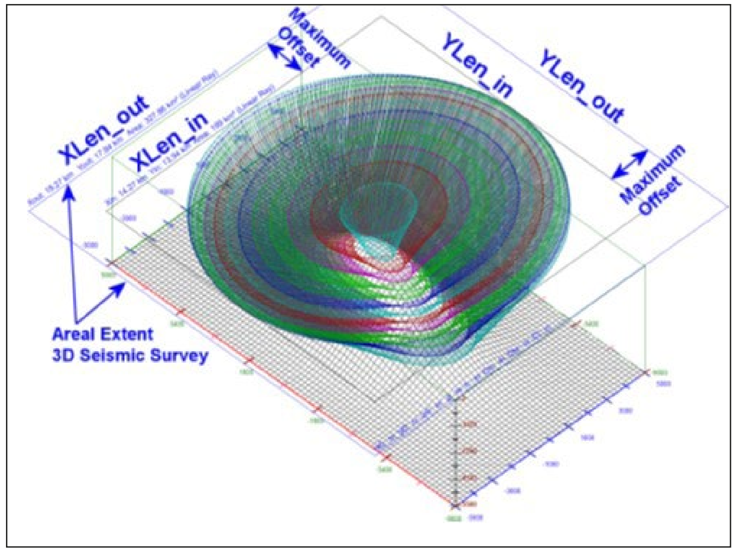

Fig. 3: Shows 3D ray tracing along linear ray paths from a structure.

Ray Tracing Structure Depth Data

Raytracing a 3D structure depth is shown in Fig. 5. This plot is generated using well depths to the top of the structure and depths from structural interpretation of seismic data. Linear 3D ray traces shown in Fig. 6 are from the structures in Fig. 5 and produces the areal extent parameters listed in the Table III below: The areal extent is, x = 15.85 km, y= 17.54

Table III: Gives the areal extent parameters

	RunID	Structure No.	XLen-in (km)	YLen-in (km)	Area-in (km)²	XLen-out (km)	YLen-out (km)	Area-out (km)²
▸	74	1	11.85	13.54	160.39	15.85	17.54	277.93

Migrated and Unmigrated Structure Maps

Migrated 3D maps are the cornerstone of 3D seismic interpretation. Simply stated, migration of 3D seismic data moves the reflected image of 3D structure to its correct subsurface position in three dimensions as in Fig. 7. A structure map of unmigrated seismic data the structure is spread out over a wide area as shown in Fig. 8. It is important to examine and compare the unmigrated and migrated maps to detect potential pitfalls. Partially migrated seismic data could lead to artifacts as pitfalls on such maps looking like anomalous stratigraphic features. Seismic data processor and interpreter should evaluate and quality control the migrated and unmigrated maps and the velocity field used in the process.

Quality Control Maps

Quality control maps to evaluate structures are generated. A 3D dip maps like the one in Fig. 9 should be consistent with the known geology of the structure and with stratigraphic features present in the map.

Benefits of Areal Extent of Geologic Structures

A good illustration of areal extent of a 3D seismic survey is a photographer taking a picture of a tall building must move far

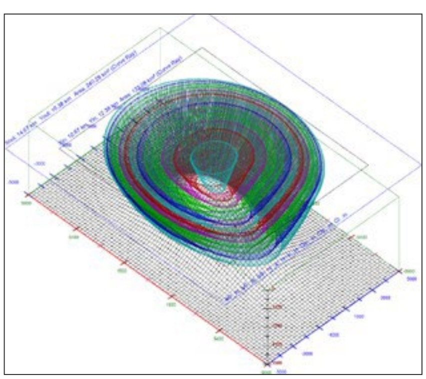

Fig. 4: Shows 3D ray tracing along curved ray paths from a structure.

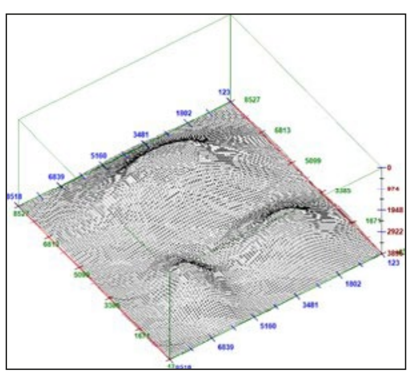

Fig. 5: Shows 3D structure display of depth data

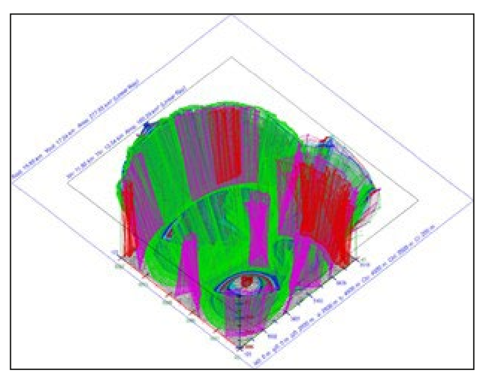

Fig. 6: Shows 3 linear ray paths from structures in Fig.

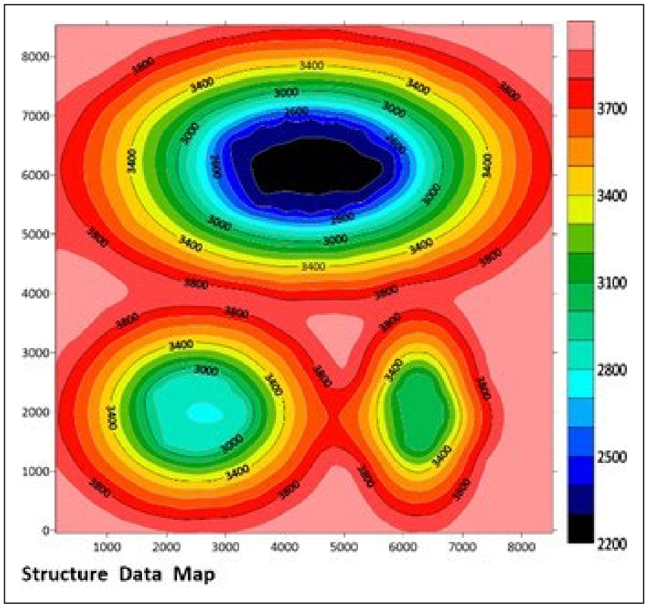

Fig. 7: Shows migrated Structure depth map

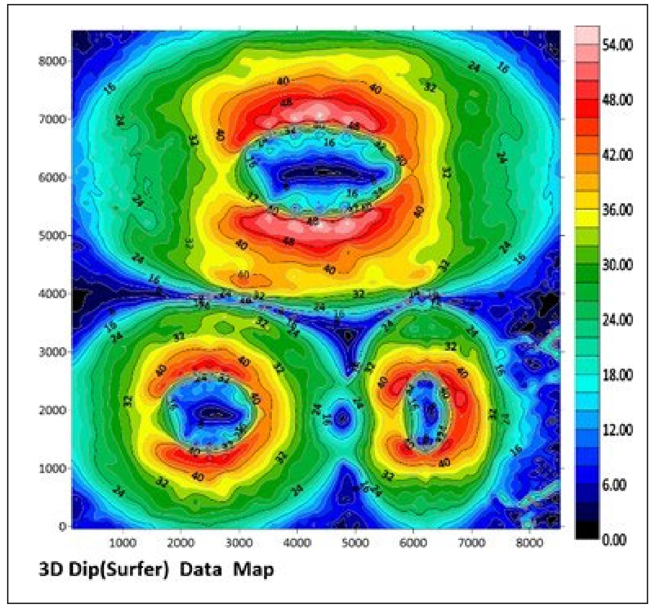

Fig. 9: Shows 3D Dip map for QC purpose using Surfer

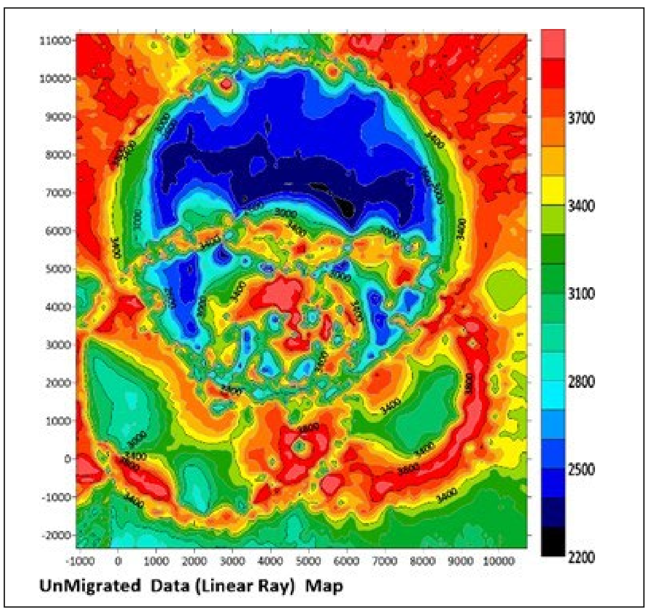

Fig. 8: Unmigrated Structure map

from the building to capture an image of the whole building. A picture taken close to the building will only show a part of the building. Similarly, 3D seismic survey will capture an image of only a part and not the whole geologic structure because of insufficient areal extent.

Survey design is not possible without the X and Y dimensions of the areal extent. X and Y dimensions of the Areal Extent must be large enough to produce a complete 3D image of the target structure.

However, if the areal extent is not large enough then the seismic image will be incomplete and the seismic reflections from steep slopes of the target structure will be missing as illustrated in Fig. 10 and Fig. 11. The missing information on steep slopes would result in incorrect interpretation and an enhanced risk in exploration. The interpreter must examine the migrated and unmigrated maps to QC for a correct areal extent in data acquisition and in processing. It is unwise to interpret structures through the missing data which will increase the risk in oil and gas exploration. Budget limitation is often the cause of insufficient areal extent of the survey design. Seismic 3D survey designed with insufficient areal extent is bound to increase exploration risk if not an exploration failure.

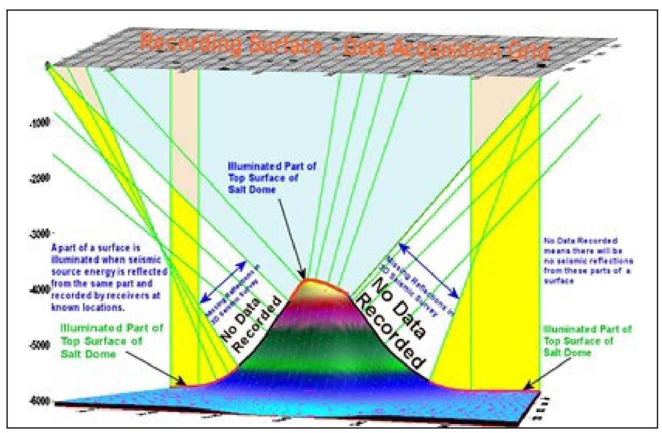

Fig. 10: Shows the effect of insuffient areal extent on seismic data acquisition and imaging

Acquisition Footprint Analysis and AVO Extraction:

Reflection amplitudes in raw seismic records are affected by: (a) Amplitude variation with offset distance between source

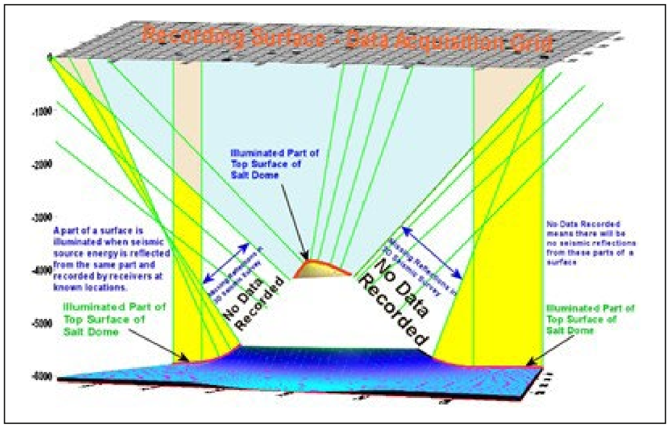

Fig. 11: reflections from slopes of the structure will be missing because of too small areal extent

and recording receivers. (b) Hydrocarbon or Water saturation. (c) Decay factors of divergence and attenuation which decrease seismic amplitudes as reflection distance increases from the source to the target and back to the surface receiver. (d) Acquisition footprints because of the layout of sources and receivers pattern geometry.

Analysis of AVO extracted from seismic recorded data are used for detection of hydrocarbon saturation. It is necessary to correct or compensate recorded seismic amplitudes for factors listed in (c) and (d) above. The process of AVO extraction is outlined in following steps.

Uncorrected raw seismic reflections and footprints are shown in Fig. 12.

(1) Calculate variation in seismic amplitudes because of source coupling and strength variation in Fig. 13

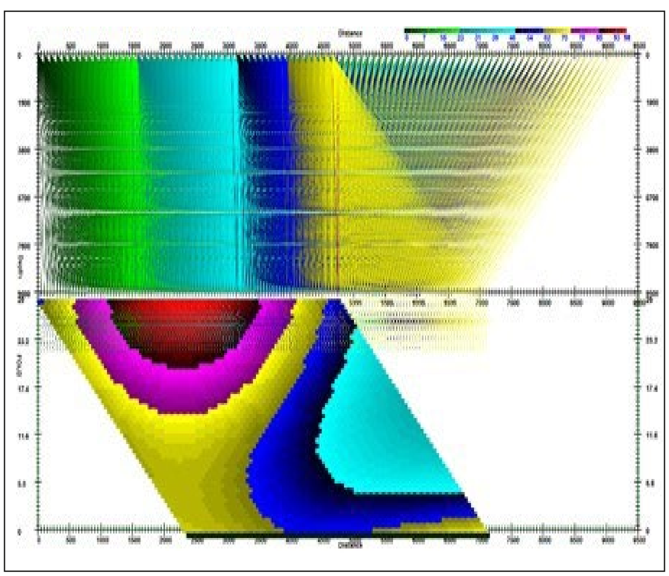

Fig. 12: is a plot of uncorrected seismic response which includes the acquisition footprint AVO and decay factors\

(2) Remove variation in seismic amplitudes because of source coupling and strength variation in Fig. 14

(3) Calculate variation in seismic amplitudes because of receiver coupling variation in Fig. 15

(4) Remove variation in seismic amplitudes because of receiver coupling variation in Fig. 16

(5) Correct for divergence and attenuation and display the extracted AVO response in Fig. 17 and Fig. 18

The next step is to compare the extracted AVO with calculated AVO response for gas/oil/water saturations. The example study in Fig. 19 shows seismic amplitude and frequency attributes over a gas field in Gulf of Mexico. The extracted AVO outside the gas field area is compared with calculated AVO curves for gas sand reservoir in Fig. 20. As expected, the extracted AVO does not correlate with calculated curves for gas sand. The extracted AVO and calculated AVO correlate for gas sand saturation in Fig. 21 over the gas field area. There are two main aspects of this method. AVO modeling for gas/oil/ water saturations and extracting AVO from raw seismic data.

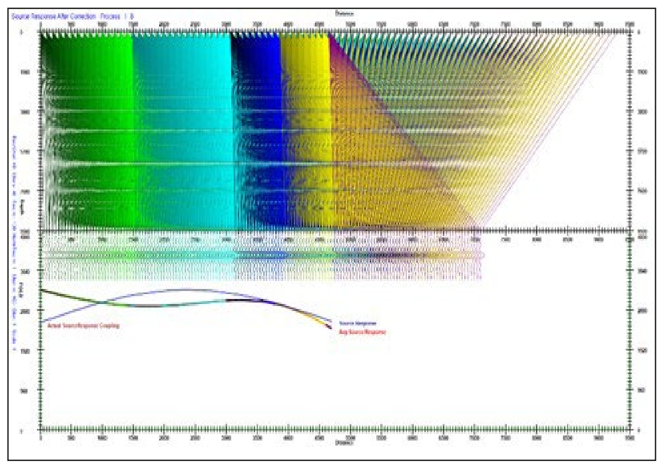

Fig. 13: Shows the source response variation.

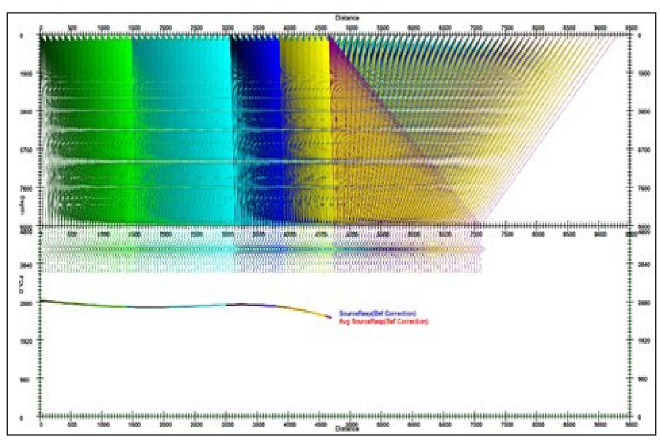

Fig. 14: Shows the source response after source correction.

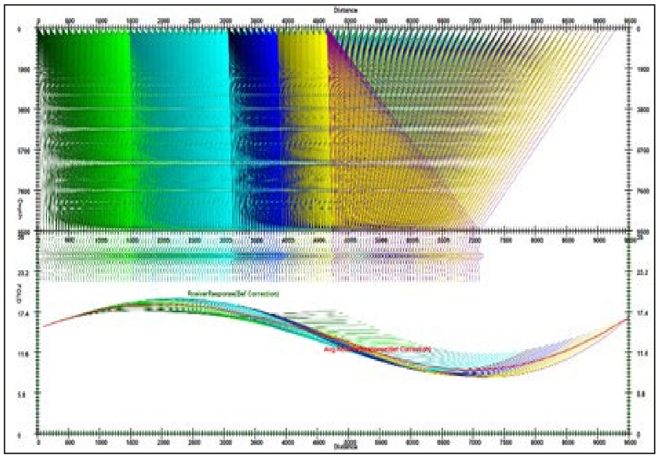

Fig. 15: Shows the receiver response variation.

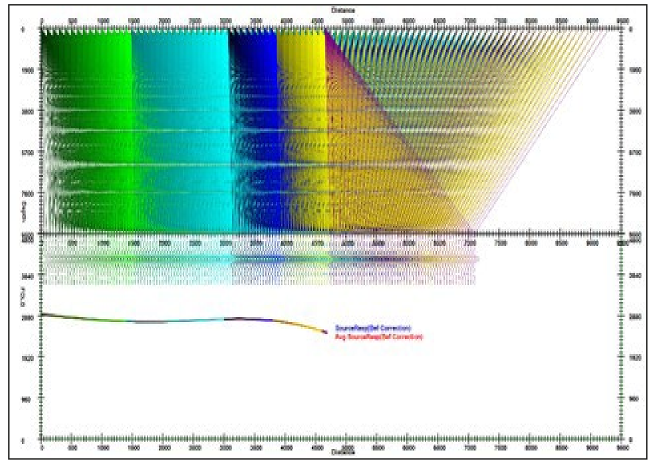

Fig. 16: Shows the receiver response after receiver coupling variation correction.

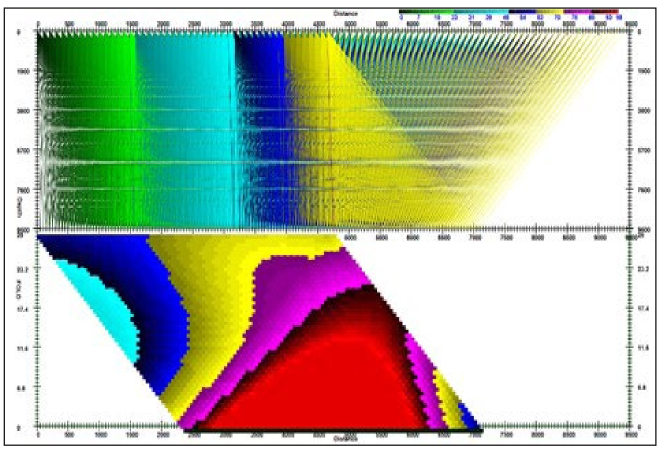

Fig. 17: Shows the extracted AVO after completing the above corrections.

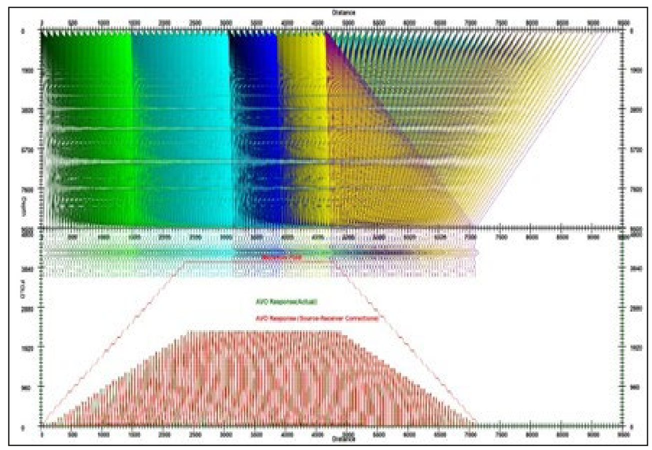

Fig. 18: Shows the extracted AVO after completing the above corrections and plotted as a curve for each CDP location.

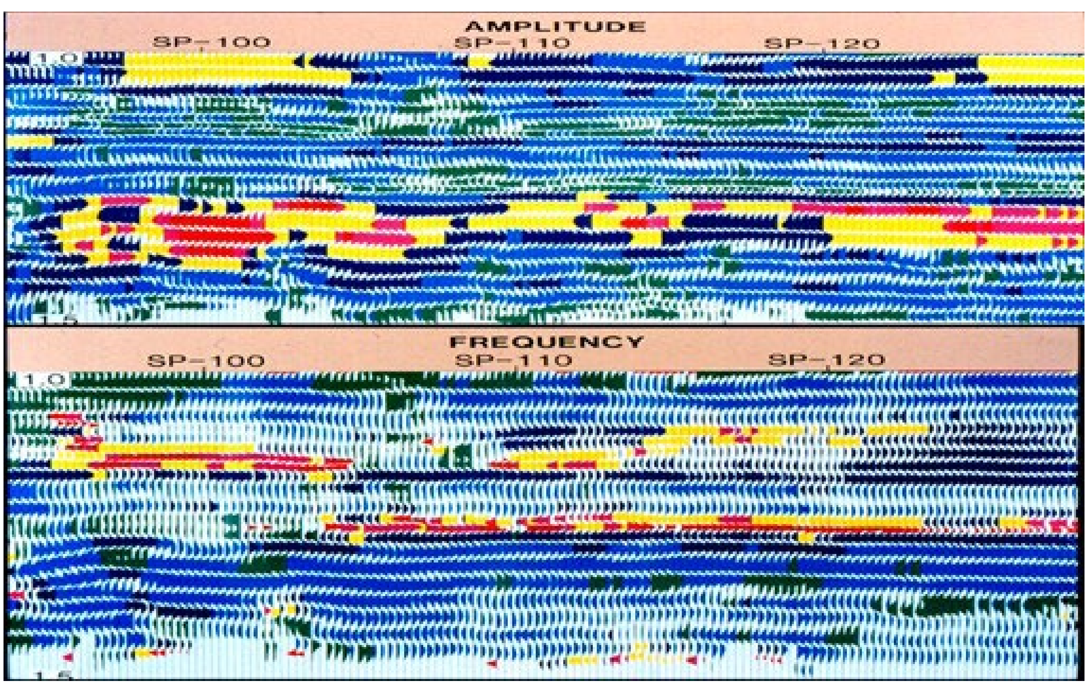

Fig. 19: Shows high seismic Amplitude and High/Low Frequency attributes for gas reservoir

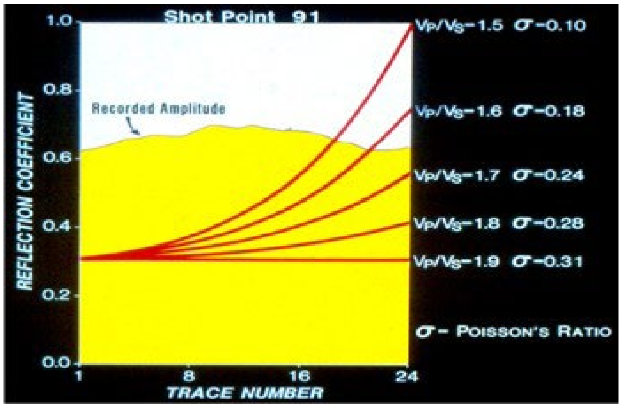

Fig. 20: AVO comparison at Shot Point 91 between the recorded AVO and modeled AVO response for gas sand.

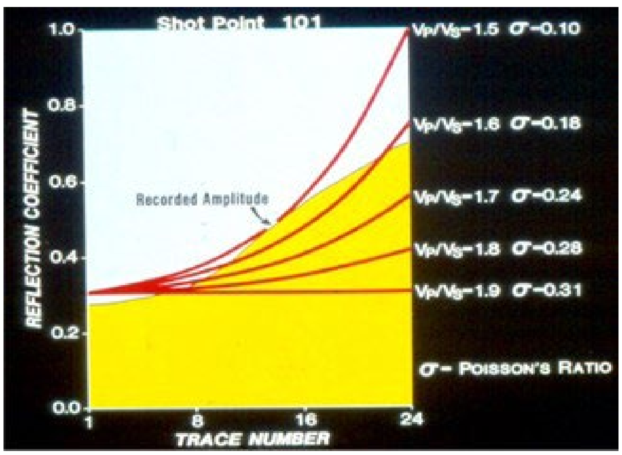

Fig. 21: AVO comparison at Shot Point 101 between the recorded AVO and modeled AVO response for gas sand.

Structure Mapping and Modeling Tools

Modeling & Mapping Fault Polygon

Interpreting fault polygons is commonly neglected or ignored. It requires skills to interpret and contour faulted structure through the polygon as shown below. Fig. 22 shows modeling a faulted structure and a fault polygon. The size and shape of the polygon will affect the estimation of gas/oil resources; therefore, it must be properly mapped.

Restore Tops Method of Contouring Faulted Structure

Restore tops method is described and documented by Tearpock, Bischke, 2003 and Jones *et al*, 1986 and numerous other books on structural interpretation. A step by step automated method of implementing a restore tops method is developed by Thapar(2009) using Surfer[8] . The discrete steps of restore tops method of contouring and volumetrics are shown in Fig. 23. This method requires mapping the displacement field for each fault and removing it from the structure depth data which restores the faulted blocks to the unfaulted state. The unfaulted structure is then contoured and mapped. The unfaulted contours are displaced by the displacement field which produces a contoured map of faulted structure as outlined in the examples in Fig. 23 to Fig. 25.

How to Select Appropriate Mapping Method

There are many computer mapping techniques available for geologists and geophysicists to choose from. The interpreters must select appropriate method for their projects. Usually, interpreters do not delve into the mathematical algorithm of each mapping method available. A good approach is to use all available methods to generate maps of the same data. It is cumbersome to run one method at a time to accomplish this task. This tool allows you to generate a map for each method with one command. The interpreter can then make an informed decision based on this comparison and the type of data used for mapping, e.g., uneven data distribution, sparse data or insufficient data. Different methods may perform better or worse depending upon the type of the data as shown in Fig. 26.

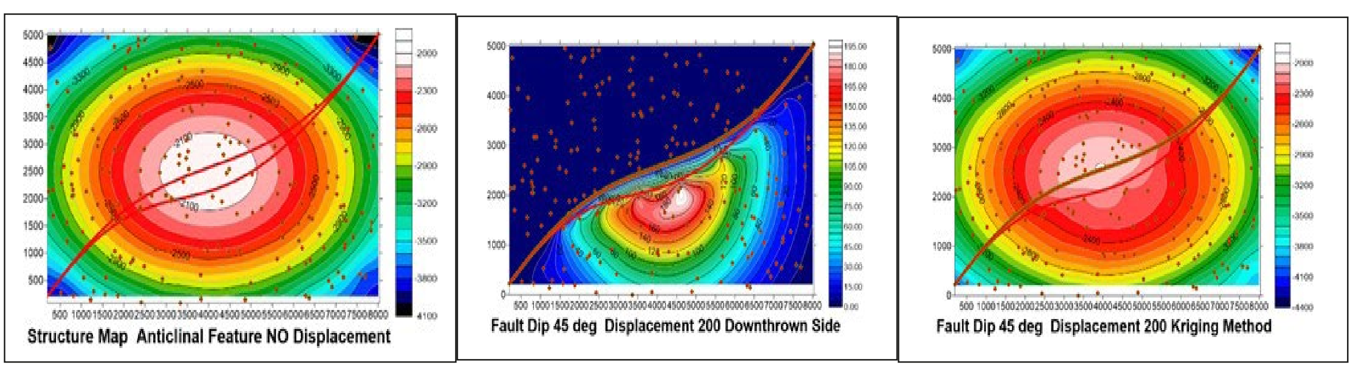

Fig. 22: (Left) Shows unfaulted structure contours in relationship to a polygon. (Middle) Shows the same polygon with the displacement field. (Right) Shows the faulted structure and contours from the upthrown block are continuing throughout the polygon to the downthrown block

8 Surfer© is Copyrighted by Golden Software, Colorado, USA

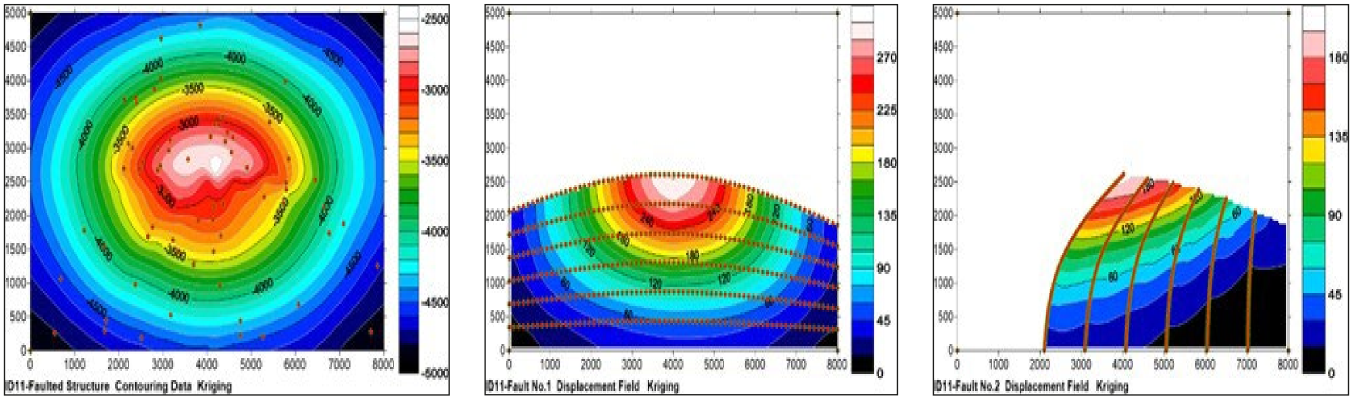

Fig. 23: Left shows contouring a faulted structure ignoring the fault locations and their displacements. A correct interpretation of faults is not possible using this structure map. (Middle) Fault displacement field for the main fault is mapped and removed from the faulted structure. (Right) Fault displacement field for the second fault is mapped and removed from the faulted structure.

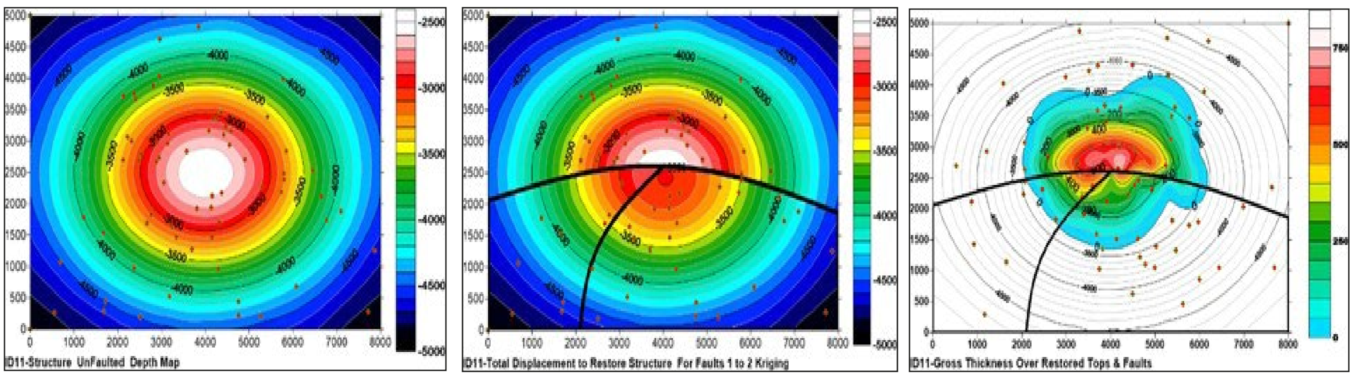

Fig. 24: (Left) After the fault displacements are removed the unfaulted structure is contoured as shown in this Fig.. (Middle) The fault displacements are added to the contoured unfaulted structure on the left to produce this Fig. along with the fault traces at correct positions. (Right) Gross thickness is displayed on restored surfaces from the previous map.

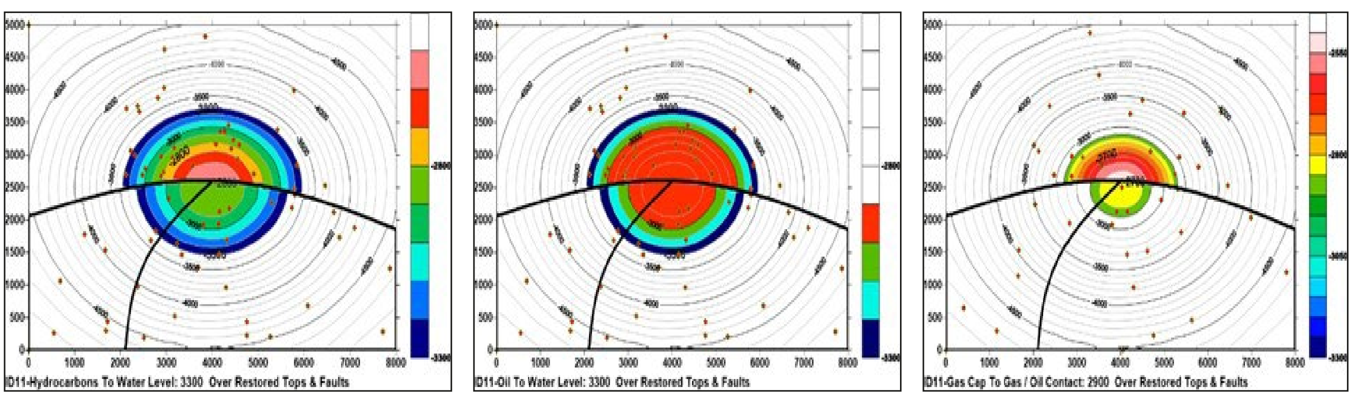

Fig. 25: (Left) shows hydrocarbons to the water level. (Middle) shows oil to the water level mapped on restored tops structure map. (Right) shows gas cap to oil contact mapped on restored tops structure map.

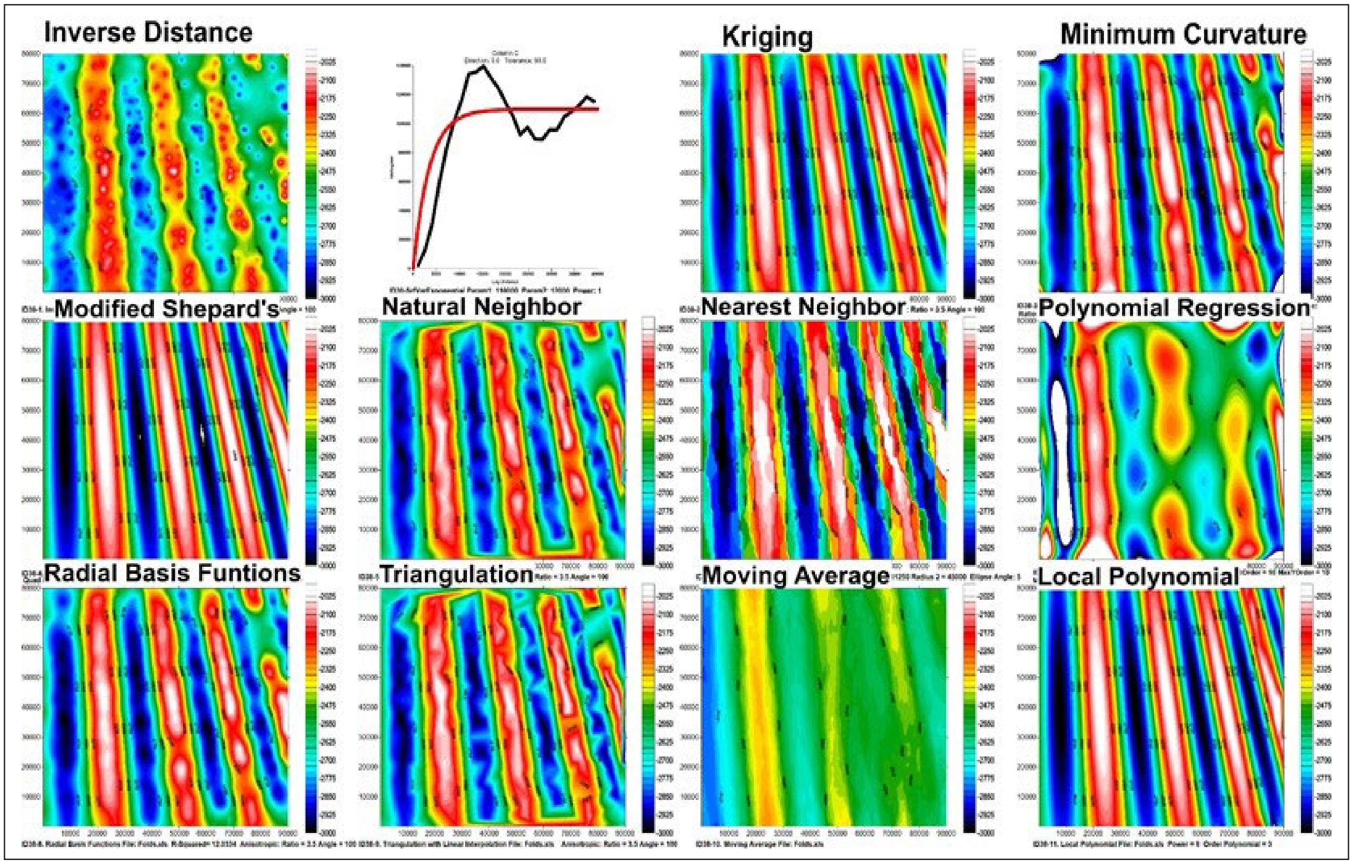

Fig. 26: Shows same depth data mapped with available mapping methods.

How to Select Appropriate Variogram for Kriging Method for Mapping:

The Kriging method for mapping is one of the preferred methods of mapping by many interpreters. Kriging is based on variation of data points as a function of the separation distance, and called a best linear, unbiased estimate at a point. It is also sometimes referred to as Geostatistical Kriging. The properties of a regionalized variable are intermediate between a random variable and a deterministic one. The complexity of the surface may not allow the description of the data using a deterministic function or a trend surface. The semi-variance is a measure of variance for equally spaced data at a distance ***h*** and it is used to find the rate of change along a specific direction. The variogram calculations are performed as follows:

$$\gamma = \frac{\sum (x_i - x_{i+h})^2}{2n}$$

where, ***n*** is the number of points, and ***h*** is the lag or distance between data points, e.g., if ***h = 10 m*** all points that are ***10 m*** apart are used. An illustration of a variogram (γ vs ***h)*** is shown in Fig. 27.

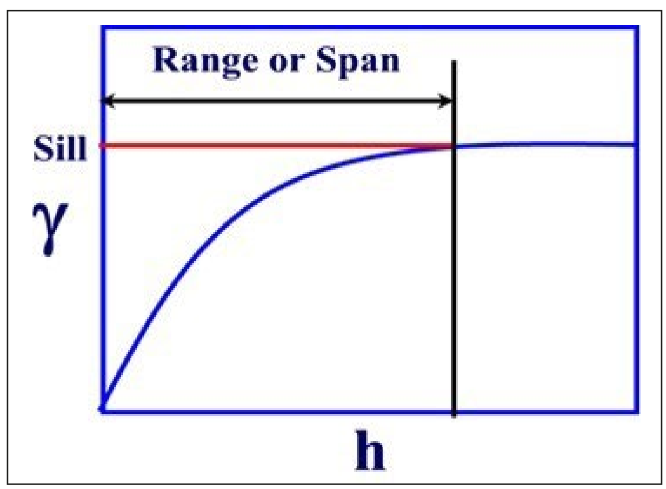

Fig. 27: Shows an illustration of a variogram.

There are 12 different variogram models to choose from as shown in Fig. 28. This mapping tool produces a map for each variogram model using the Kriging method of mapping shown in Fig. 28. The interpreter combines the limitations of the data and the type of structure with the results from different variograms to choose the variogram which satisfy the geologic requirement, e.g. shape of the structure and faulting, and shape of stratigraphic features present. The Surfer© software

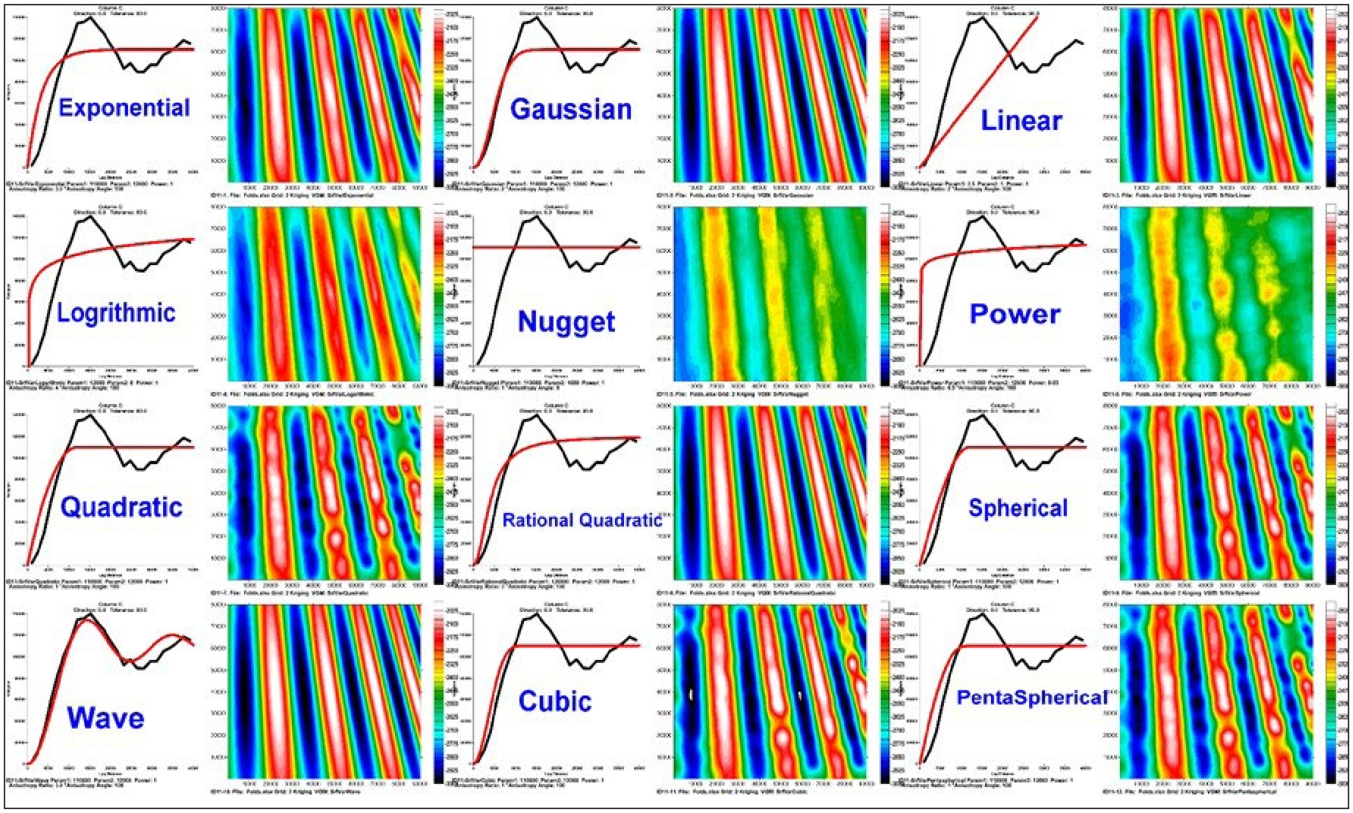

Fig. 28: Shows 12 Kriging maps produced with corresponding 12 variograms

documentation is a good source for further details on mapping methods and different variograms for the Kriging method. The variogram that fits the data variation the best and describes the shape of the structure without distortion should be selected.

Modeling and Mapping Pinchouts

Many producing reservoirs formed by the truncation of two geologic horizons are referred to as pinch-outs. Modeling and mapping are useful tools for understanding and contouring thickness variation of the pinch-out reservoirs. The following example in Fig. 29 shows pinch-out mapping due to the truncation of an anticline with a plane surface. Negative thickness contours outline the zero-thickness contour for volumetrics calculations.

The benefit of using positive and negative contours is to define the zero-thickness contour for the pinch-out.

Unconformity Modeling and Mapping

It requires skills and training to find and map unconformities on geological and geophysical maps. Modeling and mapping unconformity tool can help interpreters to quickly develop required skills and experience. A structure map of an anticlinal structure and effect of horizontal unconformity are shown in Fig. 30.

The effects of erosional angular unconformity 11.25^o to 45^o on a structure are shown in Fig. 31 (a to d).

Structure Mapping and Volumetrics

A step by step method of mapping a structure and volumetric maps are shown in Fig. 30 to Fig. 35

(1) Specify the contours defining the limits of hydrocarbons down to the water level on structure contour map as shown in Fig. 32.

(2) Gross Thickness is mapped on structure contour map as shown in Fig. 33

(3) Map net to gross thickness ratio on the structure map as shown in Fig. 34

(4) Map net thickness ratio on the structure map as shown in Fig. 35

(5) Specify and map the contour levels defining the oil limits from top to bottom as in Fig. 36.

(6) Specify and map the contour levels defining the Gas Cap limits from top to bottom as in Fig. 37

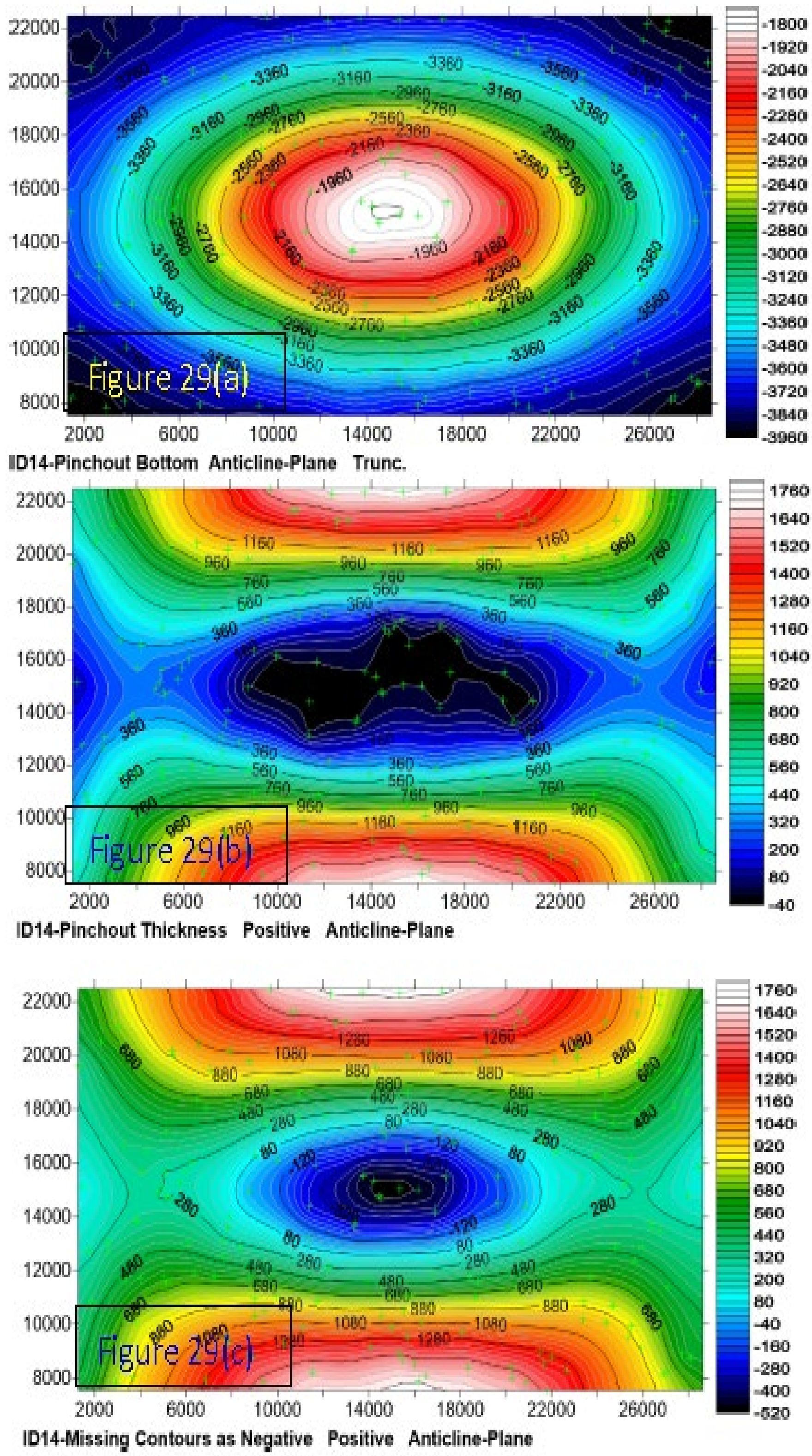

Fig. 29: (a) Shows pinch-out due to truncation of an anticline and a plane surface. It shows the surface contours of the pinch-out bottom i.e., It shows the structure of the bottom of the pinch-out. (b) This map shows positive thickness contours of the pinch-out. (c) Shows the pinch-out thickness with positive and negative contours.

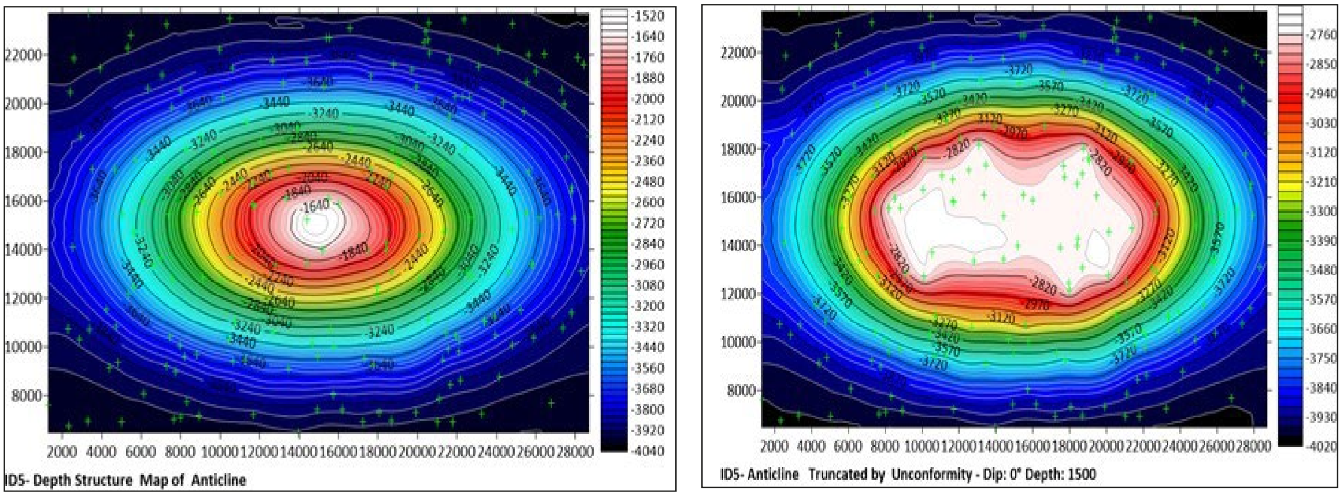

Fig. 30: (Left) Map of an anticline unaffected by the erosional unconformity. (Right) Transformation of anticlinal structure with a horizontal erosional unconformity at a depth of 2800 ft.

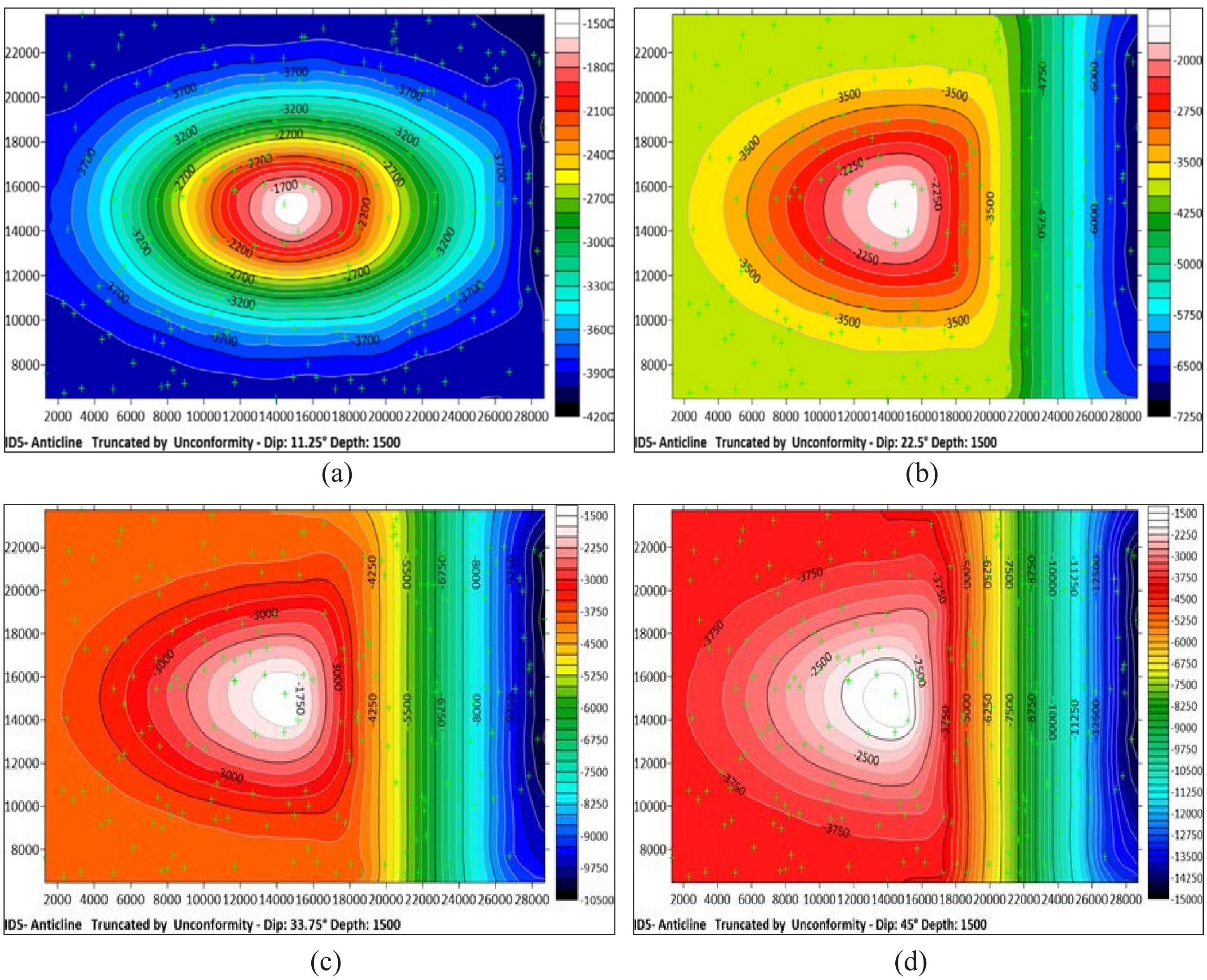

Fig. 31: (a) Shows the effect of an angular unconformity cutting through a structure at 11.25°. (b) Shows the effect of an angular unconformity cutting through a structure at 22.5° (c) Shows the effect of an angular unconformity cutting through a structure at 33.75° and (d) Shows the effect of an angular unconformity cutting through a structure at 45°.

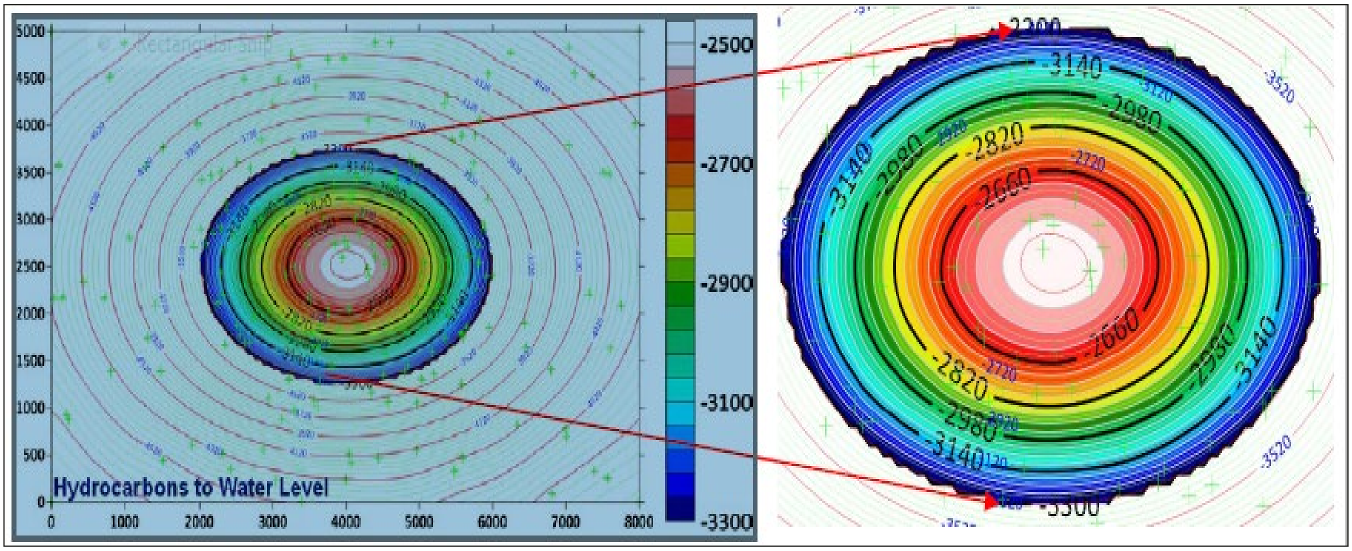

Fig. 32

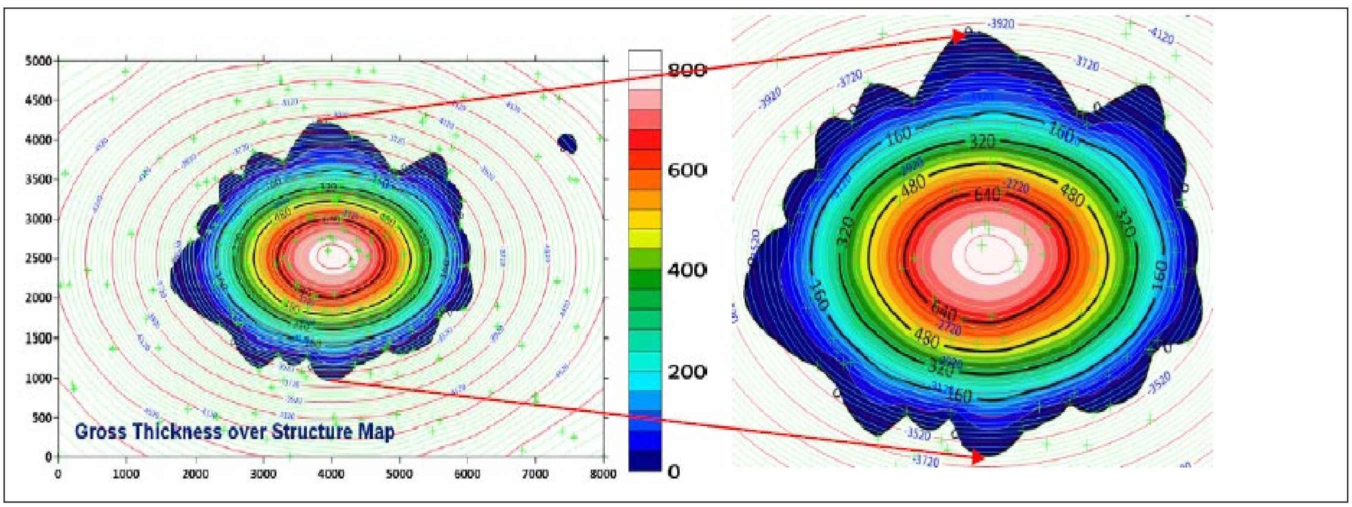

Fig. 33

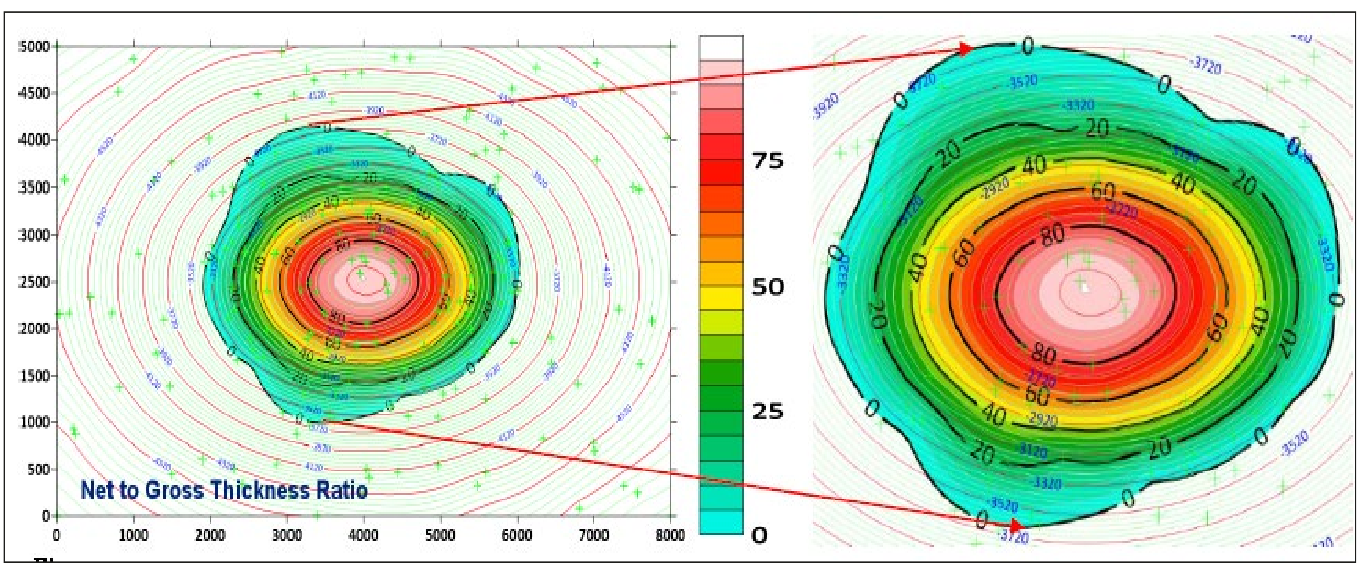

Fig. 34

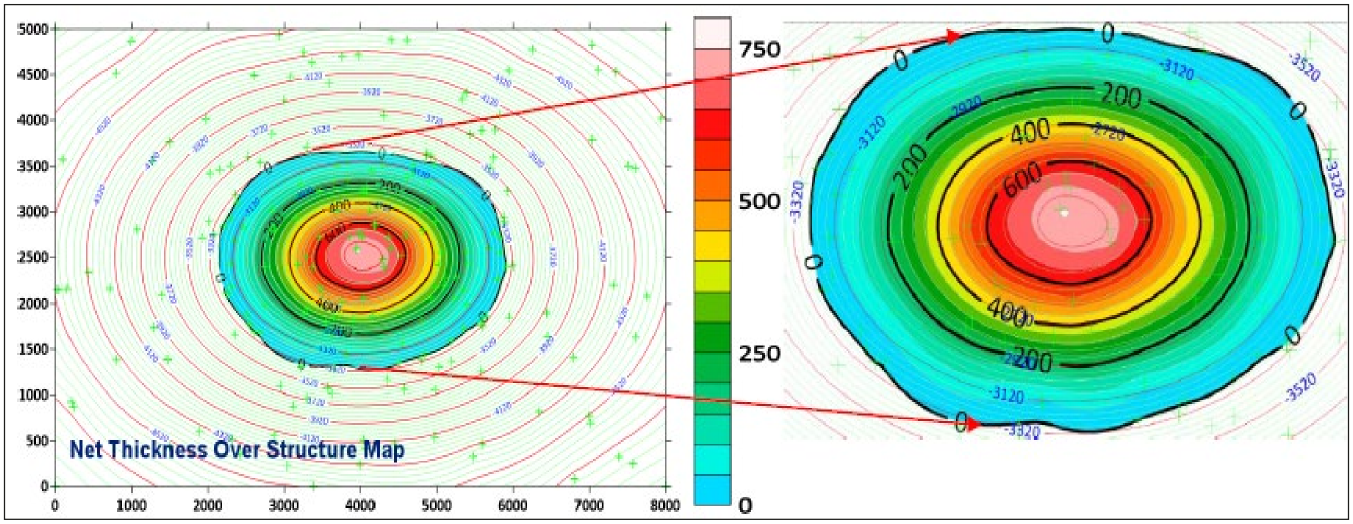

Fig. 35

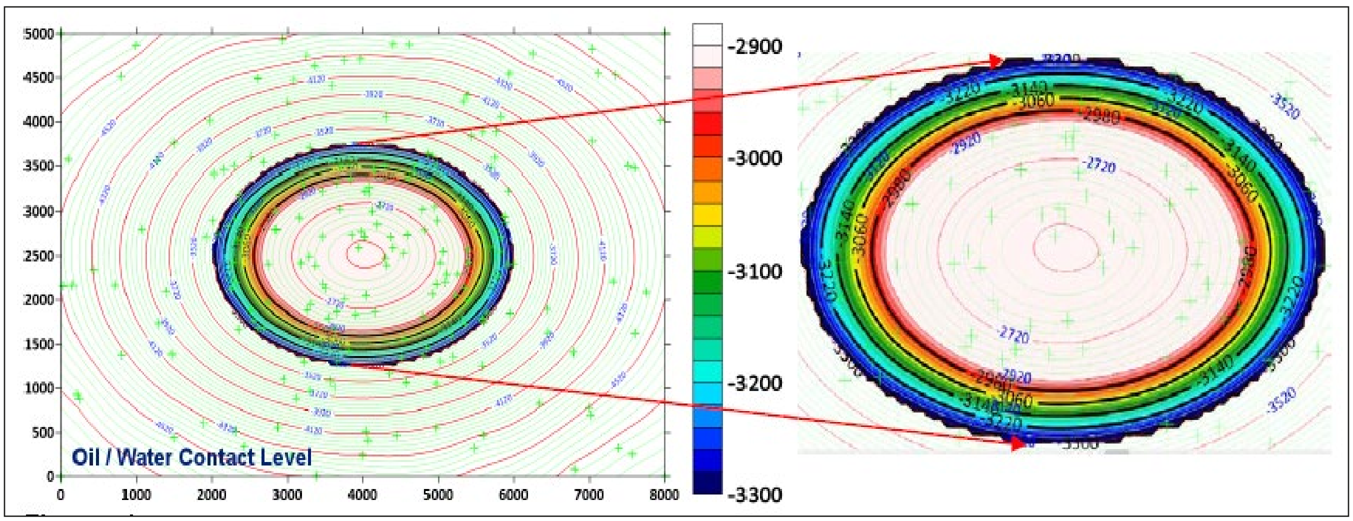

Fig. 36

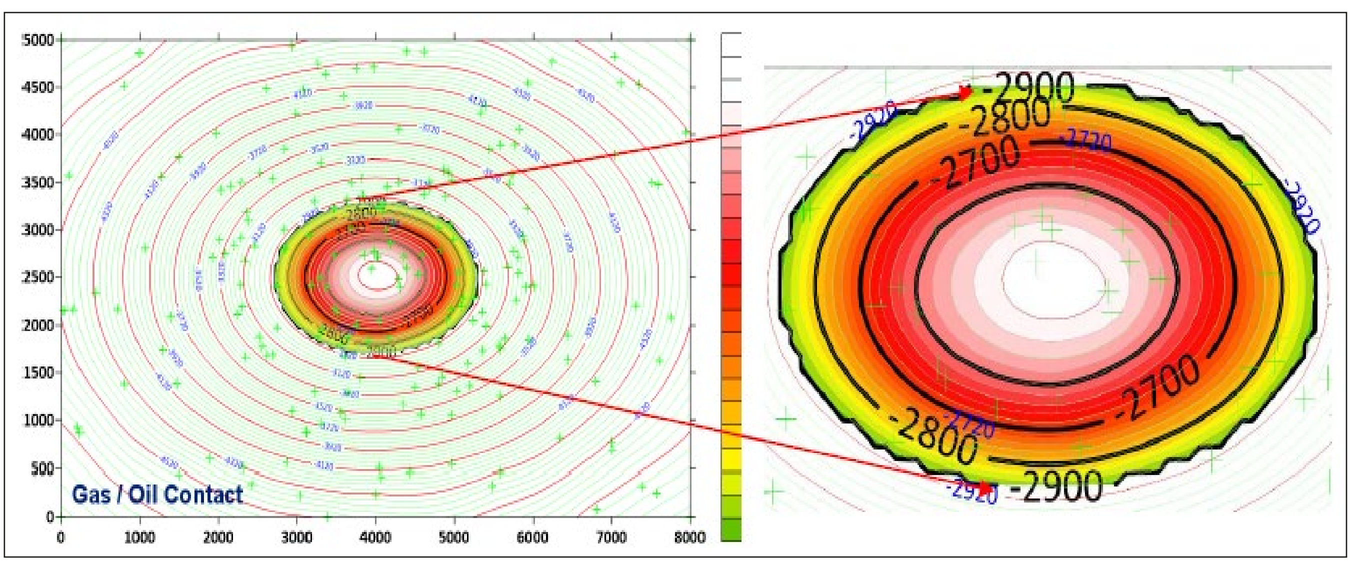

Fig. 37

The automated reservoir resources are calculated based on the defined limiting contours of oil and gas saturation:

Oil Resources to Oil/Water Contact:

= 382,213,408 barrel

Gas-Cap Resources to Gas/Oil Contact:

= 645,611,454 cu. ft.

The computer generated volumetric calculations entail positive and negative volumes. Positive volume is the volume between the top and bottom surfaces of oil or gas when bottom surface is below (deeper) the top surface. Negative volume is the volume between the top and bottom surfaces of oil or gas when bottom surface is above (shallower) the top surface. Upper and Lower surfaces for volumetric computation should be specified carefully.

It is important to verify the computer calculated resources. A simple method of estimating resources is shown below:

(1) Following the procedure outlined in Fig. 38, determine the appropriate geometric shape to approximate the contour area

(2) Interpret and identify gas and oil reflections

(3) Contour structure - top to base

(4) Identify contour relating to the top of gas

(5) Identify contour relating to the top of oil

(6) Identify contour relating to the base of oil

(7) Calculate area for each contour

(8) Calculate total volume from the top contour to each successive contour

(9) Calculate total resources

(10) Calculate total gas resources

(11) Calculate total oil resources

Gravity Modeling and Mapping

In a new exploration area, seismic data are not always available. Gravity data may be available or may be acquired at a fraction of the cost of 3D seismic surveys. The aim in Gravity modeling and mapping is to generate gravity anomaly maps before a gravity survey is conducted. For existing gravity surveys, the model parameters may be estimated based on the anomalies in the data. An illustration of a fault and parameters necessary for gravity modeling are shown in Fig. 39 (Left) and a gravity map for the fault model parameters listed below are shown on the Right. Gravity modeling and mapping can complement the seismic exploration for oil and gas.

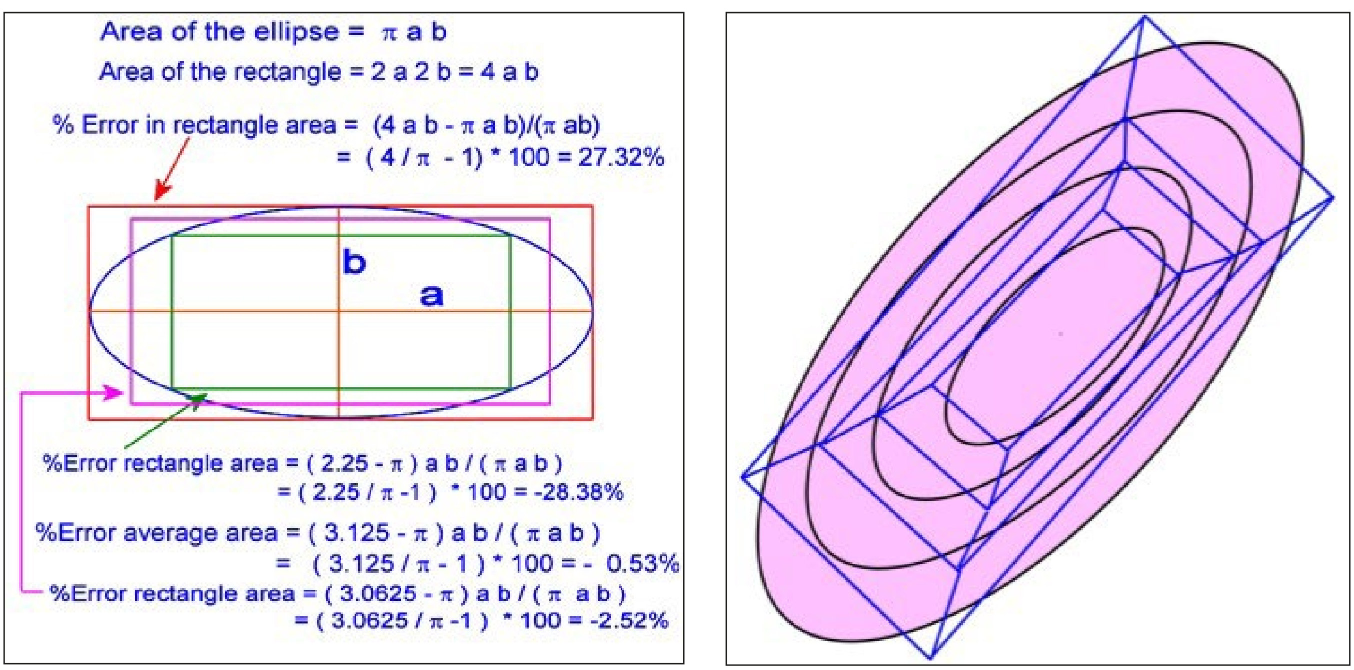

Fig. 38: (Left) shows how to calculate the area of an elliptical contour using an average rectangle with very small error. (Right) Whole or a part of the structure is approximated with a rectangular frustum.

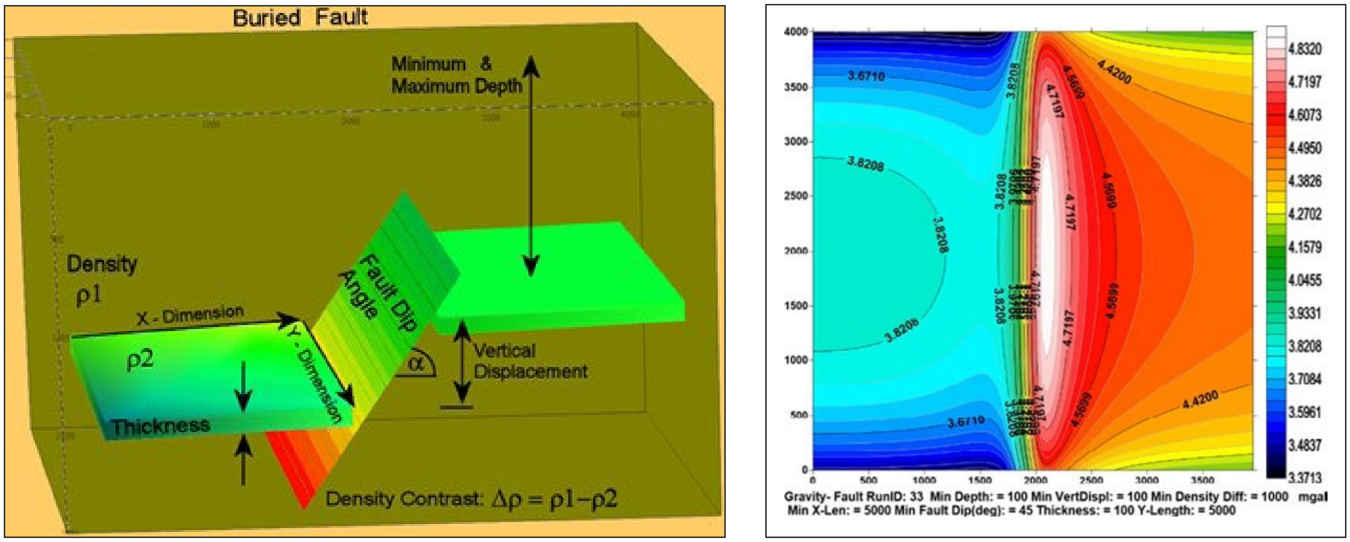

Fig. 39: (Left) shows fault model and necessary parameters for gravity modeling. (Right) shows a gravity map generated with the parameters listed below the map.

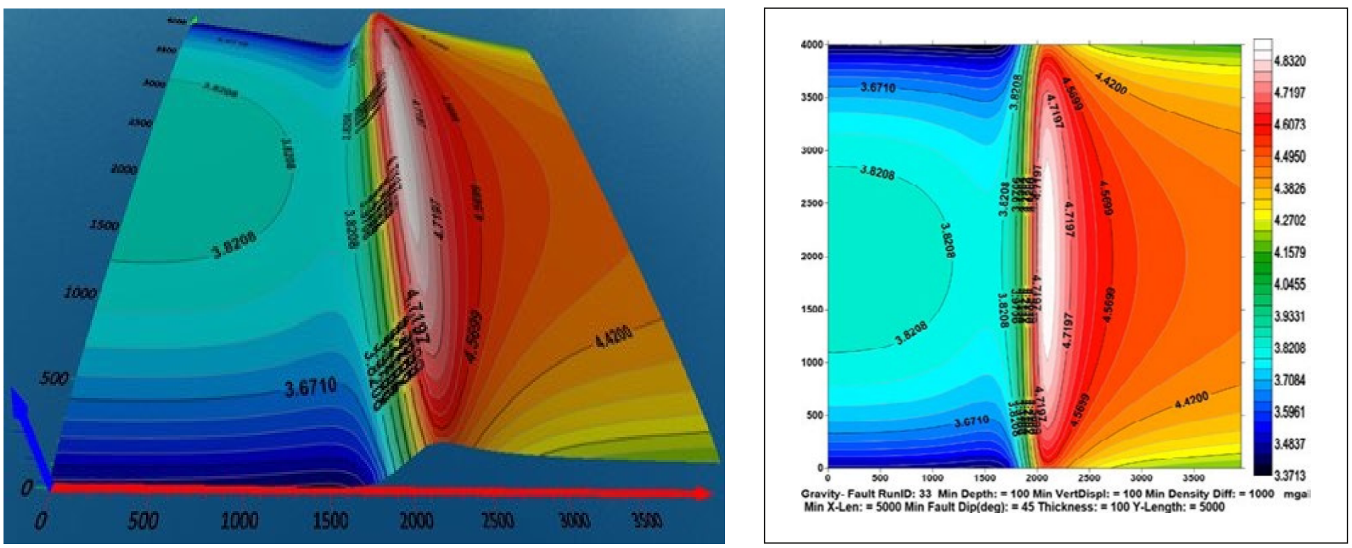

Fig. 40: (Left) is a 3D view of the same gravity map. Fig. (Right) shows 3D surface display of gravity map in Fig. 40 Left.

3D and Surface maps in Fig. 40 (Left and Right) show the gravity anomalies and their relationship to the geometric shape of the model, e.g., the upthrown side of the fault relates to the maximum gravity anomaly.

Magnetic Modeling and Mapping

Magnetic data may be available in a new exploration area or it can be acquired at a fraction of the cost of 3D seismic surveys. It is necessary to properly map the magnetic field by mapping 3-components as shown in Fig. 41. Magnetic modeling and mapping generate magnetic anomaly maps before a magnetic survey is conducted. For existing magnetic surveys, the model parameters may be estimated based on the anomalies in the data. An illustration of a fault and parameters necessary for magnetic modeling are shown in Fig. 42.

Magnetic maps for the Total Intensity (F-component) and vertical Z-component of the magnetic field generated with modeling fault model parameters are displayed in Fig. 43 Above Left and Right respectively. Magnetic modeling and mapping can also complement the seismic exploration for oil and gas.

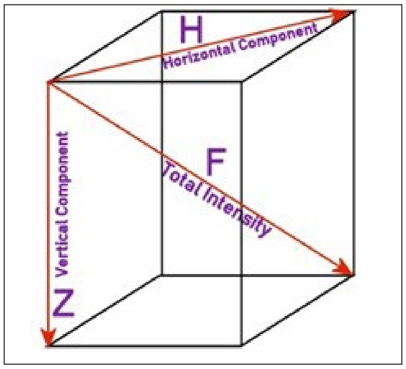

Fig. 41: Shows 3-Components of the magnetic field to model and map.

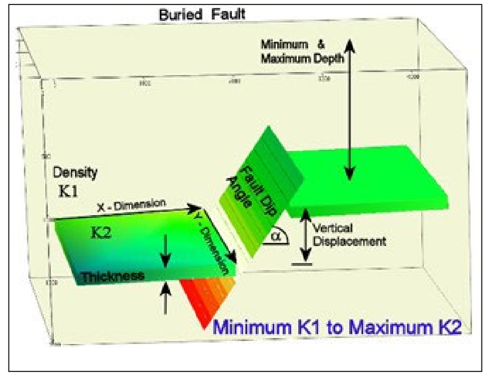

Fig. 42: Shows fault model and necessary parameters for magnetic modeling.

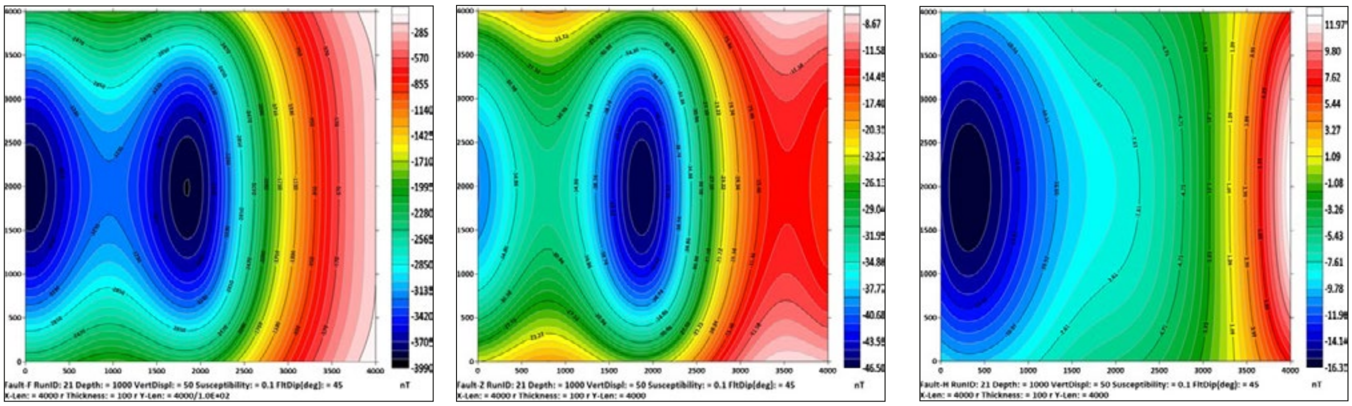

Fig. 43: (Above Left) shows a magnetic map for the Total Intensity F-component of the magnetic field generated with the parameters listed below the map. (Above Right) shows a magnetic map for the Vertical Z-component of the magnetic field generated with the parameters listed below the map. (Left) shows a magnetic map for the Horizontal H-component of the magnetic field generated with the parameters listed below the map.

Conclusions

There are numerous Geophysical Tools available to geologist and geophysicists for the oil and gas exploration. These tools will help geologists and geophysicists enhance their interpretation skills and expand their expertise in oil and gas exploration. These Geophysical Tools are valuable for professional teaching and training of new graduates and geologists and geophysicists.

Acknowledgements

The authors are thankful to Mr. S.C. Verma for recommending this paper for Krishnanunni Memoir, and appreciate Mr. Parthasaradhi formally requesting this publication. The authors acknowledge the permission from International Geophysical Company, Inc., Tulsa, OK 74135 for publishing this work based on IGCTools©[9] Geophysical Software which include the following tools: (1) Geological Structure Contour Modeling (2) Structure Mapping, (3) Acquisition Footprint Analysis & AVO, (4) Gravity Modeling and Mapping, (5) Magnetic Modeling and Mapping. The authors also acknowledge the use of Surfer©[10] mapping software to programmatically generate the maps included in this presentation.

References

Jones, T.A., Hamilton, D.E., and Johnson, C.R., 1986: Contouring Geologic Surfaces with the Computer, Van Nostrand Reinhold Company, p. 314.

Surfer User's Guide, 2002: Contouring and 3D Surface Mapping for Scientists and Engineers, Golden Software, Inc., p. 640.

Tearpock, D.J., and Bischke, R.E., 2003: Applied Subsurface Geological Mapping with Structural Methods, Prentice Hall PTR, p. 822.

Thapar, M.R., 2009: Computer Contouring and Mapping Surfaces Pitfalls and Errors, International Geophysical Company, Inc., 5-day training course, pp 3-22 to 3-26.

Indian Journal of Geosciences, Volume 74, No. 3
July - September, 2020; pp. 257-262

Invited Paper

Aeromagnetic Data Interpretation – Case Histories from Indian sub-continent

Anand S.P. and Mita Rajaram*

Indian Institute of Geomagnetism, Navi Mumbai - 410218.
Corresponding author's email: mitarajaram@yahoo.com

Abstract: The recent advancements in instrumentation, processing techniques etc has made aeromagnetic survey, a very valuable technique for the exploration of natural resources. Aeromagnetic survey is one of the oldest geophysical techniques routinely used as a reconnaissance tool to aid in geological mapping. The aeromagnetic data acquisition in a reconnaissance scale that started in the mid 70's over Peninsular India has now progressed to collecting high resolution airborne magnetic and magnetic gradiometer data which can provide subtle information of the sub as well as near surface features of an area in addition to delineating targets for mineral as well as hydrocarbon exploration. The advancement in data processing and interpretation techniques has helped extract more information from the old reconnaissance scale data. In this paper we provide basic information of magnetic method, different methods of interpretation followed by selected case histories from Indian sub-continent where magnetic data was utilized for structural mapping, crustal studies, exploration, proxy heat-flow, etc.

Key words*:* Aeromagnetic anomalies, Magnetisation, Interpretation

Introduction

In the field of aeromagnetic prospecting, the past few decades have witnessed tremendous amount of development in instrumentation technology and sophisticated data & image processing techniques. This together with the integration of different data sets: geological, geophysical and geochemical, have improved the interpretation several folds and reduced the ambiguity inherent in using a single data set for interpretation. Aeromagnetic or aerial surveys of the magnetic field of the earth are routinely used in exploration of natural resources like minerals, hydrocarbon in addition to mapping the lithology, faults/lineaments etc which can indirectly aid in hazard assessment of a region. The advantage of using aeromagnetic data lies in the fact that it has uniform and rapid data coverage and is independent of the accessibility of the region.

Aeromagnetic surveys, in general, map the variation in magnetic field resulting from the magnetic properties (susceptibility/magnetization) of the underlying rocks. The complex pattern of the earth's regional magnetic anomalies covering a broad spectrum of wavelengths is caused by a variety of geological features in the lithosphere resulting from the long and varied geological history of the earth. Many geological formations by virtue of the amount of magnetic minerals contained in them behave like tiny magnets which will be superimposed on the normal magnetic field of the Earth as anomalies, deviations from the normal pattern. The magnitudes of these anomalies primarily depend on the amount of magnetic minerals contained in the source rock in addition to the depth of burial, degree and direction of magnetization and the attitude of the formation with respect to the direction of Earth's field at the point of observation. Magnetic measurements made at any point at or above the Earth's surface contain contributions from three distinct sources: the core, the crust and the external current distribution (Blakely, 1995). The Core Field (Main Field) is the largest component of the magnetic field (99%) and is believed to be caused by electrical currents in the Earth's fluid outer core. The main field changes not only with latitude but also with time. External magnetic field is a relatively small portion of the observed magnetic field that is generated from magnetic sources within the earth's ionosphere and magnetosphere. Crustal field is the portion of the magnetic field associated with the magnetization of crustal rocks. These three fields are, in principle, separable and one can isolate the magnetic field caused by the crust termed as "Crustal Magnetic Anomalies".

Methods and techniques

Magnetic field measurements are made using magnetometers from different platforms viz ground, sea and air (fixed wing, heliborne, satellite). Improvement in instrumentation technology has led to the development of accurate magnetometers. The field obtained after applying all the necessary corrections to the measurements are plotted to produce crustal magnetic anomaly map of an area which is utilized in identifying faults, lithologic units, configuration of the subsurface, thickness of the sediments etc. The airborne magnetometers essentially map the variation of magnetic minerals in the subsurface formations, the dominant being the mineral magnetite. Magnetite loses its magnetism above 580°C, its Curie temperature & therefore, crustal magnetization normally extends from the surface of the earth to the depth at which this temperature occurs. Major rock forming minerals like quartz, feldspar etc are diamagnetic while minerals like biotite, amphibole, pyroxene, garnet, olivine etc have low magnetic susceptibilities and no remanent magnetism. Major magnetic minerals like magnetite, titanomagnetite, titanohematite, maghemite, pyrrhotite and native iron or Fe-Ni-Cu alloys give rise to magnetic anomalies because they have either large magnetization or high remanent magnetization (Grant, 1984/85). Measurements have shown that sedimentary rocks are generally non-magnetic while the igneous and metamorphic rocks, rich in iron minerals, can be highly magnetic. Crustal magnetic anomalies arising from rocks containing magnetic minerals gives rise to two kinds of magnetization- induced and remanent. Total magnetization which is sensed by the magnetometers is the resultant of the induced and remanent magnetization. The final aeromagnetic crustal anomaly map obtained after applying necessary corrections contain information from all the magnetic sources with varying wavelength that goes right from the point of observation (depending on sampling interval & flight line spacing for aeromagnetic surveys) to the Curie isotherm depth (CID).

After the preparation of an accurate crustal anomaly map, a major challenge is the proper interpretation of the map. The purpose of interpretation, which can be both qualitative and quantitative, is to estimate one or more parameters related to the causative source from observed magnetic field incorporating all available geological, geophysical and other independent information. Qualitative interpretation involves the description of the crustal anomaly maps and the explanation of the major features revealed in the map in terms of the types of likely geological formations and structures that give rise to the evident anomalies. Known geological information available from outcrop within the survey area (or nearby) is correlated with the anomalies and this knowledge is extended into areas where there is no outcrop information (i.e. extrapolation from the known to the unknown) or to extend mapped units into the depth dimension (i.e. to help add the third dimension to the mapped geology). Qualitative interpretation relies on the spatial patterns representing structures like faults, dykes, lineaments, folds etc that an interpreter can easily identify from the crustal anomaly maps. Data transformation (Blakely, 1995) operations like graphical methods, wavelength filters, matched filters, correlation filters, derivative filters, continuation filters, reduction to pole filters, pseudogravity filters etc are routinely utilized for qualitative interpretation where in certain characteristics of the crustal anomaly map, like wavelength, amplitude etc, is either enhanced or suppressed in order to derive meaningful subsurface information (Hinze *et al*., 2012). Quantitative interpretation, like forward & inverse modelling, provide estimates of the geometry, depth and magnetization of the causative magnetic sources.

Estimation of depth to the causative sources plays an important role in any geophysical interpretation. Numerous techniques including manual, semi-automated etc have been developed for the depth to basement estimation from magnetic data (Hinze *et al.*, 2012, and references therein). Early depth-to-source techniques were mostly of graphical nature and applicable only to single-source anomalies. These techniques estimate target parameters by looking at various attributes of an anomaly (curve matching, straight-slope, half-width, amplitude, horizontal extent between various characteristic points, etc). With the advent of digital aeromagnetic data, automated depth to basement methods started to develop and the number keeps growing with continual development of new algorithms. Some of these methods include: Peter's slope, Naudy, Statistical spectral techniques, Werner deconvolution, analytic signal, Euler deconvolution, Source Parameter Imaging™ (SPI™ or local wavenumber), Continuous Wavelet Transform (CWT), Tilt Angle method etc (Hinze *et al*., 2012). However, no single method is best overall. A proper or optimal method should be selected according to the data quality and the nature of the particular geologic problem. In order to produce an accurate depth solution, it is better to use more than one method, together with experience and other geologic and geophysical knowledge.

Case histories

In this section, we present some results from different geological provinces of Indian sub-continent where magnetic data interpretation has been carried out for crustal studies, lineament mapping, exploration etc. A detailed description of the development of airborne geophysics in India along with case histories using aeromagnetic data was provided by Murthy (2007). We have included few case histories from shield areas, sedimentary basins, offshore regions in addition to examples showing utility of magnetic data in exploration & generation of proxy heat flow map of the Indian sub-continent.

Rajaram and Anand (2014) has applied interpretation techniques like differential reduction to pole (Hinze *et al*., 2012), analytic signal, tilt derivative etc to the regional aeromagnetic data of Peninsular India (Rajaram *et al*., 2006, GSI, 2000) to identify magnetic source distribution, tectonic elements, terrane boundaries, suture zones and metamorphic history (Fig.1). They inferred the Chitradurga boundary shear (dividing western & eastern Dharwar) and Sileru shear (boundary between Bastar craton and Eastern Ghat Mobile belt) to represent terrane boundaries while the Palghat-Cauvery and Achankovil shear zones represent suture zones. They were also able to delineate the metamorphic facies ranging (in the region below 17°N) from Granulite to greenschists from the interpretation of the data. From the analysis, interpretation, 2.5D forward modelling and 3D magnetic susceptibility inversion of high resolution (flight altitude – 120 m agl) aeromagnetic data over the poly-deformed Paleoproterozoic Sonakhan schist belt (Central India), Sridhar *et al.* (2017) mapped the extension of Sonakhan schist belt below Singhora sedimentary rocks. Computation of depth to magnetic basement suggested a complex pattern of NNE-SSW to NE-SW trending depressions separated by linear NS trending basement ridge. The identified EW trending Trans-Chhattisgarh Aeromagnetic Lineament (TCAL) was interpreted to represent, a block fault with northern block down-thrown and affected the basement rocks comprising the Sonakhan Greenstone Belt and Sambalpur Granitoids. Results from the profile modelling combined with 3D inversion suggested the basin subsidence was controlled by NE-SW tending regional faults in an active system (Sridhar *et al*., 2017).

Indian Institute of Geomagnetism carried out ground magnetic surveys along accessible roads over the Deccan trap covered region bounded by 72° to 78°E and 16° to 19°N where a glaring gap existed in the composite magnetic anomaly map of India and its adjoining regions (Rajaram *et al*., 2006). From a combined analysis of aero (bordering the trap covered regions), ground (Fig.1) and marine (in the continental shelf) magnetic data the northward extension of the major shear zones, schist belt etc below the Deccan trap was inferred by Rajaram *et al.* (2017). They also delineated a major NE-SW lineament under the traps, extending from the west coast almost up to Godavari graben, which was inferred to represent the northern boundary of the Proterozoic Bhima-Kaladgi basins. Low pass filtered map generated from the high resolution aeromagnetic data over the seismically active Koyna region helped to delineate the sub-basalt geology and map deeper NW-SE & shallower

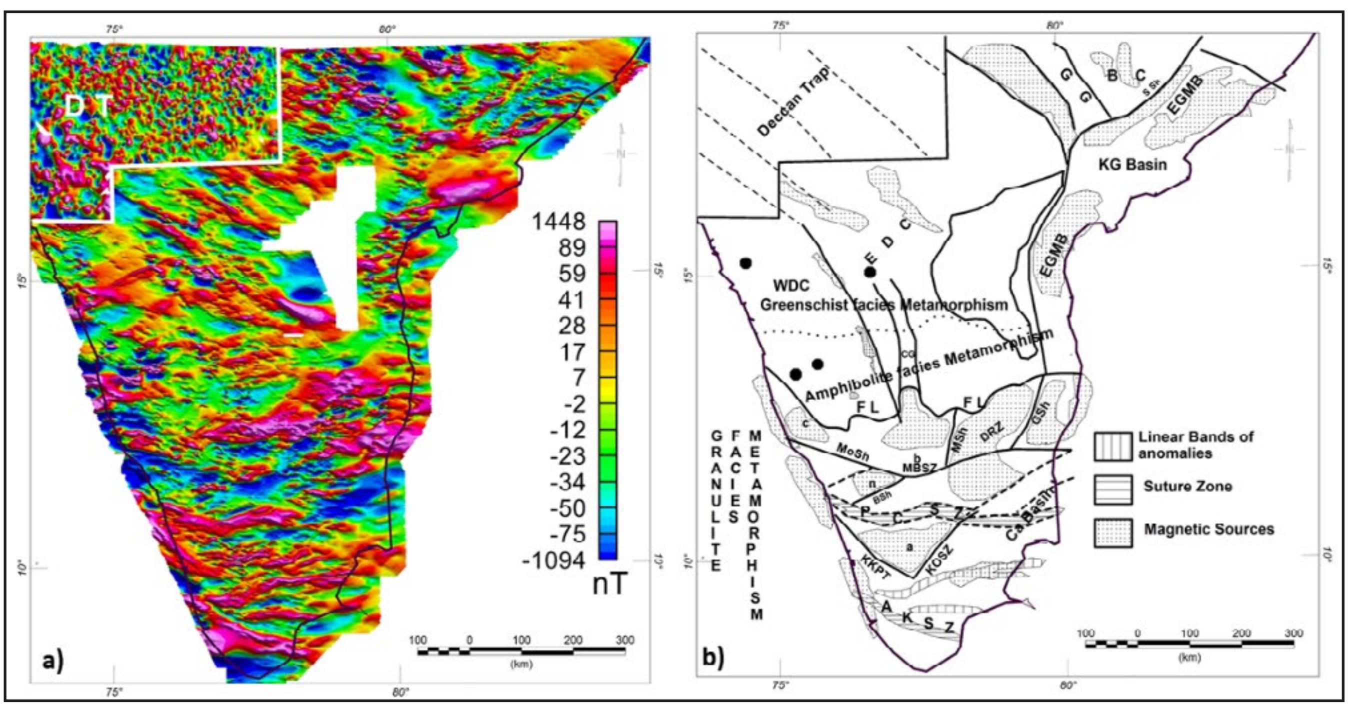

Fig. 1: (a) Differential reduction to pole (DRTP) map of the aeromagnetic anomalies over Peninsular India. The colour bar shown is for DRTP map. In the left top, above the white line, is the ground magnetic anomaly map over the Deccan Trap (DT) region. (b) Interpreted tectonic map of Peninsular India from a combination of different analysis of the DRTP map and the lineaments from ground magnetic data over the DT. The abbreviations are as follows: Basins: Ca-Cauvery, KG-Krishna Godavari, GG-Godavari graben. Lineaments/faults/shears: SSh- Sileru shear, CBS- Chitradurga boundary shear, FL- Fermor line, GSh- Gangavalli shear, MSZ-Moyar shear zone, SASh - Salem Attur shear, MSh - Mettur shear, BSh - Bhavani shear, PCSZ - Palghat Cauvery shear zone, KKPT – Karur Kambam Painvu Trichur, KOSZ – Karur Oddanchatram shear zone, AKSZ -Achankovil shear zone. Hills: c - Coorg, b - Biligrangan, n - Nilgiri, a - Anamalai. Major blocks: EGMB - Eastern Ghat mobile belt, WDC - western Dharwar craton, EDC - eastern Dharwar craton, KKB - Kerala khondalite block. DRZ – Dharmapuri Rift Zone, CG - Closepet granite. Filled circles shows location of iron ores.

EW features (Gupta *et al.,* 2016). Sub-basalt imaging of ground magnetic data over the Chikotra basin within the southern periphery of Deccan Volcanic Province, combining the results from filtering operations, Euler deconvolution and statistical depth estimation, yielded the presence of ~900 m thick Kaladgi sediments below the Deccan trap flows (Anand *et al*., 2016). Ultra high resolution helicopter borne magnetic survey with a sensor elevation of 60 m and line spacing of 200 m was carried out over the Kaladgi basin including the southern periphery of the DVP (Sridhar *et al*., 2018) which provided insight into the basement structures and their role in basin evolution. Depth to basement analysis suggested that the Kaladgi basin is an open deep basin which is divided into several sub-basins, separated by fault controlled NE-SW and NW-SE oriented basement ridges. Numerous scattered anomalies with moderate to high remanence have been interpreted to represent concealed granitic plutons with associated stocks and apophyses (Sridhar *et al*., 2018).

Interpretation of regional aeromagnetic data (flight height 1500 m & line spacing 2 km) over the Kutch Rift basin, mostly covered by inaccessible Rann of Kutch, salt plains etc, delineated seven distinct magnetic zones based on the nature of the magnetic anomalies (Chandrashekar *et al*., 2018). Integrating with remote sensing data they inferred that the central portion of Kutch mainland has undergone intense tectonic activity resulting in a number of complex geological structures. By applying the edge detection techniques like analytic signal, Horizontal Gradient Magnitude (HGM) and Euler deconvolution on the semi-detailed high resolution aeromagnetic survey data (line spacing of 1km and drape flight altitude 300 m), Radhika *et al*., (2017) delineated 14 lineaments / faults (Fig. 2) some of which do not have any surface expressions i.e., they lie within the sedimentary strata or in the Rann of Kutch. They inferred that many of these lineaments may represent basement related faults and may have been reactivated many times in the past. From depth analysis using power spectral method, located Euler Deconvolution and analytic signal method, Radhika (2019) interpreted that the Banni basin is divided into western and eastern sub-basins with average sediment thickness of 5 km & 4 km respectively while the Wagad uplift region has an average of 2.3 km thick sediments.

Aeromagnetic data individually and in conjunction with remote sensing & radiometric data is extensively used as reconnaissance tool for mineral exploration. Integrated geophysical studies (magnetic, gravity, resistivity, EM, VLF etc) were carried out in the Beldih mine area at the central part of the South Purulia Shear Zone (SPSZ), which has reported low grade uranium mineralization (Mandal *et al*., 2013). This study helped in understanding the nature of the geophysical signatures associated with Uranium mineralization which can be utilized for exploring regions of concealed uranium deposits. Atomic Minerals Directorate (AMD) has carried out aeromagnetic surveys over the Paleo-Meso Proterozoic Gwalior basin with N-S lines of 500 m interval and 120m flight altitude (Markandeyulu *et al*., 2012). First vertical derivative of TMI-RTP, tilt-angle derivative images and Euler depths were used to map precisely the location of litho-contacts, lineaments and structural features within the basin. The amplitude and textural character of the aeromagnetic data were utilized to delineate the alteration zones within the different formation that helped in narrowing down the target areas for uranium exploration.

Geological survey of India (GSI) acquired airborne magnetic and radiometric data over Ratnagiri and Mumbai offshore basins covering latitude 16^{o} to 20^{o}N, with a flight altitude of 120 m above sea & ground levels and line spacing of 2500 m (Gouda *et al*., 2019) with an aim of delineating the structural elements, the extent of the hydrocarbon bearing sedimentary basins and the basement configuration. Analysing the magnetic response using a combination of amplitude, wavelength and analytic signal they could differentiate the Archean Granite-gneiss and schistose rocks of the Dharwar Supergroup, Proterozoic sediments of Kaladgi basin, Deccan trap flows and extent of several sub-basins bearing Tertiary sediments. Depth to basement computed using Euler deconvolution, SPT^{TM} and spectral analysis suggested shallower depths in the region covered by traps and Archeans, intermediate depths in the transitional region covered by Deccan traps & sediments and deeper depths where there is thick pile of sediments (Gouda *et al*., 2019). Their analysis suggests that the basin like features delineated between 16^{o}15′ & 18^{o}N latitudes may be potential regions for oil prospects.

From an analysis of the crustal magnetic field, it is possible to make an estimate of the depth below which no magnetic sources exist, which has become synonymous with the depth to the Curie temperature though sometimes it may represent a petrological boundary. As magnetite with a Curie temperature of 580^{o}C is believed to be the dominant magnetic mineral in the deep crust within the continental region, it is reasonable to assume that below the Curie isotherm the lithosphere is virtually non-magnetic. Thus, from the magnetic field measurement it is possible to indirectly derive the temperature data that in turn can be translated to give the geothermal gradients of a region. Curie isotherm depth (CID) computed over the Indian sub-continent (Rajaram *et al*., 2009) and Peninsular India (Anand and Rajaram, 2007) suggested that it is shallow in the mobile belts and deeper in the cratons. Comparison of CID with Deep Sesimic Sounding profiles, Rajaram *et al.* (2009) inferred that CID is generally shallower than the Moho depth implying that it possibly represents a thermal boundary rather than a compositional change. Depth to the bottom of the magnetic sources computed using modified centroid method in the Central Indian region provided values ranging from 22 km in the south west part of Deccan trap to 43 km in the Chhattisgarh Basin (Bansal *et al*., 2013). A proxy

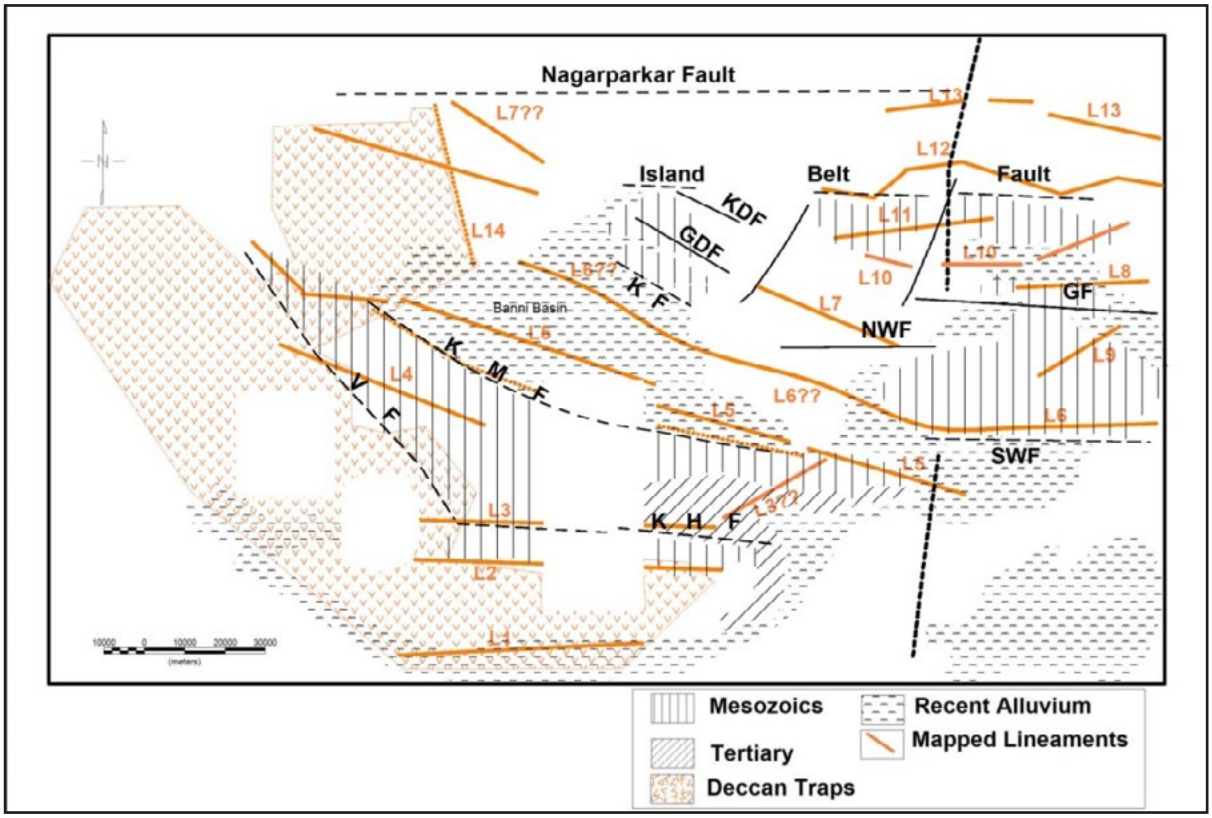

Fig. 2: Structural Framework of Kutch Rift Basin (Radhika *et al.*, 2017), KHF – Katrol Hill Fault, VF – Vigodi Fault, KMF – Kutch Mainland Fault, SWF-South Wagad Fault, NWF – North Wagad Fault, GF – Gedi Fault, KF – Khavda Fault, GDF – Gora Dongar Fault, KDF –Kala Dongar Fault. L1 to L14 are the lineaments interpreted from aeromagnetic data analysis.

heat flow map of Peninsular India from the computed CID (Anand and Rajaram, 2007,) was generated utilising the 1D heat conduction, steady state thermal model for the continental crust. Mobile belts and rift zones were characterized with higher heat flux while cratons were associated with lower heat flow values (Rajaram *et al*., 2013).

Conclusion

The last few decades have seen tremendous amount of development in aeromagnetic prospecting in terms of technology, data collection and processing techniques. The data quality and resolution of high resolution aeromagnetic (HRAM) surveys now provide levels of detail that are compatible to those derived from seismic, well and surface geological data. Sophisticated interpretation techniques have evolved to enable extraction of maximum information from the collected data. Utility of Aeromagnetic data has come a long way from being a mere reconnaissance tool to being an important method to work with. Aeromagnetic data collected over different Geological provinces are utilised to look below the subsurface and interpret them in terms of resources, tectonics, geology, heat flow, mineral exploration, hydrocarbon exploration and lineament mapping. It is the integration of different Geophysical data that lends credence to the interpretations. The Geological Survey of India has recently started acquiring high-quality multi-sensor aero-geophysical survey (including aeromagnetic) over the Obvious Geological Potential and adjoining areas. This high-resolution data coupled with improved data analysis techniques can provide valuable information that can be utilized for exploration of natural resources. In addition, covering the whole country and adjoining offshore regions on the basis of uniform parameters will go a long way in generating a seamless aeromagnetic map of Indian sub-continent.

Acknowledgement

We thank Director, IIG, for providing permission to publish this work.

References

Anand, S.P., Rajaram Mita, 2007: Aeromagnetic Signatures of the Cratons and Mobile Belts over India. *International Association for Gondwana Research, Japan, Memoir*, **10:** 233-242.

Anand, S.P., Erram, V.C., Patil, J., Pawar, N.J., Gupta, G., Suryavanshi, R.A. 2016: Structural mapping of

Chikotra Basin in the Deccan Volcanic Province of Maharashtra, India from ground magnetic data. *Journal of Earth System Science*, **125**: 301–310.

Bansal, A.R., Anand, S.P., Mita Rajaram, Rao, V.K. and Dimri V.P., 2013: Depth to the bottom of magnetic sources (DBMS) from aeromagnetic data of Central India using modified centroid method for fractal distribution of sources. *Tectonophysics*, **603**: 155-161.

Blakely, R.J., 1995: Potential theory in Gravity and Magnetic applications. Cambridge University Press, Australia.

Chandrasekhar, P., Chandra Mouli, K., Rao, D.P. and Dadhwal, V.K., 2018: Subsurface geological structure and tectonics as evidenced from integrated interpretation of aeromagnetic & remote sensing data over Kutch sedimentary basin, western India. *Current Science*, **114(1)**: 174–185

Grant, F.S. (1984 / 1985): Aeromagnetics, geology and ore environments, I. Magnetite in igneous, sedimentary and metamorphic rocks. *Geoexploration*, **23**: 303-333.

Geological Survey of India (GSI), 2000: Aeromagnetic Image of a Part of Peninsular India (Scale 1:2,000,000). GSI Publication.

Gouda, H.C., Rajaram, H, Rajeshkumar, Rao, J.A.N., Dinesh Gupta, Eswari, V, Preeti, 2019: Study of Structures & Basement configuration of Hydrocarbon bearing Offshore Regions of Ratnagiri-Mumbai Coast-An Insight from Aeromagnetic Data. *Journal of Geophysics*, **XL**, 21– 37

Gupta, H. K., Arora, K., Rao, N.P., Roy, S., Tiwari, V.M, Patro, P.K., Satyanarayana, H.V.S., Shashidhar, D., Mahato, C.R., Srinivas, KNSSS *et al*., 2016: Investigations of continued reservoir triggered seismicity at Koyna, India. *Geological Society, London, Special Publication*, **445**: 151–188.

Hinze, W. J., Ralph R. B., Saad. A. H. 2012, Gravity and Magnetic Exploration, Cambridge University Press.

Mandal, A., Biswas, A, Mittal, S., Mohanty, W.K., Sharma, S.P., Sengupta, D., Sen, J. and Bhatt, A.K., 2013: Geophysical Anomalies Associated with Uranium Mineralization from Beldih Mine, South Purulia Shear Zone, *India. Journal Geological Society of India*, **82**: 601-606.

Markandeyulu, A., Patra, I., Raju, B.V.S.N, Chaturvedi, A.K. and Parihar, P.S., 2012: Interpretation of Aero-Magnetic Data & Satellite Imagery to Delineate Structure–A Case Study for Uranium Exploration from Gwalior Basin, India. *Journal Geological Society of India*, **80**: 382-392.

Murthy, B.S.R., 2007: Airborne Geophysics and the Indian Scenario. *Journal Indian Geophysical Union*, **11(1)**: 1-28.

Radhika, P.R., 2019: A Geopotential Approach to Reveal the Buried Basement Structure of the Kutch Rift Basin, Western India. Ph D Thesis (submitted) Andhra University.

Radhika, P.R., Anand, S.P. and Mita Rajaram, 2017: Structural Mapping of Kutch Rift basin from Aeromagnetic data. Journal of Geophysics, **38(3)**: 187-197.

Rajaram, M., Anand, S.P. and Singh,K.H. 2013. Proxy heat flux and magnetization model from satellite magnetic data. Journal of Geophysics, **34(1)**: 55-61.

Rajaram, M. and Anand, S.P. 2014: Aeromagnetic signatures of Precambrian shield and suture zones of Peninsular India. *Geoscience Frontiers*, **5(1)**: 3-15.

Rajaram, M., Anand, S.P. and Balakrishna, T.S., 2006: Composite magnetic anomaly map of India and its contiguous regions. *Journal Geological Society of India,* **68**: 569-576.

Rajaram, M, Anand, S.P., Hemant, K. and Purucker M.E., 2009: Curie isotherm map of Indian subcontinent from satellite & aeromagnetic data. *Earth and Planetary Science Letters*, **281(3-4)**: 147-158.

Rajaram, M., Anand, S.P., Erram V.C. and Shinde B.N., 2017: Insight into the structures below the Deccan Trap-covered region of Maharashtra, India from geopotential data. *Geological Society, London, Special Publication*, **445**: 219–236.

Sridhar, M, Ramesh Babu,V., Markandeyulu, A., Raju, B.V.S.N., Chaturvedi, A.K. and Roy, M.K. 2017: A reassessment of the Archean-Mesoproterozoic tectonic development of the southeastern Chhattisgarh Basin, Central India through detailed aeromagnetic analysis. *Tectonophysics*, **712-713**: 289-302.

Sridhar, M, Markandeyulu, A., Chawla, A.S. and Chaturvedi, A.K., 2018: Analyses of Aeromagnetic Data to Delineate Basement Structures and Reveal Buried Igneous Bodies in Kaladgi Basin, Karnataka. *Journal Geological Society of India,* **91**: 165-173.

Indian Journal of Geosciences, Volume 74, No. 3
July - September, 2020; pp. 263-268

Invited Paper

Tectonic framework revealed by Gravity Surveys at Varkala Beach, Kerala

Dinesh Gupta[1]* and S.S. Ganguli[2]

[1]*Former Director General, Geological Survey of India*
2 Geological Survey of India, Central Headquarters, Kolkata
**Corresponding author's email: dineshguptagsi@yahoo.co.in*

Abstract: Gravity surveys are an ideal geophysical tool to understand structural as well as tectonic framework of geological domain. Regional surveys provide a broader picture but when a small area needs to be probed, a close grid detail surveys will be of paramount importance. Accordingly, at Varkala beach, Kerala, where a vertical cliff is exposed, close grid gravity surveys have been carried out with 5-10 m station interval. The cliff section runs parallel to the coast line for nearly one kilometer and expose the lithounits ranging from Tertiary to Recent.

Geologically, Varkala and surrounding area form a part of Kerala Khondalite belt (KKB) of the Southern Granulite Terrain (SGT). The Precambrian crystalline of the area is unconformably overlain by Tertiary sequence of Warkalli Formation of Mio-Pliocene age. Warkalli Formation comprises unconsolidated sand, variegated clays, white plastic clays, carbonaceous clay and lenses of lignite.

The survey reveals basement is dipping towards east resulting in thickening of sedimentary rocks away from the beach. Results of the gravity surveys identified a fault along the contact between the beach and cliff with thick sequence of sediments in the down thrown block. In next phase of tectonic event, these sediments deposited down thrown block got uplifted causing the present topography of cliff at Varkala beach.

The presence of thick clay layer is the major geological factor causing wave undercutting as well as overhang collapse.

Keywords: Varkala, Kerala, cliff, close grid gravity, down thrown block, fault.

Introduction

Close grid gravity survey has been carried out across the exposed cliff of Varkala beach to understand basement topography, structural fabric, density distribution of the litho formations overlying the basement and the possible role of these factors for the denudation of the cliff as part of land slide studies (Ganguli and Gupta, 2012)

Varkala beach, picturesque location along the south west coast of Kerala (Fig. 1), a major tourist destination, attracts large number foreign and domestic tourist. The beach is narrow silver sand beach and has a ~ 30 m cliff stands immediately to the east. A cliff adds a unique dimension to the beauty of the beach. The cliff is known as Varkala cliff and exposes all the litho units from Tertiary to recent.

The cliff section runs parallel to the coast line over a kilometer. The wave cut cliff has become vulnerable as it is experiencing severe denudation and slowly receding landwards. Both natural and anthropogenic factors are acting together for its denudation. Wave undercutting is a major cause for over hang collapse. Nature of litho units is also adding to the cause.

The area is traversed by a number of faults (Fig. 2). One major fault runs parallel to the coast is known as West Coast Fault (WCF). The tectonic features aligned parallel to the continental margin of India were formed during northwards drift of Indian plate and those traverses across the margin were formed before the drift. The pre-drift tectonic features, running across the WCF, were formed during Jurassic/Cretaceous and Tertiary period (Chandrasekhram, 2001 and references there in). From the tectonic map it is evident that the study area (Varkala) was subjected to NW-SE faulting. In a schematic model describing structural evolution along 9.15^{o} N profile; Chandrasekhram, 2001, opined that vertical movements of the blocks adjacent to the WCF during the late Tertiary is responsible for marine and continental sedimentation.

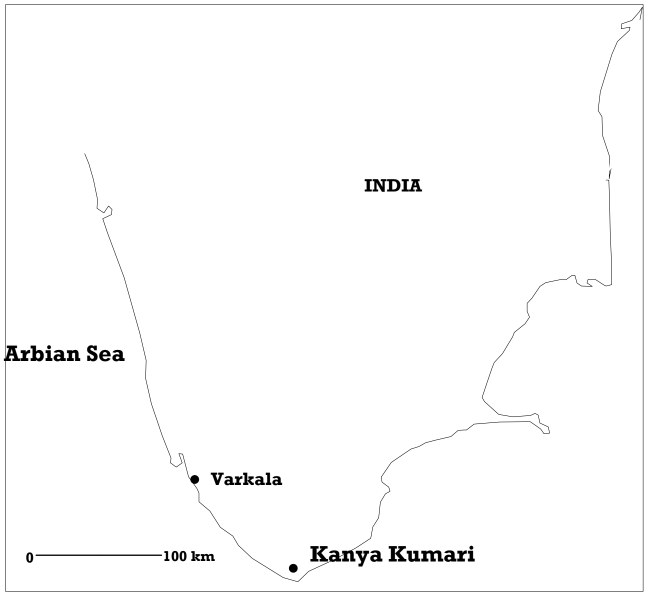

Fig.1: Location map of the study area.

Geological Set-Up

Varkala and adjacent area forms a part of Kerala Khondalite Belt (KKB) of the Southern Granulite Terrain (SGT). The Precambrian crystalline of the area is uncomfortably overlain by Tertiary sequence of Warkalli Formation. Varkala cliff exposes Warkalli formation of Mio-Pliocene age representing lithounits of unconsolidated sands, variegated clays, white plastic clays, carbonaceous clay and lenses of lignite. The beds are almost horizontal in nature. On the basis of lithology and spatial distribution, Warkalli Formation is suggested as shallow water shoreline deposit (Rao *et al.,* 1983).

The generalized stratigraphy of the area is as below

Age	Lithology
Recent (Kaddapuram Fornation)	Beach sand
Recent to sub-recent	Laterite
Unconformity	
Tertiary (Warkalli Formation)	Current-bedded friable variegated sandstone interbedded with plastic clay and variegated clays
	Carbonaceous and alum clays with lignite seams
	Gravel and pebble beds. Base marked by gibbistic clay
Tertiary (Quilon Formation)	Limestone and calcareous marl
Unconformity	
Archean	Crystalline rocks

Gravity Surveys

Close grid Gravity surveys were conducted across the cliff. The CG-3 instrument was used for Gravity survey which has inbuilt software for taking care of tidal correction. Seven profiles were laid down along the accessible tracks (Fig. 3). The longest profile runs along Papanasam beach road, in the southern part of the area where cliff is absent. The last two profiles were taken along Black beach (locally known) where the cliff ceases to exist. Rest of the four profiles laid in the stretch where cliff has maximum elevation (Helipad Profile).

The colour shaded elevation relief map of the Helipad area is shown in Fig. 4 (Ganguli et.al., 2012). At this site over hang collapse and debris slide is severe. The survey profile length and spatial distributions are mainly constraint by accessibility

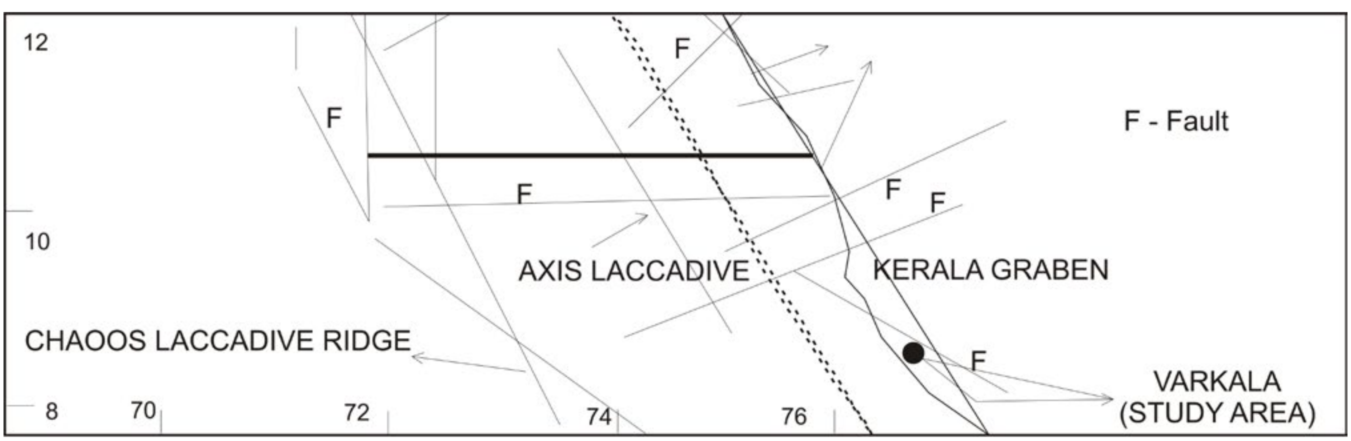

Fig. 2: Regional Tectonic map of study area (modified from Chandrasekhram, 2001).

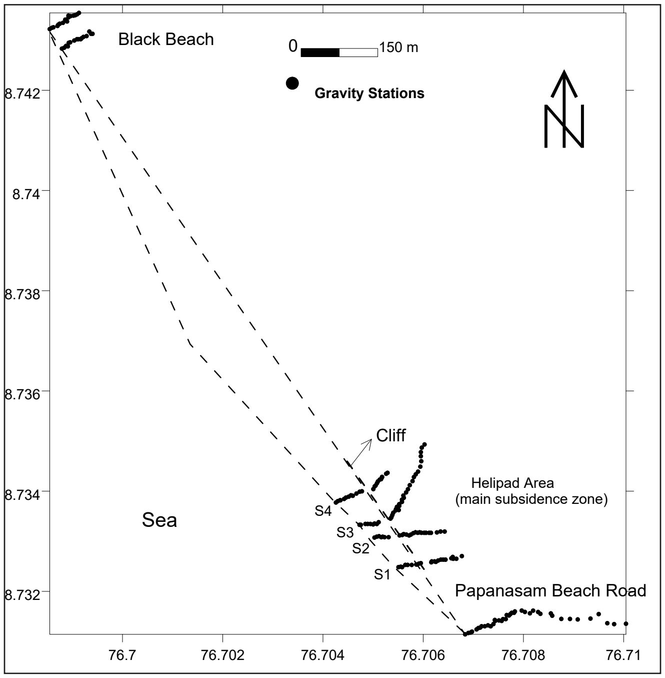

Fig. 3: Gravity Station Distribution Map, Varkala Beach, Kerala.

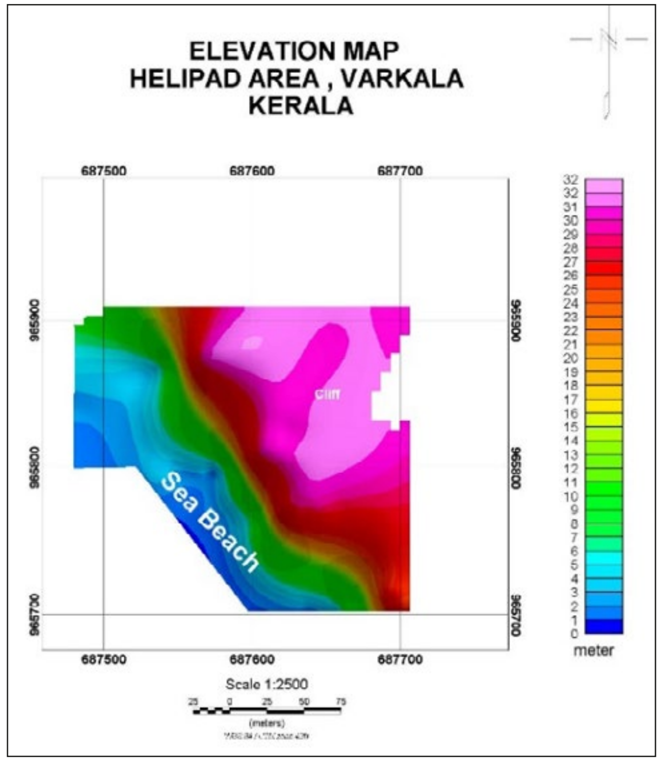

Fig. 4: Elevation Contour Map, Varkala Beach, Kerala.

since all the major hotels, restaurants have been constructed at the top of the cliff. The gravity data was acquired with 5 and 10 m station interval as per the availability of space.

After applying drift correction entire data was subjected to free air correction (0.3048 m Gal/m) and Bouguer correction, and reduced to a single standard datum at mean sea level (msl). Bouguer anomaly over the study area was computed for standard crustal density of 2.67 gm/cc. For latitude correction international gravity formula 1980 was used.

Bouguer gravity anomaly is characterized by vertical as well lateral density variation. It depends on reducing gravity measurements at Earth's surface to enhance the expression of geological targets. The anomaly derived after removal of predictable correction is termed as Bouguer gravity anomaly. Bouguer anomaly maps have been traditionally used for providing subsurface geological picture. Bouguer gravity profiles along the S1 to S4 (Fig. 3) are presented below (Fig. 5). It is quite evident from the profiles that there is sudden fall in gravity values at the contact of the sea with the continent. This leads to the inference that the contact is faulted.

Gravity anomaly profile along Papanasam beach road is presented in Fig. 6 and Bouguer gravity anomaly is of the order of 1.14 mGal ranging from -34.9 mGal to -36.04 mGal over a distance of 360 m and it is decreasing gently away from the shoreline. This indicates basement is dipping away from the sea side or dipping towards east.

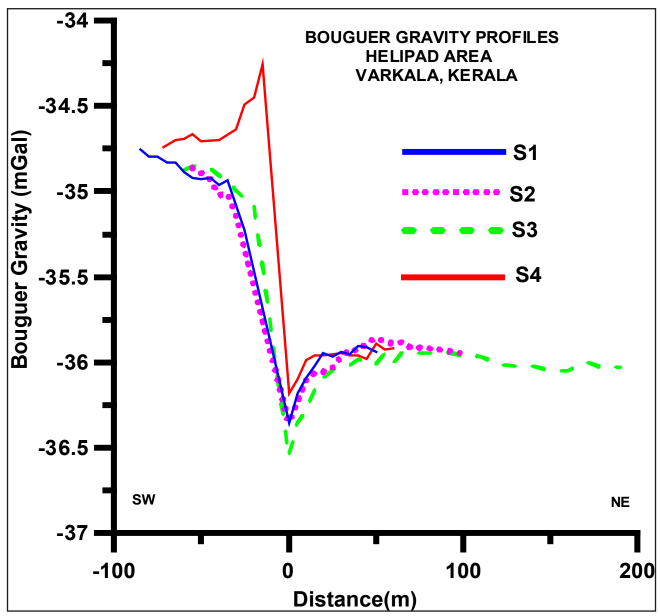

Fig. 5: Bouguer Gravity profiles along S1 to S4 lines, Varkala Beach, Kerala.

Gravity anomaly profile near Helipad Area from west to east presented in Fig. 7 shows magnitude of bouguer gravity anomaly is 1.6 mGal ranging from -34.8 mGal to -36.4 mGal over a distance of 140 m and it is decreasing away from the shoreline. This indicates basement is dipping away from the

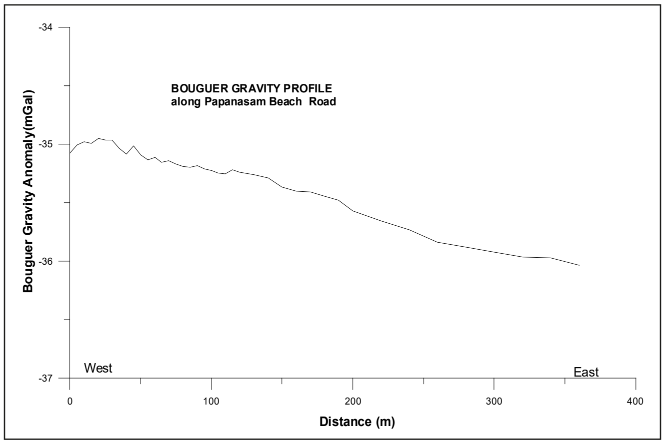

Fig. 6: Bouguer Gravity Profile along Papanasam Beach Road, Varkala Beach, Kerala.

seaside or towards east. The sudden fall of gravity value in the span of 80 meters indicates faulted contact of sea with the continents.

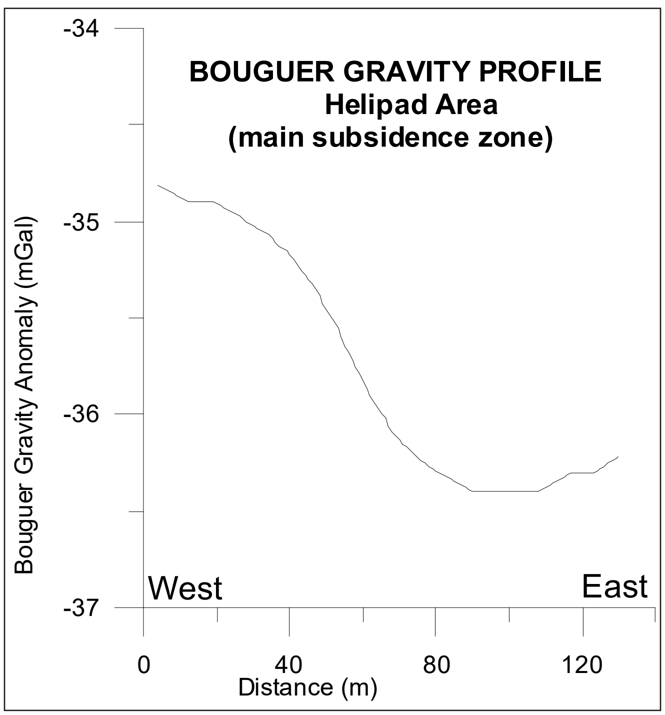

Fig. 7: Bouguer Gravity Profile Helipad Area, Varkala Beach, Kerala.

Bouguer gravity image map along the Helipad profile is presented in Fig. 8. The profiles at Helipad are showing a sharp fall of gravity value at the contact of beach and cliff. A prominent gravity low has been recorded over cliff and further east as compared to beach and further west towards sea. A diagnostic gravity low closure 'L' (Fig. 8) has been observed over cliff and an over hanging collapse was also observed at this place. This signifies a structural break or sudden increase of basement depth due to vertical faulting along the contact of beach and cliff. Beach is uplifted block and cliff is down thrown block, in which subsequent sediment deposition took place. In the second phase of tectonic disturbances, this sediment deposited in down thrown block got up lifted and the present topography is visible on the cliff.

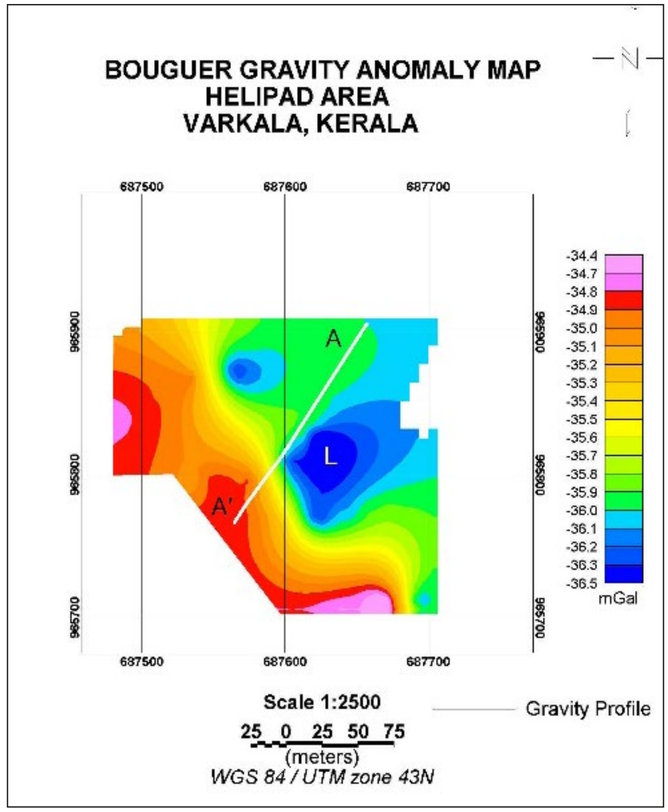

Fig. 8: Bouguer Gravity Image Map, Varkala Beach, Kerala.

Spectral Analysis of Gravity Data

Power spectrum analysis is a frequency domain approach, which is capable of separating the information from different sources at different depth. A simple relation between power spectrum and depth values of ensemble of uncorrelated gravity sources exist and the relationship is expressed as (Blakely, 1995)

$$P(w) = A\exp(-2|w|h),$$

where $P(w)$ is the power spectrum, A is the constant for randomly distributed source, w is the wave number; h is the depth to the source.

Taking logarithm in both sides the above equation yields

$$\ln(p) = -2|w|h + A$$

Thus depth can be found from slope of the plot between log power spectrum and wavenumber. The logarithmic plot of spectrum amplitude of the gravity anomaly due multiple ensembles would result multiple straight line segment. Slope at smaller wavenumbers give the depth of deeper source and subsequent slopes at higher frequency estimates the depth to the shallower sources.

The power spectrum for gravity data is displayed in Fig. 10. Gravity spectrum can be interpreted in a two linear slope segment and used to estimate the depth of the density interfaces. The deeper density interface occurs at 21.5 m while the shallower interface occurs at 8.0 m. The interface may be due to different level of compaction of litho units.

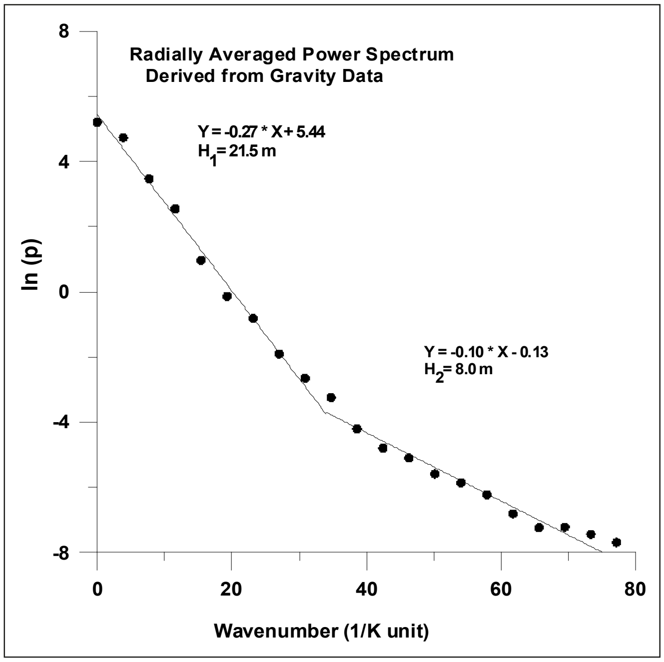

Fig. 9: Radially Averaged Power Spectrum derivative from Gravity Data, Varkala Beach, Kerala.

2D Gravity Modeling

2D modeling has been attempted over a NE-SW trending transects A-A' (Fig. 8) running across the gravity gradient of the area. The profile length is 167 m. Central Ground Water Board (CGWB) has drilled a few test drill holes at Varkala area but basement rock was not encountered up to the depth of 80 m (CGWB, personal communication). The bathymetry map (south of 9° latitude) shows that the 20 m contour line is running ~ 15 km away from the coastline and shallow sea sediments are mainly clayey (Rao *et al.,* 1983). These are the indirect evidence considered for constraining the gravity model. Density of crust was assigned standard value 2.67 gm/cc. The stratigraphy of the Varkala area shows basement is overlain by Tertiary and Quaternary formations, hence 3-layer density model is considered over the cliff however the density and thickness of the layers were modified to fit the observed gravity response.

The model (Fig. 9) shows sudden increase of basement depth along the contact of beach and cliff. This indicates a basement fault with beach as the up thrown block and cliff side as the downthrown block. The marine sedimentation took place over the downthrown block and two low density formations of total thickness ~ 120 m are present over the basement. The top lowest density (1.5 gm/cc) formation with thickness varying from ~25 to 115 m, is clayey in nature and indicating lagoonal environment of deposition. Probably vertical movement across the coast at the Helipad area had created a lagoon like structure over which sedimentation took place. The horst and graben structure as evident from the above gravity model is very much in consonance with the tectonics of the area.

However, such structure or vertical movement has not been indicated by the gravity data over traverse of Papanasam beach road as well as at the Black beach. At the same time cliff

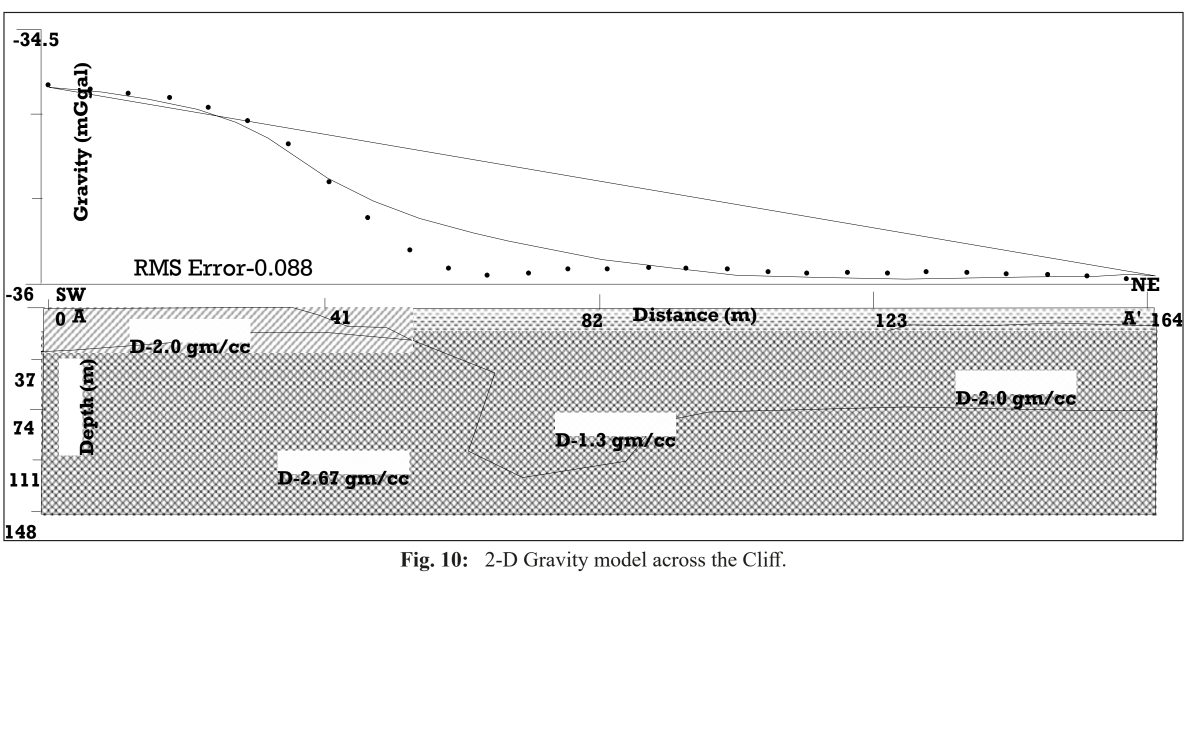

Fig. 10: 2-D Gravity model across the Cliff.

is also absent at these two places, indicating limited strike of the structure. The thick deposit of clay probably is the major contributing factor for the denudation of the cliff since the low density clay layer vulnerable to wave undercutting as well as susceptible to stress failure.

Airborne Geophysical Surveys

AMSE wing of GSI (AMSE 1982) has carried out airborne Geophysical surveys comprising magnetic and radio metric methods in the study area, and aero-magnetic map is presented in Fig. 11. A gentle magnetic low gradient has been observed from west to east i.e.as we are moving away from the sea towards land. This indicates basement is dipping towards east and sedimentary thickness also increases away from the beach. But the aeromagnetic results are not as diagnostic as gravity results particularly for the small scale survey like this mainly because of very sparse flight line spacing (4 km). However, the inference drawn from the aeromagnetic results agrees well with the gravity results.

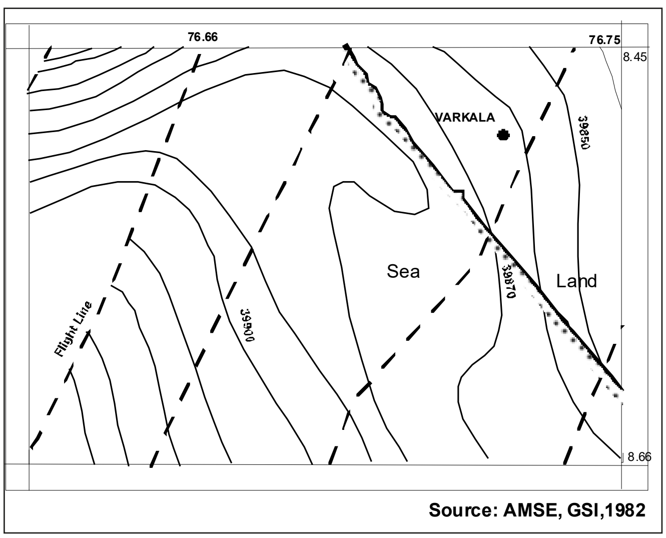

Fig. 11: Aeromagnetic Map (TF) of Varkala Area, Kerala.

Conclusion

I. Close grid gravity surveys at Varkala beach have given tectonic framework of the study area. It has identified that basement is dipping towards east i.e. away from the beach and sedimentary thickness also increases away from the beach. These results have also indicated faulted contact of sea (half graben) with continent and sediment got deposited in the down thrown block. In the second phase of tectonic disturbances, these sediment deposited in down thrown block got uplifted and the present topography is visible today on the cliff.

II. The thick clay layer present over the basement is the major geological factor causing wave undercutting as well over hang collapse.

Acknowledgement

Authors are thankful to GSI for permitting to use the data of field work carried out by them in publishing this paper.

References

AMSE, GSI, 1982: Air borne Geophysical Surveys report, GSI unpublished report.

Blakely, R., 1995: Potential theory in Gravity and Magnetic applications. Cambridge University Press, New York.

Chandrasekhram D., 2001: Structure and Evolution of the west continental margin of India deduced from gravity, seismic geomagnetic and geochronological studies. Memoir Geological Society of India, **47**: 509-521

Gupta, D., Ganguli, S.S. and Sajinkumar K.S., 2012: Close grid gravity surveys at Varkala beach, Kerala. *Journal of Geophysics*, **XXXVI (3)**:145-150.

Ganguli S. S. and Gupta D., 2012: GSI Unpublished report for the FS 2010-11.

Rao, V.P., Nair, R.R. and Hashimi, N.H., 1983: Clay Mineral distribution on the Kerala Continental Slope and Shelf. *Journal Geological Society of India*, **24**:540-546.

Indian Journal of Geosciences, Volume 74, No. 3
July - September, 2020; pp. 269-274

Invited Paper

Machine Learning Approach to Mineral Deposit Grade Modelling

B. C. Sarkar[1*] and Dipankar Ray[2]

[1]*Department of Applied Geology, IIT(ISM) Dhanbad, India*
[2]*Department of Computer Science and Engineering, IIT(ISM) Dhanbad, India*
**Corresponding author Email: bhabeshsarkar2005@gmail.com*

Abstract: Machine learning methodologies in recent time are gaining interest in mineral exploration and mineral resource modelling. Classically, machine learning algorithms construct a mathematical model on the basis of sample data known as training data to make predictions or decisions without having to explicitly program to perform a specific task. It is a method that allows one to combine several layers of data and recognize vital relationships between them, in ways that would not have been previously possible. In this paper, machine learning, in particular a deep learning model involving ensemble of regression tree has been used by the present authors to estimate iron ore grade from spatial distribution of drill hole sample values. The method employs a forward-learning algorithm to improve regression results using a flexible nonlinear regression procedure. It boosts accuracy of trees by sequentially applying weak classification algorithms to the incrementally changed data to create a series of decision trees. The model captures the spatial distribution of iron ore grade by directly training the model with sample data at borehole locations. The trained model is then used to predict the distribution of ore grade values in the region of drilling. Key benefit of this approach is that it requires no complicated mathematical modeling and makes no assumption about the spatial distribution of iron ore grade values. The approach specifies that deep learning gradient boosting model is an improved tool for solving generic block grade and ore reserve estimation problem in exploration and mining geology.

Key words: Deep Learning, Gradient Boosting Model, Regression Tree, Ore Reserve.

Introduction

Mineral exploration and subsequent grade estimation is a multifaceted exercise involving remote sensing, geochemical, geophysical and geological data to estimate ore grade and tonnage. Major advances have been made over the past few years in the fields of machine learning and geostatistics. Specifically, in the field of machine learning, deep neural network-based methods have intensely enhanced the state-of-art in pattern recognition and applications. Geostatistics, on the other hands, represents a family of methods to characterize and model spatial variability and map spatial patterns based on the regionalized variable theory. Geology integrated with Geostatistics and Artificial Neural Network (ANN) constitute a robust technique to estimate the grade of ore in a mineral deposit. Over the past 60 years, geostatistics has been the most established methodology for ore grade estimation. Geostatisitcal methods largely works on linear models based on local statistical distribution of ore body parameters whereas ANN is used to model a non-linear distribution and is widely used as a global approximator. In general, the spatial distribution of grade values in an ore deposit varies widely. Non-linear modeling using ANN provides a decent choice which delivers a robust estimation of different parameters of the deposit. It works even under noisy and extreme data value. Nevertheless, use of ANN for mineral deposit grade estimation still remains an open area of research (Wu and Zhou, 1993; Dowd and Sarac, 1994; Singer and Kouda, 1996; Yama and Lineberry, 1999; Koike and Matsuda, 2003; Samanta *et al.,* 2005).

However, shallow ANN often suffers from lack of generalized solution and fails to provide a global solution for test data set. It also lacks scalability and performs poorly for data not belonging to the sample data. To overcome these problem, a regression tree oriented weak learner based multilayered Deep Neural Network (DNN) model has been proposed to estimate grade of an iron ore deposit from a set of borehole data constituting borehole sample locations and drill core assay values.

The multilayer DNN model is used directly over the drill hole spatial assay dataset. The sample data has been split dynamically into training, validation and test datasets to train, validate and tune the network working for the best performance. Training sample has been chosen randomly from the drill hole assay data so that it can represent the entire region of the drill hole data. The trained network is then used to approximate ore grade and to estimate an overall domain of the ore body. Finally, to verify the results, DNN outputs are compared with ordinary kriged estimates in predefined grid locations.

Gradient booster model

Modern deep learning offers better training stability, generalization, and scalability than the conventional shallow neural network models. It performs quite well in a number of classification and approximation problems and is accordingly becoming widely accepted algorithm of choice for highest predictive accuracy.

To train the deep learning network, Gradient Boosting Model (GBM) has been implemented (Cheng *et al.,* 2018). Using supervised learning approach such as regression and classification, this model sequentially fits new nodes to provide a more accurate estimate of a response variable. Gradient-based optimization uses gradient computations to minimize a model's loss function in terms of the training data. This model collects a band of weak models to create a robust learning system for predicting goals. Boosting additively collects an ensemble of weak models to create a robust learning system for predictive tasks (Fig. 1). In the present case, the boosting algorithm is used for regression analysis of the used iron ore data to predict ore grade from a set of regularly distributed grid data in a 3D topology

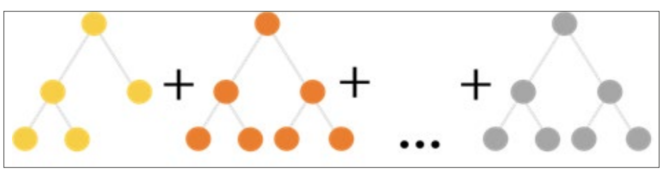

Fig. 1: Schematic diagram of Gradient Booster Model algorithm.

The multilayer decision tree captures the nonlinearity of feature space and through a regression or classification approach maps the Spatial sample data to the estimated grade values.

Data Standardization

Data standardization is carried out for eliminating influence of outlier(s), if any, which may be associated with large variance relative to other attributes as a matter of scale, rather than true contribution. Preprocessing is required for standardization so that data becomes compatible with the activation functions. As activation functions generally does not cover the full spectrum of real numbers, R, it is required to standardize the data set in the interval N (0, 1). Since activation functions may get changed from layer to layer, standardization of intermediate hidden layer data is also essential. This on-fly standardization as network propagates allows us to compute more precise errors in this standardized space than in the raw feature space.

Regularization

It is necessary to make a complex neural network uniform for different sets of field data. This method of improving the generalization is known as regularization, which aims to prevent the network to over fit to the given set during training phase. In nonlinear model of a multilayer deep learning neural network, we need an appropriate trade-off between reliability of the training data and goodness of the model. This tradeoff can be realized by minimizing the total risk:

$$J = E_s(W) + \lambda\, E_c(W)$$

$$J = E_s(W) + \lambda\, E_c(W) \qquad \text{(A)}$$

where, $E_s(W) E_s(W)$ is the performance measure and in general defined as a mean-square error. This function is carried out over the output neurons of the network and expressed as:

$$E_s(W) = \frac{1}{N}\sum_{i-1}^{N}(y^d(i) - y(i))^2$$

$$E_s(W) = \frac{1}{N}\sum_{i-1}^{N}(y^d(i) - y(i))^2 \qquad \text{(B)}$$

where, N is the total number of training samples, $y^d(i) y^d(i)$ is the desired output of the ith sample and $y(i) y(i)$ is the network output of the ith sample. $E_c(W) E_c(W)$ is the network's structural penalty term and λ is the regularization parameter, which assigns relative importance to the penalty term with respect to the performance measure of the equation (A). Zero value of λ implies unconstrained training whereas a large λ indicates complex network and implies an unreliable training phase.

$$L_{ridge}(\beta) = \|y - X\beta\|^2 + \lambda\|\beta\|^2$$

$$L_{lasso}(\beta) = \sum_{i=1}^{n}(y_i - x_i\beta)^2 + \lambda\sum_{j=1}^{n}\beta_j$$

In this regard, it has been observed that Lasso and Ridge regularization provide good results in regularization process. While Lasso penalizes the sum of their absolute values, Ridge penalizes sum of squared coefficients. Lasso adds a penalty for non-zero coefficients. As a result, for high values of λ, many coefficients get a zero value under Lasso. In case of Ridge regularization, as $\lambda \rightarrow \infty, \infty,$ coefficients are not always zero. Besides these, Dropout method (Hinton *et al.,* 2012) is another good choice to achieve regularization. Dropout constrains the optimization to achieve idle results by suppressing activation function with certain probability threshold value. With the Dropout approach, it has been found to yield good result with acceptable execution performance.

Early stopping algorithm identifies the onset of generalization loss (over fitting) through the use of cross-validation. For this, the training data are divided into estimation (training) and validation subsets. The periodic estimation followed by validation cycle continues till the generalization at epoch ***t*** exceeds a user defined threshold value on validation test. It is defined as:

G_L: Stop after first-epoch t with $G_L(t) > \alpha$

where G_L is the relative increase of the validation error over the minimum error up to epoch t, and is defined as:

$$G_L = 100\left(\frac{E_{va}(\mathbf{t})}{E_{opt}(\mathbf{t})} - \mathbf{1}\ \frac{E_{va}(\mathbf{t})}{E_{opt}(\mathbf{t})} - \mathbf{1}\right)$$

where, $E_{va}(t)$: validation error at epoch 't' and

$E_{opt}(t)$: minimum validation error up to epoch 't'.

To achieve desired generalization, training data sets are verified using cross-validation test with respect to a validation data set. In simulation involving noisy data, it is found that the validation error decreases monotonically to a minimum but then starts to increase, even when the training error continues to decrease. Cross-validation provides an effective guiding principle to identify the most suitable network parameters. Corresponding to the best training model, performance of this trained model is then measured over the test data set to confirm the best-performance parameters. It has been observed that the performance of a cross-validation test is appealing when the target is to achieve a good generalizing on a large network.

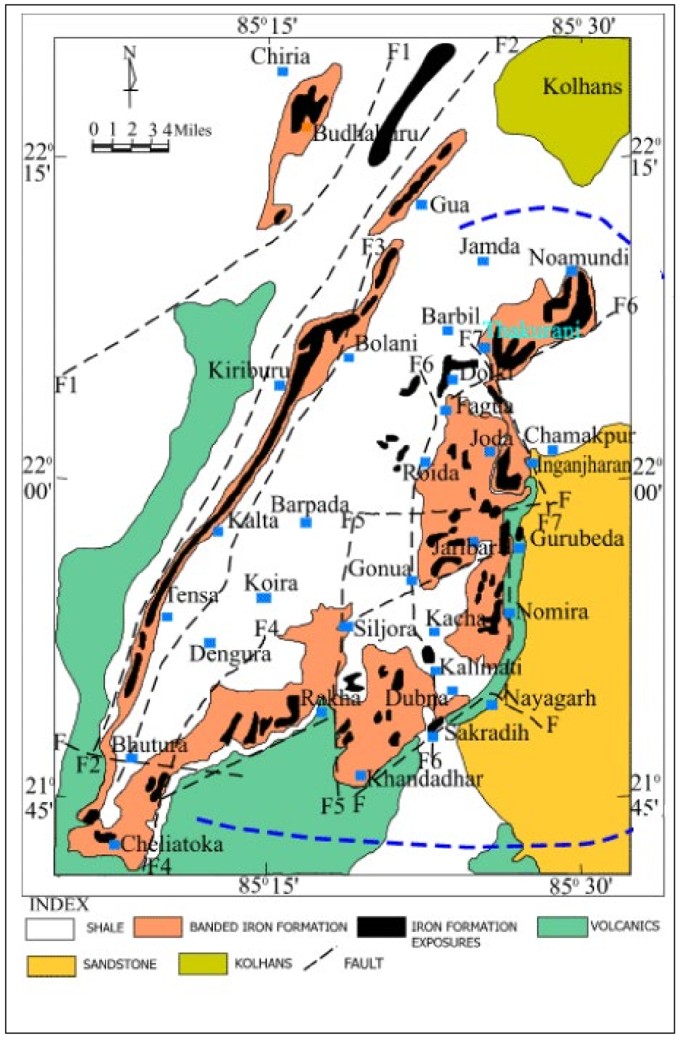

Fig. 2: Geological Map of Singhbhum-Keonjhar-Bonai Belt (Saha *et al.,* 1984).

Test case

An iron ore deposit constitute the test case for the proposed deep learning neural network-based GBM implementation. The deposit is situated on the western limb of horseshoe shaped synclinorium known as Iron Ore Group of the Singhbhum-Keonjhar-Bonai Belt and is bounded by latitude 22˚ 02′ to 22˚ 07′ N and Longitude 85˚ 14′ to 85˚ 18′ E of Toposheet no. 73F/8 (Fig.2). Genetically, the deposit is said to be related to the Banded Iron Formation (BIF).

Geological setting

It is of volcano-sedimentary origin, deposited over the eroded lower Archean basement and produced by intense supergene alteration. The iron ore body is composed of alternate layers of chert and hematite and is covered by laterite. Structurally, the Iron ore group is a horseshoe synclinorium with a regional strike of NNE-SSW and dip varying between 60˚ to 70˚, plunging towards north and is divided into three parts. The western limb consists of mainly of banded hematite jasper and quartzites. The central part is mainly composed of chert, phyllites with tuffs and lavas, while the eastern limb is mainly occupied by banded hematite and quartzite. The principal rock types comprises of laterite, goethite, limonitic ore, blue dust, ferruginous shale and banded hematite quartzite or banded hematite jasper.

Test data

The drill hole assay data of Fe collected from drill cores of a constant support of 2m from the iron ore deposit has been used in the case study. A total of 3250 drill core samples with Northing, Easting and Elevation and corresponding %Fe values constituted the dataset. Basic statistics of the drill hole data are given in Table 1.

Table 1: Basic statistics of the drill hole data

	Parameters	Range		Mean	S.D.
		Min	Max		
Input Parameters	Northing	-268	470.69	84.59	180.37
	Easting	-779.82	1501.08	399.63	621.81
	Elevation	751	895.12	826.15	29.29
Output Parameter	%Fe	45.03	69.20	60.51	5.65
No. of Samples	**3250**				

Model implementation

The proposed Deep Neural Network-based model consists of a Gradient Booster Model (GBM) with decision tree architecture having of a maximum depth of 10 and number of nodes as 1500. At the outset, assay data are processed for dimensionality and noise reduction with an unsupervised auto-encoder network. The output from the auto-encoder model, along with validation dataset are then used to train supervised GBM model. Random sampling of dataset is used to assign borehole sample field data to training, validation and test sample datasets. These datasets are then used to train, validate and test the booster model. To make the training, validation and testing of the booster model robust and representative of the entire dataset, 75% of the sample data has been allotted to training set and rest in equal division are allotted to validation and test datasets. The training dataset trains the GBM tree with respect to three spatial coordinates (predictor) and corresponding grade (response) values and continues to train the weak learner decision tree model till the given goal level is reached or the early-stopping threshold of regularization is reached. To make the approximation of spatial distribution of grade values more accurate and more robust, the booster model has been validated with a ten-fold cross-validation. Since this problem is basically a regression exercise, a logarithmic loss function is used for optimization and convergence in the solution space. Initially, rows start at node zero and in-memory Map Reduce (MR) task computes the statistics of each node then on the basis of loss function value it makes a decision. In the subsequent layers depending on decision threshold value decision moves right or left. While row wise all layers are processed, new leaf values are computed during creation of each layer.

The flow of the execution process has major eight steps which can be stated as:

Step 1- Data standardization.

Step 2- Division of data in training, validation and test sets

Step 3- Training of the booster model with training sets.

Step 4- Validation of the model with respect to the validation data set.

Step 5- If Regularization indicates less misclassification, go to the Step 3 else call Early-Stopping.

Step 6- Test the performance of the model with the test data set.

Step 7- Repeat the steps 3, 4, 5, 6 till the performance result stabilizes.

Step 8- Use the model to generate the grid point ore body grade estimation.

Step 9- Stop.

Data Pre-Processing

For dimensionality reduction an auto-encoder is used over input spatial data. This unsupervised learning algorithm learns the representation of data to reduce the dimensionality and also reproduce data from the reduced encoding as close as possible to its original input.

Learning

GBM combines two powerful tools: gradient-based optimization and boosting. Gradient-based optimization uses gradient computations to minimize a model's loss function in terms of the training data. Boosting additively collects an ensemble of weak models to create a robust learning system for predictive tasks. In a multi-class classification, a regression tree is assigned to each target class. If the regression tree is judged to be a weak learner, it is added to the current ensemble until the process provides an acceptable value for classification. A gradient based residual is then calculated for each of the bins for classification.

Cross-validation

In an attempt to establish dynamically, the network configuration and regularization parameters, a 10-fold cross-validation has been employed. This heuristic technique requires a large data set for training, validation and testing. In the present case, the data set has been divided randomly into five disjoint training sets. The cross validation process is repeated five times over the training data set. The training continues as long as the performance on validation data set keeps improving. When it ceases to improve, it calls early stopping mechanism to stop the training process. The corresponding combination of configuration and regularization parameters are selected and subsequently used for the first trained network. The test data is then used on the trained network to estimate the expected performance (generalization) of the network on field data.

Experiment and result

Acquired data was first filtered for outliers and standardized with respect to the mean and standard deviation of the sample. In order to predict the iron ore grade in the deposit, the configured GBM was trained using training datasets containing three input parameters, i.e. easting, northing and elevation and their respective Fe grades. After appropriate validation and achieving acceptable generalization with validation dataset, the model was verified with testing dataset. The estimated values at grid points were compared with the sample values. Depending on the performance, model producing the best result was selected for the final prediction of iron ore grade values. Goodness of Fit (R^2) and Mean Squared Error (MSE) of the test datasets are given in columns 3 and 4 of Table 2 while the corresponding training and testing dataset sizes of the selected models are given in columns 1 and 2 of Table 2.

Table 2: Data and model correlation results

Training No. of Samples	Validation No. of Samples	R^2	MSE
40%	60%	.8870	8.94
50%	50%	.8950	8.18
60%	40%	.9201	6.57
75%	25%	.9802	4.17

Model validation

Validation of the GBM has been done using graphical methods. Predicted Fe grade values of the grid were compared with nearby drill core Fe grade values. Fig. 3(a) displays a spatial distribution map of sample values. The grade values have been grouped into 5 classes in Fig. 3(a) and each class has a different colour code. Fig. 3(b) displays a spatially distributed map of the Fe grade values as estimated by GBM. The value of the GBM estimated map ranges between 50% Fe and 65% Fe, which correspond adequately to sample values of Fig. 3(a).

Conclusion

The deep learning neural model consisting of GBM has been used to estimate Fe grade values at grid locations. The

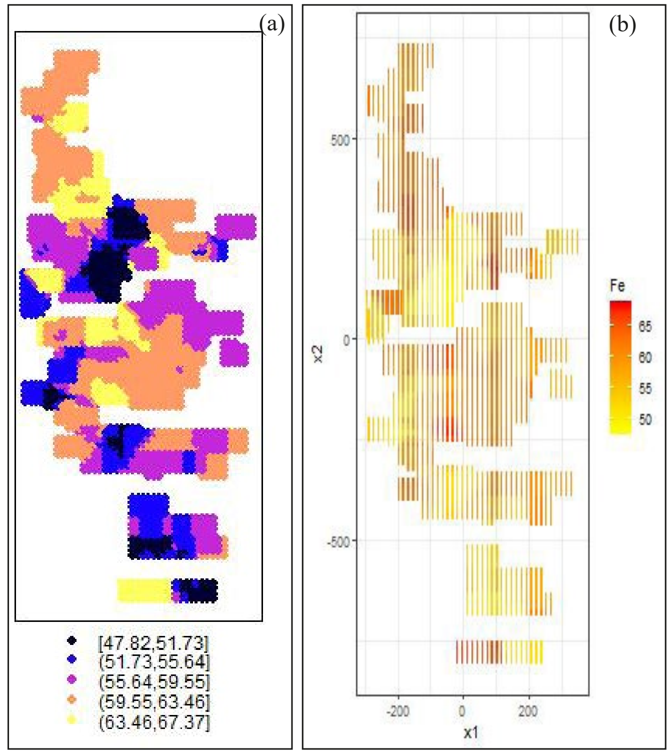

Fig. 3: Sample values and GBM estimated spatial distribution map of Fe.

resulting model shows a meaningful alternative approach compared to existing linear models. The model has been used to predict ore grades from drill hole sample values of an iron ore deposit. The results reveal a goodness of fit (R^2) value close to unity, thereby indicating a reliable robust model for prediction and is stable under noisy data. Since deep learning-based neural network model depends on the adjustment of several parameters, it is understandable that opportunities are there to improve the model by exploring different alternatives of design parameters. Furthermore, in case of large number of sample data, it is also required to handle data prudently to make time complexity within an acceptable range. However, the machine learning approach demonstrates that the rendering of prediction model could be further improved by use of present day sophisticated graphics and data rendering tools. Thus, the GBM has provided an improved technique for grade estimation. It is able to capture the non-linearity of relationships among different parameters without considering multiple assumptions and conditions on the sample data as is the case in the linear techniques of grade estimation.

Acknowledgements

The authors acknowledge the data support received from M/s Steel Authority of India and infrastructure support received from IIT(ISM) Dhanbad.

References

Cheng J., Li, G. and Chen, X . 2018: Research on Travel Time Prediction Model of Freeway based on Gradient Boosting Decision Tree. *IEEE Access*, DOI 10.1109/ACCESS.2018.2886549, 1-14.

Dowd, P.A. and Sarac, C., 1994: A neural network approach to geostatistical simulation. *Mathematical Geology*, **26(4)**: 491-503.

Hinton, G.E., Srivastava, N., Krizhevsky A., Sutskever, I. and Salakhutdinov, R.R., 2012: Improving neural networks by preventing co-adaptation of feature detectors. https://arxiv.org/abs/1207.0580, 1-18.

Koike, K. and Matsuda, S., 2003: Characterizing content distributions of impurities in a limestone mine using a feedforward neural network. *Natural Resources Research*, **12(3)**: 209-222.

Saha, A.K, Ghosh, S., Dasgupta, D., Mukhopadhyay, K. and Ray, S.L., 1984: Studies on crustal evolution of the Singhbhum Orissa Iron Ore Craton. Indian Society of Earth Sciences, 1-74.

Samanta, B., Bandopadhyay, S., Ganguli, R., and Dutta, S. 2005: A comparative study of the performance of single neural network vs. Adaboost algorithm based combination of multiple neural networks for mineral resource estimation. *Journal of South African Institute of Mining and Metallurgy*, **105(4)**: 237-246.

Singer, D.A. and Kouda, R., 1996: Application of a feedforward neural network in the search for Kuroko deposits in the Hokuroku district, Japan. *Mathematical Geology*, **28(8)**: 1017-1023.

Wu, X., and Zhou, Y., 1993: Reserve estimation using neural network techniques. *Computers & Geosciences*, **19(4)**: 567-575.

Yama, B.R. and Lineberry, G.T., 1999: Artificial neural network application for a predictive task in mining. *Mining Engineering*, **51(2)**: 59-64.

Indian Journal of Geosciences, Volume 74, No. 3
July - September, 2020; pp. 275-279

Invited Paper

Rare Earths: A concise overview of their importance, availability and geological environments of occurrence

Subhas C. Verma

Apex Exploration Research Advisory Committee AMD, Department of Atomic Energy, Govt. of India.
Email: scveragex@gmail.com

Abstract: Rare Earth Metals drive a whole range of high technologies today and fall in the category of critical metals. Though wide-spread in a variety of geological environments, rocks and minerals, the Rare Earths are 'rare' in the sense that they are not often concentrated in easily or commercially exploitable deposits. The high level of expertise required and the high cost of separating and extracting individual rare earth elements (REE) from composite rare earth minerals, further constrains their availability. New emerging frontier technologies based on application of these critical metals will lead to a spurt in demand that will outstrip supply. This calls for developing innovative exploration & exploitation methods for rare earths (RE) as well as for finding cheaper, more readily available alternatives to replace their use in the old traditional industries wherever feasible.

Keywords: Rare Earths, Critical Metals, Application, Availability, Geological Environments

Introduction

Rare Earth Metals fall in the group of critical or strategic metals. This stems from the fact of their unique metallurgical, optical, magnetic & nuclear properties. These led to their wide ranging application in high-tech & frontier technologies and in products such as advanced digital electronics, permanent magnets, wind energy turbines, solar energy, defence & space control systems, solid state lasers, optical fibres, lithium-ion/nickel-metal hydride electricity storage batteries & many more, including colour TV, electronic gadgets, glasses and LEDs in wide common or mass use. Rare earths are also used in low-carbon technologies and widely used in Y Zeolites as a fluid catalytic cracking catalyst in the cracking & refining of crude petroleum oil to extract the valuable products (Balaram, 2019; Wikipedia, 2020; Work Group GSL, 2011).

It was the advent of nuclear reactors around the mid-twentieth century, which brought about a revolutionary change in the use of rare earths. The large atomic programmes, particularly in USA & UK, provided great advantage to the rare earth industry. Rare earth elements (REE) were formed abundantly in fission products of nuclear reactors. They were examined in great detail scientifically & their separation pursued, leading to their application in frontier technologies 1960s onwards. Prior to this, rare earths were used as composites or in simply separated form in some traditional industries with a wider technical application beginning in 1930s (Greinacher, 1981).

Basics and Historical Background of REE

As we know, the rare-earths are composed of a group of seventeen chemical elements, viz., fifteen lanthanides (atomic numbers 57 to 71) – Lanthanum through Lutetium plus Yttrium (39) and Scandium (21), grouped together because of their similar chemical properties. Rarely, a broader definition that includes actinides may be used since they share some mineralogical, chemical and electron shell configuration characteristics. REEs are commonly found in minerals along with Thorium (Th) and less commonly with Uranium (U) (Brian Mason, 1966; Wikipedia, 2020; Work Group GSL, 2011).

Geochemistry of Scandium is significantly different from geochemistry of other rare earth elements (REE). Content of each individual RE element varies considerably from mineral to mineral and from deposit to deposit. The REEs are grouped as light (LREE), medium (MREE) or heavy (HREE) according to their atomic weights. Increasing atomic numbers between LREE and HREE with decreasing atomic radii, a phenomenon known as lanthanide contraction, throughout the series causes chemical variations. Europium (Eu 63) is excluded from this classification as it has two valence states Eu^{+2} and Eu^{+3}. Yttrium is grouped in HREE due to chemical similarity (Brian Mason, 1966; Wikipedia, 2020).

Even though all the RE elements have similar chemical properties, each one has its own unique metallurgical, magnetic, optical or nuclear property that determines its application in different technologies (Greinacher, E., 1981). Rare-earth elements are also useful in dating rocks, as some radio-isotopes of REE have a long half-life. In this field of geochronology, ^{138}La – ^{138}Ce, ^{147}Sm – ^{143}Nd & ^{176}Lu – ^{176}Hf systems are made use of (Work Group GSL, 2011).

Historically, the first RE mineral was found at Ytterby in Sweden in 1788 and named after it as Ytterbite and later re-named as Gadolinite after Prof. Gadolin, who first studied it. This mineral contains the RE element now called Gadolinium (Gd) atomic no. 64 along with two others RE elements Cerium and Yttrium. 1788 – 1891 is the period when the RE elements were scientifically examined, but not technologically used. The first effort to systematically analyse the mixed rare earths began in 1839. Subsequently, with the introduction of spectroscopy as a useful control instrument, the work of separation of the REEs was carried forward. The special optical properties of REE were the first to be utilized. Usage of rare earths began with lighting and in ignition by way of production of gas mantles & carbon arc/filament lamps (using both Th & REEs) and in the making of Flintstone (70% mischmetal & 30% iron) used for ignition in lighters and in the early cars. Mischmetal is composed of 95% lanthanoids & 5% iron. The other traditional use of rare earths was in the glass & ceramic industry as polishing and colouring agents and in the manufacture of high purity, high refractive index glass.

The second period is from 1891 to 1930 in which first industrial usage of mixed or simply separated REE took place. A wider usage of properties of REE came about in the period 1930-1960, in which the years 1940 to 1960 are marked by a systematic discovery of properties, separation methods and of usage of RE elements/ metals as by-products of atomic research programmes in industrial countries. The period from 1960 to the present is when the rising qualitative and quantitative application of REEs has taken place (Greinacher, 1981). So much so that REEs now have a stranglehold on all modern technologies which practically govern our lives today, directly or indirectly.

Geological Environments of Occurrence of Rare Earths

Geochemically, the REE are Incompatible, High Field Strength Elements (HFSE); REE also have a special nuclear property known as lanthanide contraction in which the ionic radii/size reduces with increase in atomic number of the rare earth elements (Brian Mason, 1966; Salters, V.J.M., 1999). These basic geochemical and electro-chemical characteristics of REE determine the geological environment of formation and distribution of the rare earths in particular types of rocks and minerals. REE minerals are formed by hypogene processes deep within the earth at depths of ~ 80 km-120 km. They are generally restricted to alkaline rocks, particularly to layered alkaline complexes, carbonatites as well as to certain types of granitoids and naturally derived placers or clays and muds from them. The REE-bearing host rocks are emplaced deep in the crust as diapirs or erupted at the surface along pre-existing fractures. Typical REE enriched deposits forming in carbonatites and in A- and M- type granitoids have a symbiotic relationship with major rifts. They tend to occur in branch faults related to the main rift (Sørensen, 1974). REE-enriched deposits emplaced in the crust above a subducting slab are typically in S-type granitoids (Wikipedia, 2020; Work Group GSL, 2011).

Monazite-bearing coastal placer deposits derived from a variety of igneous, metamorphic & sedimentary rocks of Archean to Tertiary age in the hinterland are widespread in large parts of the world. The content of thorium in these placer deposits increases with the grade of metamorphism of the source rocks and the thorium content is highest in granulite terrain-derived placers. These coastal 'Heavy Mineral Sand' deposits consist overwhelmingly of other valuable associated minerals like ilmenite, rutile, zircon, garnet and sillimanite, with monazite content generally constituting only ~ 1% to 1.5% of the total economic heavy minerals content. Modest-sized inland placer deposits enriched in xenotime derived from peralkaline granitoids and pegmatites (Nb-Y-F type) also occur in some places (Ali, *et al*., 2001).

Formation of significant REE mineralisation in hydrothermal systems has been studied (Giere, R., 1996). Recently, HREE mineralisation entirely of hydrothermal type spread across a large area has been reported from northern Australia. It occurs in the form of fault-breccia controlled, steeply dipping xenotime-rich veins close to a regional unconformity between Archean meta-sedimentary rocks and overlying Proterozoic sandstones (Nazari-Dehkordi, *et al*., 2018). Minor occurrences of hydrothermal xenotime-rich veins are also known to be present in the vicinity of some major shear zones outside Australia. A small occurrence of xenotime-rich veins is known from the SE sector of the Singhbhum Shear Zone near Kanyaluka, Jharkhand State (India). Many coal deposits also host significant amount of REE resources (Balaram, 2019). In addition to the REE minerals found in the earth's crust on land, there are some deep sea muds that contain from a few hundred to thousands of ppm rare earths (Britannica, 2020; Powell, 2011).

REE Mineralogy

Although over 250 minerals contain REE as important constituents of their chemical formula and crystal structure, only a few contain these as major or accessory minor constituents (Balaram, 2019). Idealized chemical composition of 13 minerals that are a source of rare-earths, are given in Table 1 (modified from Britannica, 2020):

NB. The 1985 International Union of Pure and Applied Chemistry "Red Book" recommends that *Lanthanoid* be used rather than *Lanthanide*. The ending '-ide' normally indicates a negative ion.

In addition to the above 13 minerals, there are a number of other REE-bearing minerals associated with rare-earth deposits. Principal ones among them are: Eudialyte, Fergusonite, Gittinsite, Limonite, Kainosite, Mosandrite, Parisite, Pyrochlore, Rinkite (Rinkolite), Steenstrupine and Synchisite (Balaram, 2019).

The crystal lattice of a mineral determines the selective incorporation of a particular rare earth element in it. Among the anhydrous rare-earth phosphates, it is the tetragonal Xenotime that incorporates yttrium & the HREE, whereas the monoclinic Monazite incorporates Cerium & the LREE preferentially.

Although REE occur in a large number of mineral species, currently principal economic sources of REE are just 4 minerals. They are: Bastnasite, Monazite, Loparite & Lateritic ion-absorption clays (Britannica, 2020). Other minerals that have been used as secondary sources of rare-earths are: Apatite, Euxenite, Gadolinite & Xenotime. In addition to Uranium & Iron tailings, Allanite, Fluorite, Perovskite, Sphene and Zircon have a potential to be future supplementary sources of rare-earths.

Economic Deposits of Rare-Earths

Although REE are widely distributed in the earth's crust (with a crustal abundance ranging from ~130 µg/g to ~ 240 µg/g), currently known significant economic reserves of rare-earths are confined to twelve countries across the globe. These principal countries in order of their share of world reserves of REE are: China (33.33%), Brazil (16.67%), Vietnam (16.67%), Russia (13.64%), India (5.23%), Australia (2.56%), Greenland (1.14%), USA (1.06%), South Africa (0.65%), Canada (0.63%), Malawi (0.11%) and Malaysia (0.02%) (Balaram, 2019).

As of 2018, the United States Geological Survey (USGS) put the world reserves of rare-earth oxides (REO) at 132,000,000 Tonnes (Te). Total world production of REO in 2019 reportedly was 212,400 Te coming from 10 countries (China, USA, Myanmar, Australia, India, Russia, Madagascar, Thailand, Brazil and Vietnam), China leading with an output of 132,000 Te (Barrera, 2020).

REE deposits have been put in four broad categories:

Alkaline igneous deposits

Residual deposits

Heavy mineral placer deposits

REE bearing coal deposits

The geological environment of occurrence of each of the first three categories has already been described above. In the

Table 1: Composition of Selected Rare-earth Minerals

Name	Idealized Composition	Primary Rare-earth Content (R)
Allanite	$(Ca,Fe^{2+})(R,Al,Fe^{3+})_3Si_3O_{13}H$	Light Lanthanoids
Apatite	$(Ca,Ln)_5(PO_4)_3(F,Cl,OH)$	Light Lanthanoids
Bastnasite	$(Ln,Y)CO_3F$	Light Lanthanoids (60-70%)
Euxenite	$R(Nb,Ta)TiO_6.xH2O$	Heavy Lanthanoids plus Y (15-43%)
Fluorite	CaF_2	Heavy Lanthanoids plus Y
Gadolinite	$R_2(Fe^{2+},Be)_3Si_2O_{10}$	Heavy Lanthanoids plus Y (34-65%)
Laterite Clays	$SiO_2.Al_2O_3.Fe_2O_3$	Heavy Lanthanoids plus Y
Loparite	$(R,Na,Sr,Ca)(Ti.Nb,Ta,Fe^{3+})O_3$	Light Lanthanoids (32-34%)
Monazite	$(R,Th)PO_4$	Light Lanthanoids (50-78%)
Perovskite	$CaTiO_3$	Light Lanthanoids
Sphene	$CaTiSiO_4X_2$ ($X = ½ O^{2-}$, OH^- or F^-)	Light Lanthanoids
Xenotime	RPO_4	Heavy Lanthanoids plus Y (54 – 65%)
Zircon	(Zr,Ln)SiO4	Both Light & Heavy Lanthanoids plus Y

first category, the Mountain Pass carbonatite in California (USA), mined between 1965 and 1980 and re-opened at the beginning of the present century, was the largest single REE deposit of its kind. Prior to this, India and South Africa were the largest suppliers of REE. With the discovery and exploitation of the massive Bayan Obo carbonatite containing a super accumulation of REE in Inner Mongolia (N. China) from the end of the last century, China overtook USA in the production and supply of REE. In the second category, the ion-absorption clay-hosted REE deposits in South China are the largest of their kind. These are particularly important as they are the biggest source of HREE in the world (Kanazawa and Kamitani, 2006; Kynicky, *et al*., 2012; Wikipedia, 2020; Yang, *et al*., 2011).

Large ore deposits of LREE are known around the world and are being exploited. Ore bodies of HREE are rarer, smaller and less concentrated. Most of the current supply of HREE comes from the ion-absorption clays of South China.

Aggregate world demand for rare-earths in 2019 was put at 149,500 Te and has been estimated to grow by ~ 8% per annum through to 2029. The growth in demand for RE metals like Neodymium and Dysprosium is projected to be much higher than for other RE metals (Barrera, P., 2020; Freedonia Group, 2020).

Other Potential & Secondary Sources of REE

Apart from the currently known and utilized sources of REE, other potential & secondary sources of supply of REE are being researched and investigated. Notably, these include:

(i) Deep Sea REE-enriched muds in different oceans [in the Pacific ocean on the seafloor at 5,600 m – 5,800 m depth ~ 250 km South of the island of Minami-Tori-Shima, a thick mud layer containing up to 0.66% REO has been discovered by Japan. A potential deposit here might compare in grade with the ion-absorption type deposits in S. China having grades from 0.05% to 0.5% REO] (Britannica, 2020; Powell, D., 2011; Wikipedia, 2020).

(ii) Recovery of REE from industrial plant waste. Red-muds, which are a hazardous waste generated in the Aluminium industry, are a potential source of REO (JNARDDC, 2020).

(iii) Coal and coal by-products are a potential source of critical elements including rare-earths with estimated amounts in the order of 50 million Te (Wikipedia, 2020).

Recovery of REE from recycling electronic waste, fluorescent lamps, magnets and batteries has an estimated potential of 300, 000 Te (Wikipedia 2020).

Exploration for REE Deposits

Exploration methods for placer REE deposits are already well established (Ali *et al*., 2001). The ion-absorption clay REE deposits can be effectively explored by using a combination of Airborne Hyperspectral, Gamma-Ray Spectral & Magnetic Surveys coupled with follow-up systematic ground gamma-ray survey, geological mapping and sampling. [The USGS, as reported in 2018, conducted extensive hyperspectral surveys in Alaska and evaluated the mineral potential for REE]. A combination of Airborne Magnetic & Gamma-Ray Spectrometric geophysical methods is ideally suited for location of Alkaline Complexes & Carbonatites hosting REE.

Conclusions and discussion

While large reserves of LREE in various types of deposits are available, there is a dearth of HREE. Exploration needs to lay an emphasis on search for deposits hosting minerals with high HREE content. Ion-absorption clay type REE deposits are favourable for hosting large resources of HREE. Airborne Hyperspectral survey is a powerful and proven technique for distinguishing between & demarcating different clay types on the ground.

Exploitation of coastal placer deposits for monazite requires a safe storage and effective commercial management of the large thorium residue left behind.

There is a whole range of regulatory, safety, environmental, commercial, political & geopolitical issues impacting exploration and exploitation of REE deposits (Balaram, V., 2019; Wikipedia, 2020). These have not been touched upon here as they are beyond the scope of this paper.

Acknowledgements

The author is thankful to Shri E.V.R. Parthasaradhi for his invitation to contribute this paper. The author also expresses his thankfulness to Shri Prakash Chandra Patra, Dy. Director General (In-charge Publications), Geological Survey of India and to the Director General, Geological Survey of India, Kolkata for kindly accepting and publishing the paper.

References

Ali, M.A., Krishnan, S., Banerjee, D.C., 2001: Beach and Inland Heavy Mineral Sand Investigations and Deposits in India- An overview. Exploration and Research for Atomic Minerals, 13.

Balaram, V., 2019: Rare earth elements: A review of applications, occurrence, exploration, analysis, recycling and environmental impact. *Geoscience Frontiers*, **10(4):** 1285-1303.

Barrera, P., 2020: 10 Top Countries for Rare Earth Metal Production. Investing News Network (INN), INN Rare Earths Investing News, May 26th 2020.

Brian Mason, 1966: Principles of Geochemistry (3rd Edition). New York, London (Wiley), vii+329 pp.

Britannica, 2020: Minerals and Ores.

Freedonia Group, 2020: World Rare Earths Industry Study.

Giere, R., 1996: Formation of rare-earth minerals in hydrothermal systems. *In:* Jones, A.P., Wall, F., Williams, T., (eds). Rare Earth Minerals: Chemistry, Origin and Ore deposits. *Mineralogical Society Series*, **7:** 105-150.

Greinacher, E., 1981: History of Rare Earth Applications, Rare Earth Market Today. Industrial Applications of Rare Earth Elements, Chapter 1. *ACS Symposium Series, American Chemical Society*, **164:** 3-17.

JNARDDC, 2020: Utilization and development of process for recovery of strategic rare-earths from industrial waste-Bauxite Residue at lab scale. On-going project P-55, Jawaharlal Nehru Aluminium Research Development and Design Centre, Nagpur, India.

Kanazawa, Y. and Kamitani, M., 2006: Rare earth minerals and resources in the world. *Journal of Alloys and Compounds*, **408-412**: 1339-1343.

Kynicky, J., Smith, M.P., Cheng Xu, 2012: Diversity of Rare Earth Deposits: The Key Example of China. *Elements*, **8(5)**: 361-367.

Nazari-Dehkordi, T., Spandler, C., Oliver, N.H.S., Wilson, R., 2018: Unconformity-related rare-earth element deposits: a regional-scale hydrothermal mineralization type of northern Australia. *Economic Geology*, **113(6)**: 1297-1305.

Powell, D., 2011: Rare earth elements plentiful in ocean sediments. *Science News* via Kurt Brouwer's Fundmastery Blog. MarketWatch.

Salters, V.J.M., 1999: Elements: High Field Strength. *In:* Marshall, C.P., Fairbridge, R.W., (eds.), Geochemistry. Springer, Dordrecht.

Sørensen, H., 1974: The Alkaline Rocks. John Wiley, London, 662 pp.

Wikipedia, 2020: Rare-earth element.

Work Group (GSL), 2011: Rare Earth Elements. A briefing note by *the Geological Society of London.*

Yang, K.F., Fan, H.R., Santosh, M., Hu, F.F., Wang, K.Y., 2011: Mesoproterozoic Carbonatitic magmatism in the Bayan Obo deposit, Inner Mongolia, North China: Constraints for the mechanism of super accumulation of rare earth elements. *Ore Geology Reviews*, **40(1)**: 122-131.

Indian Journal of Geosciences, Volume 74, No. 3
July - September, 2020; pp. 280-283

Invited Paper

Mineral Resources and Sustainable Development

Raja V. Ramani

Mining and Geoenvironmental Engineering and
George H. Jr. and Anne B. Deike Chair in Mining Engineering
The Pennsylvania State University
209 Research West Building, University Park, PA 16802, USA
E-Mail: rvr@psu.edu

Abstract: World's consumption of materials at the beginning of 2020 is 100 billion tons, about 75 billion tons of which were in minerals, ores and fossil fuels. The global material use has nearly grown four fold since the 1970 and material footprint is growing at a faster rate than population. There is almost a symbiotic relationship between growing human aspirations for enhancing quality of life, increasing demands for energy, minerals and materials, advances in science, engineering and technology for meeting these aspirations and demands, manifestations of such global problems as climate change, toxic wastes and waste disposal, and enhancing education, research and training to seek solutions to alleviate the ensuing societal issues in a sustainable manner. Mining, as one of the two primary wealth-producing industries, is associated with the extraction of the energy and mineral riches of the earth for the benefit of mankind and is often the starting point of the mineral and materials cycle. Mining as an industrial activity has come under intense criticism for the manifestations of major environmental and ecological problems. Questions have also been raised on the sustainability of the current consumption of materials. In this paper, the issue of mineral resource development and sustainable development is discussed from mining industry's need to address the long term of value of mined lands and mineral resouces.

Key Words: Land use, Material footprint, Mine environmental planning, Mined-land reclamation, Mineral resources, and Sustainable development

Introduction

The question - what are the basic needs of humans in a modern society? - is not easy to answer. One can start with identifying essential items as food and shelter, move on to easily understandable items as energy and materials, infrastructure, health, and education, and get deeply immersed in such issues as clean environment, ecological preservation, community connection, psychological needs, and so on. Here again, the definition of some of the items has been undergoing major revisions. For example, our understanding of community has not remained static and as the universe, it is ever expanding to encompass larger and larger parts of the globe with greater consideration of animate and inanimate components. Further, all our needs are not fully independent of one another and this relationship requires, on our part as individuals and as members of a community, to understand the impacts of hasty solutions to address a pressing problem to avoid disastrous consequences. For example, there is a movement, small but quite vociferous, all around the globe to "ban" mining, an action that would bring to a screeching halt the progress towards meeting the essential needs of the modern society.

Mining the energy and mineral riches of the earth is the starting point of the materials cycle, and in most cases, of the primary, secondary and tertiary industries. Directly or indirectly, it provides for every human need. The growth in the size of mines, in their use of modern technology, and achievements in production and productivity are rather impressive (Ramani, 2012). At the same time, mining has come under intense criticism, not all undeserved, for causing major environmental and ecological disasters and several human problems. Every country has plans for increasing the standards of living of its people, and all need more energy, food, materials and infrastructure. Earth is the only source for these resources and in most cases, mining is the only way to get them out of the ground. It is therefore, not surprising that the global materials footprint has been growing faster than both population and gross domestic product (Wiedmann *et al*., 2015). The urgent need to address effectively the negative issues arising from mining has never been more imminent.

Mine Environmental Issues – A Legacy

Spoil piles, waste piles, derelict lands, mine fires, water pollution, and similar other sights in mining districts around the world - still standing today from mining years ago and threatening health and safety to residents in the areas - provide evidence of little or no planning and control of these hazards in the past. Community health and safety and worker health and safety are not addressed here but are important aspects of mine social impact problems (Ramani, 1995a&b). Even to a casual observer it should be evident that the mining industry has been moving towards implementing plans and procedures to reduce the negative environmental impact of mining. In the early years of environmental movement, several cosmetic approaches were followed to make the mining areas visually less jarring without a detailed consideration of soil, groundwater and biological effects of mining-caused disturbances. Early laws and regulations requiring pollution and erosion control brought certain minimum standards to mining operations (Ramani, 1974). As the environmental movement was gaining momentum, the decades following 1950s brought land reclamation and land rehabilitation into greater prominence in mining. At the present time, it has become essential to ensure that any new mine planning include greater involvement of several interest groups, particularly additional stakeholders concerned with environment and long term sustainability. The application of principles of industrial ecology and sustainable development to address the mining project from cradle to the grave is being demanded by several parties.

Unique Aspects of Mining Industry

Mining industry, as opposed to many manufacturing industries, has several unique features. The mineral deposit on which the industry is built is evasive to detection even with very intensive search and when located, may not prove to be economic for exploitation. In addition to the geographic and geologic fixed location, the deposit has a limited amount of reserves and once exhausted, the operations have to cease. The definition of sustainable mining or mining sustainability must first acknowledge that the mining operation itself is not sustainable. Also, mining is breaking in-situ land and processing it and in most cases, vast volumes of liquid and solid wastes are by-products of the processes of mining, processing and smelting. In short, mining use of land is not the same as that by any other industry. Further, the footprint of mining is physically small, but it has big local, regional, national and global impacts as mined-raw materials are processed, manufactured, and utilized at many different locations. The increasing spatial separation of production and consumption in global supply chains leads to a shift of resource use and associated environmental pressures among countries (Wiedmann *et al*., 2015). Essentially, the footprint of mining cannot be as easily identified as those of most other industries as well.

Sustainable Development

In "Our Common Future" (Brundtland Commission, 1987), the definition of sustainable development is as follows: development that meets the needs of the present generation without compromising the ability of future generations to meet their own needs. The overall goal of sustainable development is the long term stability of the environment and economy. It is stressed that development is not synonymous with growth and includes producing more with less, and conservation. As a concept, it is simple and easy to follow and therefore, had immediate appeal and acceptance. The dimensions of sustainable development are broadly defined as economic (goods and services, government, sectors etc.), environmental (natural resources: renewable and non-renewable, cultural resources, assimilative/regenerative capacity), and social (health, education, equity in income/benefits, participation). Several aspects of the definition are worth stressing. Intergenerational equity and conserving resources for the future generation are important considerations. The integration of economic, environmental and social aspects throughout the decision-making process is essential, breaking traditional sectoral, departmental and other territorial boundaries. The application of the concept to practice is made difficult due to changing priorities placed on these dimensions, differing views on value and vulnerability of resources, and lack of specifics and understanding on what needs to be sustained for the future, what are the metrics, what are the appropriate scales for these metrics, and how and who would monitor and manage the process.

While there is a general agreement on some goals of sustainable development such as the need to ensure survival of communities, to strive to maintain biodiversity, and such, there is a lack of mutual agreement on the causes leading to threats to these goals. In fact, there is wide disagreement on human-caused and naturally occurring changes to the global environment. Industrial process does affect the natural and cultural environment and result in changes in earth resources. However, surface and subsurface of the earth are ever changing due to natural processes. Nature's ceaseless processes such as wind, water, ice, volcanoes and earthquakes are continuously at work. The goals of sustainable development must recognize that certain practices are clearly unsustainable and must be avoided. Further, there is a need to find a workable solution that addresses in an optimal way the requirements of the actors and actions in the various dimensions of sustainable development. Pursuit of major sustainable development initiatives must occur across cross-boundaries involving operations, companies, industries, countries and people. Every player must follow the dictum "think globally and act locally." Fortunately, great progress has been made in identifying the goals of sustainable development and ways and means by which countries, industries, companies and individuals can work together by major industry groups and international institutions such as World Bank (2020) and United Nations (2020). Specific to mining industry, the work of the International Institute for Environment and Development (IIED) on sustainable development practices in the mining industry is noteworthy. The Mining, Minerals and Sustainable Development Project (MMSD, 2002) was a research project looking at how the mining and minerals sector could contribute to the global transition to sustainable development. Between 2000 and 2002, the MMSD project carried out research, analysis and consultation with several stakeholders. A follow-up study ten year (2012) later found that the mining and minerals industry has made major advances towards sustainability but faced new challenges such as host governments, often lacking capacity to ensure sustainable development, reasserting control over their natural resources. Questions were also raised on how well the mining industry has put sustainable development theory into practice.

Earth scientists and mineral engineers learn early that a mineral deposit, once proven economic and starts to be exploited, would eventually be abandoned due to exhaustion, if not earlier, due to economic reasons. That a mineral deposit is a "wasting asset" and that the search for new deposits to add to its reserve and resource bases is the lifeline for the mining company are corollary lessons that are well learnt. What is probably not so well learnt are the profound implications of these facts for the community that has been or has grown around the mineral deposit's exploration and exploitation stages? When mining ceases, and the mining company moves away in search of greener pastures (sustainable development plan for the mining company), what happens to the mine property, mined-lands and structures, and more importantly, the community that lived, supported and depended on the mining operation? Indiscriminate practices of the past have left a legacy of abandoned mining areas which are generally inadequate to support human habitation. In some cases, liabilities of these operations include serious health and safety issues to miners and their families and the community (Ramani, 1988). Over the years, omnibus and mineral-industry specific environmental laws and regulations have addressed air, water and land issues. Mine closure continues to be a major issue as funds are very limited at the end-of-life stages to do an adequate job. In recent years, mine closure planning has become a key component of mine feasibility study, with requirements for frequent updates and for provisions of funds during mine operation. In fact, in some cases, the high closure cost has become a major liability for some operations, leading a senior executive to lament that "today, closing mines successfully has become more problematic than opening mines successfully." To avoid these problems, wherever possible, the reduction of costs at the end of mine life can be achieved by sequential reclamation during the production phase. The CEO of a large gold mining company stated thus the long term value of mining operations: "our success is tied to our ability to develop, operate and close mines in a manner that provides long term value. Long term value has evolved into a broad set of concepts that are now referred to as 'sustainable development' or sustainability."

While much attention has been paid to the subject of mining as a land use and the need for reclamation and land use planning for mined-lands in the last four decades (Ramani, 1978 and 2009), it is important to separate the technical issues of mined land use planning with the socio-economic issues of post-mining economic viability of the community. In fact, land, its people and the resources of the land are the primary resources of the area. Land is a resource with several uses - some one time, some multiple and some somewhat permanent and some somewhat temporary. Another unique feature is that the available lands to a community are often limited and actions that result in derelict land or affect its other resources or uses permanently should be discouraged. Lands with mineral riches are special as mining leads to a vibrant economic activity (Ramani and Sweigard, 1984). Yet, mining as a land use is temporary and with its cessation can lead to a sudden loss of the economic base, an experience that is too common in many areas of the globe. Permission for mining must be granted only after a deliberate and dispassionate consideration of the benefits of mining and the environmental and social impacts and their remedies. Even then, it is necessary to view mineral development as a "bridge between present and future generations through which the foundations for a new economic base needs to be fostered." (Ramani, 2001). For this to be realized, firstly, people, institutions and environment are to be developed for identifying the future economic base. Consideration of the needs and expectation of the future generation is essential. Secondly, mined lands, affected other resources, and needed new resources must be preserved or acquired for developing the new economic base. Finally, part of the earnings from the current operations must be dedicated to developing the identified economic base. Essentially, the value of a mine, long after it is closed, and the mineral resource, long after it is exhausted, is the preservation, if not the enhancement, of the community's livelihood.

Summary

Mining industry's technical performance indicators – health, safety, productivity and cost metrics – reflect continual progress over the years even while facing increasing competition, more complex deposit characteristics, stricter environmental and health and safety regulations, declining prices and growing aspirations of the workforce for greater standards of living. These are the result of dedication to the development and practice of highly effective and efficient operational practices to face the challenges posed by constantly changing external and internal environment. The sustainable development of mineral resources is a challenge that requires, in addition to continued superior technical and economic performance, defining the future needs of the community when there will be no mine and making plans to address them starting from the earliest stages of mine feasibility study. The paper has stressed the loss of the economic base provided by the mine and the need for a new base. The paper proposes that mining is a temporary land use and after this use, we must search for other land uses. These are only starting points for discussion. Current experience with the wide variety of successful mine reclamation/rehabilitation projects around the world points to diverse development opportunities for sustainable development.

References

Brundtland Commission, 1987: Our Common Future. The World Commission on Environment and Developement, Oxford University Press, 383 pp.

MMSD, 2002: Breaking New Ground: Mining, Minerals and Sustainable Development Project. Final Report, IIED, London. https://pubs.iied.org/G00769/ (accessed on August 24, 2020).

Ramani, R.V. and Sweigard R.J., 1984: Impacts of Land Use Planning on Mineral Resources. *Mining Engineering*, **36(4)**: 362-369.

Ramani, R.V., 1974: Environmental Concerns and Decisions for the Mining Industry. *Journal of the Institutions of Engineers [India]*, **54(2)**: 45-49.

Ramani, R.V., 1978: Integration of Land Use Planning with Surface Mining. *Earth and Mineral Sciences*, **47(5)**: 33-39.

Ramani, R.V., 1988: Air Quality in Mines: Progress and Prospects of Legal Control. *The AusIMM Bulletin and Proceedings*, **293(7)**: 27-30.

Ramani, R.V., 1995a: Mining Disasters Caused and Controlled by Mankind: the case for coal mining and other minerals, Part 1: Causes of mining disasters. *Natural Resources Forum*, **19(3)**: 233-242.

Ramani, R.V., 1995b: Mining Disasters Caused and Controlled by Mankind: the case for coal mining and other minerals, Part 2: Control of Mining Disasters. *Natural Resources Forum*, **19(4)**: 309-319.

Ramani, R.V., 2001: Environmental Planning in the Mineral Industry: Problems and Prospects. *International Mining and Minerals*, **41**: 5-12.

Ramani, R.V., 2009: Land Reclamation to Sustainable Development: the Changing Mine Planning Paradigm. *Proceedings of the International Conference on Sustainable Mining. Santiago de Compostela, Spain*, 353–360.

Ramani, R.V., 2012: Surface Mining Technology: Progress and Prospects, SYMPHOS 2011. *Procedia Engineering*, **46**: 9-21.

United Nations, 2020: https://www.un.org/sustainabledevelopment/sustainable-development-goals/ (accessed on August 24, 2020).

Wiedmann, T.O., Schandl, H., Lenzen, M., Moran, D., Suh, S., West, J., and Kanemoto, K., 2015: The Material Footprint of Nations. *Proceedings of the National Academy of Sciences (PNAS), United States of America*, **112(20)**: 6271-6276.

World Bank, 2020: https://www.worldbank.org/en/programs/sdgs-2030-agenda (accessed on August 24, 2020.

Indian Journal of Geosciences, Volume 74, No. 3
July - September, 2020; pp. 284-294

Invited Paper

The Neoarchaean Rengali Province in Eastern India: geological set up and significance

J.K. Nanda[1], M. Mohanty[2] and S. N. Mahapatro[3]

[1] *Former Deputy Director General, Geological Survey of India*
[2] *Former Deputy Director General, Geological Survey of India*
[3] *Geological Survey of India, SU: Chhattisgarh, CR, Raipur-492010*
**Corresponding author's email: jknanda49@gmail.com*

Abstract: A distinct geological terrane sandwiched between the Mesoarchaean Singhbhum and Bastar cratons respectively in the north and west, and the Proterozoic orogen of Eastern Ghats in the south, has been recognised as the Rengali Province (RP). Comparatively a new entrant to the Precambrian geological literature of eastern India, this province is situated entirely within Odisha. It is constituted of metamorphic lithoassemblages comprising granulites (charnockitic orthogneisses), amphibolite grade granitic gneisses and belts of supracrustals of low metamorphic grade. Supracrustals comprise metamorphosed quartz arenite, minor pelitic/psammopelitic sediments, volcanics and volcaniclastics. The Tikra, Malaygiri and Deogarh supracrustal belts surround a central amphibolite grade gneissic terrane known as the Pallahara – Kamakhyanagar gneisses. The southern boundary between the RP and the Eastern Ghats Province (EGP) exhibits (i) upper amphibolites to granulite facies metamorphism, (ii) crustal scale shear zones with pronounced dextral movements and strike slip components in proximity of the Ib-Talchir Gondwana basin hosting coal seams, and (iii) a discontinuous chain of deformed alkaline igneous rocks represented mainly by ~1300 Ma miaskitic nepheline syenite. This terrane with major crustal movements along all sides has a complex tectonic fabric and its overall aeromagnetic signatures are distinctly different from the adjoining Precambrian terranes.

Key words: Rengali Province, Singhbhum craton, Eastern Ghats Province, deformed alkaline rocks.

Introduction

Occurrence of terranes of contrasting high and low metamorphic grades in juxtaposition in Precambrian shields has been described and discussed in literature since long (Windley, 1977). In Peninsular India, the Proterozoic Eastern Ghats granulite belt is juxtaposed with the eastern Dharwar, Bastar and Singhbhum cratons and the nature of their boundary relations has been debated over the years (Narayanaswami, 1975; Ramakrishnan *et al.*, 1998, Biswal *et al.*, 2007). Because of the coexistence of litho-assemblages of high and low metamorphic grade in large segments of the western contact zone in Khammam region of Andhra Pradesh (presently Telangana) and Malkangiri – Koraput region of Odisha, a 'transition zone' was tentatively envisaged and shown in the compiled geological map of the Eastern Ghats Mobile Belt (EGMB) by Ramakrishnan *et al.*, (1998). In some parts of this zone a sharp tectonic (thrust) contact could also be observed especially with the Bastar craton in Khariar-Paikmal sector (Ramakrishnan *et al.*, 1998) which was subsequently documented by Biswal *et al.*, (2007 and references therein). The northern contact zone is however, highly tectonised and marked by several faults and thrusts separating the EGMB from Singhbhum craton. The nature of the contact zone between the two contrasting terranes in Riamal – Rengali region was studied by Banerjee *et al.*, (1987) and Panda and Patra (1993) but could not be conclusively established.

Mahalik (1994) identified six litho-structural assemblages in the region lying between the Singhbhum Craton and the EGMB in a transect between Rengali Dam area and Kanihan. He named them from north to south, as the Deogarh, Rengali, Malayagiri, Tikira, Jojumura and Angul assemblages. Based on the interpretation of Landsat TM data supported by field traverses, Nash *et al.* (1996) attempted to delineate different litho-structural domains in northern Odisha. The area lying between the EGMB and Singhbhum craton comprising both granulite and amphibolite facies metamorphic rock suites and displaying well defined E-W to NW-SE oriented, refolded plunging folds, was designated as the "Rengali Domain" (Nash *et al.*, 1996). Crowe *et al.*, (2001, 2003) introduced the term "Rengali Province" for this area in the tri-junction between the northern part of Eastern Ghats province, southern part of the Singhbhum craton and the eastern margin of the

Bastar craton. Bounded by thrusts and shear zones, this is a terrane distinct from the EGB in the south and the Singhbhum cratonic block in the north. Subsequently, Dobmeier and Raith (2003) divided the EGMB and adjoining parts of the cratonic areas into four Provinces e.g., the Krishna, Jeypur, Eastern Ghats and Rengali Provinces. Crowe *et al.*, (2001, 2003) and Dobmeier and Raith (2003) described the geological setting of the "Rengali Province". Recent investigations reveal that the litho-assemblages of the Rengali Province (RP) are in the age range of 3.0-2.8 Ga making the geological province distinctly different from adjoining Grenvillian (~1000 Ma) EGP and the 3.5 – 2.8 Ga Singhbhum cratonic block.

Geology of the Rengali Province

Mahalik (1994) delineated a WNW-ESE trending fault separating the Rengali and Angul litho-assemblages. He named it as the North Orissa Boundary Fault (NOBF), which passes close to the Mahanadi–Brahmani lineament, and the northern boundary fault of the Talchir Gondwana basin. He also marked another NW-SE trending fault along eastern margin of the Malayagiri supracrustal belt. The Barakot shear zone or Akul Fault zone separates it from the Singhbhum Craton in the north (Nash *et al.*, 1996). The Kerajang Fault (Nash *et al.*, 1996) broadly coincides with the North Orissa Boundary Fault described by Mahalik (1994) and the Sukinda thrust (Banerjee *et al.*, 1987; Saha, 1994). Besides, the bounding fault/shear zones, the province is traversed by many WNW-ESE, E-W and ENE- WSW trending faults and shear zones.

Crowe *et al.* (2003) classified the basement rocks of the Rengali Province (RP) into the Kansal and Badarama Complexes and the metavolcano-sedimentary sequence as the Pallahara Complex (Fig. 1). A brief description of these complexes is as follows.

Kansal Complex: This complex comprises hornblende orthogneiss, biotite ± hornblende ±garnet bearing quartzo-feldspathic migmatite and gneiss with sporadic patchy charnockite. Discontinuous elongated, commonly boudinaged bodies of amphibolite occur interlayered within the orthogneiss and quartzo-feldspathic gneiss in this complex. Pegmatitic and aplitic dykes cross-cut gneissic fabrics and are deformed by shearing.

Badarama Complex: This component of the RP includes the charnockites and the interlayered mafic granulite/ hornblende granulite occurring around Riamal – Badarama - Rengali region. Massive hornblende magnetite orthogneiss is intrusive into this complex which locally exhibits patchy charnockite.

Pallahara Complex: The Pallaharha Complex comprises meta-volcanosedimentary sequence consisting of quartzite, amphibolite and subordinate pelitic to psammopelitic units, metachert, magnetite quartzite and metaconglomerate. Metapelitic to psammopelitic schist and gneiss units represented by muscovite + biotite schist, garnet + biotite schist, garnet + staurolite + muscovite ± biotite schist and kyanite + garnet + staurolite gneiss, commonly occur interlayered with the quartzite occupying the intervening valleys. Thin bands of amphibolite (± magnetite ± garnet) and retrograded actinolite + chlorite schist occur within the metasedimentary sequence prominently in the eastern part but are rare to absent in the central and western parts of the Province. Metamorphosed conglomerate and pebbly sandstone occur as discrete units within the quartzite. These locally contain pebbles of chert and banded hematite jasper set in a matrix rich in magnetite.

The divisions of the RP into complexes as envisaged by Crowe *et al.*, (2003) are yet to be well documented and firmly established before these can effectively replace the status of these litho-assemblages in existing literature.

Lithostructural set up of Rengali Province

Litho-structurally, the central part of the Rengali Province is occupied by the Pal Lahara Gneiss containing amphibolite and granulite patches of variable dimensions (Mohanty *et al.*, 2008). This is surrounded by low-to-medium grade metavolcano-sedimentary supracrustal sequences e.g., Tikra, Malaygiri and Deogarh supracrustals. The Pal Lahara gneiss, along with the Malayagiri–Deogarh supracrustals, is juxtaposed against the Singhbhum Craton by an E-W trending ductile fault known as the Barkot Shear Zone (Crowe *et al.*, 2003). The NNW-SSE trending Akul ductile fault represents the eastern boundary of the Rengali Province separating from the Singhbhum Craton. The NE-SW trending Riamal Shear Zone separates the Pallahara Gneiss complex from the Badrama Complex. The Kerajang Fault separates the southern margin of the Rengali Province from the Proterozoic EGP. The occurrences of deformed alkaline complexes comprising nepheline syenite, in a zone between Riamal in the west, through Poipani and Badadangua (Fig. 2) to Kamakhyanagar in the east (Panda *et al.*, 1998, Panda and Panigrahi, 2009) may mark the contact between the Rengali Province and the Eastern Ghats Province. Though many workers considered this as a Precambrian suture zone (Leelanandam *et al.*, 2006; Ranjan *et al.*, 2018), Sheikh *et al.*, (2020) interpreted that the nepheline syenite intrusions were syntectonic and the ~1300 Ma alkaline magmatism is not indicative of a rift setting.

A part of the southern boundary of Rengali Province containing charnockites in Badarama area and deformed alkaline rocks in Kankrakhol and Poipani is shown in Fig. 2. The RP may extend up to Bhuban-Jenapur areas as a narrow granulite-amphibolite grade zone (Mahapatro *et al.*, 2012). A brief description of the major litho-assemblages, e.g., southern granulites, central gneisses and the peripheral supracrustal belts is briefly outlined as follows.

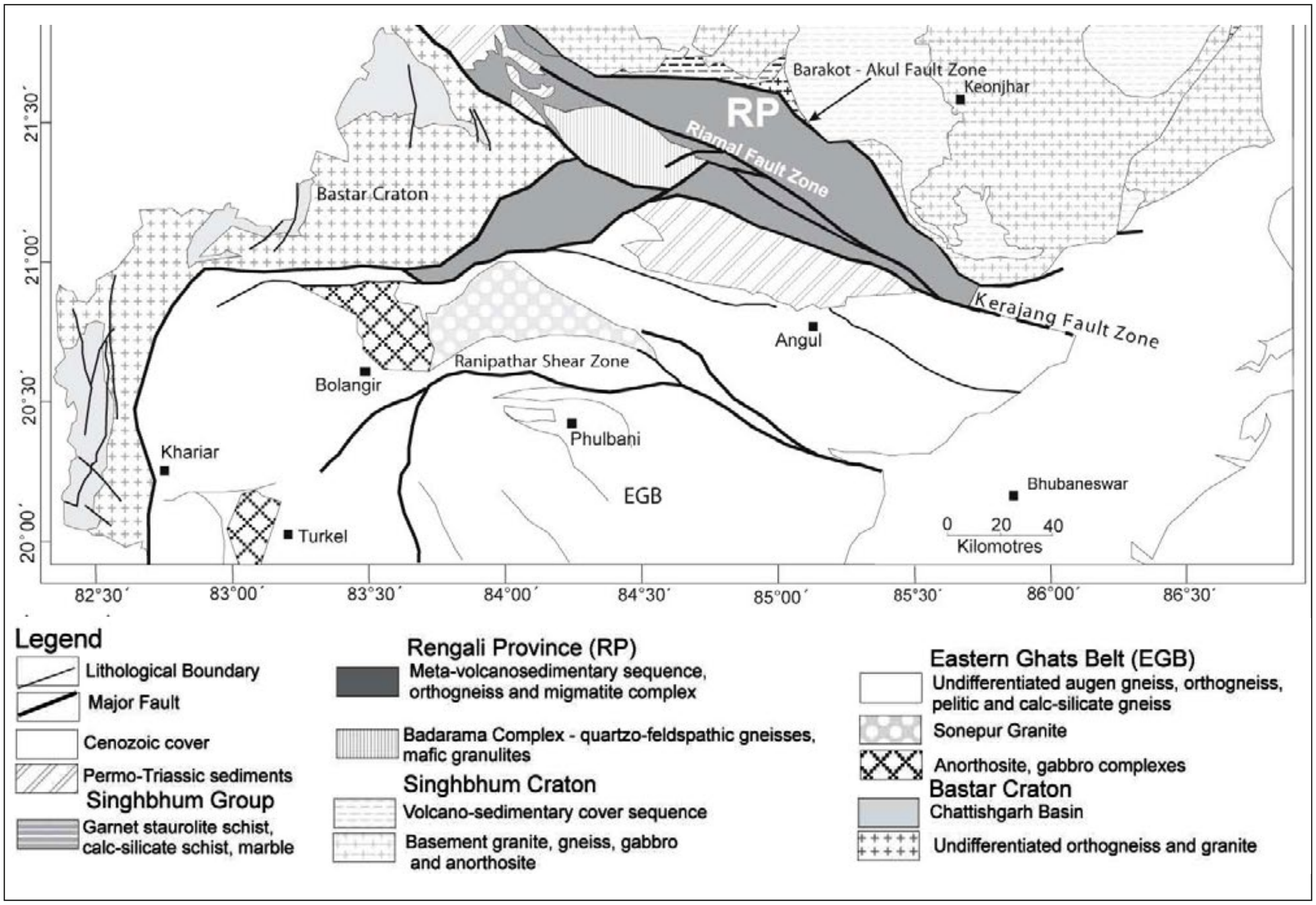

Fig. 1: Geological Map of the Rengali Province (Crowe *et al.*, 2001, Source: Mukhopadhyay and Basak, 2009).

Granulite assemblage of the southern Rengali Province

The high-grade assemblage is constituted dominantly of charnockite, enderbite and two-pyroxene mafic granulites with subordinate metasedimentary granulites which occur as bodies confined to the southern part of the RP bordering the northern margin of the EGP. These plutons of charnockite-enderbite orthogneiss, interlayered mafic granulite and felsic leucogneiss occur around Badarama, Riamal and Rengali Dam region in the western segment of its contact zone with the EGP (Fig. 2), and in Bhuban, Kabatbandh and Balrampur - Jenapur areas along and proximal to the Brahmani lineament in its eastern segment.

The charnockitic rocks are subalkalic and range in composition from granodiorite to adamellite-granite. Metamorphosed mafic (amphibolite and two-pyroxene mafic granulite) dykes traverse these charnockite bodies (Sarkar *et al.*, 2000). Besides the orthopyroxene bearing orthogneisses of the Charnockite Suite, metamorphic patchy charnockites are observed in the granitoids occurring in the neighbourhood of these charnockite-enderbite massifs in different localities of the Rengali Province (Mahalik, 1994; Nanda, 1994; Mohanty *et al*., 2007 and Ghosh *et al*., 2016). In and around Jenapore in the easternmost part of the RP, patchy charnockites in leptynite are interpreted as caught up patches or xenoliths within the granitic melt (Kar, 2001).

Geochronology of charnockitic orthogneisses and associated granulites

The ~2750 Ma (Rb-Sr Whole-rock) age data for the Riamal – Rengali chranockites were reported by Sarkar *et al*., (2000) and ~2800 Ma zircon SHRIMP ages were also obtained from two hornblende orthogneiss samples in the Rengali Province (Dobmeier and Raith, 2003). Subsequently, protolith age of charnockitic gneiss from the eastern segment (Balarampur charnockite) was reported to be 3058±15 Ma and of charnockite, mafic granulite and hornblende gneiss from the central segment (Rengali charnockite) to be in the range of 2828±9 of 2844±7 Ma (Bose *et al*., 2016). The oldest age of emplacement of charnockite magma (3.06 Ga) is similar to the oldest age of peak metamorphism (3.06 ± 0.02 Ga) reported by Mahapatro *et al*. (2012) which indicates a significant link between the two events. The 2.78 ± 0.02 Ga age from monazites in felsic granulites and high-grade paragneisses from around Bhuban in the eastern part of the province was interpreted as an event of metamorphic reheating.

Gneisses of the central Rengali Province (Pal Lahara–Kamakhyanagar Gneiss)

A vast expanse of granite gneiss occupying the central part of the Rengali Province is variously named as the Pal Lahara Gneiss (Sarkar *et al.*, 1990; Saha, 1994) or Pallahara - Kamakhyanagar (Palkam) Gneiss (Mahalik, 1994). These gneissic rocks are exposed around Pallahara, Khamar and Deogarh areas in the northern part (Saha, 1994) and Kamakhyanagar – Bhuban – Hatibari areas in the southern part (Mahalik, 1994; Mahapatro and Tripathy, 2011) in two spatially different regions occurring beween the Malayagiri, Deogarh and Tikra supracrustal belts.

The Pallahara - Kamakhyanagar Gneiss (PKG) is mainly represented by granite (monzogranite) gneiss which is locally migmatitic exhibiting stromatic structures which include petrographic variants e.g., (i) hornblende - magnetite bearing homophanous granite gneiss, (ii) hornblende -magnetite bearing banded or stromatic gneiss, and (iii) two mica (± garnet) granite gneiss. The gneissic banding is isoclinally folded both on micro- and meso-scale with the development of an axial planar foliation (Mohanty *et al*., 2008).

Geochemically, these are high-silica, metaluminous, calc-alkaline, ferroan rocks characterised by a highly fractionated REE pattern with light-REE enrichment, flat HREE and negative Eu-anomalies with overall A-type geochemical affinity (Mohanty *et al*., 2008; Topno *et al*., 2018). These are rich in both LILE and HFSE. Topno *et al*. (2018) classified Pal Lahara Gneiss as A2-type granite (i.e those representing melts derived from varied sources including continental crust and island arc basalts) with high Y/Nb ratios. The PKG at Bhuban yielded $^{207}Pb/^{206}Pb$ zircon ion probe ages of ~2.80 Ga, interpreted to be the minimum age of its formation (Misra *et al*., 2000). Broadly similar ages reported by Misra *et al.* (2000), Sarkar *et al.* (2000), Chattopadhyay *et al*., (2015) and Topno *et al*., (2018) for granites and charnockites of this region which point towards extensive Meso/Neoarchean felsic - charnockite magmatism in this region belonging to different crustal levels of emplacement.

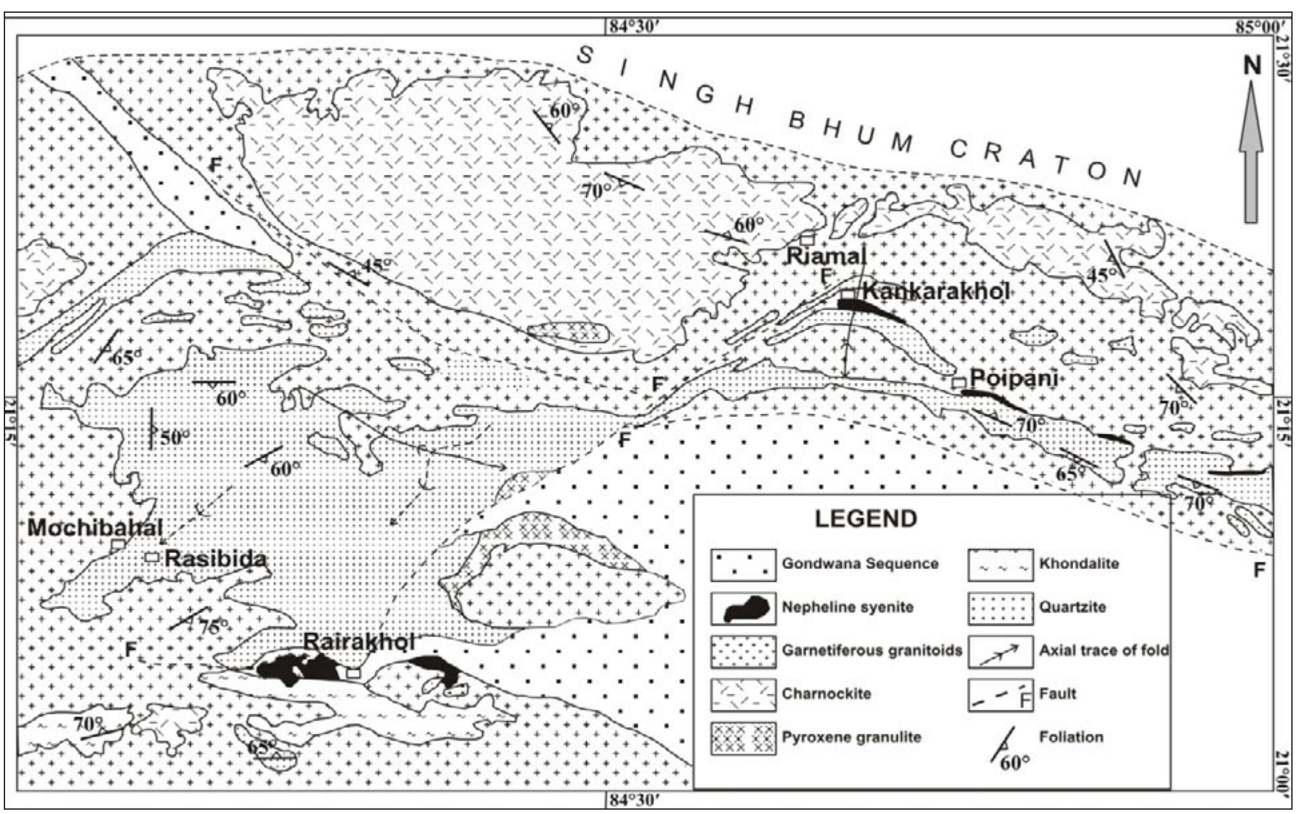

Fig.2: Geological map of the western part of the Rengali Province of the Rengali - Riamal area showing disposition of large bodies of charnockite and discontinuous lenses of deformed nepheline syenite in the southern marginal region (modified after Panda *et al.*, 1998).

The supracrustal belts

Deogarh Supracrustal Belt (DSB): This E-W to WNW-ESE trending low grade meta-volcanosedimentary sequence south of the Bonai Granite consisting of quartzites, basic lavas and BIF-bearing quartzite, form east-west trending hill ranges north and south of Deogarh town. According to Mahalik (1994), these rocks lie unconformably over the Palkam Gneiss and are intruded in the north by the Bonai Granite. Various workers viz. Ramachandran and Sinha Roy (1982), Rath *et al.* (1993), Panda and Patra (1991,1992), Dash and Das (2005) mapped different sectors of the DSB. The Barkot – Balam – Deogarh segment of this belt comprises quartz-mica schist, quartzite, quartz-wacke sequence with intermittent quartz-pebble conglomerate (QPC), thin bands of banded magnetite quartzite, Fe-rich metapelites (quartz-staurolite-kyanite-magnetite-chloritoid schist) and minor amygdular metavolcanics. Sill-like pyroxenite and gabbro occur as intrusive bodies. A majority of such occurrence is near Purunapani. Rengalbeda – Deogarh – Barakot - Purunapani road section and exposes a sequence of quartzites, fuchsite quartzite, amygdular meta-basalt and amphibolite folded together to form overturned synclinal structures and resting over a migmatite (Panda and Patra, 1992). Stratigraphy of the Deogarh Supracrustal Belt (DSB) as proposed by Mahalik (1994) is presented in the Table-2.

Table 1: Stratigraphic succession of the Deogarh assemblage (after Mahalik, 1994).

North Orissa Craton	Bonai Granite	Unfoliated granites
	Deogarh Assemblage (=Tikra Assemblage)	Quartzites, BHQ, lavas, Cherty quartzites, Micaceous quartzites
	Palkam Gneiss	Granite gneisses
---------------------------------- Faulted contact -------------------------------		
Eastern Ghats Belt	Rengali assemblage Angul assmblage	Khondalites Quartzites, gneisses, charnockites

Table- 2: Stratigraphic succession of Deogarh Supracrustal Belt (after Dash *et al.,* 2004).

Deogarh Supracrustal Belt	Younger granitoids
	Fe-rich metapelites (staurolite- Kyanite-magnetite-quartz schist)
	Metavolcanics
	Quartz schist with wacke horizons and QPC
	Banded iron formation
	Quartzite, magnetite quartzite
	Conglomerate
-------------------------------Tonalitic gneiss-------------------------------	

The tonalitic biotite gneisses exposed in the Asnali–Kalamati–Niktimal area and metatexitic stromatic gneisses exposed in the Balinali-Sunamunda areas represent the basement of the Deogarh Supracrustals (Dash *et al.*, 2004). The riebeckite-bearing alkali granite seen as WNW-ESE trending linear bodies in the Jamunali – Bhaludomar – Budhibahal – Brahmanimal –Sunidih area containing metamorphosed enclaves of the greenstone lithologies is intrusive into the DSB. Three phases of penetrative folding have been deciphered and the rocks are considered to have been preserved in nearly E-W trending doubly plunging synformal cusps occurring side-by-side without complementary antiforms due to major dislocation/ shearing (Dash *et al.*,2004). A stratigraphic succession proposed by Dash *et al.*, (2004) for the DSB is presented in the Table- 3.

Table 3: Staratigraphy of MSB after Prasad Rao *et al*., (1964)

Granite
Banded hematite quartzite
Chlorite and hornblende schists (metavolcanics)
Banded hematite quartzite
Quartzites
Mica schists
Basement (not specified)

Table 4: Stratigraphic succession of Kamakhyanagar area after Ray and Acharya, (1997).

Granitic activity
Basic intrusive / volcanics (ortho-amphibolite)
Carbonaceous phyllites
Banded para-amphibolite
Phyllites
Staurolite-garnet-mica schists
Staurolite-quartz schist
Banded Iron Formation
Sillimanite-kyanite-quartzite, quartz schists, fuchsite quartzite
Schistose ultrabasics (talc-serpentine schists)
Schistose conglomerate and pebbly quartzite
Older gneisses

Malayagiri Supracrustal Belt: The Malayagiri supracrustal belt (MSB) is represented by a highly deformed NW-SE trending linear belt extending from north of Kamakhyanagar to Pallahara area. Sarkar *et al*., (1990) have carried out detailed structural analysis of the highly folded, complex, twisted T-shaped body of Malayagiri syncline with extension towards Sundarmundi for about 40 km in a NE-SW direction. The MSB is spatially separated from the Tomka – Daitari – Mahagiri belt by granitic gneisses possibly related tothe Pal Lahara Gneiss. The Malayagiri sequence mainly consists of metaconglomerate, pebbly quartzite, fuchsite quartzite, schistose quartzite, sillimanite – kyanite - quartzite, garnet-biotite-muscovite schist, staurolite-quartz schist, quartz-kyanite-muscovite-staurolite-ilmenite schist, staurolite-garnet-mica schist, phyllites, carbonaceous phyllites, banded iron formation and garnet- bearing as well as garnet-free amphibolite. This is delimited in the east by the prominent NW- SE trending Malayagiri Shear Zone (Barakot Shear Zone of Crowe *et al*., 2003).

Prasad Rao *et al*., (1964), Iyengar and Murthy (1982) and Ray and Acharya (1997) considered the BIF bearing Malayagiri sequence to be equivalent to Gorumahisani – Badampahar Group. Prasad Rao *et al.*, (1964) included this belt in the older sequence (I and II). The stratigraphic sequence suggested by them is given in Table- 4. Ray and Acharya (1997) observed a Barrovian type metamorphic zoning in the southern part of the MSB in Kamakhyanagar segment and proposed a stratigraphic succession for the area as presented in the Table-5.

Many intrusive bodies of mafic and ultramafic rocks comprising gabbro, pyroxenite, orthopyroxenite, peridotite and dunite occur near Kaliahata around Ramiala Dam area (close to Kankadahad, NNE of Kamakhyanagar) possibly within the Malayagiri shear zone (Kartikeyan and Nayak, 2017). A lensoid patch of detrital chromite bearing sedimentary quartzite displaying current bedding occurs in the proximity near Ghotrigan (Banerjee, 1972). Nelson *et al.*, (2014) reported a dacite tuff from the Malayagiri IOG basin south of Pallahara which yielded an igneous crystallisation date of 2806±6 Ma based on which it was considered as the youngest of the BIF bearing supracrustals of Singhbum craton (including the RP).

Tikra Supracrustal Belt (TSB): A metasediment dominated belt in the southernmost part of the Rengali Province is named as the Tikra Assemblage by Mahalik (1994), after the Tikra river, a tributary of Brahmani. This belt is delimited by the Talchir basin in the south and the Pallahara - Kamakhyanagar Gneiss in the north. The Kerajang Fault Zone separates this assemblage from the Proterozoic Eastern Ghats Province and is constituted of a medium to low-grade litho-assemblage represented by quartzites, mica-schists and metabasic rocks (chlorite ± actinolite schist). Mahalik (1994) suggested that the Tikra Assemblage could be equivalent of the Deogarh assemblage and younger to both Rengali and Malyagiri assemblages. He inferred unconformable relation of the Tikra assemblage with Rengali and Malayagiri assemblages.

The tectonic set up of the area around Samal – Baruan - Mahabirorh where the eastern part of Tikra assemblage joins with the southeastern part of the Malayagiri schist belt is very complex (Mohanty and Mahapatro, 2004) (Fig. 3) and is marked by rotation of structural elements due to interplay of the Kerajang Fault and the Akul Fault (Malayagiri shear zone). This area is mainly represented by two very prominent quartzite bands with intervening mica schist. Quartzo-feldspathic gneisses occur at places as basement. The southern quartzite band is highly recrystallized fine- to medium-grained quartzite with occasional muscovite-sericite-rich laminae. It forms WNW-ESE trending linear broad strike ridges in the southernmost part. Its tectonised contact zone with the stromatic migmatites (PKG) is exposed near Baruan and Dadara Ghati. The northern quartzite band contains laminae / partings of segregated fibrolite / sillimanite and muscovite. The WNW-ESE trending quartzite units takes an eastward swing from east of Pakatamunda, after which these are truncated by a series of NE-SW trending faults parallel to the Ramiala River.

The valley portions between the two quartzite ridges are occupied by schistose metapelites and meta-psammopelites often containing 2-polymorphic Al-silicates. Besides, one or more phases like garnet, stauraolite and quartz may be present. At Durgapur, one such schist is composed of quartz, muscovite, andalusite, kyanite, minor fibrolite and opaques. The metamorphosed arenite-psammopelite-pelite sequence occurs as several discrete and thick bands co-folded with metabasic rocks surrounded by gneissic rocks in localities like Sana Khuntia, Jararha-Bam, Parapuri Pahar, Amelijharan Parbat and Kaimati Parbat. Interbanded garnetiferous amphibolite and sillimanite quartzite occur near Jangu and Pangatira within the Pal Lahara Gneiss.

Crowe *et al.*, (2003) argue that the greenschist facies assemblage observed in the southernmost part of the Rengali Province to north of the Kerajang Fault, is a result of retrogression from a former amphibolite facies assemblage. In contrast, Dutta *et al.* (2010) consider that though these rocks have been involved in tectonism, they may not have experienced metamorphic conditions beyond the greenschist facies. Based on structural and metamorphic dissimilarity, they suggested that these lithologies in the southern part of the Rengali Province could be of allochthonous origin. Alternatively, this region may represent laterally extruded allochthonous material that was emplaced in its present position during a period of crustal convergence between the Rengali Province and EGP. Mahapatro (2013) pointed that the entire >500 km long contact zone of the RP with EGMB and SC is marked by interdigitation of disparate lithological assemblages of different age and metamorphism.

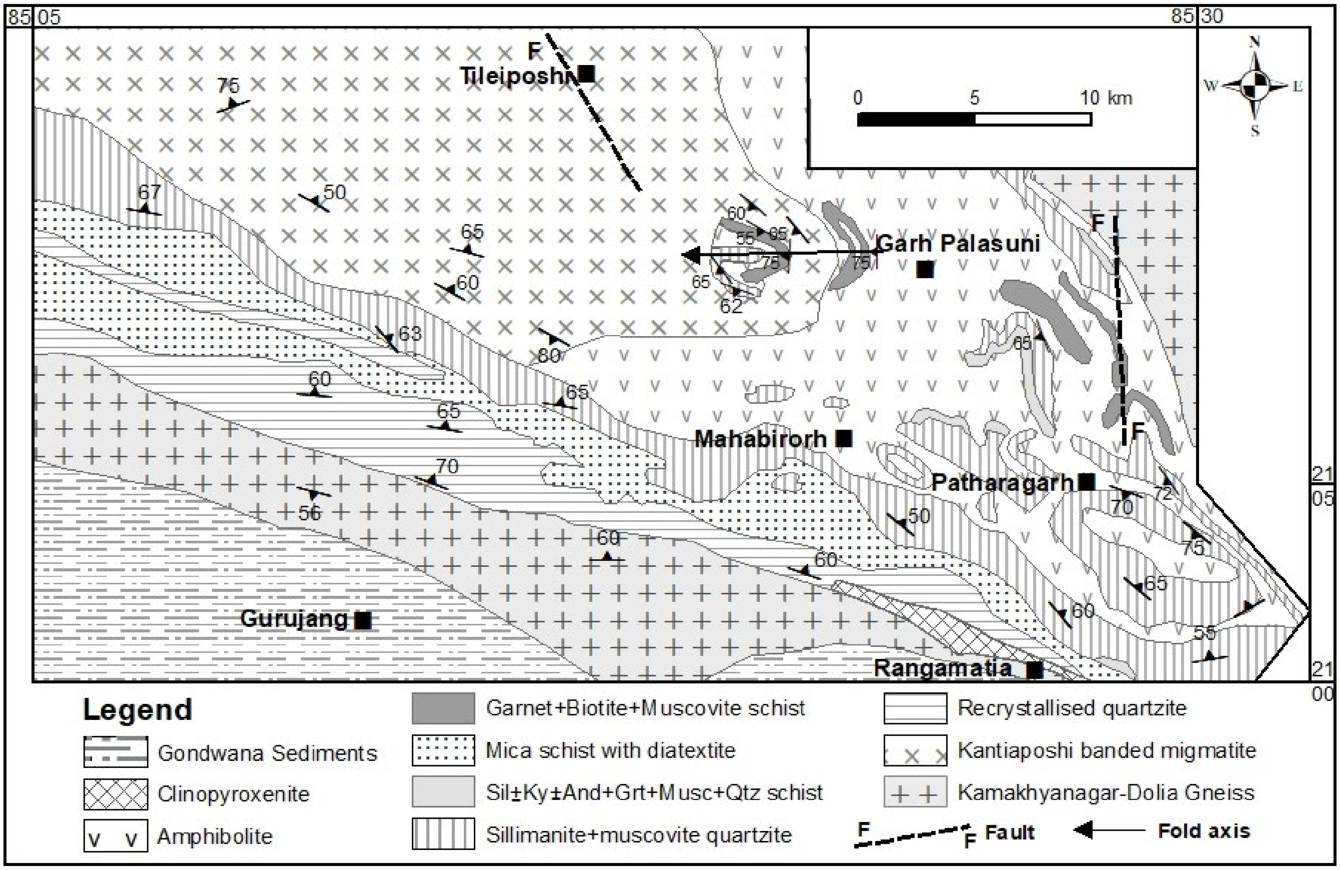

Fig. 3: Geological Map of Kamakhyanagar – Malaygiri Sector (after Mohanty and Mahapatro, 2004).

Evolution of Rengali Province

The Rengali Province separated from the Singhbhum Craton and the Eastern Ghat Belt by crustal scale tectonic zones forms a Neoarchaean geological entity in the East Indian Peninsula recognized by the geoscientist community (Nanda *et al.,* 2020). Its structural attributes in restricted corridors although have been brought out, divergent views are expressed regarding the evolution of the terrane vis-à-vis suturing with the Proterozic Eastern Ghat Belt with the cratons. Some of the views expressed by different workers are summarized as follows.

This crustal segment containing an amphibolite facies sequence with intercalated basement gneiss and metavolcano-sedimentary lithologies was described as a transitional zone (Ramakrishnan *et al*., 1998), a transitional belt (Crowe *et al*., 2001), a suspect terrane (Chetty, 1995, 2001), an exotic/ reworked terrane (Dutta *et al*., 2010) or an accreted arc terrane wherein granulites represent the thrusted deep crustal section of the Singhbhum Craton (Mahapatro *et al*., 2012; Mahapatro, 2013). Nash *et al*., (1996) inferred that this region is characterised by N-S shortening (E-W fold/thrust packages with associated NE and NW strike-slip faulting) followed by regional dextral transpression, manifested in the form of major strike-slip faults. They inferred Palaeozoic-Mesozoic dextral motion associated with coal basin along the Kerajang Fault coinciding with the NOBF. Misra and Gupta (2014) considered Rengali Province as a rotated fragment of the Bastar Craton having a dilational step-over zone within a continental strike slip system. They suggested that the Archaean Singhbhum Province juxtaposed against the Proterozoic Eastern Ghats Belt at 490-470 Ma through a dextral strike-slip system. Chetty (2010) interpreted a crustal-scale ‘flower structure’ in a N–S structural cross-section across the Province, comprising crustal components having distinctive internal structures with widely varying geological evolution history and strain partitioning spatially close to each other separated by crustal-scale shear zones. His interpretation is also based on deep seismic imaging and gravity signatures. Ghosh *et al*., (2016) also interpreted the overall structural disposition as a positive flower structure bounded between the longitudinal and transverse faults with vertical extrusion and symmetric juxtaposition of mid-crustal amphibolite grade basement gneisses over low-grade upper crustal rocks emanating from the central axis of the transpressional belt. Ghosh *et al*., (2016) also inferred that deformational, metamorphic, fabric data and monazite age from Rengali Province, converge towards a multi-scale transpressional deformational episode at ca. 498-521 Ma. Their detailed study suggest that deformation was regionally partitioned into fold-thrust dominated shortening zones alternating with zones of dominant transcurrent deformation bounded between the Barkot Shear Zone (thrust) in the north and the dextral Kerajang Fault Zone in the south. The strain partitioned zones are restricted between the sinistral Riamal Shear Zone in the west and the dextral Akul Fault Zone in the east which are interpreted as synthetic R and antithetic R' Riedel shear planes, respectively (Ghosh *et al*., 2016).

Misra *et al*., (2000) and Sawant *et al*., (2017) inferred that both the Rengali charnockite and the hornblende orthogneiss intruded the Rengali Province at around 2.8 Ga, and underwent metamorphism simultaneously at around 2.5 Ga. Dasgupta *et al*., (2017) proposed that the protoliths of orthogneissic rocks (charnockite - enderbite, migmatitic hornblende gneiss and granite gneiss) occupying the central part of the Rengali Province were emplaced in the deep to middle crust (8-10 kbar; 800-860 ^{o}C) and crystallized as fractionated magma in within-plate syncollisional setting during the ca. 2860–2780 Ma Rengali orogeny. They interpreted that the charnockite magma was synkinematically emplaced followed by post-kinematic emplacement of the hornblende granite and leucogranite. The Rengali high-grade rocks are brought in contact with the low-grade rocks of the Singhbhum Craton by thrusting and shearing with a top-to-the-north vergence. This entire evolutionary history further demarcates the southward growth of the Singhbhum Craton during Meso-Neoarchean era. Chattopadhyay *et al.* (2015) have interpreted that the Rengali supracrustal rocks were deposited between 2.79 and 2.42 Ga on the ~2.80 Ga Pal Lahara Gneiss basement. This age is broadly similar to the emplacement of the protolith of the charnockite, granite gneiss and leucogranite in the central part of the Rengali Province. Several Neoproterozoic zircon/monazite age populations (0.98–0.94 Ga, 0.85–0.80 Ga and 0.62–0.50 Ga) found common between the Eastern Ghats Granulites and the Rengali supracrustal units indicate a common geological history shared by the Rengali Province with the granulites of the EGP since the early Neoproterozoic (Chattopadhyay *et al*., 2015). Sheikh *et al*., (2020) concluded that the Rengali Province and Jeypur Province (between the Bastar craton and the EGP) share a common geological history. Axelsson *et al*., (2020) inferred that U–Pb rutile, Rb–Sr biotite and $^{40}Ar – ^{39}Ar$ amphibole ages of ca. 500 Ma occurring on a regional scale throughout the EGB and the Rengali Province is indicative of a thermal overprint belonging to the Kunga Orogeny which is a key geological feature of Gondwana.

Two divergent views are expressed regarding the cratonic lineage of the Rengali Province. Mishra and Gupta (2014) and Bhattacharya *et al.* (2016) opined that the Rengali Province is a part of Bastar craton. On the other hand, geological evidences from the central and eastern parts of Rengali Province suggest its lineage with the Singhbhum Craton (Mahapatro *et al.,* 2012; Bose *et al*., 2015, 2016; Ghosh *et al*., 2016).

Significance of the Rengali Province

Though the geochronological investigations involving modern techniques fairly established the Rengali Province as a Neoarchaean block, distinct from the Singhbhum and Bastar cratons and also the EGP, a lot more detailed geological ground mapping and meaningful integration with products of National Geochemical and Geophysical mapping programmes is necessary to delineate the actual limits of the RP and evaluate its significance. The bounding shear zones need special attention since these could be sites of movements of the mineralizing fluids derived from the precursor crustal blocks. The Cu ($\pm$ Au) prospect of Adash area, near Riamal, in its southwestern marginal part is an indication. The shear zones close to and conformable with the Kerajang shear zone host lenses of deformed nepheline syenite between Chhatabar and Kamakhyanagar (Panda *et al.*, 1998; Panda and Panigrahi, 2009; Ranjan *et al.*, 2018; Sheikh *et al.*, 2020). The recent interpretation by Sheikh *et al*., (2020) indicate that the curvilinear shear zone hosting ~1300Ma miaskitic nepheline syenite continues from Chhatabar near Riamal through Rairakhol, Sonepur, Bolangir and encompassing the Khariar alkaline complex to Koraput Complex in the Jeypur Province. This enhances the possible significance of the study of this zone (or zones) especially for mineralization commonly related to Proterozoic alkali magmatism and also for locating lamproite and kimberlite bodies if any. Areas between Maulabhanj and Bhuban through Birasal and Kathpal is important for the known occurrence of pods and lenses of chromite associated with boudinaged ultramafic and associated gabbro-anorthosite intrusives which may have a potential host rock for PGE. The shear zone passing between Malaygiri and Tomka-Daitari supracrustal belt in the eastern boundary of RP has many mafic and ultramafic bodies near Kaliahata and Benamunda close to the Ramiala Dam where investigation for PGE was recently undertaken by GSI. The zone may continue further towards NW. The areas to the north and NW of the Rengali Province have 2.8 Ga plutons of A-type granites in Tamparkola, Bamra and Jharsuguda. Some of these granite and pegmatite bodies in Pandkimal areas of Sundargarh district are investigated by Atomic Mineral Directorate (AMD) for rare-metals and radioactive elements. The possible linkage of this Kerajang shear zone may be studied in the context of the initiation of the Gondwana basin and also the correlation of the Mahanadi rift zone with the Lambert rift of East Antarctica. This is an important topic of research in deciphering geological events of Eastern Ghats-Rengali-Reyner orogens. Bose *et al.*(2016) inferred that a Pan-African tectonic front along the northern (Rengali orogen) and the western margin of the Eastern Ghats belt (EGB) extends eastwards towards the Prydz Bay region in Antarctica and they argued that the Pan African accretion front located along the northern margin and continuing along the western margin of the Grenvillian-age domain in EGB (a dismembered part of the Rayner Complex) is the loci along which the EGB integrated with the Greater India landmass as late as the Pan African, coinciding with the final assembly of the Gondwanaland.

Acknowledgement

Authors thank Shri P. C. Patra, Deputy Director General, Geological Survey of India for invitation to submit this paper for the special volume of the Indian Journal of Geosciences.

References

Axelsson, E., Mezger, K., Ewing, T. 2020: The Kunga Orogeny in the Eastern Ghats Belt: evidence from geochronology of biotite, amphibole and rutile, and implications for the assembly of Gondwana. *Precambrian Research*, **347**: 105805.

Banerjee, P. K. 1972: Geology and geochemistry of the Sukinda Ultramafic field, Cuttack District, Orissa. *Memoirs of the Geological Survey of India*, **103**: 171 p.

Banerjee, P.K., Mahakud, S.P., Bhattacharya, A.K., Mohanty, A. K., 1987: On the northern margin of the Eastern Ghats in Orissa. *Records Geological Survey of India*, **118(2)**: 1–8.

Bhattacharya, A., Das, H.H., Bell, E., Bhattacharya, A., Chatterjee, N., Dutt, A. and Saha, L., 2016: Restoration of Late Neoarchean-early Cambrian tectonics in the Rengali orogen and its environs (eastern India): the Antarctic connection. *Lithos*, **263**:190–212.

Biswal, T.K., De Waele, B., Ahuja, H., 2007: Timing and dynamics of the juxtaposition of the Eastern Ghats mobile belt against the Bhandara Craton, India: a structural and zircon U-Pb SHRIMP study of the fold-thrust belt and associated nepheline syenite plutons. *Tectonics*, **26(4)**: TC4006, 1-21.

Bose, S., Guha, S., Ghosh, G., Das, K., Mukhopadhyay, J., 2015: Tectonic juxtaposition of crust and continental growth during orogenesis: example from the Rengali Province, eastern India. *Geoscience Frontiers,***6(4)**: 537–555.

Bose, S., Das, K., Kimura, K., Hidaka, H., Dasgupta, A., Ghosh, G., Mukhopadhyay, J.: 2016. Neoarchean tectonothermal imprints in the Rengali Province, eastern India and their implication on the growth of Singhbhum Craton: evidence from zircon U-Pb SHRIMP data. *Journal of Metamorphic Geology*, **34(8)**:743–764.

Chattopadhyay, S., Upadhyay, D., Nanda, J. K., Mezger, K., Pruseth, K. L., Berndt, J., 2015: Proto-India was a part of Rodinia: evidence from Grenville-age suturing of the eastern Ghats Province with the Paleoarchean Singhbhum craton. *Precambrian Research*, **266**: 506–529.

Chetty, T.R.K., 1995: A correlation of Proterozoic shear zones between Eastern Ghats, India and Enderby Land, EastAntarctica. *In*: India and Antarctica during the Precambrian. (Eds.) Santosh, M. and Yoshida, M., *Memoirs Geological Society of India*, **34**: 205-220.

Chetty, T.R.K., 2001: The Eastern Ghats Mobile Belt, India: a collage of juxtaposed terranes (?). *Gondwana Research*, **4(3)**: 319–328.

Chetty, T.R.K., 2010. Structural architecture of the northern composite terrane, the Eastern Ghats Mobile Belt, India: Implications for Gondwana tectonics. *Gondwana Research*, **18(4)**: 565–582.

Crowe, W.A., Cosca, M. A., Harris, L.B., 2001: $^{40}Ar/^{39}Ar$ geochronology and Neoproterozoic tectonics along the northern margin of the Eastern Ghats Belt in north Orissa, India. *Precambrian Research*, **108(3-4)**:237–266.

Crowe, W.A., Nash, C.R., Harris, L.B., Leeming, P.M., Rankin, L.R., 2003: The geology of the Rengali Province: implications for the tectonic development of northern Orissa, India. *Journal of Asian Earth Science*, **21(7)**: 697–710.

Dash, C. R. and Das, P. K., (2005) Report on Deogarh Supracrustal Sequence and spatially associated granitoids in parts of Deogarh District, Orissa, *Unpublished Progress Report for the F.S. 1998-1999 & 1999-2000 (UE 13434), Operation: Orissa, GSI.*

Dash, C. R., Das, P. K., and Mohanty, S. D., 2004: Evolution of Deogarh supracrustal sequence and spatially associated granitoids in Balam – Rajamunda – Tikaitpal – Tangra –Ambgaon segment, Deogarh district, Northern Orissa. *Records Geological Survey of India*, **134(3)**: 169-174.

Dasgupta, A., Bose, S., Das, K., Ghosh, G., 2017: Petrological and geochemical evolution of the Central Gneissic Belt, Rengali Province, eastern India: Implications for the Neoarchean growth and orogenesis. *Journal of Asian Earth Science*, **146**: 1–19.

Dobmeier, C.J. and Raith, M.M., 2003: Crustal architecture and evolution of the Eastern Ghats Belt and adjacent regions of India. *In*: Proterozoic East Gondwana: Supercontinent Assembly and Breakup. Yoshida, M., Windley, B.F., Dasgupta, S. (Eds.). *Geological Society, London, Special Publication,* **206**: 145–168.

Dutta, A., Gupta, S., Panigrahi, M.K., 2010: The southern Rengali province – a reworked or exotic terrane? *Indian Journal of Geology*, **80(1-4)**: 81-96.

Ghosh, G., Bose, S., Das, K., Dasgupta, A., Yamamoto, T., Hayasaka, Y., Chakrabarti, K., Mukhopadhyay, J., 2016: Transpression and juxtaposition of middle crust over upper crust forming a crustal scale flower structure: insight from structural, fabric, and kinematic studies from the Rengali Province, eastern India. *Journal of Structural Geology*, **83**: 156–179.

Iyengar, S.V.P. and Murthy, Y.G.K. 1982: The evolution of the Archaean-Proterozoic crust in parts of Bihar and Odisha, Eastern India. *Records Geological Survey of India*, **112(3)**:1-5.

Kar, R., 2001: Evidence of Structural reworking in the Eastern Ghats Granulite belt, India: Implication for a Contiguous Supercontinent in the Proterozoic. *Gondwana Research*, **4(4)**:650.

Kartikeyan, A. and Nayak, K. K., 2017: Search for PGE in the mafic-ultramafic plutonic bodies in Patakhali – Balijori and Ghuturigan – Mundasahi areas, Kendujhar and Dhenkanal districs, Odisha. *Records of the Geological Survey of India*, **150 (3).**

Leelanandam, C., Burke, K., Ashwal, L.D. and Webb, S.J. 2006: Proterozoic mountain building in Peninsular India: An analysis based primarily on alkaline rock distribution. *Geological Magazine,* **143(2)**:1-18.

Mahalik, N.K., 1994: Geology of the contact between the Eastern Ghats Belt and North Orissa Craton, India. *Journal Geological Society of India*, **44**:41-51.

Mahalik, N.K., 1995: Geology of Rengali assemblage, an off shoot of Eastern Ghats Mobile Belt within Iron Ore Craton of north Odisha. *Vistas in Geological Research, Utkal University Special Publication in Geology*,**1**: 104-114.

Mahapatro, S.N., Tripathy, A.K, (2011): Final report on the specialised thematic mapping of the northern contact region between Eastern Ghats Mobile Belt and Singhbhum Craton around Kamakhyanagar – Bhuban – Hatibari – Nihalprasad areas in Jajpur and Dhenkanal Districts, Orissa. *Unpublished Progress Report for the Geological Survey of India, F.S. 2008-2010.*

Mahapatro, S.N., Pant, N.C., Bhowmik, S.K., Tripathy, A.K., Nanda, J.K., 2012: Archaean granulite facies metamorphism at the Singhbhum Craton–Eastern Ghats Mobile Belt interface: implication for the Ur supercontinent assembly. *Geological Journal*, **47**: 312–333.

Mahapatro, S.N. 2013: Geology of the northern contact zone between the Eastern Ghats Mobile Belt and the Singhbhumcraton in Odisha sector. *Journal Geological Society of India*, **82:** 724-725.

Misra, S., Moitra, S., Bhattacharya, S., Sivaraman, T.V., 2000: Archaean granitoids at the contact of Eastern Ghats Granulite Belt and Singhbhum–Orissa Craton, in Bhubaneswar-Rengali sector, Orissa, India. *Gondwana Research*, 3: 205–213.

Misra, S., Gupta, S., 2014: Superposed deformation and inherited structures in an ancient dilational step-over zone: post-mortem of the Rengali Province, India. *Journal of Structural Geology*,**59**: 1–17.

Mohanty, M., Mahapatro, S.N., 2004: Tectono-stratigraphic relationship between Kamakhyanagar gneisses and Malaygiri greenstones in Kendujhar, Anugul anddhenkanal districts, Orissa. *Records of the Geological Survey of India*, **138(2)**: 126-129.

Mohanty, M., Mahapatro, S.N. and Nanda, J.K., 2007: Nature and stratigraphic status of metasedimentary lithopackage in the Terrane boundary between Singhbhum craton and Eastern Ghats Mobile Belt in Pal Laharha –Kamakhyanagar sector,Central Odisha. *Vistas in Geological Research, Utkal University Special Publication in Geology*, **6**: 147-154.

Mohanty, M., Panda, P.K. and Mohanty, B.K., 2008: Petrogenesis of Pal Laharha Granitic Gneiss in Eastern Indian Craton: evidence from field relations and petrochemistry. *Journal Geological Society of India*, **72**: 415-431.

Mukhopadhyay, D. and Basak, K., 2009: The Eastern Ghats Belt – a polycyclic granulite terrain. *Journal Geological Society of India*, **73:**489-518.

Nanda, J.K., 1994: Gneiss-charnockite relation in parts of northern fringes of Eastern Ghats granulite belt in Riamal sector Orissa. Proceeding Volume Workshop on Eastern Ghats Mobile Belt, Visakhapatnam, 16-18.

Nanda, J. K., Mohanty, M., and Mahapatro, S. N., 2020: Geology of Odisha. Geological Society of India, Bangalore (*in Press*).

Narayanaswami, S., 1975: Proposal for charnockite-khondalite system in the Archean Shield of Peninsular India. *Miscellaneous Publication, Geological Survey of India*, **23(1)**: 1-16.

Nash, C., Rankin, L., Leeming, P., Harris, L., 1996: Delineation of lithostructural domains in northern Orissa (India) from Landsat Thematic Mapper imagery.

Tectonophysics, **260(4)**: 245–257.

Nelson, D.R., Bhattacharya, H., Thern, E.R., Altermann, W., 2014: Geochemical and ionmicroprobe U-Pb zircon constraints on the Archaean evolution of Singhbhum Craton, eastern India. *Precambrian Research*, **255(1)**: 412–432.

Panda, P.K. and Panigrahi, D., 2009: Petrochemistry and REE mineralogy of Kankarakhol -Lodhajhari Alkaline Complex, Deogarh district, Orissa. *Indian Journal of Geosciences*, **63(3)**: 249-274.

Panda, P.K. and Patra, P., (1991): Progress report on geotraverse along Bauda – Deogarh -Panposh transect across Eastern Ghat, Iron Ore and Gondwana Supergroups (Rairakhol-Naktideola section). *Unpublished Progress Report for the F.S. 1990-1991(UE 11889), Operation: Orissa, GSI.*

Panda, P.K. and Patra, P., (1992) Progress report on geotraverse along Bauda – Deogarh -Panposh transect across Eastern Ghat, Iron Ore and Gondwana Supergroups, Rengalbeda-Deogarh - Barakot - Purunapani section**,** Sambalpur District, Orissa. *Unpublished Progress Report for the F.S. 1991-1992, (UE 11909), Operation: Orissa, GSI.*

Panda, P.K., Patra, P.C., and Nanda, J.K., 1998: Petrochemistry of the Alkaline rocks of Rairakhol-Kankarakhol belt, Sambalpur and Deogarh districts, Orissa. *Geological Survey of India, Special Publication*, **44**: 307-314.

Prasad Rao, G. H. S. V., Murthy, Y. G. K. and Deekhshitulu, M. K., 1964: Stratigraphic relations of Precambrian Iron formations associated sedimentary sequences in parts of Keonjhar, Cuttack, Dhenkanal and Sundergarh districts, Orissa, India. Proceeding International Geological Congress, New Delhi, **X**: 72-87.

Ramachandran, K. V. and Sinha Roy, R. N. (1982): Report on the systematic geological mapping in parts of Deogarh sub-division, Sambalpur District, Orissa *Unpublished Progress Report for the F.S. 1981-1982, (UE 11565), Project (North): Orissa, GSI.*

Ramakrishnan, M., Nanda, J.K. and Augustine, P.F., 1998: Geological evolution of the Proterozoic Eastern Ghats Mobile Belt. *Geological Survey of India, Special Publication*, **44**: 1-21.

Ranjan, S., Upadhyay D., Kumar A., Pruseth, K. L. and Nanda, J.K., 2018: Zircon geochronology of deformed alkaline rocks along the Eastern Ghats Belt margin: India–Antarctica connection and the Enderbia continent. *Precambrian Research*, **310**: 407-424.

Rath, S.C., Behera, S.N. and Som, S.K. 1993: Contact zone between Eastern Ghats and Iron Ore Supergroup / Chhatisgarh Supergroup with special emaphasis on petrology and mineral association in parts of Western Orissa in Sambalpur, Dhenkanal and Kalahandi districts (Kansar-Jamankera Area). *Records of the Geological Survey of India*, **125(3)**: 50-51

Ray, P. and Acharya, S., 1997: Medium pressure metamorphism of BIF-I and associate rocks, North of Kamakhyanagar, Dhenkanal district, Orissa. *Special Publication in Geology (2), Utkal University*. p.99-112.

Saha, A., 1994: Crustal evolution of Singhbhum-North Orissa, India. *Memoirs Geological Society of India*, **27**: 341p.

Sarkar, S. N., Saha, A. K. and Sen, S., 1990: Structural pattern of Pala Lahara area, Dhenkanal district based on aerial photointerpretation and ground data. *Indian Journal Earth Science*, **17(2)**: 128-137.

Sarkar, A., Pati, U.C., Panda, P.K., Patra, P.C., Kundu, H.K. and Ghosh, S., 2000: Late Archaean charnockitic rocks from the northern marginal zones of the Eastern Ghats belt: a geochronological study. Proceedings Volume, International Seminar on Precambrian Crust in Eastern and Central India, IGCP-368, Bhubaneswar, 171-179.

Sawant, A.D., Gupta, S., Clark, C., Misra, S., 2017: The Rauer-Rengali connection in the Indo-Antarctica amalgam: evidence from structure, metamorphism and geochronology. *In*: Crustal Evolution of India and Antarctica: the Supercontinent Connection. (Eds.) Pant, N.C. and Dasgupta, S., *Geological Society London, Special Publications*, **457**: 171–196

Sheikh, J. M., Patel, S. C., Champati, A. K., Madhavan, K., Behera, D., Naik, A., Gerdes, A., 2020: Nepheline syenite intrusions from the Rengali Province, eastern India: Integrating geological setting, microstructures, and geochronological observations on their syntectonic emplacement. *Precambrian Research*, **346**: 105802.

Topno, A., Dey, S., Liu, Y. and Zong, K., 2018: Early Neoarchaean A-type granitic magmatism by crustal reworking in Singhbhum craton: evidence from Pala Lahara area, Orissa. *Journal of Earth System Science*, **127(43)**: 1- 22.

Windley, B. F., 1977: The evolving Continents. John Wiley & Sons, London, 385p.

Indian Journal of Geosciences, Volume 74, No. 3
July - September, 2020; pp. 295-306

Invited Paper

Ductile shear zones along the margins of Neoarchaean Chitradurga Schist Belt with particular reference to tectonic status of Ghattihosahalli Belt of Dharwar Craton, India

Siladitya Sengupta[1*], H.M. Ramachandra[2] and Abhinaba Roy[3]

[1] NCEGR, Geological Survey India, Faridabad
[2] Former Director, Geological Survey India
[3] Former Sr. Dy. DG. Geological Survey India
*Corresponding author's email: senguptasiladitya@gmail.com

Abstract: Major ductile shear zones delimit the Neoarchaean NNW-trending Chitradurga schist belt (CSB) of West Dharwar Craton (WDC) in southern India. The authors present the tectonic set up along the sheared margins of the schist belt. These shear zones are important in the structural evolution of the poly-deformed CSB. The Sargur-type older Ghattihosahalli Belt (GH Halli Belt), occurring close to the western margin of CSB, shows characteristics of a shear belt that got tectonically incorporated within the PGC. The linear GH Halli Belt and adjacent PGC show undeniable evidences of a sinistral strike-slip dominated subvertical shear zone (Chitradurga Western Margin Shear Zone). The western margin of CSB, having tell-tale evidences of a basement (PGC) - cover (CSB) relationship, has been tectonised during this late shear.

In contrast, the eastern margin of CSB is unmistakably a tectonic one, defined by a prominent crustal scale ductile shear zone (Gadag Mandya Shear Zone) along which the amphibolite grade Javanahalli Belt (JB) of uncertain age is juxtaposed with the green schist grade CSB. No basement-cover relationship exists at the eastern margin. An early thrusting and late sinistral shearing along this contact were earlier reported by these authors. The early top-to-west movement is modified into a major late sinistral transurrent shear either in continuum or in phases. Regional scale strain partitioning as a result of the major E-W directed oblique transpressional tectonism is manifested by narrow simple shear dominated high strained eastern and western margins of the CSB and pure shear dominated, poly-deformed supracrustal rocks in the wider central part of the CSB.

Keywords: Ductile shear, Dharwar craton, GH Halli, Strain partitioning.

Introduction

The Archaean to Proterozoic Dharwar Craton in southern India comprises western (Western Dharwar Craton or WDC) and eastern (East Dharwar Craton or EDC) cratonic blocks that are separated by either the ductile shear zone east of the Chitradurga Belt or the Closepet Granite (Swami Nath and Ramakrishnan, 1981); 3.4-3.1 Ga Archaean TTG gneiss-supracrustals (including Sargur Complex) and younger Neoarchaean 3.0-2.6 Ga greenstone belts that are intruded by 2.6-2.4 Ga granites (Chadwick *et al.*, 2007; Ramakrishnan and Vaidyanadhan, 2008; Jayananda *et al.*, 2013). Based on differences in lithological set up, metamorphic characters, structural features and nature of intrusive Neoarchaean to Palaeoproterozoic granites the WDC and EDC are believed to have had separate evolutionary histories. However, certain common features in the two cratons and overlapping geochronological ages have prompted some workers to propose that they evolved as a single terrain (Maibam *et al.*, 2011). Many models for evolution of WDC and EDC have been proposed and critically reviewed (e.g. Chardon *et al.*, 1998; Chadwick *et al.*, 2007; Sengupta and Roy, 2012; Maibam *et al.*, 2011; Jayananda *et al.*, 2013).

Ductile shear zones have an important role in providing crucial information on relative movement of large crustal blocks or plates in geologic past and thereby on tectonic reconstruction of an area (Passchier and Coelho, 2005). Large scale strain partitioning is a characteristic feature of transpressional tectonics, particularly in an oblique convergence set up. The role of strain partitioning has been discussed while proposing a plate tectonic model for the evolution of the Dharwar Craton by Chadwick *et al*. (2003, 2007). Shear Zones in the WDC were first described by Drury and Holt (1980) and Rollinson *et al*., (1981) who interpreted that margins of most greenstone belts and the gneiss-supracrustal contacts in the craton were sheared in nature. The interpretation of shallow, sub-crustal seismic discontinuity at the eastern contact between the Chitradurga Schist Belt and older gneiss-supracrustals (Kaila *et al.*, 1979) provide geophysical support for presence of a major shear zone in that area. In a recent contribution (Roy *et al*., 2020), we have shown that ENE-WSW directed oblique transpressional tectonism resulted in development of boundary shears and intra- and interformational ductile shear zones having dominant sinistral transcurrent component within the Chitradurga Schist Belt (CSB). In this paper, we present new data from the GH Halli Belt on the western margin of the CSB and show that the CSB flanked by the Chitradurga Western Margin Shear Zone (CWMSZ) in the west and the Gadag-Mandya Shear Zone (GMSZ) in the east affords a good example of manifestation of strain partitioning on small and large scales during structural evolution.

The Chitradurga Schist Belt

The Neoarchaean Dharwar Supergroup in the WDC comprises mainly N-S to NNW-SSE trending granite-greenstone belts separated by screens of Older gneiss (>3.0 Ga Peninsular Gneissic Complex, or PGC) and associated older supracrustals placed in the Sargur Complex (Swaminath and Ramakrishnan, 1981). The Dharwar Supergroup unconformably overlies the PGC as documented by presence of quartz-pebble conglomerate at many places in the WDC. It is divisible into lower Bababudan and upper Chitradurga Groups based on well-developed stratigraphic way-up criteria. Both these groups show common polyphase structural and tectonic history and greenschist to lower amphibolite grade of metamorphism.

The Chitradurga Schist Belt (CSB, or Chitradurga-Gadag Superbelt, Ramakrishnan and Vaidyanadhan, 2011) is the easternmost supracrustal belt of WDC exposing a typical WDC association of closely spatially associated N-S to NNW-SSE trending PGC, older supracrustals and Dharwar Supergroup of rocks that extend over a length of 400 km from Gadag in the north to Mandya in the south in Karnataka. The Mesoarchaean Ghattihosahalli Belt (GH Halli Belt) forms the western margin of the Chitradurga Schist Belt (CSB) and is considered to be a part of the Sargur Schist Complex (Swaminath and Ramakrishnan, 1981) that is older to the Neoarchaean Dharwar Supergroup. The Dharwar Supergroup of rocks form the central part of the CSB, and the Javanahalli Belt (JB) of uncertain stratigraphic status, forms the eastern tectonic margin of CSB (Sengupta and Roy, 2012). Well-developed basement-cover relationship exists on the western margin of the CSB in the study area between the Peninsular Gneissic Complex (PGC) component of the GH Halli Belt on the west and the Dharwar Supergroup of rocks on the east attested by the presence of quartz-pebble conglomerate at Nerlakatte (Swaminath *et al*., 1976). Above this unconformity, a stable, platformal sequence of the Bababudan Group follows in the east which is in turn succeeded by rocks of the Chitradurga Group. Sinistral shear zones at the margins of CSB have been reported by many authors (Sengupta and Roy, 2012; Roy *et al*., 2020; Roy and Bhattacharyya, 2014, Mohakul and Pattanaik, 2015) and discontinuous, discrete shear zones on different scales and dimensions, mostly along formational/ lithological contacts have been reported from within the CSB.

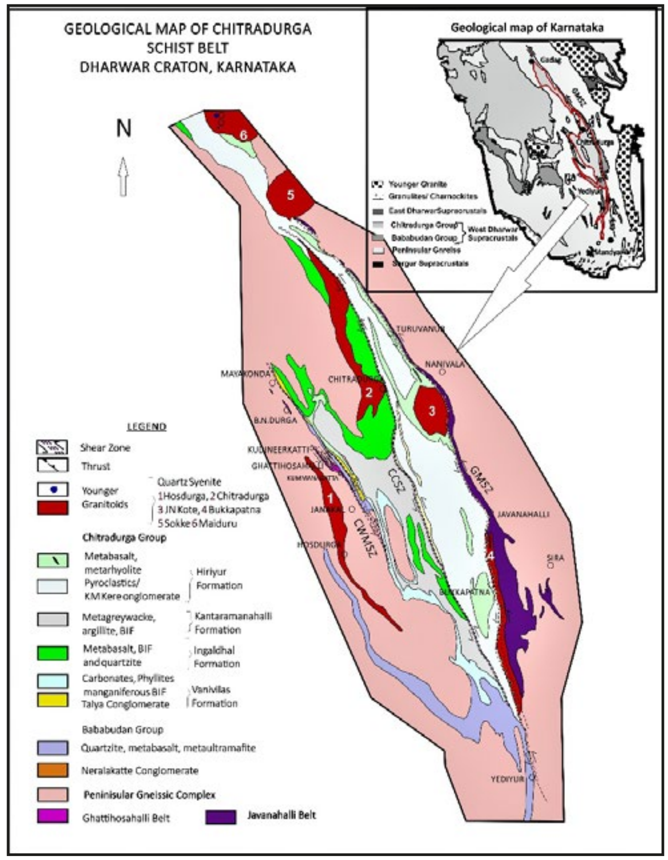

Fig.1: Geological Map of Chitradurga Schist Belt (CSB) in Karnataka showing the Chitradurga Western Margin Shear Zone (CWMSZ), Gadag Mandya Shear Zone (GMSZ) and Chitradurga Central Shear Zone (CCSZ).

Western margin of Chitardurga Schist Belt

The lithotectonic ensemble at the western margin of Chitradurga Schist Belt comprises the older Sargur type Ghattihosahalli Belt, the PGC and rocks of the Dharwar Supergroup including those of the Bababudan and Chitradurga Groups and has earlier been studied among others by Seshadri *et al*., (1981), Chadwick *et al*., (1981) and Paranthaman (2005).

1. Ghattihosahalli Schist belt

The narrow, linear Ghattihosahalli Belt (GH Halli Belt) trends approximately NW-SE, extends discontinuously over a length of nearly 50 km from Mayakonda in the north to Janakal in the south (Paranthaman, 2005) at the western margin of CSB (Fig.1). The proportion of gneisses adjoining the belt increases towards north and in the BN Durga and Mayakonda areas, the supracrustal rocks occur as barely mappable to outcrop scale patches within gneisses. GH Halli Belt is surrounded by 3.1 Ga PGC (Taylor *et al.,* 1984) with the gneisses also occurring as thin slivers within the schist belt in the eastern part with the Dharwar Supergroup exposed to further east. The GH halli Belt is constituted by a sequence of metaultramafics, amphibolite, metapelites, orthoquartzite and aluminous quartzite that contain thin seams of barite at places (Radhakrishna and Srinivasaiah, 1974; Viswanatha *et al.,* 1977; Chadwick *et al.,* 1981; Paranthaman, 2005). Our studies have shown that a coherent stratigraphic order in the GH Halli Belt cannot be established due to multiple deformation, granite invasion, tectonism and amalgamation with the Dharwar Supergroup.

Quartzites with impersistent metapelite patches in the belt are tectonically interlayered with other rocks of the belt without a coherent stratigraphic order. They contain a mineral assemblage of quartz-kyanite-sillimanite-staurolite-garnet-muscovite-chloritoid-chlorite and sericite, along with accessory tourmaline, chromite, iron oxides and zircon (Raase *et al.,* 1983). Petrographic studies indicate that aluminosilicates may have formed during pre- to early-tectonic period whereas staurolite and garnet could have formed much later during early schistosity development. Relics of rare sillimanite now largely replaced by white mica occur in quartzites in both Kummanagatta and Ghattihosahalli areas. Pseudomorphs of andalusite and probably sillimanite occur in the Kudineerkatte outcrop (Fig.2a) associated with coarse pegmatite within granite gneiss. However microscopic and XRD studies done by us have shown presence of only secondary white mica in these samples indicating complete retrogression of suspected andalusite and sillimanite. Fuchsite, is characteristically present in quartzite. A characteristic association of thin, cm-scale, impersistent barite layers chiefly with the fuchsite quartzite in this area was first reported by Radhakrishna and Srinivasaiah (1974). Though barite is mainly associated with quartz, Devaraju *et al.,* (1999) report presence of minor chromian mica, uvarovitic garnet, K-Ba Feldspars, pyrite, plagioclase, tourmaline and epidote in these layers.

The ultramafic components of the GH halli Belt include STPK komatiite (of Kummanagatta), ultramafic schists with varying modal proportions of talc-tremolite-actinolite-chlorite-serpentine (talc-serpentine or serpentine rocks and hornblendite. Though many publications on the GH halli Belt show large map areas covered by ultramafics as komatiite based on chemical data (Chadwick *et al.,* 1981; Devaraju *et al.,* 1999; Paranthaman, (2005); GSI unpublished map of Ghattihosahalli area) deformation and retrogressive recrystallizations have erased any igneous primary structures or mineral assemblages in these ultramafics. The sole exception is the relict spinifex texture in the peridotitic komatiite (STPK) recorded in the hill southwest of Kummanagatta (Viswanatha *et al.,* 1977). That as the proper STPK and hence the only example of ultramafic lava occurs in the hill southwest of the Kummanghatta. Other ultramafics of the area show large variations in their modal assemblage of tremolite-actinolite and chlorite suggesting that, like in other Sargur type ultramafics (Swaminath and Ramakrishnan, 1981), these too form a part of dismembered original layered complexes. Jayananda *et al.,* (2008) have interpreted that ultramafic rocks of the Ghattihosahalli (and those from other Sargur Complexes in WDC including Banasandra, Nuggihalli, JC Pura, Kalyadi) define a 16-point Sm–Nd whole-rock isochron age of 3352±110 Ma. Amphibolite and rare hornblendite occur mainly in the western part of the area also tectonically layered with other rock types in the belt. The amphibolites show a prograde mineral assemblage of hornblende-relic moderate to high An plagioclase-rare quartz and iron oxides that is retrogressed to secondary amphiboles-low An plagioclase-quartz-epidote/zoisite-chlorite and iron oxides.

2. Peninsular Gneissic Complex (PGC) and Younger Hosdurga Granite

Gneissic rocks in the western part of the GH Halli Belt are mainly granite gneisses of quartz-tonalite, trondjehmite and granodiorite composition having banded and stromatic partial melt migmatitic structures at places. The migmatite sheet at BN Durga includes tonalitic gneisses containing granitic leucosomes along with relict TTG and amphibolite bands, schlierens and restites. The gneisses are considered to be of pre-Dharwar age with their younger structures in conformity with that of the Dharwar Supergroup.

PGC with TTG composition generally show earlier equant, granoblastic fabric overprinted by a strong foliation defined by biotite. The retention of mafic selvedges around leucosomes and coplanar deformation attest to in-situ generation of melt veins. This anatectic episode is believed to pre-date Dharwarian metamorphism and deformation. The ductile shearing of the PGC on both sides of the GH Halli Belt show overprinting of partial melt migmatitic structures by mylonitic fabric. Taylor *et.al,* (1984) have reported Rb-Sr whole-rock isotopic data for gneisses of the Chitradurga area that define a poorly fitted 2970±100 Ma isochron. Pb whole rock isotope data define a well fitted 3028±28 Ma $^{207}Pb/^{206}Pb$ isochron. There is no significant difference between the Pb/Pb ages of the two groups within this suite of Peninsular Gneisses.

3. Dharwar Supergroup

The younger Dharwar supracrustals (stratigraphically known as the Dharwar Supergroup), which unconformably overlie the PGC at the western margin of CSB, constitute the main

Fig. 2: (a) Large Pseudomorphs of andalusite and probably sillimanite in metapelites near Kudineerkatte, GH Halli Belt. (b) Isoclinal $^{G}F_2$ folding in outcrop scale; Bedding defined by alternate psammitic and pelitic layers and early schisotsity ($^{G}S_1$) both are folded by $^{G}F_2$, indicating complete transposition of pre-existing bedding and schistosity subparallel to late $^{G}S_2$ fabric, GH Halli Belt. (c). Microsection showing early schistosity ($^{G}S_1$) defined by mica grains is crenulated to give rise to second generation crenulation cleavage ($^{G}S_2$) in metapelitic rocks, GH Halli Belt. (d) Microsection showing sinistral CS fabric and mica fish in mylonitised quartzite, GH Halli Belt. € Fold axial planes (yellow dashed lines) are deformed and curved by the shear deformation to produce strongly asymmetrical non-plane noncylindrical folds (C-planes in blue lines), GH Halli Belt

part of the Chitradurga Schist Belt. The Dharwar Supergroup of rocks is divided into an older Bababudan overlain by the younger Chitradurga Group. Both the basal Neralakatte oligomict Conglomerate of the older Bababudan Group and the basal Talya Conglomerate of the younger Chitradurga Group are in contact with the PGC of the GH halli Belt in separate segments of the western boundary along strike. This feature is interpreted by us (Roy *et al.,* 2020) to be due to delimited occurrence of Bababudan Group of rocks by the fault controlled deposition of Talya Conglomerate at the base of the overlying Chitradurga Group.

4. Structural characteristics of the western margin of CSB

The rocks of the GH Halli Belt at the western margin of the CSB are strongly sheared and mylonitised resulting in a linear, lensoid, disposition of the belt within the PGC. Hence, we denote this belt as a shear belt at the Chitradurga Western Margin Shear Zone (CWMSZ), which has been brought in contact with the CSB by a late sinistral shear. The CWMSZ shows two main shear splays, the western one passing over the GH Halli Belt and its adjacent gneisses and the eastern one mainly passing through the Talya Conglomerate horizon in the east (Fig.1). In the northern part, the shear splay has affected both the gneisses and the Talya Conglomerate near Mayakonda, with less strained domains occurring between the two. The two major shear splays coalesce east of Janakallu in the south (Fig.1).

Presence of relict primary bedding plane in quartzite (with rare metapelite) within the later strong ductile shear zone indicates distinct strain partitioning in the area. The bedding is completely transposed parallel to the second generation crenulation banding ($^{G}S_2$) (Fig.2b). The earliest deformation structures recognizable in the GH Halli rocks include a strong penetrative schistosity ($^{G}S_1$), preserved only on microscopic scale and rare small scale isoclinal intrafolial folds ($^{G}F_1$). Presence of crenulation fabric ($^{G}S_2$) over an earlier mineral assemblage provide evidence for multiple deformation and metamorphism in these rocks (Fig.2c). These earlier fabrics of GH Halli Belt are overprinted by mylonitic and other shear deformation fabrics related to the CWMSZ developed during deformation of the Dharwar Supergroup. Early structures also include cm-scale subparallel clots and patches of kyanite and sillimanite blades and sheaves, fuchsite flakes and oriented aggregates of baryte that attest to presence of an earlier granoblastic schistosity ($^{G}S_1$) associated with amphibolite facies metamorphism. The prograde minerals recorded above are retrogressed into secondary muscovite, sericite and chlorite during later shearing and uplift related processes. The extensive reorientation and neocrystallization of the entire mineral assemblage along planes subparallel to that of the later ductile shear zone make difficult interpretation of mineral orientation fabrics in the area. The early penetrative fabric in the metaultramafics and amphibolites in the study area is represented by varied granoblastic aggregates, schistose prisms, blades and sheaves of hornblende, epidote, chlorite, tremolite and actinolite that formed during amphibolite grade metamorphism. These minerals show grain growth during metamorphism attaining sizes of up to a few cms at places and now mainly occur as relict patches in a mileu of fibrous secondary amphiboles, chlorite, talc and serpentine. The STPK komatiite at Kummanghatta now shows a mineral assemblage of serpentine, talc and chlorite with no clue to original mineralogy and does not show penetrative schistose fabric.

The second generation deformation in GH Halli Belt as observed in the quartzites (with rare metapelite) is also manifested by a set of tight or isoclinal upright to inclined (rarely reclined), low to moderately plunging (10° to 30°→N to N32° W) small outcrop scale folds ($^{G}F_2$) on sub-vertical to steep easterly dipping, NW to NNW striking axial planes. Structural characteristics indicate the above features may have formed by a ENE-WSW (approx.) shortening. $^{G}F_2$ and $^{G}S_2$ are often modified due to superposition of a strong shear fabric due to the later shearing event along CWMSZ. Shear fabric is represented by excellent development of mylonitic foliation, CS fabric and stretching lineation with or without mineral lineation (Fig.2d). Fold axes and axial planes are, at places, deformed and curved by the shear deformation to produce strongly asymmetrical non-plane noncylindrical folds showing variation from upright to reclined geometry (Fig.2e). The strike of the mylonitic foliation and shear bands vary from N25°W to N45°W and dip moderate to steep (46° to 85°) to the east. The stretching lineation plunges gently (0 to 28°) towards N to NNW. Sense of shear is consistently sinistral strike slip (to slightly oblique) in nature. This is well demonstrated by the map pattern of the GH Halli Belt, which shows left lateral shifting towards north as a result of which the distance between the GH Halli Belt and the CSB widens towards north and narrows down southward. The earlier amphiboles have been retrogressed into an assemblage of chlorite-talc-serpentine suggesting their formation during greenschist grade (Dharwarian) metamorphism.

The PGC, to the west of the GH Halli Belt supracrustals, shows similar imprints of the strong ductile shearing superposed on pre-existing gneissic banding along a narrow zone traced for more than 40 km along NW-SE strike. A gneiss may not reveal all aspects of its history clearly, because deformation processes, particularly the ductile shearing event, tend to reorient and flatten older structures, thereby obscuring or even erasing them. The gneisses are considered to be of pre-Dharwar age (>3000 Ma) but their structural features are in conformity with those of the Dharwar Supergroup. The ductile shearing in the gneisses show overprinting of partial melt migmatitic structures by mylonitic fabric.

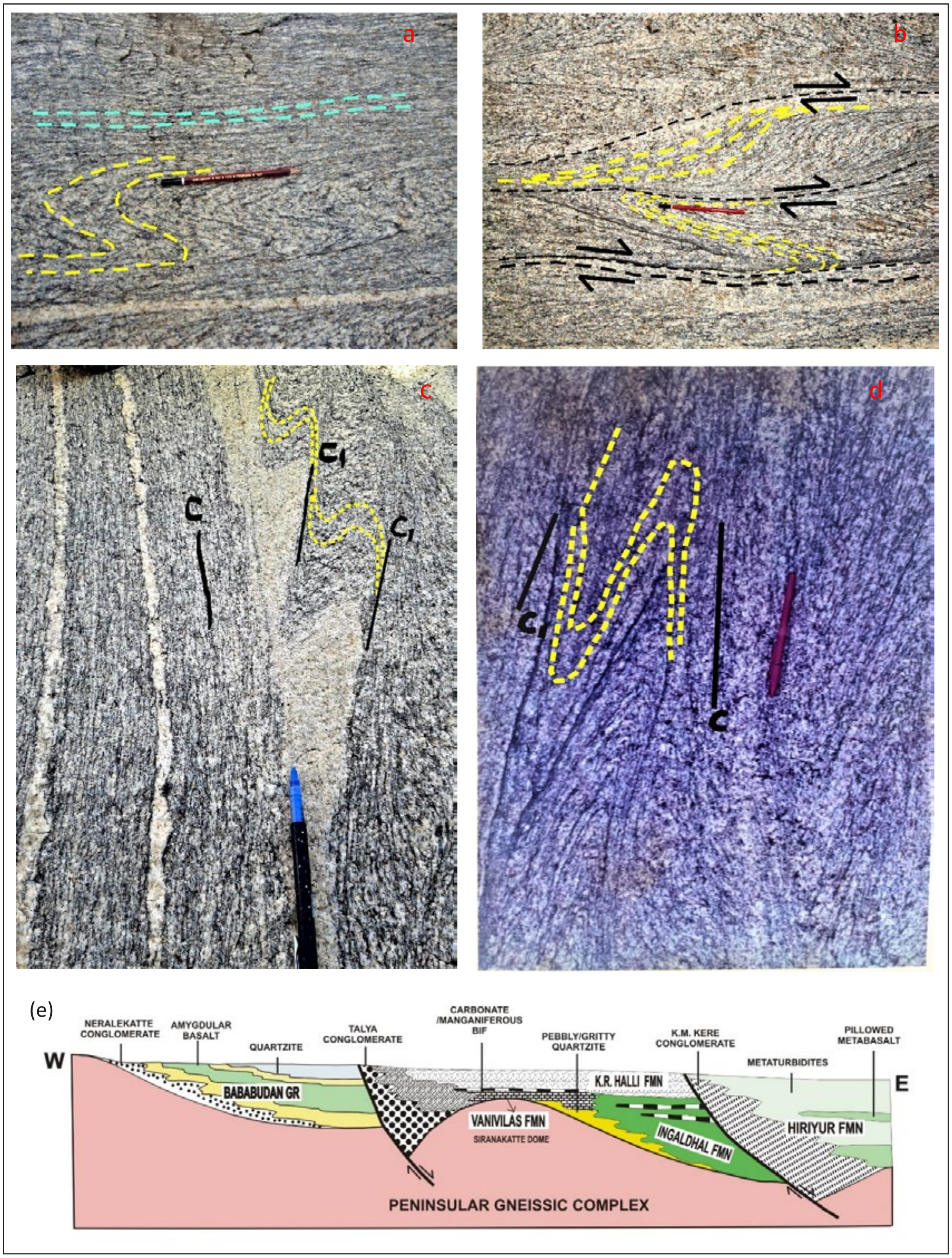

Fig.3: (a) Sinistral folding developed in pre-existing gneissic fabric (yellow lines) due to sinistral shearing (C-planes in blue lines) in the gneisses, W of GH Halli Belt. The C-planes have N40°W-strike. (b) Antithetic C_1-shear band (black lines) showing dextral dragging of the early gneissic foliation (yellow dashed lines). Note that folding of gneissosity as a result of progressive shortening of space between two C_1-shear bands. C_1-shear bands strike at N-S to NNW-SSE. (c) Acute angle (av.30°) between C-and C_1-plane indicating moderate to high shear strain in the gniesses. Note the termination of the folding (of pre-existing gneissic banding) and C_1 planes at the contact with C planes. (d) Angle between C-and C_1-planes progressively decreases and tightness and amplitude/wavelength ratio of folds increase with increasing strain. (e) Fault controlled debris flow deposits of Talya and K. M. Kere Conglomerate horizons at the base of Chitradurga Group and Hiriyur Formation (from Roy *et al.*, 2020)

Shearing has given rise to very well developed consistently asymmetric S-folds and both simple shear (C) and secondary (C_1 of Ramsay and Lisle, 2000) shear bands in gneisses (Fig.3a). Grain size reduction along the shears is discernible but not prominent. The overall shear sense in ductile shear zone resulted from the dominantly simple shear deformation is unambiguously sinistral, the dominant secondary shears are the antithetic shear bands (C_1-bands of Ramsay and Lisle, 2000) and the sense of the displacement is opposite to that of the sense of shear along the C-planes. In our study area, west of Ghattihosahalli, while the main C- shear as demonstrated by sinistral asymmetric folds on gneissic foliation indicate sinistral sense of kinematics, the secondary C_1-shear shows dextral sense of movement (Fig. 3b). The general trend of C-shear is N30°W to N50°W and dip is sub-vertical and that of the antithetic C_1-shear is N-S to N10°W. Synthetic secondary shears (C_2 shears of Ramsay and Lisle, 2000) could not be recognized. The angle between C-and C_1-plane is generally low varying from 20° to 38° (av.30°) indicating moderate to high shear strain. According to Ramsay and Lisle (2000) the angle between these two planes progressively decreases with increasing strain (Fig.3c&3d). Concomitant with this change of angle is a closing up of the spacing between zones together with an increase in length. The zonal narrowing implies that the gneissic banding within the C_1-zones become acutely attenuated along the sub-shears and strongly shortened in the inter-shear domains. They have explained that these C_1- and C_2-shear band structures might form due to progressive simple shear deformation. The gneissic banding in the study area is intensely stretched in the strongly sheared sectors and folded in the inter-shear portions (Fig.3a, b, c, d). Although the late shearing event recorded in the gneisses and GH Halli Belt is contemporaneous with the shearing episode of the Dharwar Supergroup of rocks, the well-developed granoblastic texture, complete ductile nature of the deformation of both plagioclase and K-feldspar, ductility of the shear bands, absence of any noticeable brittle structural feature, lack of prominent stretching lineation in the strongly sheared gneiss possibly hint at a slightly higher grade of metamorphism during the shearing event compared to that in the Dharwar Supergroup. This mismatch of metamorphic grade needs to be further worked out.

As mentioned earlier, the eastern shear splay passes through the contact between the PGC and CSB in the northern part in Mayakonda area (Fig.1). This shear splay in the southern part becomes marginally oblique to the above, following all along the western boundary of the Talya Conglomerate horizon which has been interpreted by these authors in an earlier publication as a fault controlled debris flow deposit (Roy *et al*., 2020). We thus interpret that the locus of this shear splay actually trailed the pre-existing Chitradurga Basinal fault that triggered the deposition of the thick polymictic Talya Conglomerate horizon (Fig.3e). Second generation pure shear deformation (D_{2a}) followed by a dominant sinistral simple shear deformation (D_{2b}) has also been demonstrated by the authors in the Talya Conglomerate and surrounding litho-units. Shear kinematics similar to that recorded in the GH Halli Belt indicates that these shears, recorded at the western margin of CSB, are parts of an anastomosing network of shears having narrow zones of high strain of sinistral simple shear nature, enclosing weakly deformed lenses, controlled by the rheological properties and pre-existing discontinuities in the rocks.

Eastern margin of the Chitradurga Schist Belt

Geology and structure of eastern margin of the CSB are recorded in Seshadri *et al*., (1981), Sengupta and Ramachandra, 2002, Roy *et al.,* (2008), and Sengupta and Roy (2012). Litho-components flanking the Chitradurga Group of the Dharwar Supergroup on this margin include the rocks of the Javanahalli Belt (JB) showing uncertain age relation with that of the Dharwar Supergroup, older PGC and younger intrusive granites.

1. Javanahalli Belt (JB)

The Javanahalli Belt (an allochthonous belt, Sengupta and Roy, 2012) is a large supracrustal lens juxtaposed with the eastern margin of the CSB in the Javanahalli area that tapers in both ends and comprises amphibolite, gabbroic amphibolite, calc-silicates, crystalline limestone, quartzite, BIF, quartz biotite schist, cordierite-anthophyllite rock and quartz-sillimanite schist (Ghosh Roy and Ramakrishnan, 1985; Sengupta and Roy, 2012). However, northern part of JB the belt is represented mainly by a thin slice of amphibolite persisting all along the eastern margin of CSB (Fig.1). The mineral assemblages in different lithologies in the JB indicate lower to middle amphibolite grade of metamorphism.

2. Chitradurga Schist Belt (CSB)

The Dharwar Supergroup on the eastern margin of the CSB is represented by the Chitradurga Group including metagreywacke-argillite and metabasalt sequences interspersed with bands of rhyolite, quartzite, intraformational conglomerate and BIF of the Hiriyur Formation. Metaultramafites and metabasic intrusives occur at places, for example, southwest of Javgondanahalli, east of Chitradurga (near Turuvanur) and west of JN Kote. The mineral assemblage of albitic plagioclase-fibrous amphiboles-epidote/zoisite-chlorite-minor quartz-iron oxides in metabasalt and prograde quartz-chlorite-biotite-low An-plagioclase in variable modal abundance in argillite–greyacke unit indicate a low greenschist grade of metamorphism of the Chitradurga Group of rocks.

3. 1. PGC on the eastern margin of the CSB

PGC on the eastern margin of the CSB is characterized by restricted presence of banded migmatite showing evidence of insitu partial melting as in quarry sections at Nannivala and Sira and adjoining areas. Intense shearing of the gneisses and granitoids has resulted in a strong mylonitic fabric obscuring pre-existing fabric in the above rocks at most places. Although Mesoarchaean ages equivalent to that of PGC from the western margin are recorded in the eastern part as well, Neoproterozoic ages ($^{207}Pb/^{206}Pb$ age of 2562 ± 4 Ma) are reported in the gneisses from the Sira area by Chardon *et al.,* (2011).

PGC, exposed east of the Javanahalli belt, include banded and stromatic migmatites associated with foliated granodioritic gneisses (Sengupta and Ramachandra, 2002). Stromatic migmatitic gneisses in the Nannivala quarry, about 8 km east of the eastern margin of the Chitradurga belt contain amphibolite bands that evidently intruded in different basic magma pulses. The anatectic episode in the eastern margin too is believed to pre-date Dharwarian metamorphism and deformation.

3.2. Intrusive Granitoids along the eastern margin of the CSB

The eastern margin intrusive granites mainly include the Bukkapatna and JN Kote granites. The linear Bukkapatna Granite is a dominantly porphyritic alkali feldspar granite unit syntectonically emplaced between the CSB and the JB along the crustal scale GMSZ, near Javanahalli. Field evidences clearly show this granite to be younger than the Chitradurga Group though it has yielded older ages of 2988 ± 5 Ma (zircon U-Pb, Chardon *et al*., 2011). The possibility of presence of older xenocrystic zircon within the younger granite melt or partially melted basement component within the granite might be the cause of above older ages. A large portion of the oval shaped, JN Kote Granite on the eastern margin of the CSB is constituted by mingling between sheets of granitoids that show modal differences in their quartz-K feldspar-low An plagioclase-biotite assemblages. The granite is associated with a differentiated suite of dominantly gabbro-rare anorthosite-minor ultramafic and tonalite that occurs partly rimming the granite body. The Bukkapatna and JN Kote granites, in contrast to the Chitradurga and Hosdurga granites occurring in the central and western part of the CSB are slightly calc-alkaline in nature. All these granites are believed to have been emplaced at 2.61 Ga based on zircon dating of the Chitardurga Granite (Taylor *et al.,* 1984; Jayananda *et al.,* 2006).

4. Structural characteristics of the eastern margin of CSB

A detailed account of the structural features and tectonic interpretation of the eastern margin of the CSB, emphasizing on the crustal scale GMSZ in Javanahalli and other domains has earlier been presented by Sengupta and Roy, 2012. It was shown that there is a significant difference in the structural patterns between rocks of the Javanahalli belt and those of the Dharwar Supergroup in the CSB.

4.1. Differences in structural features between the JB and the Dharwar Supergroup

The structures in the Javanahalli Belt are characterized by stacking of recumbent (F1) folds of different scales having subhorizontal to gentle easterly dipping axial planar schistosity and mylonitic foliation (Fig. 4a) and mesoscopic to large mappable scale asymmetric (westward vergence) overturned (F2) folds overprinted on the former, signifying a dominant thrust/updip movement. On the contrary, the structural pattern of the Dharwar Supergroup in the CSB is controlled mainly by the D_{2a} deformation that gave rise to NNW-SSE to N-S striking subvertical to steep easterly dipping axial planar (S2) foliation and noncylindrical, generally gentle to moderately plunging F2 folds superposing on rootless tight isoclinal mesoscopic early folds (F1). An early top to west thrusting has brought the amphibolite grade Javanahalli Belt in juxtaposition with the greenschist grade CSB along the crustal scale GMSZ. Subsequent to the thrusting, a dominant late sinistral transcurrent movement (D_{2b}) along the GMSZ continued to accommodate the overall east-west/ENE-WSW transpression.

4.2. Late Sinistral transcurrent shearing along GMSZ between CSB and JB

The 2 to 3 km wide, N-S striking, ductile shear zone (GMSZ) has affected the metabasalts and the argillites of CSB and the amphibolites and quatzites of JB including the Bukkapatna granite at the eastern margin.

We present here some important structural features of amphibolite of the JB, which has been mylonitized along with syntectonic granites in the GMSZ. Protolith for this amphibolite is debatable but presence of relict igneous texture in coarse grained metagabbro within the mylonitized amphibolites indicates gabbroic parentage at least in places. The amphibolites and the granite in the shear zone show a very strong L-S tectonite fabric defined by a NNW-SSE to N-S striking subvertical to steep easterly dipping mylonitic foliation (Sm) and sub-horizontal mineral lineation (Lm) representing the dominant latest sinistral shearing event. Consistent sinistral asymmetric folds of the mylonitic fabric with variable axial planar orientation and axial plunge are conspicuous. Shear lenses are common, and are mostly bound by very well developed anastomosing shear bands (Fig.4b). Stacking of shear lenses is common. Often the shear lenses are represented by small scale rootless S-folds. The development of the shear zone in a brittle – ductile transitional domain at greenschist metamorphic grade is evident from the actinolite-chlorite-albitic plagioclase mineralogy of the sheared amphibolite, brittle-ductile deformation of both K-feldspar and plagioclase porphyroclasts and simultaneous occurrence of mylonite and pseudotachylyte in the sheared granite (Roy *et al*., 2008). Recrystallised ribbon quartz in granite and actinolite needles define the stretching lineation that is mostly horizontal but also varying in plunge up to 25^{o} both towards N and S. Very well developed S-C and C-$C^{/}$ fabrics, recorded in granitoids and amphibolites of JB and metabasalts and argillites of CSB establish the sinistral sense of shear (D_{2b}) equivalent to that of the sinistral shearing in the western margin (Fig.4c).

Tectonic evolution of the CSB

The Neoarchaean evolution of the Chitradurga Schist belt in particular and the Dharwar Craton as a whole is a critical example of current debate between uniformitarian plate tectonic model with crustal shortening (Chadwick *et al.,* 2000, 2003) or a fold-thrust model (Chadwick *et al.*, 2007) and non-uniformitarian plume-related or gravity driven sagduction model (Goodwin and Smith, 1980), either with or without E-W crustal shortening and transcurrent shearing (Bouhallier *et al.,* 1995, Choukroune *et al.,* 1995, 1997, Chardon *et al.*1996, 1998, 2002, Jayananda *et al.,* 2000). In the above attempt, the present work records structural and petrographic characteristics of two major shear zones (CWMSZ and GMSZ) occurring at the western and eastern margins of the CSB and their role in the tectonic evolution of the belt and in a larger context that of the Dharwar Craton. We have earlier recorded (Roy *et al.,* 2020) that the eastern margin of the CSB is tectonic in nature, evidenced by the presence of a major crustal scale shear zone, namely the Gadag Mandya Shear Zone (GMSZ) (Sengupta and Roy, 2012), and also by the absence of any basement-cover relationship all along the 400 km long stretch of the belt from Gadag in the north to Mandya in the south. The fact that the gneisses and granites at the margin are in contact with the rocks of the youngest Hiriyur Formation of Chitradurga Group for a major stretch of the eastern margin and the older Bababudan group has not been repeated in the eastern margin is also indicative of the tectonic nature of the eastern margin of CSB.

Based on the presence of recumbent and overturned folds with gentle easterly dipping foliation in gneisses and JB rocks, an early top to west thrusting event was recognised at the eastern margin in the Javanahalli, Sira and other areas (Sengupta and Roy, 2012) which brought the allochthonous JB in juxtaposition with the CSB. Similar up-dip movement at the eastern margin of Gadag Schist Belt (the northernmost stretch of the CSB) was also inferred by Chadwick *et al.*, 2003 who proposed a duplex thrust system as a result of the Archean oblique convergence

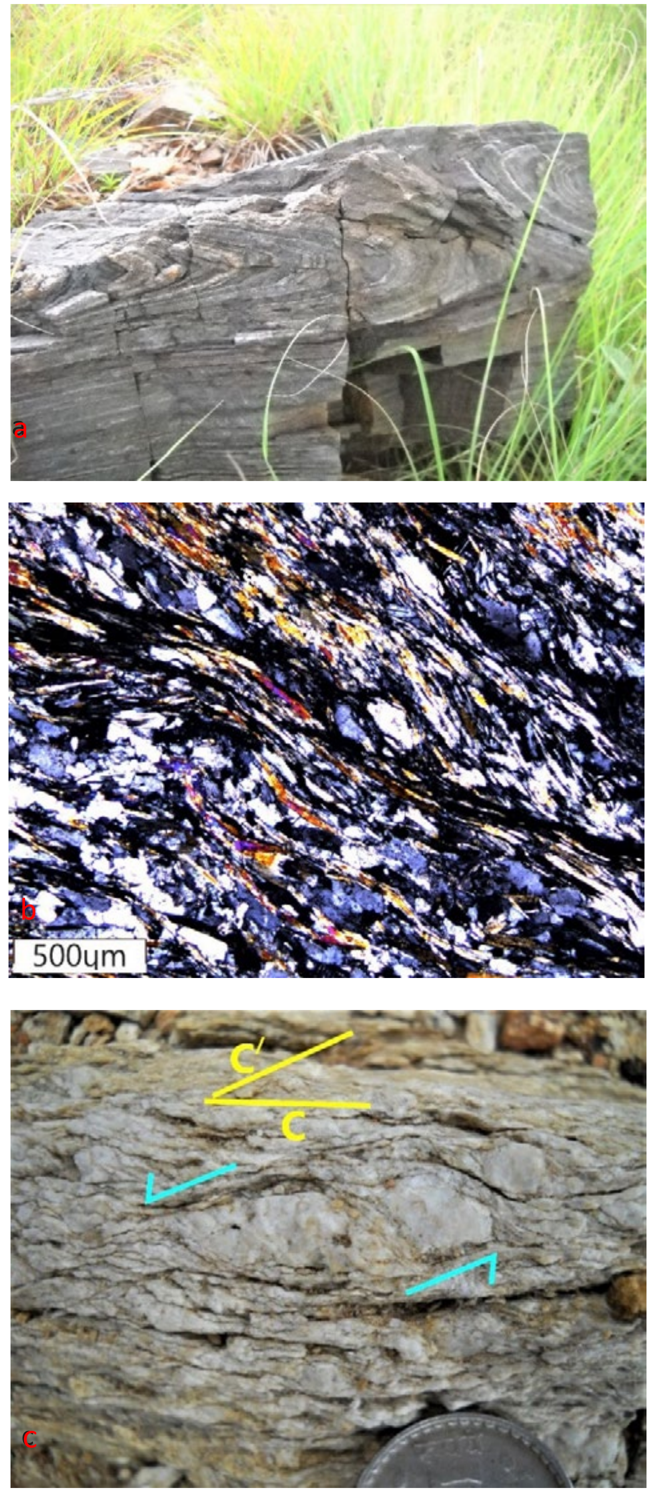

Fig.4: (a) Stacking of recumbent (F1) folds having subhorizontal to gentle easterly dipping axial plane in BIF of Javanahalli Formation, east of the Chitradurga Schist Belt (CSB). (b) Microsection of sheared amphibolite having anastomosing shear bands defined by elongated actinolite grains in Javanahalli Belt at the eastern margin of CSB. (c) Granite proto-mylonite showing very well developed C-$C^{/}$ fabric, Bukkapatna Granite at the eastern margin of CSB.

in the Dharwar Craton. The E-W transpression at the eastern margin resulted in shortening of the schist belt rocks giving rise to early (D1) and late (D2) pure shear related structures. Thrusting and subsequent sinistral shearing along the GMSZ also resulted due to this transpression at the eastern margin of CSB. A similar narrow zone of shear in the central part of the CSB has been termed the Chitradurga Central Shear Zone (CCSZ) by Mohakul and Pattanaik (2015). Our study shows that this central shear zone occurs between the northern arm of the CSB and the Chitradurga Granite and passes along the formational boundary at the base of Hiriyur Formation (KM Kere Conglomerate) simulating the pre-existing basin development fault in the central part of the belt. Based on mineral assemblages in the shear zone rocks it can be shown that the shearing in both GMSZ and CCSZ took place under greenschist facies of metamorphism.

At the western margin, we recognize the Ghattihosahalli Belt (GH Halli Belt) as a shear belt (CWMSZ) based on the narrow, linear, lensoid shape and its occurrence as mesoscopic enclaves having invariable tectonic contact with the adjacent gneisses, as well as intense shear fabric development. The shear zone in the western margin of CSB has a slightly variable but average NNW-SSE strike and steep easterly to subvertical dip with subhorizontal stretching lineation indicating a similar transcurrent shear. No features, indicating a thrust or up-dip movement, could be recorded here. Thus there are some important differences between the GMSZ and CWMSZ attributable to differences in the geological set up of the two shear zones as described earlier. However, both these shears form a part of the same shear system generated during the second generation of progressive deformation in the Dharwar Supergroup.

Our study indicates that the CSB is characterized by a conspicuous regional partitioning of strain in the form of a pure shear dominated wide central part and narrow zones of intense simple shear strain at the margins of the schist belt where mechanical and rheological contrasts are expectedly quite large. A prominent horizontal transpressional tectonics due to an E-W/ ENE-WSW shortening has resulted in multiple deformation phases with a late shearing event in the CSB.

However, to subscribe to a typical plate tectonic model, as envisaged by Chadwick *et al.*,(2003, 2007) remains conjectural although a major component of subhorizontal strain resulting in arc-parallel sinistral displacement and arc-normal shortening is discernible. The lateral constrictional flow (LCF) proposition of Chardon *et al*., (2011), a combination of plate tectonic and plume-related sagduction models, is more speculative than demonstrative from field evidences. Our studies establish that the tectonic evolution of CSB is due to major horizontal transpressional tectonics at the eastern marginal zone of the CSB resulting from a far field contractional stress.

Conclusion

In summary, the following concluding remarks can be made from the present study:

i. The NNW trending Archaean CSB of Dharwar Craton manifests conspicuous strain partitioning of regional dimension with the presence of major NNW-SSE to N-S striking, subvertical to steep easterly dipping flanking shear zones (CWMSZ and GMSZ) dominated by transcurrent sinistral shear component and wide subparallel domains of multiply deformed supracrustal rocks dominated by pure shear deformation in the central part during the Dharwar Orogeny.

ii. The marginal sinistral transcurrent shears record the final phase of polyphase deformation of the CSB and adjacent lithotectonic units. Components of both flattening and simple shearing indicate a transpressional tectonics caused by a huge far field differential stress induced by accretion or collision of crustal blocks resulting in extreme strain partioning.

iii. Although the late sinistral shearing events in CWMSZ and GMSZ are grossly conformable and contemporaneous, there is a significant difference in their evolution. The Ghattihosahalli Belt is a shear belt tectonically brought into its present disposition and contact with neighboring gneisses and CSB by the late sinistral transcurrent shear without evidence of any up-dip or thrust component. On the contrary, there is clinching evidence of a top to west early thrusting event that effected a westward translation of the allochthonous and higher grade Javanahalli Belt that overrides the low grade CSB, followed by the late sinistral shearing along GMSZ at the eastern margin.

iv. The granite gneisses of the GH Halli Belt spectacularly preserve different stages of a progressive ductile shear zone having a pre-existing anisotropy in the rock. The geometry and kinematics of the shearing in gneisses and the adjacent supracrustals are in conformity with that of the Dharwar deformation at the western margin.

v. At the western margin, the normal erosional basin margin, represented by Neralakatte oligomict Conglomerate is subsequently tectonised by the CWMSZ. In contrast, the eastern contact of the CSB between the youngest Hiriyur Formation and the granites and gneisses itself was originally tectonic.

Acknowledgement

We express our gratitude to the Director General, Geological Survey of India, for allowing to publish the paper. We sincerely acknowledge the contribution of a number of workers, especially of Geological Survey of India, in shaping the concept of tectonic evolution of the Chitradurga Schist Belt. We are highly indebted to Prof. Tapas Bhattacharya and Prof Dhruba Mukhopadhyay for their valuable suggestions and discussions during preparation of the manuscript.

Reference

Bouhallier, H., Chardon D., and Choukroune, P. 1995: Strain patterns in Archaean dome-and-basin structures: The Dharwar craton (Karnataka, South India). *Earth and Planetary Science Letters*, **135(1-4)**: 57 – 75.

Chadwick, B., Ramakrishnan, M. and Viswanatha. M.N., 1981: Structural and Metamorphic relations between Sargur and Dharwar Supracrustal rocks and Peninsular Gneiss in central Karnataka. *Journal Geological Society of India*, **22**: 557 - 569.

Chadwick, B., Vasudev, V.N. and Hegde, G.V., 2000: The Dharwar Craton, southern India, interpreted as the result of late Archaean oblique convergence. *Precambrian Research*, **99(1-2):** 91-111.

Chadwick, B., Vasudev, V.N. and Hegde G.V., 2003: The Chitradurga schist belt and its adjacent plutonic rocks, NW of Tungabhadra, Karnataka: A duplex in the late Archean convergent setting of the Dharwar craton. *Journal Geological Society of India,* **61(6):** 645–663.

Chadwick, B., Vasudev, V., Hegde, G.V. and Nutman, A.P., 2007: Structure and SHRIMP U/Pb zircon ages of granites adjacent to the Chitradurga schist belt: Implications for Neoarchean convergence in the Dharwar craton, southern India. *Journal Geological Society of India***, 69(1):** 5–24.

Chardon, D.H., Choukroune, P. and Jayananda, M., 1998: Sinking of the Dharwar Basin (South India); implications for Archaean tectonics. *Precambrian Research*, **91(1-2)**: 15-39.

Chardon, D., Peucat J.J., Jayananda, M., Choukroune, P. and Fanning, C.M., 2002: Archean granite-greenstone tectonics at Kolar (South India): Interplay of diapirism and bulk inhomogeneous contraction during juvenile magmatic accretion. *Tectonics*. **21(**3): 7(1-17).

Chardon, D., Jayananda, M. and Peucat, J.J., 2011: Lateral constrictional flow of hot orogenic crust: insights from the Neoarchean of South India, geological and geophysical implications for orogenic plateau. *Geochemistry Geophysics Geosystem*, **12(2):** 1-24.

Choukroune, P., Bouhallier, H. and Arndt, N.T.,1995: Soft lithosphere during periods of Archaean crustal growth or crustal reworking. *In*: Early Precambrian processes. M.P. Coward and A.C. Reis (Eds.), *Geological Society, London, Special Publication*, **95**: 67- 86.

Choukroune, P., Luden, J.N., Chardon, D., Calvert, A.J. and Bouhallier, H., 1997: Archaean crustal growth and tectonic processes: a comparioson of the Superior Province, Canada and the Dharwar Province, India. *In*: Orogeny through time. J.P. Burge and M. Ford (Eds.), *Geological Society, London, Special Publication*, **121**: 63-98.

Devaraju, T.C., Raith, M.M. and Spiering, B., 1999: Mineralogy of the Archaean Barite deposit of Ghattihosahalli, Karnataka, India. *The Canadian Mineralogist*, **37(3)**: 603-617.

Drury, S.A. and Holt, R.W., 1980: The tectonic framework of the south Indian craton: a reconnaissance involving LANDSAT imagery. T*ectonophysics*, **65**: T1-T15.

Ghosh Roy, A.K. and Ramakrishnan, M., 1985: Stratigraphic status of Javanahalli belt in the Archaean geology of Karnataka. *Journal Geolgical Society of India*, **26**: 567-579.

Goodwin, A. M. & Smith, I. E. M. 1980: Chemical discontinuities in Archean metavolcanic terrains and the development of Archean crust. Precambrian Research, **10**: 301-311.

Jayananda, M., Chardon, D., Peucat, J. J. and Capdevila, R., 2006: 2.61 Ga potassic granites and crustal reworking in the western Dharwar craton, southern India: Tectonic, geochronologic and geochemical constraints. *Precambrian Research*, **150(1-2)**: 1–26.

Jayananda, M., Kano, T., Peucat, J.-J. and Channabasappa, S. 2008: 3.35 Ga komatiite volcanism in the western Dharwar craton, southern India: Constraints from Nd isotopes and whole-rock geochemistry. *Precambrian Research*, **162(1-2)**: 160–179.

Jayananda, M., Moyen, J.-F., Martin, H., Peucat, J.-J., Auvray, B. and Mahabaleswar, B., 2000: Late Archaean (2550–2520 Ma) juvenile magmatism in the eastern Dharwar craton, southern India: constraints from geochronology, Nd–Sr isotopes and whole rock geochemistry. *Precambrian Research*, **99(3-4)**: 225–254.

Jayananda, M., , J J, Chardon D, Krishna Rao B, Fanning C M and Corfu F 2013 Neoarchean greenstone volcanism and continental growth, Dharwar craton, southern India: Constraints from SIMS U–Pb zircon geochronology and Nd isotopes. *Precambrian Research*, **227**: 55–76.

Kaila, K.L., Roy Chowdhury, K., Reddy, P.R., Krishna, V.G., Hari Narain, Subbotin, S.I., Sollogub, V.B., Chekunov, A.V., Kharetchko, G.E., Lazarenko, M.A. and Ilchenko, T.V. 1979: Crustal structure along Kavali–Udipi profile in the Indian Peninsular Shield from deep seismic sounding. *Journal Geological Society of India*, **20**: 307–333.

Maibam, B., Goswami, J. and Srinivasan, R., 2011: Pb–Pb zircon ages of Archaean metasediments and gneisses from the Dharwar Craton, southern India: Implications for the antiquity of the eastern Dharwar craton. *Journal of Earth System Science*, **120(4)**: 643–661.

Mohakul, J. and Pattanaik, D.S., 2015: Characterisation of the chitradurga western shear zone in mayakonda sector, chitradurga schist belt, dharwar craton. *International Journal of Earth Sciences and Engineering,* **8(1)**: 31-38.

Paranthaman, S., 2005: Geology and geochemistry of Archaean Ghattihosahalli mafic-ultramafic complex, Chitradurga, Karnataka. *Journal Geological Society of India,* 66(5): 653-657.

Passchier, C. and Coelho, S., 2006: An outline of shear-sense analysis in high-grade rocks. *Gondwana Research*, 10(1-2): 66–76.

Raase, P., Raith, M., Ackermand, D., Viswanatha, M.N. and Lal, R.K., 1983: Mineralogy of chromiferous quartzites from south India. *Journal Geological Society of India*, **24**: 502-521.

Radhakrishna, B.P. and Srinivasaiah, G. 1974: Bedded barytes from the Precambrian of Karnataka. *Journal Geological Society of India*, **15**: 314-315.

Ramakrishnan, M. and Vaidyanadhan, R. 2008: Geology of India. Geological Society of India, Bangalore, **1**: 556p.

Ramsay, J.G. and Lisle, R.J., 2000: The techniques of modern structural geology. Applications of continuum mechanics in structural geology (3). Academic Press, London.

Rollinson, H.R., Windley, B.F. and Ramakrishnan, M., 1981: Contrasting high and intermediate pressures of metamorphism in the Archaean Sargur schists of southern India. *Contributions to Mineralogy and Petrology*, **76**: 420–429.

Roy, A., Ramachandra, H.M. and Sengupta, S., 2020: Interpretation of stratigraphy and structure of the Neoarchaean Dharwar Supergroup of rocks in Chitradurga area, Dharwar Craton. *Journal of Earth System Science*, **129**: 98(1-28).

Roy, A. and Bhattacharya, H. N., 2014: Overprinting of simple shear strain on pure shear deformation: Evidences from the western margin of the Chitradurga schist belt of Dharwar craton. Abstract: Rock Deformation Structure III: 57–60.

Roy, A., Sengupta, S. and Mandal, A., 2008: Synchronous development of mylonite and pseudotachylyte: An example from the Chitradurga Eastern Margin Shear Zone, Karnataka. *Journal Geological Society of India*, **72(4)**: 447–457.

Sengupta, S. and Ramachandra, N.D. 2002: A Report on Specialised Thematic Mapping of Chitradurga Schist Belt, chitradurga and davanagere districts, Karnataka. *Unpublished Report Geological Survey of India*.

Sengupta, S. and Roy, A., 2012: Tectonic amalgamation of crustal blocks along Gadag–Mandya Shear Zone in Dharwar Craton of southern India. *Journal Geological Society of India*, **80(1)**: 447–457.

Seshadri, T., Chaudhuri, A., Harinadha Babu, P. and Chayapathi, N., 1981: Chitradurga belt. *In*: Early Precambrian supracrustals of southern Karnataka. Swami Nath, J. and Ramakrishnan, M (Eds.), *Memoirs Geological Survey of India*, **112**: 163-198.

Swaminath, J., Ramakrishnan, M. and Viswanatha, M.N., 1976: Dharwar stratigraphic model and Karnataka craton evolution. *Records of the Geological Survey of India,* **107(2)**: 149-175.

Swami Nath, J. and Ramakrishnan, M. 1981: Early Precambrian supracrustals of southern Karnataka. *Memoirs Geological Survey of India*, **112**: 308.

Taylor, P.N., Chadwick, B., Moorbath, S. Ramakrishnan, M. and Viswanatha, M.N., 1984: Petrography, chemistry and isotopic ages of Peninsular Gneiss, Dharwar acid volcanic rocks and the Chitradurga granite with special reference to the late Archaean evolution of the Karnataka craton, southern India. *Precambrian Research*, **23(3-4)**: 349-375.

Viswanatha, M.N., Ramakrishnan, M. and Narayanan Kutty, T.R. 1977: Possible spinifex texture in a serpentinite from Karnataka. *Journal Geological Society of India*, 18: 194-197.

Indian Journal of Geosciences, Volume 74, No. 3
July - September, 2020; pp. 307-314

Invited Paper

Glacier Studies in India: Remote Sensing Applications and Challenges

Anil V. Kulkarni and Tejal Shirsat

Divecha Centre for Climate Change, Indian Institute of Science, Bengaluru, 560012
Corresponding author's email: anilkulkarni@iisc.ac.in

Abstract: In the paper, we discuss application of remote sensing methods to study Himalayan cryosphere in India. Satellite data in combination with field is used to develop models, which can estimate numerous glacier parameters as area, velocity, depth, mass balance, debris cover, glacier lakes and risk assessment of Glacier Lake Outburst Flood. Digital Elevation models are extensively used to estimate glacier mass balance at regional scale and have improved our understanding of spatial heterogeneity in mass loss. Surface velocity and slope are combined with laminar flow to estimate spatial distribution of glacier depth. This has significantly improved estimate of glacier stored water and glacier lakes. Applications of remote sensing data in mass balance and runoff models help in assessing the impact of climate change on water availability. These investigations suggest indispensable role of remote sensing techniques to understand Himalayan cryosphere.

Keywords: Remote Sensing; Himalaya; Glaciers; Snow; Mass Balance; Velocity; GLOF

Introduction

The Himalayan and Karakoram mountain ranges consist one of the largest concentration of glaciers outside the Polar Regions. In addition, large area is also covered by snow in winter. Meltwater from glaciers and snow along with rainfall and groundwater feed the three major Himalayan rivers *viz.,* Indus, Ganga, and Brahmaputra, which sustain water requirements of 800 million people living in the Indian sub-continent (Kulkarni *et al*., 2017). However, these frozen water resources are vulnerable to changing climate (Azam *et al.*, 2018; Kulkarni *et al*., 2011). Therefore, distribution and volume of glaciers and seasonal snow is crucial for management of Himalayan water resources. However, conventional field methods are often challenging due to the rugged terrain and severe climatic conditions. Therefore, field methods can provide data at few locations, inadequate considering the vast and transboundary extent of Himalayan cryosphere. Remote Sensing (RS) technique can provide valuable information about Himalayan cryosphere due to significant improvement in the sensor characteristics like temporal frequency, spatial coverage, spectral bands, radiometric, and spatial resolutions. In addition, unique reflectance and emission characteristics of snow and ice in optical and microwave region have helped in generating reliable information about Himalayan cryosphere (Kulkarni *et al*., 2017). In addition, recently unmanned Aerial Vehicle and helicopter-borne ice penetrating radar were also used to study the Himalayan glaciers (Ramsankaran *et al*., 2020). Due to these advances, RS techniques are extensively used to map snow cover, glacier extent, glacier lakes, glacier velocity and debris cover. The satellite data along with models is being extensively used to estimate mass balance, glacier thickness, contribution in runoff and potential hazard from glacier lake outburst flood (GLOF); which is discussed in subsequent sections.

Snow

Snow Cover Area (SCA)

Snow has high reflectance in the optical region and low in the Short-Wave Infrared (SWIR) region (Fig.1). This characteristic is used in Normalized Differential Snow Index (NDSI) to separate snow from other features. (Kulkarni *et al.*, 2006; Fig.2). SCA can be mapped using various sensors such as AWiFS, LISS-II and III of Indian Remote Sensing satellite (IRS) and Landsat MSS, TM, ETM+ and OLI and MODIS Terra and Aqua at a spatial resolution of 30-500 m and temporal frequency of 1-16 days. SCA in the entire Himalayan region show large variability due to altitude, season, and region; but suggests no significant trend in inter-annual variability (Gurung *et al*., 2011; Rathore *et al*., 2018; Singh *et al*., 2014). However, study in Western and Central Himalaya show negative correlation with temperature (Gurung *et al.*, 2017; Sahu and Gupta, 2020). SCA mapping using AWiFS sensor in Ravi and Bhaga basins from 2004 to

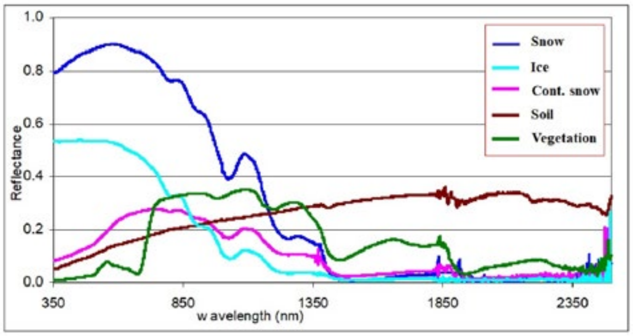

Fig. 1: Variation in reflectance with respect to wavelength for various features. Snow has high reflectance in visible and low in SWIR wavelengths (Source: Kulkarni, 2007).

2007 showed depletion in low altitude Ravi basin from 90% to 55% in mid-winter, whereas in high altitude Bhaga basin no significant snow depletion occurred (Kulkarni *et al*., 2010).

Snow Albedo

Optical wavelengths are generally used to estimate Snow albedo. Changes in albedo can influence snow melt and investigation in the Baspa basin suggest 29 % drop in albedo during April - May 2009; potentially due to black carbon deposits from forest fires (Kulkarni *et al*., 2013). MODIS Terra satellite provides daily blue and white sky albedo (Riggs *et al*., 2015). However, not many studies are reported in India on albedo modeling and mapping.

Snow Depth (SD)

SD is a useful parameter to assess water equivalent but is difficult to retrieve from RS data. In Himalaya, SD is usually estimated by combining field station and remote sensing data. It can be estimated using airborne lidar surveys, passive microwave sensors such as (Special Sensor Microwave/Images (SSM/I), Scanning Multichannel Microwave Radiometer (SMMR), and Advanced Microwave Scanning Radiometer-Earth Observing System (AMSR-E/2)) at spatial resolution of 25 km and active microwave sensors such as SAR at finer spatial resolution of <5km; however active sensors provide the most reliable data due to their ability of retrieving images during night as well (Patil *et al*., 2020). Patil *et al*., 2020 utilized TerraSAR-X to obtain SD maps at 90 m resolution and validated them at Dhundi observatory in Beas basin.

Glacier Area

Glacier features as accumulation area, ablation area, snowline, moraines, crevasses and snout are visible on a satellite imagery (Fig.3) and can be mapped using automatic, semi-automatic and manual techniques. Numerous satellite sensors as IRS-LISS-III, The Landsat ETM+, OLI and Sentinel-2 have been used. This can also be further complimented by DEMs and high spatial resolution (1-5 m) google earth imagery. Numerous glacier inventories at basin, regional or mountain range scale have been carried out to estimate glacier area. Some of the earliest inventories of the Indian Himalaya

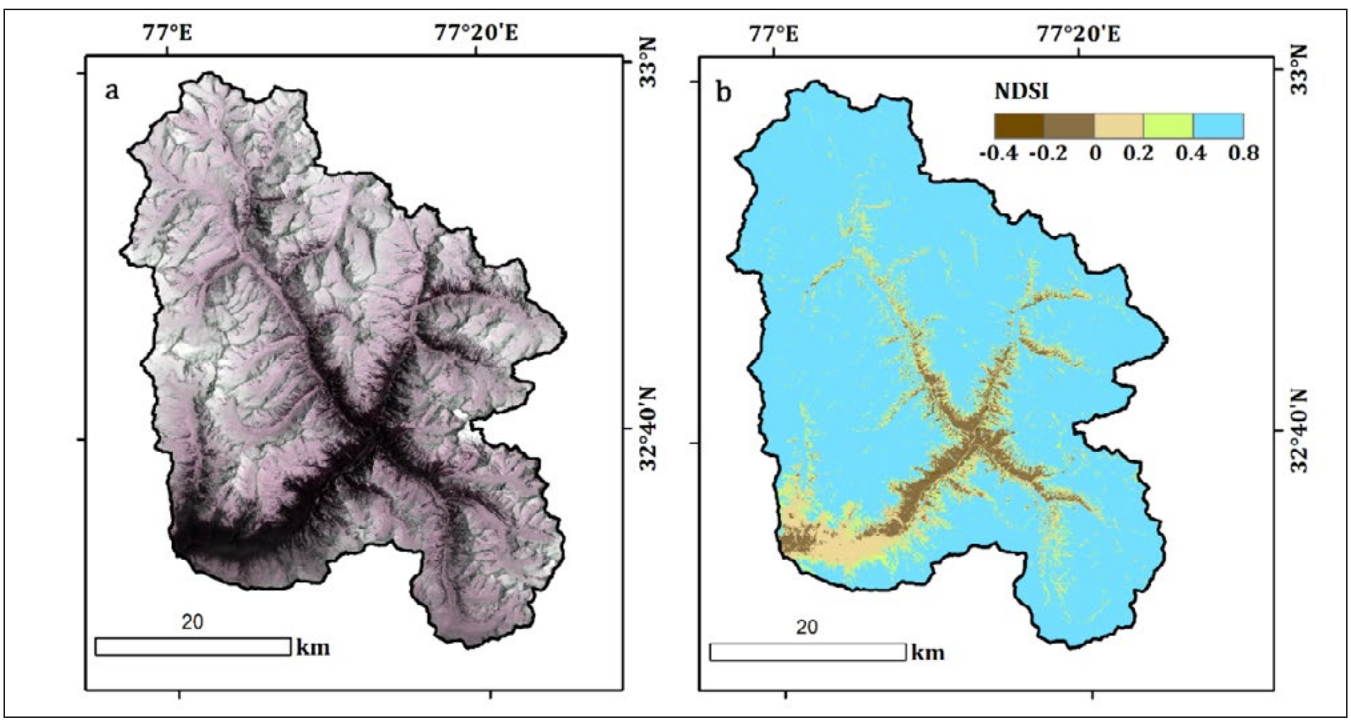

Fig. 2: (a) Color composite of Landsat OLI dated 10 May 2015 in Bhaga basin. (b) NDSI image obtained from Green and SWIR bands (Kulkarni *et al*., 2002).

prepared using satellite data of 1987 and topographical maps and aerial photographs taken in 1962-63 by Space Application Centre (SAC) and Geological Survey of India (GSI) suggests glacier area of 23,314 and 26,775 km^2, respectively (Kulkarni and Buch, 1991; Sangewar and Shukla 2009). The mean glacier extent in Indus, Ganga and Brahmaputra basins is 26253±3,746 km^2, 11109±4038 km^2 and 14399±3782 km^2 based on 5 basin wide inventories by ICIMOD, SAC, IWMI, GAMDAM and RGI6.0 (Bajracharya and Shrestha, 2011; Nuimura *et al*., 2015; Sharma *et al*., 2013). The large deviation in the estimates could be due to the differences in the dataset, geographical area covered, period of satellite data acquisition, scale of mapping, methodology and glacier classification. Glacier area loss and retreat can be estimated by temporal assessment of glacier boundaries. Long term monitoring of 83 glaciers in Himalayan region indicates the average retreat rate is 15.5±11.8 ma^{-1} whilst the mapping of around 20,060 km^2 glacier area suggest area loss of 3.4 ± 2%/decade (Kulkarni and Pratibha, 2018).

Glacier Velocity

Velocity of Himalayan glaciers can be estimated using feature tracking technique and generally COSI-Corr program is used (Gantayat *et al*., 2014). Assessment of surface velocities of Himalayan glaciers have shown decreasing trend and it is associated increasing mass loss (Bhushan *et al*., 2017). The velocity is further used to estimate the spatial distribution of ice thickness using laminar flow method (Gantayat *et al*., 2014; Fig.4). The method in combination with region-specific volume-area scaling is used to estimate the volume of glacial stored water in Satluj and Beas basins as 62.3± 11.5 and 22.5±4 Gigatons, respectively (Prasad *et al.*, 2019).

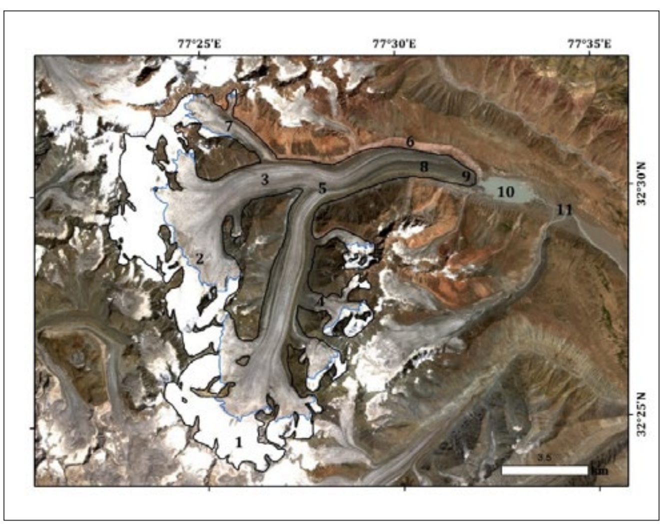

Fig. 3: Features of Samudra Tapu glacier, Chandra basin, Himachal Pradesh on a true color composite of Sentinel-2 imagery dated 22 August 2018. 1. Accumulation Area 2. Snowline 3. Ablation Area 4. Crevasse 5. Medial moraine 6. Lateral moraine 7. Tributary glacier 8. Supraglacial debris cover 9. Snout 10. Glacier lake 11. Meltwater stream

Velocity can also be estimated using Differential Interferometry (DInSAR). High resolution SAR data such as ALOS-2 and PALSAR-2 with time interval of a few days was used to detect glacier motion (Singh *et al*., 2020). Velocity derived using this method in Chandra and Bhaga basins have provided interesting insights on anomalous disintegration of glaciers. The meltwater from tributary glaciers to the main trunk of the glacier can enhance the velocity and melting in the frontal zone, which lead to formation of dead ice near snout and leading to disintegration of glaciers (Singh *et al.*, 2020).

Glacier Mass Balance

Glacier mass balance can be estimated at individual glacier, basin or mountain scale using various RS techniques as Geodetic, gravimetric, Equilibrium line altitude (ELA) and Accumulation Area Ratio (AAR). In geodetic method, DEMs obtained at two or more time periods are subtracted to estimate thickness change. This method is used to estimate changes in spatial distribution of surface elevation and mass balance. In last decade mass balance is estimated as -0.41 ± 0.11 m.w.e.a^{-1} in the eastern, −0.58 ±0.01 m.w.e.a^{-1} in the central (Fig.5), -0.55±0.37 m.w.e.a^{-1} in the western Himalaya and −0.08 ± 0.13 m.w.e.a^{-1} in Karakoram (Maurer *et al*., 2016; Bandyopadhyay *et al*., 2019; Vijay and Braun, 2016 and Kumar *et al*., 2019).

Satellite data was used to estimate ELA, and AAR and then mass balance (Kulkarni,1992; Kulkarni *et al*., 2004). The method was further improved using temperature and precipitation and called Improved AAR (IAAR) methods (Tawde *et al*., 2017). AAR/IAAR and ELA approaches can provide inter-annual variation in the mass balance (Fig.6) and can be forced with climate condition to estimate future changes in glacier mass (Tawde *et al*., 2019; Prasad *et al*., 2019)

Supraglacial Debris Cover (SDC)

Numerous techniques have been developed to estimate supraglacial debris cover (Pratibha *et al*., 2018; Shukla *et al*., 2009, 2010). NDSI and band ratio of NIR and SWIR was used to estimate changes in SDC for 48 glaciers in Baspa basin. An increase by 15% was observed from 1997 to 2014 (Pratibha *et al*., 2018). Another study was carried out using artificial neural network which suggests increase in SDC by 20% for 3 glaciers in Chandra basin from 1993 to 2014 (Garg *et al*., 2017).

Glacier Lakes and Glacier Lakes Outburst Flood

RS techniques have been extensively used to study high-altitude glacier lakes; these are a) glacier lake area mapping, b) identification of future lake sites, c) estimation of maximum expansion of present and future lakes and d) hazard potential of GLOF (Basnett *et al*., 2013; Maanya *et al*., 2016; Patel *et*

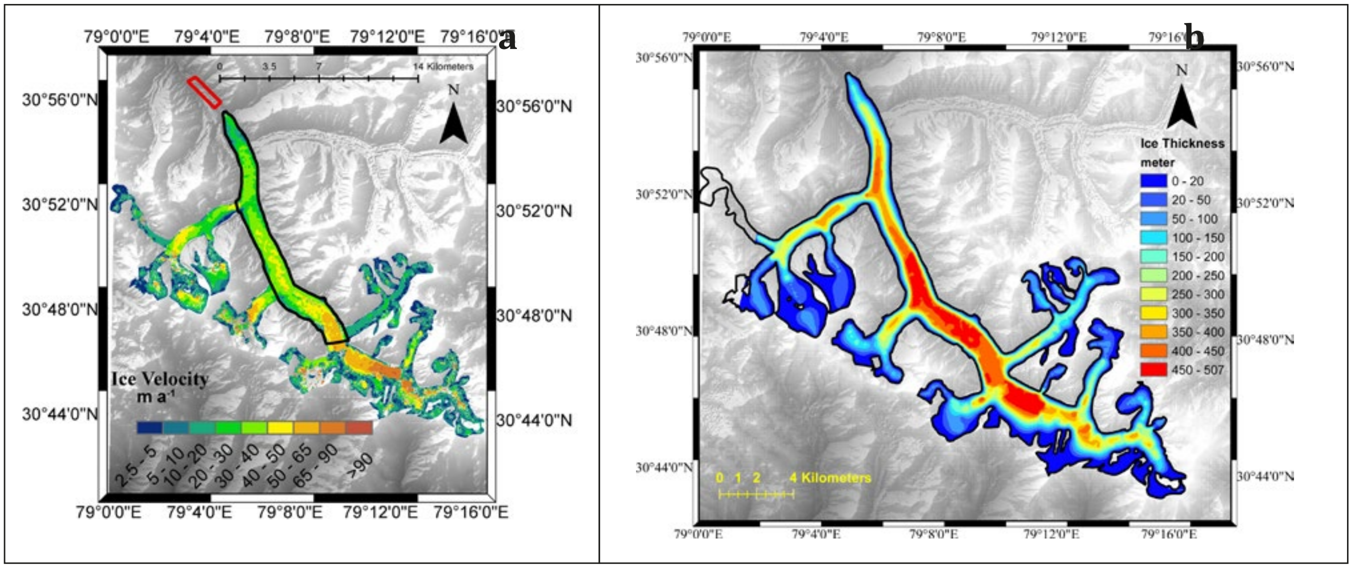

Fig. 4: (a) Spatial distribution of velocity at Gangotri glacier for year 2013-14 and (b) spatial distribution of ice thickness (Source: Bhushan *et al*., 2017)

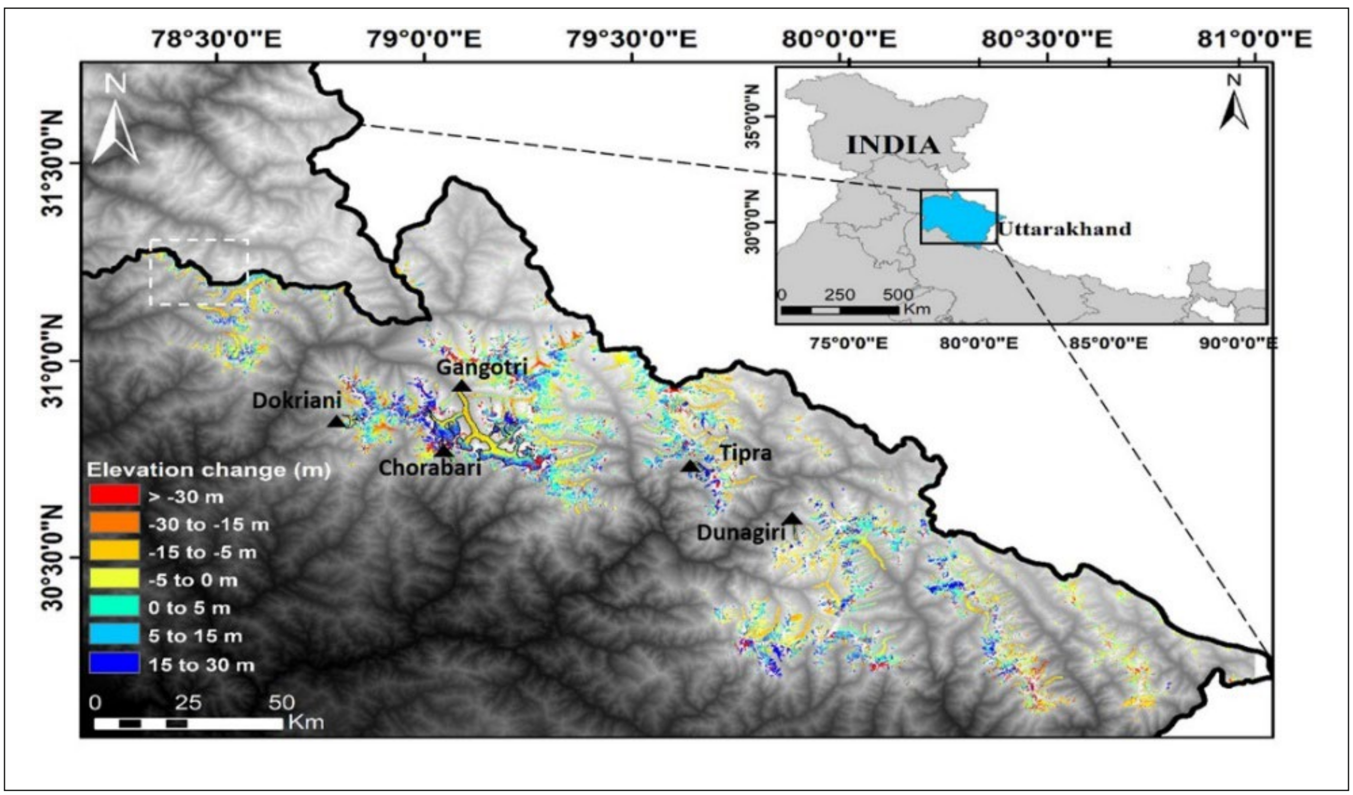

Fig. 5: Spatial distribution of surface elevation change (m) during 2000-2014 using TanDEM-X and SRTM DEM translates into the mass loss rate of −1.21 ± 0.11 Gta^{-1} for glaciers in Uttarakhand state (Source: Bandyopadhyay *et al*., 2019).

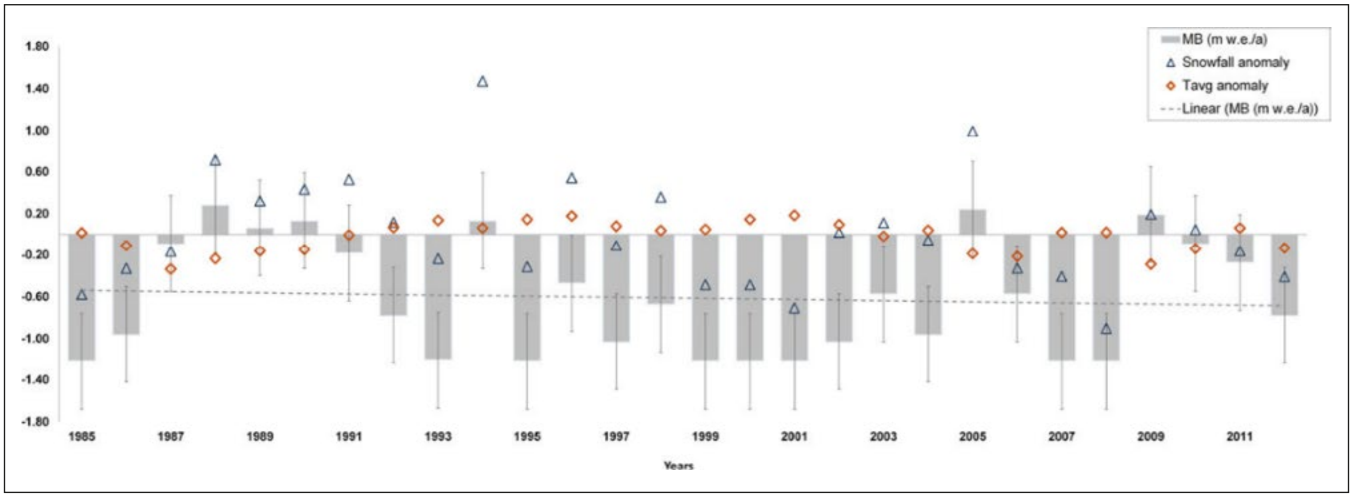

Fig. 6: Inter-annual variation in specific glacier mass balance shown with snowfall and temperature anomaly in Chandra basin. The mass balance is estimated using IAAR method. Mass loss between 1985 and 2013 for Chandra and Satluj basins is estimated as 11.1 Gt and 16.4 Gt, respectively.

al., 2017; Remya *et al*., 2019; Sattar *et al*., 2019). Glacier lakes can be mapped due to the contrast between ice, rock, and water (Fig.3a). These can be digitized manually or by automated techniques as Normalized Differential Water Index (NDWI).

A new technique has also been developed to estimate lake volume, expansion of existing and potential lakes. In this method, ice thickness obtained from laminar flow is subtracted from DEM to obtain bottom topography and over deepening (Bhushan *et al*., 2017; Maanya *et al*., 2016; Remya *et al*., 2019; Fig.7). The methodology is automated in a python-based tool called Himalayan Glacier Thickness Mapper (HIGTHIM), which can be used to estimate expansion of present and future glacier lakes (Kulkarni *et al*., 2018; Fig.7). These inputs have been used in hydrological models to assess GLOF, which can help in mapping vulnerable sites and developing mitigation strategy (Sattar *et al*., 2019).

Conclusion and discussion

Remote sensing data can provide information on numerous parameters of Himalayan cryosphere. We have seen explosion of new data and its application in last decades, making remote sensing as an indispensable tool for cryospheric studies. Remote sensing data in combination with field observations has led to numerous models which can provide information on different spatial and temporal scales. For example, techniques can estimate reliable information on glacier stored water for individual glaciers, for group of glaciers and for entire mountain range. In addition, we can combine these estimates with mass balance to assess changes in storage and assess

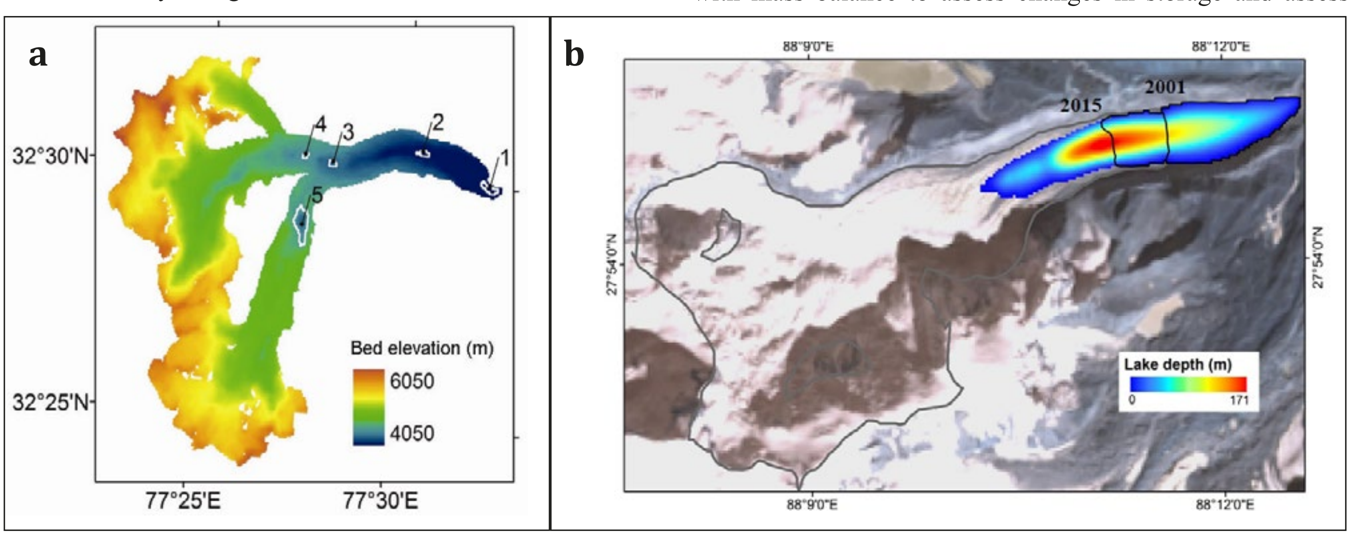

Fig. 7: (a) Potential lake sites at Samudra Tapu glacier, mean depth varying between 35 and 95 m (Source: Maanya *et al*., 2016). (b) Lake extent of South Lhonak lake in 2001, 2015 and predicted maximum expansion. The lake has a volume of 60±10.8 million m^3 in 2015, which is likely to expand to 90±16.2 million m^3 (Source: Remya *et al*., 2019).

spatial heterogeneity. This provides a unique opportunity to assess changes in water availability. Remote sensing can also provide information on glacier lakes, snow cover, snow albedo and debris cover. It can be used in numerous hydrological models to assess impact of climate change on livelihood of people living in mountains and to assess water and food security of India.

Acknowledgement

This work was carried out at Divecha Centre for Climate Change at IISc, Bengaluru. The Landsat OLI and Sentinel-2 images used in the study are acquired from U.S.G.S. Earth Explorer data portal. RGI boundaries were provided by Global Land Ice Measurements from Space initiative.

References

Azam, M. F., Wagnon, P., Berthier, E., Vincent, C., Fujita, K. and Kargel, J. S., 2018: Review of the status and mass changes of Himalayan-Karakoram glaciers. *Journal of Glaciology*, **64(243)**: 61-74.

Bajracharya, S. R. and Shrestha, B. R., 2011: The status of glaciers in the Hindu Kush-Himalayan region. International Centre for Integrated Mountain Development (ICIMOD).

Bandyopadhyay, D., Singh, G. and Kulkarni, A. V., 2019: Spatial distribution of decadal ice-thickness change and glacier stored water loss in the Upper Ganga basin, India during 2000–2014. *Scientific reports*, ***9*(1)**: 1-9.

Basnett, S., Kulkarni, A. V. and Bolch, T., 2013: The influence of debris cover and glacial lakes on the recession of glaciers in Sikkim Himalaya, India. *Journal of Glaciology*, **59(218)**: 1035-1046.

Bhushan, S., Syed, T. H., Kulkarni, A. V., Gantayat, P. and Agarwal, V., 2017: Quantifying changes in the Gangotri Glacier of Central Himalaya: Evidence for increasing mass loss and decreasing velocity. *IEEE Journal of Selected Topics in Applied Earth Observations and Remote Sensing*, **10(12)**: 5295-5306.

Gantayat, P., Kulkarni, A. V. and Srinivasan, J., 2014: Estimation of ice thickness using surface velocities and slope: case study at Gangotri Glacier, India. *Journal of Glaciology*, **60(220)**: 277-282.

Garg, P. K., Shukla, A., Tiwari, R. K., and Jasrotia, A. S., 2017: Assessing the status of glaciers in part of the Chandra basin, Himachal Himalaya: a multiparametric approach. Geomorphology, **284**, 99-114.

Gurung, D. R., Giriraj, A., Aung, K. S., Shrestha, B. R. and Kulkarni, A. V., 2011: Snow-cover mapping and monitoring in the Hindu Kush-Himalayas. International Centre for Integrated Mountain Development (ICIMOD).

Gurung, D. R., Maharjan, S. B., Shrestha, A. B., Shrestha, M. S., Bajracharya, S. R. and Murthy, M. S. R., 2017: Climate and topographic controls on snow cover dynamics in the Hindu Kush Himalaya. *International Journal of Climatology*, **37(10)**: 3873-3882.

Kulkarni, A. V. and Buch, A. M., 1991: Glacier Atlas of Indian Himalaya. Ahmedabad, Space Application Centre (ISRO).

Kulkarni, A. V., 1992: Mass balance of Himalayan glaciers using AAR and ELA methods. *Journal of Glaciology*, **38(128)**: 101-104.

Kulkarni, A. V., Srinivasulu, J., Manjul, S. S. and Mathur, P., 2002: Field based spectral reflectance studies to develop NDSI method for snow cover monitoring. *Journal of the Indian Society of Remote Sensing*, **30**: 73-80.

Kulkarni, A. V., Rathore, B. P. and Alex, S., 2004: Monitoring of glacial mass balance in the Baspa basin using accumulation area ratio method. *Current science*, **86(1)**: 185-190.

Kulkarni A. V., S. K. Singh, P. Mathur and V. D. Mishra, 2006: Algorithm to monitor snow cover using AWiFS data of RESOURCESAT for the Himalayan region. *International Journal of Remote Sensing*, **27(12)**: 2449-2457.

Kulkarni, A. V., 2007: Effect of global warming on the Himalayan cryosphere. *Jalvigyan Sameeksha*, **22**: 93-108.

Kulkarni, A. V., Rathore, B. P., Singh, S. K. and Ajai, 2010: Distribution of seasonal snow cover in central and western Himalaya. *Annals of Glaciology*, **51(54)**: 123-128.

Kulkarni, A. V., Rathore, B. P., Singh, S. K. and Bahuguna, I. M., 2011: Understanding changes in the Himalayan cryosphere using remote sensing techniques. *International journal of Remote Sensing*, **32(3)**: 601-615.

Kulkarni, A. V., Vinay Kumar, G., Negi, H. S., 2013: Srinivasan, J. and Satheesh, S. K.: The effect of black carbon on reflectance of snow in the accumulation area of glaciers in the Baspa basin, Himachal Pradesh, India. *The Cryosphere Discussions*, **7(2)**: 1359–1382, https://doi.org/10.5194/tcd-7-1359-2013.

Kulkarni, A. V., Nayak, S. and Pratibha, S., 2017: Variability of Glaciers and snow cover. *In*: Observed Climate Variability and Change over the Indian Region, M.N. Rajeevan and S. Nayak (eds.), Springer, Singapore, 193-219.

Kulkarni, A, V., Goswami, A., Ramsanakaran R., Singh, G., Dashora, A., Srinivasalu, P., Remya S., Krishnamurthy., N., Arya A.R. and Godha, A., 2018: HIGTHIM User Manual, Divecha Centre for Climate Change, Indian Institute of Science, Bengaluru, India.

Kulkarni, A. V. and Pratibha, S., 2018: Assessment of glacier fluctuations in the Himalaya. *In*: Science and Geopolitics of The White World, P.S. Goel, R. Ravindra and S. Chattopadhyay (eds.), Springer, 183-195.

Kumar, A., Negi, H. S., Kumar, K., Shekhar, C. and Kanda, N., 2019: Quantifying mass balance of East-Karakoram glaciers using geodetic technique. *Polar Science*, **19**: 24-39.

Maanya, U. S., Kulkarni, A. V., Tiwari, A., Bhar, E. D. and Srinivasan, J., 2016: Identification of potential glacial lake sites and mapping maximum extent of existing glacier lakes in Drang Drung and Samudra Tapu glaciers, Indian Himalaya. *Current Science*, **111(3)**: 553-560.

Maurer, J. M., Rupper, S. B. and Schaefer, J. M., 2016: Quantifying ice loss in the eastern Himalayas since 1974 using declassified spy satellite imagery. *The Cryosphere*, **10**: 2203-2215.

Nuimura, T., Sakai, A., Taniguchi, K., Nagai, H., Lamsal, D., Tsutaki, S., Kozawa, A., Hoshina, Y., Takenaka, S., Omiya, S., Tsunematsu, K. and Fujita, K., 2015: The gamdam glacier inventory: a quality-controlled inventory of Asian glaciers. *The Cryosphere*, **9**: 849–864.

Patel, L. K., Sharma, P., Laluraj, C. M., Thamban, M., Singh, A. and Ravindra, R., 2017: A geospatial analysis of Samudra Tapu and Gepang Gath glacial lakes in the Chandra Basin, Western Himalaya. *Natural Hazards*, **86**: 1275-1290.

Patil, A., Singh, G. and Rüdiger, C., 2020: Retrieval of Snow Depth and Snow Water Equivalent Using Dual Polarization SAR Data. *Remote Sensing*, **12(7)**: 1183.

Prasad, V., Kulkarni, A. V., Pradeep, S., Pratibha, S., Tawde, S. A., Shirsat, T., Arya, A.R., Orr, A. and Bannister, D., 2019: Large losses in glacier area and water availability by the end of twenty-first century under high emission scenario, Satluj basin, Himalaya. *Current Science*, **116(10)**: 1721-1730.

Pratibha, S. and Kulkarni, A. V., 2018: Decadal change in supraglacial debris cover in Baspa basin, Western Himalaya. *Current Science*, **114(4)**: 792-799.

Ramsankaran, RAAJ., Navinkumar, P. J., Dashora, A. and Kulkarni, A., 2020: UAV-based Survey of Glaciers in Himalayas: Opportunities and Challenges. https:/doi: 10.20944/preprints202002.0442.v1

Rathore, B. P., Bahuguna, I. M., Singh, S. K., Brahmbhatt, R. M., Randhawa, S. S., Jani, P., Yadav, S.K.S. and Rajawat, A. S., 2018: Trends of snow cover in Western and West-Central Himalayas during 2004-2014. *Current Science*, **114(4)**:800-807.

Remya, S. N., Kulkarni, A., Pradeep, S. and Shrestha, D. G., 2019: Volume estimation of existing and potential glacier lakes, Sikkim Himalaya, India. *Current Science*, **116(4)**: 620-627.

Riggs, G. A., Hall, D. K. and Román, M. O., 2015: MODIS snow products collection 6 user guide. National Snow and Ice Data Center: Boulder, CO, USA, 66.

Sahu, R. and Gupta, R. D., 2020: Snow cover area analysis and its relation with climate variability in Chandra basin, Western Himalaya, during 2001–2017 using MODIS and ERA5 data. *Environmental Monitoring and Assessment*, **192(8)**: 1-26.

Sangewar, C. V. and Shukla, S. P., 2009: Inventory of the Himalayan glaciers. *Geological Survey of India Special Publication, **34***.

Sattar, A., Goswami, A. and Kulkarni, A. V., 2019: Hydrodynamic moraine-breach modeling and outburst flood routing-A hazard assessment of the South Lhonak lake, Sikkim. *Science of the total environment*, **668**: 362-378.

Sharma, A. K., Singh, S. K., Kulkarni, A. V. and Ajai, 2013: Glacier Inventory in Indus, Ganga and Brahmaputra Basins of the Himalaya. *National Academy Science Letters*, **36(5)**: 497-505.

Shukla, A., Gupta, R. P. and Arora, M. K., 2009: Estimation of debris cover and its temporal variation using optical satellite sensor data: a case study in Chenab basin, Himalaya. *Journal of Glaciology*, **55(191)**: 444-452.

Shukla, A., Gupta, R., and Arora, M. K., 2010: Delineation of debris-covered glacier boundaries using optical and thermal remote sensing data. *Remote Sensing Letters*, **1(1)**: 11-17.

Singh, G., Nela, B. R., Bandyopadhyay, D., Mohanty, S. and Kulkarni, A. V., 2020: Discovering anomalous dynamics and disintegrating behaviour in glaciers of Chandra-Bhaga sub-basins, part of Western Himalaya using DInSAR. *Remote Sensing of Environment*, **246**: 111885.

Singh, S. K., Rathore, B. P., Bahuguna, I. M. and Ajai, 2014: Snow cover variability in the Himalayan–Tibetan region. *International Journal of Climatology*, **34(2)**: 446-452.

Tawde, S. A., Kulkarni, A. V. and Bala, G., 2017: An estimate of glacier mass balance for the Chandra basin, western Himalaya, for the period 1984–2012. *Annals of Glaciology*, ***58*(75-2)**: 99-109.

Tawde, S.A, Kulkarni, A. V. and Bala, G., 2019: An assessment of climate change impacts on glacier mass balance and geometry in the Chandra Basin, Western Himalaya for the 21st century. *Environmental Research Communications*, **1(4)**: 041003.

Vijay, S., & Braun, M., 2016: Elevation change rates of glaciers in the Lahaul-Spiti (Western Himalaya, India) during 2000–2012 and 2012–2013. *Remote Sensing*, **8(12)**: 1038.

Indian Journal of Geosciences, Volume 74, No. 3
July - September, 2020; pp. 315-326

Invited Paper

Sub-ice Geology of East Antarctica- the supercontinent connection and its context to the East Antarctic Ice Sheet

Rasik Ravindra[1], Devsamridhi Arora[2], Naresh Chandra Pant[2] and S.K. Roy[3]

[1]Former Deputy Director General, Geological Survey of India;
Former Director, National Centre for Polar and Ocean Research (NCPOR), Goa
[2] Department of Geology, University of Delhi, New Delhi
[3]Geological Survey of India, Central Region, Nagpur
Corresponding author's email: rasikravindra@gmail.com

Abstract: Defining sub-ice geology of the east Antarctic shield (EAS), holding the largest concentration of ice on planet earth, has assumed importance on account of its role in predicting its behaviour in a warming world. Significant gaps as well as challenges remain in mapping sub-ice geology of EAS despite continued efforts. Status of geology of EAS is discussed considering the continuity from adjacent terrains in the most accepted continental fits as well as by incorporation of recently acquired data. In the central Dronning Maud Land (cDML) sector, continuation of East African Orogen (EAO) is indicated up to ~200km inland. The suturing of East and West Gondwana at ~640 Ma is also correlated as well as extensive pan African age anorogenic magmatism. Description and correlation of a Tonian age arc is also well described recently from east of cDML. In the Princess Elizabeth Land (PEL) sector, existence of a recently proposed ~800 Ma orogeny prior to the pervasive ~500 Ma Kunga orogeny is recorded. Despite area specific efforts, need for integrated and, major multinational collaborative efforts to describe the sub-ice geology is acutely felt.

Keywords: East Antarctica Shield, Gondwana assembly, Kunga orogeny, East African Orogen (EAO), Tonian and Pan-African metamorphic events

Introduction

Antarctica, especially the east Antarctic craton, has remained a key constituent in several attempts to build a best fit assembly of pre-Gondwana break up (Crawford, 1974; Grew and Manton, 1986; Hoffman, 1991; Stern,1994; Yoshida 1995; Dalziel, 1997; Jacobs *et al*., 1998; 2015; Fitzsimmons, 2000a,b; Zhao *et al.*, 2003; Boger and Miller, 2004; Ravikant *et al*., 2004, 2007; Collins and Pisarevsky, 2005; Boger, 2011; Pant *et al*., 2013; Harley, 2003, 2013; Roy *et al*., 2017; Chatterjee *et al*., 2017; Mikhalsky *et al*., 2017; Arora *et al*., 2020; Wang *et al*., 2020 among others). Given the inhospitable climate, inaccessible terrain conditions and with only 2 percent of the ice-free area being available to unravel the details, the geological investigations are often challenging. The Antarctic continent is comprised of two distinct physiographic and tectonic domains: the West Antarctica and the East Antarctica- that are divided into two unequal parts by a 3500 km long Transantarctic Mountains chain extending across the continent between the Ross and the Weddell Sea (Fig. 1). In the East Antarctica, rock outcrops are exposed in discontinuous mountain chain, along the coastal fringes of the Dronning Maud land, Enderby Land, Princess Elizabeth Land, Wilkes Land and Victoria Land (Fig.1). The interiors of the East Antarctica rise as ice plateau, attaining maximum height of around 3233 m above mean sea level (m.s.l.) with thick ice sheet throwing an apron of ice that conceals the outcrops and subsurface topography.

Understanding of the sub-ice geology, geomorphology and heat flow constrains has important bearing on the future behaviour of the East Antarctic Ice Sheet (EAIS) (DeConto and Pollard, 2003; Pollard *et al.*, 2015). The complex issue of reconstructing the sub-ice geology involves multiple approaches including the direct observations as well as indirect inferences. In this paper we discuss progress of sub-ice geology reconstruction in selected sectors of east Antarctic shield and link it to the Rodinia to Gondwanaland supercontinent reconstruction.

The East Antarctic Shield

East Antarctic shield (EAS) is a complexly interweaved Precambrian basement rock body that is buried by the East Antarctic Ice sheet. The Precambrian EAS is considered as a key component of both Rodinia and Gondwana (Fitzsimons, 2000a; Boger, 2011). Geologically, EAS comprises of preserved Archean nuclei separated by Proterozoic suture belts (Fig. 2; e.g., Dalziel, 1992; Fitzsimons, 2000a, b). EAS has become a quintessential continental cratonic block to test supercontinent formation and rifting models (Fitzsimons, 2000a; Boger 2011) and to investigate and understand the nature of high-grade metamorphism (Harley, 2003; Boger and Miller, 2004; Kelsey *et al.*, 2007). It is suggested that post Gondwana amalgamation at~500 Ma, EAS was not directly affected by the subsequent orogenic activities that resulted in the final assembly of Pangea at 250 Ma, as Gondwana accreted to Laurasia as a coherent block.

Broadly, EAS preserves a history of ~4 billion years and has generally been considered as a collage of different terranes having affinities with several other continents (Fig. 3; Boger, 2011), amalgamated during global orogenic activities. Boger (2011) divided Antarctic cratons into five broad tectonic domains on the basis of age similarities and orogenic history, four of which lie in EAS and the fifth one is Phanerozoic rocks making the basement of West Antarctica (Fig. 3). The five domains are:

Fig. 1: Map of Antarctica the Southern Ocean (Landsat Image Mosaic of Antarctica), http://lima.nasa.gov/pdf/A3_overview.pdf.

1. Domain 1: Terrane with close geological affinity with south-eastern Africa (marked by green colour in Fig. 3), comprising of the Dronning Maud Land.

2. Domain 2: Terrane with close geological affinity with eastern India (marked by purple colour in Fig. 3), comprising parts of Enderby land to PEL.

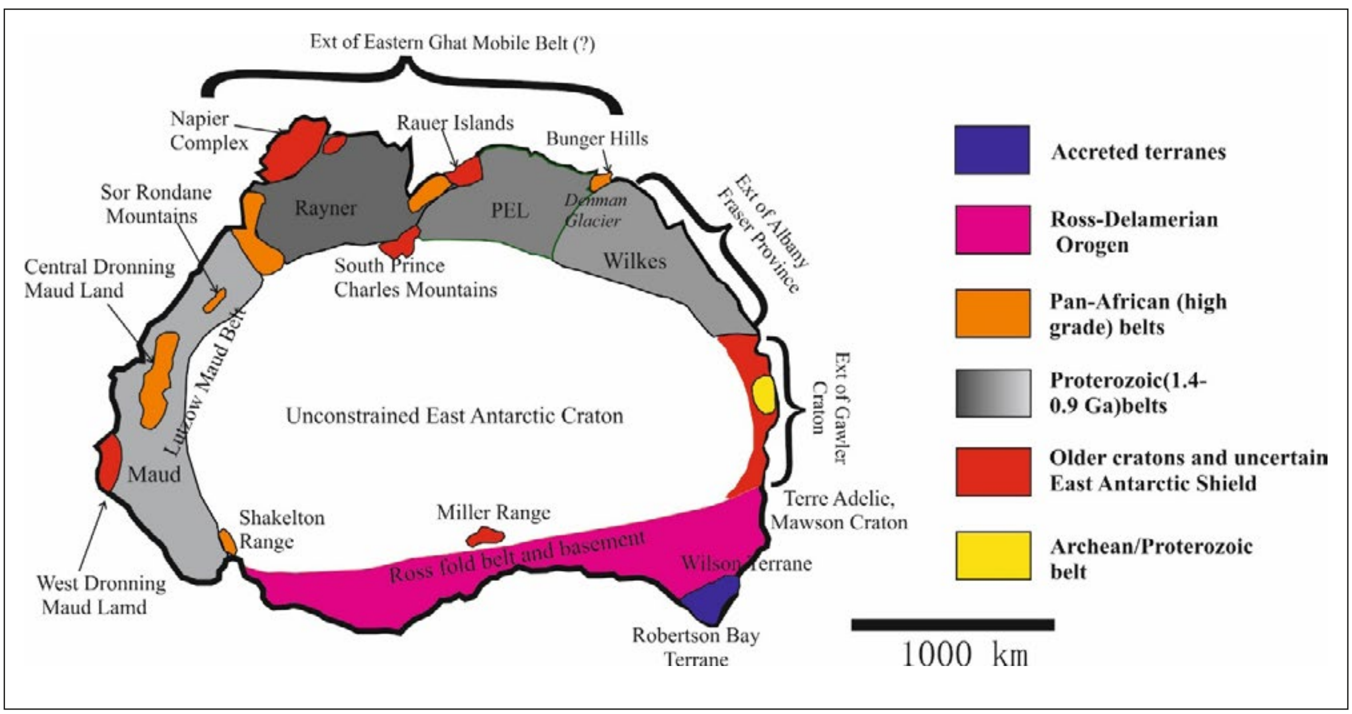

Fig. 2: Map of East Antarctic Shield showing the major geological terrains based on inferences from exposures of rock mountains in the coastal areas. (Modified from Fitzsimons, 2000b)

3. Domain 3: Terrane with close geological affinity with southern Australia (marked by pink colour in Fig. 3), comprising of Wilkes Land and Terre Adelie Land.

4. Domain 4: Ice covered centre of EAS which has no known affinity (marked by peach colour in Fig. 3). Very little knowledge of subglacial geology of this domain is known, mainly on account of lack of outcrops.

5. Domain 5: Phanerozoic rocks accreted on the margin of Gondwana (marked by blue colour in Fig. 3), comprising of Ross fold belt and Ellsworth Land.

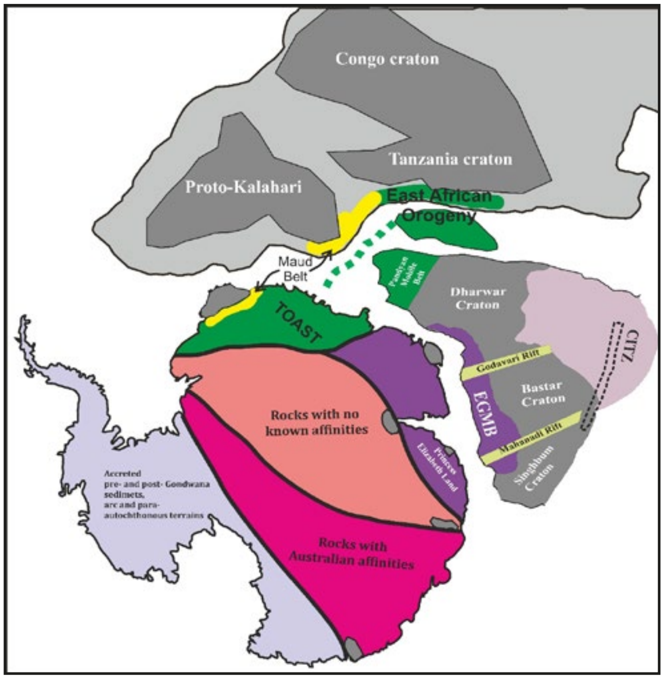

Fig. 3: Map showing the proposed position of Antarctica and other adjacent continents in archetypal models Gondwana (c. 0.5 Ga) assembly. Redrawn from Harley *et al*. (2013). Tectonic domains of Antarctica are redrawn from Boger (2011). Location of TOAST and Maud Belt are from Jacobs and Thomas (2004) and Jacobs *et al.* (2015).

The boundaries between these domains are well constrained in coastal outcrops, however, their continuation into interior of EAS is unclear, except the one between domain 3 and 5 (Finn *et al*., 2006). Domain 1 and 2 defining Africo-Antarctic and Indo-Antarctic are the final addictions that were made to the EAS during Ediacaran and early Cambrian (Boger 2011). The two most important orogenic collisions related to this are known as the East African-Antarctic Orogen (EAAO) or Mozambique Belt (e.g. Jacobs *et al*., 1998; Meert and Van der Voo, 1997; Boger, 2011) and the Kunga Orogeny (e.g. Meert *et al*., 1995; Boger *et al*., 2011; Fitzsimons, 2000b, 2003). EAAO marks the boundary between the African affinity domain and domain 4 (Coats Land) while the Kunga Orogeny differentiates the Indo–Antarctic and Australo–Antarctic terranes. The Kunga orogeny is the Ediacaran-Cambrian (~570-530 Ma) aged orogeny, considered to document the collision between north and south Gondwana, or what is today Dronning Maud Land in Antarctica and northern Mozambique in Africa. The term was given by Meert *et al.* (1995). A number of alternate routes have been hypothesised for the Kunga orogeny (Boger, 2011). The three main proposed routes are by Meert, (2003); Fitzsimons, (2003) and Boger and Miller (2004) (Fig. 4).

Meert (2003) proposed that the east Gondwana assembled in two phases (as shown in Fig. 4 a). The first phase is defined by collision of north and central parts of East Africa with parts of India, Madagascar and Antarctica at ~650Ma (Stern, 1994). This was followed by another collision at ~570-530 Ma, between the Africo-Indo-Antarctic and the Australo-Antarctic sectors, defining the Kunga orogeny. In this model, the amalgamation of Kalahari craton with Gondwana is proposed to have occurred at the same time along the Kunga orogeny (Meert, 2003). A number of structural problems makes this model inappropriate, e.g.: The proposed route of Kunga orogeny cuts southern sectors of Madagascar at a high angle to its structural orientation (Boger, 2011). Also, the coastal belt of EAS from Lützow–Holm Bay and Prydz Bay-PEL preserve evidences of Indian affinity and very little Pan-African reworking is been reported from this domain (e.g.: Mezger and Cosca, 1999).

Fitzsimons (2003) proposed two alternative routes for Kunga orogeny (as shown in Fig. 4 b), both traverse the Gamburtsev Subglacial mountain range and end near Shackleton range. The south trending boundary of the Lambert rift defined the western flank of the Kunga suture in both these routes. The problem with this model is that the route to the Shackleton ranges tends to cut the Transantarctic Mountains in between, which is unlikely because Nimrod-Kimban orogeny marks the eastern margins of the Mawson craton (Boger, 2011). Another problem with this model is the routes proposed trend south whereas the structural orientation in the southern Prince Charles mountains is west to southwest (surface observations e.g.: Phillips *et al*., 2005a, b; Boger and Wilson, 2005; Corvino *et al*., 2008 and airborne geophysical evidence: McLean *et al*., 2009).

Boger and Miller (2004) proposed a roughly similar route for Kunga orogeny (as shown in Fig. 4 c). Unlike Fitzsimons (2003), it did not cover much of the interior of EAS and terminated along the PEL coast. Its western flank is consistent with the west-southwest structural trends of southern Prince Charles Mountains and runs along the PEL coast till West Ice shelf, covering all the coastal outcrops of PEL as well as Grove mountains. However, it did not incorporate the Pan-African orogenic signatures from the Shackleton range (Kleinschmidt and Boger, 2009).

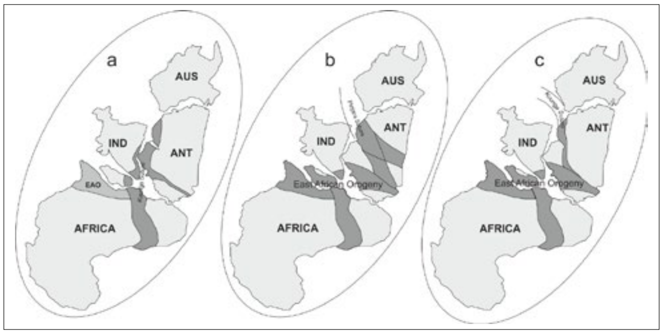

Fig. 4: Illustration showing different proposed routes of the Kunga orogeny. Redrawn from Boger, (2011). (a) by Meert, (2003), (b) by Fitzsimons, (2003) and (c) by Boger and Miller, (2004).

Contributions by the Indian Antarctic Program

Though the international efforts in exploring the geology of eastern Antarctica commenced with International Geophysical Year, 1957-58 (Ravich and Soloviev, 1966; Ravich and Kamenev, 1975; Grew, 1981; Bormann and Fritzsche 1995, etc.), the Indian efforts towards geological studies in this region were initiated in Schirmacher Oasis – the northernmost ice free area of cDML during 1983, which continued with emphases on special themes such as structure and tectonics, metamorphism, lamprophyres, shear zone etc. around Schirmacher and later extended gradually to other interior areas of cDML and the Prydz Bay Region especially, Larsemann Hills and Princess Elizabeth land.

Four decades of sustained Indian contributions towards understanding the crustal evolution of eastern Antarctica and paleoclimate, geomorphology and glaciological studies of the region saw the extension of investigations in deep interior parts of central Dronning Maud land and Prydz Bay- Amery Ice shelf (Fig. 1), leading to publications of a series of geological maps of Wholthat Mountains (1991), Schirmacher Oasis (1998), Orvin fjella (2006), Muhligg-Hoffman Mountains (2010) and geomorphological map of Schirmacher in 2006 by Geological Survey of India (Fig. 5). An elaborate bibliography of the work has been given in several publications (such as Ravindra and Mohan, 2011; Ravindra 2012; Nayak 2017; Pant and Dasgupta, 2017a; Pant, *et al*., 2017b; Ravindra and Rajan, 2020; Mohan *et al*., 2020).

Schirmacher Oasis and Central Dronning Maud land

The northernmost extension of cDML are seen exposed in and around Schirmacher Oasis in the form of low lying undulatory rolling topography. The rocks exhibit polymetamorphic, deformed terrain (Fig. 6) exposing garnet- biotite gneiss, augen gneiss; inter-banded mafic granulite, khondalite, calc–silicate, charnockite, enclaves of mafic granulite with hypersthene-plagioclase and/or two- pyroxene plagioclase, garnet-sillimanite gneiss as dominant litho-units. (Sengupta, 1988; Singh, 1986; Kaul *et al*., 1987; Bose and Hazra, 2000; Bose and Sengupta, 2003, Ravikant *et al*., 2004). The chronology of deformation and metamorphic events is summarised by Ravikant and Kundu (1998) as per which the first phase of metamorphism took place at 750-800^{o}C temperatures under 8kbar pressure followed by an isothermal decompression at 750^{o}C during which charnockite intrusions took place. An isobaric cooling of rocks at 5-6 kbar pressure followed. A later metamorphism, responsible for a retrogressive phase has also been widely recognized.

The main mountain chain of cDML exposed from west to east and comprising Gjelsvkfjell , Muhlig-Hoffmannfjella, Orvin-fjella, - Humboldt - Petermann Ranges of Wholthat Mountains and Gruber massif (Fig. 5) have been mapped systematically on 1:50,000 scale by GSI (Dharwadkar *et al*., 2017; D'Souza *et al*., 2006; Bejarniya *et al*., 1995; Ravindra *et al*., 1994; Joshi and Pant, 1995; Kaul, *et al*., 1987 respectively).

The lithostratigraphy, as built up by D'Souza *et al*. (1997) in parts of cDML has been shown below at Table 1.

The dominant Meso-Neoproterozoic rock types exposed in cDML have been classified as high-grade granulite to amphibolite facies rocks, para gneisses with calc- silicates, migmatised gneiss, charnockite and amphibolite as seen in the Humboldt Mountains (Ravindra *et al.,* 1994). Pant *et al.* (2013) considered the ~640Ma granulites to be representing the suture between east and west Gondwana representing the extension of East African Orogen (EAO) inland in east Antarctica. The Gruber anorthosites have intruded the Late Mesoproterozoic orthogneiss and have been shown to be alkali and silica rich (Mukerji *et al*., 1988). Ravikant *et al.* (2011) have classified the rocks marginal to the anothosites massif as ferro-monzodiorite and ferro-monzonite, invoking contamination of the parent magma by crustal material that now occurs as enclaves within it. PGM bearing meta-ultramafites have been reported from northern parts of Humboldt (Ravindra *et al*., 1989), from the EPMA scan of the meta-ultramafite assemblages. Ravindra and Pandit (2000) also assign whole rock Rb- Sr isochoron age of 514$\pm$59 Ma to the Nordvestoya granites exposed in the northern parts of the Humboldt Mountains.

Late Proterozoic granitic orthogneisses in the Payer-Weyprecht Mountains, south of Gruber and Petermann ranges, have been assigned an age of 749$\pm$61 Ma by whole rock Rb-Sr (Ravikant *et al*., 1997). In the eastern part of cDML, the granites of Muhlig-Hofmannfjella (Fig. 5) have been correlated with the Svarthmaren charnockite of western Muhlig-Hoffmanfjella that have been dated at 500$\pm$24 Ma by Ohta *et al*. (1990). The Gjelsvikfjella area located in the farthest western parts of the cDML exposes predominantly para and orthogneisses

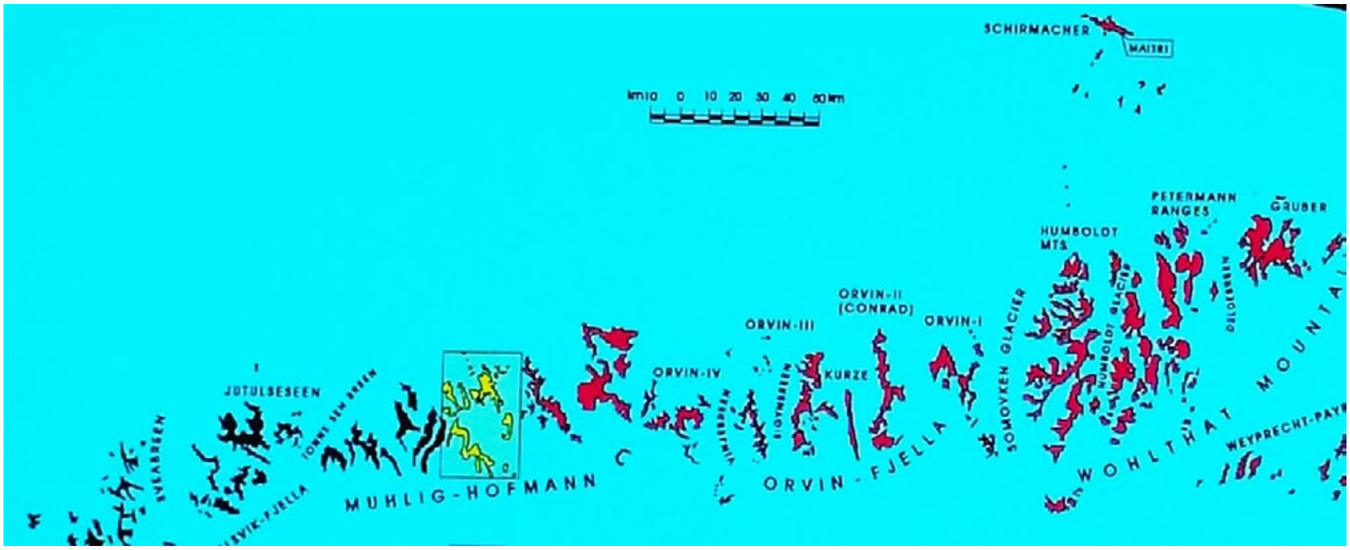

Fig. 5: Area of detailed geological mapping by GSI in CDML, east Antarctica (modified after GSI)

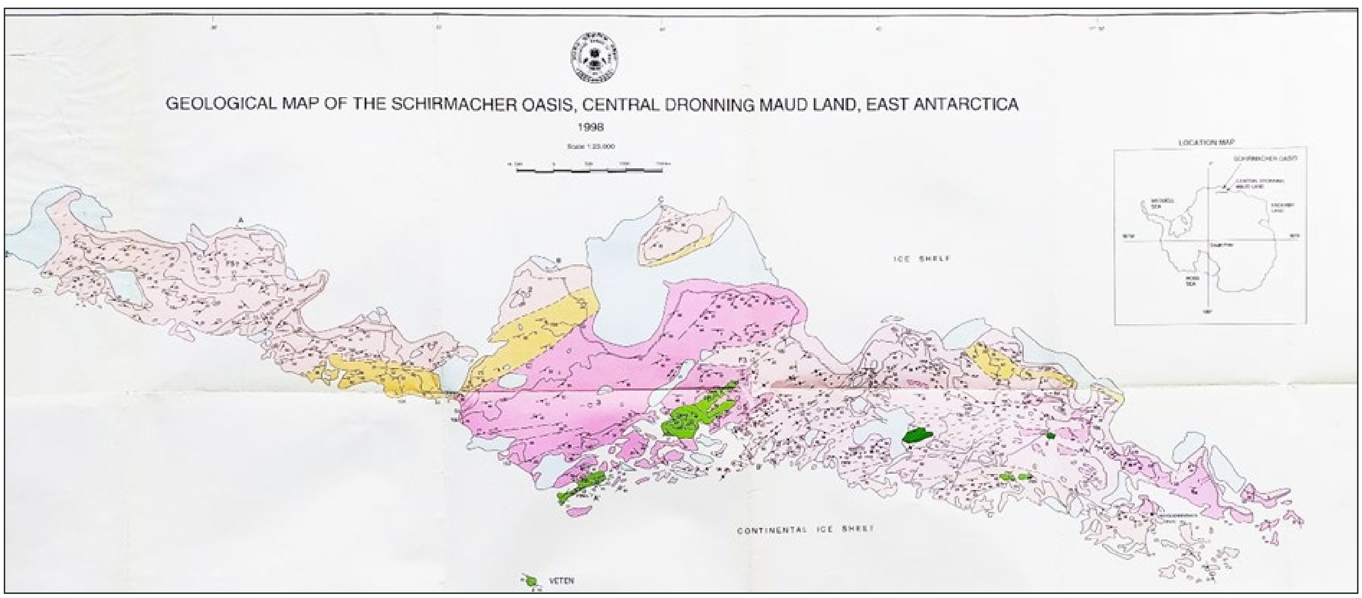

Fig. 6: Geological map of the Schirmacher Oasis depicting lithological and structural details.The major rock units mapped (from left to right) are quartzofelspathic augen gneiss, khondalite, charnockite-enderbite with pyroxene granulite and enclaves of mafic and ultra-mafic dykes (GSI).

represented by biotite gneiss, biotite-garnet gneiss, quartzo-feldspathic and granite gneiss (Dharwadkar *et al*., 2017).

Princess Elizabeth Land

Princess Elizabeth Land (PEL) constitutes part of eastern Antarctica bounded by Amery Ice Shelf/Lambert Glacier and Mac. Robertson Land in the west and Wilhelm II Land in the east (Fig. 1). There are several isolated nunataks and mountain ranges exposed within the Amery basin- Lambert Glacier, collectively called as the Prince Charles Mountains. The ice-free outcrops in Princess Elizabeth Land include coastal fringe of east Prydz Bay in form of island groups, peninsulas and bluff and are exposed along the ~250 km long coastal fringe of PEL. The major outcrops in the east are Vestfold Hills, Rauer Group, the Brattstrand Bluffs, the Larsemann Hills and the Bollingen Islands. Landing Bluff westwards, adjacent to the Lambert graben, exposes the un-deformed granites of Pan African age. Further east from the Vestfold Hills, most of the interior sector of PEL lacks rock outcrops except one isolated nunatak exposed near the West Ice Shelf called Mount Brown.

An inland group of scattered mountains and nunatak called Grove mountains is exposed in interior PEL which is reported

Table 1: Lithostratigraphy in cDML (after D'Souza *et al*., 1997).

Unit	Lithology	Area of exposure
Late Intrusive	Dolerite, basalt, lamprophyres, melasyenite, norite	Schirmacher, many parts of cDML
Granite	Porphyritic alkali granite with rafts of country rocks	Petermann, Nordvestoya , northern Humboldt, Conrad, Kurze and Dalmann fjellet
C-Type magmatic suite	Charnockite and its variants-ferrogabbro, monzonite, monzosyenite, anorthosite	Zwiessel, Northern Humboldt, Kurze
Orthogneisses	Quartzofelspathic gneiss with biotite, contains enclaves of earlier granulites	Payer and Weyprcht Mountains
Anorthosites and foliated Charnockite	Coarse grained and other variants of anothosites with marginal norite, Charnockite (foliated) enderbite, granulite, inter banded pyroxene granulie and amphibolite.	Gruber Anorthosite massif, Skeid, Muhlig-Hoffmann fjella, Schirmacher. various parts of cDML
Skeidd Orthogneiss	Hornblende-biotite quartzofelspathic gneisses with migmatites. Essentially migmatised gneiss of amphibolite facies	Skid Conrad Mountain, North Humboldt
Calc-gneisses	Garnet-clinopyroxene bearing gneiss associated with calc- silicate rocks. Metamorphosed under granulie facies	Humboldt and Dalmannfjellet
Para-gneisses	Garnet-sillimanite gneiss, garnetiferous quartzo-felspathic gneiss, migmatites associated with early meta basics,	Petermann, Humboldt, Dalmannfjellet, Schirmacher

to have similar metamorphic history as the Northern Prince Charles Mountains and other Pan-African dominated domains of Prydz Bay sector (e.g.: Liu *et al*., 2009). The Vestfold block consists of high-grade metamorphic rocks of Archean age dominantly derived from igneous protoliths with subordinate metasediments while the Rauer Group block comprises of both Archean as well as Proterozoic geological history and possesses distinct ages and metamorphic history as compared to other outcrops of the PEL coast (e.g.: Kinny *et al*., 1993; Harley *et al*., 1998). A westward younging sequence is evident and the large time gap of >2000 Ma suggests presence of complex geological history and interleaved distinct terrains. The Larsemann Hills area along the eastern coastal margin of Prydz Bay, encircling the Ingrid Christensen Coast, lies along the northern extension of the eastern Indian Cratonic belts of Bastar, EGMB, Singhbhum, etc. of the East Gondwanaland-East Antarctica tectonic framework.

Geological studies undertaken by Mandal and Roy (2008) and Nath *et al*. (2016) have shown that the major rock types exposed in the Larsemann Hills area are: garnetiferous granite; granodiorite gneiss; orthopyroxene bearing granite representing the metamorphosed acid igneous suite; pyroxene granulite representing the metamorphosed basic igneous suite and the pelitic granulite representing the metamorphosed sedimentary suite.

Small scale quartzo-feldspathic melts (migmatite) are also preserved at a few locations. The post tectonic igneous suite is represented by small patches of granitoids. Relicts of older amphibolites and mafic enclaves occur as rafts and enclaves within the garnetiferous gneiss. The rocks document a diachronous geological evolutionary history that shows a Palaeoproterozoic felsic/ gneissic basement over which supracrustal sequence of pelitic, psammitic paragneisses were deposited (Pandit, 2016). The rocks have undergone two major phases of metamorphism at ca ~ 1 Ga and during early Palaeozoic- the latter, a medium to low pressure granulite facies metamorphism at ~ 7 kbar pressure and 800-850°C temperature. Detailed work on the complicated basement-cover rocks of the Larsemann Hills area, their relationship and the time frame was carried out by Ghosh *et al.* (2017). However, Arora *et al*. (2020) while confirming the presence of pan-African mountain building event accompanied by extensive decompression, propose that the preceding orogeny was ~800 Ma and represented a Rodinian amalgamation.

East Antarctic Shield and the supercontinent connection

The rock outcrops along the coast of East Antarctica initially considered to be a single, continuous Grenvillian age Circum-East Antarctic mobile belt (Tingey, 1981; Stuwe *et al*., 1989; Yoshida, 1995 etc), was later proposed to be divided in three segments by two Pan African domains, one across the coast of the Dronning Maud Land and other across the Princess Elizabeth land (PEL) coast (Fitzsimons, 2000). The former has been proposed as the southward continuation of the East African Orogen (EAO) in Antarctica (Jacobs *et al*., 1998; Pant *et al*., 2013; Roy *et al*., 2017) while the northward continuation of the PEL domain into the Eastern Ghats Mobile Belt remains ambiguous though recent studies have reported Pan African ages from EGMB (e.g.: Nanda *et al*., 2018).

The ~ 3000 km long East African Orogen (EAO), extending from Jordan and Israel in the North (Arabian Nubian Shield, ANS) to Madagascar –Mozambique in the South has been suggested to extend into East Antarctica through the Lutzow-Holm Bay to cDML. A large number of individual cratonic segments viz., India (in the East) and Kalahari, Sahara etc (in the West) were sutured in the world's largest Neoproterozoic orogen. The passage of EAO and attempts to provide the missing links have been made by several workers (e.g. Jacobs *et al*., 1998, Jacobs and Thomas, 2004; Jacobs *et al*., 2003, 2008; Mikhalasky *et al*., 2006; Pant *et al*., 2013 etc).

Investigations pertaining to crustal evolutionary history of parts of east Antarctica especially, cDML and the Larsemann Hills, and their correlation with the Indian landmass under pre Gondwana set up, have also been carried out by Indian scientists in last three decades (Ravikant *et al*., 2007; Baba *et al*., 2006; Pant *et al*., 2013; Roy *et al*., 2017, and references therein), who recognise the southern extension of the EAO, comprising Mesoproterozoic rocks of Grenvillian orogeny into the coastal mountain ranges of cDML through the NNW-SSE trending rocks of Schirmacher Oasis, Wohlthat Mountains and the isolated exposures between these, such as Baalsrudfjellet. The western and central Dronning Maud Land represents a tectonically reworked rim of the Kalahari craton comprising the Grenvillian continental arc called the Maud Belt (Fig. 3) signifying Rodinia amalgamation (Marschall *et al*., 2013), whereas the Eastern section of Dronning Maud Land is proposed to be constituting a 1000-900 Ma juvenile oceanic arc (Tonian Oceanic Arc Super Terrane, TOAST, Jacobs *et al*., 2015; Fig. 3), that was amalgamated to the easternmost margin of the Archean Kalahari craton during final collision of East and West Gondwana.

Both the cDML and Larsemann Hills regions expose Mesoproterozoic poly-deformed, magmatic rocks that have undergone granulite grade of metamorphism. The southern extension of EAO is believed to have acted as a suture between the east and west Gondwana blocks during Neoproterozoic (Pant *et al*., 2013 and references therein). Based on electron microprobe dating of the monazite grains, Pant *et al*. (2013) have opined that metamorphic neo-crystallisation began in at~640-650 Ma time and continued up to 580 Ma. The 500-600 Ma magmatic activity is widespread in cDML. Wang *et al.* (2020) have also given whole-rock Sm–Nd isotopic age for dominant magmatism of 530–485 Ma and 650–600 Ma age for charnockite and anorthosites of eastern cDML.

The extension of EAO to Antarctica through Schirmacher has been cited depending upon the similarities of granulites representing 660 Ma-600 Ma (Stern, 1994) to those of Schirmacher (Ravikant *et al*., 2004, 2007; Baba *et al*., 2006). Though there are differences in the interpretation of the metamorphic paths in rocks of the Schirmacher Oasis, from isobaric heating isothermal decompression-isobaric cooling (Ravikant and Kundu, 1998) to isobaric cooling during retrograde metamorphism (Baba *et al*., 2006), there is a general consensus about the clockwise P–T–t paths and the timing of peak metamorphism to be significantly younger than was envisaged earlier (Baba *et al*., 2008, 2010). The oldest date of ~584 Ma obtained from monazite within the metapelite of Baalsrudfjellet nunatak (situated between the Schirmacher and Wohlthat Mountains) indicates that the area is part of EAO (Roy *et al*., 2017). The P-T fluid histories inferred from the study of calc-silicate rocks of Baalsrudfjellet have been correlated with those from Kerala- Khondalite Belt (KKB) and the Highland complex of Sri Lanka (D'Souza *et al*., 2012).

The Larsemann Hills in the Prydz Bay region offers a key setting for correlation between the Princess Elizabeth Land sector of East Antarctica and the Eastern Ghat Mobile Belt of eastern India. The geochronological similarities between Larsemann-Brattstrand sector and Eastern Ghat Mobile Belt of India were first cited by Crawford (1974) as a strong evidence of India-Antarctic connection. The study of Grenvillian (~1000 Ma)-Pan-African (~500 Ma) high grade tectono-metamorphic evolutionary history of the Prydz Bay, including Larsemann Hills and its adjoining areas like Sostrene Islands, Bolingen Islands, Brattstrand Bluffs, Rauer Islands, Vestfold Hills etc. is significant in the present-day reconstruction and correlation with India and East Antarctica. Nath *et al.* (2016) have drawn a marked similarity between the metamorphic history of the rocks of Larsemann Hills and that of Anantagiri-Araku areas of the Eastern Ghats of India that show the peak metamorphic P-T condition of 843°C at ~6 kb for the pyroxene granulites and 805°C at ~6 kb for the metapelites. Dates, similar to Pan-African ages of 490+14 Ma from dating of monazite are also reported from various pockets of the Eastern Ghats of India. In a recent study, Arora *et al.* (2020) have demonstrated that there are marked similarities between pelitic granulites of Princess Elizabeth land and Eastern Ghat belt of India. The authors have reported two granulite grade events at ~800 Ma and~500 Ma from coastal outcrops of PEL that correspond to Tonian and Pan-African metamorphic events, later marking the collision of Indo-Australo-Africo-Antarctic cratons.

Boger (2011) presented events that represent the separate collision events that amalgamated the final domains of EAS and proposed that these events were closely spaced in time and hence, divided the events into time zones such as: Ediacaran events, Ediacaran–early Cambrian events and Cambrian events. The model supported that the rocks of domain 1, 2 and Coats Land section of domain 4 were amalgamated with rest of the EAS during formation of Gondwana and the subsequent Kunga orogeny stitched these sectors into the Australo-Antarctic plate along the Crohn margin. This hypothesis is challenged later by e.g.: Phillips *et al*., (2009); Mikhalsky *et al*., (2010) who proposed that these terranes amalgamated at ~1000 Ma during the Grenvillian and were reactivated during the Pan African collision.

Increasing geochronological and petrological evidence from EAS and its contiguous terrains of EGMB and sections of African shield suggest that the time period between the assembly of Rodinia (~1100 Ma) and Gondwana (~500 Ma) is clearly not as simple as it is commonly accepted. The present configuration of EAS is a result of multiple Neoproterozoic tectonic events with its Rodinia and Gondwana geological neighbours. The extensive geological research work undertaken in late three decades in the Dronning Maud Land unravels the complexly coalesced Neoproterozoic zones, whereas the interior regions of Princess Elizabeth Land largely remains enigmatic. An improved understanding of the ice-covered subglacial interior and tectonic configuration of EAS will not only address the unresolved questions regarding the supercontinental assemblies but will also enhance our knowledge about the geological controls on the growth, dynamics and stability of the overlying East Antarctic Ice Sheet (Goodge and Fanning 2010).

Concluding Remarks

Reconstruction of sub-ice geology in the EAS is problematic on account of extremely limited direct observations. The "adjacent contiguous terrain" theory has limited applicability as demonstrated by non-continuation of several major features from the nearby continental landmasses as well as problems of crust loss. Extension of EAO up to ~200 km inland in Antarctica appears to be one significant feature in this context in the cDML. Identification of Tonian age arc east of cDML is also a new addition to the existing knowledge. Further east, in the PEL sector, identification of ~800 Ma orogenic signatures also point out to necessity of revising geology of this sector of EAS. However, it is quite apparent that the sub-ice geology and structure, increasingly important in context of assessing the stability of the East Antarctic Ice Sheet, is far from well understood. The need for major, integrated multinational campaigns is imperative in this context.

Acknowledgement

Indian Antarctic Program is a multi-institutional Program involving several organisations and universities. Author record their gratitude to all earth scientists whose work has formed the base of the current paper. The support and encouragement provided by Geological Survey of India and National Centre for Polar and Ocean Research is gratefully acknowledged.

References

Arora, D., Pant, N., Pandey, M., Chattopadhyay, A., Greenbaum, J., Siegert, M., Bo, S., Blankenship, D., Chalapathi Rao, N.V., and Bhandari, A., 2020: Insights into geological evolution of Princess Elizabeth Land, East Antarctica-clues for continental suturing and breakup since Rodinian time. *Gondwana Research*, **84:** 260-283.

Baba, S., Hokada, T., Kaiden, H., Dunkley, D.J., Owada, M., and Shiraishi, K., 2010: SHRIMP Zircon U–Pb dating of sapphirine-bearing granulite and biotite-hornblende gneiss in the Schirmacher Hills, East Antarctica: implications for Neoproterozoic ultrahigh temperature metamorphism predating the assembly of Gondwana. *The Journal of Geology,* **118(6):** 621-639.

Baba, S., Owada, M., and Shiraishi, K., 2008: Contrasting metamorphic P-T path between Schirmacher Hills and Mühlig- Hofmannfjella, central Dronning Maud Land, East Antarctica. *Geological Society of London Special Publications,* **308(1):** 401-417.

Baba, S., Owada, M., Grew, E.S., and Shiraishi, K.: 2006: Sapphirine – orthopyroxene – garnet granulite from Schirmacher Hills, Central Dronning Maud Land. *In:* Fütterer, D.K., Damaske, D., Kleinschmidt, G., Miller, H., and Tessensohn, F., (Eds.). *Antarctica: Contributions to Global Earth Sciences, Springer-Verlag, Berlin Heidelberg New York,* 37- 44.

Bejarniya, B.R., Ravikant, V., Mukerji, S., Nautiyal, S.C., Oberoi, L.K., and Gill, A.S., 1995: Geology of the Payer-Weyprecht Mountains, Central Dronning Maud Land, East Antarctica. *Eleventh Indian Expedition to Antarctica Scientific Report, Department of Ocean Development, Technical Publication,* **9:** 121-144.

Boger, S.D., and Miller, J.McL., 2004: Terminal suturing of Gondwana and the onset of the Ross–Delamerian Orogeny: the cause and effect of an Early Cambrian reconfiguration of plate motions. *Earth and Planetary Science Letters,* **219(1-2):** 35–48.

Boger, S.D., and Wilson, C.J.L., 2005: Early Cambrian crustal shortening and a clockwise P–T–t path from the southern Prince Charles Mountains, East Antarctica: implications for the formation of Gondwana. *Journal of Metamorphic Geology*, **23(7):** 603-623.

Boger, S.D., 2011: Antarctica—before and after Gondwana. *Gondwana Research,* **19(2):** 335–371.

Krynauw, J., 1997: The Schirmacher Oasis, Queen Maud Land, East Antarctica, and its surroundings, *In:* Bormann, P., and Fritzsche, D., (Eds.), *Polar Record,* **33(184):** 72-73.

Bose, S., and Hazra, S., 2000: Structural analyses of the western part of the Schirmacher hills, east Antarctica. *Sixteenth Indian Expedition to Antarctica, Scientific Report, Department of Ocean Development, Technical Publication,* **14:** 1-36.

Bose, S., and Sengupta, S., 2003: High Temperature Mylonitization of Quartzofeldspathic gneisses: Example from the Schirmacher Hills, East Antarctica. *Gondwana Research,* **6:** 805-816.

Chatterjee, A., Das, K., Bose, S., Ganguly, P., and Hidaka, H., 2017: Zircon U–Pb SHRIMP and monazite EPMA U–Th–total Pb geochronology of granulites of the western boundary, Eastern Ghats Belt, India: a new possibility for Neoproterozoic exhumation history. *Geological Society, London, Special Publications*, **457:** 105-140.

Collins, A. S., and Pisarevsky, S. A., 2005: Amalgamating eastern Gondwana: The evolution of the Circum-Indian Orogens. *Earth-Science Reviews,* **71(3-4):** 229-270.

Corvino, A.F., Boger, S.D., Henjes-Kunst, F., Wilson, C.J.L. and Fitzsimons, C.W., 2008: Superimposed tectonic events at 2450 Ma, 2100 Ma, 900 Ma and 500 Ma in the North Mawson Escarpment, Antarctic Prince Charles Mountains. *Precambrian Research*, **167(3-4):** 281-302.

Crawford, A.R., 1974. Indo-Antarctica, Gondwanaland, and the distortion of a granulite belt. *Tectonophysics,* **22(1-2):** 141–157.

D'Souza, M.J, Nath, A.K., Swain, A.K., Shrivashtava, P.K., Mandal, A., and Dharwadkar, A., 2012: Modeling the Pan-African Calc-Silicate rocks of Central Dronning Maud Land, East Antarctica with reference to CaO-Al_2O_3-SiO_2-CO_2 System. *Unpublished report of the Geological Survey of India, FS 2010-2012.*

D'Souza, M.J., Keshava Prasad, A.V., and Ravindra, R., 2006: Genesis of ferropotassic A-Type granitoids of Muhlig- Hofmannfjella, Central Dronning Maud Land, East Antarctica, *In:* Fütterer, D.K., Damaske, D., Kleinschmidt, G., Miller, H. and Tessensohn, F., (Eds.), Antarctica: contributions to global earth sciences, *Springer, Berlin, Heidelberg, New York*, 45-54.

D'Souza, M.J., Kundu, A., and Kaul, M.K., 1997: The geology of a part of Central Dronning Maud Land (cDML), East Antarctica. *Indian Minerals,* **50(4):** 323-338.

Dalziel, I.W.D., 1992: Antarctica; a tale of two supercontinents?. *Annual Review of Earth and Planetary Sciences,* **20(1):** 501-526.

Dalziel, I.W.D., 1997: OVERVIEW: Neoproterozoic-Paleozoic geography and tectonics: Review, hypothesis, environmental speculation. *Geological Society of America Bulletin*, **109(1):** 16-42.

DeConto, R.M. and Pollard, D., 2003: Rapid Cenozoic glaciation of Antarctica induced by atmospheric CO_2. *Nature*, **421(6920):** 245-249.

Dharwadkar, A., Shrivastava, P.K., and Shrivastava, H.B., 2018: Tectonometamorphic Evolution of Jutulsessen, Gjelsvikfjella, cDML, East Antarctica. *Journal of the Geological Society of India,* **92:** 265–280.

Finn, C.A., Goodge, J.W., Damaske, D., and Fanning, C.M., 2006: Scouting craton's edge in paleo-Pacific Gondwana. *Antarctica*, 165-173.

Fitzsimons, I.C.W., 2000a: A review of tectonic events in the East Antarctic Shield and their implications for Gondwana and earlier supercontinents. *Journal of African Earth Sciences,* **31 (1):** 3–23.

Fitzsimons, I.C.W., 2000b: Grenville-age basement provinces in East Antarctica: Evidence for three separate collisional orogens. *Geology,* **28(10):** 879–882.

Fitzsimons, I.C.W., 2003: Proterozoic basement provinces of southern and southwestern Australia, and their correlation with Antarctica. *Geological Society London Special Publications,* **206(1):** 93–130.

Ghosh, J.G., Roy, S.K., Krishna, K.V.S.S., Sadiq, Md., Raghuram, and Ayemi, K. K., 2017: Report on Relationship between the Paragneiss and Orthogneiss in the Larsemann Hills, Antarctica. *Unpublished report of the Geological Survey of India, FS 2015-17.*

Goodge, J.W., and Fanning, C.M., 2010: Composition and age of the East Antarctic Shield in eastern Wilkes Land determined by proxy from Oligocene-Pleistocene glaciomarine sediment and Beacon Supergroup sandstones, Antarctica. *GSA Bulletin,* **122(7-8):** 1135-1159.

Grew, E.S., and Manton, W.I., 1986: A new correlation of sapphirine granulites in the Indo-Antarctic metamorphic terrain: Late Proterozoic dates from the Eastern Ghats Province of India. *Precambrian Research,* **33(1-3):** 123-137.

Grew, E.S., 1981: Surinamite, taaffeite, and beryllian sapphirine from pegmatites in granulite-facies rocks of Casey Bay, Enderby Land, Antarctica. *American Mineralogist*, **66(9-10):** 1022-1033.

Yoshida, M., Windley, B.F., Dasgupta, S., 2003: Proterozoic East Gondwana: Supercontinent Assembly and Breakup. *Geological Society London, Special Publications*, 206.

Harley, S.L., Fitzsimons, I.C.W., and Zhao, Y., 2013: Antarctica and supercontinent evolution: historical perspectives, recent advances and unresolved issues. *Geological Society of London, Special Publications*, **383:** 1-34.

Hoffman, P.F., 1991: Did the breakout of Laurentia turn Gondwanaland inside-out?. *Science,* **252(5011):** 1409–1412.

Jacobs, J., and Thomas R. J., 2004: Himalayan-type indenter-escape tectonics model for the southern part of the late Neoproterozoic–early Palaeozoic East African–Antarctic orogen. *Geology,* **32(8):** 721–724.

Jacobs, J., Bauer, W., and Fanning, C.M., 2003: Late Neoproterozoic/Early Palaeozoic events in central Dronning Maud Land and significance for the southern extension of the East African Orogen into East Antarctica. *Precambrian Research*, **126(1-2):** 27-53.

Jacobs, J., Elburg, M., Läufer, A., Kleinhanns, I.C., Henjes-Kunst, F., Estrada, S., Ruppel, A.S., Damaske, D., Montero, P., and Bea, F., 2015: Two distinct Late Mesoproterozoic/Early Neoproterozoic basement provinces in central/eastern Dronning Maud Land, East Antarctica: The missing link, 15–21°E. *Precambrian Research*, **265:** 249-272.

Jacobs, J., Fanning, C. M., Henjes-Kunst, F., Olesch, M., and Paech, H.J. 1998: Continuation of the Mozambique Belt into East Antarctica: Grenville-age metamorphism and polyphase Pan- African high-grade events in Central Dronning Maud Land. *The Journal of Geology,* **106(4):** 385-406.

Jacobs, J., Pisarevsky, S.A., Thomas, R.J., and Becker, T., 2008: The Kalahari Craton during the assembly and dispersal of Rodinia. *Precambrian Research,* **160(1-2):** 142-158.

Joshi, A., and Pant, N.C., 1995: Petrology, geochemistry and evolution of the charnockite suite of the Petermann Ranges, East Antarctica. *Memoirs of the Geological Society of India,* **34:** 241-258.

Kaul, M.K., Singh, R.K., Srivastava, D., Jayaram, S., and Mukerji, S., 1987: Petrological and structural characteristics of a part of east Antarctic Craton, Queen Maud land, Antarctica, In: M.R.A. Thompson., J.A. Crane and J.W. Thomson (Eds.) *Geological Evolution of Antarctica, Cambridge University Press, Cambridge,* 89-94.

Kelsey, D.E., Hand, M., Clark, C., Wilson, C.J.L., 2007. On the application of in situ monazite chemical geochronology to constraining P–T–t histories in high-temperature (>850°C) polymetamorphic granulites from Prydz Bay, East Antarctica. *Geological Society Publication House, London,* **164:** 667–683.

Kinny, P.D., Black, L.P., and Sheraton, J.W., 1993: Zircon ages and the distribution of Archaean and Proterozoic rocks in the Rauer Islands. *Antarctic Science,* **5(2):** 193-206.

Kleinschmidt, G., and Boger, S.D., 2009: The Bertrab, Littlewood and Moltke Nunataks of Prinz-Regent-Luitpold-Land (Coats Land) - Enigma of East Antarctic Geology. *Polarforschung*, **78(3):** 95-104.

Liu, X., Hu, J., Zhao, Y., Lou, Y., Wei, C., Liu, X., 2009: Late Neoproterozoic/Cambrian high- pressure mafic granulites from the Grove Mountains, East Antarctica: P–T–t path, collisional orogeny and implications for assembly of East Gondwana. *Precambrian Research,* **174(1-2):** 181–199.

Nath, A.K., D'souza, M.J., and Mandal, A., 2011: Correlation of crustal evolutionary history of Larsemann Hills, East Antarctica and Eastern Ghats, India. *Unpublished Report of the Geological Survey of India, FS 2008-2009.*

Marschall, H.R., Hawkesworth, C.J., and Leat, P.T., 2013: Mesoproterozoic subduction under the eastern edge of the Kalahari-Grunehogna Craton preceding Rodinia assembly: The Ritscherflya detrital zircon record, Ahlmannryggen (Dronning Maud Land, Antarctica). *Precambrian Research*, **236:** 31-45.

McLean, M.A., Wilson, C.J.L., Boger, S.D., Betts, P.G., Rawling, T.J., and Damaske, D., 2009: Basement interpretations from airborne magnetic and gravity data over the Lambert Rift region of East Antarctica. *Journal of Geophysical Research: Solid Earth*: **114(B6).**

Meert, J.G., 2003: A synopsis of events related to the assembly of eastern Gondwana. *Tectonophysics*, **362(1-4):** 1-40.

Meert, J.G., Van Der Voo, R., 1997: The assembly of Gondwana 800–550 Ma. *Journal of Geodynamics,* **23(3-4):** 223–235.

Meert, J.G., Van Der Voo, R., Ayub, S., 1995: Paleomagnetic investigation of the Neoproterozoic Gagwe lavas and Mbozi complex, Tanzania and the assembly of Gondwana. *Precambrian Research,* **74(4):** 225–244.

Mezger, K., and Cosca, M.A., 1999: The thermal history of the Eastern Ghats belt (India) as revealed by U-Pb and ^{40}Ar / ^{39}Ar dating of metamorphic and magmatic minerals: implications for the SWEAT correlation. *Precambrian Research,* **94(3-4):** 251-271.

Mikhalsky, E.V., Sheraton, J.W., Hahne, K., 2006: Charnockite composition in relation to the tectonic evolution of East Antarctica. *Gondwana Research,* **9(4):** 379–397.

Mikhalsky, E., Krylov, D., Rodionov, N., Presnyakov, S., Skublov, S., and Myasnikov, O., 2017: Refined geological history of the polyphase plutonometamorphic complex in the Thala Hills area (Enderby Land, East Antarctica) from zircon SHRIMP dating and implications for Neoproterozoic amalgamation of Gondwanaland. *Geological Society, London, Special Publications,* **457(1):** 7-36.

Mikhalsky, E.V., Henjes-Kunst, F., Belyatsky, B.V., Roland, N.W., and Sergeev, S.A., 2010: New Sm–Nd, Rb–Sr, U–Pb and Hf isotope systematics for the southern Prince Charles Mountains (East Antarctica) and its tectonic implications. *Precambrian Research,* **182(1-2):** 101-123.

Mohan, R., Roy, S.K., Meloth, T., Anilkumar, N., Krishnan, K. P., Sabu, P., Kumar, A., Mahesh, B. S., Patil, S.M., Venkatachalam, S., and Pant, N.C., 2020: Recent Indian Contributions from the Polar Realm. *Proceedings of the Indian National Science Academy,* **86(1):** 569-583.

Mukerji, S., Kaul, M.K., Singh, R.K., Srivastava, D., and Jayaram, S., 1988: Anorthosites of Gruber Massif, Central Queen Maud Land, East Antarctica-An appraisal. *Fifth Indian Expedition to Antarctica, Scientific Report, Department of Ocean Development Technical Publication,* **5:** 99-108.

Nanda, J., Gupta, S., Hacker, B., 2018: U-Pb zircon and titanite ages from granulites of the Koraput area–evidence for Columbia, Rodinia and Gondwana from the Eastern Ghats Province, India. *Precambrian Research,* **314:** 394–413.

Nath, A.K., Dharwadkar, A., and Shrivastava, P.K., 2016: Preliminary geological Investigation at Larsemann Hills, East Antarctic during 26th Indian Antarctic Expedition, *National Centre for Antarctic and Ocean Research, Goa, India, Technical Publication,* 24.

Nayak, S., 2017: Recent Antarctic Research in India: The National Committee Report to SCAR. *Proceedings of the Indian National Science Academy*, **83(2):** 245-512.

Ohta, Y., Torudbakken, B.O., and Shiraishi, K., 1990: Geology of Gjelsvikfjella and western Muhlig-Hofmannfjella, Dronning Maud Land, east Antarctica. *Polar Research,* **8(2):** 99-126.

Pandit, M.K., 2019: Magnetic fabric studies in Larsemann Hills, Prydz Bay region, East Antarctica. *National Centre for Polar and Ocean Research, Ministry of Earth Sciences, Govt. of India, Technical Report*, **24:** 279-287.

Pant, N.C., Roy, S., Ravikant, V., and Ravindra, R., 2017b: Recent contributions to the Antarctic Geology - An Indian Perspective. *Proceedings of the Indian National Science Academy,* **83(2):** 269-278.

Pant, N.C. and Dasgupta, S., 2017a: An introduction to the crustal evolution of India and Antarctica: the supercontinent connection. *Geological Society, London, Special Publications,* **457(1):** 1-6.

Pant, N.C., Kundu, A., D'souza, M.J., and Saikia, A., 2013: Petrology of the Neoproterozoic granulites from Central Dronning Maud Land, East Antarctica–Implications for southward extension of East African Orogen (EAO). *Precambrian Research*, **227:** 389-408.

Phillips, G., Corvino, A.F., Boger, S.D., McLean, M.A., and Wilson, C.J.L., 2005a: Crustal Cross-Sections along the Mawson Escarpment and Mount Stinear, Southern Prince Charles Mountains (East Antarctica): Correlating the Ruker Complex across the Lambert Glacier. *Terra Antartica,* **12(2):** 51-53.

Phillips, G., Kelsey, D.E., Corvino, A.F., and Dutch, R.A., 2009: Continental reworking during overprinting orogenic events, Southern Prince Charles Mountains, East Antarctica. *Journal of Petrology,* **50(11):** 2017-2041.

Phillips, G., Wilson, C.J.L., and Fitzsimons, I.C.W., 2005b: Stratigraphy and structure of the southern Prince Charles Mountains, East Antarctica. *Terra Antartica,* **12(2):** 69-86.

Pollard, D., DeConto, R. M., and Alley, R. B., 2015: Potential Antarctic Ice Sheet retreat driven by hydrofracturing and ice cliff failure. *Earth and Planetary Science Letters*, **412:** 112-121.

Ravich, M.G., and Kamenev, E.N., 1975: Crystalline Basement of the Antarctic Platform, *John-Wiley, New York*, 582p.

Ravich, M.G., and Soloviev, D.S., 1966: Geology and petrology of the Mountains of Central Dronning Maud Land (Eastern Antarctica). *Transactions of the Scientific Research Institute of the Geology of the Arctic, Ministry of Geology, Leningrad,* 141.

Ravikant, V., and Kundu, A., 1998: Reaction textures of retrograde pressure temperature-deformation paths from granulites of Schirmacher Hills, East Antarctica. *Journal of the Geological Society of India,* **51:** 305-314.

Ravikant, V., Bejarniya, B.R., Mukerji, S. and Kaul, M.K., 1997: Late Proterozoic granitic orthogneisses from Payer-Weyprecht Mountains, East Antarctica: their tectonometamorphic history and regional correlation, *In:* C.A. Ricci (ed.) *The Antarctic Region: Geological Evolution and Processes, Siena, Italy,* 55-63.

Ravikant, V., Bhaskar Rao, Y.J., Gopalan, K., 2004: Schirmacher Oasis as an extension of the Neoproterozoic East African Orogen into Antarctica: new Sm–Nd isochron age constraints. *The Journal of Geology,* **112(5):** 607–616.

Ravikant, V., Dharwadkar, A., Golani, P.R., and Ravindra, R., 2011: Petrology and geochemistry of the Grubergebirge anorthosite and marginal rocks, Central Dronning Maud Land: Further characterization of the Late Neoproterozoic magmatic event in East Antarctica. *Journal of the Geological Society of India*, **78(1):** 7-18.

Ravikant, V., Laux, J.H., and Pimentel, M.M., 2007: Sm–Nd and U–Pb isotopic constraints for crustal evolution during Late Neoproterozoic from rocks of the Schirmacher Oasis, East Antarctica: geodynamic development coeval with the East African Orogeny. *US Geological Survey,* Open-File Report: 5p.

Ravindra, R., and Mohan, R., 2011: Three Decades of Polar Science in India. *Journal of the Geological Society of India,* **78(1):** 5-6.

Ravindra, R., Dey, A., D'Souza, M.J., Beg, M.J., and Kaul, M.K., 1994: On the gneisses and associated rocks from South Humboldt Mountains, Central Dronning Maud Land, East Antarctica. *Ninth Indian Expedition to Antarctica, Scientific Report, Department of Ocean Development, New Delhi, India, Technical Publication,* **6:** 133-159.

Ravindra, R., and Pandit, M.K., 2000: Geochemistry and Geochronology of A-type Granite from Northern Humboldt Mountain, East Antarctica: Vestige of Pan-African magmatism. *Journal of the Geological Society of India*, **56:** 253-262.

Ravindra, R., and Rajan, S., 2020: Advances in Antarctic geoscience studies: Indian contributions. *Episodes*, **43(1):** 563-574.

Ravindra, R., 2012: National Centre for Antarctic and Ocean Research. *Proceedings of the Indian National Science Academy,* **78(3):** 591-600.

Ravindra, R., Pant, N.C., and D'Souza, M.J., 1989: A note on the PGM-bearing metaultramafite from Humboldt Mountains in East Antarctica. *Indian Minerals,* **43(2):** 157-161.

Roy, S.K., Pant, N.C., Kundu, A., Dharwadkar, A., Kumar, P.K., Joshi, S., Raghuram, Sadiq, M., and Pandey, M., 2017: Geological studies in the Baalsrudfjellet nunatak between the Schirmacher Oasis and the Wohlthat Mountains to establish the continuation of the East African Orogen (EAO) in central Dronning Maud land, East Antarctica. *In:* Pant, N.C., and Dasgupta, S., (Eds.), Crustal Evolution of India and Antarctica: The Supercontinent Connection. *Geological Society of London Special Publications,* **457:** 37-60.

Sengupta, S. (1988) History of successive deformation in relation to metamorphism-migmatitic events in the Schirmacher Hills, Queen Maud Land, East Antarctica. Jour. Geol. Soc. India, v.32, pp.295-319

Singh, R.K., 1986: Geology of Dakshin Gangotri hill range, Antarctica. *Third Indian Expedition to Antarctica Scientific Report, Department of Ocean Development, New Delhi, India*, *Technical Publication,* **3:** 181-186.

Stern, R.J., 1994: Arc assembly and continental collision in the Neoproterozoic East African Orogen: implications for the consolidation of Gondwanaland. *Annual Review of Earth and Planetary Sciences*, **22:** 319-351.

Stüwe, K., Braun, H.M., Peer, H., 1989: Geology and structure of the Larsemann Hills area, Prydz Bay, East Antarctica. *Australian Journal of Earth Sciences*, **36(2):** 219–241.

Tingey, R.J., England, R.N., Sheraton, J.W., 1981: Geological investigations in Antarctica 1973–the Southern Prince Charles Mountains. *Bureau of Mineral Resources, Record*, 43.

Wang, C.C., Jacobs, J., Elburg, M.A., Läufer, A., and Elvevold, S., 2020: Late Neoproterozoic–Cambrian magmatism in Dronning Maud Land (East Antarctica): U–Pb zircon geochronology, isotope geochemistry and implications for Gondwana assembly. *Precambrian Research*, 350.

Yoshida, M., 1995: Assembly of East Gondwanaland during the Mesoproterozoic and its Rejuvenation during the Pan-African period. *In:* Yoshida, M., and Santosh, M., (eds.) India and Antarctica during the Precambrian. *Geological Society of India, Memoir*, **34:** 25–45.

Zhao, Y., Liu, X.H., Liu, X.C., Song, B., 2003: Pan-African events in Prydz Bay, East Antarctica, and their implications for East Gondwana tectonics. *Geological Society, London, Special Publications*, **206:** 231–245.

Indian Journal of Geosciences, Volume 74, No. 3
July - September, 2020; pp. 327-331

Invited Paper

Coal Mine Fire: Monitoring Through Thermal Remote Sensing Technique

Asis Bhattacharya

Former Deputy Director, NRSC, ISRO, Hyderabad;
Former Emeritus Professor, Presidency University, DB – 31/121, Salt Lake, Kolkata – 700064.
Email: asisbh@yahoo.co.in

Abstract: Surface and sub-surface coal fire is a great concern in the coal mining districts all over the world. Around the world, many of the coal fields have severe coal mine fire problems due to the spontaneous combustion of organic matters in the coal. In India, Jharia coalfield is worst affected by coal mine fires. Whether started by human activity or natural causes, coal mine fires continue to burn coal seams for decades or even centuries until either the fuel source is exhausted or is controlled by human intervention. It is very difficult to follow the conventional ways of measuring anomalous surface temperature resulting from sub-surface coal fire, by inserting normal thermometers in the different fire affected areas, because, by the time we encounter the results, fire spreads very fast to other areas. Hence, satellite remote sensing thermal infrared technique is followed to solve such problem because the technique itself is highly dynamic due to its spectral, spatial, temporal and radiometric characteristics. TM, ETM+ and ASTER thermal IR satellite data have been used for the monitoring study.

***Keywords**:* Coal mine fire, Spontaneous combustion, Thermal remote sensing, TM, ETM+ and ASTER satellite data

Introduction

Coal mine fire is a serious concern in all the coal mining districts around the world. Spontaneous combustion of organic matters in the coal is responsible for coal mine fire problems. In the world, coal mine fires have been encountered in China, USA, Australia, South Africa and Germany. In India, Jharia coalfield is worst affected by coal mine fires. Coal fire phenomenon is so dynamic that satellite remote sensing thermal infrared survey is the most effective technique to map and monitor the coal fires because the technique itself is highly dynamic due to its spectral, spatial, temporal and radiometric characteristics.

Spontaneous combustion and coal fire

There is a complex mechanism involved in the spontaneous combustion of coal. The exact process is yet to be apprehended fully (Misra *et al*., 1996). Air (oxygen) flow rate, particle size, rank of coal, humidity, ambient temperature, pyrite content, mining practices followed, etc. are some of the important factors responsible for the spontaneous combustion of coal. The main sources of heat include heat from oxidation of coal, heat from pyrite oxidation, latent heat of water vapour, etc. (Misra *et al*., op.cit). Spontaneous combustion of coal producing fires is mainly controlled by three important factors among others such as temperature or heat, fuel like coal and oxygen meaning air. It may simply be expressed as follows (Rosema *et al*., 1999):

$$\text{Coal } (C_xH_x) + O_2 \rightarrow CO_2 + H_2O + \text{Heat}$$

Spontaneous combustion normally starts as 'hot spots' deep within the coal reserves (Chatterjee and Bhattacharya, 2010). The hot spots appear when coal absorbs oxygen from the air. As a result, the temperature of the coal gets rising above the ambient temperature. The coal temperature thus continue to climb up to a point known as temperature of ignition, which varies with the coal rank, mainly its high carbon content that is called high ranking coal or coking coal. After attaining the ignition or flash points, coal starts burning.

Coal fires around the world

Coal mine fires have been reported from the different parts of the world as follows (Bhattacharya and Reddy, 1992):

(1) Witbank coalfield in the Eastern Transvaal of South Africa (Bakker *et al*., 1978)

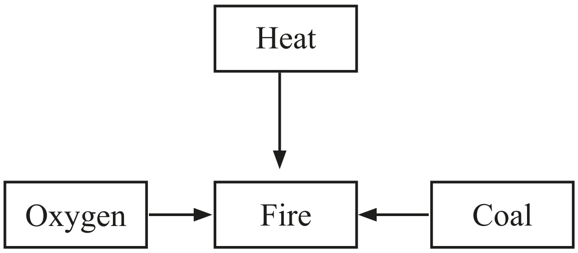

Fig.1: Shows the influence of heat, oxygen and coal for spontaneous combustion of coal, resulting coal fire

(2) Pennsylvanian coalfields of United States (Fisher and Knuth, 1968)

(3) Burning Mounting region of Australia (Ellyet and Fleming, 1974)

(4) Baskiria region in erstwhile USSR (Ming, IRS, 1987)

(5) China (Guan Hai-yan, 1984).

In India, the Late Permian (Raniganj Formation) coal seams in the Raniganj and Singrauli Coal fields and Early Permian (Barakar Formation) Coal Seams in Jharia, Bokaro, North and South Karanpura, Korba, Talchir and Ib valley Coalfields are susceptible to spontaneous combustion. Among these coalfields, Jharia coalfield is worst affected by coal mine fires, partly followed by Raniganj Coalfield.

Satellite Remote sensing Thermal IR Survey in Jharia Coal field

The Jharia Coal Field (JCF) lies about 260 km. northwest of Kolkata (erstwhile Calcutta), in the state of Jharkhand in the eastern part of India. Since 1988 up to 2011, the author was intimately associated with the coal mine fire problems of the Jharia Coal field, where he extensively used satellite thermal IR data for coal fire mapping.

Whether started by human activity or natural causes, coal mine fires continue to burn coal seams for decades or even centuries until either the fuel source is exhausted, a permanent ground water table is encountered or controlled by human intervention (Chatterjee and Bhattacharya, 2010). Coal fire cannot occur if the coal seams occur at greater depth and where no mining activity has started because in such case, no oxygen can reach at that depth and hence, no spontaneous combustion of coal can take place. So, for virgin coal, coal fire problem is not supposed to crop up.

Sharma, 1989, suggested that coal mine fires in Jharia coal field was initiated due to the following reasons:

(1) In underground mine workings, substantial quantity of coal was left in form of roof and pillars. Subsequently, these unsealed roofs had established ventilation through secondary fractures, and finally coal fires had spread like wild fire.

(2) Coal seams were exposed in abandoned open cast mine workings.

(3) Direct contact of coal seams with hot ash or heated quarry debris.

(4) In mine dumps or mine refuge, particularly when they contain sufficient quantity of carbonaceous matters.

Under the above situation where the fire spread is so fast, thermal remote sensing technique is the best way to understand and map the fire dynamics.

It is very difficult to follow the conventional ways of measuring anomalous surface temperature resulting from sub-surface coal fire (Fig. 2), by inserting normal thermometers in the different fire affected areas, because, by the time we encounter the results, fire spreads very fast to other areas. Further, it requires huge man power to cover the entire coal field following conventional methods. Hence, satellite remote sensing thermal infrared technique is followed to solve such problem because the technique itself is highly dynamic due to its spectral, spatial, temporal and radiometric characteristics.

Fig. 2: Smoke emanating from underground coal fire, Jharia

Data used

For JCF fire mapping and fire dynamic study, multi-date day and night time thermal IR data of ASTER (5 TIR spectral bands within 8.125-11.05 µm) sensor on-board Terra Satellite along with Landsat Thematic Mapper (TM) and Enhanced Thematic Mapper (ETM+) have been used and analyzed. Fig. 3 shows the night time ASTER TIR data of JCF.

In JCF, apart from using the satellite TIR data, airborne Daedalus TIR scanner data was also used for coal fire mapping during 1989-90 (Bhattacharya and Reddy, 1992).

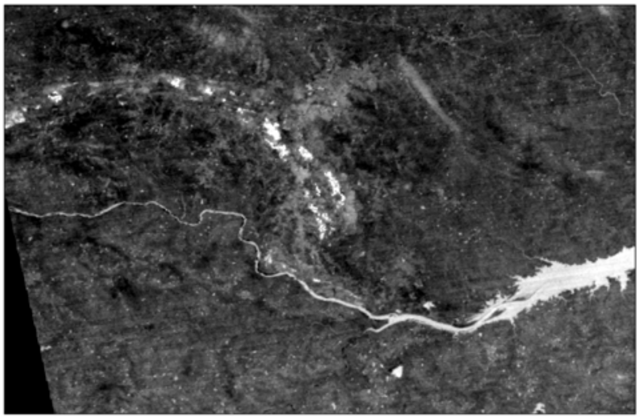

Fig. 3: ASTER night time image of JCF dt. 21.11.2007

Analysis

Geo-referenced Satellite data of the above sensors were processed, analysed and integrated with GPS data in a GIS environment for surface and underground coal fire detection and establishing the trend of fire dynamics.

It is that thermal properties of a substance which decide how the heat received from the different sources are spread as temperature in the surface layers and how the temperature varies as a function of time and depth in response to heating. In this context, two thermal properties like thermal conductivity and thermal capacity are very important. Thermal energy of a material is usually indicated by its kinetic temperature (that is internal: measured by normal thermometers) or its radiant temperature (that is external: measured by radiometers). Remote Sensors usually measure the quantity of radiant temperature.

On the ground, coal fire temperatures were measured by hand held digital infra-red thermometer (Fig. 4) and they are correlated with the DN values also.

Finally, coal fire temperatures have been calculated using DN values from ASTER, TM and ETM$^+$ TIR data. DN values were converted to surface temperature, following three steps (Chatterjee and Bhattacharya, 2010) as below.

Step-1: Converting the radiance values (DN) to spectral radiance.

Step-2: Converting the spectral radiance to radiant temperature.

Step-3: Converting the radiant temperature to surface temperature.

Result

After deriving the surface temperature, coal fire map is generated (Fig. 5). Time series data analysis produced the fire dynamics map (Fig. 6). In Fig. 3, brighter signatures are warmer, of which some are coal fires, which is known after DN conversion to temperature as mentioned above.

Fire depth is also calculated considering the temperature profile. Coal seams at the surface under fire are traced to the depth, considering the dip of underlying coal seams. On the surface, fires are coming from depth through the process of convection along some fractures (Fig. 7a-c).

Fig. 4: Digital Infra-red Thermometer

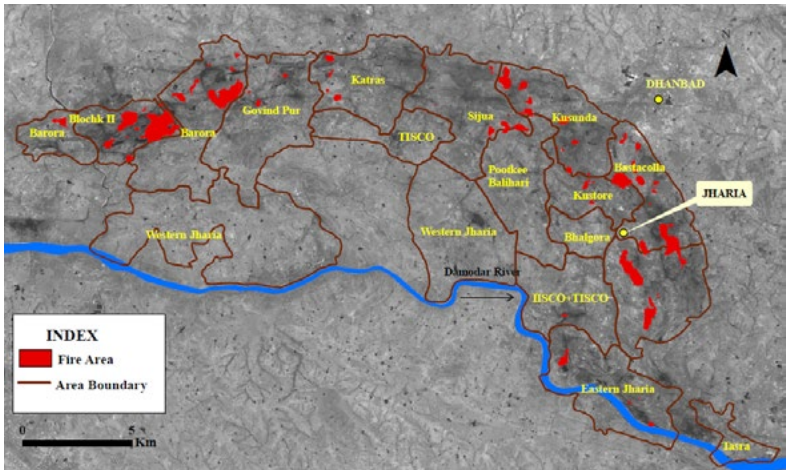

Fig. 5: Coal Mine fire map of Jharia coal field, Jharkhand using ETM TIR day time data (24.01.2003) superimposed on ASTER IR image

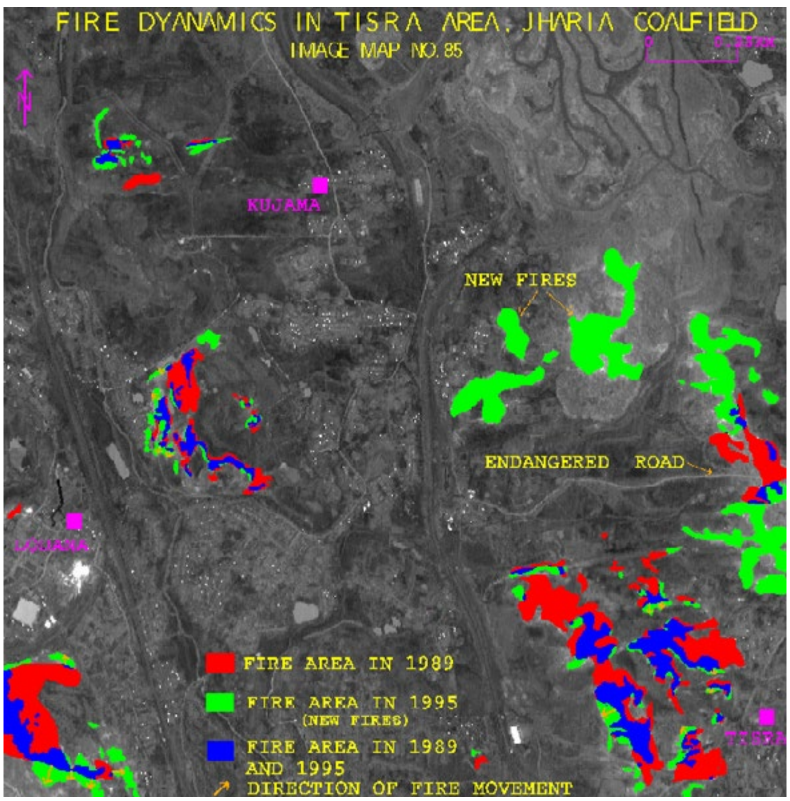

Fig. 6: Coal Fire dynamics map using Daedalus airborne TIR scanner data, Jharia, Jharkhand.

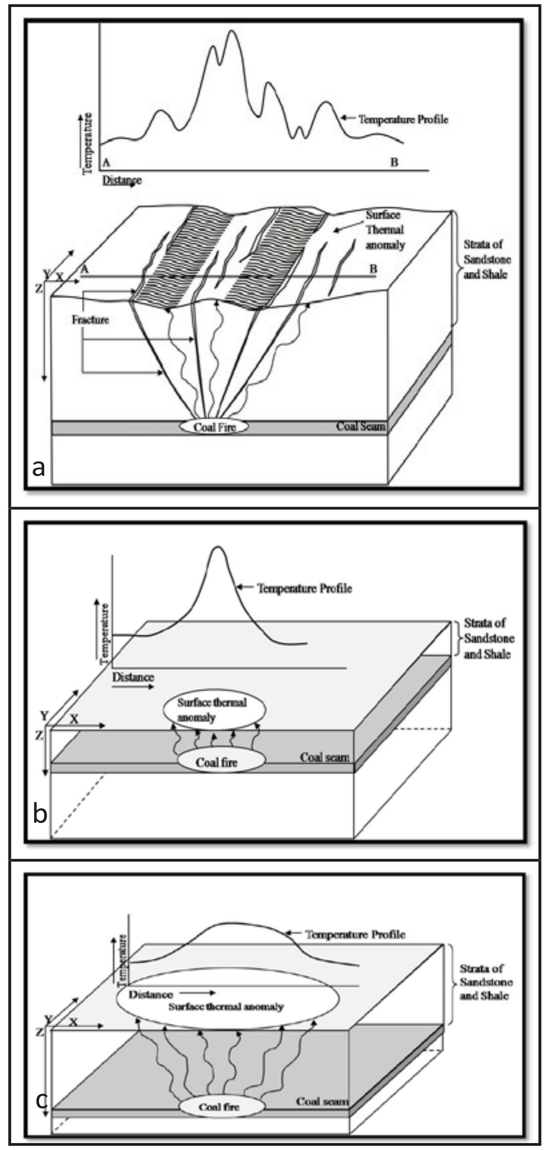

Fig. 7: (a) Schematic diagram showing Temperature profile generated from the surface thermal anomalies due to underground coal fires and fractures on the overlying strata mainly through the process of convection and also some conduction, (b) Schematic diagram showing temperature profile (in sharp peak) generated from the Surface thermal anomalies due to shallow depth underground coal fires and (c) Schematic diagram showing temperature profile (broad peak) generated from the Surface thermal anomalies due to deep underground coal fires

Conclusion

Finally, it may be concluded that the TIR data is very useful to mitigate the coal fire disaster after preparing coal mine fire map and knowing the fire dynamics. Though coal fire is a natural disaster due to spontaneous combustion, but it is largely aggravated by human inactions, particularly in Jharia Coal Field.

Acknowledgement

The author is grateful to Dr C.S.S. Reddy, Shri Manoj Dangwal, Dr A. Chatterjee, Dr Amitava Mukherjee and Shri Tanmoy Pramanik for providing their valuable technical inputs.

References

Bakker, P., Church, D.J., Feuchtwanger, T. F., Grooterboer, J., Lee, C.A., Longshaw, T. G. and Viljoen, R. P., 1978: Some practical applications of Thermal Infrared Line Scanning. *Mining Mag,* October, 398-413.

Bhattacharya, A. and Reddy, S., 1994: Underground and surface coal mine fire detection in India's Jharia Coalfield using airborne thermal IR data. *Asian-Pacific Remote Sensing Journal*, **7**: 59-63.

Chatterjee, Alokesh and Bhattacharya, Asis, 2010: Inventory and Monitoring of Underground and Surface Coal Mine Fire for modeling Fire dynamics and rate of fire movement, Jharia Coal Field, Jharkhand, using satellite Thermal Remote Sensing data. *Dept. of Geology, Presidency Univ., Kolkata - 700073. Unpulished Project Report, Project* Code No.CIL/R&D/1/23/06.

Ellyett, C.D. and Fleming, A.W., 1974: Thermal infrared imagery of the Burning Mountain Coal Fire. *Remote Sensing of Environment,* **3(1)**: 79-86.

Fisher, W. Jr. and Knuth, W. M., 1968: Detection and delineation of subsurface coal fires by aerial infrared scanning. *Abstracts for 1967, Geological Society of America Special Paper,* **115**: 67-68.

Guan Hai-yan, 1984: The research of coal bed thermal IR radiation. *Proceeding of Seminar on RS for Geological application, Beijing.*

Ming, IRS, 1987: Engineering and services in carrying out thermal infrared air survey, ground thermometry of Mukunda Open Cast Project (OCP), Jharkhand, India, with a view to Localize fire zones in coal seams. *Technical report on contract No. 05-022/02208, Leningrad, USSR.*

Misra, B. K., Singh, B. D. and Anand Prakash, 1996: Biopetrographic approach to the spontaneous combustion susceptibility of Indian Gondwana Coals: with reference to some coals of Raniganj and Singrauli coalfields, in Gondwana nine: *Ninth International Gondwana Symposium, Geological Survey of India,* 2: 1257-1264.

Rosema, A., Van Genderen, J.L. Veld, H., Vekerdy, Z., Ten Katen, A. M., Prakash, A., and Sharif, M., 1999: Manual of Coal fire detection and monitoring: report of the project: Development and implementation of a coal fire monitoring and Fighting system in China. *The Netherlands Institute of Applied Geoscience*, 99-221-C.

Sharma, S.D., 1989: Integrated fire control plan of Jharia coalfield, Jharkhand, India. *Minetech*, **10(2)**: 7-32.

Indian Journal of Geosciences, Volume 74, No. 3
July - September, 2020; pp. 332-344

Invited Paper

Efficient Burning Area Identification Using Image Classification and Optimization Techniques

T. Ashwin Kumar[1*] and K. Mruthyunjaya Reddy[2]

[1]*IIC Technologies Limited, 8-2-350/5/B-22, Banjara Hills, Hyderabad - 500034, Telangana, India*
[2]*FIDG & Rural Development and Watershed Monitoring Division, NRSC, Hyderabad - 500037*
[*]*Corresponding author's email: ashwinkumar.thumma@iictechnologies.com.*

Abstract: Recently, forest fires have drawn utmost attention throughout the globe. The detection of such forest fires at an early stage can create precise alerts that may pave the way for preventing widespread loss of lives and resources. This thesis has contributed three approaches for spotting forest fires from the satellite images. In the first work, a technique was planned and constructed for identifying burning area utilizing image segmentation and IHS (I (Intensity), H (Hue), S (Saturation)) transformation. The steps executed in this work are i) IHS transformation, ii) object segmentation, iii) smoke area identification utilizing FFNN (Feed-Forward Neural Network) and iv) burning areas identification as of the smoke segments. The satellite images are transmuted to IHS images. This is followed by object segmentation utilizing K-means clustering algorithm. These segmented objects are then fed to FFNN. This step is done for the smoke area identification. In the secondary approach, the image from the database is preprocessed. This step is done utilizing the Histogram equalization and decorrelation stretching. Then, clustering is done using FCM. A finite count of features is extorted. Then those features are classified utilizing the ANFIS classifier. Moreover, the two categories of classification are non-fire and fire areas. This categorization facilitates easier recognition of the fired area in the satellite image. In the third work, a proficient method was introduced for detecting forest fire utilizing optimized ANFIS classification. This method was executed using the subsequent steps. Preprocessing was done using the median filter (MF) and linear contrast stretching (LCS) process. The modified-FCM is then implemented to the preprocessed image. A set of features were extorted from the clustered image. These features were optimized using the CSO algorithm (Cuckoo Search Optimization). The optimized features were supplied to the ANFIS classifier. This classifier provides two classes of images, namely non-fire and fire images. Grounded on this categorization, the area with forest fire could be easily identified.

Keywords: Burning Area, Segmentation, K-means, FFNN, ANFIS, Histogram equalization, Decorrelation stretching, Clustering, Features extraction, Classification.

Introduction

A natural tragedy called "forest fire" damages the forest area which could turn out to be a great peril to wildlife and individuals who have their livelihood in forests. Such fires are usually started via lightning or through human arson or negligence. Forest fires, also termed as a Grassfire, wildfires, vegetation fire, are most recurrent on the vegetated locale of South Africa, Canada, Australia in addition to the United States in which climates are amply moist to permit trees growth, however, have extensive dry as well as hot times. Fire is a result of chemical reaction termed oxidation, i.e., the combination of oxygen and material like woods or leaves. Fire is quick and aggressive amid oxidation which releases water, heat, light and smoke into the air and leaves ashes on the ground.

Remote Sensing (RS) is a versatile tool for probing the Earth. It encompasses the application of instruments/ sensors to 'capture' the spatial along with spectral relations of materials and objects in a perceptible distance. Satellite and Aerial images (Mohamad Awad, 2010, Mahi *et al.*, 2014), termed as tenuously sensed images, let precise mapping of land-cover and make landscape traits comprehensible on continental, regional, and also universal scales. It is extensively utilized for observing the earth surface and the alterations on land-cover and land-use (Tansey *et al.*, 2009). It is also employed to produce of mapping products for i) civil and military applications, ii) assessment of environmental damage, iii) perceiving land use, iv) monitoring radiation, v) urban planning, vi) forest monitoring, vii) crop yield appraisal, viii) growth regulation and ix) soil assessment (James and Daniel, 2002).

Forest fires are drawing utmost attention on account of their remarkable effect on wildlife, humans, the environment, climate, ecosystem, and weather. Precise monitoring along with mapping of the ST dissemination of forest fires is imperative since it leads to fire effect estimation and also control, as well as to a count of ongoing studies on alterations on land usage, climate, land cover, et cetera. (Wang *et al.*, 2012).

Chief causes are unpredictable changes in climate, lingering dry season, lower winter rainfall, etc. but these conservative fire extinguishing schemes are inadequate to take relevant action amid fire and saving a life. The traditional manual scheme doesn't assure 24/7 monitoring as of fire protection. Forest fire completely devastates the abundant Forest and disturbs the 'plants and animals' balance state, ecology, biodiversity, and environment. These gigantic flames could spread and alter the course rapidly as of its source (Ganesan *et al.*, 2016).

Different methods are utilized for recognizing forest fire. Albeit, the existing methodologies identified the forest fire beforehand, but some algorithms found it difficult to identify forest fires due to the oversampling problem, generates delayed responses when applied to large scale images, low classification accuracy. This creates a need for an efficient means of FFD. This is taken as the motivation for this research. The detecting forest fires in advance can lessen the adversarial effects on the ecosystem. This work copes with an effective technique of FFD utilizing satellite images.

Several methodologies were recommended for the technique termed 'Burning Area Identification' (BAI). The motivation for examining the forest fires early detection & prevention systems is to increase the accuracy. The chief objectives are presented in the statements given below.

- To design and construct a strategy for BAI utilizing IHS transformation and also image segmentation methods.
- To attain an efficient classification and recognition of fires in satellite images for the successful identification of the burning region.
- To augment the performance of burning area identification, effective classification of the forest fire along with fire territory identification in satellite images is proposed using optimized ANFIS classifier.

The above efforts were taken to apply a runtime digital system with minimized power consumption, elevated throughput, diminished chip area, and lowered time.

Study Area and Dataset Description

Three study places like Sierra National Forest (California, USA), Salmon-Challis National Forest (Idaho, USA) and Nallamala Forest (Srisailam, Andhra Pradesh, India) are considered for the current research work. The US datasets which are acquired from NASA's AQUA Satellite, MODIS (Moderate Resolution Imaging Spectroradiometer) Sensor and having a resolution of 250m are established from NASA website that covers only smoking centered burning conditions. The Indian datasets which are acquired from IRS P6 Satellite (RESOURCESAT-1), AWiFS Sensor and having a resolution of 56m are procured from NRSC, Balanagar, Hyderabad. The uses of such disparate study sites enhance the competency to extrapolate and generalize our findings. The downloaded satellite image obtained would have multispectral (R, G, B, NIR) bands and those images transmuted to TIFF format. This is done utilizing Multispec32, a freeware multi-spectral image data analysis scheme.

Methodology

Three approaches were followed for spotting forest fires from the satellite images.

(A) Technique for Burning Area Identification Using IHS Transformation and Image Segmentation

In the first approach, a technique is built for BAI utilizing 'Intensity, Hue, Saturation' (IHS) transformation together with IS. Here, NASA's satellite images are utilized for the experiential study of this proposed research. The images attained as of the NASA is sent for IHS transformation which transmutes the RGB [red, green and blue] image into IHS image. After the image transformation, object segmentation is performed centered on 'K-means clustering' algorithm. Consequently, FFNN is utilized for Smoke Area Identification as of the segments. After detecting the smoke area, the BAI is done via directional examination.

The process of proposed BAI technique encompasses four steps like a) IHS transformation, b) object segmentation, c) detection of Smoke Area utilizing FFNN d) finding BAs from the smoke segments using directional examination (Ashwin and Kamireddy, 2015). The diagram for the proposed BAI technique is delineated in Fig. 1.

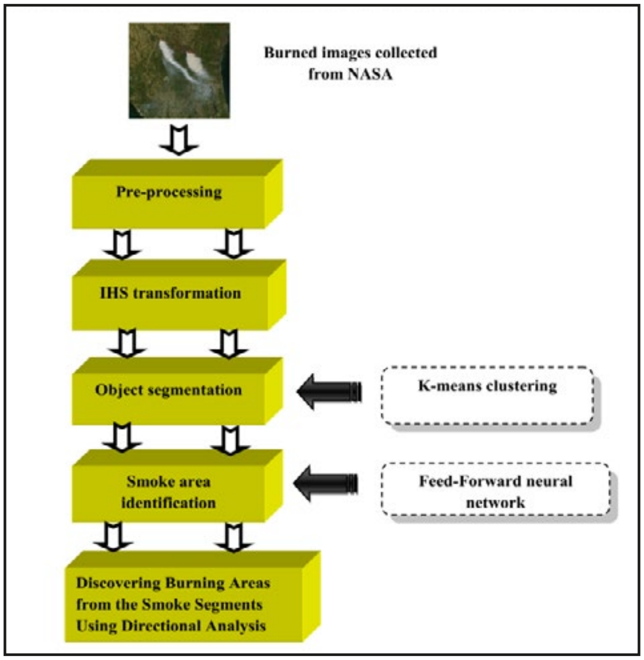

Fig. 1: Overall Block diagram of Burning Area Identification (BAI) process.

Pre-Processing

The inputted burning image is primarily transmuted to RGB. Then, the resulted RGB image is transmuted to LAB color space. Afterward, by contrasts fine-tune the L layer in lab image utilizing imadjust operation and lastly, transform it back to the RGB.

IHS Transformation

Intensity: Intensity signifies the color brightness. It differs as of black (= 0) to white (=255 in an 8bit scheme). Hue: Hue signifies the dominant light wavelength contributing to the color. It differs as of 0 - 255 equivalent to a different gamut of 'red, blue and green.' Saturation: Saturation signifies color purity. A value 0 means entirely impure color with all wavelengths evenly shown in it (gray tones). The maximal value (255 in an 8bit scheme) means the wholly pure color (red, blue or green).

Object Segmentation

Object segmentation is carried out using K-means Clustering algorithm. It is simpler and faster. It Splits burned image datasets to "K" groups/ clusters. It groups similar data objects in one cluster and different data objects in separate cluster. K-means classification groups all pixels to specified classes. Every class is a cluster of pixels. It groups appropriate clusters into 1 single group. From the groups, smoke areas are recognized.

Smoke Area Identification

Feed forward Neural Network (FFNN) is considered for identifying smoke areas. In FFNN, data goes through input layer, travels via Network (hidden layer) and gets the output. Here, there is no Feed-Back between the layers hence it is termed as Feed-Forward Neural Network. FFNN decides the number of neurons to be in input & output layer, number of hidden layers and the number of neurons in each hidden layer. FFNN process flow include Detecting Smoke areas from Segmented Regions by computing the required features (Mean, Entropy). Feature Matrix is developed and the matrix contains Input & Output parameters which are chosen for Training & Testing purpose, which is displayed in Fig. 2. Output Target Smoke Region=2, Other Region=1

Discovering Burning Areas using Directional Analysis

After combining all the smoke segments using segmentation, Morphological Dilation process is implemented for identifying Red Zone. For this, smoke segments are converted into Binary image for applying Dilation process and smoke areas are dilated. Smoke segments are converted to IHS color space and from "H" layer, Red region is identified. The chief target of this section is to recognize the red region (i.e., Burning area) from the smoke segments as provided in Fig. 3.

(B) Efficient Forest Fire Image Classification and Fire Area Detection

In the second approach, the proposed 'forest fire area identification' method is done in subsequent stages. Primarily, the satellite forest fire images are fetched from the database for pre-processing (Ashwin *et al.*, 2018a). Next, the Modified FCM is employed in preprocessed images for the clustering. Then from the clustered images, features like a) Local tetra pattern (LTrP), b) Contrast, cluster shade, c) cluster prominence, d) Area, e) Standard deviation along with f) Color feature is extorted. Finally, the extorted features are inputted to the optimized ANFIS classifier for classifying the images as Non-fire or fire, and then the fire area is recognized in the images. The proposed strategies block diagram is exhibited in Fig. 4.

Preprocessing

The input images are preprocessed using Histogram Equalization (HE) and De-correlation Stretching (DS) to upgrade the images. HE is used to enhance image contrast and acquires uniform spreads of Histogram. Each gray scale value has a measure to number of pixels. DS is used for image improvement. It improves color difference found in each pixel of an image. It lessens Spatial Redundancy because of strong Correlation among neighboring pixels.

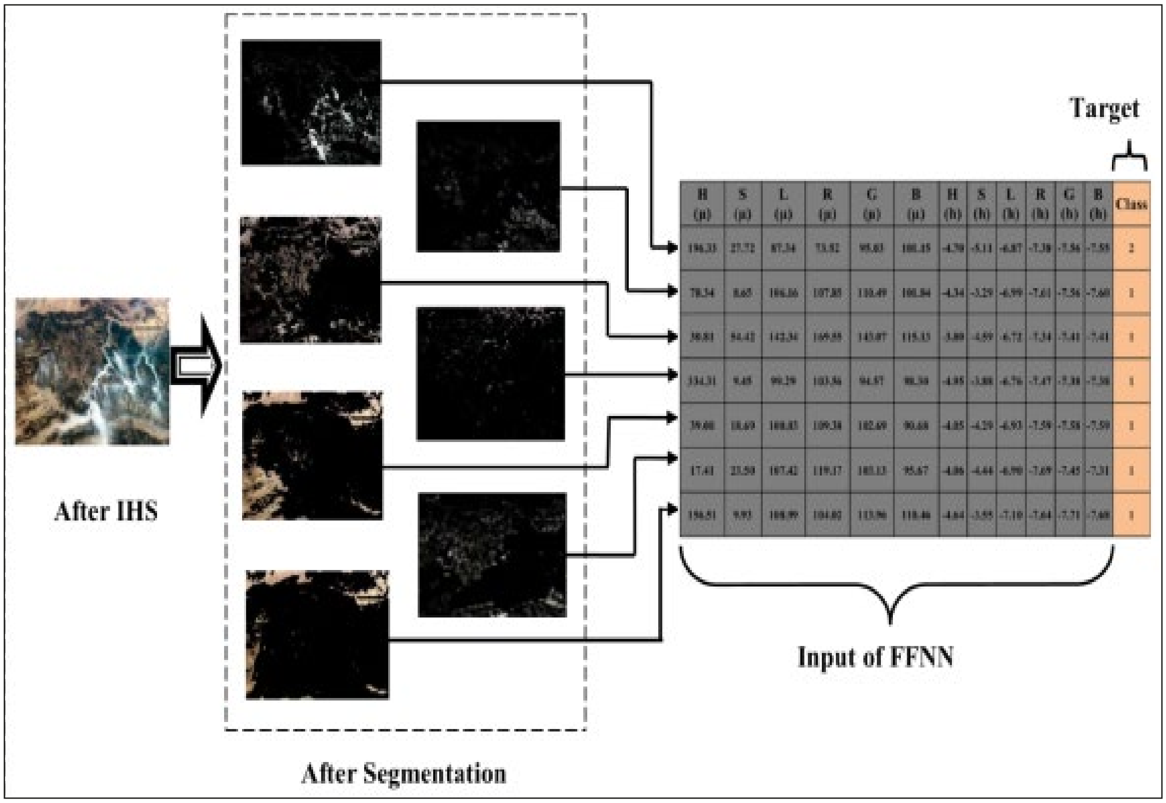

Fig. 2: Input and Target output of FFNN.

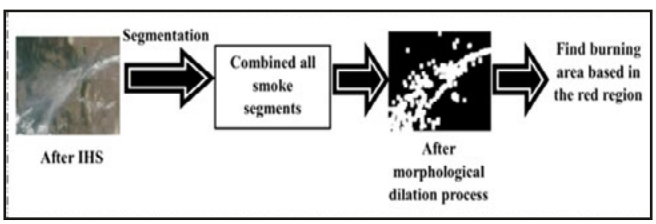

Fig. 3: Discovering burning areas using Directional Analysis.

Clustering

Fuzzy C-Means (FCM) executes clustering by iteratively discovering a set of fuzzy clusters and the related cluster centers that signify the structure of the data. This algorithm is contingent on the user to state the count of clusters existent in the set of data to be clustered. It stands as a powerful unsupervised technique for the analysis of data. Most of the time, it is incredibly natural on comparing to hard clustering. Initially, Dunn presented the FCM, afterward was advanced by Bezdek. FCM is valuable when the needed quantities of clusters are pre-determined; consequently, the algorithm endeavors to put every data points to the clusters. What makes FCM distinctive is that it doesn't choose the absolute membership of a data point to a specified cluster; instead, it figures the membership (likelihood) degree where it would encompass a place with that cluster. Here, the preprocessed image experiences M-FCM for the efficient clustering.

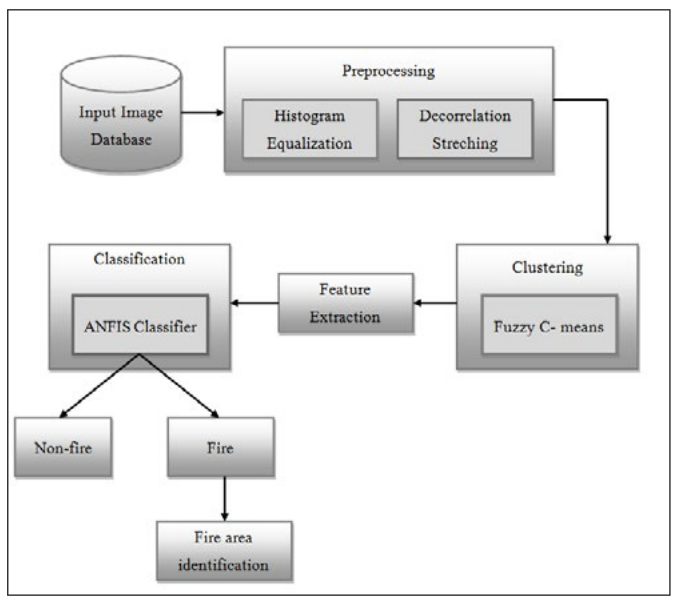

Fig. 4: Block diagram of the proposed method.

Feature Extraction

The effective features like cluster prominence, LTrP, cluster shade, Contrast, Area, Standard deviation, and Color feature, are extracted from the images after FCM clustering.

Classification

Fire image classification is implemented using Adaptive-Neuro Fuzzy Inference System (ANFIS) Classifier. It is an adaptive network that uses supervised learning on learning algorithm. It is a FUZZY Model which encourages learning & adaptation. It is used for productive image examination, classification and analysis. The features like i) LTrP feature, ii) Contrast, iii) Cluster shade, iv) Cluster prominence, v) Area, vi) Standard deviation and vii) Color feature are extracted from FCM clustered images and are classified using ANFIS classifier. There are 5 layers of ANFIS classifier. Layer 1: Square Node, Layer 2: Fixed/ Non-Adaptive, Layer 3: Fixed/ Non-Adaptive, Layer 4: Square Node and Layer 5: Fixed/ Non-Adaptive (Circle Node).

All the features which are extracted are classified using ANFIS. Using ANFIS, a pre-defined threshold value "ω" is set. If output of Neural Network is greater than "ω", it is classified as FIRE, else NO-FIRE.

Fire Area Identification

The ANFIS classifier classifies the processed input images into non-fire and fire images. At that point, the fire region is recognized from the classified fire images. If the red (R) band value is equal to 255 besides blue (B) band or green (G) band is equal to 0; it ought to be red area; otherwise, it is a non-red locale.

(C) Proficient Forest Fire Identification Using Optimized ANFIS Classification

In the third approach, the forest fire is precisely classified, and even the fire territory is identified in satellite images by utilizing MFCM and also enhanced ANFIS classifier. The proposed technique is processed in succeeding stages as; primarily, the satellite forest fire images are taken from the database is subjected to the pre-processing. The preprocessing incorporates MF along with LCS procedure for upgrading the images. Next, the MFCM is connected in preprocessed images for the clustering. Here, from the resulting clustered images, features namely, LGXP, Color Features, entropy feature, Homogeneity feature, ASM features are extorted. The extracted features are optimized by employing CS algorithm, and then those optimized features are inputted into the ANFIS classifier for classifying images into Non-fire or fire. Lastly, the fire zone is accurately recognized from the classified fire images. The proposed technique's block diagram is exhibited in Fig. 5.

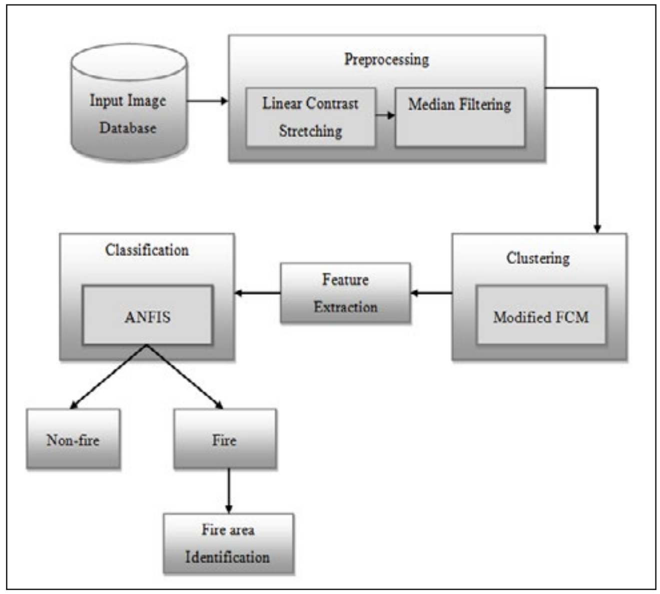

Fig. 5: Block diagram of the proposed method.

Preprocessing

The input images are preprocessed using Median Filtering (MF) and Linear Contrast Stretching (LCS) to upgrade the images. MF is used to remove Salt and Pepper Noises (SPN) to improve results. It operates over the window by selecting Median Intensity. SPN would have dark pixel in bright zone and bright pixel in dark zone. LCS improves the image by stretching the range of intensity values. Contrast Stretching comprises of two types. Global Contrast Stretching (GCS) and Linear Contrast Stretching (LCS). GCS enhances image with Luminance information. LCS upgrades Noise filtered images.

Clustering

The preprocessed image is now free from the noise. Then, the noise removed image is further clustered utilizing Modified Fuzzy C-Means Clustering (MFCM). Based on this clustering technique, the property of the images that resemble the same belongs to one cluster, while the images with different properties belong to different clusters. FCM is regarded as a robust un-supervised methodology for examining data and constructing models. In several scenarios, fuzzy clustering is utmost natural on considering hard clustering (Ashwin *et al.*, 2018b). Objects on the boundaries betwixt numerous classes are not forced to wholly fit into one of the classes, but instead, are allotted membership degrees betwixt 0 & 1 denoting their partial membership. FCM is an extensively utilized algorithm. In 1974, FCM was initially reported in the literature for a particular scenario (m=2). In 1973, the general situation (for any m >1) was proffered by Jim Bezdek in his Ph.D. at Cornell University. In 1981, it was augmented by Bezdek.

Feature Extraction

The clustered data images may contain much irrelevant and redundant information. Feature extraction paves the way for reducing the number of resources needed for processing without losing essential or relevant information. Feature extraction can also reduce the amount of redundant data for a given analysis. The effective features like i) contrast, ii) sum average, iii) variance, iv) sum variance, v) Information measures of correlation I, vi) correlation, vii) difference variance, viii) difference entropy, ix) sum entropy, x) Information measures of correlation II are extracted.

Cuckoo Search (CS) Optimization Algorithm

The extracted features are then optimized utilizing the Cuckoo Search (CS) algorithm to reduce the complexity of a model and makes it easier to interpret. It improves the accuracy of a model based on the selected subset and enables the machine learning algorithm to train faster. It is a Heuristic Search Algorithm. It is kindled by the Cuckoos' reproduction strategy. It upgrades the reliability and robustness. Extracted features are optimized using Cuckoo Search Algorithm. Optimized features are most effective, non-redundant & most relevant for fire image classification and is given as input to ANFIS Classifier.

Classification

The optimized feature set is provided as the input to the ANFIS. The optimized ANFIS primary target is like other fuzzy models, i.e., building a fuzzy model with higher interpretability and accuracy. The ANFIS stands as a fuzzy model placed in the adaptive framework's structure to encourage learning and also adaptation. Such structure composes the ANFIS to be more systematic besides less-contingent on professional knowledge. The ANFIS features on the data set modify the framework parameters as indicated by an error criterion. ANFIS classifier's Effective implementation is meant for productive image examination and classification.

The ANFIS contains five layers. In the five layers, the layer-1 and layer-4 has adaptive nodes whereas 2nd, 3rd and fifth layers holds fixed nodes. Utilizing the ANFIS, the images are sorted as fire & non-fire.

Fire Area Identification

In the former section, ANFIS classifier classifies the provided images into non-fire and fire images. In this section, using the red band value, the fire area and the fire territory identified correctly from the classified fire images. If the red band value is equivalent to 255 and blue band or green band is equal to 0, it ought to be red area otherwise it is non-red region.

Results and discussion

The proposed methodology is executed in a windows machine with configurations 3.20 GHz Intel (R) Core i5 processor, 4 GB RAM and the OS platform, which is Microsoft Window 7 Professional. The downloaded satellite image obtained would have multispectral (R, G, B, NIR) bands and those images transmuted to TIFF format. This is done utilizing Multispec32, a freeware multi-spectral image data analysis scheme.

(D) Implementation of Burning Area Identification using IHS Transformation and Image Segmentation

The proposed approach introduced a technique for BAI utilizing IHS transformation along with IS. Here, the experiments are done utilizing the satellite images taken as of the forest fire image database. The proposed structure is contrasted to the prevailing clustering techniques and classification methodologies centered on the performance metrics. By performing sensitivity, accuracy, and also specificity, the proposed hotspot fire detection's performance is examined. This proposed approach is designed for BAI in burnt satellite images. The attained experimental results are delineated from Fig. 6 to Fig. 12.

Performance Evaluation

Here, the performance assessment and comparative analysis of proposed and prevailing techniques are delineated. Here,

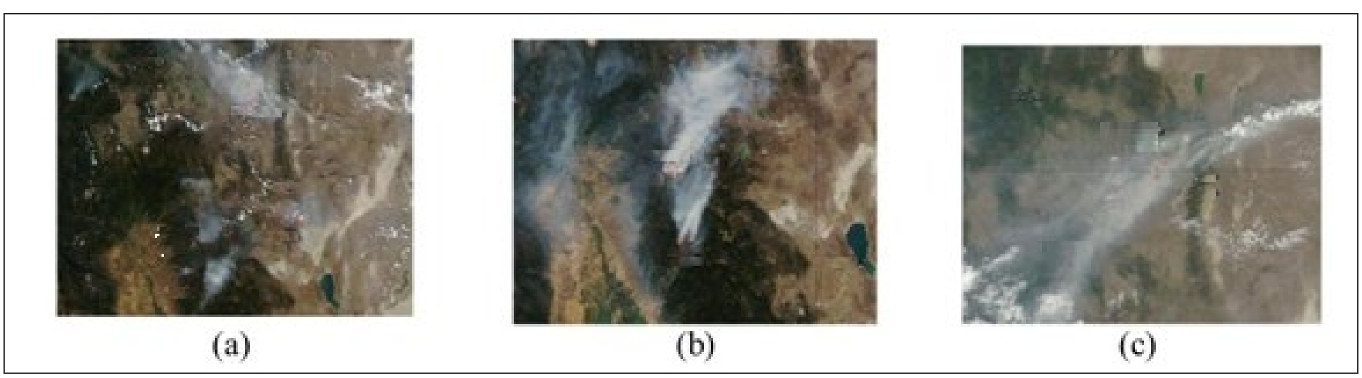

Fig. 6: Sample dataset images of the proposed technique.

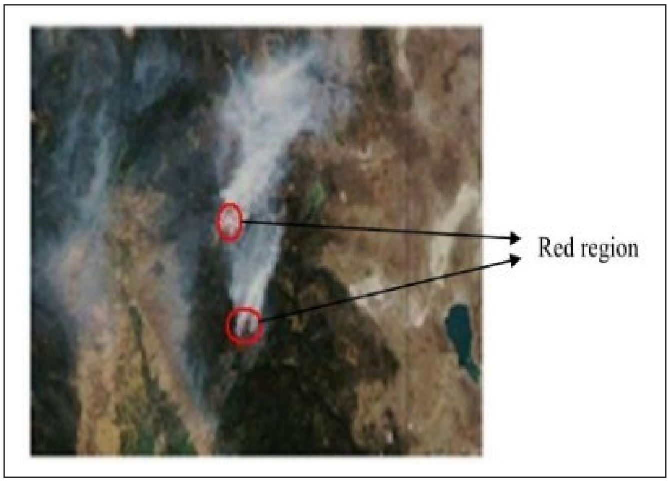

Fig. 7: Burnt image of NASA.

Fig. 8: Post IHS.

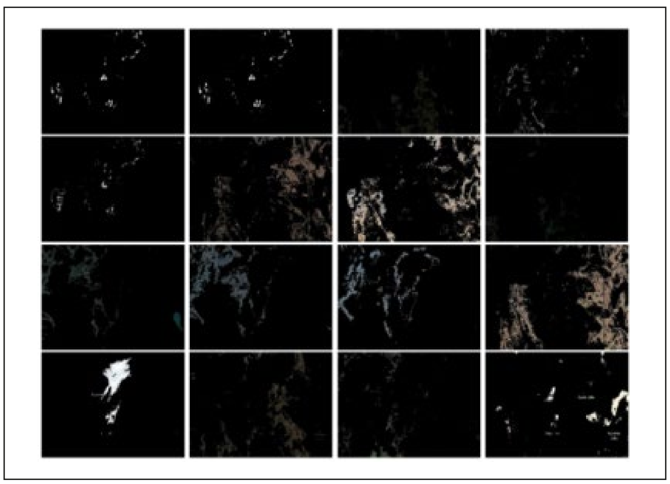

Fig. 9: Post segmentation using K-means.

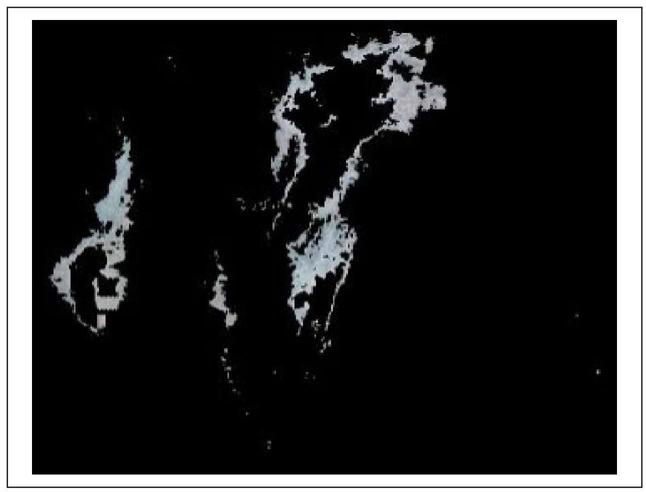

Fig. 10: Combined all smoke regions.

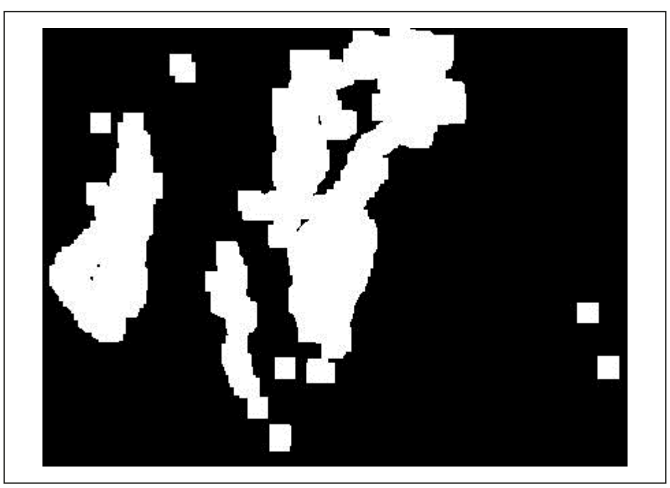

Fig. 11: Post Morphological dilation process.

Fig. 12: Red region identified (represented in yellow shade).

the proposed approach is contrasted with the 'Bayesian classifier' (BC) aimed at BAI. The experimental results were evaluated based on the metrics like Precision, Recall, Sensitivity, Specificity, Accuracy, FNR, FDR, MCC, Dice, Correlation, FAR and FRR. The metrics evaluated for object segmentation is based on precision, recall, FNR, FDR, MCC, Dice, Correlation, FAR and FRR is depicted in Table 1, and the graphs are delineated in Fig. 13 and Fig. 14. The evaluation metrics for smoke area identification is based on specificity, sensitivity and accuracy, which is depicted in Fig. 15, Fig. 16 and Fig. 17.

The Sensitivity, specificity and accuracy values are measured to prove better identification of smoke area using FFNN approach.

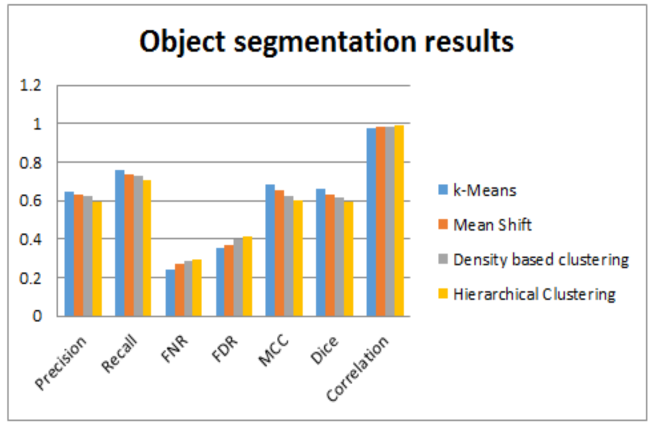

Fig. 13: Object segmentation results obtained for Precision, Recall, FNR, FDR, MCC, Dice & Correlation measures.

Table 1: Values obtained during object segmentation for performance metrics

Measures	K-Means	Mean Shift	Density based clustering	Hierarchical Clustering
Precision	0.645	0.631	0.621	0.59
Recall	0.759	0.739	0.728	0.705
FNR	0.241	0.268	0.286	0.294
FDR	0.355	0.369	0.395	0.417
MCC	0.681	0.652	0.623	0.601
Dice	0.662	0.631	0.615	0.596
Correlation	0.975	0.981	0.986	0.991
FAR	57	58.6	59	58.4
FRR	49	56	52	60

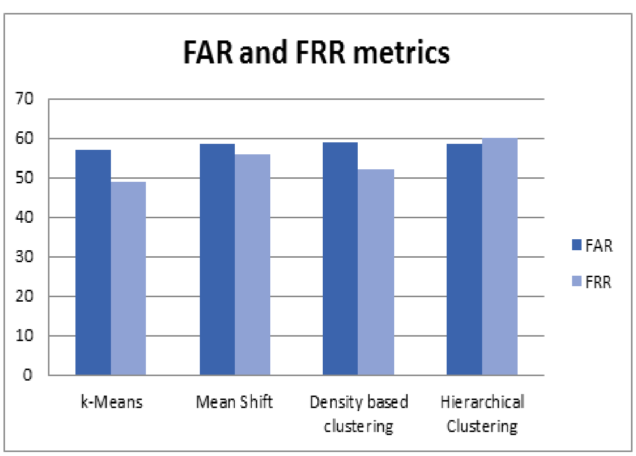

Fig. 14: Object segmentation results obtained for FAR & FRR measures.

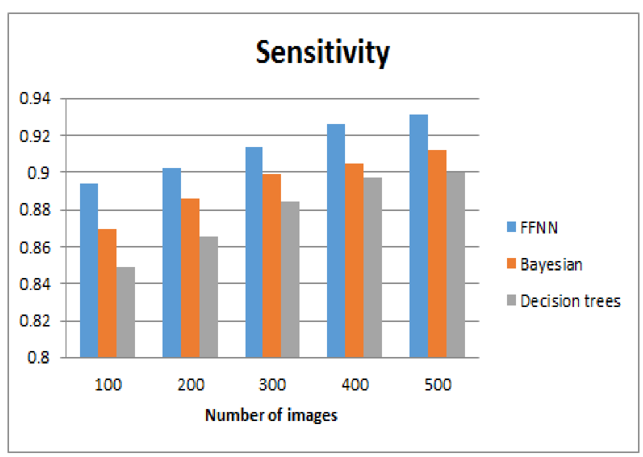

Fig. 15: Sensitivity values obtained for smoke area identification.

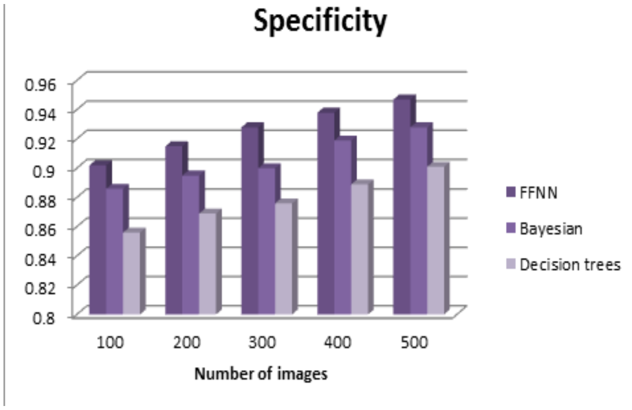

Fig. 16: Specificity values obtained for smoke area identification.

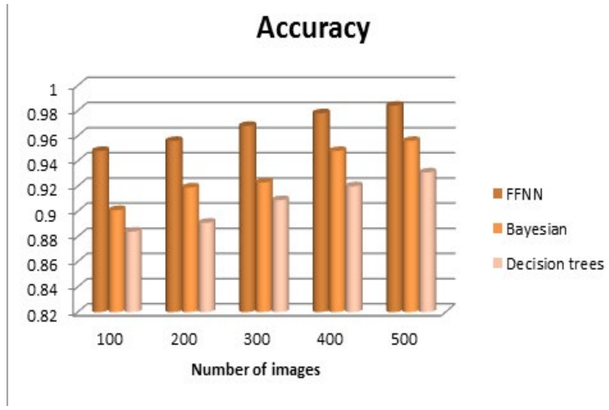

Fig. 17: Accuracy values obtained for smoke area identification.

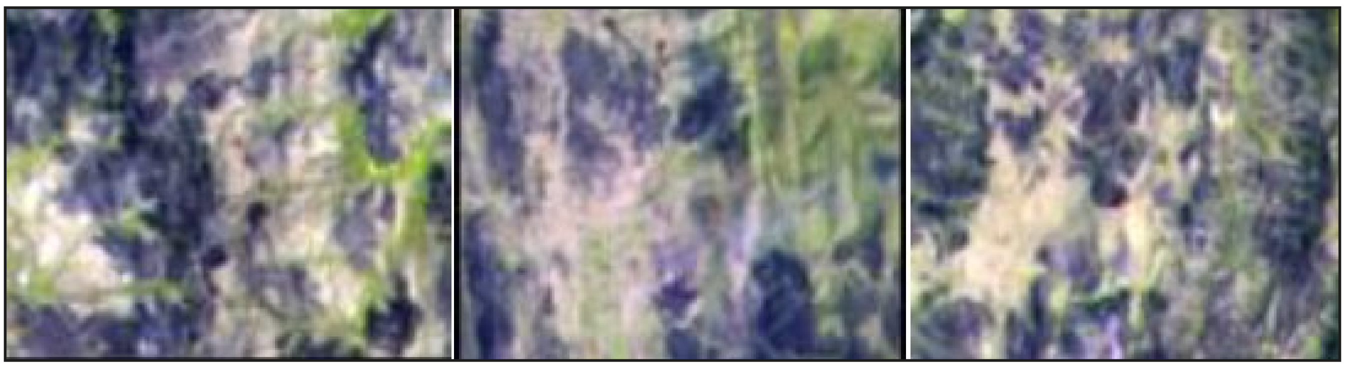

Fig. 18: Sample input images.

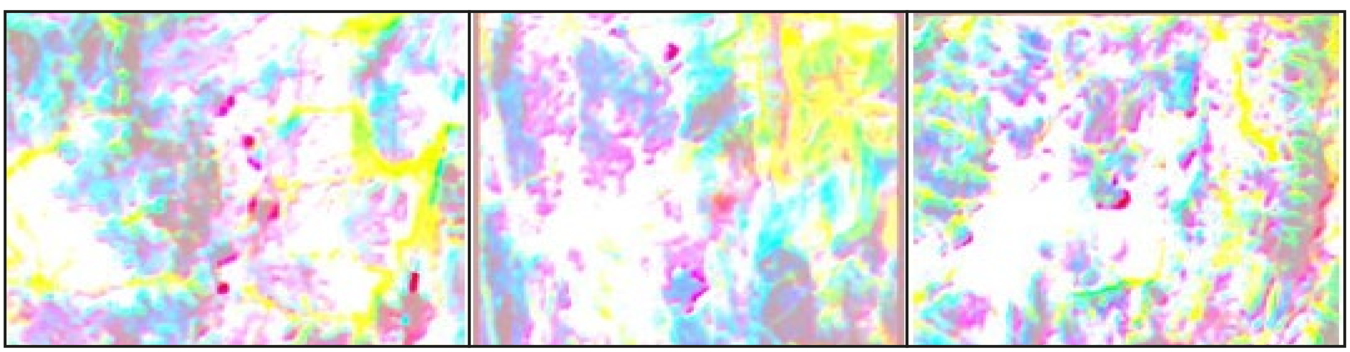

Fig. 19: Preprocessed images.

Fig. 20: Fire detected images.

(E) Implementation of Forest Fire Image classification and Fire Area Detection

In the proposed system, initially, the satellite images fetched from the database undergoes preprocessing to eliminate the noise. The pre-processing encompasses smoothening and sharpening process to enhance the very fine and minute details and also to eradicate the redundant information. Then the satellite image in RGB is transmuted to LAB-CS. This is a perceptually uniform. The independent CS is utmost effectual for color segmentation and machine vision on contrasting with any other CS. Then the resulting image is segmented utilizing modified 'watershed segmentation algorithm.' From the segmented image, features like texture feature using LTrPs, color feature utilizing HE, Intensity feature (standard deviation), shape feature (area), wavelet feature (orthogonal) are extorted. Finally, those features are given as input to the classifier. The 'krill-herd optimization algorithm' utilized ANFIS classifier is deployed for the classification. The proposed fire image classification and fire territory detection are executed in the working platform of MATLAB.

The experiments are done utilizing the satellite images taken from the forest fire image database and are delineated from Fig. 18 to Fig. 20. The proposed structure is contrasted to that of the prevailing clustering techniques and classification methodologies centered on the performance metrics.

Performance Analysis

The detail explanation of the implementation result and its performance are analyzed. By performing sensitivity, accuracy, and also specificity, the proposed hotspot detection's performance is examined. Error rate regarding TP (true positive), FP (false positive), FN (false negative), TN (true negative) are computed.

Comparative Analysis

The Comparative analysis incorporates the correlation of the proposed MFCM clustering strategy with the prevailing strategies. Also, it includes the correlation of the proposed ANFIS classifier with the prevailing classifiers.

a. Clustering

The performance metrics, for example, precision, accuracy, recall, specificity, FDR, FNR, FPR (False Positive Rate), MCC, Dice, and Correlation are utilized for the contrast of the proposed MFCM with the prevailing strategies, for example, k-Means, FCM and also Mean Shift.

b. Classification

The proposed ANFIS classifier is contrasted with NB, SVM and NN.

Table 2: Performance metrics evaluation with proposed MFCM, existing FCM, Mean shift and K-means.

Measures	FCM	Mean Shift	k-Means	Proposed MFCM
Precision	0.654982	0.619835	0.644719	0.6651
Recall	0.736402	0.346304	0.759207	0.77592
Accuracy	0.999479	0.999406	0.999377	0.999527
Specificity	0.99965	0.99957	0.99964	0.99965
FNR	0.263598	0.653696	0.240793	0.22408
FDR	0.345018	0.380165	0.355281	0.3349
MCC	0.688886	0.411105	0.6813	0.711014
Dice	0.682681	0.366957	0.661862	0.702173
Correlation	0.998606	0.999378	0.998612	0.998519
FAR	56.667	66.667	57	56.6667
FRR	26.6667	52.77	68	19

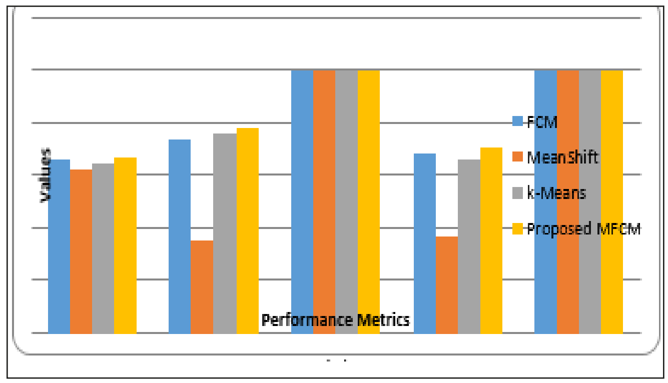

Fig. 21: Performance comparison of Precision, Recall, Accuracy, Dice, Specificity.

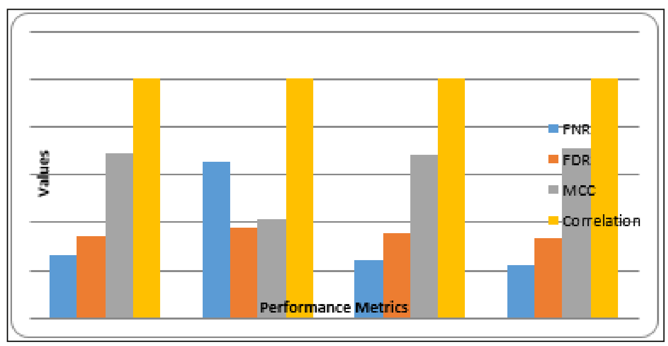

Fig. 22: Performance comparison of FNR, FDR, MCC, Correlation.

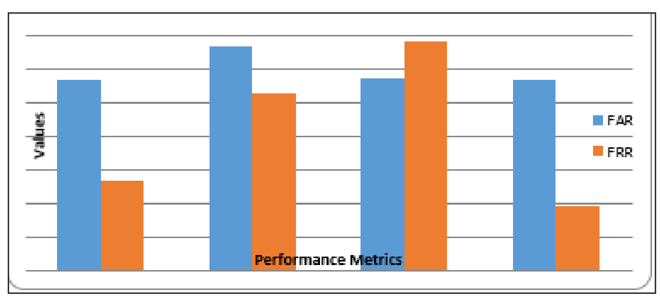

Fig. 23: Performance comparison of FAR, FRR.

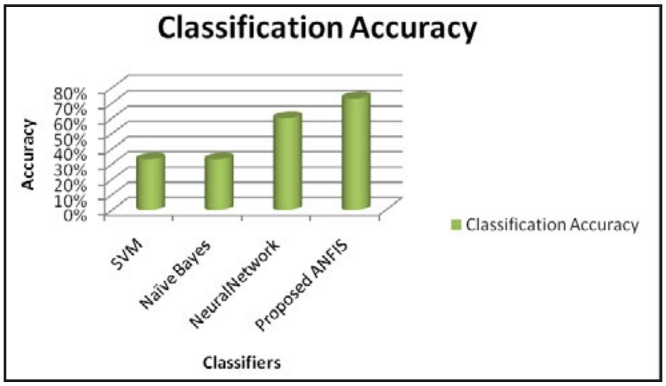

Fig. 24: Comparison of Classification accuracy.

Table 3: Performance evaluation of accuracy in classification

Classifiers	Classification Accuracy
ANFIS	73%
NN	60%
NB	33%
SVM	33%

From Table 3, the accuracy of the classification for the proposed ANFIS is more noteworthy when contrasted to the prevailing classifiers. While deducing the prevailing systems, NB along with SVM exhibits low accuracy of around 33%. Nevertheless, the proposed ANFIS classifier evinces progress in accuracy, which is 73%.

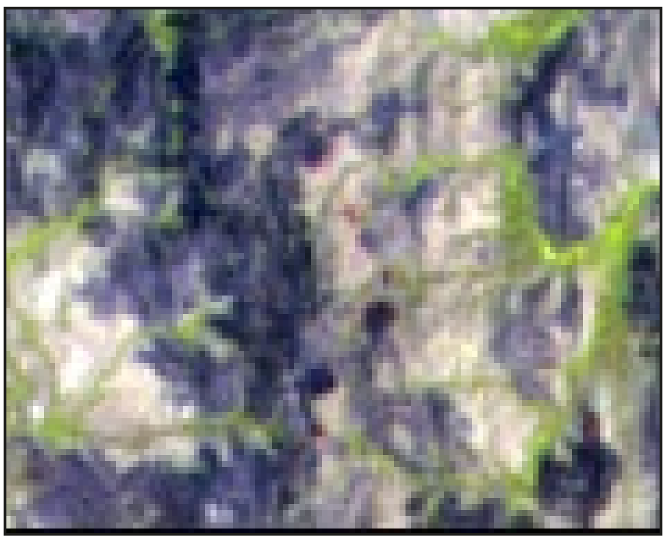

Fig. 25: Sample input image.

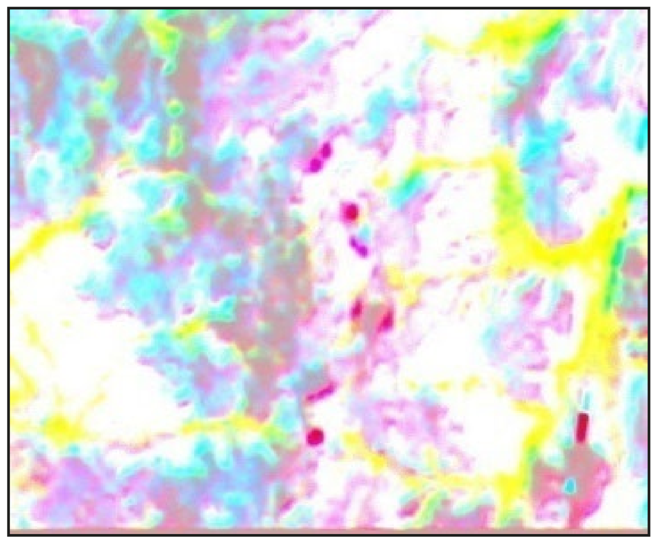

Fig. 26: Preprocessed image.

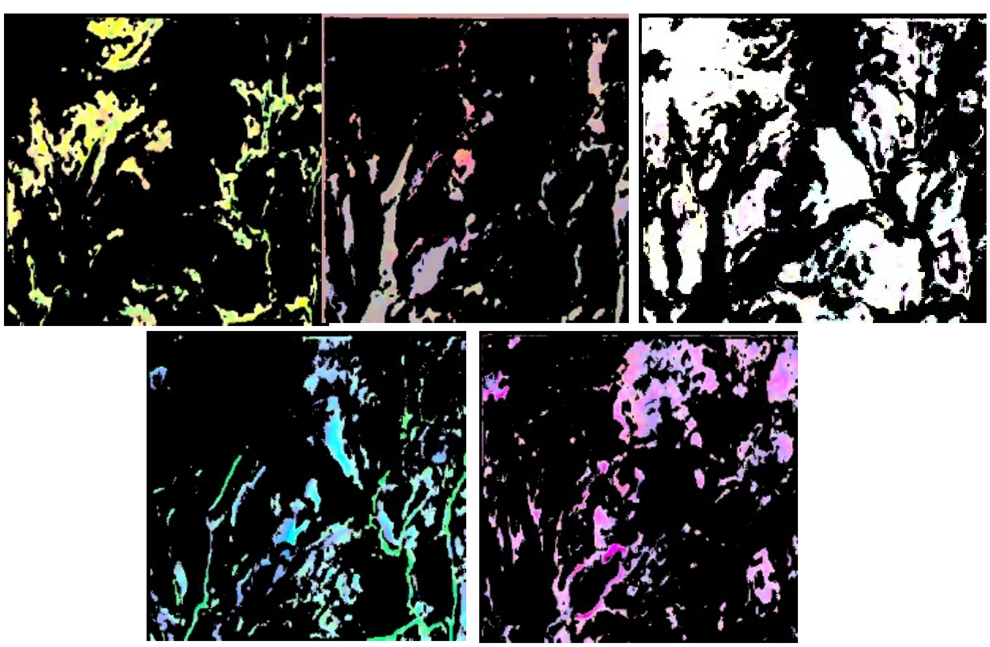

Fig. 27: Clustered images of preprocessed images.

(F) Implementation of Forest Fire Identification using Optimized ANFIS Classification

The pre-processing incorporates median filtering along with LCS procedure to upgrade the images. Subsequently, the MFCM is connected in pre-processed images for the clustering. Here, from the resulting clustered images, features are extracted. The extracted features are optimized by employing CS algorithm, and then those optimized features are inputted into the ANFIS classifier for the classifying images into Non-fire or fire. Lastly, the fire zone is accurately recognized from the classified fire images. In this proposed work, satellite forest fire data utilizing the ANFIS framework has been actualized in the MATLAB working platform.

Grounded on optimized CS algorithm, the planned forest fire identification strategy is assessed by utilizing images acquired from the satellite forest fire database. The proposed system performance attained by the performance metrics. The extorted features like LGXP, Color Features, Entropy feature, Homogeneity feature, ASM features are optimized utilizing CS algorithm. Eventually, to distinguish the fire region and non-fire region, the optimized features are classified by utilizing ANFIS classification.

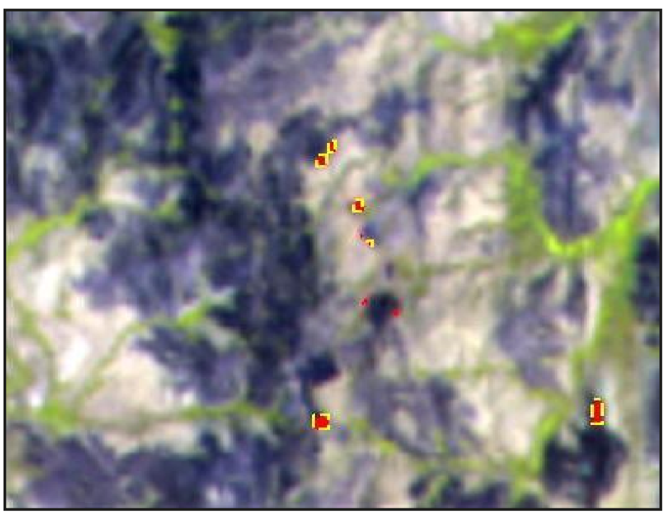

Fig. 28: Fire detected images.

Fig. 25 delineates the sample image taken from the satellite forest fire database. Fig. 26 demonstrates the image that has experienced median filtering along with the LCS process in the preprocessing stage. Fig. 27 demonstrates the clustered images of the image attained after preprocessing. Fig. 28 demonstrates the fire identified images. The red regions existing in the image is the fire detected area.

Performance Analysis

Here, the detail explanation of the implementation result and its performance are analyzed. By performing the sensitivity, specificity, along with accuracy, the proposed hotspot detection's performance is analyzed. Performance evaluation depends on performance metrics, say, precision, recall, accuracy, specificity, and F-measure.

Table 4: Comparison of existing and proposed classifiers

Measures	SVM	NB	NN	ANFIS	Proposed Optimized ANFIS
Precision	65	61	64	66	69
Recall	60	50	62	70	72
Accuracy	55	56	60	73	75
Specificity	52	49	65	72	78
F-measure	68	46	54	59	70

Table 4 demonstrates the comparison of the prevailing classifiers, for example, SVM, NB, NN, ANFIS, and proposed Optimized ANFIS. It is deduced that this proposed Optimized ANFIS delineates superior performance on considering the prevailing ones.

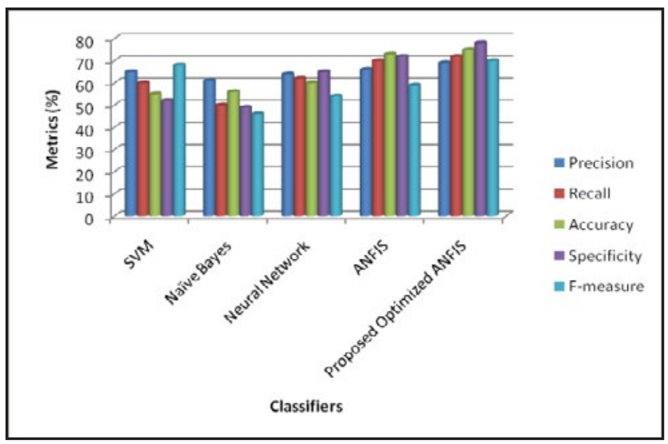

Fig. 29: Performance evaluation of existing and proposed classifiers.

Conclusion

In the first work, a technique was intended and constructed for BAI. Here, the input to this system was the satellite images from NASA, which are transmuted to IHS images. This is followed by object segmentation utilizing k means clustering algorithm. Subsequently, these segmented objects are then fed to an FFNN for the smoke area identification. The burning area is detected using the directional analysis. This approach was analyzed with respect to performance metrics like sensitivity, specificity, along with accuracy. From the experiential results, it was observed that the proposed work attained accuracy, which was 2.6% higher on considering the prevailing approach.

In the second work, an efficient method was introduced for the classification and recognition of forest fires from satellite images. This is done for the successful BAI. Primarily, the satellite image is preprocessed utilizing the HE along with the decorrelation stretching. The resulting image is clustered by employing the FCM technique. A collection of features are extorted and are categorized utilizing the ANFIS classifier. The results in two categories are the i) Non-fire and ii) Fire area. The area with fire is identified. The proposed classifier was contrasted to the prevailing classifiers and it is deduced that the proposed work renders propitious results.

In the third approach, an effectual approach was demonstrated for the recognition of the area with a forest fire. The pre-processing integrates median filtering with LCS to upgrade the images. Subsequently, the resulting preprocessed images undergo MFCM for the clustering and features are extorted. The extorted features are optimized by employing CS algorithm and are classified using the ANFIS classifier. The forest fire area was recognized. From the results, the performance metrics was evaluated. The proposed work was contrasted with the prevailing work. It is deduced that this approach produces notable results while compared with the prevailing work.

Acknowledgement

A special thanks to National Remote Sensing Centre (NRSC) for sharing the Forest Fire data of the study area territory. The authors are thankful to Dr. C. S. Jha, Chief General Manager, Regional Centres (RC), NRSC for providing logistic and Imagery support.

References

Ashwin, T.K. and Kamireddy, R., 2015: A technique for burning area identification using IHS transformation and image segmentation. *International Arab Journal of Information Technology*, 12(6A): 764-771.

Ashwin, K.T., Reddy, K.M. and Vidyavathi, S., 2018a: An efficient forest fire image classification and fire area detection. *Jour of Advanced Research in Dynamical & Control Systems*, 10(06).

Ashwin, K.T., Reddy, K.M. and Vidyavathi, S., 2018b: An proficient forest fire identification using optimized ANFIS classification. *International Journal of Pure and Applied Mathematics*, 119(12): 239-258.

Ganesan P., B. S. Sathish, and G. Sajiv., 2016: A comparative approach of identification and segmentation of forest fire region in high-resolution satellite images. *In Futuristic Trends in Research and Innovation for Social Welfare (Startup Conclave), World Conference on, IEEE*, 1-6.

James A. Shine and Daniel B. Carr, 2002: A comparison of classification methods for large imagery data sets, JSM 2002 *Statistics in an ERA of Technological Change-Statistical computing section*, New York City, 3205-3207.

Mahi H., Isabaten H. and Serief C., 2014: Zernike moments and SVM for shape classification in very high-resolution satellite images, 11(1).

Mohamad Awad, 2010: An unsupervised artificial neural network method for satellite image segmentation. *Int. Arab J. Inf. Technol*, 7(2): 199-205.

Tansey K., Chambers I., Anstee A., Denniss A., Lamb A., 2009: Object-oriented classification of very high-resolution airborne imagery for the extraction of hedgerows and field margin cover in agricultural areas. *Applied Geography*, 29(2): 145-157.

Wang Shi-Dong, Miao L.L. and Guang-Xiong Peng, 2012: An improved algorithm for forest fire detection using HJ data. Procedia Environmental Sciences, 13: 140-150.

Indian Journal of Geosciences, Volume 74, No. 3
July - September, 2020; pp. 345-353

Invited Paper

The role of Marine Wing, GSI in India- an appraisal

P.C. Shrivastava

Retired Deputy Director General, Marine Wing, Geological Survey of India
Email: prem.shri1943@gmail.com

Abstract: The Marine Wing of GSI was established in August, 1965 to carry out mapping and mineral exploration of the continental margin and other applied aspects of the coastal areas. In the absence of a research vessel, the survey programmes were implemented by chartering vessels, motor boats and participating in the cruises of Naval Hydrographic and NIO vessels. About 288 million tonnes of calcareous sand deposit suitable for cement and other industries found in lagoons and shallow offshore areas of Lakshawadeep. Detailed studies of ferro-manganese nodules from the Indian Ocean found nodules of eastern Indian Ocean rich in Mn, Ni, and Cu, and Central Indian Basin as potential for future exploration. The bottom sediments map of the seas bordering India was compiled on 1:2.0 million scale and presented in the International Geological Congress (IGC) held at Montreal (Canada) in the year 1972. Geoscientists of Marine Wing participated in Oceanographic Expedition (ONCEANAVEX-I) in the Arabian Sea and in the different cruises of *R.V. Gaveshani, M.V. Fernella, M.P. Skandi Surveyors* from 1981 until the arrival of GSI research vessel *Samudra Manthan* in the mid-1983 as a part of National Project of ferromanganese nodules of the Central Indian Basin of Department of Ocean Development (D.O.D). Systematic mapping of the seabed and mineral exploration within EEZ of India started from mid-1983 after the acquisition of research vessel *Samudra Manthan* and two coastal research launches *Samudra Kaustubh* and *Samudra* Shaudhikama in 1984. More than 35 sheets of 2° x 2°maps of the seabed within EEZ of India were compiled and released. Vast resources of lime mud has been found off Andhra Pradesh, Gujarat and Maharashtra coasts. Heavy minerals (HM) of economic importance have been delineated within territorial waters (TW) off east and west coast. Phosphorites found off Ratanagiri, Okha on the west coast and off Chennai on the east coast. Sand useful for the construction purposes have been located in the shelf area off Kerala coast. Manganese micro-nodules with Mn, Fe, Cu, Ni, Zn, Co have been found in a very wide area west of Lakshadweep in water depths of 2,800-4,400 m. Ferro-manganese encrustation samples have been recovered from Chetlat (Lakshawadeep) and Tillan Chand and Batti Lav (Andaman) areas. Eight channels and levee systems have been recognized in the Bengal Fan area. Sponsored programmes for Single Buoy Mooring (SBM) systems, pipeline surveys, tidal energy, casion for export of iron ores, geotechnical surveys prior drill sites for oil/gas exploration were undertaken. Special programmes were carried out for defense needs. There is need to expedite compilation and release of maps, collection of high resolution data from identified mineral potential zones for resource evaluation, basic data on environment, modelling for shoreline changes due to mining.

Keywords: Marine, seabed, EEZ, ferro-manganese nodules, exploration, sediments map, coastal landforms, magnetic, OBMs SBMs, Seamounts.

Introdution

The Geological Survey of India (GSI) has been carrying out mapping and mineral exploration on the land since its inception in March 1851. Its activities on marine geology was confined to coastal investigations and studies of seabed samples of phosphorite (Tipper, 1911) and barium nodules (Jones, 1887), etc. collected by other Organizations. An Indian National Committee for Research (INCOR) in oceanography was constituted by the Govt. of India in the year 1960 to coordinate the research activities and provide infrastructural support needed during the proposed programmes of the International Indian Ocean Expedition (IIOE). The geoscientists of GSI participated in the cruises of IIOE (1960-65). Realizing the importance of marine geology and resources of the seabed of the continental margin of India, covering an area of about 0.9 million sq.km. (Chaterji, *et al.,* 1968), and other applied aspects such as sediment tracing in coastal areas and its application in coastal engineering, the GSI created a three member team of Marine Geology Unit in August, 1965 under Central Petrological Laboratories, at Kolkata. The present author of this paper, P.C. Shrivastava, was one of the three members of this Unit. A programme for exploration of mineral resources of the eastern continental margin of India was planned in September, 1965 onboard a Naval Vessel but, unfortunately the vessel was withdrawn as Pakistan had attacked India. The Unit was given a status of a separate Offshore Mineral Exploration and Marine Geology Division (OME & MG Division) in the year 1971 and raised its status by opening two new Centres at Visakhapatnam and Mangalore in the year 1979. Later on another Centre was opened at Cochin. Dr. M.V.N. Murty was the First Director of OME & MG Division. The OME & MG Division was re-named as Marine Wing of GSI.

Marine surveys, mineral exploration and other related activities (August, 1965- Mid 1983).

In the absence of research vessels, Marine Wing, GSI commenced its programme of seabed surveys, mineral exploration and other coastal programmes by chartering vessels, motor boats and participating in the cruises of Naval Hydrographic and NIO vessels. Some achievements are given here.

Investigation for calcareous sand deposits in lagoons and shallow offshore areas of Lakshadweep: Eleven lagoons, shallow offshore areas and four submerged banks were surveyed by hiring mechanized boats for calcareous deposits and inferred a reserve of about 288 million tonnes, suitable for cement, lime, iron and steel and other industries (Siddiquie and Mallik, 1973; Mallik, 1976).

Ferro-manganese nodules from Indian Ocean

During International Indian Ocean Expedition (IIOE, 1960-65) different Research Institutions collected large number of seabed samples including ferro-manganese nodules. Marine Wing, GSI obtained these nodule samples from USSR and USA institutions and carried out detailed studies on morphology, thin and polished sections, Differential Thermal Analysis (DTA) and chemical analysis of nodules. The nodules vary in shape from spherical, ellipsoidal, tabular, and prismatic to irregular with average specific gravity of 1.72. DTA curves resemble those of vernadite or manganese manganite. X - ray data show that the nodules are mainly consist of 10Å manganite or todorokite and 7Å manganite or bernesite (Siddiquie, *et al.,* 1968). Nodules found in the eastern Indian Ocean are rich in Mn, Ni and Cu. The Central Indian Ocean Basin appeared to be potential area for future exploration of ferro-manganese nodules in the Indian Ocean (Siddiquie, *et al.,* 1978).

National Project of D.O.D. on the exploration of ferro-manganese nodules from Central Indian Basin

Geoscientists of Marine Wing, GSI participated in the different cruises of *R.V. Gaveshani, M.V. Fernella, M.P. Skandi Surveyor* from 1981 until the arrival of GSI research vessel *Samudra Manthan* in mid-1983 for collection of ferro-manganese nodules and chemical analysis of the same in the Central Chemical Laboratory of GSI, Kolkata under the above National Project of D.O.D. (Shrivastava, 2013).

Bottom sediments map of the seas bordering India for IGC, Montreal (Canada) 1972: The bottom sediments map of the seas bordering India on 1:2.0 million scale was compiled with the help of data collected on the types of sediments, mineral occurrences on the beaches and offshore areas, C^{14} Th^{230} and U^{234} Dates, etc. from research papers, memoirs and records of Organizations, Institutions. Naval Hydrographic and Admiralty charts under the guidance of Dr. M.V.N. Murty, Director, OME & MG Division, GSI. Shri M.S. Balasundaram, Director General, GSI presented this map in the International Geological Congress (IGC) held at Montreal (Canada) in the year 1972 (Closs, *et al*. 1974). This map with additional data was published by GSI in the year 1975 (Fig. 1; Siddiquie, *et al.,* 1975).

Coastal landforms of India

Coastal landforms classified into (i) Rocky coastline, (ii) Barrier, (iii) Lagoon, (iv) Coralline coastline, (v) Delta, (vi) Alluvial plains, (vii) Low Dunes, (viii) Dune Hills, (xi) Mangrove Marshy Bushes, (x)Salt Marsh and Mud Flats, and (xi) Embayments oblique and perpendicular to the coast were plotted on 1:5.0 million scale map of India and the same was published by GSI in the year, 1972 under the guidance of Dr. M.V.N. Murty, Director, OME & MG Division (Rao, 1972).

Cruises off Mangalore

A large number of seabed samples were collected on board Mangalore Harbour Project launch *M.V. Rohini* in the month of April, 1966. The sand is confined to a narrow strip along the coast and major part of the area surveyed is covered with silt and clay. The heavy minerals consist of hornblende, tremolite/actinolite, garnet, sillimanite, zircon, monazite, rutile and opaques (Chandra, *et al.,* 1978). Siddiquie and Chowdhury (1968) reported phosphate content of 0.06% to 0.4%. A radial movement of sediment off Netravati River mouth with prominent movement towards northwestward was deciphered (Shrivastava and Viswanathan, 1979). Fluorescent tracer studies have also indicated northwestward movement (Siddiquie, *et al.,* 1971).

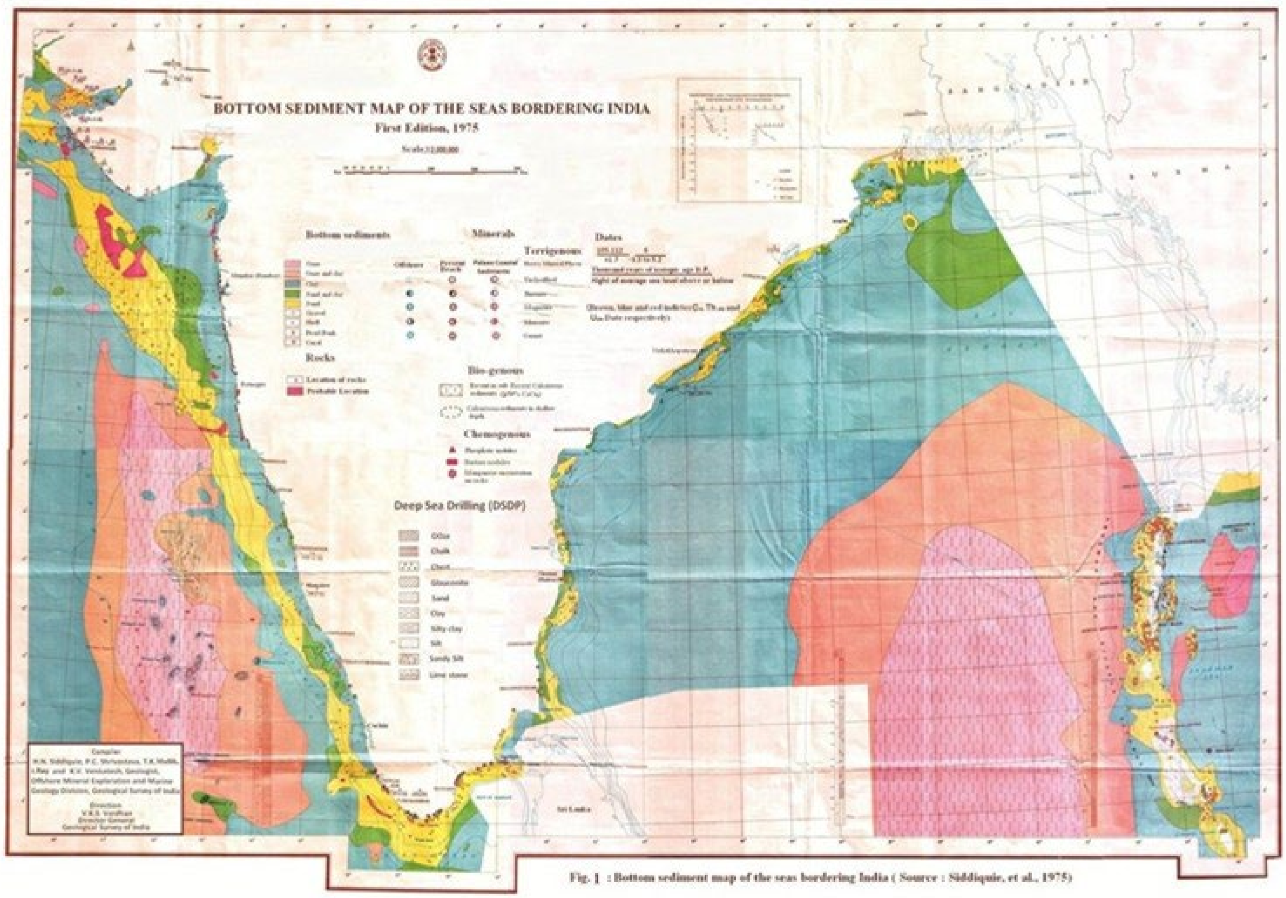

Fig. 1: Sediment map of the seas bordering India (Source: Siddiquie, *et al.,* 1975)

Oceanographic Expedition (OCEANAVEX-I) in the Arabian Sea

A multi-disciplinary Oceanographic Expedition was organised by the Indian Navy in the northwestern Arabian Sea onboard *INS Darshak* between November, 1973 and May, 1974. Geoscientists of OME & MG Division, GSI also participated in the expedition and collected a large number of seabed samples from over 200 stations. Mineralogical and micro-palaeontological studies on the selected samples were undertaken. Heavy mineral assemblages suggest a mixed igneous and metamorphic source with major contribution from the igneous rocks. Illite is the major contributions from the western continental shelf (Chandra, *et al.,* 1978). Four foraminifera biofacies were recognised from the faunal assemblages in the area. The larger foraminifera identified include *Operculina* Sp*., Alveolinella* Sp. *and Borelis,* Sp. (Sen, *et al.,* 1975).

Cruises off Ratnagiri-Vijay Durg

Bathymetric, shallow seismic, magnetic and side scan sonar surveys were taken up, as a part of NIO-GSI collaboration programmes, onboard *R.V. Gaveshani* during 1978-79. A bunch of calcareous ridges parallel to the coast were found on the outer shelf. Oolitic sand was found beyond 50-60m water depth. Samples of algal limestone off Ratnagiri-Vengurla analysed > 5% P_2O_5.

Cruises off Hooghly River mouth

Survey off Hooghly River mouth was taken up in March**,** 1967 by chartering *R.V. Anusandhani* of Calcutta Port Trust and Sediments samples were collected between mouths of the Hooghly and Mahanadi Rivers (Siddiquie, *et al.,* 1971). The northeastern part is admixture of fine sand and grey clay brought by Ganga and Brahmaputra river systems. The sediments on the west are clay and to the south they are mixed with calcareous concretions (Kankar like) which might have formed during low sea level. The southwestern part of the area is occupied by coarse sand which is quite different from the sand reported from northern area and might have been brought by Mahanadi river. Mallik, (1976) reported mineral assemblages of opaques, biotite, muscovite, garnet, hornblende, chlorite, sillimanite, zircon, epidote, monazite, rutile, sphene, etc. which suggests a mixed igneous and metamorphic source. X-ray diffraction data of the clay (<2 μm) from the shelf sediments revealed the predominance of illite and quartz with minor amounts of montmorillonite, kaolinite and feldspar (Rama Murty and Shrivastava, 1979). High concentration of illite near Hooghly river mouth and offshore area indicated the source of clay minerals from Ganga-Brahmaputra river systems and direction of movement of sediments towards southeast.

Fluorescent Tracer Studies

Fluorescent tracer studies have assumed importance due to their usefulness in the development of Harbour and other marine structures. A new simple and indigenous technique for the preparation of fluorescent tracers of short and long duration was developed in the Laboratory (Shrivastava, 1975). For releasing tracer on the river bed/seabed, a mechanical device was fabricated in Surveys Workshop (Shrivastava, 1970). The first experiment was carried out successfully at Haldia Anchorage in the Hooghly River on 07.01.1968 (Siddiquie and Shrivastava, 1970). Such studies were also taken up in Tuticorin, Mangalore, Gopalpur, Kavarati lagoon, etc. (Shrivastava, 1975; Venkatesh, 1974; Shrivastava and Rao, 1976). Fluorescent tracer studies carried out off Paradip Port during February, 1972 suggested that the disposal of dredged material may be done far away towards northeast during northeast monsoon to avoid re-entry of the dredged material into the navigational channel (Shrivastava, 1976).

Systematic Seabed mapping, Mineral Exploration, other activities onboard GSI research vessels and major achievements (Mid-1983 onwards): The Marine Wing of the Geological Survey of India started its systematic geological, geophysical and geochemical mapping of the seabed within Exclusive Economic Zone (EEZ) of India covering an area of about 20,14,900 sq.km with the acquisition of research vessel *Samudra Manthan* in mid-1983 and two coastal research launches *Samudra Kaustubh* and *Samudra Shaudhikama* in later half of 1984. About 98% of the seabed within EEZ of India has already been surveyed on reconnaissance scale (GSI Annual Report 2015-16) and huge geoscientific data collected on the morphology, sediments, minerals and other applied aspects (Fig. 2).

Seabed maps of EEZ of India

The entire EEZ of India has been divided into 63 sheets of $2^\circ \times 2^\circ$and more than thirty five maps compiled on 1:500,000 scale using geological, geophysical and geochemical data collected during systematic mapping of the seabed onboard *R.V. Samudra Manthan*. The maps depict sediment types, bathymetry, sample description with locations, carbonate content of surface sediments and magnetic anomaly with short notes. The sub-surface geological data including stratigraphic logs of deep bore holes wherever available and obtained from ONGC are included in the map. Maps with ONGC data are published and released jointly.

Minerals within Territorial Waters (TW) of India

The area of Territorial Waters (TW) is about 0.15 million sq. km and restricted to 12 nautical miles (NM) from shore. *Samudra Kaustubh* carried out mapping and mineral exploration on the east coast and Andaman Islands whereas *Samudra Shaudhikama* was deployed on the west coast of India.

Heavy minerals off Orissa Coast: A zone of sand with heavy minerals varying from 5 to 35% was delineated around 30m water depth off Gopalpur-Chhattarpur-Malud (Fig. 2). Sengupta,*et al.,* (1992) estimated reserve of 17.2, 6.8, 4.8 and 1.6 million tonnes of ilmenite, sillimanite, garnet and zircon + rutile + monazite respectively.

Heavy minerals off Andhra coast: The inner shelf sediments are predominantly sand and contain heavy minerals from 0.04 to 23.63% (Fig. 2). Ilmenite and sillimanite predominate in nearshore areas whereas garnet, ilmenite are rich beyond 20m isobaths. Zircon, monazite and rutile vary from 0 to 0.47%, 0 to 0.43% and 0 to 0.23% respectively. Sub-surface sediments contains heavy minerals from 0.59 to 15.97%. About 17.3 million tonnes of heavy minerals are estimated from Kapasukuddi to Karipeta off Andhra coast. Ravi Kumar, *et al.,* (2002) estimated a reserve of ilmenite (3.59 million tonnes), sillimanite (1.21 million tonnes), garnet (1.09 million tonnes) and monazite (0.37million tonnes) respectively from the northern Andhra Pradesh.

Heavy minerals off Kerala and adjoining Tamil Nadu coast: Preliminary mapping of the seabed from Alleppey to Kolachal revealed the presence of sand containing heavy minerals from 4% to 7% in selected sectors (Fig. 2). Detailed surveys in Chavara, Varkala and Taingapatnam-Vizhinzham areas found heavy minerals from 1.57% to 32.86%. Senthiappan, *et al.,* (1992) estimated reserve of ilmenite (1.41 million tonnes),

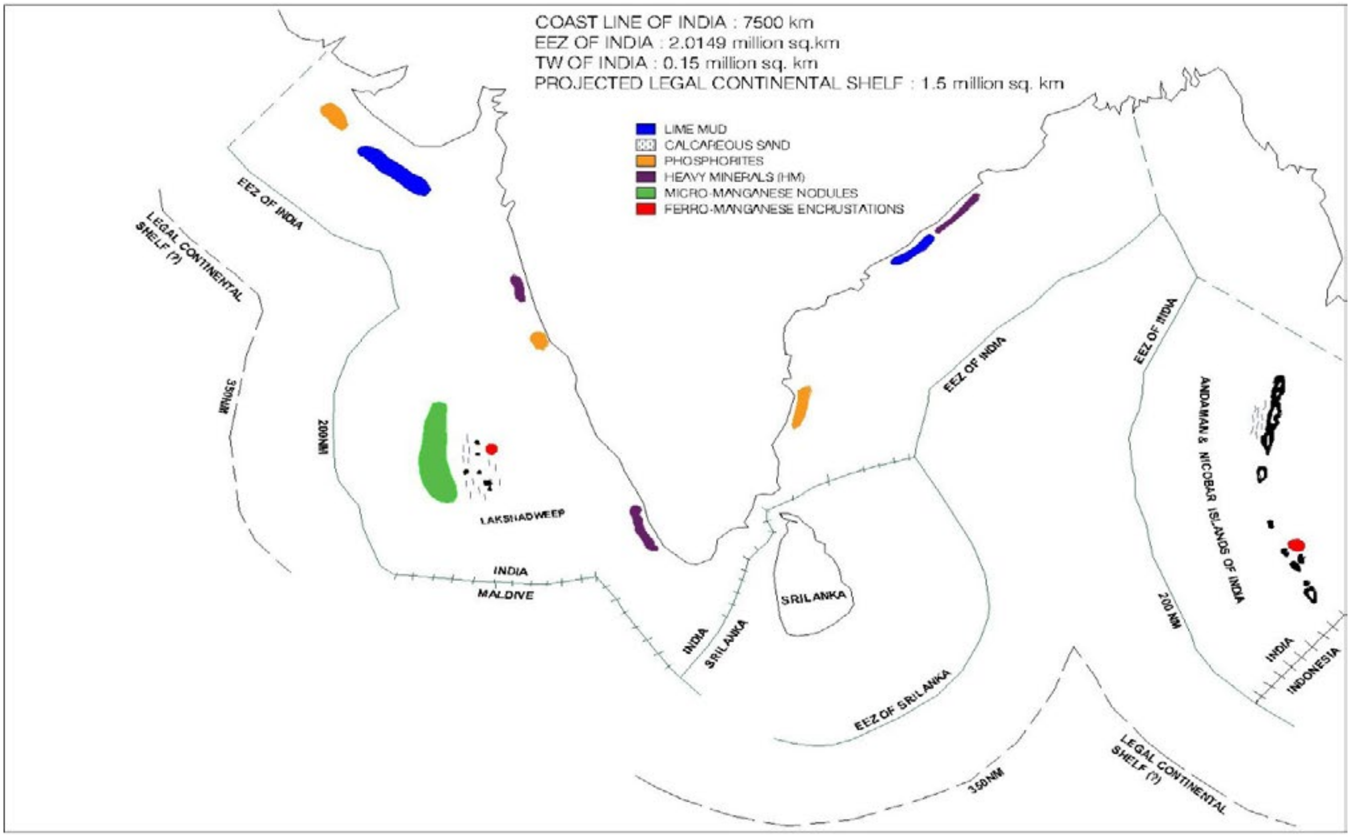

Fig. 2: Sketch map of India showing boundary of EEZ, Legal continental shelf (?) and minerals delineated by Marine Wing, GSI within EEZ of India.

zircon (0.11 million tonnes), rutile (0.113 million tonnes) and sillimanite (0.520 million tonnes) from Varkala and Chavara sectors. Nambiar, *et al.,* (2002) estimated reserve of ilmenite + leucoxene + rutile (3.05 million tonnes), zircon (1.08 million tonnes) and garnet (0.24 million tonnes) from Taingapatnam to Vizhinzham areas.

Heavy minerals off Konkan coast: Kalba Devi, Mirya and Ratnagiri Bays off Konkan coast were surveyed and ilmenite and titano-magnetite, two economic minerals were found (Fig. 2). Ilmenite varies from 1 to 40% and magnetite 0.8 to 8% in the sediments. The estimated reserve of ilmenite and magnetite in the Kalba Devi Bay is around 3.12 million and 0.68 million tonnes respectively (Nambiar, *et al.,* 1992).

Sand off Kerala coast: The sand found in the shelf area of Quilon and Chavara contains less heavies. Balakrishnan and Gangadharan (2003) reported fine sand in water depths of 20-25 m off Kollam and Kochi. According to them good quality sand of more than 2.0m thickness is found in a large area which might be used in the construction works. Zaheer, *et al.,* (2005) and Shrivastava (2005) suggested relook of sand deposits of shelf regions of Orissa and Andhra Pradesh coasts also for use in the construction industry.

Minerals beyond T.W. and within EEZ of India

Lime mud deposit*s*: Pure calcareous clay like plaster of Paris is called Lime Mud. For the first time such clay samples were collected off Visakhapatnam-Pentakota onboard *R.V. Samudra Manthan* from 80 m to 300 m water depths (Fig. 2). Detailed surveys identified four lime mud deposits in an area of about 1,000 sq. km. The thickness of the lime-mud varies between 0.06m and 2.04 m below a layer of about 0.1 to 1.8m thick clay mixed with calcareous sand. CaO and MgO of lime-mud vary from 46.36% to 50.9% and 0.4% to 1.2% respectively. A calcareous ridge was found around 90m water depth which might have contributed to the formation of lime-mud when sea level was lower during Pleistocene. Similar lime-mud deposit has been found in fifteen areas in water depths of 100- 1,000 m from Okha to Mumbai (Fig. 2). The thickness of lime-mud varies from 1.5 m to 3.0 m and the CaO content from 43% to 52% (Vaz, *et al.,* 1993; Rao and Vaz, 1998). Kalluraya *et al.* (2003) reported lime-mud deposit from north-northwest of Angaria Bank.

Phosphorite*s*: NIO-GSI joint cruise of *R.V. Gaveshani* in 1978, collected algal limestone samples off Ratnagiri-Vengurla and found P_2O_5 content >5%. Phosphatised limestone with oolite, fish teeth, skeleton of fishes and shells, etc. were collected from water depth of 300-500 m off Okha onboard *R.V. Samudra Manthan* (Fig. 2). The chief minerals of phosphatised limestone are ankerite and carbonate flour apatite.P_2O_5 content of phosphatised limestone vary from 24.25% to 30.4% (Rao and Vaz, 1998). For the first time phosphatised rock pieces were recovered from water depth of about 195 m off Chennai-Mahabalipuram sector during 80th cruise of *R.V. Samudra Manthan*. Detailed surveys identified two terraces in water depths of 100-200 m and 350-500 m from where phosphorite samples were collected. P_2O_5 content varied from 8.10% to 20% (Vaz, 1995). Rao, *et al.* (2001) also reported phosphatic concretions from Point-Calimere off east coast of India.

Manganese micro-nodules west of Lakshadweep: While mapping the seabed west of Lakshadweep onboard *R.V. Samudra Manthan,* a 0.5 to 20 cm thick layer of manganese micro-nodules was found several centimeters below the surface sediments in water depths of 2,800-4,400m (Fig. 2). Adiga and Kalluraya (1997) carried out detailed studies of these nodules. Micro-nodules vary from 2.6% to 24% of the coarser part of the sediments, and birnesite is the chief manganese mineral.

Ferro-manganese encrustations: Ferro-manganese encrustation samples were collected from 1,562 m water depth around Chetlatisland (Lakshadweep) and also from Tillanchand and BattiMalv islands in the Andaman sea (Chandra, *et al.,* 1996; Fig. 2). Charlu and Kalluraryya (1997) reported average content of Co, Ni, and Pt 0.254%, 0.263% and 0.3 ppm respectively in the samples of Chetlat area. Ferro-manganese, encrustation samples from Andaman area contain Ni (0.402%), Pb (0.128%) and Co (0.083%).

Other achievements

Barren Volcano in Andaman Sea: The study of magnetic profiles prior and post eruptions of Barren Volcano in 1991 indicated Curie point about 2km below seabed and that the lava source was through thin fissures from northeast of island. Lava could not spread westward due to internal hindrance (Banerjee *et al.,* 1998). Ocean Bottom Magnetometers (OBMS) studies also found Curie depth of 3 to 5 km on the eastern sector and 5 to 12 kms on the western side of Barren Island. Saha *et al*. (1997) discovered a submerged ridge of about 450-700m in height from west, south and eastward side of Barren Island.

Channel and levee system in the Bengal Fan: Bengal Fan is one of the well-known Fans of the world. It is built by sediments of Ganga-Brahmaputra river systems in the Bay of Bengal. The survey data collected during different cruises of *R.V. Samudra Manthan* in the Bay of Bengal were studied by Rao and Faruque (2002) and they identified eight channels and levee system in the area. Most of them emerge from Middle Fan and get divided into several branches. Channel No.1 is about 500 km long.

Legal Continental Shelf: The Coastal States may demarcate their outer limit of the continental shelf in accordance with the Article 76 of the United Nations UNCLOS-III. The outer limit may extend up to 350 nautical miles from the coast (Baseline). India is likely to get a large area of about 1.5 million sq.km under this claim. Department of Ocean Development (D.O.D.; now Ministry of Earth Science) was pursuing this claim in association with GSI, NIO, NHO, ONGC, NGRI and other Agencies. *R.V. Samudra Manthan* collected about 159 bathymetric profiles data from shore to EEZ boundary running into thousands of nautical miles and the same were utilized in the Demarcation of *Foot of the slope* as well as 2500 m isobath line as the first step towards the programme of the *legal continental shelf*. The Ministry of Earth Science, Govt. of India submitted its claim of Continental Shelf beyond 200 nautical miles (EEZ) to the concerned International Seabed Authority (ISBA) on the 13th May, 2009.

Holocene sea level curve of east coast: Hashimi, *et al.,* (1995) prepared Holocene sea level curve based on C^{14}data from coastal and offshore areas. There was no such curve for the east coast. C^{14} data were collected from oolites off Visakhapatnam (Naidu, 1968), off Gopalpur-Chilka lake (Sanjeev Raghav, 2002), *Acropora* sp. collected from coral reef in water depth of 125 m off Karaikal east coast (Vaz, 2000), coral reef off Mahabalipuram, and algal ridges found at -85m and -100 m, other places. According to Narassayya, *et al.,* (2002) sea level reached at +6 m around 6000yr. BP and there was regression during 6000-3500yr BP when sea cliffs, tidal flats, beach ridges were formed. Based on these C^{14} dates and other observations, a sea level curve for east coast of India was generated (Fig. 3; Faruque, 2002).

Seamounts in Andaman Sea:GSI, first research vessel *Samudra Manthan* with its active service of about three decades was decommissioned and replaced by a most modern research vessel *Samudra Ratnakar* in October, 2013. Surveys in the Andaman sea identified several seamounts (Annual Report of GSI, 2014-15), and further probing is going on.

Off-shore Areas Mineral (Development and Regulation) Act, 2002: Marine Wing of GSI provided necessary geoscientific information on the continental shelf, slope, continental rise, abyssal plain, seamounts, mid ocean ridges, mineral resources of the sea, legal limits of Territorial Water (TW), Contiguous Zone, Exclusive Economic Zone, Legal Continental Shelf, etc. for framing the rules and regulations for the development and regulation of offshore Areas Mineral Act. The above OAMDR Act-2002 was notified in Spl. Gazette dated 31.01.2003 (IBM, Year Book- 2003).

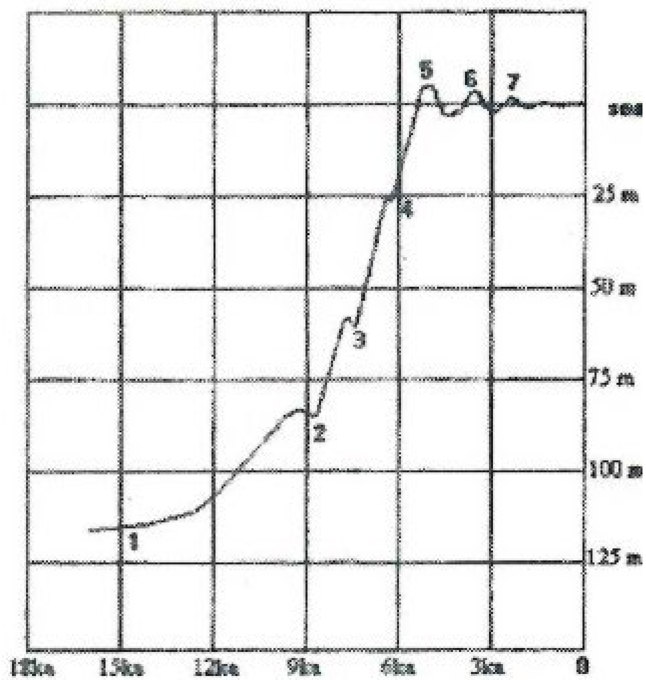

Fig. 3: Sea level curve of east coast of India (Source : Faruque, 2002).

Seabed sample preservation Centres: First sample preservation Centre was created at Mangalore office. The samples are preserved under controlled temperature. The samples were kept systematically and maintained proper register for quick retrieval of the samples. Second Centre was created at Visakhapatnam office.

Sponsored programmes

During the year 1991, Govt. of India issued circulars to Departments including Scientific Departments to generate some financial support for their programmes. Marine Wing took initiative in this direction and, the first MOU was signed with Hydraulic Study Department of Calcutta Port Trust in the year 1992 to carry out geotechnical surveys for the proposed Oil Terminal (Single Bouy Mooring –SBM systems) off Digha coast in the Bay of Bengal. The programme was taken up in early 1993 on board *R.V. Samudra Kaustubh* and completed successfully within the stipulated time frame. After this other Agencies/ Organizations' started approaching Marine Wing for their programmes. Geotechnical surveys were taken up for M/s Black Gold Refinery Ltd., Visakhapatnam; Southern L.P.G. Ltd., Madras; Southern Petrochemical Industries Ltd. (SPIC); tidal energy in the Sunderbans for IIT Madras, Drill Sites for ONGC on the east coast of India onboard *R.V. Samudra Kaustubh*. Surveys for selection of suitable sites for Casion in water depths of 25-30m off Goa onboard R.V. *Samudra Shaudhikama*was taken up for M/s Murmagoa Maritime Ltd., Goa for export of iron ore. Pipeline route survey for British Gas International in the Gulf of Khambat was taken up with D.O.D. Special and strategic surveys were taken up for Defence needs onboard *R.V. Samudra Manthan* and *R.V. Samudra Shaudhikama* jointly or individually.

Now, there is need for Marine Wing, GSI to expedite compilation and release of EEZ maps, high resolution data collection from already identified mineral potential zones for resource evaluation for future exploration; collection of basic data on various parameters of environment in collaboration with other agencies engaged in environmental studies prior to exploitation of seabed minerals; computer modelling on the effect of shore changes due to mining in shallow water (erosion and deposition); with the new vessel *Samudra Ratnakar* look for gas hydrates within EEZ and other valuable minerals beyond EEZ also.

Acknowledgements

Author is grateful to Shri E.V.R. Parthasaradhi, Dy. Director General (Rtd), GSI and Secretary of Krishnanunni Mermorial charitable Trust for the suggestion to write an article on the role of Marine Wing, GSI for the Special Publication in memory of Shri Krishnanunni. He also expresses his thanks to all his colleagues and friends of Marine Wing who had provided reprints of their papers and other publications earlier.

References

Adiga, K.S. and Kalluraya, V.K.K., 1997: On the occurrence of manganese micronodules in the deep-sea sediment west of Lakshadweep Ridge, Arabian Sea. *Current Science,* **72(3)**: 206-210.

Anonyomous, 2016: Ministry of Mines, Annual report of GSI, 2015-16.

Balakrishnan, P. and Gangadharan, A.V., 2003: Bharat ke paschmi aptatiye chhetra mein ret ke nichhep ke sanket. *Samudrika,* **10 (1)**: 15-16.

Banerjee, B., Rao, V., Gupta, G, Joseph, E.J. and Singh, B.P., 1998: *Earth Planets Space,* 50, pp. 327-328.

Chandra, P.R., Shrivastava, P.C. and Mallik, T.K., 1978: Marine geosciences in the Geological Survey of India. *Records of the Geological Survey of India*, **110(2):** 125-150.

Chandra, P.R., Rao, B.R.J and Shrivastava, P.C., 1996: Minerals within the EEZ of India, India's exclusive economic zone: resources, exploitation,management. (Eds.) Qasim, S.Z. and Roonwal, G.S., Omega Scientific Publishers, New Delhi

Charlu, T.K. and Kallurayya, V.K.K., 1997: Ferro-manganese encrustations from Lakshadweep area, Arabian sea. *Journal of the Geological Society of India*, **49**: 389-394

Chaterji, G.C., Karunakaran, C. and Siddiquie, H.N., 1968: Exploration for minerals on the continental margin of India: an appraisal of the existing data: Symp. Indian Ocean, *Bulletin National Institute of Science, India*, **38**: 552-562.

Closs, H., Narain, H. and Garde, S.C. 1974: Continental Margins of India. *In*: The Geology of Continental Margins, (Eds.) C.A. Burk and C.L Drake. Springer Science+Business Media, New York: 629-639.

Faruque, B.M., 2002: Bharat ke purvi tat ke ek prayogatmak pura chaturtha kal samundra star vakra rekha. *Samudrika*, **9(1)**:29

Hashimi, N.H., Nigam, R., Nair, R.R. and Rajagopalan, G., 1995: Holocene Sea Level Fluctuations on Western Indian Continental Margin: An Update. *Journal Geological Society of India,* **46**: 157-162.

Jones, E.J., 1887: Natural History notes from HM's Indian Marine Survey Steamer 'Investigator' No. 5, on some noduler stones obtained by trawling off Colombo in 675 fathom of water, *Journal Asiatic Society of Bengal,* **LVI**: 209-212.

Mallik, T.K., 1976: Grain size variation in the Kavaratti lagoon sediments, Lakshadweep, Arabian Sea. *Marine Geology*, **20(1)**: 57-75.

Mallik, T.K., 1976: Shelf sediments of the Ganges delta with special emphasis on the mineralogy of the western part, Bay of Bengal, Indian Ocean. *Marine Geology*, **22(1)**: 1-32.

Naidu, A.S., 1968: Radiocarbon data of an oolitic sand collected from the shelf off the East Coast of India. *Bulletin National Institute of Science, India*, **38**: 467-471.

Nambiar, A.R., Abdulla, N.M., Dinesh, A.C., Gangadharan, A.V., Jayakumar, R., Jayaprakash, C., Kannan, S., Rao, M.K.,Charlu, T.K., Kumaran, K., Ramachandran K.V., Pai, P.R., Rahothman, V.K., Adiga, K.S., Unnikrishnan, E., Nair, E.V., Venkataramana, P. and Zaheer, B., 2002: Prospecting for offshore placer deposits in the area between Inayam (Tamilnadu) and Vizhinjam (Kerala) in southwest coast of India. *Geological Survey of India, Special Publication* **74**: 146-155.

Nambiar, A.R., Sukumaran, P.V. , Zaheer, B., Venkataramana, P., Kannan, S. Pai, P.R., Rahothman, V.K., Gujar, S, and Srinivas, K., 1992: Status of heavy mineral investigation off Konkan Coast *Marine Wing Newsletter*, *Geological Survey of India*, **VIII (1)**: 5-6.

Narasayya, B.L., Hari Prasad, M. and Vaz, G.G., 2002: Quaternary records and sea level oscillations along the east cost of India. *Marine Wing, Newsletter, Geological Survey of India*, **16(1)**: 10-11.

Rama Murty, M. and Shrivastava, P.C., 1979: Clay minerals in the shelf sediments of the northwestern part of the Bay of Bengal. *Marine Geology,* **33(1-2)**: M21-M32.

Rao, B.L., Ramamurthy, M., Vaz, G.G., Vijaykumar, P., Sankar, J., Maharana, C., Krishna Rao, J.V. and Murthy, P.S.N., 2001: Progress report on the search for phosphate and glauconite in the outer shelf and slope off Andhra and Tamil Nadu Coast. *Unpublished Report Geological Survey of India*.

Rao, B.R. and Faruque, B.M., 2002: Physiography of the Deep Seafloor of the western part of the Bay of Bengal. *Geological Survey of India, Special Publication* **74**: 17-23.

Rao, B.R. and Vaz, G.G., 1998: Gujarat ke aptatiye chhetra mein chuna mitti ke nichhep. *Samudrika,* **5(1)**: 31.

Rao, B.R., 1972: Coastal land forms of India. Geological Survey India, Publication.

Ravi Kumar, V., Khan. M.I.A., Vaz, G.G., Vijay Kumar, P., Sankar, J., Devdas, V. and Subba Rao, V., 2002: Offshore Placer Minerals Off Iduvanipalem of North Andhra Coast. *Geological Survey of India, Special Publication* 74: 183-186.

Saha, B.K., Rakshit , S., Majumdar, S., Sinha, J.K., Deb Roy, D.K. and Bhattacharya, D., 1997: Morphology and Sediment character of seamounts and undersea ridges in Andaman Sea. *Indian Minerals*, **50(4)**: 339-360.

Sanjeev, Raghav, 2002: Orissa aptat per Holocene Samudri charav evem bhitari Mahadwipiymagnatat per pura paryavarn mein parivartan ke kuchh praman. *Samudrika*, 9 (1).

Sen, M.K., Shrivastava, P.C., Dasgupta, T. and Chandra, P.R. 1978: Study of benthic foraminifera from the bottom sediments of the continental shelf of the west coast of India: *Abstract : 5th Micropalaeontological Colloquim, Aligarh.*

Sengupta, R., Khalil, S.M., Deb Roy, D.K., Mitra, S.K. and Bhattacharya, S., 1992: Heavy mineral placers off Orissa coast prospects and potential. *Marine Wing*

Newsletter, Geological Survey of India, **VIII(1)**: 7-10.

Senthiappan, M, Michael, G.P., Charlu, T.K., Jayakumar, R., Abdulla, N.M., Kumaran, K., Unnikrishnan, E. and Bhat, K.K., 1992: Multi mineral placer deposits off Kerala coast, *Marine Wing Newsletter, Geological Survey of India,* **VIII(1)**: 2-4.

Shrivastava, P.C., 1970: A mechanical device for releasing fluorescent tracers. *Marine Geology,* **9(5)**: M43-M46.

Shrivastava, P.C. 1975: Preparation of fluorescent tracer with indigenous dyes and binding media. *Indian Journal of Marine Sciences* **4(1)**: 95-96.

Srivastava, P.C. 1976: Study of movement of sediments by fluorescent tracers at Paradip Port, east coast of India. *Indian Journal of Marine Sciences,* **5(1)**: 121-124.

Shrivastava, P.C. and Rao, B.R., 1976: A note on the relict sand (?) and movement of sediments of Gopalpur, Orissa coast, India. *Journal of the Geological Society of India*, **17**: 401-404.

Shrivastava, P.C. and Viswanathan, T.V., 1978: The shelf sediments off Mangalore, West Coast of India. *Indian Minerals*, **32(1)**:43-49.

Shrivastava, P.C., 1975: A note on the study of movement of beach sand by fluorescent tracer at Paradip and Gopalpur, Orissa coast, India. *Journal of the Geological Society of India*, **16 (1)**: 78-83

Shrivastava, P.C., 2005: The possibility of exploitation of sand deposit within EEZ of India. All India Scientific and Administrative Workshop organized by the Geological Survey of India on 30-31 August, 2005 at Bangalore.

Shrivastava, Prem Chandra, 2013: Bharat Mein Samudri Bhuvigyan KaItihas (1871-2012). Shilalekh Publishers, Delhi, 358 pp.

Siddiquie, H.N. and Choudhury A.N., 1968: The distribution of phosphate in some samples of the shelf sediments off the west coast of India. *Bulletin National Institute of Science, India,* 38 (1): 483-490.

Siddiquie, H.N. and Mallik, T.K., 1973: Report on the investigation of the calcareous sand deposits in the lagoons of the Laccadives. Unpublished Report Geological Survey of India.

Siddiquie H.N., Dasgupta, D.R., Sengupta, N.R., Paul, J.C., Shrivastava, P.C. and Mallik, T.K. 1968. Unpublished Report Geological Survey of India.

Siddiquie, H.N. Shrivastava, P.C. and Vankatesh, K.V., 1971: A fluorescent tracer investigation of movement of beach sand in the Mangalore Harbour Project area. Unpublished Report Geological Survey of India.

Siddiquie, H.N., Dasgupta, D.R., Sengupta, N.R., Shrivastava, P.C. and Mallik T.K., 1978: Manganese –iron Nodules from the Indian Ocean. *Indian Journal of Marine Sciences*, 7: 239-253

Siddiquie, H.N., Shrivastava, P.C. and Mallik, T.K. 1971: Cruise Report – Marine geological cruises of R.V. Anusandhani. *Indian Minerals*, **24(4)**:383-386.

Siddiquie, H.N., and Shrivastava, P.C., 1970: Study of sediment movement by fluorescent tracers at Haldia Anchorage. *Current Science,***39 (20)**: 451-454.

Siddiquie, H.N., Shrivastava, P.C., Mallik, T.K., Ray, I. and Venkatesh, K.V., 1975: Bottom sediments map of the Seas bordering India. Geological Survey India Publication.

Tipper, G.H., 1911: The Geology of the Andaman lslands, with references to the Nicobars. *Memoirs of the Geological Survey of India*, **35 (4):** 195-216.

Vaz, G.G., Misra, U.S., Biswas, N.R., Vijaykumar, P.V., Krishna Rao, J.V.,Sankar, J. and Faruque, B.M., 1993: Lime mud in continental shelf edge and slope off Kachch. *Indian Journal of Marine Sciences,* **22(3)**: 209-215.

Vaz, G.G., 1995: Phosphatic nodules in the outer continental shelf off Madras, Bay of Bengal. *Indian Journal of Marine Sciences,* **24(1)**: 8-12.

Venkatesh, K.V., 1974: A note on the movement of sediments in the Kavaratti lagoon, Lakshadweep. *Indian Minerals*, **28(3):** 94-97.

Zaheer, B., Gangadharan, A.V. and Balakrishnan, P., 2005: National Seminar on mineral exploration, mining and mineral beneficiation and road map to vision 2020 held on 20-12 May, 2005 at Anna University, Chennai.

Indian Journal of Geosciences, Volume 74, No. 3
July - September, 2020; pp. 354-362

Invited Paper

Geoheritage sites and potential geoparks in India strategies for sustainable development

Sudesh Kumar Wadhawan

Adjunct Professor, Amrita Vishwa Vidyapeetham University, Kollam, Kerala-690525
Former Director General, Geological Survey of India
Email: wadhawansk.leo@gmail.com

Abstract: Indian terrain is bestowed with spectacular geodiversity showcasing geological phenomena and geomorphic landscapes. In 2015, the International Union for Conservation of Nature (IUCN) adopted a Resolution that affirmed Geodiversity and Geoheritage as integral parts of Natural Diversity and Natural Heritage. Thus, it is imperative to treat geodiversity and geoconservation as inseparable from biodiversity and nature conservation. The designated area of the Geopark incorporates not only geodiversity and geoheritage sites, but also the cultural, historical and biodiversity aspects, and it needs to be administered with specified management plan involving the local community. Sustainable economic development plans for the area covered by Geoparks are pursued through management of low-impact recreational, scientific, and educational activities. Achievement of sustainable development goals hinges on geotourism that is based on appreciation and conservation of natural geological features of the terrain and aesthetic values of landscape. In addition to the fauna and flora, geotourism thrives on abiotic dimension of the environment. As each geoheritage site has its own distinctive set of attributes - both natural geological as well as associated cultural, together with the socio-economic regional factors. Guidelines and a coordinated approach need to be adopted with defined roles and responsibilities of all concerned stake-holders, tour-operators and local community for long term engagements and societal benefits.

Adopting international good practices on application of geosciences and bottoms-up approach with well-informed support and involvement of local community will promote long awaited development of potential geoparks in India for sustainable development. Present contribution elaborates on strategies for integrated geoconservation and utilizing potential of delineating, protecting and conserving the geodiversity as part of the natural heritage resources for sustainable development of local communities. It is sought to be achieved through programmed management plan and geotourism by collective efforts of Government and non-government stakeholders.

Keywords: Geodiversity, Geoheritage sites, Geoparks, Geotourism, Sustainable Development, India

Introduction

Indian subcontinent is bestowed with spectacular geodiversity and a variety of geoheritage sites. Several natural sites of geological significance and landscapes aesthetic qualities have been delineated in the lofty young mountain ranges of the Himalaya in the north, dissected rugged rocks of the continental volcanic eruptions of the Deccan Traps in the central region, the Precambrian rocks and landscapes of Indian peninsula in the south, the dryland sedimentary environment of the Thar Desert in the west and the rain soaked geomorphic features and geological treasures of north-eastern India have universal appeal and hold important position in Earth's geological history (GSI, 2001, 2012; Kale, 2009, 2010; Singh and Anand, 2013; Bhargava, *et al.* 2010; Wadhawan, 2013; 2016; 2020; Govt. of India-GSI, 2016; Ranawat and Soni, 2019; Shekhar *et al.*, 2019; Patnaik, 2019).

Ever since the International Union for Conservation of Nature (IUCN) has adopted a Resolution in 2015, that affirmed Geodiversity and Geoheritage as integral parts of Natural Diversity and Natural Heritage; it is imperative to treat geodiversity and geoconservation as inseparable from biodiversity and nature conservation. Presently development of the Geoparks has become major international theme implying application of geosciences for inclusive growth of society and protection/ conservation of unique Geoheritage.

As per Charter of Functions, Geological Survey of India (GSI) has been mandated to identify, preserve and make initial and sustained efforts in conservation and protection of the unique Geoheritage sites in the country (Government of India, 2009). Consequently, GSI has been making programmed attempts in studying and protecting natural geoheritage sites of rare and unique geological and geomorphologic significance (GSI, 2001; Wadhawan, 2013). Such endeavours were initiated way back in 1951 and presently 38 Geoheritage sites have been part of an integrated concept of protection, education and sustainable development. However, in Indian context, lot more needs to be accomplished for systematic promotion and upkeep of geoheritage sites/ and integrated development of geoparks beyond identification and declaration of a geological monuments or geoheritage sites (INTACH, 2016; Dowling and Newsome, 2010). It is realised that geotourism is based on appreciation of natural geological features of the terrain and aesthetic values of landscape. In addition to the fauna and flora, geotourism thrives on abiotic dimension of the environment and is treated as an integral part of the UNESCO's Geopark programmes (UNESCO, 1999; 2015; Eder, 2008; Lazzari and Aloia, 2014). Besides, geotourism and recreational activities based on geodiversity elements were completely integrated in the aims of the International Year of Sustainable Tourism, as was proclaimed by the United Nations for 2017 (Shekhar *et al.* 2019). In the following sections I have attempted to elaborate on definitions and unique characteristics of geodiversity, geoheritage sites and suggest some of the potential and eligible geoparks in India. It is followed by a synthesis on significance of geoconservation and strategies for sustainable development are enumerated.

Geodiversity, geoheritage and geoparks

In order to increase awareness about geological heritage (together with biological heritage) that forms part of natural heritage, it is imperative to appreciate the basic concepts about the geoheritage, geodiversity, geoparks and geoconservation (Patzak and Eder, 1998; Eder, 1999; Brocx and Semeniuk 2007; Henriques *et al.*, 2011; Hose, 2012; Reddy and Sarma, 2013; Wadhawan, 2020). These are enumerated below: -

Geodiversity is defined as the variety of non-living elements of nature. Geodiversity is expressed in geological formations as variety of rock formations, minerals, fossils, tectonic structures; geohydrological features such as rivers and lakes, soils and geological processes that created distinctive minerals and rock assemblages and landscapes. It is the major abiotic component of lithosphere that supports geomorphic processes and landforms, biodiversity and ecosystems (Stanley, 2000; Gray, 2004). Geodiversity underpins biodiversity, but has its own intrinsic values independent of biodiversity. Geodiversity is essential to human well-being and provides the foundations and habitats for all living things. It is the source of materials that build our towns and cities, it provides our energy resources, including renewable energy and the materials mined to manufacture the wind turbines, solar panels, etc.; it allows us to bury our waste, provides us with freshwater and attenuates our pollution; it inspires our artists and provides us with incredible landscapes from mountains to coasts.

Geoheritage is the abbreviated version of the term geological heritage. It includes any area/ place/ mining site located inland and/or offshore within the territorial waters of the country containing distinctive examples of geological materials (e.g. sediments, rocks, minerals and fossils) and phenomena, stratigraphic type sections, geological structures and geomorphic landforms including caves, natural rock-sculptures of national/ international interest. It is part of the natural heritage of a certain area constituted by geodiversity elements with particular geological value and hence worthy of safeguard for the benefit of present and future generations. Geoheritage can include both in situ elements (geosites) or ex situ elements (collections of geological specimens) having paleontological, geomorphological, mineralogical, petrological or stratigraphic significance, etc. Studying, protection and development of geoheritage sites achieve its goals through a three-pronged approach: conservation, education and geotourism respectively (Hose, 2012; Gray *et al.* 2013)**.**

A **Geopark** means single unified geographical area where natural heritage sites and landscapes of national/ international geological significance are managed with a holistic concept of protection, education and sustainable development (Eder and Patzak, 2004). Geopark is a distinctive area that advances the protection and use of geological heritage in a sustainable way, and promotes the economic well-being of the people who live there. Therefore, geoparks are places (delineated and designated area in contrast to a singular specific Geosite or the Geological Monument) where rare geoheritage sites with geomorphic landscapes and geological phenomena are preserved intact with local community involvement and where sustainable economic development plans are pursued through low-impact recreational, scientific, and educational activities. Geoparks can be of National and/or Global significance (Eder, 1999; 2004; 2008; McKeever and Zouros, 2005; Ahluwalia, 2006; Mazumdar, 2007). As on July 2020 there are 161 Global Geoparks in 44 countries.

Geoheritage sites in India

As the National custodian, it is the bounden duty of GSI to delineate and maintain the Geoheritage sites in India either on its own or in collaboration with the State Government authorities who have been convinced for its intrinsic worth and geotourism potential. GSI has been making concerted efforts in studying and protecting natural sites of rare and unique geological and geomorphologic significance. Such endeavours were formally initiated way back in 1951 when two major geosites: Fossil wood occurrences near Thiruvakkarai, South Arcot district and Sattanur area near Tiruchirapalli district in Tamilnadu in southern India were declared National Geological Monuments by GSI. Thereafter, between 1974 and 1981, over 20 geosites were declared as geological monuments by GSI. A comprehensive account of 26 geological monuments was compiled by GSI in a Special Publication No.61 in 2001 (GSI, 2001; Wadhawan, 2013; INTACH, 2016). Several other prominent geoheritage features and landscapes have also been added to make the list go up to 40 geosites and landscapes that need to be preserved as part of geoconservation and promoted as geotourism hotspots. An attractive book on the 40 nos. of Geotourism Hotspots in India as published under aegis of 36th IGC Secretariat and released during the 35th IGC at Cape Town, South Africa in September 2016 (Government of India - GSI, 2016). Out of these 40 listed Geotourism Hotspots in India, four are large geo-ecological zones/ regions namely: Kerala Backwaters, Kerala; Sundarban Mangrove Forests, West Bengal; Thar Desert, Rajasthan (Wadhawan, 2016; Mathur *et al.* 2017) and Shyok-Nubra Valley, Ladakh that also preserve the pristine natural beauty, landscapes, geodiversity and biodiversity. Although there are many more potential geosites, such as the Bellum Caves in Kurnool district, Andhra Pradesh, Ajanta and Ellora Caves in Maharashtra (Sheth *et al.* 2017), Deccan Trap landscapes of distinctive volcanic lava flows in Maharashtra (Kale, 2010), Zawar (Udaipur) ancient mining and oldest metallurgical sites, Rajasthan (Ranawat, 2019), etc., that are already well known geotourists hotspots and maintained by the concerned State Governments, the other 38 officially recognised National Geological Monuments/ Geoheritage sites and under consideration in India (**Fig.1**) are categorised here in the following genetic, geoscientific and geomorphic groups:-

I. Large and unique rock assemblages, geological formations and rare mineral deposits

1. Peninsular Gneiss, Lalbagh, Bengaluru, Karnataka
2. Charnockite, St. Thomas Mount, Chennai, Tamilnadu
3. Laterite near Angadipuram PWD Rest House premises, Malappuram district, Kerala.Volcanogenic bedded Barytes, Mangampeta, Cuddapah district, Andhra Pradesh
4. Gossan in Rajpura-Dariba Mineralised Belt, Rajsamand district [formerly part of Udaipur district], Rajasthan
5. Kishangarh Nepheline Syenite, Ajmer district, Rajasthan
6. Naga Hill Ophiolite Suite, near Pungro, Nagaland
7. Panjal Volcanics in Srinagar district, Jammu & Kashmir

II. Geological boundaries and contacts of stratigraphic significance

1. Eparchaean Unconformity, Tirumala - Tirupati Road, Chittoor district, Andhra Pradesh.
2. Barr Conglomerate, Pali district, Rajasthan
3. Malani Igneous Suite of rocks contact with Jodhpur Group of sedimentary rocks, Jodhpur district, Rajasthan

III. Tectonic structures of regional significance

1. Great Boundary Fault at Satur in Bundi district, Rajasthan

IV. Meteorite Impact structures

1. Lonar Lake Buldana district, Maharashtra
2. Dhala Impact Structure – a geoheritage site in Shivpuri district, Madhya Pradesh
3. Ramgarh Large Complex Impact Structure, Baran district, Rajasthan, India

V. Significant volcanic features of past geologic events of eruption

1. Pyroclastic and Pillow Lavas, Kolar Gold Fields, Kolar district, Karnataka
2. Columnar Lava, St. Mary Island, Karnataka
3. Pillow lavas near Mardihalli, Chitradurga district, Karnataka
4. Pillow Lava in Iron ore belt at Nomira, Keonjhar district, Odisha
5. Welded Tuff, Malani Igneous Suite, Jodhpur district, Rajasthan

VI. Rare sedimentary structures

1. Sedimentary Structures – Eddy Markings, Kadana Dam, Panch Mahals district, Gujarat.

VII. Fossils and fossiliferous stratigraphic markers

1. Fossil Wood Park near Tiruvakkarai, South Arcot district, Tamil Nadu
2. National Fossil Wood Park, Sattanur, Perambalur district, Tamil Nadu
3. Siwalik Fossil Park, Saketi, Sirmur district, Himachal Pradesh

4. Stromatolite Fossil Park, Jharmarkotra Rock Phosphate deposit, Udaipur district, Rajasthan:
5. Stromatolite Park near Bhojunda, Chittaurgarh district, Rajasthan
6. Akal Fossil Wood Park, Jaisalmer district, Rajasthan
7. Lower Permian Marine Beds at Mahendragarh, Surguja district, Chhattisgarh [formerly part of Madhya Pradesh]
8. Stromatolite bearing Dolomite Limestone of Buxa Formation at Mamley, near Namchi, South Sikkim district, Sikkim
9. Salkhan Stromatolite Fossil Park, Sonbhadra district, Uttar Pradesh
10. Plant Fossil bearing Inter-Trappean beds of Rajmahal Formation, Upper Gondwana sequence around Mandro, Sahibganj district, Jharkhand
11. Raiyoli- Balasinor dinosaur Fossil Park, Kheda district, Gujarat
12. Karai badlands -Kulakkalnattam Geological Section, Perambalur district, Tamilnadu.

VIII. GEOMORPHIC SCULPTURES AND LANDSCAPES

1. Sendra Granite, Pali district, Rajasthan
2. Natural Geological Arch, Tirumala Hills, Chittoor district, Andhra Pradesh
3. Varkala Cliff, Thiruvananthapuram district, Kerala
4. Erra Matti Dibbalu, Vishakhapatnam district, Andhra Pradesh
5. Arwah – Lumshynna Cave, East Khasi Hills district, Meghalaya

1. A.P. - Eparchaean Unconformity
2. A.P. - Erra Matti Dibbalu
3. A.P. - Mangampeta Baryte
4. A.P. - Natural Rock Bridge
5. Chhattisgarh - Marine Fossils
6. Gujarat - Eddy Current
7. H.P. - Siwalik Fossil Park, Saketi
8. Jharkhand - Mandro Plant Fossils
9. Karnataka – St. Mary Columnar Basalt
10. Karnataka - Maradihalli Pillow Lava
11. Karnataka - Peninsular Gneiss
12. Karnataka - Pyroclastic Rocks
13. Kerala - Angadipuram Laterite
14. Kerala - Varkala Cliff
15. Maharashtra - Lonar Lake
16. Nagaland - Nagahill Ophiolite
17. Odisha - Nomira Pillow Lava
18. Rajasthan - Akal Fossil Wood Park
19. Rajasthan - Bar Conglomerate
20. Rajasthan - Bhojunda Stromatolite
21. Rajasthan - Great Boundary Fault
22. Rajasthan - Jhamer Kotra Stromatolite
23. Rajasthan - Jodhpur-Malani Contact
24. Rajasthan - Nepheline Syenite
25. Rajasthan - Rajpura-Dariba Gossan
26. Rajasthan - Sendra Granite
27. Rajasthan - Welded Tuff
28. Sikkim - Mamley Stromatolite
29. T.N. - Karai- Kulakkalnattam Badlands
30. T.N. - Sattanur Fossil Wood
31. T.N. - St. Thomas Mount Charnockite
32. T.N. - Tiruvakkrai Fossil Wood

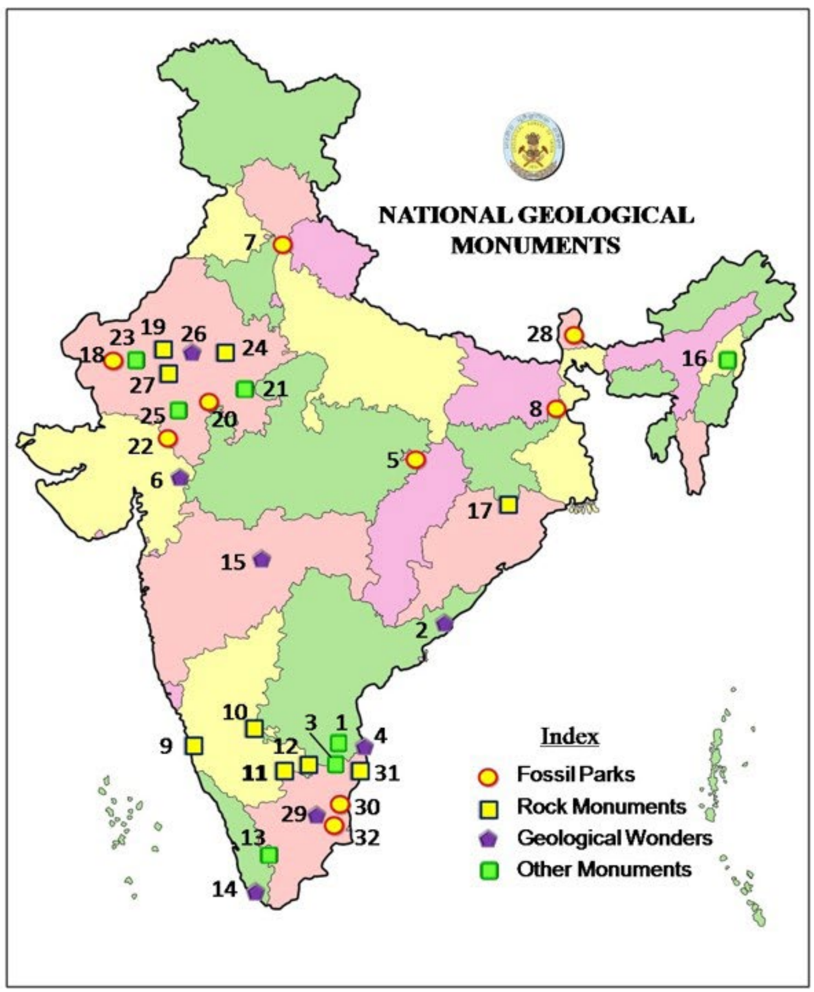

Fig.1: Geoheritage sites in India (as declared by GSI).

Geoconservation and potential geoparks in India

It is worth recording that the geoparks initiative was formally launched by UNESCO in response to the perceived need for an international initiative that recognizes sites representing an earth science interest, while at the same time creating employment opportunities and promoting regional socio-economic development (UNESCO, 1999; 2015). The Global Geoparks Network (GGN) works in synergy with UNESCO's World Heritage Centre and Man and the Biosphere (MAB) World Network of Biosphere Reserves (Eder and Patzak, 2004; Brocx and Semeniuk, 2007; Henriques and Brilha, 2017).

Geoconservation of geoheritage sites and geoparks is intimately linked to the concept of global sustainable development goals for overall harmonious living with and protection of natural heritage. It is increasingly realised that geoheritage is a non-renewable natural resource and gets adversely affected by natural factors such as: weathering, erosion, climate change as well as human interventions for changed land-uses that can result in a partial or total loss of geological sites. The risk of its damage is triggered also by urban development, vandalism, smuggling of geological samples owing to absence of a proper legal protection and international agreements, or lack of expertise and poor understanding by local and national authorities. Therefore, proper identification of geosites and landscapes, their characterization, publicity and suitable management of these localities will enable their preservation and for reaping the benefits of promoting geotourism, thereby building mutually beneficial relationships between geoscientists, site owners and/or local and regional authorities and communities (Robinson, 1998; Dowling, 2011; Shekhar, *et al.* 2019; Wadhawan, 2020).

Geoconservation deals with effective mechanisms for preservation of significant earth science features – the geoheritage sites, for purposes of education, science and heritage and value added recreation (Sharples, 2002; Henriques, *et al.* 2011; Hose, 2012). It means the conservation of geodiversity for its intrinsic ecological and heritage values in such a manner so as to prevent all forms of excavation, removal, damage, defacement, or any other forms of interference. Well-managed geoheritage sites can support different types of sustainable use with clear benefits for the society, such as educational, scientific and economic uses. Geoconservation needs to promote geotourism circuits for sustainable growth of the locally involved communities. This is already happening in many territories around the world through the establishment of Global Geoparks which have recently been fully recognized by UNESCO.

There are several regions in India that are bestowed with a spectacular geodiversity containing one or more geosites of particular geological/ geomorphological importance, with associated sites of biodiversity, cultural and archaeological importance, and where educational, scientific and tourism activities can be promoted through geoconservation and geotourism means in a designated Geopark. What has been lacking perhaps is the drive and political will to make concerted efforts to devise legal framework for their protection and conservation and promotion of organised geotourism that would enable generation of resources for their maintenance and sustainable development of local community. Nevertheless, it is heartening to note that the Government of India is presently sieged of the matter and a suitable legislation is being finalised on "Conservation of Geoheritage Sites and Development of Geoparks" (Government of India, 2020). The Bill seeks to constitute a nodal organization at the Centre and a statutory Board at the State levels respectively for regulating various activities pertaining to geoheritage conservation, management and promotion, primarily through setting of a network of geoparks in the country.

Accordingly, several potential Geopark in India, at State and National levels, need to be put in place the management plans focussed on geoconservation linked to geotourism and designed to foster sustainable socio-economic development. A Geopark, at State/National level or subsequently at the global level, must inform and educate people about the broader environmental issues with respect to Earth heritage conservation, sustainable use and need for natural resources, whether they are mined, quarried or harnessed from the surrounding environment, while at the same time promoting respect for the geological environment and the integrity of the landscape.

There are several known Geoheritage sites that are of regional importance for geoscience education and recreation purpose (and may not necessarily be of National importance). However, these Geoheritage sites also need to be conserved. Consequently, several State level Geoheritage sites and Geoparks that are not formally recognised as natural heritage resources of national importance, but have been duly recognised as rare geodiversity sites and Nature (Fossil) Parks of regional significance. These geosites and geoheritage parks are well known and have been promoted for geotourism, for instance: the Arwah – Lumshynna Cave, East Khasi Hills district, Meghalaya; Kolodyne Castle, Mizoram; Amkhoi Fossil Park near Illambazar, Birbhum district and Gongoni Grand Canyon of West Bengal; Urvakal Rock garden and Belum Caves in Kurnool district; Borra Caves and Gandhikota Gorge, Pennar River, Andhra Pradesh; Dinosaur Fossil Park at Raiyoli - Balasinor, Kheda district, Gujarat; Natural Coral Bridge, Neil Island, Andamans; Narmada River Gorge through Marble Rocks, Bhedaghat, Jabalpur, M.P.; Narmada Dinosaur Fossils and petrified Egg-nests and fossilised Wood Park (large tree trunks) at Mandu, Bagh-Lameta in Dhar District, M.P.; Balancing Rocks, Hampi, and Yana Rocks near Yana village in Karnataka, etc., (INTACH, 2016; Ranawat and Soni, 2019; Ravi Vundavalli, personal communication). Similarly, there are several other candidates in India that fulfil the requirements to be considered as Geoparks at the State and National levels to begin with. Subsequently as the geoconservation and management plans take roots and fructify with support of local community and organised geotourism, the Geopark is ready to be considered and approved as part of GGN. Some such potential Geoparks that have well established unique geodiversity, biodiversity and associated cultural/ historical heritage include the following:

1. **Aravalli Geopark:** Udaipur - Zawar Lead-Zinc Mines – oldest Zinc metallurgical sites, Precambrian rocks and landscapes of Aravalli Hills, Rikhabdeb Serpentinite (commercially called Green Marble) quarries – Stromatolites Fossils Park at Jhamarkotra, and Mewarh cultural heritage of Udaipur, Rajasthan.

2. **Thar Desert Geopark:** Welded Tuff (700 Ma old) acid volcanic rocks and, stratigraphic disconformity between Malani Igneous Suite of rocks in contact with Jodhpur Group of sedimentary rocks, Mehrangarh Fort hill, palaces and desert rock gardens**,** Jodhpur; Desert Landscapes golden active sand dune fields and landscapes, unique dryland biodiversity, Akal Fossil Wood Park and Dinosaur foot-prints and fossiliferous yellow Jurassic rocks and cultural heritage sites, UNESCO's World Heritage Hilltop Fort and temples, Jaisalmer. Thar Desert preserves records of past climate change in their deposits and landforms and are educators on current climate change besides showcasing modern generation of renewable energy, Solar PV panels and Wind-mills.

3. **Jaipur Uplands and Desert Margin Geopark:** Achrol - Ajitgarh –Sambhar Salt Lake, Jaipur UNESCO's World Heritage City and Palaces, world's oldest and largest stone astronomical observatory (Jantar Mantar), Aravalli Hills (Precambrian Fold Mountain range), Palaeoclimatic indicators preserved by Quaternary formations and intensely dissected obstacle dunes, Sambhar: the Ramsar Wetland of inland Salt Lake, with geoarchaeological Palaeolithic sites; Ajitgarh-Viratnagar Granite Hills and landscapes and Kishangarh Syenite Geoheritage site and important cultural heritage, traditional bazars in planned historic city, international centre of gems and jewellery, diamond and gemstones cutting and polishing theme parks etc., Rajasthan.

4. **Himalayan Geopark Splendour:** Glaciated Spiti Valley is a natural Geopark of cold dryland environments; the rugged landscapes and fossiliferous geological formations of the Tethyan Sea, 250 million year old section recording Triassic catastrophic mass extinction, near Spiti, Quaternary terraces and landforms, tracking trails, etc., Himachal Pradesh.

5. **Eastern Ghats and Coastal environment Geopark:** Konark Sun temple - Chilka Lake biodiversity, coastal Quaternary tracts, Palaeo-strandlines and Neogene evolutionary history - Dholagiri- Khandagiri Jain and Buddhist temples Khondalite Hills, Unique tracts of Gondwanaland; East Coast bauxite and industrial revolution, cultural heritage, arts and crafts, etc., Odisha

6. **Deccan Traps Geopark of Large Igneous Province:** volcanic rocks and landscapes – Pune Forts and palaces-Mahabaleshwar – Koyna Crater Lake, Geo-archaeological sites, Palaeolithic human implements, etc., Maharashtra.

7. **Andaman & Nicobar Islands Geopark –** Landscapes, features of live volcanic eruptions, seismotectonics, ophiolite of Mesozoic age and 55Ma evolutionary history of earth and cultural and historical heritage sites associated with colonial rule and of Indian independence provide the required unique geodiversity and biodiversity ingredients to develop and conserve a Geopark in selected and demarcated areas. It is further emphasised that such Geopark would promote awareness of geological hazards, including volcanoes, earthquakes and tsunamis, and may help prepare disaster mitigation strategies and resilience among local communities.

8. **Vishakhapatnam- Erra Matti Debbalu – Khondalite Hills Geopark:** Unique Coastal deposition, sandy pocket beaches and erosional features, cliffs and a bridge; Quaternary geological and geomorphic evolution and highly dissected coastal red sands dune fields - Rajahmundry Deccan Traps- volcanic rocks and inter-trappean sedimentary beds hosting a variety of Cretaceous age fossils geoheritage sites, cultural heritage and historical Buddhist and Hindu temples, Andhra Pradesh.

9. **Varkala Cliff - Thiruvananthapuram Geopark:** Varkala Cliff is a unique major cliff in the state of Kerala facing the Arabian Sea. It exposes a geological type section of the Tertiary sedimentary rocks, coarse sandstone and shale with minor thin seams of lignite (Mio-Pliocene age of 15-23 million years) of the Warkalli Formation. It provides a great scenic view of shoreline littoral deposits, beaches of shallow marine – estuarine environment and Neogene tectonics. Janardana Swami Temple is more than 2,000 years old. Thiruvananthapuram has rich cultural heritage, palaces and museums, traditional Ayurveda Research Centres and very ancient Hindu temples and old churches.

10. **10. Kachchh Jurassic and Cenozoic Geoparks:** It is a natural Geopark for a variety of typical sedimentation in a Jurassic rift-basin preserving rock types with distinctive fossils assemblages of macro-invertebrate fauna and rare exposures of Dhosa Golden Oolite Member of Oxfordian age. Well exposed successions of Cenozoic

Type Sections with diagnostic fossils show spectacular landscape of dryland environment. Besides, the famous white salt encrusted vast Ranns – the tidal flats of the sabkha environment, seasonally inundated with sea water and features of active seismotectonics provide a treasure of interesting rock types, structures and evolutionary geological history to geoscience researcher and visitors alike. Associated geoarchaeological finds of Dholavira (equivalent to Harappa settlements), cultural heritage, Bhuj Fort, palaces, traditional water reservoirs (S*arovars*) and various old temples and small traditional ports and excellent accessibility make Kachchh a bright candidate to be declared as a Geopark of global significance.

These potential Geoparks and geoheritage sites with outstanding universal values and cultural attributes and are accessible with good infrastructure and have already been on the general tourism circuits with thriving hotel and hospitality industry. However, modern concepts of geotourism need to be popularized with good literature providing authentic interpretations, in situ protection, and emphasising on the crustal evolution and earth history (Fursich *et al.*, 2013; Shekhar *et al*., 2019; Wadhawan 2016; 2020). An attempt has been made to popularise these thematic Geoparks and geoheritage sites therein on a series of Webinars delivered recently by different authors/ experts on the subjects that can be accessed at: https://www.youtube.com/playlist?list=PLXLRRyPdGXkD1uoGoRPP9gL4obh2JqlkW (courtesy: Ravi Vundavalli, personal communication).

Strategies for sustainable development

Strategies for sustainable development must promote geoconservation of geodiversity through involvement of all stake holders - both government and non-government. It is realised the world over that geotourism has proven to be essential support system for overall regional sustainable development that can leverage creation of employment and service industry, boosting economic growth and rise in living standards of local communities. Therefore, it is imperative to appreciate that geotourism is knowledge based tourism, an interdisciplinary integration of the tourism industry with conservation and interpretation of abiotic attributes of nature, besides considering related cultural issues, associated with the geosites for the general public. It is a form of natural area tourism that specifically focuses on landscape and geology. Geotourism involves the provision of interpretative facilities and services to enable tourists to acquire knowledge and understanding of the geology and geomorphology of a site (including its contribution to the development of the Earth Sciences), beyond the level of mere aesthetic appreciation and recreation.

UNESCO's agenda on Sustainable Development Goals (SDGs) consist of 17 goals and 169 targets, covering topics as diverse as food security, education, gender equality, energy supply and sustainable consumption and production patterns (UNESCO, 2015). However, in the context of Geoheritage sites, geoparks and related geotourism, some SDGs have direct relevance and responsibility for achieving the targets by 2030. Therefore, geoconservation of biodiversity and geodiversity will help address issues of ending poverty in all its forms (Goal No.1), improve quality educational activities for all ages and to spread awareness of our geological heritage and its links to other aspects of our natural, cultural and intangible heritages (Goal No. 4); achieve gender equality and empower all women and girls through educational programmes or the development of women's cooperatives (Goal No. 5). The promotion of sustainable local economic development needs to be through sustainable (geo) tourism and local culture and products (Goal No. 8). Geoparks will necessarily encourage human settlements and cities around them inclusive, safe, resilient and sustainable and teach the local communities and visitors to live in harmony with nature (Goal Nos.11&12). Finally, the geoparks will promote creating awareness towards impacts of and take action to combat climate change (Goal No. 13) and strengthen the means of implementation and revitalize the regional and global partnership for sustainable development (Goal No. 17). These emerging considerations need to be developed and followed in conformity with the international best practices and for regional sustainable development.

Concluding remarks

I have analysed and discussed various aspects and need for geoconservation of geodiversity, geoheritage sites and development of listed potential geoparks in India. It is recognised that Geoparks play an innovative and important role in the protection and conservation of natural and geological heritage for cultural sustainability in rural areas. A formally declared Geopark has the potential to stimulate local socio-economic and socio-cultural development and accelerate growth of infrastructural support thereby attracting an increasing number of visitors.

It is expected that emerging economies including that of Indian society, would gear up to fully recognize and optimally utilise the great potential of geodiversity and geoheritage sites through geotourism. As each geoheritage site has its own distinctive set of attributes - both natural geological as well as associated cultural, together with the socio-economic regional factors, guidelines and coordinated approaches need to be adopted with well-defined roles and responsibilities of all concerned stake-holders, tour-operators and local community for societal benefits. However, protection and conservation of such rare and unique geodiversity and natural heritage resources need to be buttressed by legal enactments.

GSI being a National survey organisation and as an attached department of Ministry of Mines, with its country-wide presence/ network and trained Geoscientists having diverse specialisation and national resources at their command, should continue to be recognised as the Nodal Agency by Government of India. GSI must also be strengthened on a continuing basis to remain the chief custodian of immense geodiversity and geoheritage sites, tasked with identification, delineation and granting formal approval or recognition to such geological monuments or the geoheritage sites and regions of unique geo-ecological and earth science values.

As ownership of the land rests with the State Governments, the declaration of geoparks will rely largely on how the States rise to the occasion and put in place a well-planned comprehensive management model to enhance the value and conservation of the various biotic and abiotic components of the potential geoparks. There are several international good practices that provide guidelines and standard operating procedures which can be formulated to suit local conditions (Henriques, *et al.,* 2011; Hose, 2012).

Where GSI has the ownership of the allocated land**,** it must be maintained by it. Involvement of professional geoscience conservation experts and consultants will add value to the project, improve upkeep, awareness campaigns, help increase visitor footfalls for selected Geoheritage sites / Geoparks and promote geotourism and fulfilment of SDGs. Refurbishing of attractive & info-loaded Signage and Display Boards that unfold the narrative as captivating stories and well-stocked Geoheritage Museum with explanatory notes are needed to be displayed within the Geopark.

Acknowledgements

The Director General, GSI is thanked for his encouragement and providing a credible platform and Shri Prakash C. Patra, Dy. DG, CHQ, GSI Kolkata and his team for bringing out this publication in a record time. Shri EVR Parthasaradhi is thanked for launching the Late K. Krishnaunni Trust and steering the entire movement to admire and enthuse commemorative publication in memory of Late K. Krishnaunni**,** former DG, GSI.

References

Ahluwalia, A.D., 2006: Indian Geoheritage, geodiversity: Geosites and geoparks. *Current Science*, **91(10)**: 1307.

Bhargava, O.N., Kumbkarni, S. and Ahluwalia, A.D., 2010: Geomorphology and landforms—Illustrations from Himachal Himalayas. Technology Publications, Dehradun, 211 p.

Brocx, M. and Semeniuk, V., 2007: Geoheritage and geoconservation—history, definition, scope and scale. *Journal of the Royal Society of West Australia*, **90**:53–87

Dowling, R.K., 2011: Geotourism's Global Growth. *Geoheritage*, **3(1)**, 1-13.

Dowling, R.K. and Newsome D., 2010: Global geotourism perspectives. Goodfellow Publishers, Oxford.

Eder, W., 1999: UNESCO Geoparks' – A new initiative for protection and sustainable development of the Earth's heritage. *Neues Jahrbuch für Geologie und Paläontologie - Abhandlungen,* **214(1)**: 353-358.

Eder, W., 2008: Geoparks – Promotion of Earth Sciences through Geoheritage Conservation, Education and Tourism. *Journal Geological Society of India*, **72(2):** 149-154.

Eder, W. and Patzak, M., 2004: Geoparks – geological attractions: tool for public education, recreation and sustainable economic development. *Episodes*, 27(3), 162-164.

Fursich, F.T., Matthias Alberti and Pandey Dhirendra K., 2013: Stratigraphy and palaeo-environments of the Jurassic rocks of Kachchh – Field Guide. Beringeria Special Issue-7, Erlangen, 174p.

Geological Survey of India (GSI), 2001: National Geological Monuments (Anantharamu, T.R., Bellur, D., Bhasker, A.A., Eds.). *Geological Survey of India, Special Publication*, **61**, 98 p

Geological Survey of India (GSI), 2012: Travel brochure on National Geological Monuments of India: Region South. Geological Survey of India, Hyderabad, 12 p

Government of India, 2009: Report on the functioning of Geological Survey of India, Ministry of Mines. New Delhi. 369 p.

Government of India, 2016: Geotourism Hotspots of Indian Subcontinent, 36th International Geological Congress (IGC), C/o Geological Survey of India. New Delhi, 101p.

Government of India, 2020: Minutes of the 1st Meeting of the Task Group for drafting Geoparks/Geo-heritage Bill/ Legislation, held on 1st April, 2020, Ministry of Mines, New Delhi, 5p.

Gray, M, 2004: Geodiversity: Valuing and Conserving Abiotic Nature. John Wiley & Sons, Chichester UK, 434p

Gray, M., Gordon, J. E. and Brown E.J., 2013: Geodiversity and ecosystem approach: the contribution of geoscience in delivering integrated environmental management. *Proceedings of the Geologists' Association*, **124(4):** 659-673.

Henriques, M.H., Pena dos R., R., Brilha, J., and Mota, T.S., 2011: Geoconservation as an emerging geoscience. *Geoheritage*, **3(2)**: 117–128.

Henriques, M.H. and Brilha, J., 2017: UNESCO Global Geoparks: strategy towards global understanding and sustainability. *Episodes,* **40(4)**: 349-355.

Hose, T. A., 2012: 3G's for Modern Geotourism. *Geoheritage*, **4**, 7-24

Indian National Trust for Art and Cultural Heritage (INTACH), 2016: A monograph on National Geoheritage Monuments of India. Natural Heritage Division, New Delhi. 146p.

Kale, V.S., 2009: DEM-based studies of some outstanding fluvial landforms in India. *In*: Geomorphology of India, Sharma H.S., Kale V.S. (Eds.). Prayag Pustak Bhavan, Allahabad, 59–68.

Kale, V.S., 2010: The Western Ghats: the great escarpment of India. *In*: Geomorphological landscapes of the world, Migon P (Ed.). Springer, New York, 257–264.

Lazzari, M. and Aloia A., 2014: Geoparks, Geoheritage and Geotourism: Opportunities and Tools in Sustainable Development of the Territory. *GeoJournal of Tourism and Geosites,* **13(1)**, 8-9.

Mathur, S.C., Pradip. K., Rathore, S.S. and Mathur, S., 2017: Mehrangarh Ridge of Jodpur City, Western Rajasthan, India: Its Geoheritage and Geotourism Sites, In Proceedings of International Geopark Conference in Taiwan, 45-51.

Mazumdar, M.K., 2007: The Geopark Initiative. *Current Science*, **92(1):** 13.

McKeever P.J. and Zouros N., 2005: Geoparks: Celebrating earth heritage, sustaining local communities. *Episodes*, **28(4)**: 274-278.

Ranawat, P.S., 2019: Zawar- world's oldest Zinc mining and metallurgical site. Geography & You, 87-94.

Ranawat, P.S. and Soni G., 2019: Potential Geoheritage & geotourism sites in India. *International Journal of Scientific and Research Publications*, **9(6)**: 91-96.

Patnaik, R., 2019: Popularising geosciences in India. *Current Science,* **116(11)**: 1779-1780.

Patzak, M. and Eder, W., 1998: UNESCO Geopark, a new programme—a new UNESCO label. *Geologica Balcania*, **28(3–4)**: 33–35.

Reddy, D.R. and Sarma, R., 2013: Proceedings of National Workshop and Brainstorming Session on Geoheritage Sites in India- Need for an Indian Activism. Department of Geology, Andhra University and INTACH, Visakhapatnam, 30–31 May 2013, 94p.

Robinson, E., 1998: Tourism in geological landscapes. *Geology Today,* **14(4)**: 151–153.

Sharples, C., 2002: Concepts and principles of Geoconservation. Tasmanian Parks & Wildlife Service, Hobart.

Shekha,r S., Kumar, P., Chauhan, G. and Thakkar, M.G., 2019: Conservation and sustainable development of Geoheritage, Geopark and Geotourism: a case study of Cenozoiic successions of Western Kutch, India. *Geoheritage*, **11**: 1475-1488.

Sheth, H., Samant, H., Patel, V. and D'Souza, J., 2017: The Volcanic Geoheritage of the Elephanta Caves, Deccan Traps, Western India. *Geoheritage,* **9(3)**: 359–372.

Singh, R.B. and Anand, S., 2013: Geodiversity, geographical heritage and geoparks in India. *International Journal of Geoheritage,* **1**:10–26.

Stanley, M., 2000: Geodiversity. *Earth Heritage*, **14**: 15-18.

UNESCO, 1999: UNESCO Geoparks Programme – a new initiative to promote a global network of geoparks safeguarding and developing selected areas having significant geological features: Document 156 EX/11 Rev., Executive Board, 156th session, UNESCO, Paris, 3p.

UNESCO, 2015: Statutes of the International Geoscience and Geoparks Programme and Operational Guidelines for UNESCO Global Geoparks: UNESCO, Paris, 6 p.

Wadhawan, S.K., 2013: Conservation, Protection and Maintenance of National Geoheritage sites – contributions from Geological Survey of India. In: Reddy, D. R., Sarma, Rani (Eds.), Proceedings of the National Workshop & Brainstorming Session on Geoheritage Sites in India – Need for Indian Activism, Andhra University & INTACH, Vishakhapatnam, 30-31 May 2013. 23-45p

Wadhawan, S.K., 2016: Jaisalmer Basin in Thar Desert - Potential for Developing Geopark in Rajasthan, West India. *In*: Proceedings of the 35th International Geological Congress, IUGS, Cape Town South Africa. *Association of Geoscience Societies of America*. Paper No. 1770.

Wadhawan, S.K., 2020: Responsible Mining and Conservation of Geodiversity through Geotourism in India – a perspective. *Mining Engineers' Journal*. **21(10)**: 22-26.

Indian Journal of Geosciences, Volume 74, No. 3
July - September, 2020; pp. 363-368

Invited Paper

Geo-Information in Ancient Indian Literature

Prithvish Nag

Department of Civil Engineering, Indian Institute of Technology (Banaras Hindu University), Varanasi
Email: prithvishnag@hotmail.com

Abstract: India is very rich in ancient literature. The literary works were philosophical or religious but they do contain valuable information on geographical and geological features. Most of the works are in Sanskrit from Hindu, Buddhists and Jain sources. They provide information and descriptions on the regions, geology and rocks, water, soil, forests, land and its use, climate and the like. The classifications of these features do indicate the strength of information, depth of analysis and their interrelationships. Vedas, Kautilya's Arthasastra, epics and the likes have to be studied and analyzed for understanding the geo-information contained in such literature. Further, this ancient wisdom and the modern knowledge go in different directions. Convergence of both the sources will help in generating new knowledge.

Keywords: Geo-information, Rig Veda, Arthasastra, Mahajanapadas, Markandya Purana, forests, land, climate and agriculture.

Introduction

Boundaries depict continuity and change. They are compromise of several historical, cultural, social and administrative processes over space, which may be a nation, state, district or even a revenue village. In an old settled country like India, such processes are complicated but essential to understand and analyse the socio-economic composition; and to use them as a basis to administrative change for development (Singh *et al.*, 1971). .

In the ancient Indian literature we do get some indications of aerial units by the way of describing different characteristics, customs and civilization, *e.g. Kautilya's* description about gems in *Arthasastra*; or *Vatsyayana's* enumeration of different customs in *Kamasutra* and the like (Sharma, 1980). However, the boundaries were not precise. Nevertheless, Kalidas in *Meghadutam* and *Raghuvansa* described the boundaries with a fair accuracy with the help of hills, rivers, plains, mountains and settlements. In fact, he is considered to be the earliest Indian geographer. Though, the *Ramayana*, the *Mahabharata*, the *Puranas* and the *Katha Saritsagara* do provide some geographical descriptions, they are not always accurate to the extent which we understand now Dube, 1967).

Geographical Regions

India has been described as a geographical entity and hence attempts have been made to understand its boundaries. One of the earliest references we get is in *Vishnu Purana*. It defines the extent of India between the snowy Himalayas and the ocean. Further, during different historical phases, various regions and sub-regions got prominence, which do have some sort of continuity either in conceptual or in spatial form. *Aryavarta*, *Aparanta*, *Dakshinapatha* and *Prachya*were frequently referred in the ancient literature. Bounded on the north by chains of mountains and on the other three sides by seas and oceans, this part of Asia has been considered as a distinct geographical unit since time immemorial (Nag and Sengupta, 1992). The exploration of the entire country has been completed in or about the fourth century B.C.

Literatures of this period show acquaintances with the realm of the *Pandyas* in the south and even beyond up to the island Tamraparni (Sri Lanka). The name *Jambudvipa* was used by that time to denote this region. The term "India" has been derived at a much later date from the name of the River Sindhu or the Indus. References from ancient literature reveal a five-fold division of India. In the centre of the Indo-

Ganga plain was the *Madhya-Desha* stretching according to the *Brahminical* account, from the River Saraswati, which flowed past Thaneshwar and Pehoa (ancient Prithudaka), to Allahabad and Varanasi and according to the early records of the Buddhists, to the Rajmahal hills. The western part of this area was known as the *Brahmarshi-Desa,* and the entire region was roughly equivalent to *Aryavarta,* as described in the grammar of Patanjali but according to other references *Aryavarta* means the whole of the territory lying between the Himalayas in the north and the Vindhyas in the south. To the north of the *Madhya-Desa* lays *Uttarapatha.* The entire Indus valley being cradle of Rigvedic culture was included in the *Uttarapath. Aparanta* or *Pratichya* (western India) was Saurashtra, and the northern Konkan. *Dakshinapatha* was the upper Deccan, north of the Krishna River, the region between the Satpura hills and Rameshwaram. The south was also termed as Tamilakam or the Tamil country. *Purva Desha* or *Prachya* was the eastern region. To the five primary divisions, the *Puranas* also add two others, namely, the *Parvasrayin* or the Himalayan tract, and the Vindhyan region (Law, 1968).

In the sixth century B.C., references from Buddhist literature show India had sixteen large states called *Mahajanapadas*. The administrative unit at district level was called *Janapada.* Of the *Mahajanapadas*, Magadha, Kosala, Vatsa and Videha were powerful states in eastern India. In the west, the states of importance are Avanti, Panchala, Surasena, Matsya and Kuru (adjoining areas of western Uttar Pradesh, Rajasthan and Haryana).

Geological Background

The earliest reference of the knowledge of Indian geology is available from *Vaidika* literature, referring the origin of earth from its primary gaseous state. In the *Satapatha Brahmana*, descriptions of various earth materials (*Sristayah)* are found. They are: (i) *Fena* (foam), (ii) *Mrid* (clay), (iii) *Suskapa* (vapours), (iv) *Usa* (saline earth), (v) *Sikata* (sand, silica), (vi) *Sarkara* (primary crystalline rocks), (vii) *Asman* stones, consolidated rocks), (viii) *Loha* (iron), (ix) *Hiranya* (gold) and (x) *Oshadhi, Vanaspati* (herbs and plants).

Mineral civilization of India dates back to approximately 3,000 years before the birth of Christ, the Bronze Age, which replaced the Neolithic age. The mineral civilization, which evolved simultaneously in Egypt, Mesopotamia, India, Greece and China, became more elaborate and extensive as urban civilization needed for a constant supply of minerals. Ancient Indian literature, the *Atharvaveda* classified rocks, forming the earth's crust in the section namely, the *Prithivisukta (Shilabhumirashmapangsusabhumihsangghritaghrita/ tasyeyhiranyabakshaseprithibyahakarangnamah)*,which means: Rock, earth and stone, and dust, this earth is held together firmly bound. (Pandey and Sukla, 1962).

Atharvaveda classified rocks, forming the earth's crust composed of hard (*Sila),* argillacious (clayey or *Bhumi*), arenaceous (sandy and pebbly and *Asma*and *Pamsuh*) rocks. Mentions are also made of different coloured, hard and soft types of rocks in *Ramayana* and *Vamana Purana.* Rocks, found in India are classified into three broad categories, *viz.* igneous, sedimentary and metamorphic. Their occurrences vary from widespread stretches to small patches or pockets throughout the country (Wadia, 1953).

Soils

Soil, which is the outer mantle of the earth's crust, is influenced by climatic factors. Soils of India extending from the temperate regions through the sub tropical and torrid regions show remarkable differences in character which in turn are reflected in the vegetation pattern of the country. *Satapatha Brahamana* the ancient Indian literature describes the earth materials *(Sristayah*) in their various forms. In the *Taihiya Aranyaka*, the soil is devoted to be pious as it promotes welfare giving vitality. The study of soils was made from the point of agriculture and building purposes. The *Agni Purana* has studied the soil according to their colour and smell.

Water Resources

From the very beginning of history, all civilizations were based on water resources. The ancient Indian literature has repeatedly mentioned about the importance of rivers and other water bodies. According to *Markandya Purana*, "all rivers are sacred, all flows towards the sea. All are like mothers, all purge away sins." The whole Aryan land was described in terms of rivers called Ganga, Yamuna, Godavari, Saraswati, Narmada, Sindhu and Kaveri. The traditional Indians chanted hymns when offering prayers as "*let all the sacred waters of Ganga, Yamuna, Godavari, Narmada, Sindu and Kaveri* be represented together in my offered (*puja)* water to thee" ("*Om Gangech Yamunechaiba Godavari Saraswati / Narmada, Sindhu, Kaveri/Jaleisminsannidhing kuru*"). Similarly, the Buddhist-heartland was represented by the seven sacred rivers (Ganga, Yamuna, Sarabhu, or Sarayu, Saraswati, Aciravati and Mahi or Mahanadi). Further, the rivers as per their origin, which are mostly mountains, have been grouped by Ptolemy, the Greek explorer, and also in the great epic, the *Puranas* and in Jain and Buddhist books. In *Rajanirghanta*, the quality of water having different origin has been described.

Water conservation and management has been embedded in the Indian civilization. The *Vedas,* the earliest reference of Indology (more than 3,000 years old) refer to different sources of this valuable resource, such as *avata* (or well*), Kuliya* (canal) and *Sarsi* (dam). Manu, the great law maker mentions about *tataka* (artificial water storage) or upkeep of aquatic resources in general, conservation of moisture, water quality, equitable distribution and water balance, laws and punishment for polluting the water and the like. One of the greatest Indian epic, *Mahabharata* (C3150 B.C.), referred about the enquiring of availability of water in different parts of the Kingdom. Kautilya (fourth century B.C.) in *Arthashastra* mentions about the management of dams and their repairs. In the classical Sanskrit literature the categorization of water courses has been included. Water and irrigation was looked after by a specialist, *jalasutrada* or water director. In fact there are references to *Patha Shastra* or hydrology in the ancient Indian inscriptions.

Climate

An Indian conception of atmosphere, weather and climate are vividly described in literary sources like the *Atharva Veda*, the *Brahamanas*, the Epics (*Ramayana* and *Mahabharata*) and many other Hindu, Buddhist and Jain chronicles. Ancient Indians discovered that the earth is surrounded by a cover called *Antariksha* or *Bhuvah* (earth) and *Svah*or *Dyavh* (heaven). Bhaskaracharya conceived (in *Siddhanta Siromani*) the thickness of the atmosphere to be 12 *yojanas* (15 km approx.) round the earth where winds, clouds, lightning, rain etc. occur. *Mahabharata* mentions seven layers of atmosphere, *viz*. *Pravaha, Avaha, Udvaha, Samvaha, Parivaha* and *Paravaha.* The *Atharva Veda* mentions terrestrial radiation and the insolation received from the sun which determines the season or *Ritu*. The *Rig Veda* lucidly describes *Grishma Ritu* (Summer), occur in *Jeystha* and *Asadha* (May & June); *Varsa Ritu* in the months of Shravana and Bhadrapada (July and August); Sarada Ritu in the months of *Asvina* and *Kartika* (September and October); *Hemonta Ritu* in *Margasirsa* and *Pausa* (November and December); and *Sisir Ritu* in *Magh*a and *Phalguna* (January and February) with their all sorts of combination, temperature, precipitation, wind condition, the prevailing disaster out of them as well as the crops and other vegetation grown through the period. *Vedic* scholars classified three different types of winds, namely, *Vayu*, the gentle breeze; *Marudgna*, the Monsoon wind and *Rudra*, denoting thunder storms and gales. Geographers in the *Bhagbata Purana* used the term *Chakravata* for cyclone. Through ages observations on meteorological phenomena about the insolation, condensation, precipitation and their distribution become helpful in agricultural activities.

Forests

There are twelve mega-diversity countries in the world and India is one of them where, the eco-climatic zones, from cold deserts to rich-dense topical forests are there. Moreover, Indian culture had its roots in forests. The forests of ancient India not only contained valuable timber, fuel wood, medicinal plants but also provided the suitable environment of meditation and higher studies. *Brihad-aranyakopanishad* actually the last of the ten *Upanishad*, as its name connotes, was composed in the solitude of deep forests. Girija Prasanna Majumdar prepared a list of the trees, shrubs, herbs and other plants mentioned in the Vedic literature. This list is based upon the classical work on Vedic index by two Europeans, McDonnell and Keith (Chatterjee, 2004). The list comprises the following species.

(a) *Asvattha*, growing wild in the Siwalik hills

(b) *Spandana*

(c) *Svadhiti*, a hard wood tree,

(d) *Kakambira*

(e) *Khadira*, a hard wood tree on which Arundhati, a creeper with healing properties climb

(f) *Kharjura,* growing wild in the Indus basin

(g) *Haridru*, a coniferous tree, growing in Uttarakhand

(h) *Pitudaru*, Pine

(i) *Putudru,* Pine

(j) *Nyagradha* etc.

Asvavati, Somavati, Udojasa and *Urjayanti* are the four important medicinal herbs indicated in *Rig Veda.* 'There is no wonder then, that India was also worshipped by the Aryans as the mother of many herbs and repository of many potent drugs (Chatterjee 2004). There is also mention of forestry in *Rig Veda*. The use of axe which perhaps was used to cut trees, the mentioned by *Taksana* and *Tvastri* (carpenters) working on woods are also there. In the epic there are references to the exploitation of forest resources. In the *Ramayana,* the *Mahabharata* and in the *Jataka*s, there are indications of the use of forests economically. At that time forests were governed by the kings and they provided a great source of economic prosperity to the society. There is evidence in literature, of the existence of a guild of weavers near Varanasi, which collected timber from the forests and made household furniture (*Anilachitta Jataka*). The *Puranas* laid great importance to afforestation and also provided with classification of trees. The following are the advantages of forests realized by ancient India (Chatterjee, 2004).

1. Forests were used as pasture lands.
2. It was a great source of fuel, dwellers used to cut them.
3. Wood was in use for making houses, chariots and cots. Sala, Audunibara, Bamboo, Tala, and Deodar were considered very important trees for their economic utility.
4. Honey from forest trees and certain types of juices like *Niryasa* were also received from sandal trees.

5. Fruits and roots were the main item of food for hermits in the forest. They also used *Valkalavastra* made from the barks of trees.

Thus, in India, forest exploitation was done by man since the very beginning for shelter, food and fulfillment of their needs. But in recent days, the forest resource has been cut down rapidly. The soft wood coniferous trees *i.e*. *Pitudaru* mentioned in the *Rig Veda* represent very small percentage of share now-a-days. The bulk of the present day forests comprise hard wood trees like *spandana* and *svadhiti* of the Rig Veda.

Land and its Use

The earliest evidence of land use can be quoted from *Rig-Veda* (R.III.3.2.15) as "wide fields, vast treasures, spacious pastures, have Indra bestowed on his friends." In the Vedic age land was laid out into regular fields, ploughed and sown and crops were reaped and stored. The Vedic farmers knew the method of improving fertility of the soil by crop rotation (*Taittiriya Samhita*). The plough land was called *Urbara*or *kshetra.* Classification of land became elaborate in the Buddhist period (sixth century B.C.) when *khetta* or pastures and woodland or uncleared jungles were kept around the *Janapada* or *Gama* (cluster of two or three houses to an indefinite number). Adjoining those wilder tracts were the supplementary grazing pastures of cattle and goat (Aiyer, 1950). The arable land of the *Gama* were surrounded by fences and guarded by watchmen. Internal boundaries of each house holders plot were apparently made by channels, dug for co-operative irrigation.

During the Mauryan administration the divisions of lands for various purposes were well classified. Kautilya's (prime minister of Chandragupta Maurya) *Arthashatra* accounts cultivated plot of lands (*krsta*), uncultivated fields (*akrsta*), high and dry ground (*sthala*), grovel (*arama*), horticultural plantation (*sanda*), field for growing roots (*mulavapa*), sugar cane plantation *(vata*), wet lands (*kedara*), gardens, vegetable gardens fenced plots, forests, alters, temples, irrigation works, cremation grounds, feeding houses, piaos where water was supplied to travellers, places of pilgrimage, pastures grounds (*vivita*), roads (*pathi*), boundary plots, threshing floors, house site and stables of domestic animal. The age of the Guptas, (AD 300-AD 500) as the *Amarakosha* written by great scholar Amar Singha classified 12 types of land in its chapter on *Bhumivarga*. Depending upon the feasibility of the soil, irrigation facilities and physical characteristics of the land the 12 divisions made are: *urbara* (fertile), (2) *usara* (barren), (3) *maru* (desert), (4) *aprahata* (fallow), (5) *sadvala* (grassy), (6) *pankila* (muddy), (7) *jalaprayamanupa* (watery), (8) *kaccha* (land contiguous to water), (9) *sarkara* (landfall of pebbles and pieces of limestone's), (10) *sarkaravati* (sandy), (11) *nadimatrka* (land watered from a river) and (12) *devamatrka* (rain fed). The kingdoms of southern India, specially the Chola dynasty (AD985-AD1205), showed the most glorious phase in the history. Prosperity resulted from irrigated agriculture. All lands were carefully classified into tax bearing and taxable lands. The taxable were graded according to their natural fertility and the nature of the crops of the ground

Irrigation

Agriculture has been the principal occupation with the Indians since time immemorial. Earliest reference goes with Aryan civilization. In many sutras of *Rig-Veda*, watering of fields from canals and walls are found. Mauryan empire, from the sixth century B.C., paid attention to irrigated crops. Kauitlya in *Arthashastra* mentions:

"Those who irrigate land by manual labour shall pay 1/5th of the produce as water rate *(Udakabhagam*); by carrying water on shoulders, 1/4th of the produce; by water lifts 1/ 3 rd of the produce; and by raising water from rivers, lakes, tanks and wells 1/4 of the produce."

Megasthenese, the ambassador at the court of Chandragupta wrote:" The whole country is under irrigation and very prosperous because of the double harvest which they are able to reap each year because of irrigation". Irrigation system, developed in southern India from 985 to 1205 AD under Chola dynasty. The proud achievement of southern India in this period is irrigation system by building anicuts across rivers and the chains of tanks in the courses of small streams. The most famous of the Chola public work is the great anicuts, in the south of the island of Srirangam, consisting of a massive dam of uneven stone, 329 m long and from 12 to 18 m broad. There were chain tanks in Andhra Pradesh, Karnataka, and Telegana and hence the area was known as the land of thousands tanks. In the tenth century a vast majority of tanks are constructed on a connected system and their feeders in the undulating plateau of Karnataka. Tank supervision committee looked after the maintenance of the irrigation works. During the medieval period, towards the middle of the 14th century Great Plains witnessed memorable feats of irrigation-engineering regarding application of agriculture.

Agriculture

History of Indian agriculture dates back to Harappan Chalcolithic culture in India (c 2200 B.C.-1600 B.C.). Food grains and fibers recovered from excavations of Mohan-jo-daro, Harappa, Lothal and Chandigarh are the best evidences found along with the granaries found in Harappa and Lothal. The Indo-Aryans appear to have brought with them their staple food grain (*Java),* the wheat and barley, which was adopted by the Indus people, generating new variability required for more intensive cultivation. The carbonized grains of gram *or* chana *(cicer arietinum*), peas *(pisumsativum),* sesame, rape and mustered are recovered from the excavated granaries of Kalibangan (Harappan site of Rajasthan) and are carefully preserved in the Genetics Museum of the Indian Agricultural Research Institute, New Delhi. Both Neolithic and Chalcolithic cultures were developed in South India in Andhra, Karnataka and Tamil Nadu with different genera and species of *jawar* (sorghum bicolor), *bajra (pennisetumty phoides*) and *ragi (eleusinecoracana*). Carbonized seeds of pulses have been recovered from neolithic site of Tekkalakota in Karnataka, dated to 1780 B.C to 1500 B.C. Navdatoli, the key site of this culture of the Narmada basin show evidences of pulses like *masur*or lentil *(lens culinari) urad* or mash *(vigna mungo),mug* or green gram (*vignaradiata) and khesari (lathyrussatives*) are the first record of pulses from India showing their antiquity (Randhawa, 1980).

The Neolithic culture of eastern India *viz.* Assam (excavated site Daojali Hading), north Bihar (Chirand), West Bengal (Pandu Rajar Dhibi) and Orissa (Kuchai) can claim the origin of cultivation of rice. Eastern India can also claim the origin of multiplication and selection of clones for vegetative propagation. References regarding agricultural practices, implements and crops show a fair knowledge of fertility of the land, selection and treatment of seeds, seasons of sowing and harvesting, rotation and other cultural practices. The pursuit of agriculture was not associated with either social prestige or social stigma in the 6th century B.C, *i.e.* the Buddhist period. Both *Jatakasuttas* and *Brahamans* are frequently found pursuing agricultural practice. Kautilya wrote in *Arthashastra,* a vivid account of social, political and economic conditions of India. Classification of different lands for different crops mentioned by Kautilya is as follows:

(a) Lands, that are beaten by foam *(Phenaghata*) are suitable for growing pumpkin, gourd etc.;

(b) Frequently flooded lands are suitable for pepper, grapes and sugar cane when the vicinity of the wells for vegetables and root crops in the moist beds of lakes etc. for green crops and

(c) The marginal furrows between any two rows of crops are suitable for the plantation of fragrant plants, medicinal herbs, *khus-khus* roots etc

From all these accounts it is found that India knew the art and operations of farming seed treatment, growing of crops, inter-culture control of pastes, plant diseases and irrigation techniques etc. Kautilya refers to sluice gates of tanks for regulation of water flow. Agricultural activities flourished and implements of iron started in 200 B.C.-AD300, the period of Sungas to the Satbahanas and Kushans. The people of Deccan cultivated cotton. According to R.S. Sharma (1980), the art of transplanting rice seedlings was widely practiced in the first two centuries in the deltas of Krishna and Godavari which become the rice bowl of southern India.

Gupta period (A.D.300-A.D.500) is known as the "golden age" of Indian history. Renaissance in art, literature, science, high level iron technology and progressive agriculture took place. Varahamihira (AD 505-587) records information of detailed agriculture in *Brhatsamhita*. The book *Agnipurana* deals with the selection of land manuring, cultivation the treatment of seed, sowing, planting, reaping and grafting. *Amarkosha* of Amarsimha, a scholar of Chandra Gupta II contains information on soil irrigation and agricultural implements. The life of the people of India and their agriculture is described in Hiuen Tsang's *Si-Yu-K* and Bana's *Harshacharita* during the Kanauj Empire of Harshabardhana (AD 606-AD 647). From all their accounts it appears that cereals like wheat, rice, millets, various fruits and vegetables were extensively cultivated.

River Narmada was the conventional boundary between the northern and southern India. Southern states are subdivided into two groups; (a) kingdoms of the Deccan plateau and (b) Tamil kingdoms. The dynasty of the Chalukyas, Rashtrakutas, Pallavas, Cholas, Pandyas, Hoysalas and Kakatiyas (AD 535-AD 1300) all contributed immensely to the different fields of improvement of the country. With the expansion in irrigation, rice cultivation was extended over a large area. Millets continued to be cultivated in rain fed areas of the Deccan and Mysore plateau. The names of crops are mentioned in relation to the land revenue payable to the government and the rent payable to the landowner. These are paddy, millets, sugarcane, mango, coconut, plantain, jackfruit, ginger, pumpkin and yams. Cardamom *(elettriacardamomum)* produced in southern India was highly prized and exported to Middle-East countries along with cloves *(syzygiumaromaticum*), sesame *(sesamumindicum)*, indigo varieties of barberry, opium, rhubarb and fruits like coconut, banana, melon, peaches, apricot and vegetables as cucumber and onion.

The sources of information on agriculture in India from the ninth to eleventh centuries are the writings of Medhathithi, Parasar and Kashyap. In *Abhidhariratriamala*, Medhalithi classifed soil as fertile (*urvara*), barren, (*irina*), fallow (*khit*a), desert (*maru*) and excellent (*mritsa*). Different kinds of fields were selected for different crops like varieties of rice (*vrihi, sali,odrava*), of beans (*mudga* and *masha*), oilseeds (sesame and linseed) as well as those producing hemp, barley and vegetables. *Krishi Parashara* deals with the then existing system and knowledge of agricultural such as soil classification, land use, manuring, rotation of crops, irrigation tillage implements, protection of crops from pests and diseases and agricultural meteorology.

Conclusion

The information on geography, geology and other spatial features in the ancient Indian literary works is enormous. Such valuable sources of knowledge have been overshadowed by the modern concepts and ever improving technologies. *Rig Veda* itself contains precious description about the universe, earth and other geo-information. The attempt should be to bring closer the ancient knowledge wisdom and the modern concepts and technology. We can no longer ignore the possible integration of both the approaches. Perhaps the motto should be to generate new knowledge by convergence. There are other fields of proficiency as well where similar approach is required. Geospatial information should be considered as an example in this direction.

Acknowledgement

This research paper has been extracted from a major work entitled P. Nag (Eds.) (2006), *India by the turn of Millennium*, National Atlas & Thematic Mapping Organisation, Kolkata.

References

Aiyer. A.K.Y.N., 1950: Dairying in Ancient India. NIS, New Delhi.

Chatterjee, S.P. 2004: Geography and culture of India over time and space. *In*: Selected works of Professor S.P. Chatterjee, National Atlas & Thematic Mapping Organisation, Kolkata. Lecture delivered in Sri Sathya Sai Summer Course in the year 1974 and 1978, (Eds.) P. Nag and G.N. Saha.

Dube, B. 1967: Geographical Concepts in Ancient India. The National Geographical Society of India, Banaras Hindu University.

Law, B.C., 1968: Mountains and Rivers of India. National Committee for Geography, Calcutta.

Nag, P. and Sengupta S. 1992: Geography of India. Concept publishing Company, New Delhi.

Pandey, I.C. and Sukla V.D. 1962: Geology of ancient India. *Prajna*, B.H.U. Journal.

Randhawa, M.S., 1980: A History of Agriculture in India. Department of Agriculture, I.C.A.R, Government of India, New Delhi, **I &II**.

Sharma, Rajendranath, 1980: Ancient India According to Manu. Nag Publisher, Delhi.

Sharma, R.S. 1980: Ancient India. National Council of Educational Research and Training, New Delhi.

Singh, R.L. *et al.* (Eds.) 1971: India: A Regional Geography. National Geographical Society of India, Varanasi.

Wadia, D.N. 1953: Geology of India. National Book Trust, New Delhi.

Indian Journal of Geosciences, Volume 74, No. 3
July - September, 2020; pp. 369

Scientific Note

DOVEMAP - Development of village economy through Mineral Appraisal Program

Sri. K. Krishnanunni, the then HOD of the the Northeastern Region, Geological Survey of India (GSI) conceived and proposed DOVEMAP, a grassroot, practical program in 1996 with following objectives:

(1) Keeping in view the rapid urbanization and industrial growth in the Northeastern Region, particularly in Brahmaputra and Barak basins in Assam, it was envisaged that there would be increased demand for building and construction material.

(2) Localization, assessment and utilization of these resources will generate employment opportunities for weaker sections of the rural society and improve their living standards.

(3) Program was envisaged at generating rural employment and discourage their migration towards urban areas.

(4) Identify and suggest remedial measures for various environmental and natural hazards.

(5) Assess and suggest proper land use in consideration with soil type, soil cover and forest/vegetation covers in various areas.

The methodology involved in the project was to map and transfer the geoscientific knowledge and data about terrain evaluation to grassroot level, i.e., on cadastral base village revenue maps (on 16" inch = 1 mile scale) and to educate rural population at village panchayat levels about natural/ mineral potential, soil erosion, ground water, natural water conditions and various hazards problems - proposed and possible remedial measures for substantial development and generating rural employment. The dataset collection included details on socio-economic scenarios of villages, their geological, geomorphological setup, soil types, distribution, land use pattern maps, search, localization and assessment of low-value high volume minerals.

Development and finalization of working methodology and implementation of the programme was initiated through a pilot project in 10 villages covered in Kamrup, Darrang, Nagaon and Majuli Island of Zorhat districts in Assam during 1996-97 field season. All the villages covered under this project are located in the Quaternary sediments. In Kamrup districts, basement rocks are encountered at variable depths. During Pilot project implementation, natural resources of plastic clay bands suitable for pottery making and sand pockets and hard rock boulders useful as building material were located. Water table conditions and land-use pattern maps were prepared depicting geo-environmental hazards and suggested remedial measures.

Based on the results obtained during the pilot studies followed by critical reviews of proposed data collection methodology. Parameters and factors held during the in-house workshops at Guwahati, Shillong and Itanagar. The programme was extended as a regular project in parts of Assam, Meghalaya and Tripura states. About 165 villages, were covered during 1997-98 field session, 98 villages in 1998-99, 168 villages in 1999-2000, and 178 villages during 2000-01 were covered under the extended program. Similar type of work was also taken up in other parts of India.
During the subsequent years, shallow drilling for water and water analysis by rapid mobile water testing kits were also added in the working process. Assessment of sub-surface lithology and ground water quality with a possible correlation to the land-use pattern and suggested or modified land-use pattern.

Important problems and hazards identified in different areas were related to land and soil erosion by flood waters, frequent shifting of channels, river bank erosion, slope erosion, deforestation. Various measures suggested include sope stabilization by plantation of suitable trees, soil binding grass and vegetation cover and providing micro drainage outlet channels to minimize slope wash and soil erosion.

Z.G. Ghaveriya
Former Director, Geological Survey of India

SOME RECENT PUBLICATION OF GSI

Record Vol. 152 Pt. 9

Annual Report for F.S. 2017-18 ₹ 3744.00/$ 132.00/£ 100.00/€ 116.00

Bulletin Series C. No. 10

Compilation of Geotechnical Database ₹ 387.00/$ 15.02/£ 11.12

Bulletin Series A. No. 68

Diamond Fields of Southern India ₹ 3109.00/$ 121.31/£ 85.10

Bulletin Series A. No. 66

Limestone deposits of Ukhrul District, Manipur ₹ 919.00/£ 26.47/$ 35.65

Bulletin Series A, No. 45, Volume-VI

Geology and coking coal resources of Jharia coalfield, Dhanbad and Bokaro districts, Jharkhand, February 2019

₹ 442.00/$ 16.00/ £ 12.00/€ 14.00

Bulletin Series B, No. 71

A comprehensive report on pre-construction and construction stage geotechnical investigations of Maneri-Bhali hydro electric project, Stage-II, Uttarakhand, 2019 ₹ 1223.04/$ 42.51/£ 33.90/€ 37.51

Special Publication No. 111

Landslide Compendium of Maharashtra ₹ 511.00/$ 20.07/£ 14.25/€ 16.19

Indian Journal of Geosciences

Vol. 73, No. 1 (January - March, 2019) ₹ 250.00/$ 10.25/£ 6.25/€ 7.50

Vol. 73, No. 2 (April - June, 2019) ₹ 250.00/$ 10.25/£ 6.25/€ 7.50

Vol. 73, No. 3 (July - September, 2019) ₹ 250.00/$ 10.25/£ 6.25/€ 7.50

Vol. 73, No. 4 (October - December, 2019) ₹ 250.00/$ 10.25/£ 6.25/€ 7.50

Vol. 74, No. 1 (January - March, 2020) ₹ 250.00/$ 10.25/£ 6.25/€ 7.50

Vol. 74, No. 2 (April - June, 2020) ₹ 250.00/$ 10.25/£ 6.25/€ 7.50

The Geological Survey of India products are sold on advance payment; payment is to be remitted by
Bank Draft drawn in favour of
The Director General, Geological Survey of India
27, Jawaharlal Nehru Road, Kolkata- 700 016

For further details visit us at: www.gsi.gov.in

GUIDANCE TO AUTHORS

Policy

Indian Journal of Geosciences (formerly Indian Minerals) is the official journal of the Geological Survey of India and aims to publish quality research articles and notes dealing with all aspects of Earth sciences. Anyone - both from within and outside the Department - can contribute to the journal, provided that the contribution is of interest to Earth scientists. The papers are accepted on the merit of quality and originality of the research work and its significance to the readership. Names of two referees may be suggested at the time of submission of the manuscript. Submission in the Journal is understood to imply that the same is not published or submitted for publication elsewhere. The Editor reserves the right to accept or reject any material for publication or to modify a manuscript towards improving its communication and polishing the language. Author should retain copies of manuscript and other documents as material once submitted cannot be returned.

Peer Review

This journal follows a double blind review process. All contributions will be initially assessed by the editor for suitability for the journal. Papers deemed suitable are then sent to independent expert reviewer/s to assess the scientific quality of the paper. The Editor is responsible for the final decision regarding acceptance or rejection of articles.

Manuscript Preparation and Submission guidelines

(a) Manuscript should be written in English and spellings should conform to the Concise Oxford Dictionary of Current English.

(b) The typescript should preferably be prepared on a word processor with 12 font size, double spacing and wide (about 3cm) margins only on one side of A4 size paper.

(c) The typescript should include a title page with a concise, informative title and a list of author's names and affiliations with respective addresses (postal as well as e-mail); corresponding author should also be clearly specified. It should include an abstract of not more than 500 words. Abstract should not contain abbreviations or reference. Three to 10 key words should also be provided for indexing purpose.

(d) The main body of the text should be arranged under up to four different levels of heading.

(e) The use of S.I. units is recommended.

(f) Authors should not indulge in formatting (e.g. bi-column, etc.) while preparing the typescript.

(g) Tables and figures must be numbered consecutively in Arabic numerals in accordance to the order of their appearance in the text. The word 'figure' should be shortened to 'Fig.' except when starting a sentence. All illustrations (line drawings and photographs) are to be classified as figures.

(h) The actual tables and figures may be kept separate from the text and presented with captions in separate sheets of A4 size. Tables and figures should be self-contained and understandable without the reference to the text. Sources of tables and figures taken from already published material must be properly acknowledged.

(i) In the tables, vertical lines should not be used to separate columns.

(j) Captions of maps and other line drawings must not be included within the artwork.

(k) All references cited in the text should be given in the reference list and vice versa. References in the text should follow the author (date) system. In the list, references should be listed in the alphabetical order of the first author(s), citing the names of all the co-authors as well. The Journal style for listing the references is as follows:

Glaessner, M.F., 1984: The dawn of animal life. Cambridge University Press, Cambridge, 244p.

Singh A.K., and Singh R.K.B., 2011: Zn- and Mn-rich chrome-spinels in serpentinite of Tidding Suture Zone, Eastern Himalaya and their metamorphism and genetic significance. *Current Science*, **100 (5):** 743-749.

Grotzinger, J.P., Bowring, S.A., Saylor, B.Z. and Kaufman, A.., 1995: Biostratigraphic and geochronologic constraints on early animal evolution. *Science*, **270:** 598-604.

Harley, S.L, 1998: On the occurrence and and characterization of ultrahigh temperature and crustal metamorphism. *In*: What drives metamorphism and and metamorphic reactions? P.J. treloar and P.J. O'Brian (eds.), *Geological Society, London, Special Publications*, **138:** 81-107.

(l) Authors are encouraged to submit manuscripts electronically. Electronic submissions should be sent as e-mail attachments as a MS-Word document with figures incorporated, and should be no more than 15 MB including figures and tables. Figures are to be incorporated as JPEGs.

(m) Submission of the manuscript is through www.gsi.gov.in /Core Apps module or can be mailed to the above given e-mail address.

(n) At the time of submission of the final revised versions electronic files of the complete paper may be sent, bearing in mind the following points:
- The software program (and version) used to generate the text, tables and figures must be specified.
- Each figure should be saved as a separate file of manageable size (less than 2 MB). If a figure has multiple sub-figures, all the sub-figures and sub-figure numbers should be given as single image file. Figures are to be submitted in .jpg format. Files must be submitted at a resolution of at least 300 d.p.i at full size. Powerpoint and PDF files are not acceptable.
- It must be ensured that files are not saved as read only.

Proofs

The corresponding authors will be e-mailed an edited PDF file of their articles. Authors are requested to check this file carefully for errors and to answer any queries. Corrections in the proofs may be listed quoting page / line nos. and returned preferably in an e-mail. The Journal authority may proceed with the publication of an article if no response is received within stipulated time.

Offprints

The corresponding author will receive PDF file of the article via e-mail.

Subscription Information

The subscription rates are as follows: Annual subscription: ₹ 1000.00 / £ 25.00 / $ 41.00
Single Issue: ₹ 250.00 / £ 6.25 / $ 10.25 / € 7.50
Subscription is accepted both in Indian and foreign currencies and is payable by D.D. (payable at Kolkata Branch) drawn in favour of the Director General, Geological Survey of India, 27, Jawaharlal Nehru Road, Kolkata-700016, India.

Indian Journal of Geosciences is Abstracted in AGI's Bibliography and Index to Geology, Economic Geology, INIST (France), Geoabstracts, Geotitles, India Science Abstracts (INSDOC), SCOPUS, Mineralogical Abstract, Journal of Asian Earth Science, Chemical Abstract Service (ACS).

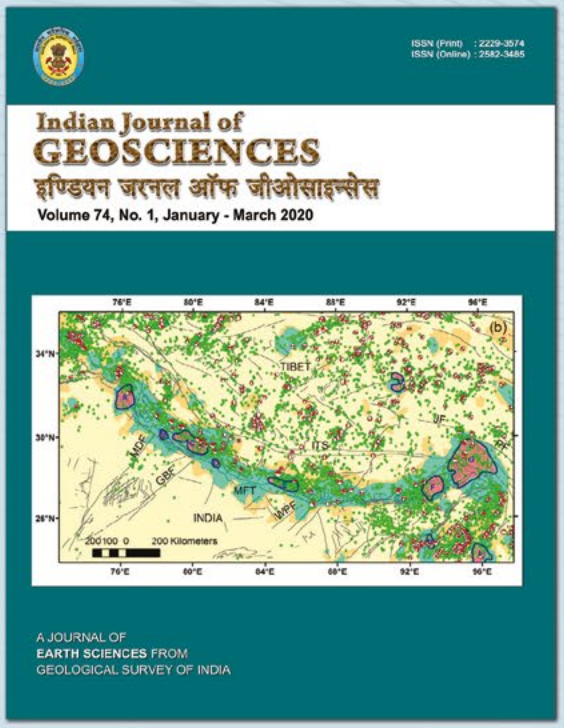

Indian Journal of GEOSCIENCES

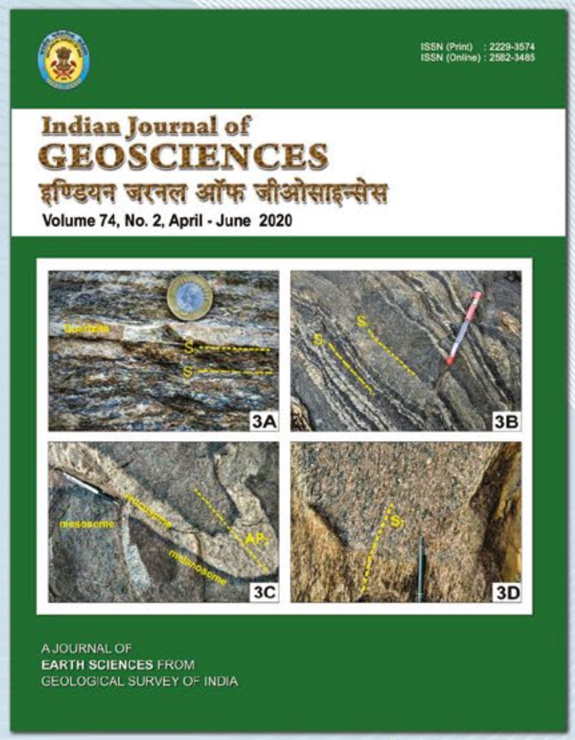

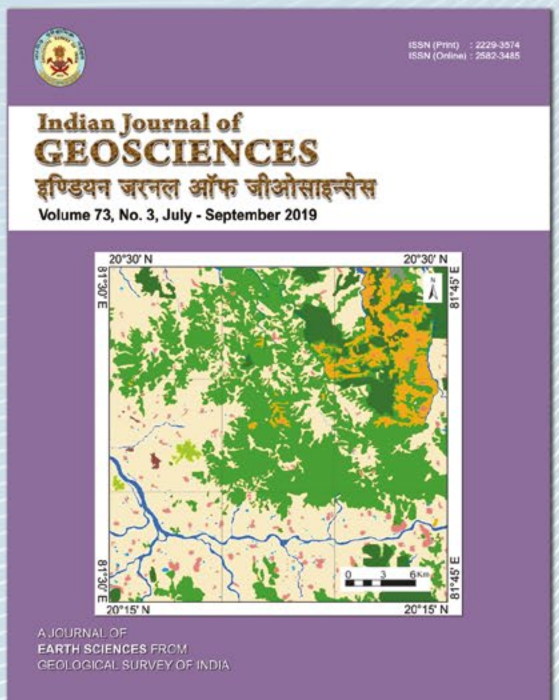

Published by the Director General, Geological Survey of India, 27 Jawaharlal Nehru Road, Kolkata - 700 016

Printed by Semaphore Technologies Pvt. Ltd., 3, Gokul Baral Street, Kolkata - 700012

Price of this issue :
₹250/ £6.25 / $10.25 / € 7.50

PGSI - 15 - 3 - 2020